PENNSTATE

THE DEVELOPMENT OF COAL-BASED TECHNOLOGIES FOR DEPARTMENT OF DEFENSE FACILITIES

Semiannual Technical Progress Report for the Period 09/28/1994 to 03/27/1995

Volume 1. Technical Report

By DOE/PC/92162--T9

Bruce G. Miller, David A. Bartley, Patrick Hatcher, Heike Knicker, Jessel McConnie, Bradley Molton, Joel L. Morrison, Sarma V. Pisupati, Roger L. Poe, Reza Sharifi, Joséph F. Shepard, Jianyang Xie, Guheng Xu, and Alan W. Scaroni
Energy and Fuels Research Center
The Pennsylvania State University;
Richard Hogg, Subhash Chander, Heechan Cho, M. Thaddeus Ityokumbul, Mark S. Klima, and Peter T. Luckie
Mineral Processing Section
The Pennsylvania State University;
Adam Rose, Sam Addy, Patrick Chidley, Timothy J. Considine, Richard L. Gordon, Kim Harley, Gi C. Jung, Ahmet E. Kocagil, Jeffrey Lazo, Katherine McClain, and A. Michael Schaal
Department of Mineral Economics
The Pennsylvania State University;
Paul C. Painter and Boris Veytsman
Polymer Science Program
The Pennsylvania State University; and
Donald Morrison, Donald Englehardt, and Todd M. Sommer
Energy and Environmental Research Corporation

October 15, 1996

Work Performed Under Cooperative Agreement No. DE-FC22-92PC92162

For
U.S. Department of Energy
Pittsburgh Energy Technology Center
Pittsburgh, Pennsylvania

By
The Consortium for Coal-Water Slurry Fuel Technology
The Pennsylvania State University
University Park, Pennsylvania

PENNSTATE

THE DEVELOPMENT OF COAL-BASED TECHNOLOGIES FOR DEPARTMENT OF DEFENSE FACILITIES

Semiannual Technical Progress Report for the Period 09/28/1994 to 03/27/1995

By

Bruce G. Miller, David A. Bartley, Patrick Hatcher, Heike Knicker, Jessel McConnie, Bradley Molton, Joel L. Morrison, Sarma V. Pisupati, Roger L. Poe, Reza Sharifi, Joseph F. Shepard, Jianyang Xie, Guheng Xu, and Alan W. Scaroni
Energy and Fuels Research Center
The Pennsylvania State University;
Richard Hogg, Subhash Chander, Heechan Cho, M. Thaddeus Ityokumbul, Mark S. Klima, and Peter T. Luckie
Mineral Processing Section
The Pennsylvania State University;
Adam Rose, Sam Addy, Patrick Chidley, Timothy J. Considine, Richard L. Gordon, Kim Harley, Gi C. Jung, Ahmet E. Kocagil, Jeffrey Lazo, Katherine McClain, and A. Michael Schaal
Department of Mineral Economics
The Pennsylvania State University;
Paul C. Painter and Boris Veytsman
Polymer Science Program
The Pennsylvania State University; and
Donald Morrison, Donald Englehardt, and Todd M. Sommer
Energy and Environmental Research Corporation

October 15, 1996

Work Performed Under Cooperative Agreement No. DE-FC22-92PC92162

For
U.S. Department of Energy
Pittsburgh Energy Technology Center
Pittsburgh, Pennsylvania

By
The Consortium for Coal-Water Slurry Fuel Technology
The Pennsylvania State University
University Park, Pennsylvania

THE DEVELOPMENT OF COAL-BASED TECHNOLOGIES FOR DEPARTMENT OF DEFENSE FACILITIES

Semiannual Technical Progress Report for the Period 09/28/1994 to 03/27/1995

By

Bruce G. Miller, David A. Bartley, Patrick Hatcher, Heike Knicker, Jessel McConnie, Bradley Molton, Joel L. Morrison, Sarma V. Pisupati, Roger L. Poe, Reza Sharifi, Joseph F. Shepard, Jianyang Xie, Guhung Xu, and Alan W. Scaroni
Energy and Fuels Research Center
The Pennsylvania State University;
Richard Hogg, Subhash Chander, Heechan Cho, M. Thaddeus Ityokumbul, Mark S. Klima, and Peter T. Luckie
Mineral Processing Section
The Pennsylvania State University;
Adam Rose, Sam Addy, Patrick Chidley, Timothy J. Considine, Richard L. Gordon, Kim Harley, Gi C. Jung, Ahmet E. Kocagil, Jeffrey Lazo, Ping-Cheng Li, Katherine McClain, and A. Michael Schaal
Department of Mineral Economics
The Pennsylvania State University;
Paul C. Painter and Boris Veytsman
Polymer Science Program
The Pennsylvania State University; and
Donald Morrison, Donald Englehardt, and Todd M. Sommer
Energy and Environmental Research Corporation

October 15, 1996

Work Performed Under Cooperative Agreement No. DE-FC22-92PC92162

For
U.S. Department of Energy
Pittsburgh Energy Technology Center
Pittsburgh, Pennsylvania

By
The Consortium for Coal-water mixture Technology
The Pennsylvania State University
University Park, Pennsylvania

DISCLAIMER

EXECUTIVE SUMMARY

The U.S. Department of Defense (DOD), through an Interagency Agreement with the U.S. Department of Energy (DOE), has initiated a three-phase program with the Consortium for Coal-Water Mixture Technology, with the aim of decreasing DOD's reliance on imported oil by increasing its use of coal. The program is being conducted as a cooperative agreement between the Consortium and DOE.

Activities this reporting period are summarized by phase.

PHASE I

Phase I is nearly completed. During this reporting period, coal beneficiation/preparation studies, engineering designs and economics for retrofitting the Crane, Indiana boiler to fire coal-based fuels, and a 1,000-hour demonstration of dry, micronized coal were completed. In addition, a demonstration-scale micronized-coal water mixture (MCWM) preparation circuit was constructed and a 1,000-hour demonstration firing MCWM began. Preparation of the Phase I final report has started.

PHASE II

Work in Phase II focused on emissions reductions, coal benefication/preparation studies, and economic analyses of coal use.

Emissions reductions investigations involved literature surveys of NO_x, SO_2, trace metals, volatile organic compounds, and fine particulate matter capture. In addition, vendors and engineering firms were contacted to identify the appropriate emissions technologies for the installation of commercial NO_x and SO_2 removal systems on the demonstration boiler. Information from the literature surveys and engineering firms will be used to identify, design, and install a control system(s).

Work continued on the refinement and optimization of coal grinding and MCWM preparation procedures, and on the development of advanced processes for beneficiating high ash, high sulfur coals.

Work also continued on determining the basic cost estimation of boiler retrofits, and evaluating environmental, regulatory, and regional economic impacts. In addition, the feasibility of technology adoption, and the public's perception of the benefits and costs of coal usage was studied. A coal market analysis was completed.

PHASE III

Work in Phase III focused on coal preparation studies, emissions reductions, and economic analyses of coal use.

Coal preparation studies were focused on specific coal-cleaning options and their associated ancillary operations and integration of processing/cleaning operations for overall system optimization.

Emissions reductions investigations included algal studies for trace metal capture and CO_2 uptake.

The economic study focused on determining cost and market penetration, selection of incentives, and regional economic impacts of coal-based fuel technologies. In addition DOD's fuel mix is being determined and a national energy portfolio is being constructed.

TABLE OF CONTENTS

TABLE OF CONTENTS (cont.)

TABLE OF CONTENTS (cont.)

TABLE OF CONTENTS (cont.)

LIST OF FIGURES

LIST OF TABLES

1.0 INTRODUCTION

The U.S. Department of Defense (DOD), through an Interagency Agreement with the U.S. Department of Energy (DOE), has initiated a three-phase program with the Consortium for Coal-Water Mixture Technology, with the aim of decreasing DOD's reliance on imported oil by increasing its use of coal. The program is being conducted as a cooperative agreement between the Consortium and DOE. The first phase is nearly completed; work is underway in the other two phases.

To achieve the objectives of the program, a team of researchers was assembled and the current members of the Consortium are from Penn State (Energy and Fuels Research Center (EFRC), Mineral Processing Section, Department of Mineral Economics, and Polymer Science Program) and the Energy and Environmental Research Corporation (EER). AMAX Research and Development Center was a charter member but has subsequently withdrawn. ABB Combustion Engineering was invited to join but declined.

Phase I activities are focused on developing clean, coal-based combustion technologies for the utilization of both micronized coal-water mixtures (MCWMs) and dry, micronized coal (DMC) in fuel oil-designed industrial boilers. Phase II research and development continue to focus on industrial boiler retrofit technologies by addressing emissions control and pre-combustion (i.e., slagging combustion and/or gasification) strategies for the utilization of high ash, high sulfur coals. Phase III activities evaluate current DOD boiler operation and emissions, and examine coal-based fuel combustion systems that cofire wastes. Each phase includes an engineering cost analysis and technology assessment. The activities and status of the phases are described below.

The objective in Phase I is to deliver fully engineered retrofit options for a fuel oil-designed watertube boiler located on a DOD installation to fire either MCWM or DMC. This will be achieved through a program consisting of the following five tasks: 1) Coal Beneficiation and Preparation; 2) Combustion Performance Evaluation; 3) Engineering Design; 4) Engineering and Economic Analysis; and 5) Final Report/Submission of Design Package. Following is an outline of the project tasks that comprise Phase I:

Task 1: Coal Beneficiation/Preparation

- Subtask 1.1 Identify/Procure Coals
- Subtask 1.2 Determine Liberation Potential
- Subtask 1.3 Produce Laboratory-Scale Quantities of Micronized Coal-Water Mixtures (MCWMs)
- Subtask 1.4 Develop Dry Coal Cleaning Technique
- Subtask 1.5 Produce MCWMs and Dry, Micronized Coal (DMC) From Dry Clean Coal
- Subtask 1.6 Produce MCWM and DMC for the Demonstration Boiler
- Subtask 1.7 Project Management and Support

Task 2: Combustion Performance Evaluation

- Subtask 2.1 Boiler Retrofit

Subtask 2.2 Fuel Evaluation in the Research Boiler
Subtask 2.3 Performance Evaluation of the MCWM and DMC in the Demonstration Boiler
Subtask 2.4 Evaluate Emissions Reductions Strategies
Subtask 2.5 Project Management and Support

Task 3: Engineering Design

Subtask 3.1 MCWM/DMC Preparation Facilities
Subtask 3.2 Fuel Handling
Subtask 3.3 Burner System
Subtask 3.4 Ash Removal, Handling, and Disposal
Subtask 3.5 Air Pollution Control
Subtask 3.6 Integrate Engineering Design
Subtask 3.7 Project Management and Support

Task 4: Engineering and Economic Analysis

Subtask 4.1 Survey Boiler Population/Identify Boilers for Conversion
Subtask 4.2 Identify Appropriate Cost-Estimating Methodologies
Subtask 4.3 Estimate Basic Costs of New Technologies
Subtask 4.4 Process Analysis of MCWM and DMC
Subtask 4.5 Analyze/Identify Transportation Cost of Commercial Sources of MCWM and Cleaned Coal for DMC Production
Subtask 4.6 Determine Community Spillovers
Subtask 4.7 Regional Market Considerations and Impacts
Subtask 4.8 Integrate the Analysis
Subtask 4.9 Project Management and Support

Task 5: Final Report/Submission of Design Package

The Phase I activities include:

Task 1: The coal beneficiation and preparation effort is being conducted by Penn State's Mineral Processing Section with assistance from Penn State's Polymer Science Program. This task involves identifying and procuring six coals that can be cleaned to <1.0 wt.% sulfur and <5.0 wt.% ash which have been, or possess the characteristics to enable them to be, made into MCWMs. The coals are being subjected to detailed characterization and used to produce laboratory-scale quantities of MCWM. A fundamental study of MCWM stabilization is being conducted. Additional activities include developing a dry coal cleaning technique and producing MCWMs and DMC from the resulting cleaned coal.

Task 2: The EFRC is conducting the combustion performance evaluation with assistance from EER and Penn State's Fuel Science Program. The technical aspects of converting a fuel oil-designed boiler at a DOD facility will be identified in this task. All appropriate components will be evaluated, including the fuel, the fuel storage, handling and delivery equipment, the burner, the boiler, the ash handling and disposal equipment, the emissions control system, and the boiler control system. Combustion performance as indicated by flame stability, completeness of combustion, and related issues such as system derating, changes in system maintenance, the occurrence of slagging, fouling, corrosion and erosion, and air pollutant emissions will be

determined. As part of this task, MCWM and DMC will be evaluated in EFRC's 15,000 lb steam/h watertube boiler. EER will provide a proven coal-designed burner for retrofitting Penn State's boiler. In addition, EER will design the burner for the DOD boiler identified for retrofitting.

Task 3: An engineering study will be performed for a complete retrofit of a DOD boiler facility to fire either MCWM or DMC. The designs will be performed by EER with input from the other project participants. The designs will include the coal preparation, the fuel handling, the burner, the ash removal, handling, and disposal, and the air pollution control systems. The two designs will be for the DOD boiler identified in Task 4. The retrofits will be designed for community/societal acceptability. The deliverables for this task will be a detailed design that can be used for soliciting bids from engineering/construction firms to retrofit the candidate DOD boiler.

Task 4: An engineering cost analysis and technology assessment of MCWM and DMC combustion will be performed by Penn State's Department of Mineral Economics and the EFRC with assistance from the industrial participants. The effort will involve surveying the DOD boiler population, identifying boilers for conversion, identifying appropriate cost-estimating methodologies, estimating basic costs for new technologies, developing a process model, analyzing and identifying transportation costs for commercial sources of MCWM and cleaned coal, determining community spillovers, and determining regional market considerations and impacts.

Task 5: The results from each of the tasks will be summarized in a final report. In addition, the design packages for the boiler retrofits will be submitted. These will include the engineering design and economic analysis.

The original objectives of Phase II were to: (a) extend the Phase I boiler retrofit options by including designs to achieve further reductions in gaseous and particulate emissions, (b) prepare and characterize fuels compatible with coal precombustors, and (c) investigate precombustion as a means of using high ash, high sulfur coals. Upon investigating precombustion options for installing a system on either the demonstration boiler (15,000 lb steam/h) or research boiler (1,000 lb steam/h), it became apparent that there were limited viable options and that the complexity of the systems will likely preclude their use on small-scale, industrial boilers. A similar conclusion was presented by the U.S. Corps of Engineers regarding the use of slagging combustors in the Army [1]. Consequently, the Phase II work has been revised by eliminating the precombustion fundamental, pilot-scale, and demonstration-scale studies and focusing the effort towards fundamental, pilot-scale, and demonstration-scale emissions reduction strategies. An economic analysis of precombustion strategies will be conducted, as originally planned, in order to compare precombustion strategies with (low ash) MCWM and DMC combustion retrofits. The revised Phase II consists of four tasks as outlined below:

Task 1. Emissions Reduction

- Subtask 1.1 Evaluation of Emissions Reduction Strategies
- Subtask 1.2 Fundamental Emissions Studies
- Subtask 1.3 Installation of an Emissions Reduction System on the Demonstration Boiler
- Subtask 1.4 Evaluation of an Emissions Reduction System

Task 2. Coal Preparation/Utilization

- Subtask 2.1 Optimization of Particle Size Consist for CWM Formulation
- Subtask 2.2 Fine Grinding/Classification/Liberation
- Subtask 2.3 Fine Gravity Concentration
- Subtask 2.4 Agglomeration/Flotation Studies
- Subtask 2.5 Fundamental Studies of Surface-Based Processes
- Subtask 2.6 Column Flotation
- Subtask 2.7 Dry Cleaning of Fine Coal
- Subtask 2.8 CWM Density Control
- Subtask 2.9 Stabilization of CWM

Task 3. Engineering Design and Cost; and Economic Analysis

- Subtask 3.1 Determination of Basic Cost Estimation of Boiler Retrofits
- Subtask 3.2 Determination of Process Analysis
- Subtask 3.3 Determination of Environmental and Regulatory Impacts
- Subtask 3.4 Determination of Transportation Cost Analysis
- Subtask 3.5 Determination of Technology Adoption
- Subtask 3.6 Determination of Regional Economic Impacts
- Subtask 3.7 Determination of Public Perception of Benefits and Costs
- Subtask 3.8 Determination of Social Benefits
- Subtask 3.9 Determination of Coal Market Analysis
- Subtask 3.10 Integration of Analyses

Task 4. Final Report/Submission of Design Package

The Phase II activities include:

Task 1: In Task 1, strategies will be developed to provide for ultra-low emissions when firing coal-based fuels in industrial-scale boilers. Emissions to be addressed include SO_2, NO_x, fine particulate matter (<10 μm), and air toxics (volatile organic compounds and trace metals). Post-combustion and during-combustion technologies to reduce SO_2 and NO_x emissions from coal-fired industrial boilers will be investigated. Novel technologies that are under development but are not commercially available will be evaluated as well as proven technologies such as limestone/lime injection, selective catalytic reduction, and nonselective catalytic reduction. Options to remove the submicron particulates will also be investigated. In addition, methods to remove air toxics from the flue gas, such as scrubbing, will be investigated.

Task 2: Emphasis in Task 2 will be on the refinement and optimization of coal grinding and CWM preparation procedures, and on the development of advanced processes for beneficiating high ash, high sulfur coals. CWM formulation is still an art and there is a clear need for scientifically-based guidelines for slurry design. This involves determining the optimum particle

size distribution, how and why the optimum particle size distribution varies from coal to coal, and the specific roles of chemical dispersing and stabilizing agents. Extensive, physical pre-cleaning of coal is especially important in small-boiler applications. The research effort will build on work conducted in Phase I and will be carried out in concert with the efforts in combustion engineering, emissions control and cost analysis.

Task 3: Task 3 focuses on determining the basic cost estimation of boiler retrofits, evaluating environmental, regulatory, and regional economic impacts, and analyzing the coal market.

Task 4: The results from each of the tasks will be summarized in a final report.

The objectives in Phase III are to: (a) develop coal-based fuel/waste cofiring technologies, and (b) assist DOD in improving the combustion performance and reducing emissions from existing stoker-fired boilers. This will be achieved through a combination of fundamental, pilot-scale, and demonstration-scale studies, field testing, and an engineering design and cost analysis of a stoker retrofit. Phase III consists of six tasks outlined below:

Task 1. Coal Preparation/Utilization

- Subtask 1.1 Particle Size Control
- Subtask 1.2 Physical Separations
- Subtask 1.3 Surface-Based Separation Process
- Subtask 1.4 Dry Processing
- Subtask 1.5 Stabilization of Coal-Water Mixtures

Task 2. Stoker Combustion Performance Analysis and Evaluation

- Subtask 2.1 Determine DOD Stoker Operability and Emissions Concerns
- Subtask 2.2 Conduct Field Test of a DOD Stoker
- Subtask 2.3 Provide Performance Improvement Analysis to DOD
- Subtask 2.4 Evaluate Pilot-Scale Stoker Retrofit Combustion
- Subtask 2.5 Perform Engineering Design of Stoker Retrofit

Task 3. Emissions Reduction

- Subtask 3.1 Demonstrate Advanced Pollution Control System
- Subtask 3.2 Evaluate Carbon Dioxide Mitigation and Heavy Metal Removal in a Slipstream System
- Subtask 3.3 Study VOC and Trace Metal Occurrence and Capture

Task 4. Coal-Based Fuel/Waste Cofiring

- Subtask 4.1 Coal Fines Combustion
- Subtask 4.2 Coal/Rocket Propellant Cofiring

Task 5. Economic Evaluation

- Subtask 5.1 Cost and Market Penetration of Coal-Based Fuel Technologies
- Subtask 5.2 Selection of Incentives for Commercialization of the Coal-Using Technology
- Subtask 5.3 Community Sensitivity to Coal Fuel Usage

Subtask 5.4 Regional Economic Impacts of New Coal Utilization Technologies
Subtask 5.5 Economic Analysis of the Defense Department's Fuel Mix
Subtask 5.6 Constructing a National Energy Portfolio which Minimizes Energy Price Shock Effects
Subtask 5.7 Proposed Research on the Coal Markets and their Impact on Coal-Based Fuel Technologies
Subtask 5.8 Integrate the Analysis

Task 6. Final Report/Submission of Design Package

The Phase III activities include:

Task 1: Research conducted under Phase I and Phase II of this project has revealed a number of specific areas where continued and/or more focused effort is required in order to develop more effective and more reliable coal processing systems. Specific objectives of Task 1 are centered around:

- focused investigations into specific coal-cleaning options and their associated ancillary operations and
- integration of processing/cleaning operations for overall system optimization.

As in the previous phases, emphasis will be on fine-coal processing for the production of high-quality, micronized coal for dry coal and coal-water mixture (CWM) applications.

Task 2: DOD operates several large World War II-vintage stoker-fired boilers for steam production. The objective in Task 2 is to address DOD's concern that they are difficult to operate properly, which results in poor combustion performance and excessive emissions. Ultimately, there is the possibility that the boilers may be converted from coal to another fuel form. The objective will be achieved by surveying the operability of the stoker-fired boilers, identifying a candidate boiler for improvement, conducting field testing to determine the combustion performance and emissions, providing a performance improvement analysis to DOD, if applicable, evaluating pilot-scale stoker retrofit combustion technologies, and performing an engineering design of a stoker retrofit to fire coal in a form that is most conducive to achieve operability and environmental goals.

Task 3: In Task 3, three levels of effort investigating emissions reductions will be performed. An advanced pollution control system will be tested at the demonstration level, CO_2 mitigation and heavy metal removal will be evaluated at the pilot-scale level, and fundamental studies of VOC and trace metal occurrence and capture will be conducted.

Task 4: The activities in Task 4 will address advanced/novel combustion techniques. This involves coal fines combustion and cofiring wastes with coal-based fuels.

Task 5: The activities in Task 5 will focus on determining cost and market penetration, selection of incentives, and regional economic impacts of coal-based fuel technologies. In addition, DOD's fuel mix will be determined and a national energy portfolio constructed.

Task 6: The results from each of the tasks will be summarized in a final report. In addition, the design package for the stoker retrofit will be submitted. This will include the engineering design and economic analysis.

The accomplishments and status of Phase I, Tasks 1, 2, 3, 4, and 5 are presented in Sections 2.0, 3.0, 4.0, 5.0, and 6.0, respectively. The accomplishments and status of Phase II, Tasks 1, 2, 3, and 4 are presented in Sections 7.0, 8.0, 9.0, and 10.0, respectively. The accomplishments and status of Phase III, Tasks 1, 2, 3, 4, 5, and 6 are presented in Sections 11.0, 12.0, 13.0, 14.0, 15.0, and 16.0, respectively. Section 17.0 discusses miscellaneous activities that were conducted. Activities planned for the next semiannual period are listed in Section 18.0. Selected nomenclature is given in Section 19.0. References and acknowledgments are contained in Sections 20.0 and 21.0, respectively. The project schedule for Phases I, II, and III is given in Figures 1-1, 1-2, and 1-3, respectively, with a description of the milestones contained in Tables 1-1, 1-2, and 1-3, respectively.

2.0 PHASE I, TASK 1: COAL BENEFICIATION/PREPARATION

The initial objectives of this activity were to select appropriate coals which could meet the specific requirements of the project and to prescribe the necessary cleaning steps. Longer-term objectives are to develop improved cleaning procedures which can be used to increase the yield of usable coal and to expand the reserve base of candidate fuels for retrofitted boilers.

2.1 Subtask 1.1 Identify/Procure Coals

This subtask is complete, and the results are contained in the Phase I Final Report which is under preparation.

2.2 Subtask 1.2 Determine Liberation Potential

This subtask is complete, and the results are contained in the Phase I Final Report which is under preparation.

2.3 Subtask 1.3 Produce Laboratory-Scale Quantities of Micronized Coal-Water Mixtures

The preparation of micronized coal-water mixture (MCWM) is presented as laboratory-scale and pilot-scale activities. Laboratory-scale activities include the cleaning of the coal feedstock to targeted coal specifications and the preparation of a stable, low viscosity MCWM from the cleaned coal feedstock. Barrel quantities of MCWM were produced and tested in the laboratory-scale efforts. Pilot-scale activities focused on producing ton quantities of MCWM from a cleaned coal feedstock for testing in the 15,000 lb steam/h demonstration boiler.

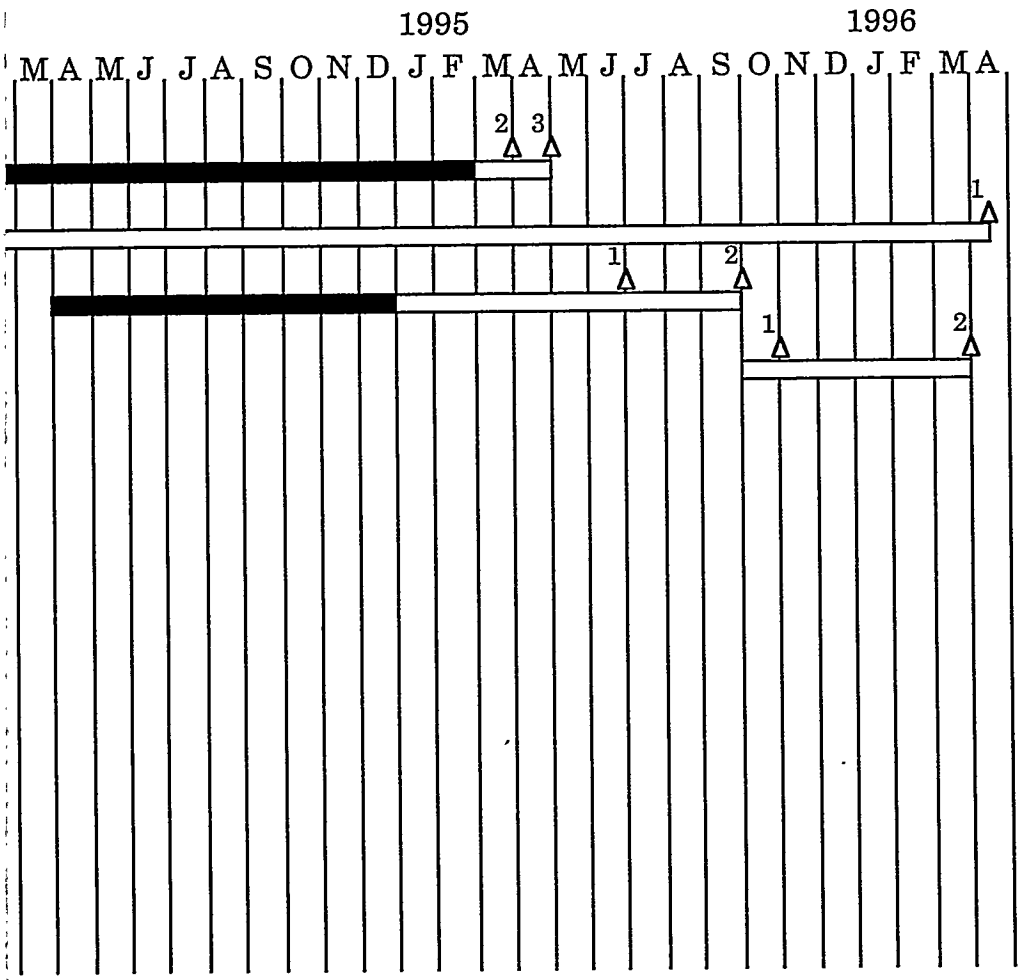

edule

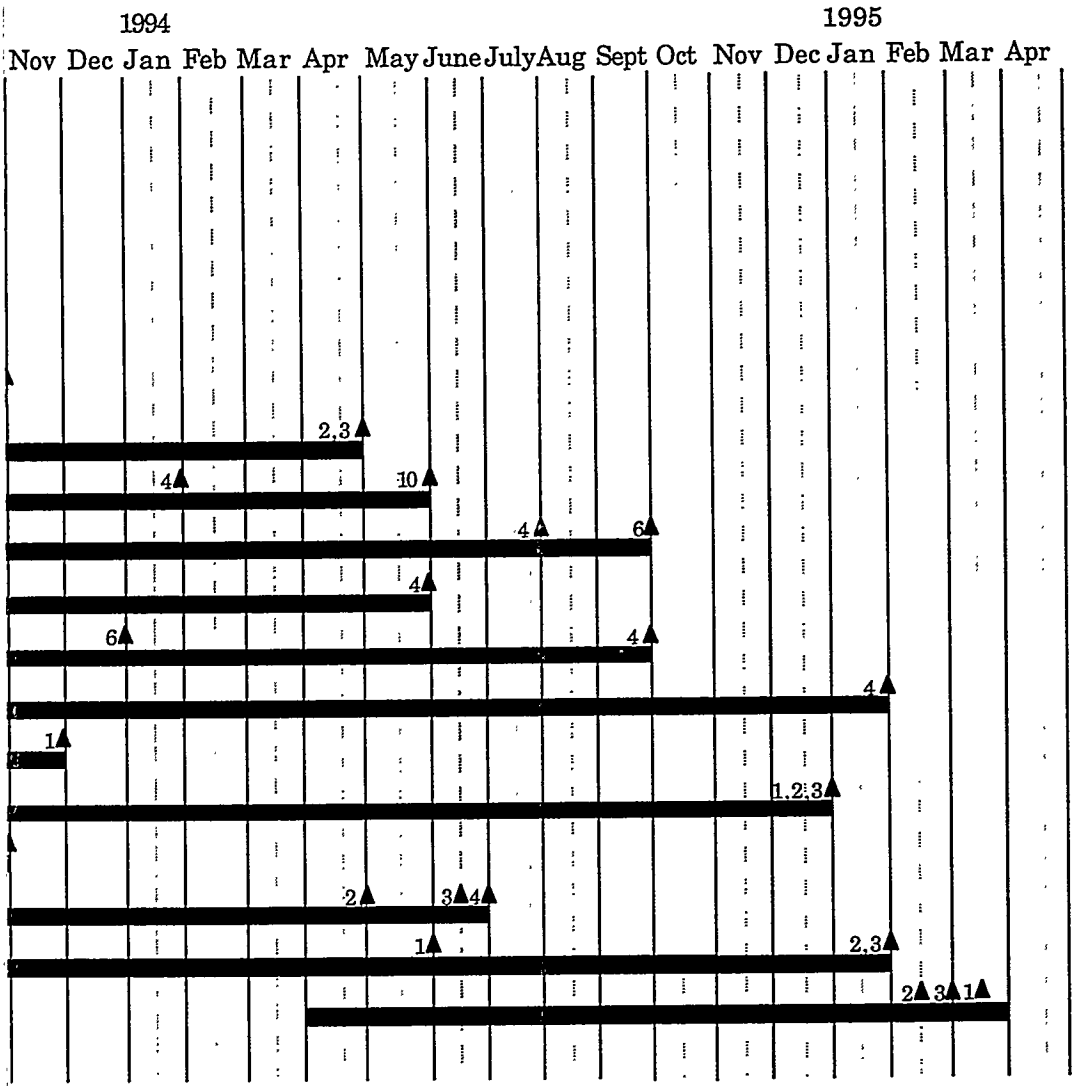
1994
1995
Nov Dec Jan Feb Mar Apr May June July Aug Sept Oct Nov Dec Jan Feb Mar Apr
2,3
4
10
4
6
4
6
4
4
1
1,2,3
2
3
4
1
2,3
2
3
1

Schedule

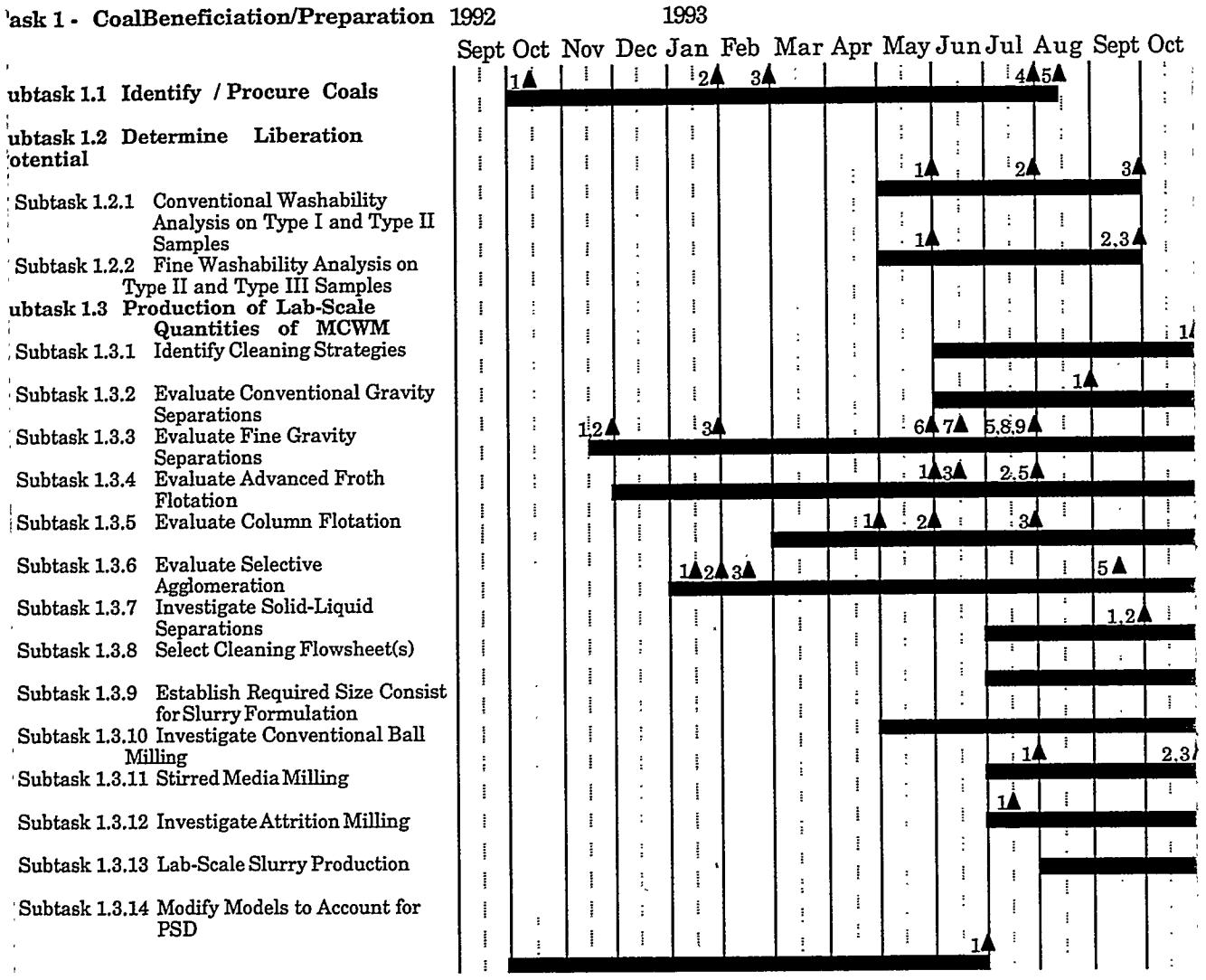

Figure 1-1. DOD Phase I Milestone

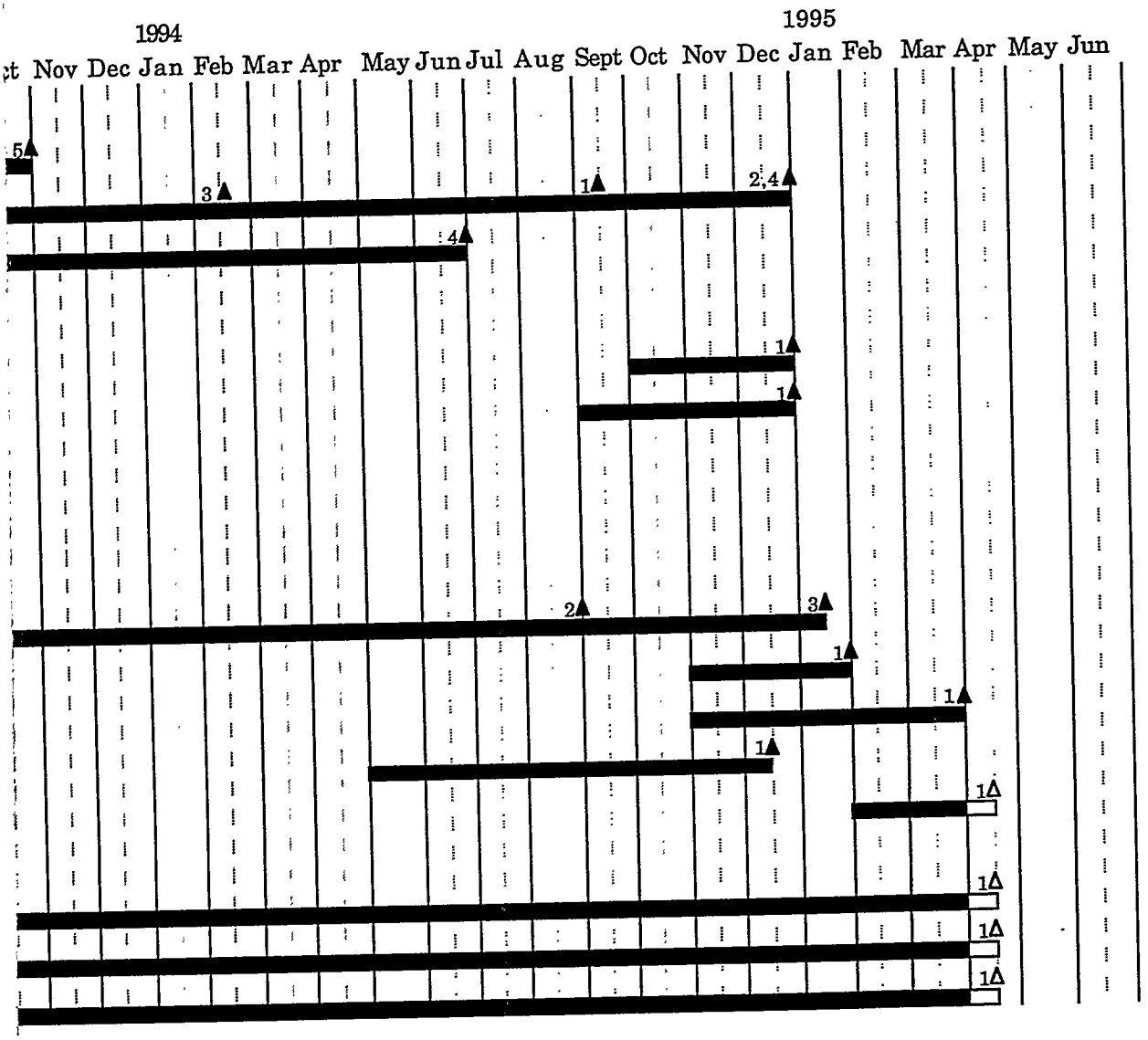
1994
1995
ct Nov Dec Jan Feb Mar Apr May Jun Jul Aug Sept Oct Nov Dec Jan Feb Mar Apr May Jun
5
3
1
2,4
4
1
1
2
3
1
1
1
1Δ
1Δ
1Δ
1Δ

Task 1 - CoalBeneficiation/Preparation (cont.)

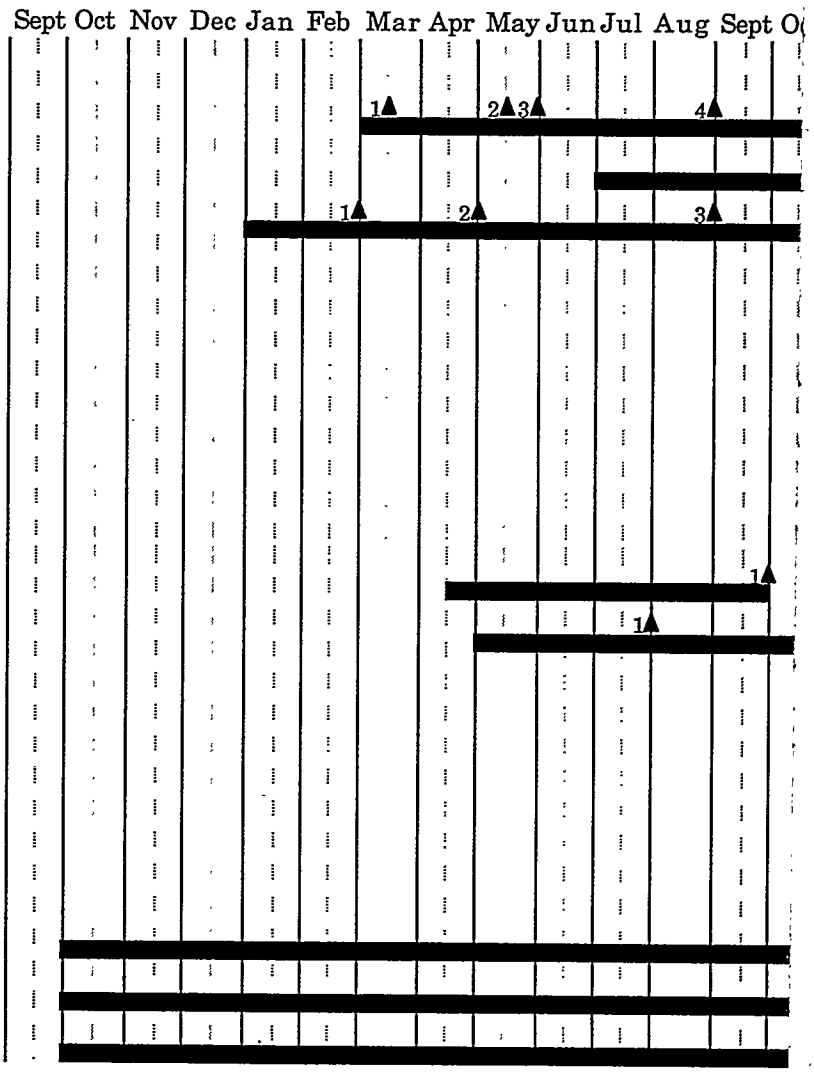

Subtask 1.4 Develop Dry Coal Cleaning Technique

Subtask 1.4.1 Dry Grinding Studies

Subtask 1.4.2 Deagglomeration Studies

Subtask 1.4.3 Dry Separations

Subtask 1.5 Produce MCWMs and Micronized Coal from Dry, Clean Coal

Subtask 1.5.1 Produce Micronized Coal from Dry, Clean Coal

Subtask 1.5.2 Produce MCWM from Dry, Clean Coal

Subtask 1.6 Produce MCWM and Dry, Micronized Coal for the Demonstration

Subtask 1.6.1 Shakedown Dry, Micronized Coal Circuit

Subtask 1.6.2 Install MCWM Equipment

Subtask 1.6.3 Shakedown MCWM Equipment

Subtask 1.6.4 Coal Cleaning

Subtask 1.6.5 CoalMicronizing

Subtask 1.6.6 MCWM Preparation

Subtask 1.7 Project Management and Support

Subtask 1.7.1 Project Management and Technical Advisement

Subtask 1.7.2 Drafting / Technical Secretarial Support

Subtask 1.7.3 Budget Management / Project Administration

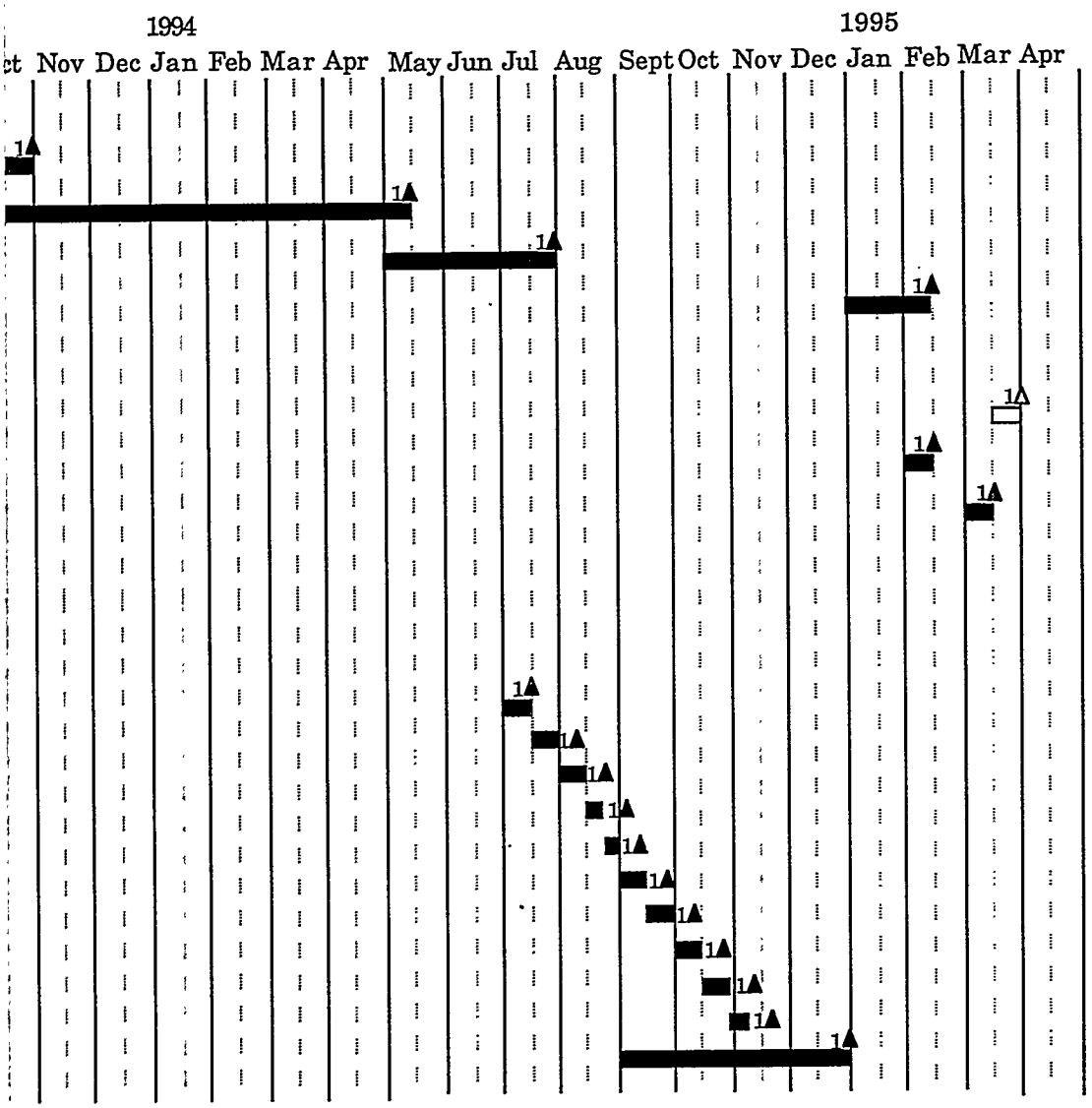
1994
1995
ct Nov Dec Jan Feb Mar Apr May Jun Jul Aug Sept Oct Nov Dec Jan Feb Mar Apr

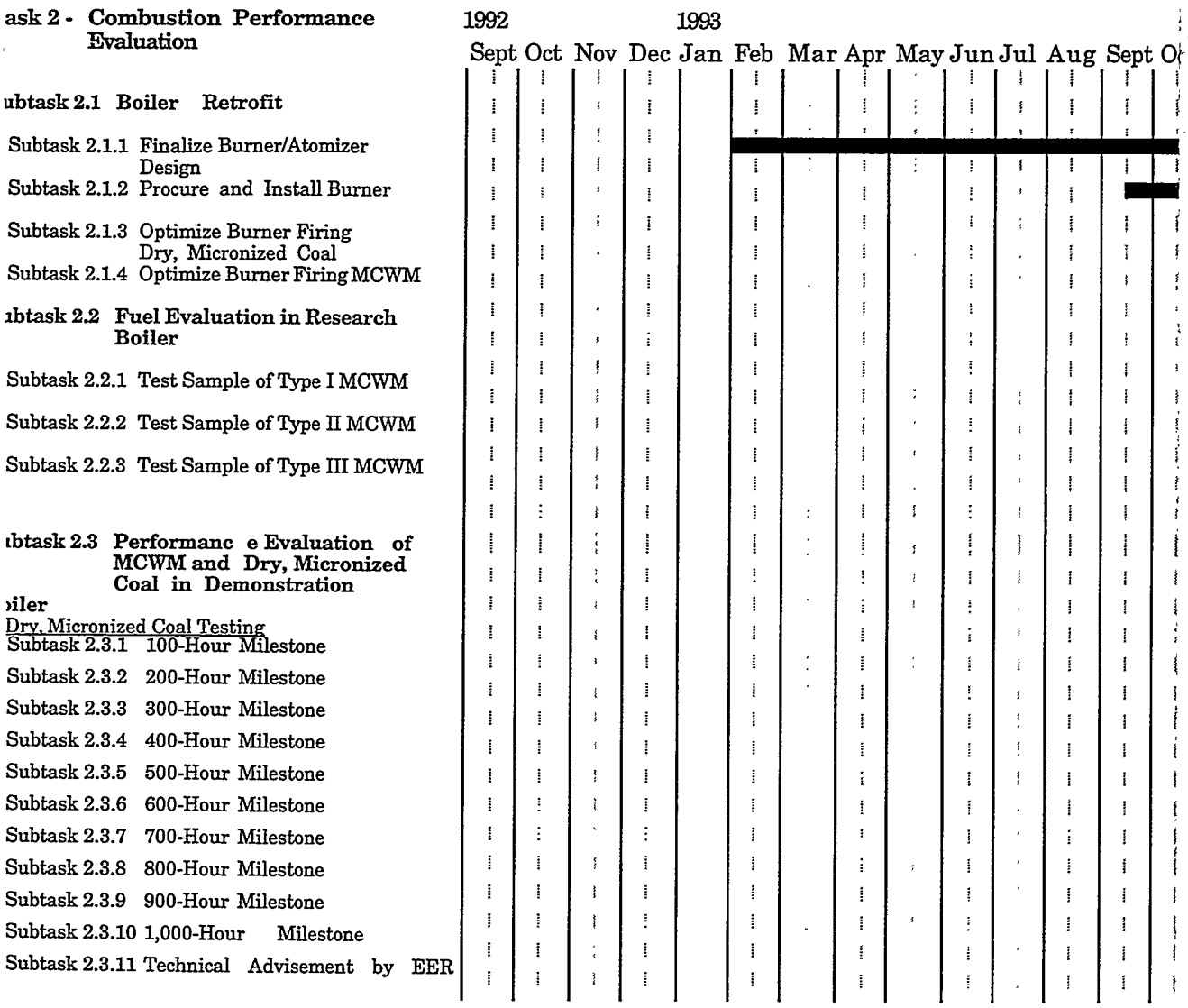
1992
1993
Sept Oct Nov Dec Jan Feb Mar Apr May Jun Jul Aug Sept O
ask 2 - Combustion Performance Evaluation
ubtask 2.1 Boiler Retrofit
Subtask 2.1.1 Finalize Burner/Atomizer Design
Subtask 2.1.2 Procure and Install Burner
Subtask 2.1.3 Optimize Burner Firing Dry, Micronized Coal
Subtask 2.1.4 Optimize Burner Firing MCWM
ıbtask 2.2 Fuel Evaluation in Research Boiler
Subtask 2.2.1 Test Sample of Type I MCWM
Subtask 2.2.2 Test Sample of Type II MCWM
Subtask 2.2.3 Test Sample of Type III MCWM
ıbtask 2.3 Performanc e Evaluation of MCWM and Dry, Micronized Coal in Demonstration
ıiler
Dry, Micronized Coal Testing
Subtask 2.3.1 100-Hour Milestone
Subtask 2.3.2 200-Hour Milestone
Subtask 2.3.3 300-Hour Milestone
Subtask 2.3.4 400-Hour Milestone
Subtask 2.3.5 500-Hour Milestone
Subtask 2.3.6 600-Hour Milestone
Subtask 2.3.7 700-Hour Milestone
Subtask 2.3.8 800-Hour Milestone
Subtask 2.3.9 900-Hour Milestone
Subtask 2.3.10 1,000-Hour Milestone
Subtask 2.3.11 Technical Advisement by EER

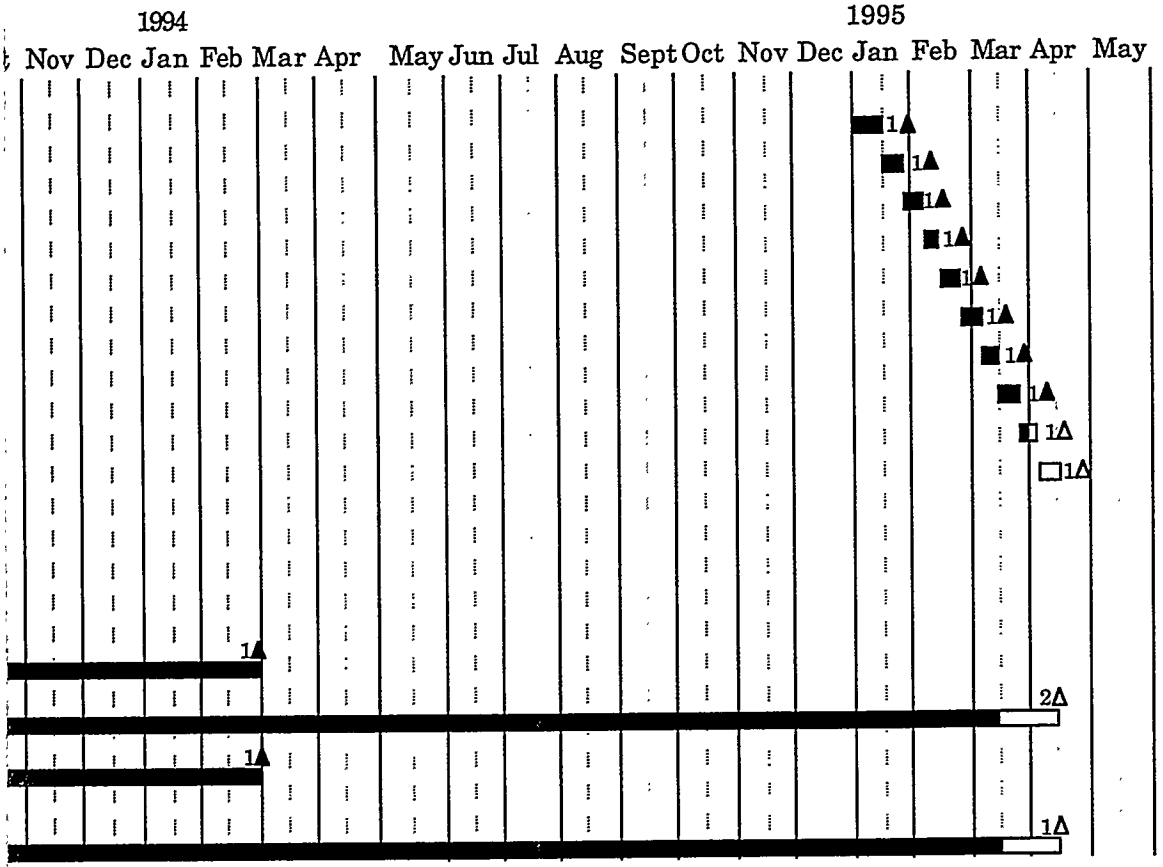
1994
1995
Nov Dec Jan Feb Mar Apr May Jun Jul Aug Sept Oct Nov Dec Jan Feb Mar Apr May
1▲
1▲
1▲
1▲
1▲
1▲
1▲
1▲
1Δ
1Δ
1▲
2Δ
1▲
1Δ

Task 2 - Combustion Performance Evaluation(cont.)

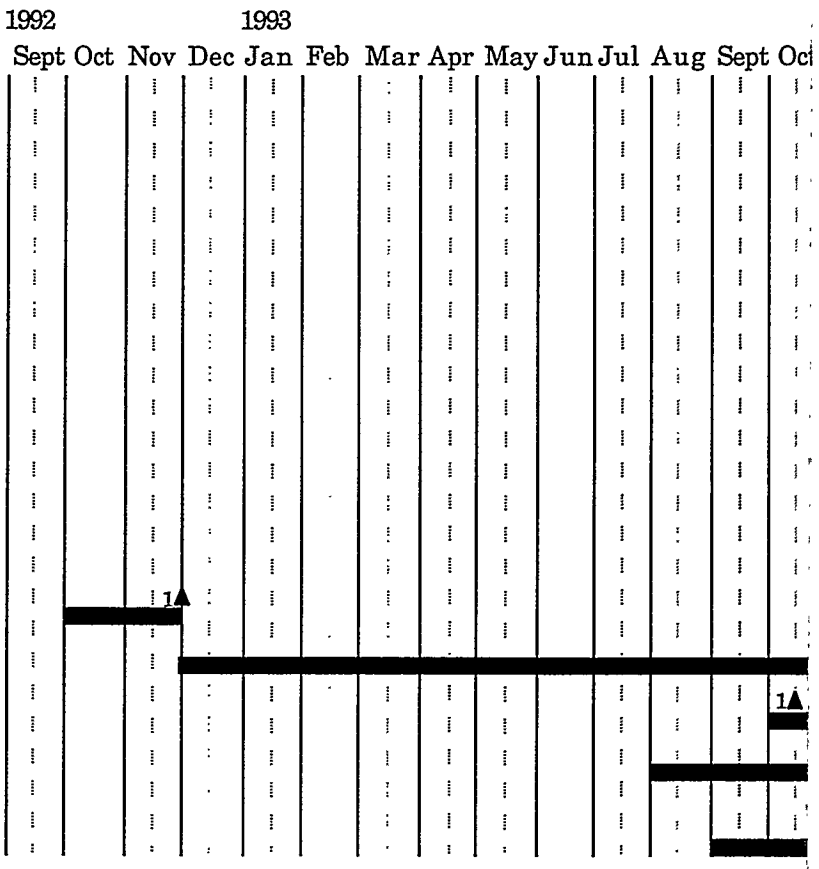

MCWM Testing

Subtask 2.3.12 100-Hour Milestone

Subtask 2.3.13 200-Hour Milestone

Subtask 2.3.14 300-Hour Milestone

Subtask 2.3.15 400-Hour Milestone

Subtask 2.3.16 500-Hour Milestone

Subtask 2.3.17 600-Hour Milestone

Subtask 2.3.18 700-Hour Milestone

Subtask 2.3.19 800-Hour Milestone

Subtask 2.3.20 900-Hour Milestone

Subtask 2.3.21 1,000-Hour Milestone

Evaluate Erosion / Deposition Characteristics

Subtask 2.3.23 Identify Erosion and Deposition Regimes

Subtask 2.3.24 Model Simultaneous Erosion and Deposition

Subtask 2.3.25 Compare Heat Transfer Surface Performance

Subtask 2.3.26 Procedure for Determining Optimum Convective Section Gas Velocity

Subtask 2.3.27 Comparison of Performance of Various Coals

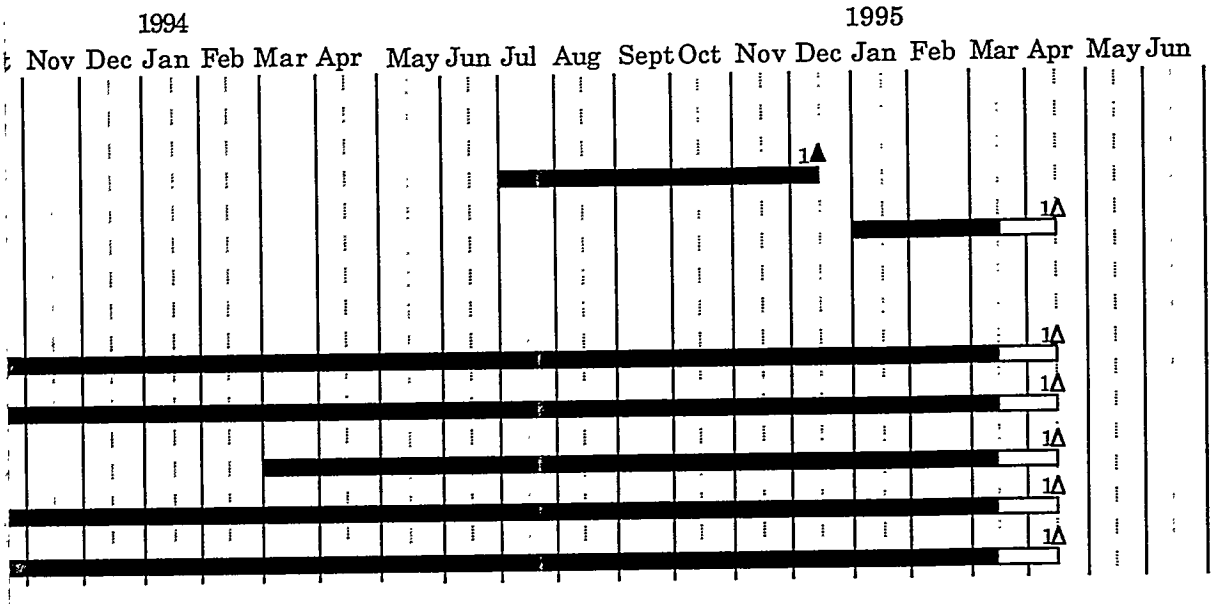
1994
1995
t Nov Dec Jan Feb Mar Apr May Jun Jul Aug Sept Oct Nov Dec Jan Feb Mar Apr May Jun
1
1
1
1
1
1
1

Task 2 - Combustion Performance Evaluation (cont.)

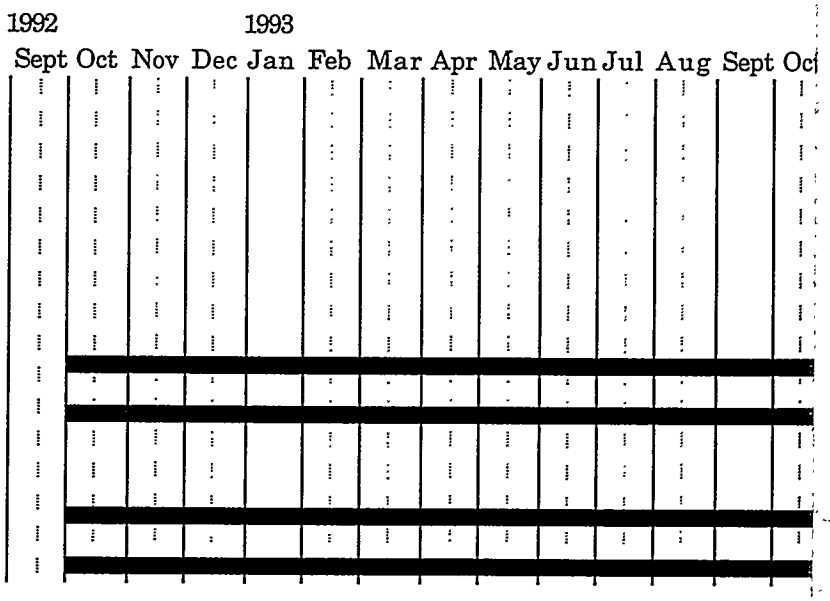

Subtask 2.4 Evaluate Emissions Reduction Strategies

Subtask 2.4.1 Dry, Micronized Coal Testing

Subtask 2.4.2 CWSF Testing

Subtask 2.5 Project Management and Support

Subtask 2.5.1 Project Management and Advisement

Subtask 2.5.2 Staff Supervision Test Planning and Quality Control

Subtask 2.5.3 Data Reduction and Interpretation

Subtask 2.5.4 Drafting / Technical Secretarial Support

Subtask 2.5.5 Budget Management / Project Administration

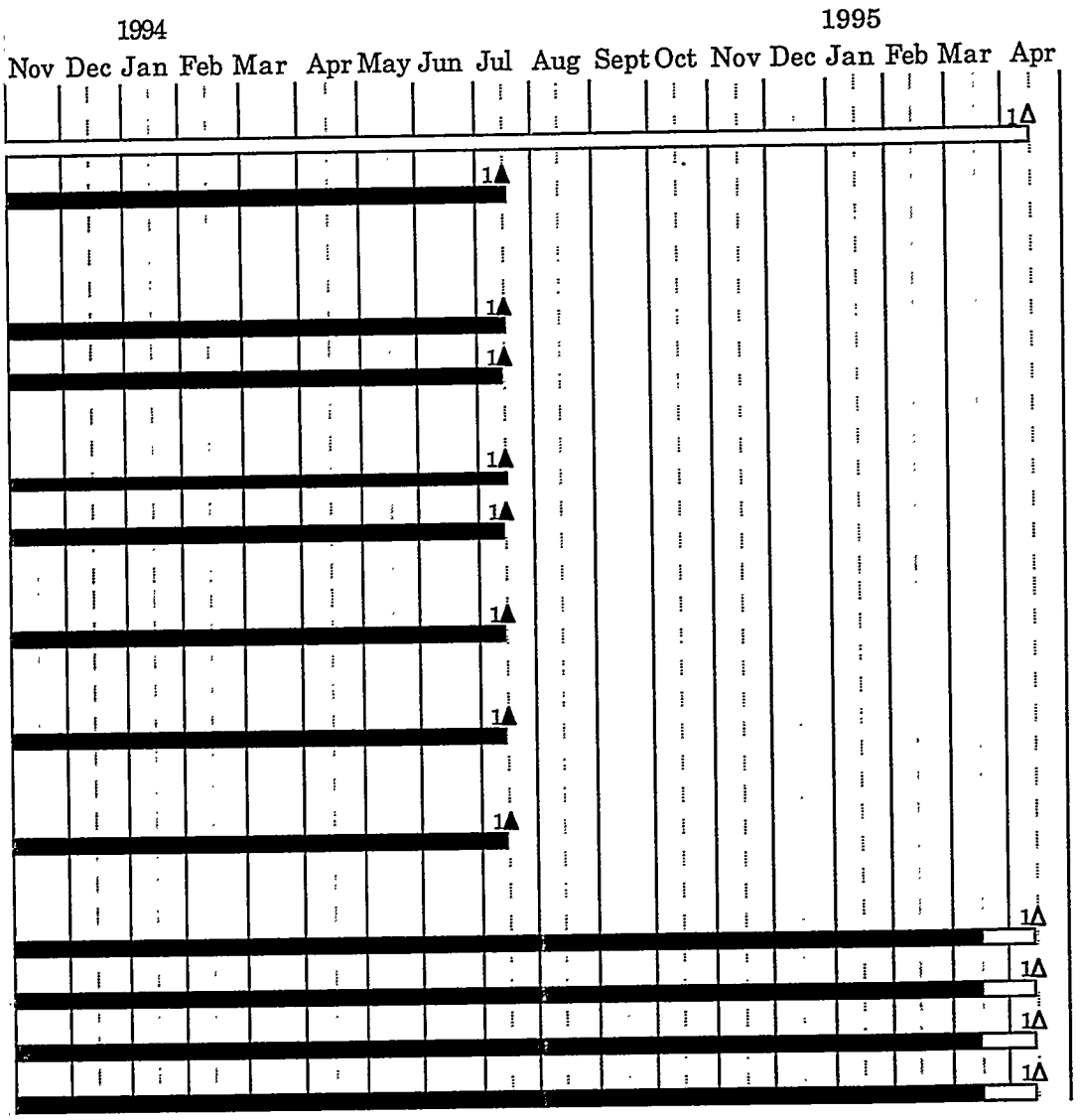
1994
1995
Nov Dec Jan Feb Mar Apr May Jun Jul Aug Sept Oct Nov Dec Jan Feb Mar Apr

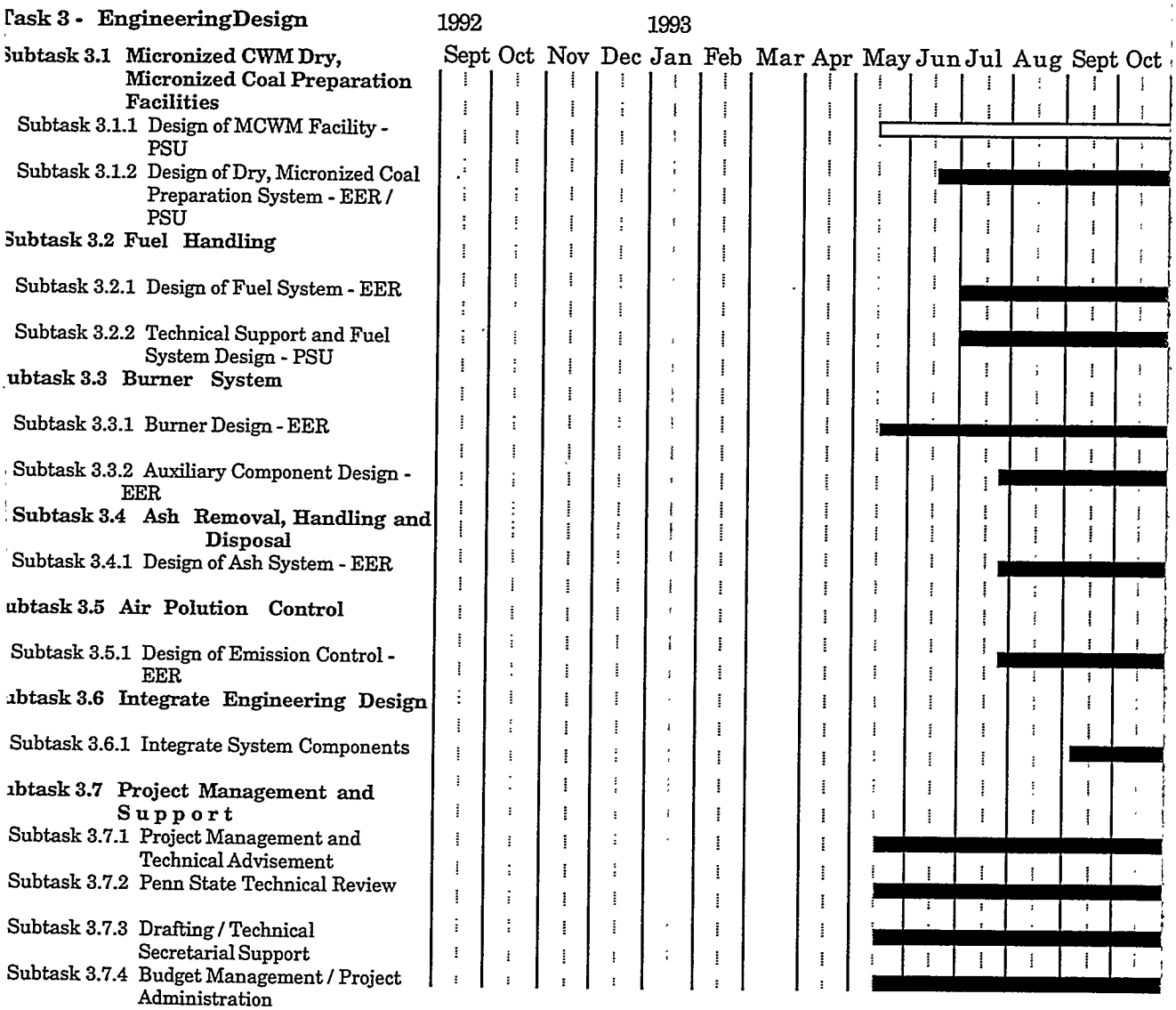
Task 3 - EngineeringDesign
1992
1993
Sept Oct Nov Dec Jan Feb Mar Apr May Jun Jul Aug Sept Oct
Subtask 3.1 Micronized CWM Dry, Micronized Coal Preparation Facilities
Subtask 3.1.1 Design of MCWM Facility - PSU
Subtask 3.1.2 Design of Dry, Micronized Coal Preparation System - EER / PSU
Subtask 3.2 Fuel Handling
Subtask 3.2.1 Design of Fuel System - EER
Subtask 3.2.2 Technical Support and Fuel System Design - PSU
ubtask 3.3 Burner System
Subtask 3.3.1 Burner Design - EER
Subtask 3.3.2 Auxiliary Component Design - EER
Subtask 3.4 Ash Removal, Handling and Disposal
Subtask 3.4.1 Design of Ash System - EER
ubtask 3.5 Air Polution Control
Subtask 3.5.1 Design of Emission Control - EER
ıbtask 3.6 Integrate Engineering Design
Subtask 3.6.1 Integrate System Components
ıbtask 3.7 Project Management and Support
Subtask 3.7.1 Project Management and Technical Advisement
Subtask 3.7.2 Penn State Technical Review
Subtask 3.7.3 Drafting / Technical Secretarial Support
Subtask 3.7.4 Budget Management / Project Administration

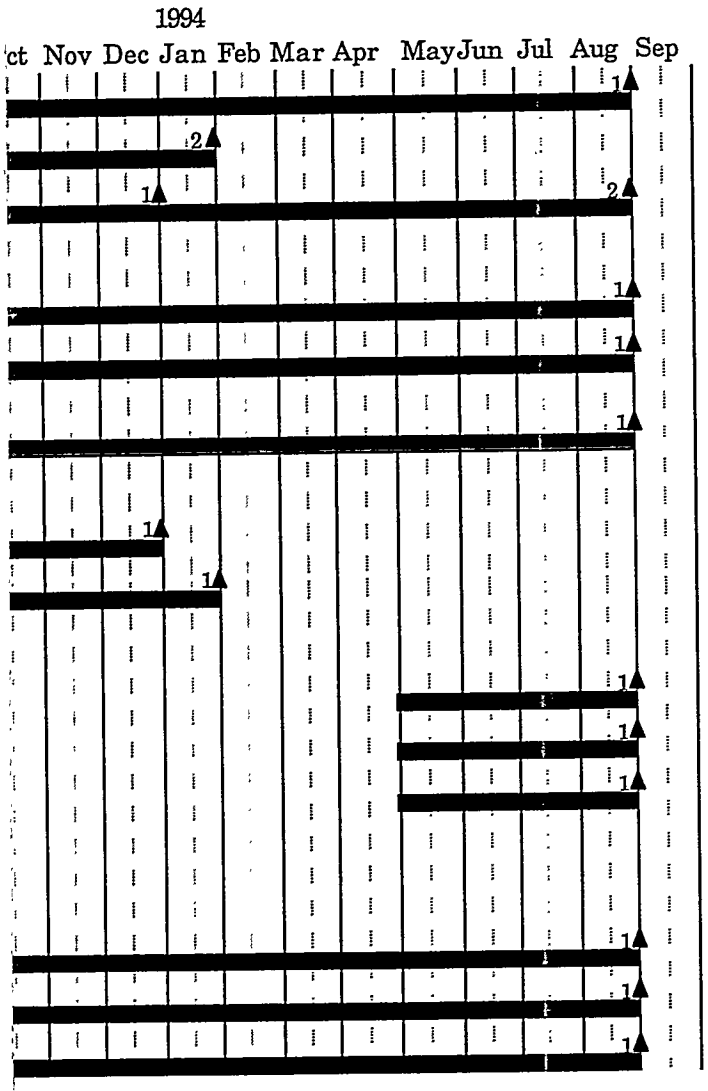
1994
ct Nov Dec Jan Feb Mar Apr May Jun Jul Aug Sep

Task 4 - Engineering and Economic Analysis

1992 1993

Sept Oct Nov Dec Jan Feb Mar Apr May Jun Jul Aug Sept O

Subtask 4.1 Survey Boiler Population / Identify Boilers for Conversion

Subtask 4.2 Identify Appropriate Cost - Estimating Methodologies

Subtask 4.3 Estimate Basic Costs of New Technologies

Subtask 4.4 Process Analysis of MCWSF and Dry, Micronized Coal

Subtask 4.4.1 Penn State Analysis

Subtask 4.4.2 Industrial Participants Assistance / Advisement

Subtask 4.5 Analyze/Identify Transportation Cost of Commercial Sources of MCWSF and Cleaned Coal for Dry, Micronized Coal Production

Subtask 4.6 Determine Community Spillovers

Subtask 4.7 Regional Market Considerations and Impacts

Subtask 4.8 Integrate the Analysis

Subtask 4.8.1 Penn State Review of Industrial Participants Contribution

Subtask 4.8.2 Penn State Integrate the Analysis

Subtask 4.8.3 Industrial Participants Assistance in Preparing, and Review of, the Integrated Analysis

Subtask 4.9 Project Management and Support

Subtask 4.9.1 Project Management and Advisement

Subtask 4.9.2 Drafting / Technical Secretarial Support

Subtask 4.9.3 Budget Management / Project Administration

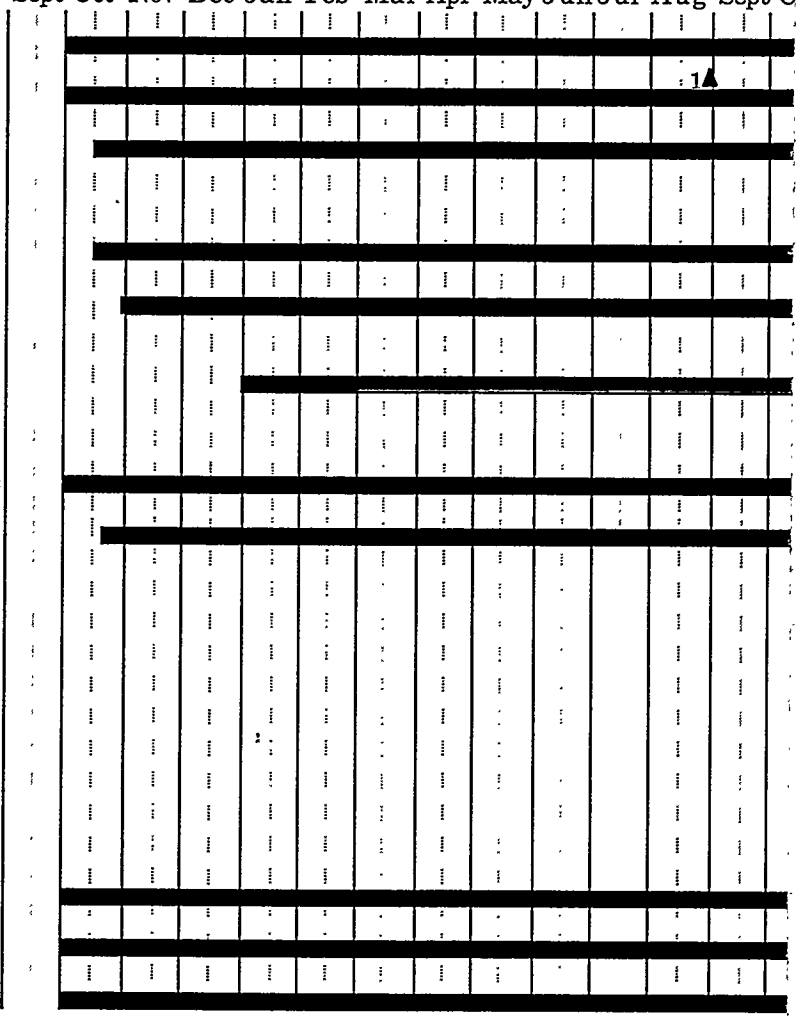

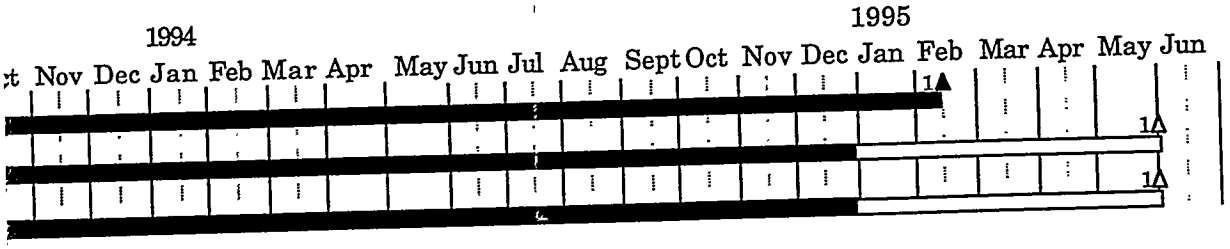
1994
1995
ct Nov Dec Jan Feb Mar Apr May Jun Jul Aug Sept Oct Nov Dec Jan Feb Mar Apr May Jun
1
1
1

		1992				1993									
		Sept	Oct	Nov	Dec	Jan	Feb	Mar	Apr	May	Jun	Jul	Aug	Sept	Oct
Task 5 -	**Final Report / Submission of DesignPackage**														
Subtask 5.1	**Industrial Participants Submission**														
Subtask 5.2	**Penn State Technical Preparation**														
Subtask 5.3	**Report Preparation Support Services**														

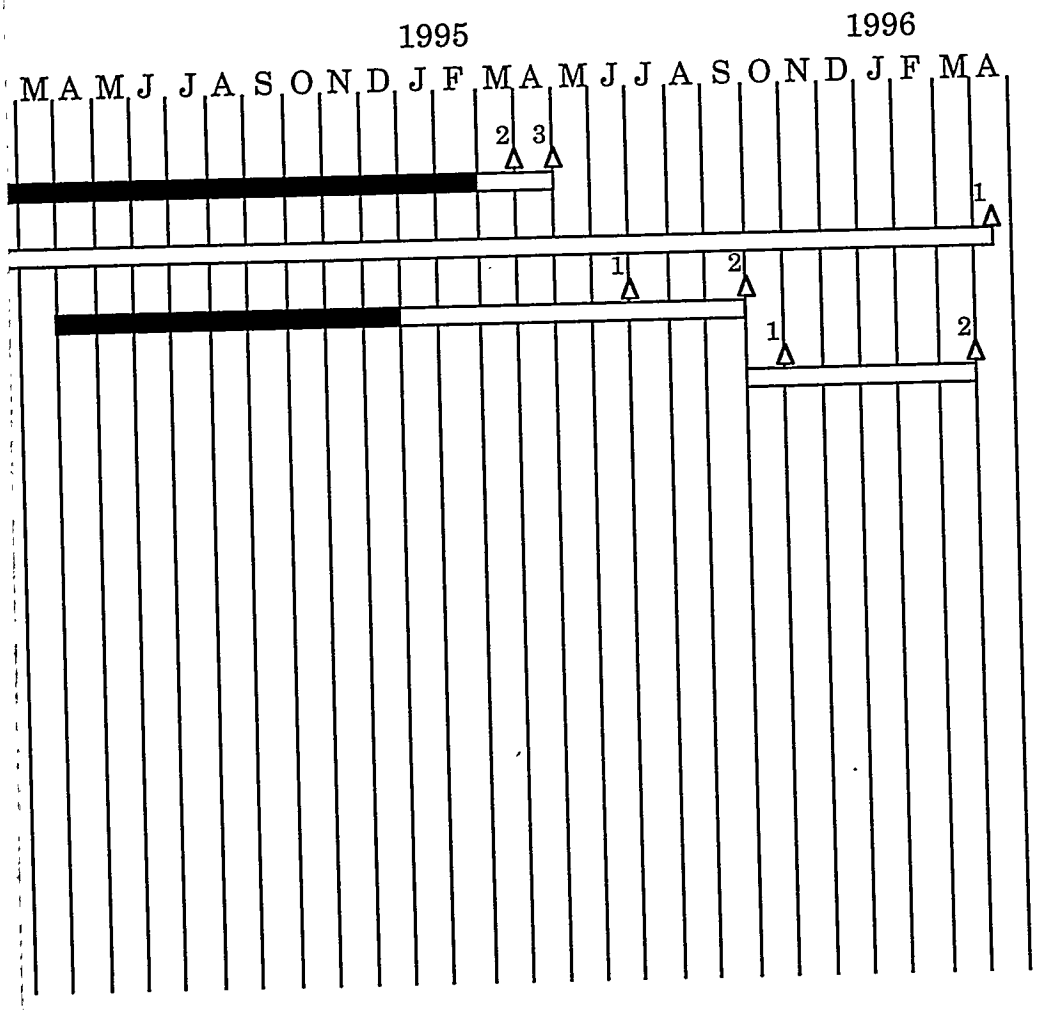

edule

Task 1. Emissions Reductions

Subtask 1.1 - Evaluate Emissions Reductions Strategies

Subtask 1.2 - Conduct Fundamental Emissions Studies

Subtask 1.3 - Install System on Demonstration Boiler

Subtask 1.4 - Evaluate Emissions Reduction System

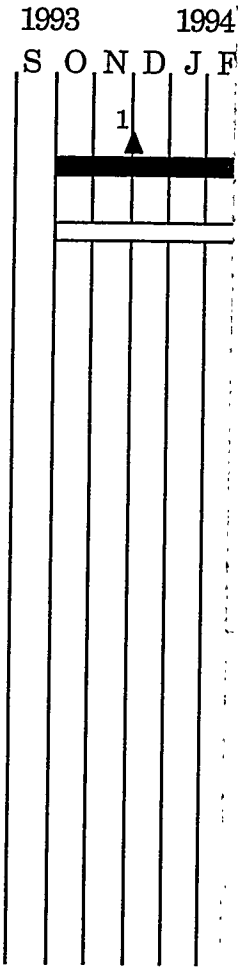

Figure 1-2. DOD Phase II Milestone Sch

Task 2. Coal Preparation / Utilization

Subtask 2.1 - Optimization of Particle Size Consist for Slurry Formulation

Subtask 2.2 - Fine Grinding / Classification / Liberation

Subtask 2.3 - Fine Gravity Concentration

Subtask 2.4 - Agglomeration / Flotation Studies

Subtask 2.5 - Fundamental Studies of Surface-Based Processes

Subtask 2.6 - Column Flotation

Subtask 2.7 - Dry Cleaning of Fine Coal

Subtask 2.8 - Slurry Density Control

Subtask 2.9 - Stabilization of CWSF

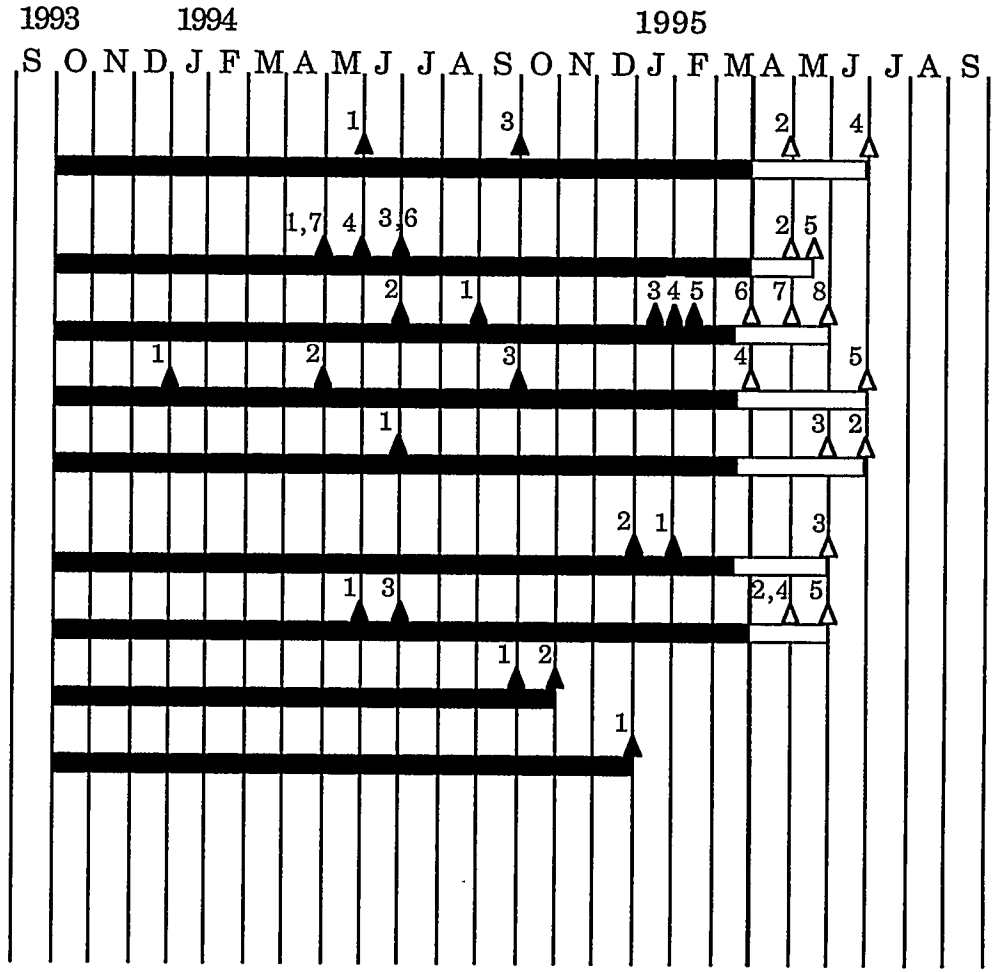

Task 3. Engineering Design and Cost and Economic Analysis

Subtask 3.1 - Basic Cost Estimation of Boiler Retrofits

Subtask 3.2 - Process Analysis

Subtask 3.3 - Environmental and Regulatory Impacts

Subtask 3.4 - Transportation Cost Analysis

Subtask 3.5 - Technology Adoption

Subtask 3.6 - Regional Economic Impacts

Subtask 3.7 - Public Perception of Benefits and Costs

Subtask 3.8 - Social Benefits

Subtask 3.9 - Coal Market Analysis

Subtask 3.10 - Integration of Analyses

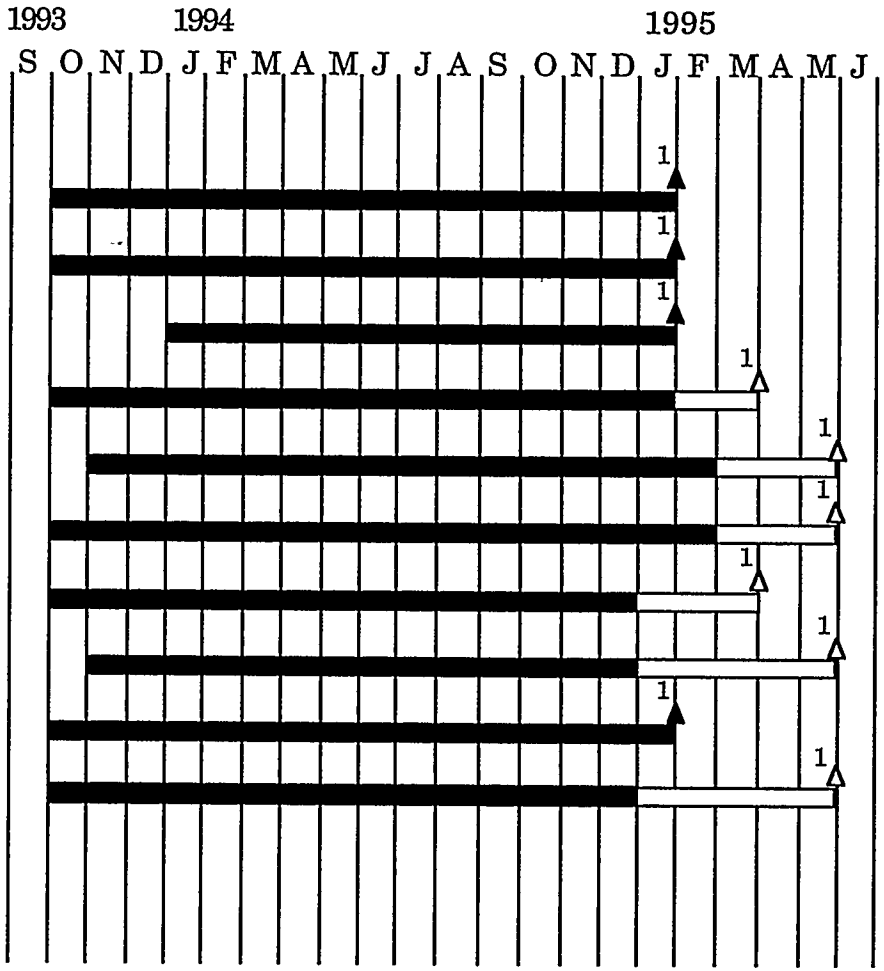

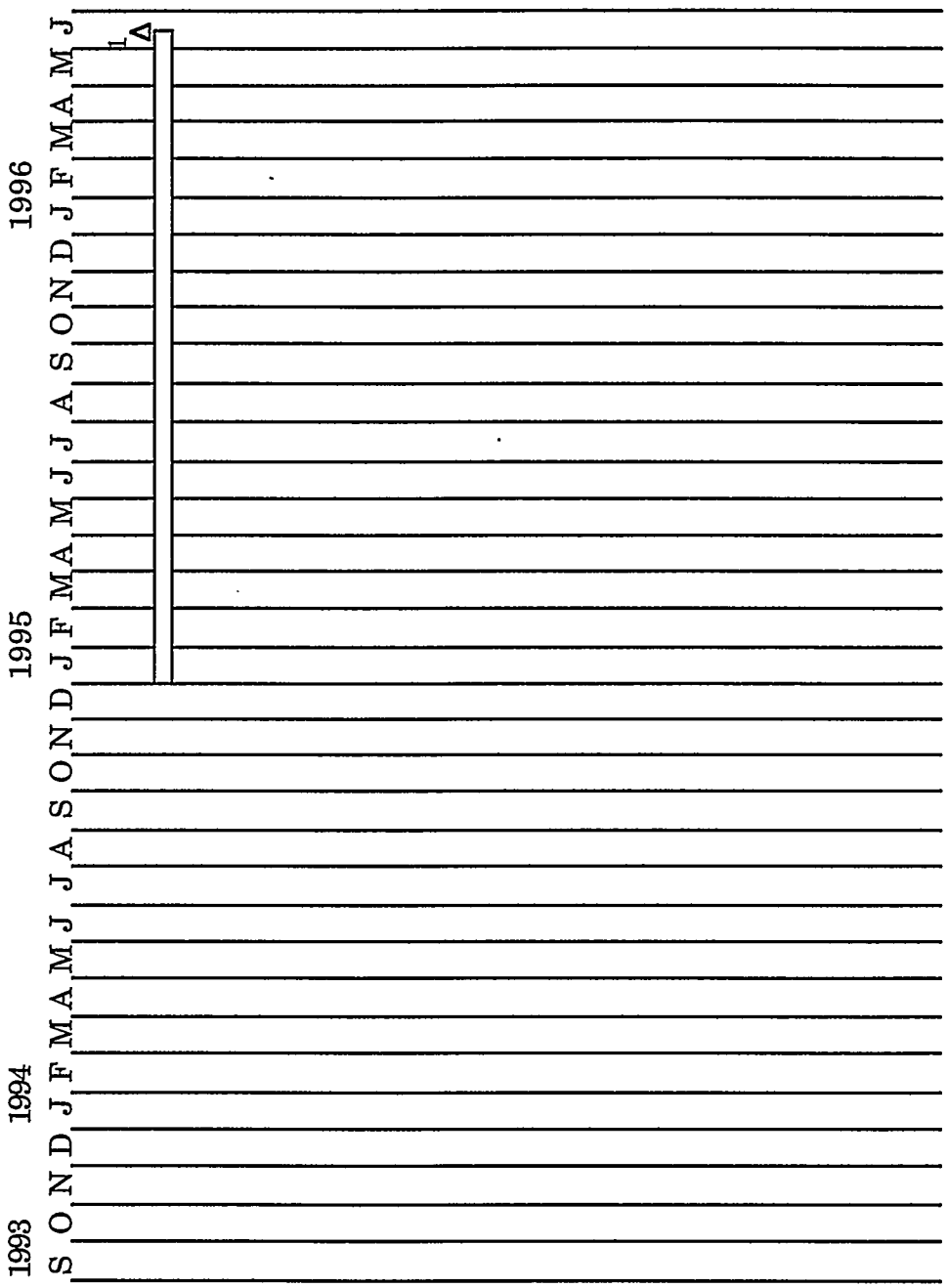

Task 4. Final Report

Task 1. Coal Preparation Utilization

Subtask 1.1 - Particle Size Control

Subtask 1.2 - Physical Separations

Subtask 1.3 - Surface-Based Separation Process

Subtask 1.4 - Dry Processing

Subtask 1.5 - Stabilization of Coal-Water Mixtures

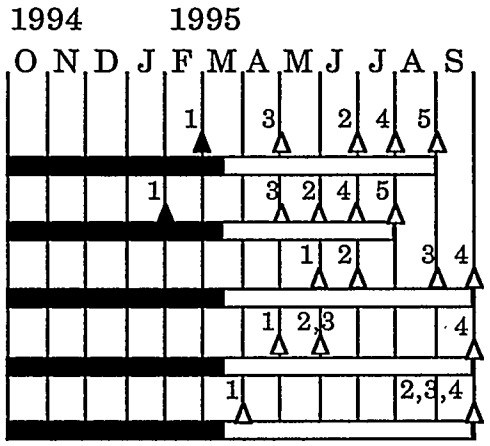

Task 2. Stoker Combustion Performance Analysis and Evaluation

Subtask 2.1 - Determine DOD Stoker Operability and Emissions

Subtask 2.2 - Conduct Field Test of a DOD Stoker

Subtask 2.3 - Provide Performance Improvement Analysis to DOD

Subtask 2.4 - Evaluate Pilot-Scale Stoker Retrofit Combustion

Subtask 2.5 - Perform Engineering Design of Stoker Retrofit

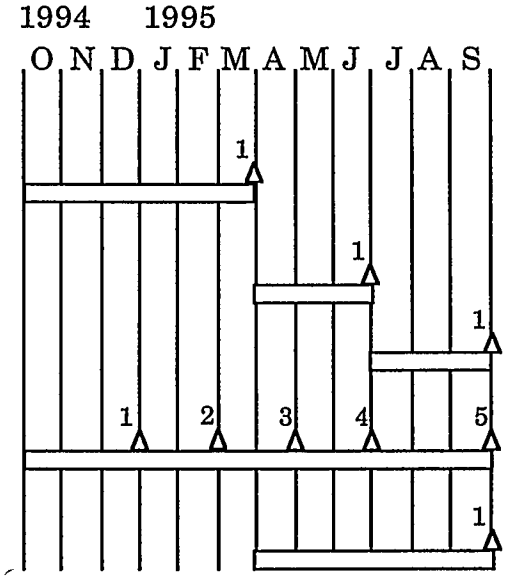

Figure 1-3. DOD Phase III Milestone Schedule

Task 3. Emissions Reduction

Subtask 3.1 - Demonstrate Advanced Pollution Control System

Subtask 3.2 - Evaluate CO_2 Mitigation and Heavy Metal Removal in a Slipstream System

Subtask 3.3 - Study VOC and Trace Metal Occurrence and Capture

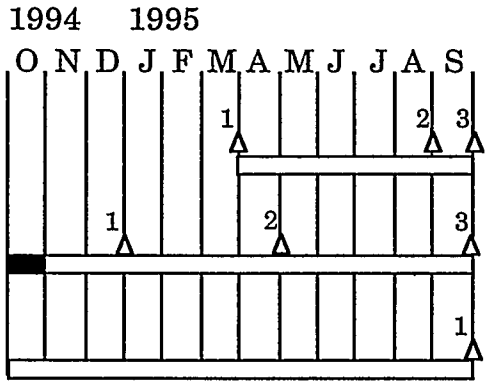

Task 4. Coal-Based Fuel Waste Cofiring

Subtask 4.1 - Coal Fines Combustion

Subtask 4.2 - Coal/Rocket Propellant Cofiring

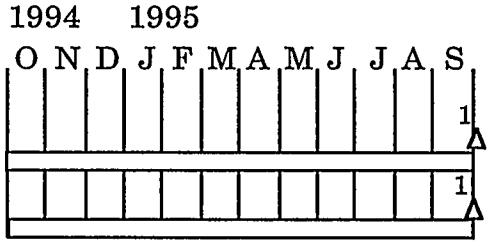

Task 5. Economic Evaluation

Subtask 5.1 - Cost and Market Penetration of Coal-Based FuelTechnologies

Subtask 5.2 - Selection of Incentives for Commercialization of the Coal Using Technology

Subtask 5.3 - Community Sensitivity of Coal Fuel Usage

Subtask 5.4 - Regional Economic Impacts of New Coal UtilizationTechnologies

Subtask 5.5 - Economic Analysis of the Defense Department's Fuel Mix

Subtask 5.6 - Constructing a National Energy Portfolio which Minimizes Energy Price Shock Effects

Subtask 5.7 - Proposed Research on the Coal Markets and their Impact on Coal-Based Fuel Technologies

Subtask 5.8 - Integration of Economic Analysis

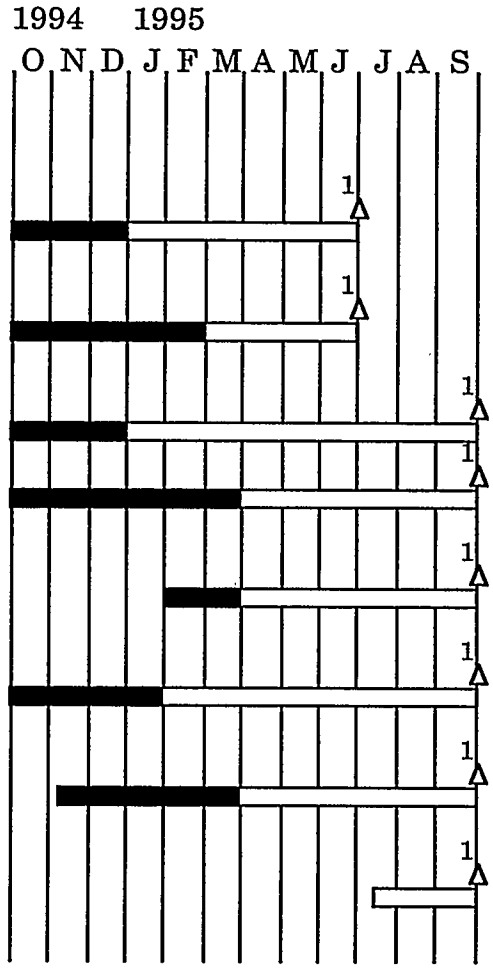

Task 6. Final Report / Submission of Design Package

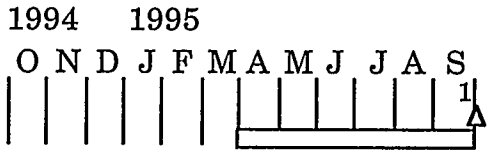

Table 1-1. Phase I. Milestone Description

Milestone	Description	Planned Completion Date	Actual Completion Date
Task 1. Coal Beneficiation/Preparation			
Subtask 1.1. Identify/Procure Coals			
Subtask 1.1, No. 1	Establish selection criteria	10/15/92	10/15/92
Subtask 1.1, No. 2	Preliminary list of candidate coals	02/01/93	02/01/93
Subtask 1.1, No. 3	Short list	03/01/93	03/01/93
Subtask 1.1, No. 4	Final list based on boiler selection	05/01/93	08/10/93
Subtask 1.1, No. 5	Procure samples	06/01/93	08/15/93
Subtask 1.2. Determine Liberation Potential			
Subtask 1.2.1.	Conventional Washability Analysis on Type I and Type II Samples		
Subtask 1.2.1, No. 1	Review of published data	06/01/93	06/01/93
Subtask 1.2.1, No. 2	Analysis of Type I complete	06/15/93	07/27/93
Subtask 1.2.1, No. 3	Analysis of Type II complete	09/30/93	09/30/93
Subtask 1.2.2.	Fine Washability Analysis on Type II and Type III Samples		
Subtask 1.2.2, No. 1	Review of published data	06/01/93	06/01/93
Subtask 1.2.2, No. 2	Analysis of Type II complete	07/01/93	09/30/93
Subtask 1.2.2, No. 3	Analysis of Type III complete	09/30/93	09/30/93
Subtask 1.3. Produce Laboratory-Scale Quantities of MCWM			
Subtask 1.3.1, No. 1	Identify Cleaning Strategies	10/30/93	10/30/93
Subtask 1.3.2,	Evaluate Conventional Gravity Separations		
Subtask 1.3.2, No. 1	Test work on Type I complete	09/01/93	09/01/93
Subtask 1.3.2, No. 2	Test work on Type II complete	04/30/94	04/30/94
Subtask 1.3.2, No. 3	Test work on Type III complete	04/30/94	04/30/94
Subtask 1.3.3.	Evaluate Fine Gravity Separations		
Subtask 1.3.3, No. 1	Cyclone test rig set-up	11/30/92	11/30/92
Subtask 1.3.3, No. 2	Initiate magnetite classification studies	12/01/92	12/01/92
Subtask 1.3.3, No. 3	Initiate batch centrifuge testing	02/01/93	02/02/93
Subtask 1.3.3, No. 4	Preliminary centrifuge data evaluation	01/31/94	01/31/94
Subtask 1.3.3, No. 5	Procure continuous centrifuge	08/01/93	07/14/93
Subtask 1.3.3, No. 6	Initiate selectivity studies on Type III coals	06/01/93	06/01/93
Subtask 1.3.3, No. 7	Magnetite classification studies complete	06/15/93	06/15/93
Subtask 1.3.3, No. 8	Procure saturation magnetization analyzer	08/01/93	07/29/93
Subtask 1.3.3, No. 9	Procure variable speed pump	08/01/93	07/29/93
Subtask 1.3.3, No. 10	Preliminary test work complete	04/01/94	05/31/94
Subtask 1.3.4.	Evaluate Advanced Froth Flotation		
Subtask 1.3.4, No. 1	Reagent selection	06/01/93	06/01/93
Subtask 1.3.4, No. 2	Initiate test work on Type II samples	06/15/93	08/31/93
Subtask 1.3.4, No. 3	Initiate test work on Type III samples	07/01/93	06/15/93

Milestone	Description	Planned Completion Date	Actual Completion Date
Subtask 1.3.4, No. 4	Type II test work complete	09/30/94	07/31/94
Subtask 1.3.4, No. 5	Type III test work complete	08/31/93	07/31/93
Subtask 1.3.4, No. 6	Data evaluation completed	11/30/94	09/30/94
Subtask 1.3.5. Evaluate Column Flotation			
Subtask 1.3.5, No. 1	Complete column design	05/01/93	05/01/93
Subtask 1.3.5, No. 2	Procure bubble generators	06/01/93	06/01/93
Subtask 1.3.5, No. 3	Complete column fabrication	07/31/93	09/01/93
Subtask 1.3.5, No. 4	Complete test work	05/31/94	05/31/94
Subtask 1.3.6. Evaluate Selective Agglomeration			
Subtask 1.3.6, No. 1	Initiate wetting studies	01/15/93	01/15/93
Subtask 1.3.6, No. 2	Initiate 3-phase aggregation studies	01/31/93	01/31/93
Subtask 1.3.6, No. 3	Fabricate test cell	02/15/93	02/15/93
Subtask 1.3.6, No. 4	Complete preliminary test work on Type II samples	09/30/94	09/30/94
Subtask 1.3.6, No. 5	Complete preliminary test work on Type III samples	09/15/93	09/15/93
Subtask 1.3.6, No. 6	Complete detailed studies on Type III samples	03/01/94	03/01/94
Subtask 1.3.7. Investigate Solid-Liquid Separations			
Subtask 1.3.7, No. 1	Preliminary evaluation complete	09/30/93	09/30/93
Subtask 1.3.7, No. 2	Initiate studies on test coals	09/30/93	09/30/93
Subtask 1.3.7, No. 3	Complete studies on test coals	09/30/94	01/31/95
Subtask 1.3.8. Select Cleaning Flowsheet(s)			
Subtask 1.3.8, No. 1	Establish flowsheet for Type I sample	12/01/93	12/01/93
Subtask 1.3.9. Establish Required Size Consist for Slurry Formulation			
Subtask 1.3.9, No. 1	Complete for Type I samples	10/31/94	12/31/94
Subtask 1.3.9, No. 2	Complete for Type II samples	12/31/94	12/31/94
Subtask 1.3.9, No. 3	Complete for Type III samples	12/31/94	12/31/94
Subtask 1.3.10. Investigate Conventional Ball Milling			
Subtask 1.3.10, No. 1	Complete test work for Type I samples	07/31/93	07/31/93
Subtask 1.3.10, No. 2	Complete test work for Type II samples	10/31/93	10/31/93
Subtask 1.3.10, No. 3	Complete test work for Type III samples	10/31/93	10/31/93
Subtask 1.3.11. Stirred Media Milling			
Subtask 1.3.11, No. 1	Procure stirred media mill	07/15/93	07/15/93
Subtask 1.3.11, No. 2	Complete test work on Type I samples	04/30/94	04/30/94
Subtask 1.3.11, No. 3	Complete test work on Type II samples	05/15/94	06/15/94
Subtask 1.3.11, No. 4	Complete test work on Type III samples	05/31/94	06/30/94
Subtask 1.3.12. Investigate Attrition Milling			
Subtask 1.3.12, No. 1	Establish test procedure	04/30/94	05/31/94
Subtask 1.3.12, No. 2	Evaluate preliminary data	09/30/94	12/31/94
Subtask 1.3.12, No. 3	Complete evaluation	10/31/94	12/31/94

Milestone	Description	Planned Completion Date	Actual Completion Date
Subtask 1.3.13. Lab-Scale Slurry Production			
Subtask 1.3.13, No. 1	Type I produced	03/15/95	03/24/95
Subtask 1.3.13, No. 2	Type II produced	02/07/95	02/07/95
Subtask 1.3.13, No. 3	Type III produced	03/01/95	03/03/95
Subtask 1.3.14, No. 1	Modify viscosity and sedimentation rate models to account for PSD; compare model predictions to experimental observations	06/30/93	03/01/94
Subtask 1.4. Develop Dry Coal Cleaning Technique			
Subtask 1.4.1. Dry Grinding Studies			
Subtask 1.4.1, No. 1	Procure compressor system	03/15/93	03/15/93
Subtask 1.4.1, No. 2	Set up closed-circuit grinding system	05/15/93	05/15/93
Subtask 1.4.1, No. 3	Procure pilot-scale jet mill	05/30/93	05/30/93
Subtask 1.4.1, No. 4	Procedure established for Type III samples	08/31/93	08/31/93
Subtask 1.4.1, No. 5	Produce micronized product for dry beneficiation studies	11/01/93	11/01/93
Subtask 1.4.2. Deagglomeration Studies			
Subtask 1.4.2, No. 1	Establish standardized test procedure	07/31/94	09/15/94
Subtask 1.4.2, No. 2	Initiate humidity and reagent testing	09/30/94	09/30/94
Subtask 1.4.2, No. 3	Procure laser diagnostic system	10/15/93	02/08/94
Subtask 1.4.2, No. 4	Complete humidity testing	10/01/94	11/31/94
Subtask 1.4.3. Dry Separations			
Subtask 1.4.3, No. 1	Procure power supplies	03/01/93	03/01/93
Subtask 1.4.3, No. 2	Fabricate prototype test unit	05/01/93	05/01/93
Subtask 1.4.3, No. 3	Complete preliminary testing	08/31/93	08/31/93
Subtask 1.4.3, No. 4	Complete testing	06/30/94	06/30/94
Subtask 1.5. Produce MCWMs and Micronized Coal from Dry, Clean Coal			
Subtask 1.5.1, No. 1	Produce Micronized Coal from Dry, Clean Coal	11/01/94	12/31/94
Subtask 1.5.2, No. 1	Product MCWM from Dry, Clean Coal	12/01/94	12/31/94
Subtask 1.6. Produce MCWM and Dry, Micronized Coal for the Demonstration			
Subtask 1.6.1, No. 1	Shakedown dry, micronized coal circuit	07/31/93	09/30/93
Subtask 1.6.2, No. 1	Complete CWM Preparation Facility	07/31/93	07/31/93
Subtask 1.6.2, No. 2	Procure automated valves	09/01/94	09/01/94
Subtask 1.6.2, No. 3	Install CWM equipment	01/15/95	01/27/95
Subtask 1.6.3, No. 1	Shakedown CWM circuit	01/31/95	01/27/95
Subtask 1.6.4, No. 1	Coal Cleaning	03/29/95	03/29/95
Subtask 1.6.5, No. 1	Coal Micronizing	01/01/95	12/15/94
Subtask 1.6.6, No. 1	MCWM Preparation	04/15/95	

Milestone	Description	Planned Completion Date	Actual Completion Date
Subtask 1.7. Project Management and Support			
Subtask 1.7.1, No. 1	Project Management and Technical Advisement	04/15/95	
Subtask 1.7.2, No. 1	Drafting/Technical Secretary Support	04/15/95	
Subtask 1.7.3, No. 1	Budget Management/Project Administration	04/15/95	
Task 2. Combustion Performance Evaluation			
Subtask 2.1. Boiler Retrofit			
Subtask 2.1.1, No. 1	Finalize burner/atomizer design	05/31/93	11/01/93
Subtask 2.1.2, No. 1	Procure and install burner	05/01/94	05/15/94
Subtask 2.1.3, No. 1	Optimize burner firing dry, micronized coal	07/31/94	07/31/94
Subtask 2.1.4, No. 1	Optimize burner firing CWM	02/15/95	02/15/95
Subtask 2.2. Fuel Evaluation in Research Boiler			
Subtask 2.2.1, No. 1	Test sample of Type I CWM	03/31/95	
Subtask 2.2.2, No. 1	Test sample of Type II CWM	02/15/95	02/15/95
Subtask 2.2.3, No. 1	Test sample of Type III CWM	03/10/95	03/10/95
Subtask 2.3. Performance Evaluation of MCWM and Dry, Micronized Coal in Demonstration Boiler			
	Dry, Micronized Coal Testing		
Subtask 2.3.1, No. 1	100-hour milestone firing dry, micronized coal	07/19/94	07/19/94
Subtask 2.3.2, No. 1	200-hour milestone firing dry, micronized coal	07/28/94	07/28/94
Subtask 2.3.3, No. 1	300-hour milestone firing dry, micronized coal	08/05/94	08/05/94
Subtask 2.3.4, No. 1	400-hour milestone firing dry, micronized coal	08/22/94	08/22/94
Subtask 2.3.5, No. 1	500-hour milestone firing dry, micronized coal	08/30/94	08/30/94
Subtask 2.3.6, No. 1	600-hour milestone firing dry, micronized coal	09/14/94	09/14/94
Subtask 2.3.7, No. 1	700-hour milestone firing dry, micronized coal	09/30/94	09/30/94
Subtask 2.3.8, No. 1	800-hour milestone firing dry, micronized coal	10/14/94	10/14/94
Subtask 2.3.9, No. 1	900-hour milestone firing dry, micronized coal	10/25/94	10/25/94
Subtask 2.3.10, No. 1	1,000-hour milestone firing dry, micronized coal	11/09/94	11/09/94
Subtask 2.3.11, No. 1	Technical Advisement by EER	12/31/94	12/31/94
	MCWM Testing		
Subtask 2.3.12, No. 1	100-hour milestone firing micronized CWM	01/15/95	01/15/95
Subtask 2.3.13, No. 1	200-hour milestone firing micronized CWM	01/23/95	01/23/95
Subtask 2.3.14, No. 1	300-hour milestone firing micronized CWM	02/07/95	02/07/95
Subtask 2.3.15, No. 1	400-hour milestone firing micronized CWM	02/15/95	02/15/95
Subtask 2.3.16, No. 1	500-hour milestone firing micronized CWM	02/23/95	02/23/95
Subtask 2.3.17, No. 1	600-hour milestone firing micronized CWM	03/07/95	03/07/95
Subtask 2.3.18, No. 1	700-hour milestone firing micronized CWM	03/15/95	03/15/95
Subtask 2.3.19, No. 1	800-hour milestone firing micronized CWM	03/23/95	03/23/95
Subtask 2.3.20, No. 1	900-hour milestone firing micronized CWM	04/07/95	
Subtask 2.3.21, No. 1	1,000-hour milestone firing micronized CWM	04/15/95	
	Evaluate Erosion/Deposition Characteristics		
Subtask 2.3.23, No. 1	Identify erosion and deposition regimes	11/30/92	11/30/92
Subtask 2.3.24, No. 1	Model simultaneous erosion and deposition	09/30/93	03/01/94

Milestone	Description	Planned Completion Date	Actual Completion Date
Subtask 2.3.25, No. 1	Procure Zirconia/Platinum sensor/recorder	10/15/93	10/15/93
Subtask 2.3.25, No. 2	Compare heat transfer surface performance firing micronized dry coal and CWM	04/15/95	
Subtask 2.3.26, No. 1	Develop procedure for determining optimum convective section gas velocity	02/28/94	03/01/94
Subtask 2.3.27, No. 1	Comparison of performance of various coals	04/15/95	
Subtask 2.4. Evaluate Emissions Reduction Strategies			
Subtask 2.4.1, No. 1	Determine emissions from micronized coal testing	12/15/95	12/15/95
Subtask 2.4.2, No. 1	Determine emissions from CWM testing	04/15/95	
Subtask 2.5. Project Management and Support			
Subtask 2.5.1, No. 1	Project management and advisement	04/15/95	
Subtask 2.5.2, No. 1	Staff supervision, test planning, and quality control	04/15/95	
Subtask 2.5.3, No. 1	Data reduction and interpretation	04/15/95	
Subtask 2.5.4, No. 1	Drafting/technical secretarial support	04/15/95	
Subtask 2.5.5, No. 1	Budget management/project administration	04/15/95	
Task 3. Engineering Design			
Subtask 3.1. Micronized CWM/Dry, Micronized Coal Preparation Facilities			
Subtask 3.1.1, No. 1	Design of micronized CWM preparation facility by PSU	04/15/95	
Subtask 3.1.2, No. 1	Design of dry micronized coal preparation system by EER	09/01/94	07/15/94
Subtask 3.2. Fuel Handling			
Subtask 3.2.1, No. 1	Design of fuel system by EER	09/01/94	07/15/94
Subtask 3.2.2, No. 1	Technical support and design of fuel system by PSU	09/01/94	07/15/94
Subtask 3.3. Burner System			
Subtask 3.3.1, No. 1	Design of burner by EER for selected boiler	09/01/94	07/15/94
Subtask 3.3.2, No. 1	Design of auxiliary components by EER	09/01/94	07/15/94
Subtask 3.4. Ash Removal, Handling, and Disposal			
Subtask 3.4.1, No. 1	Design of ash system by EER	09/01/94	07/15/94
Subtask 3.5. Air Pollution Control			
Subtask 3.5.1, No. 1	Design of emission control by EER	09/01/94	07/15/94
Subtask 3.6. Integrate Engineering Design			
Subtask 3.6.1, No. 1	Integrate system components	09/01/94	07/15/94

Milestone	Description	Planned Completion Date	Actual Completion Date
Subtask 3.7. Project Management and Support			
Subtask 3.7.1, No. 1	Project management and technical advisement	04/15/95	
Subtask 3.7.2, No. 1	Penn State technical review	04/15/95	
Subtask 3.7.3, No. 1	Drafting/technical secretarial support	04/15/95	
Subtask 3.7.4, No. 1	Budget management/project administrtaion	04/15/95	
Task 4. Engineering and Economic Analysis			
Subtask 4.1, No. 1	Survey Boiler Population/Identify Boilers for Conversion	09/01/94	09/01/94
Subtask 4.2, No. 1	Identify Appropriate Cost-Estimating Technologies	05/31/93	09/01/93
Subtask 4.2, No. 2	Prepare Final Draft	01/31/94	01/31/94
Subtask 4.3, No. 1	Estimate Basic Costs of New Technologies	12/31/93	12/31/93
Subtask 4.3, No. 2	Prepare Final Draft	09/01/94	09/01/94
Subtask 4.4. Process Analysis of MCWM and Dry, Micronized Coal			
Subtask 4.4.1, No. 1	Penn State Analysis	09/01/94	09/01/94
Subtask 4.4.2, No. 1	Industrial Participants Assistance/Advisement	09/01/94	09/01/94
Subtask 4.5, No. 1	Analyze/Identify Transportation Cost of Commercial Sources of MCWM and Cleaned Coal for Dry, Micronized Coal Production	12/31/93	09/01/94
Subtask 4.6, No. 1	Determine Community Spillovers	12/31/93	12/31/93
Subtask 4.7, No. 1	Regional Market Considerations and Impacts	01/31/94	01/31/94
Subtask 4.8. Integrate the Analysis			
Subtask 4.8.1, No. 1	Penn State Review of Industrial Participants Contribution	09/01/94	09/01/94
Subtask 4.8.2, No. 1	Penn State Integration of the Analysis	09/01/94	09/01/94
Subtask 4.8.3, No. 1	Industrial Participants Assistance in Preparing, and Review of, the Integrated Analysis	09/01/94	09/01/94
Subtask 4.9. Project Management and Support			
Subtask 4.9.1, No. 1	Project Management and Advisement	09/01/94	09/01/94
Subtask 4.9.2, No. 1	Drafting/Technical Secretarial Support	09/01/94	09/01/94
Subtask 4.9.3, No. 1	Budget Management/Project Administration	09/01/94	09/01/94
Task 5. Final Report/Submission of Design Package			
Subtask 5.1, No. 1	Industrial Participants Submission to Penn State/Review Final Package	02/15/95	02/15/95
Subtask 5.2, No. 1	Penn State Technical Preparation	06/01/95	
Subtask 5.3, No. 1	Report Preparation Support Services	06/01/95	

Table 1-2. Phase II. Milestone Description

Milestone	Description	Planned Completion Date	Actual Completion Date
Task 1. Emissions Reduction			
Subtask 1.1. Evaluation of Emissions Reduction Strategies			
Subtask 1.1, No. 1	Receive proposals for pollution control system	12/01/93	12/01/93
Subtask 1.1, No. 2	Complete summary report of pollution control technologies	03/31/95	
Subtask 1.1, No. 3	Select pollution control system	04/30/95	
Subtask 1.2. Conduct Fundamental Emissions Studies			
Subtask 1.2, No. 1	Prepare summary of emissions studies	04/15/96	
Subtask 1.3. Install System on Demonstration Boiler			
Subtask 1.3, No. 1	Design pollution control system	06/30/95	
Subtask 1.3, No. 2	Complete installation of system	10/01/95	
Subtask 1.4. Evaluate Emissions Reduction System			
Subtask 1.4, No. 1	Shakedown system	11/01/95	
Subtask 1.4, No. 2	Complete system evaluation	04/01/96	
Task 2. Coal Preparation/Utilization			
Subtask 2.1. Optimization of Particle Size Consist for Slurry Formulation			
Subtask 2.1, No. 1	Samples of fine and coarse slurry components prepared	04/30/94	05/30/94
Subtask 2.1, No. 2	Rheological characterization of components completed	04/30/95	
Subtask 2.1, No. 3	Models for rheology of binary mixtures developed	09/30/94	09/30/94
Subtask 2.1, No. 4	Optimization studies complete	06/30/95	
Subtask 2.2. Fine Grinding/Classification Liberation			
Subtask 2.2, No. 1	Grinding kinetics data for wet ball milling obtained	04/30/94	04/30/94
Subtask 2.2, No. 2	Wet classifier performance evaluated	04/30/95	
Subtask 2.2, No. 3	Dry classifier performance evaluated	04/30/94	06/30/94
Subtask 2.2, No. 4	Grinding kinetics data for stirred media milling obtained	05/31/94	05/31/94
Subtask 2.2, No. 5	Closed-circuit jet-milling data obtained	05/15/95	
Subtask 2.2, No. 6	Slurry production simulations initiated	06/30/94	06/30/94
Subtask 2.2, No. 7	Liberation data on Type III coal obtained	04/30/94	04/30/94
Subtask 2.3. Fine Gravity Concentration			
Subtask 2.3, No. 1	Initiate magnetic fluid separation of Type III coal	07/31/94	08/15/94
Subtask 2.3, No. 2	Complete batch centrifuge testing	04/30/94	06/30/94
Subtask 2.3, No. 3	Continuous centrifuge test rig set-up	09/30/94	01/15/95
Subtask 2.3, No. 4	Initiate magnetite classification studies	10/15/94	01/31/95
Subtask 2.3, No. 5	Initiate separations of Type III coals	02/28/95	02/28/95

Milestone	Description	Planned Completion Date	Actual Completion Date
Subtask 2.3, No. 6	Initiate micronized coal classification studies	04/30/95	
Subtask 2.3, No. 7	Evaluate dense-medium separation data	04/30/95	
Subtask 2.3, No. 8	Evaluate size classification data	05/31/95	
Subtask 2.4. Agglomeration/Flotation Studies			
Subtask 2.4, No. 1	Set-up device to size separate flotation products of micronized coal	12/31/93	12/31/93
Subtask 2.4, No. 2	Set-up equipment for larger scale tests using 2.2 cu.ft. flotation cells	04/30/94	04/30/94
Subtask 2.4, No. 3	Conduct agglomeration-flotation tests for micronized Type III coal	09/30/94	09/30/94
Subtask 2.4, No. 4	Conduct agglomeration-flotation tests in larger cells	03/31/95	
Subtask 2.4, No. 5	Determine parameters for scale-up	06/30/95	
Subtask 2.5. Fundamental Studies of Surface-Based Processes			
Subtask 2.5, No. 1	Conduct interface characterization studies to determine flotation reagent-coal interactions	06/30/94	06/30/94
Subtask 2.5, No. 2	Measure contact angles in the coal-oil-surfactant-water system	06/30/95	
Subtask 2.5, No. 3	Determine effect of surfactants on slurry stability	05/31/95	
Subtask 2.6. Column Flotation			
Subtask 2.6, No. 1	Test work on Type II coals	11/30/94	01/31/95
Subtask 2.6, No. 2	Test work on Type III coals	09/30/94	12/31/94
Subtask 2.6, No. 3	Determine scale-up parameters	05/31/95	
Subtask 2.7. Dry Cleaning of Fine Coal			
Subtask 2.7, No. 1	Complete evaluation of Type III coal in batch separator	04/30/94	05/31/94
Subtask 2.7, No. 2	Integration of closed dry grinding circuit with TES	04/30/95	
Subtask 2.7, No. 3	Initiate investigation of continuous TES	04/01/94	06/30/94
Subtask 2.7, No. 4	Complete charge measurements on Type II coal	04/30/95	
Subtask 2.7, No. 5	Complete charge measurements on Type III	05/31/95	
Subtask 2.8. Slurry Density Control			
Subtask 2.8, No. 1	Evaluate procedures for reversible flocculation of fine coal	09/30/94	09/30/94
Subtask 2.8, No. 2	Establish process engineering for thickening of fine-coal slurries	10/31/94	10/31/94
Subtask 2.9. Stabilization of CWSF			
Subtrask 2.9, No. 1	Complete stabilization study	12/31/94	12/31/94

Milestone	Description	Planned Completion Date	Actual Completion Date
Task 3.	**Engineering Design and Cost; and Economic Analysis**		
Subtask 3.1.	Determine Basic Cost Estimation of Boiler Retrofits	02/01/95	02/01/95
Subtask 3.2.	Determine Process Analysis	02/01/95	02/01/95
Subtask 3.3.	Determine Environmental and Regulatory Impacts	02/01/95	02/01/95
Subtask 3.4.	Determine Transportation Cost Analysis	04/01/95	
Subtask 3.5.	Determine Technology Adoption	06/01/95	
Subtask 3.6.	Determine Regional Economic Impacts	06/01/95	
Subtask 3.7.	Determine Public Perception of Benefits and Costs	04/01/95	
Subtask 3.8.	Determine Social Benefits	06/01/95	
Subtask 3.9.	Determine Coal Market Analysis	02/01/95	02/01/95
Subtask 3.10.	Complete Integration of Analyses	06/01/95	
Task 4.	**Final Report**	06/15/96	

Table 1-3. Phase III. Milestone Description

Milestone	Description	Planned Completion Date	Actual Completion Date
Task 1. Coal Preparation/Utilization			
Subtask 1.1. Particle Size Control			
Subtask 1.1, No. 1	Evaluate conventional ball milling circuit	02/28/95	02/28/95
Subtask 1.1, No. 2	Evaluate stirred-media milling circuit	06/30/95	
Subtask 1.1, No. 3	Complete baseline testing of attrition milling for the production of broad size distributions	07/31/95	
Subtask 1.1, No. 4	Complete preliminary evaluation of dry grinding/ cleaning circuit	07/31/95	
Subtask 1.1, No. 5	Initiate investigation of an integrated grinding/cleaning circuit	08/31/95	
Subtask 1.2. Physical Separations			
Subtask 1.2, No. 1	Complete preliminary investigation of magnetic fluid-based separation for fine coal cleaning	01/31/95	01/31/95
Subtask 1.2, No. 2	Complete baseline testing of dense-medium separation using the continuous, solid-bowl centrifuge	05/31/95	
Subtask 1.2, No. 3	Initiate investigation of magnetic fluid cyclone separations	04/30/95	
Subtask 1.2, No. 4	Complete baseline testing of solid-bowl centrifuge for micronized coal classification	06/30/95	
Subtask 1.2, No. 5	Initiate testing of integrated centrifugal/flotation system	07/31/95	
Subtask 1.3. Surface-Based Separation Processes			
Subtask 1.3, No. 1	Set up and evaluate continuous flotation circuit	05/31/95	
Subtask 1.3, No. 2	Evaluate effectiveness of alternative bubble generators in flotation column	06/30/95	
Subtask 1.3, No. 3	Baseline testing on selected coal	08/31/95	
Subtask 1.3, No. 4	Evaluate flotation system performance	09/27/95	
Subtask 1.4 Dry Processing			
Subtask 1.4, No. 1	Complete deagglomeration testing using the batch triboelectrostatic separator	04/30/95	
Subtask 1.4, No. 2	Complete baseline testing of continuous triboelectrostatic separator unit	05/31/95	
Subtask 1.4, No. 3	Initiate investigation of alternative approaches to charging/deagglomeration	05/31/95	
Subtask 1.4, No. 4	Complete preliminary testing of integrated grinding and triboelectrostatic separator unit	09/27/95	

Milestone	Description	Planned Completion Date	Actual Completion Date
Subtask 1.5 Stabilization of Coal-Water Mixtures			
Subtask 1.5, No. 1	Complete PSD model extension	04/01/95	
Subtask 1.5, No. 2	Complete construction of computer program	09/27/95	
Subtask 1.5, No. 3	Complete PSD model comparison to experimental results	09/27/95	
Subtask 1.5, No. 4	Complete coal oxidation study	09/27/95	
Task 2. Stoker Combustion Performance Analysis and Evaluation			
Subtask 2.1. Determine DOD Stoker Operability and Emissions			
Subtask 2.1, No. 1	Complete stoker survey, identify stoker for evaluation	03/31/95	
Subtask 2.2. Conduct Field Test of a DOD Stoker			
Subtask 2.2, No. 1	Complete stoker field test	07/01/95	
Subtask 2.3 Provide Performance Improvement Analysis to DOD			
Subtask 2.3, No. 1	Complete performance improvement analysis	09/27/95	
Subtask 2.4. Evaluate Pilot-Scale Stoker Retrofit Combustion			
Subtask 2.4, No. 1	Complete modifications to stoker system	12/31/94	
Subtask 2.4, No. 2	Complete evaluation of anthracite micronized coal	02/28/95	
Subtask 2.4, No. 3	Complete evaluation of anthracite/water mixtures	04/30/95	
Subtask 2.4, No. 4	Complete evaluation of bituminous micronized coal	06/30/95	
Subtask 2.4, No. 5	Complete evaluation of bituminous/water mixtures	09/27/95	
Subtask 2.5. Perform Engineering Design of Stoker Retrofit			
Subtask 2.5, No. 1	Complete retrofit design	09/27/95	
Task 3. Emissions Reduction			
Subtask 3.1. Demonstrate Advanced Pollution Control System			
Subtask 3.1, No. 1	Identify low-temperature catalysts	03/31/95	
Subtask 3.1, No. 2	Install catalyst-coated filter and SO_2 removal system	08/31/95	
Subtask 3.1, No. 3	Complete demonstration of unit	09/27/95	
Subtask 3.2. Evaluate Carbon Dioxide Mitigation and Heavy Metal Removal in a Slipstream System			
Subtask 3.2, No. 1	Identify CO_2 mitigation technique	01/01/95	
Subtask 3.2, No. 2	Install slipstream	05/01/95	

Milestone	Description	Planned Completion Date	Actual Completion Date
Subtask 3.2, No. 3	Complete evaluation of CO_2 mitigation/heavy metal removal	09/27/95	
Subtask 3.3. Study VOC and Trace Metal Occurrence and Capture			
Subtask 3.3, No. 1	Complete evaluation of VOC and trace metals	09/27/95	
Task 4. Coal-Based Fuel Waste Cofiring			
Subtask 4.1. Coal Fines Combustion			
Subtask 4.1, No. 1	Complete coal fines combustion evaluation	09/27/95	
Subtask 4.2. Coal/Rocket Propellant Cofiring			
Subtask 4.2, No. 1	Complete cofiring testing	09/27/95	
Task 5. Economic Evaluation			
Subtask 5.1. Cost and Market Penetration of Coal-Based Fuel Technologies			
Subtask 5.1, No. 1	Complete study of cost and market penetration of coal-based fuel technologies	06/01/95	
Subtask 5.2. Selection of Incentives for Commercialization of the Coal Using Technology			
Subtask 5.2, No. 1	Complete selection of incentives for commercialization of the coal-using technology	06/01/95	
Subtask 5.3. Community Sensitivity to Coal Fuel Usage			
Subtask 5.3, No. 1	Complete evaluation of community sensitivity to coal fuel usage	09/27/95	
Subtask 5.4 Regional Economic Impacts of New Coal Utilization Technologies			
Subtask 5.4, No. 1	Complete study of regional economic impacts of new coal utilization technologies	09/27/95	
Subtask 5.5 Economic Analysis of the Defense Department's Fuel Mix			
Subtask 5.5, No. 1	Complete economic analysis of the defense department's fuel mix	09/27/95	

Milestone	Description	Planned Completion Date	Actual Completion Date
Subtask 5.6 Constructing a National Energy Portfolio which Minimizes Energy Price Shock Effects			
Subtask 5.6, No. 1	Complete construction of a national energy portfolio which minimizes energy price shock effects	09/27/95	
Subtask 5.7 Proposed Research on the Coal Markets and their Impact on Coal-Based Fuel Technologies			
Subtask 5.7, No. 1	Complete research on the coal markets and their impact on coal-based fuel technologies	09/27/95	
Subtask 5.8 Integrate the Analysis		09/27/95	
Subtask 5.8, No.1	Complete integration of the analysis	09/27/95	
Task 6. Final Report/Submission of Design Package		09/27/95	

Five coals were examined in the laboratory-scale activities. They are the Taggart, Upper Freeport, Lower Kittanning, Indiana VII, and Pittsburgh coal seams. Table 2-1 summarizes the sampling localities and suppliers for these five coals. In the pilot-scale activities, the Upper Freeport coal was utilized throughout the duration of the MCWM production efforts.

LABORATORY-SCALE ACTIVITIES

The targeted specifications for the coal and MCWM are presented in Table 2-2. The methodology by which the various coals were cleaned was coal specific and therefore will be described when discussing each individual coal. The methodology by which MCWMs are prepared may be generalized despite differences in the coal feedstock (e.g., particle size). A systematic laboratory approach was undertaken to determine how particle size distribution, solids loading, slurry pH, and concentration of chemical additives (e.g., viscosity and pH modifiers, stabilizers) affected the MCWM's apparent viscosity and stability and how they may be manipulated to meet the desired MCWM properties. This approach is often referred to as the MCWM formulation methodology. The status of the coal cleaning and MCWM formulation efforts for the laboratory-scale activities is summarized in Table 3-3. A brief summary of the Upper Freeport formulation efforts and the Lower Kittanning coal cleaning efforts are presented below.

Upper Freeport Coal

The Upper Freeport coal was procured from Rawlee Fuels of Indiana, PA. This coal was transported to a coal cleaning facility located near Osceola Mills, PA which is owned and operated by Power Operating Company, Inc.. The Upper Freeport coal was cleaned using heavy media cyclones operating at a media gravity of 1.30.

The cleaned 1.5" x 0 Upper Freeport coal stockpile was sampled by taking approximately 2 fifty gallon barrels of coal around the perimeter of the coal stockpile from the top, middle, and toe sections. The material was crushed and sample splits taken for chemical analysis. A typical analysis of the cleaned Upper Freeport coal is presented in Table 2-4. An additional split was taken for MCWM formulation efforts. The coal was further reduced in size to a nominal top size of 1/8" to 1/16". Approximately 1 kg. of coal was wet milled at a 68 wt.% solids loading in a 12" diameter by 12" long ball mill to determine how particle size varied with grind time. Milling was performed in a batch mode. Dispersant levels were adjusted to permit the MCWM to discharge from the mill. Solids loadings were determined using a CEM AVC-80 microwave moisture analyzer. Particle size was determined using a Malvern 2600 Droplet and Particle Size Analyzer. Figure 2-1 illustrates how particle size varied with grind time for the Upper Freeport coal when milled at approximately 68 wt.% solids, a 0.6 wt. % dispersant level, and a slurry pH of approximately 9. In an effort to determine if the particle size distribution of the coal was near that

Table 2-1. Sampling Locality

Coal Seam	State	County
Taggart	Virginia	Wise
Upper Freeport	Pennsylvania	Armstrong
Lower Kittanning	Pennsylvania	Jefferson
Indiana VII	Indiana	Sullivan
Pittsburgh	Pennsylvania	Greene

Table 2-2. Targeted Coal and MCWM Specifications.

Parameter	Targeted Specification
Coal Feedstock	
Total Sulfur	< 1.0 wt.% (d.b.)
Ash	< 5.0 wt. % (d.b.)
Volatile Matter	Maximize, > 30 wt.%
Nicronized Coal-Water Mixture	
Coal Particle Size (Top Size)	100 wt.% passing 200 μm (~ 65 mesh)
Coal Particle Size Distribution	Broad, optimize using Farris-Furnace Equation
Apparent Viscosity	< 500 cp. at 100 sec^{-1} at 25° C
CWSF Flow Behavior	Yield psuedoplastic
Solids Loading	Maximize to targeted viscosity, < 50 wt. %)
Stability/ Sedimentation Type	Maximize stability without the use of a stabilizer/ softpack sedimentation)

Table 2-3. Laboratory-Scale Coal Cleaning and MCWM Production Status Summary

Coal Seam	Coal Cleaned	MCWM Formulated	Formulation Data Compiled	Barrel Quantities Prepared
Taggart	Not required	Yes	On-going	Yes
Upper Freeport	Yes	Yes	Yes	Yes
Lower Kittanning	On-going	Yes	On-going	Yes
Indiana VII	Yes	Yes	On-going	No
Pittsburgh	No	No	No	No

Table 2-4. Typical Analysis of the Cleaned Upper Freeport Coal.

Parameter	Wt.% (dry basis)
Particle Size	1.5" x 0
Coal Cleaning Methodology	Heavy Media Cyclone
Proximate Analysis	
Volatile Matter	31.7
Fixed Carbon	61.7
Ash	6.6
Ultimate Analysis	
Carbon	79.5
Hydrogen	5.2
Nitrogen	1.3
Sulfur	0.5
Oxygen	6.9
Higher Heating Value (Btu/lb)	14,062
Hardgrove Grindability Index	58.0
Alkali Extraction	94.3
Free Swelling Index	6.5
Equilibrium Moisture	3.37

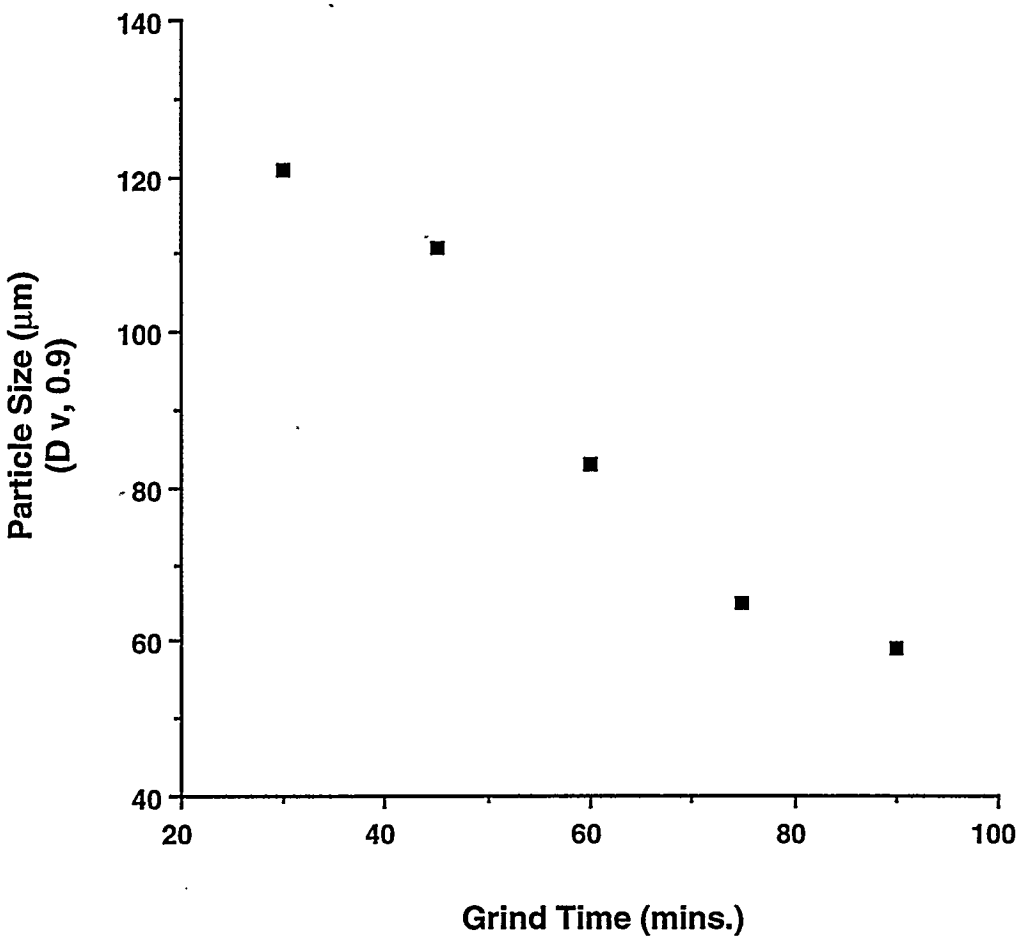

Figure 2-1. GRINDING TIME VS. PARTICLE SIZE FOR THE UPPER FREEPORT COAL

required for optimum packing density, the particle size distributions were plotted against the calculated theoretical particle size distribution[2];[3]) using the following mathematical expression:

$$CPP = (100)\ (D^n - Ds^n)/Dl^n - Ds^n) \qquad (1)$$

where:

CPP = Cumulative weight percent of particles smaller than a given size
D = Particle diameter
Dl = Largest diameter coal particle
Ds = Smallest diameter coal particle
n = Distribution modulus (0.19 to 0.25)

The particle size distribution for the 30, 45, 60, 75, and 90 minute grinds were examined and compared to the calculated theoretical particle size distribution needed to achieve optimum packing density. Figure 2-2 illustrates the "measured" vs. "calculated" particle size distribution for the 75 minute test grind. The 75 minute grind was used throughout the remaining portion of the formulation effort because it produced a top size of less than the 100 % passing 200 μm target specification while most closely approximating the theoretical particle size distribution.

The effect of slurry pH on the apparent viscosity was examined after determining the grind time to document if additional reductions in apparent viscosity could be realized if slurry pH was modified. The slurry pH was varied from approximately 6.5 to 9.0. Slurry pH was measured with an Orion Model 420 pH meter. Apparent viscosity was measured using a Bohlin Visco-88 rotational viscometer. Figure 2-3 illustrates the effect of slurry pH on apparent viscosity. A marked decrease in apparent viscosity occurred as slurry pH increased.

The effect of dispersant level on the MCWM's apparent viscosity was determined by varying dispersant concentration from 0.6 to 1.2 wt.% (wt.% active solids, dry coal basis). Figure 2-4 illustrates the effect of dispersant concentration on apparent viscosity. A dramatic decrease in apparent viscosity can be clearly identified between the 0.6 to 0.7 wt.% dispersant levels. At a dispersant level greater than approximately 0.8 wt.% there was little benefit of adding additional dispersant and would most likely over-disperse the slurry, eventually leading to the deleterious formation of "hardpack".

The effect of solids loading on the MCWM's apparent viscosity was determined by varying solids loading from approximately 59 to 66 wt.%. Dispersant concentration was held constant at 0.7 wt. %. Figure 2-5 illustrates the sudden increase in apparent viscosity when the solids loading exceeds approximately 63 to 64 wt.%.

The effect of stabilizer on the MCWM's apparent viscosity was determined by varying stabilizer concentration from 0 to 1,000 ppm (active solids, dry coal basis). Dispersant

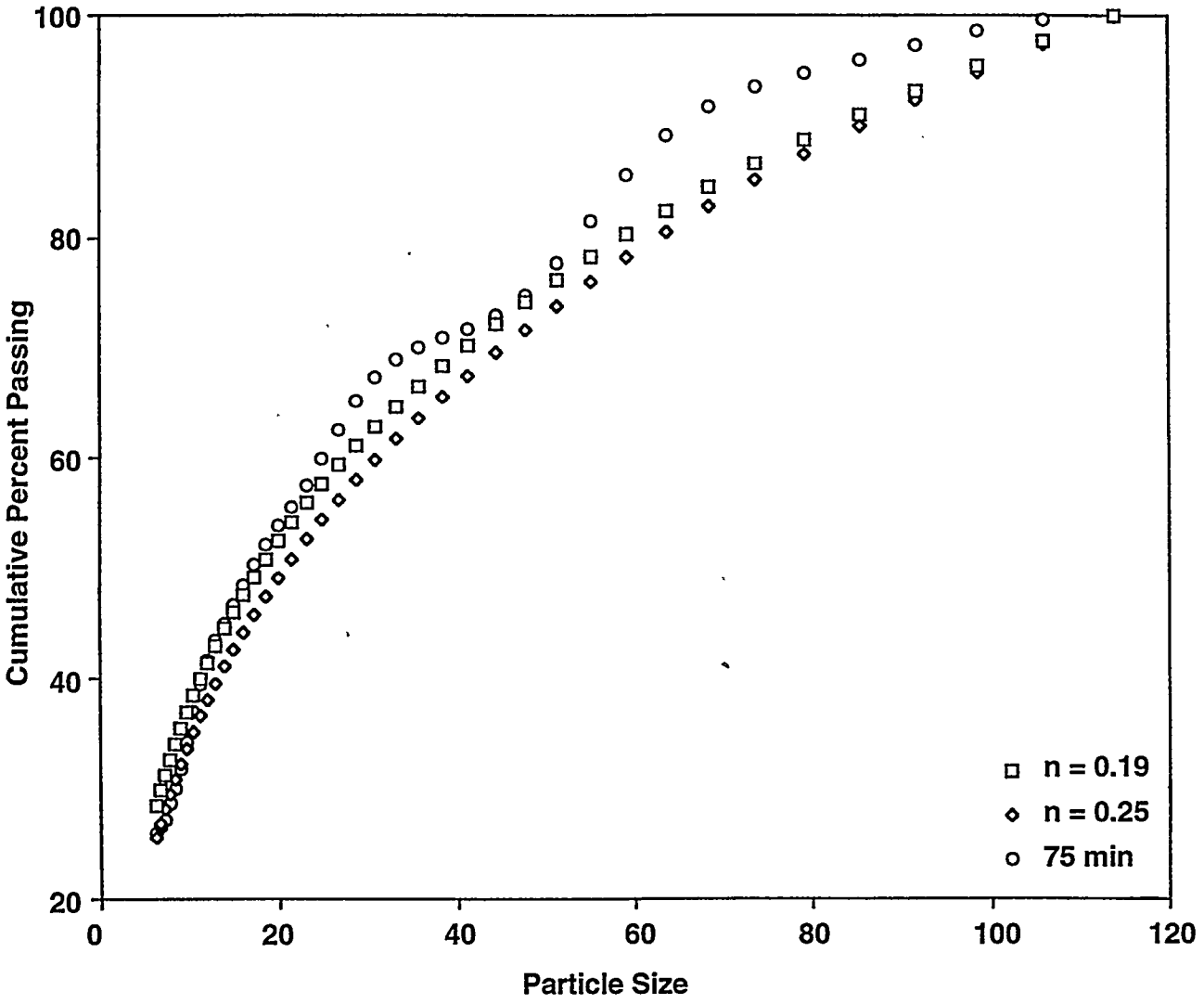

Figure 2-2. FARRIS-FURNAS DISTRIBUTION FOR A 75 M GRIND TIME FOR UPPER FREEPORT MCWM

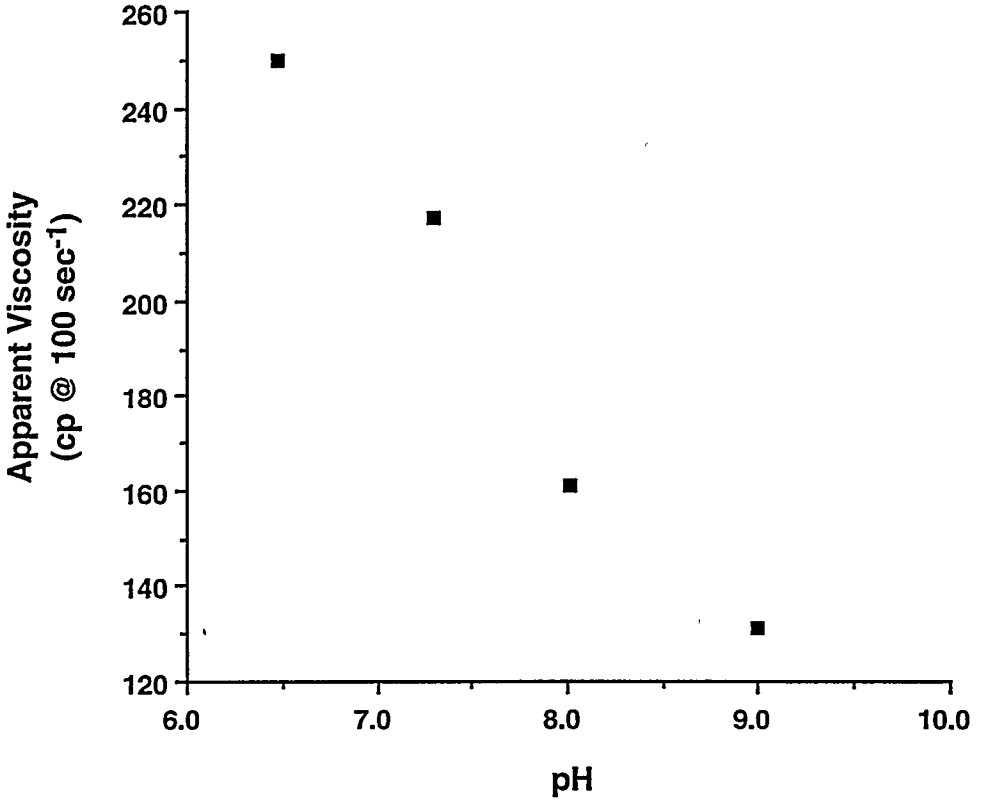

Figure 2-3. EFFECT OF SLURRY pH ON APPARENT VISCOSITY FOR THE UPPER FREEPORT COAL

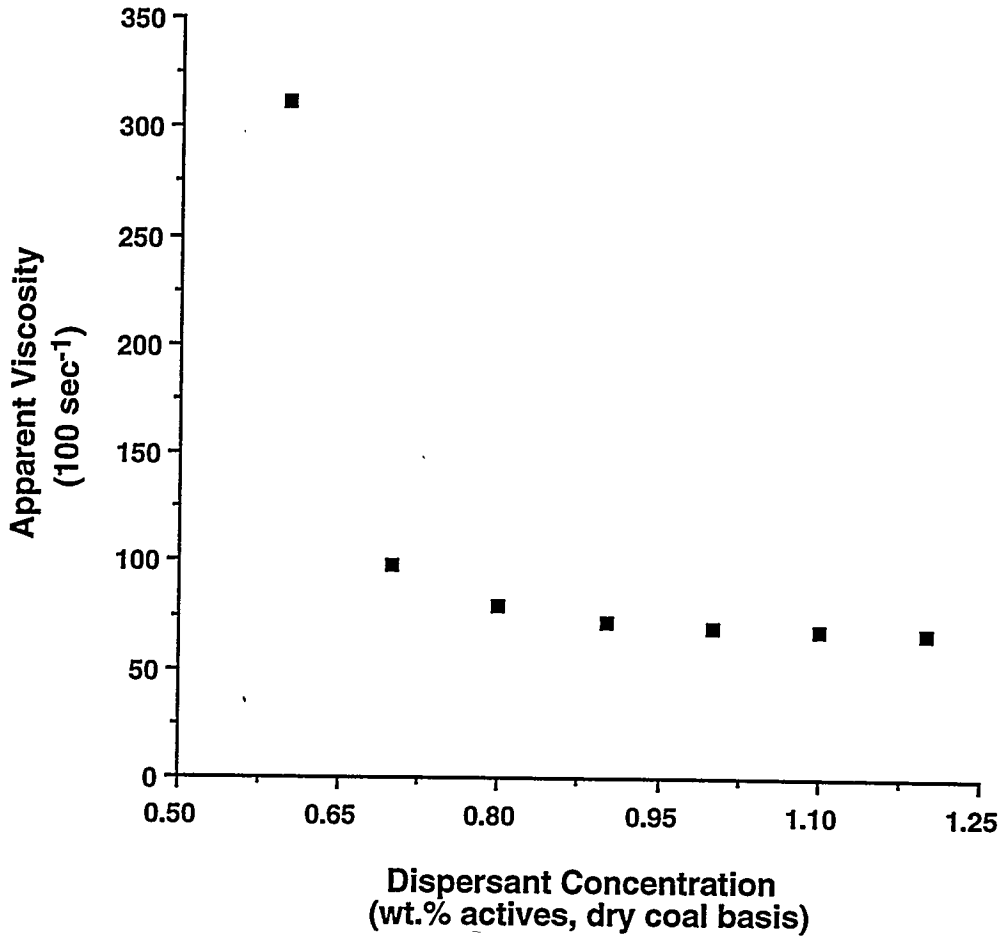

Figure 2-4. EFFECT OF DISPERSANT CONCENTRATION ON APPARENT VISCOSITY FOR THE UPPER FREEPORT COAL.

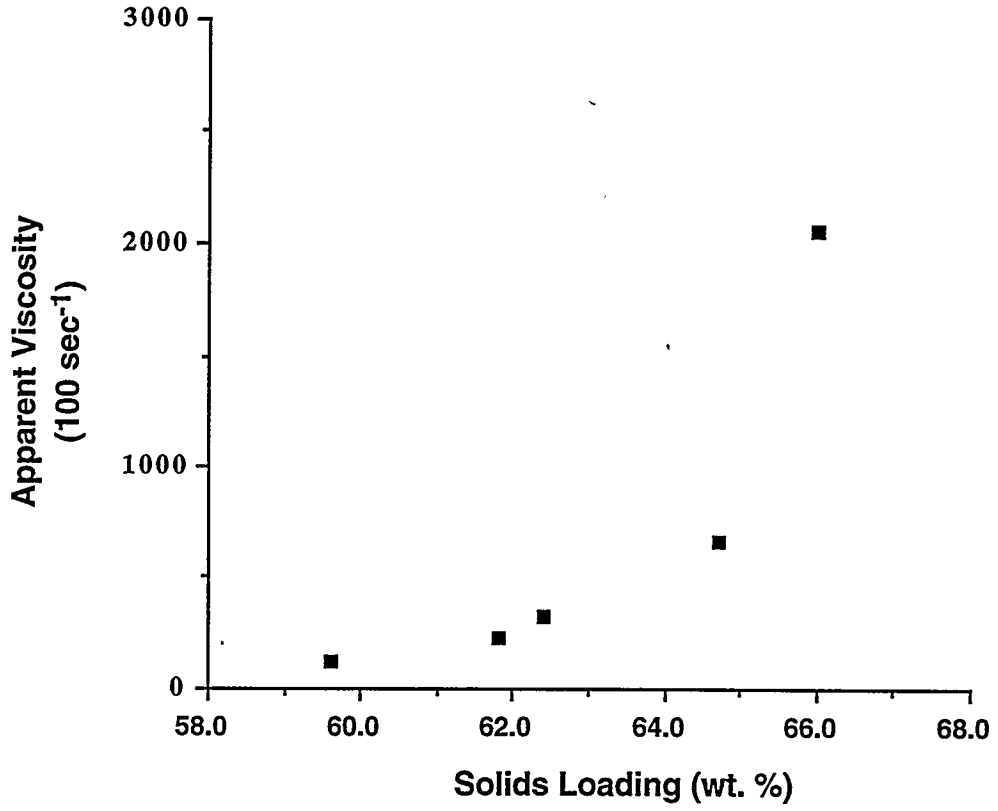

Figure 2-5. EFFECT OF SOLIDS LOADING ON APPARENT VISCOSITY FOR THE UPPER FREEPORT COAL

concentration was held constant at 0.7 wt.% and solids loading constant at approximately 61 wt.%. The effect of stabilizer concentration on apparent viscosity is illustrated in Figure 2-6. Apparent viscosity increased as stabilizer concentration increased.

Based on the laboratory-scale MCWM formulation, the following formulation was targeted in the pilot-scale MCWM production for the Upper Freeport coal:

Solids Loading: 62 wt.%
Slurry pH: 9.0
Dispersant Concentration: 0.7 wt.%
Stabilizer Concentration: 400 ppm

Lower Kittanning Coal

The Lower Kittanning coal was collected from Jefferson County, PA. and cleaned using the continuous two stage froth flotation circuit shown in Figure 2-7. A froth flotation feedstock was produced by crushing and sizing the parent coal into a 28 x 400 mesh size fraction. This size fraction was then slurried to a solids loading to approximately 25 wt. %. The feed slurry was pumped to, and stored in a 500 gallon tank, which served as the main feed tank to the froth flotation circuit.

The Lower Kittanning feed slurry was pumped into a nominal 20 gallon conditioning tank where froth flotation reagents were introduced and slurry solids loading adjusted to approximately 5 wt.%. Methisobutidechloride (MIBC) was introduced to the conditioning tank as the frothing reagent at a dosage of 0.3 kg/ ton of coal. Dodecane was introduced into the conditioning tank as the collector at a dosage of 0.05 kg/ton of coal. The conditioned slurry exited the conditioning tank through an overflow port at a rate of approximately 8 gpm into a single rougher flotation battery consisting of four Wemco flotation cells. The rougher concentrate then, if needed, underwent additional cleaning in a single cleaner flotation battery consisting of two Wemco flotation cells. The froth from both the rougher and cleaner cells averaged approximately 20 wt.% solids. The froth was dewatered using a continuous Denver disk filter consisting of two 24 inch disks. After the initial shakedown and optimization of the froth flotation circuit, the cleaner cells were not operated because the targeted cleaned coal specification of < 1.0 wt.% total sulfur and < 5.0 wt.% ash could be achieved by cleaning the coal in the rougher circuit alone. A typical analysis of the cleaned Lower Kittanning coal filter cake is presented in Table 2-5. Cleaning efforts are on-going to produce barrel quantities of cleaned coal filter cake for MCWM production efforts.

PILOT-SCALE ACTIVITIES

Pilot-scale activities focused on preparing ton quantities of MCWM in a single stage wet grinding circuit. A generalized schematic diagram of this circuit is presented in Figure 2-8. A discussion of the circuit's construction is given in Section 2.6. The Upper Freeport coal was utilized throughout the pilot-scale activities.

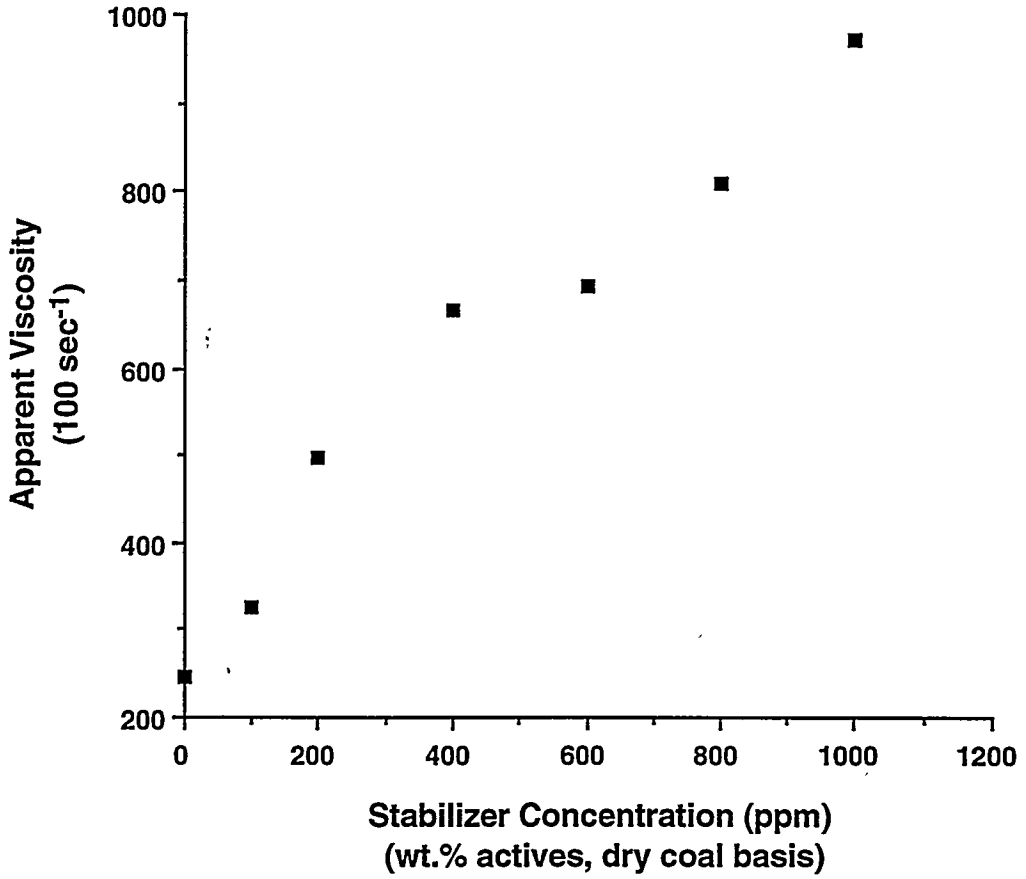

Figure 2-6. EFFECT OF STABILIZER CONCENTRATION ON APPARENT VISCOSITY FOR THE UPPER FREEPORT COAL

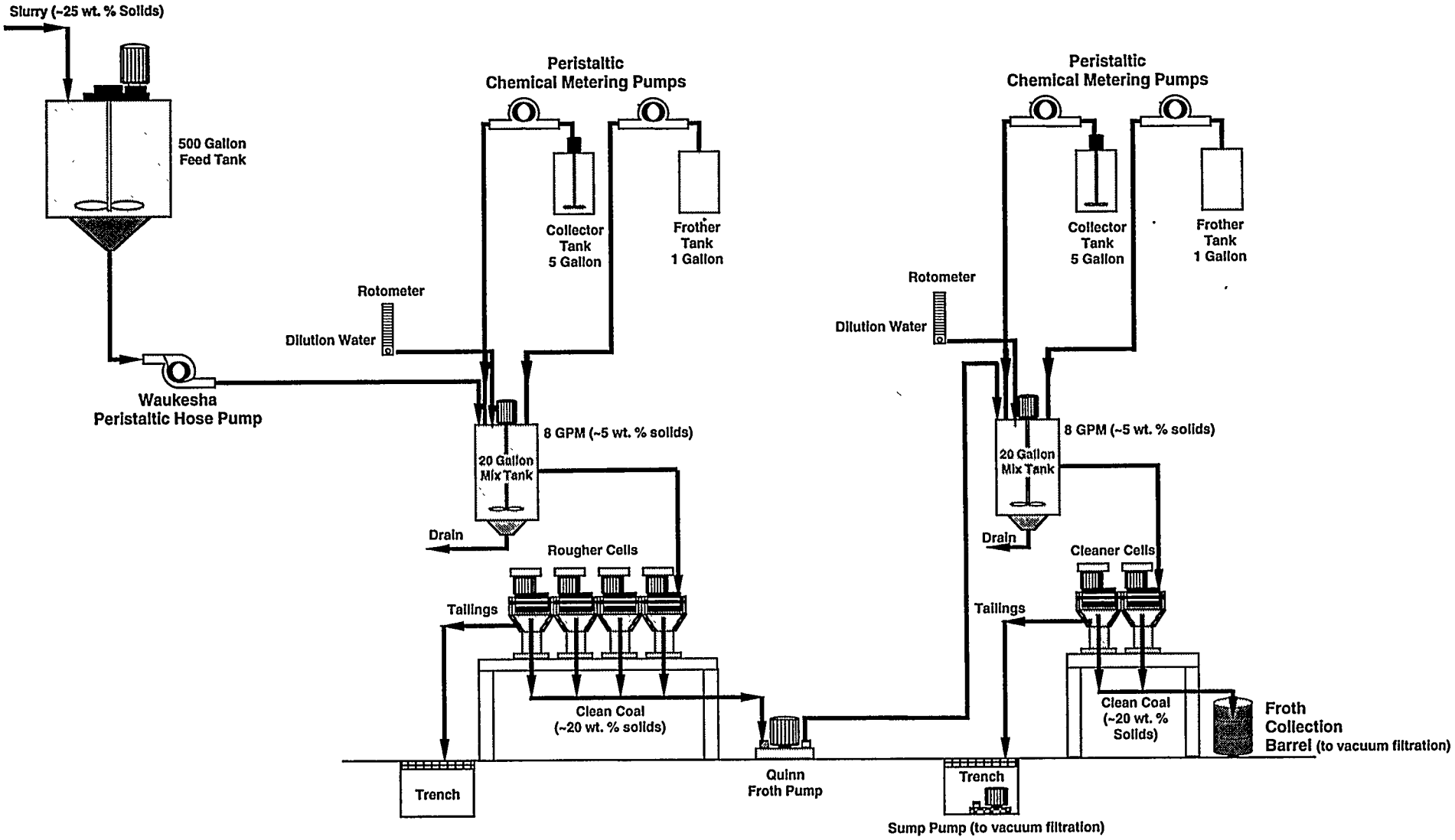

Figure 2-7. SCHEMATIC DIAGRAM OF THE DOUBLE STAGE FROTH FLOTATION CIRCUIT

Table 2-5. Typical Analysis of the Lower Kittanning Coal Utilized in the MCWM Formulation Efforts.

Parameter	Wt.% (dry basis)
Particle Size	28 x 400 mesh
Coal Cleaning Methodology	Conventional Froth Flotation
Proximate Analysis	
Volatile Matter	30.6
Fixed Carbon	65.8
Ash	3.6
Ultimate Analysis	
Carbon	84.5
Hydrogen	5.2
Nitrogen	1.6
Sulfur	0.8
Oxygen	
Higher Heating Value (Btu/lb)	On-going Analyses
Hardgrove Grindability Index	On-going Analyses
Alkali Extraction	On-going Analyses
Free Swelling Index	8.5
Equilibrium Moisture	On-going Analyses

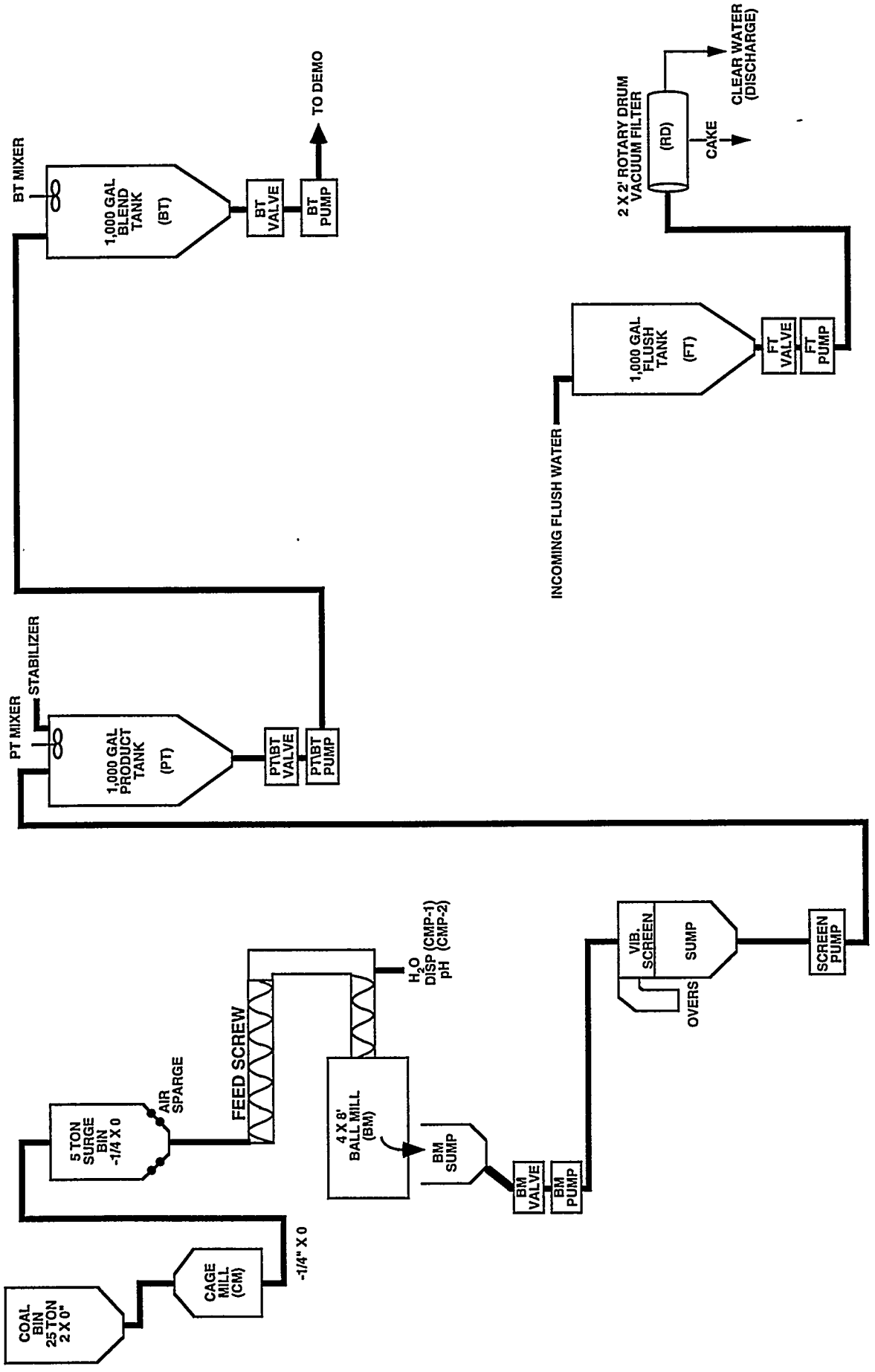

Figure 2-8. SCHEMATIC DIAGRAM OF THE MCWM PREPARATION CIRCUIT

The Upper Freeport coal was transported from Power Operating Company's coal cleaning facility in Osceola Mills, PA to a covered outdoor storage area owned and operated by Bradford Coal Company in Bigler, PA. The coal was then trucked on a as-needed basis to the MCWM preparation facility. Incoming truck loads of coal were dumped into a covered 25 ton hopper. The coal was crushed to minus 1/4" and conveyed to a 5 ton surge bin. The minus 1/4" coal was fed to the ball mill at a rate of approximately 600 to 650 lb/h. Water, dispersant (A-23M), and pH modifier (NH_4OH) were introduced into the ball mill feed screw. The coal was milled at a solids loading of 68 to 72 wt.%, while running the mill at 65% critical speed. The MCWM was produced using a targeted dispersant level of 0.7 wt. % (active solids dry coal basis) and a pH target of 8.5 to 9.5. The MCWM discharged into nominal 175 gallon sump and was diluted to a solids loading of approximately 64 wt.%. The MCWM was agitated in the ball mill sump by an in-situ air sparge system. The MCWM was pumped from the ball mill sump to a Liquidtix vibratory screen to remove oversize particles (plus 30 mesh). From the screen sump, the MCWM was pumped into a baffled 1,000 gallon stainless steel process mixing tank (PT). Stabilizer (Flocon 4800 C) was added to the MCWM in the process tank at a dosage level of 400 ppm (active solid dry coal basis). The MCWM was allowed to mix in the process tank for 4 to 8 h. Mixing was accomplished using a variable speed, center mounted 5 Hp Lightnin mixer (model 15Q5) having a lower 18" 6 bladed R-100 impeller and an upper 30" 3 bladed A-305 impeller. The MCWM was pumped from the process tank (PT) to another baffled 1,000 gallon stainless steel mixing tank (BT). This tank provided intermediate storage between the fuel production facility and the demonstration boiler. The MCWM was mixed in this tank using a fixed speed, center mounted 5 Hp Lightnin mixer (model 15Q5) having dual 30" 3 bladed A-305 impellers.

The MCWM production circuit began operation on January 30, 1995. Production data are currently being compiled.

2.4 Subtask 1.4 Develop a Dry Coal Cleaning Technique

This subtask is complete, and the results are contained in the Phase I Final Report, which is under preparation.

2.5 Subtask 1.5 Produce MCWMs and Micronized Coal from Dry, Clean Coal

This subtask is complete, and the results are contained in the Phase I Final Report, which is under preparation.

2.6 Subtask 1.6 Produce MCWM and Dry, Micronized Coal for the Demonstration Boiler

FUEL PREPARATION FACILITY

Work on this subtask focused on completing the fuel preparation facility (which contains the MCWM and DMC preparation circuits) associated with the demonstration boiler (15,000 lb

steam/h boiler). There are two circuits in the facility, one for producing DMC and one for producing MCWM. The construction of the fuel preparation facility that will contain the MCWM preparation circuit and the DMC circuit was previously completed. During this reporting period, the MCWM preparation circuit was completed.

Dry, Micronized Coal Preparation Circuit

The DMC preparation circuit is complete and was used during this reporting period to complete the DMC demonstration (see Section 2.3 for results). A schematic diagram of the DMC equipment train in the fuel preparation facility is shown in Figure 2-9.

MCWM Preparation Circuit

Construction of the MCWM preparation circuit was completed during this reporting period. Figure 2-8 is a schematic diagram of the MCWM preparation circuit. The installation of the MCWM circuit was conducted in conjunction with another program (Cooperative Agreement No. DE-FC22-89PC88697).

Items that were installed or constructed during this reporting period are listed below:

- Moyno pumps were received and installed;
- Two stainless-steel tanks were received and installed;
- Two mixers for the stainless-steel tanks were received and installed;
- MCWM, water lines, and flush lines within the Fuel Preparation Facility were installed;
- Chemical metering pumps and their associated tubing were installed;
- Piping for compressed air and water lines was installed to each major piece of equipment (pumps, tanks, etc.) ;
- The 4 x 8' Centrix ball mill was refurbished. Allis Mineral Systems of York, Pennsylvania fabricated a new main bearing for the ball mill. A new lubrication system, screw feeder, and a 50 hp motor were procured and installed. Installation of these components and controls for the ball mill was conducted by Beitzel Corporation;
- Pneumatic valves for tanks T1, T2, T3, and T4 were installed;
- The sump for the ball mill was fabricated and installed; and
- The rotary drum vacuum filter for cleaning the purge water was installed.

3.0 PHASE I, TASK 2: COAL COMBUSTION PERFORMANCE

3.1 Subtask 2.1 Boiler Retrofit

In this subtask, an EER low-NO_x burner capable of firing natural gas, DMC, and MCWM was constructed for Penn State's 15,000 lb steam/h demonstration boiler. The burner was installed on the boiler during the previous reporting period.

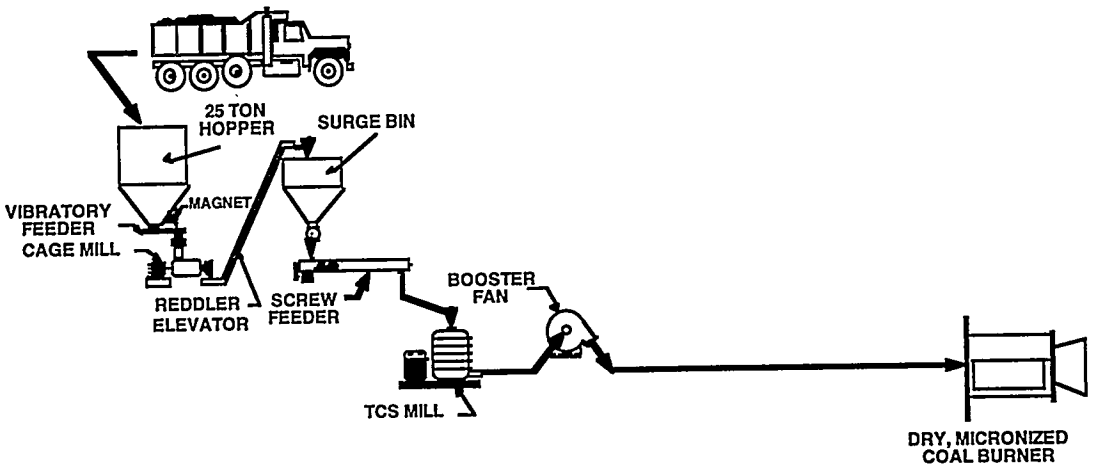

Figure 2-9. SCHEMATIC DIAGRAM OF THE DRY, MICRONIZED COAL EQUIPMENT TRAIN IN THE FUEL PREPARATION FACILITY

3.2 Subtask 2.2 Fuel Evaluation in the Research Boiler

Tests are underway to evaluate and compare the combustion characteristics of the five program coals fired as DMC and MCWM. The evaluation is being conducted in a 1000 lb/h (steam) Research Boiler at Penn State. The following is the test matrix:

Test #1 Upper Freeport seam coal - fired as a DMC
Test #2 Taggart seam coal - fired as a DMC
Test #3 Upper Freeport seam coal - fired as a MCWM
Test #4 Indiana VII seam coal - fired as a MCWM
Test #5 Taggart seam coal - fired as a MCWM
Test #6 Lower Kittaning seam coal - fired as a MCWM
Test #7 Pittsburgh seam coal - fired as a MCWM

The Indiana VII, Lower Kittaning, and Pittsburgh seam coals will not be tested in dry, micronized coal form. They are being cleaned using fine coal, wet cleaning methods are which produce a wet filter cake and, from a practical stand point, they would not be dried and fired as a DMC.

The combustion behavior is being characterized in terms of carbon burnout, temperature profiles resulting from heat release rates, and char/ash morphology. The gas temperature profiles inside the boiler are being measured using a suction pyrometer. The combustion gas profile is being measured with a portable gas analyzer. The total heat flux measurements are made using a total heat flux meter. Radiation heat flux measurements are made using an ellipsoidal radiometer from Land.

DMC tests with the Upper Freeport and Taggart seam coals were performed in December 1994 and in January 1995, respectively. A discussion of the sample preparation and fuel analyses are presented in Section 1.3. The remaining combustion tests will be conducted in February, March, and April 1995.

COMBUSTION TEST PROCEDURE

The coals were fired in the 1,000 lb/h watertube research boiler, described in Appendix A. This ceramic quarl was preheated by a natural gas flame until the surface temperature was approximately 900°F. The coal was then admitted slowly by dilute phase transport (1 lb of air/lb of coal). Slowly, the coal firing rate was increased while simultaneously reducing the natural gas rate until the desired load was obtained on coal. A thermal input of approximately 1.6 million Btu/h (MM Btu/h) was held constant throughout the testing. The boiler was operated on coal for about half an hour before ash samples were collected. A test was continued thereafter for about four to six hours while collecting ash samples from the hoppers and the baghouse every fifteen minutes. Data were collected at 30 seconds intervals on pressures, temperatures, emissions, and air flow rates. The data during steady-state operation were then averaged. The ash samples were analyzed for moisture and unburned carbon to calculate the carbon burnout using the ash tracer technique:

$$\text{Combustion Efficiency (\%)} = \left[1 - \frac{A_c(100 - A_r)}{A_r(100 - A_c)}\right] \times 100 \qquad (3\text{-}1)$$

where, A_c = wt percent ash in the coal
and A_r = wt percent ash in the residue

The flue gas analysis was obtained by a continuous emissions monitoring system interfaced with a data acquisition system. The flue gas analyzers and the data acquisition system used are listed below. The analyzers included: Beckman Oxygen Analyzer, model 755; Beckman Carbon Dioxide Analyzer, model 864 infrared; Thermo Electron Pulsed Fluorescent SO_2 Analyzer, series 40; Thermo Electron Chemiluminescent NO-NO_2-NO_X Analyzer. A computer was used to collect the temperatures, flow rates, and the flue gas concentration at the economizer outlet. All the signals were relayed to a Texas Microsystems industrial grade computer and processed through a Viewdac software package. The Viewdac display was updated every second and data were recorded from each signal every 30 seconds.

TEST RESULTS

Data reduction and alanysis are currently being carried out. Table 3-1 gives a summary of the test conditions.

3.3 Subtask 2.3 Performance Evaluation of MCWM and DMC in the Demonstration Boiler

Activities in Subtask 2.3 included conducting DMC and MCWM testing, addressing deposition in the furnace and convective pass during coal firing, redesigning the coal storage and handling capabilities in the coal milling area, evaluating erosion-corrosion and deposition characteristics when firing coal in an oil-designed boiler, determining the erosion characteristics of materials subjected to atomized MCWM, and conducting theoretical and experimental studies of particle behavior in the demonstration boiler. These activities are discussed in the following subsections.

SUMMARY OF ACTIVITIES

During this reporting period, the DMC demonstration was completed on December 31, 1994, construction and shakedown of the MCWM preparation circuit was completed on January 27, 1995, after which time the MCWM demonstration was started. A summary of activities from October 1994 through February 1995 is presented.

October Activities

The boiler was shutdown most of this month for repair and maintenance of equipment and buildings. EER personnel were on site to improve burner performance. Also, the Beitzel

Table 3-1. Summary of Test Conditions When Firing the Upper Freeport and Taggart Coals as DMC in the Research Boiler

Fuel	Upper Freeport Micronized Coal	Upper Freeport Micronized Coal	Upper Freeport Micronized Coal	Upper Freeport Micronized Coal	Taggart Micronized Coal	Taggart Micronized Coal
Date	12/6/94	12/8/94	12/19/94	12/21/94	1/12/95	1/16/95
Duration on coal (hrs)	2.25	6	6	5.25	4	4.5
Firing Rate (MMBtu/h)	1.56	1.58	1.78	1.48	1.69	1.52
Combustion Air (lb/h)	900	863	997	807	919	855
Transport Air (lb/h)	107	114	118	112	112	112
Tertiary air (lb/h)	324	316	316	324	316	316
Cooling Air (lb/h)	31	31	31	31	31	31
Average Quarl Temp (°F)	1,266	1,349	1,425	1,280	1,330	1,318
Average Combustion Air Temperature (°F)	183	259	217	237	161	202
Average Oxygen Concentration[a]	7.49	6.84	5.84	6.94	5.94	6.97
Average Baghouse Carbon Burnout (%)	97.4	97.9	97.6	97.6	98.4	98.6
Average Baghouse Carbon Burnout (%)	96.5	96.3	96.4	96.6	97.8	98.1

[a]Concentration at the economizer inlet.

Corporation (a construction firm) finished preliminary reworking of the large ball mill. A day-by-day synopsis of the activities associated with the boiler is presented:

- October 3 -- No testing was conducted. Personnel attempted to fit a model of the coal weigh-belt feeder into the coal milling area. This was part of a coal storage and handling redesign effort that was performed and is reported below.
- October 4 -- No testing was conducted.
- October 5 -- No testing was conducted. Personnel started mounting the shafts and impellers on the MCWM tanks.
- October 6 -- No testing was conducted. Personnel finished mounting the shafts and impellers in the MCWM tanks. Personnel hydro-tested the boiler to check for leaks.
- October 7 -- No testing was conducted.
- October 10 -- Personnel fired the boiler on natural gas. The boiler was not operated for most of September because of steam line work conducted by the University. Difficulties were experienced in lighting the boiler due to the extended shutdown. Personnel from EER were on-site this week (10/10/94 to 10/14/94) to modify the burner in order to improve burner performance.
- October 11 -- Coal testing was conducted.
- October 12 -- No boiler testing was conducted. Ports were installed on the coal feed line in order to perform pitot tube measurements. The objective was to measure pressure differential with time to determine if there was coal feed slugging. Three 1-1/2" diameter ports with valves were installed on the coal feed line; one on the TCS mill outlet, one on the booster fan outlet, and one near the entrance of the burner.
- October 13 -- A delivery of coal was received from Bradford Coal Company. This was the first shipment of Upper Freeport seam coal. All testing to date with the EER burner (May 1994 to October 12, 1994) was done using Brookville seam coal. A heater in the TCS mill control panel needed replacement prior to operation. The boiler was fired for 2 hours on 100% coal. Later, the boiler was shut down and the burner was removed from the boiler. A cone was installed on the secondary zone of the burner. The cone was designed to increase flame stability in the secondary zone.
- October 14 -- The boiler was fired for 3 hours on 100% coal. Highly erratic CO readings were observed with values ranging from 1,500 ppm to about 5,000 ppm.
- October 17 -- A new coal curve was generated for the coal screw feeder. The boiler was operated and poor flame stability was observed. EER personnel were on-site this week (10/17/94 to 1//21/94) to evaluate burner performance.
- October 18 -- Testing was conducted but the boiler was shut down due to erratic CO readings and poor flame stability. The cone was removed from the burner.

- October 19 -- Testing was conducted but the boiler was shut down due to low UV signal readings and a detached flame. Coal piping at the burner interface was modified by replacing a portion of hard pipe with flexible hose to allow for burner repositioning. The modification allowed the burner to be moved backward and forward a few inches. After this modification the boiler was fired successfully for 3 hours on 100% coal.
- October 20 -- The boiler was fired for 3 hours on 100% coal. MCWM preparation circuit construction was also conducted.
- October 21 -- Testing was conducted and poor flame stability and erratic CO readings were observed.
- October 24 - 31 -- No testing was conducted. Repair and maintenance of equipment and buildings were conducted.

November Activities

During the first part of the month, the primary focus was repair and maintenance of equipment and buildings. Personnel fabricated and repaired equipment in the coal preparation facility to reduce fugitive dust. After reducing fugitive dust, the boiler was brought on line for testing. During the three day period prior to Thanksgiving, the boiler was operated continuously for 72 hours. A day-by-day synopsis of the activities associated primarily with the boiler is:

- November 1 -- No boiler testing was conducted. Work began on repairing the dust collection system in the coal milling area. Maintenance of the dust collector was performed and its rotary valve was repaired. Preliminary plans for installing a filtering system on the top of the surge bin were prepared. The filtering system is a series of baghouse filters and cages installed on top of the surge bin to allow air from the sparge system to escape without fugitive dust emissions. The reason for these repairs was an attempt to decrease the amount of fugitive dust in the coal preparation facility.
- November 2 -- No boiler testing was conducted. Work continued on the dust collection system and surge bin. Work also began on installing a dust cover around the seals of the Redler Conveyor. General site maintenance and repair was also conducted.
- November 3 -- No boiler testing was conducted. Work continued on the dust collection system, surge bin filtering system, and Redler Conveyor. General site maintenance and repair was also conducted.
- November 4 -- No boiler testing was conducted. Work on the dust collection system, surge bin filtering system, and Redler Conveyor were completed. General site maintenance and repair was also conducted.
- November 7 -- The boiler was fired for 2 hours on 100% coal. Data and samples were collected. Coal combustion efficiency averaged 89.7%. Due to excessive coal dust from the cage mill, the boiler was shut down and the cage mill was repaired. A new coal curve

was generated for the coal screw feeder and general site maintenance and repair were conducted.

- November 8 -- No boiler testing was conducted. Repairs to the cage mill continued. Related repair work was started on the dust collection system. General site maintenance and repair were also conducted.
- November 9 -- No boiler testing was conducted. Repairs of the dust collection system and cage mill continued. General site maintenance and repair were also conducted.
- November 10 -- No boiler testing was conducted. Repairs of the dust collection system and cage mill continued. General site maintenance and repair were also conducted.
- November 11 -- No boiler testing was conducted. Repairs of the dust collection system and cage mill continued and general site maintenance and repair were conducted. Construction of the MCWM preparation circuit was performed.
- November 14 -- No boiler testing was conducted. Boiler operational problems were encountered with the emissions monitoring system and the feedwater pump. Also, the cage mill required additional repairs. The boiler was eventually fired on natural gas. Working continued on the MCWM preparation circuit. General site maintenance and repair were also conducted.
- November 15 -- No boiler testing was conducted. Repairs of the emissions monitoring system and the feedwater pump continued. Work continued on the MCWM preparation circuit. General site maintenance and repair were also conducted.
- November 16 -- The boiler was fired for 2 hours on 100% coal. Data and samples were collected. Coal combustion efficiency averaged 86.3%. Highly erratic CO analyzer readings were observed. In particular, the CO readings showed dramatic upward spikes that were often off-scale.
- November 17 -- The boiler was difficult to light. The ignitor burner was removed and repaired. Additional problems were encountered with the continuous emissions system. A portable analyzer (Land Analyzer) was connected while the continuous emissions system was repaired. The boiler was fired for 4 hours on 100% coal. Data and samples were collected. Coal combustion efficiency ranged from 89.5-91.3% with an average of 90.4%.
- November 18 -- A delivery of Upper Freeport seam coal was received. The boiler was fired for 7 hours on 100% coal. Data and samples were collected. Coal combustion efficiency ranged from 91.6-95.2% with an average of 93.9%.
- November 21 -- The first shift began at 0000 h (military time) in an attempt to continuously operate the boiler over a 24 hour period. The boiler was brought on full rate by 0200 h. The boiler was fired for a total of 22 hours on 100% coal. Data and

samples were collected. Coal combustion efficiency ranged from 93.8-96.0% with an average of 94.7%. Personnel observed heavy ash build-up on the boiler walls.

- November 22 -- Personnel continued 24-hour operation. The boiler was fired for an additional 10 hours on 100% coal. Data and samples were collected. Coal combustion efficiency ranged from 93.5-93.8% with an average of 93.7%. The test was terminated because the convective pass was observed to be heavily packed with ash. The continuous test lasted for a total of 32 hours. A delivery of Upper Freeport seam coal was received. Maintenance and repair activities were performed and construction of the MCWM preparation circuit was conducted.
- November 23 -- Ash was removed from the furnace floor and walls. A total of 855 pounds of ash was removed from the furnace. Maintenance and repair activities were performed.
- November 24 -- University Holiday; Thanksgiving Day
- November 25 -- Operational personnel were on vacation.
- November 28 -- The boiler was fired for 3 hours on 100% coal. Data and samples were collected. Coal combustion averaged 89.0%. The cage mill and rotary valve plugged with coal. Personnel dismantled the equipment and repaired the problem. The vibrating switch on the cage mill required replacement.
- November 29 -- No boiler testing was conducted. Replacement of the vibrating switch on the cage mill was completed. The boiler was operated on natural gas. Additional problems were encountered with the SO_2 analyzer. The instrumentation and controls group was on site to repair the analyzer. Maintenance and repair activities were performed and construction of the MCWM preparation circuit was conducted.
- November 30 -- Personnel unplugged coal from the cage mill. The boiler was fired for 4 hours on 100% coal. Data and samples were collected. Coal combustion efficiency ranged from 87.1-90.8% with an average of 89.5%.

December Activities

At the beginning of December, the boiler was operated on 100% micronized coal to complete the DMC demonstration. Continuous 24-hour operation of the boiler was conducted from December 5 to 7, 1994. The middle of December was dedicated to construction of the MCWM preparation circuit. A day-by-day synopsis of the activities associated with the boiler is:

- December 1 -- Personnel encountered problems with the continuous emissions monitoring system. A portable analyzer (Land Analyzer) was connected while the continuous emissions analyzers were repaired. The boiler was fired for 7 hours on 100% coal. Data and samples were collected. Coal combustion efficiency ranged from 89.7-92.6% with an average of 90.9%.

- December 2 -- The continuous emissions monitoring system was repaired. The boiler was fired for 2 hours on 100% coal. Data and samples were collected. Coal combustion efficiency averaged 94.1%.
- December 5 -- The first shift began at 0000 h (military time) to operate the boiler continuously over a 24-hour period. Personnel experienced low feedwater temperature in the morning. Upon notification, the power plant corrected the feedwater problem. The boiler was on full rate by 0600 h. The boiler was fired for 12 hours on 100% coal. Boiler operation was interrupted at 1800 h because the forced draft fan belt broke. During the period of 100% coal operation, personnel collected data and samples. Coal combustion efficiency ranged from 93.2-94.9% with an average of 93.2%. The boiler was on coal only again at 2330 h for continuous operation into December 6. During the day, a delivery of coal was received.
- December 6 -- 24-hour operation continued. The boiler was fired for 24 hours on 100% coal. Data and samples were collected. Coal combustion efficiency ranged from 92.5-95.2% with an average of 94.2%.
- December 7 -- 24-hour operation continued. The boiler was fired for an additional 21 hours on 100% coal. Data and samples were collected. Coal combustion efficiency ranged from 91.5-95.2% with an average of 93.6%. The test was terminated because the boiler's outer steel skin began warping. The convective pass was observed to be heavily packed with ash. The continuous test lasted for 45 hours. During the day, a delivery of coal was received.
- December 8 -- Personnel entered the boiler and removed ash from the furnace floor and walls. A total of 740 pounds of ash were removed from the furnace. In addition, personnel replaced the bearing on the ash screw. They also conducted general site maintenance and repair.
- December 9 -- The outside skin of the boiler was removed to check for damage caused on December 7. A representative from Kibbe Boiler Works arrived on site to inspect the boiler. He entered the furnace to inspect the tubes and saw no sign of tube problems. Site maintenance and repair were conducted.
- December 12 -- No boiler testing was conducted. Efforts were focused on constructing the MCWM preparation circuit.
- December 13 -- Construction of the MCWM circuit continued.
- December 14 -- Construction of the MCWM circuit continued.
- December 15 -- Construction of the MCWM circuit continued.

- December 16 -- Construction of the MCWM circuit continued. Modifications to the boiler were started. In particular, the manhole into the boiler's furnace was being enlarged.
- December 19 -- Construction of the MCWM circuit and modifications to the boiler continued.
- December 20 -- Construction of the MCWM circuit and modifications to the boiler continued.
- December 21 -- Construction of the MCWM circuit and modifications to the boiler continued.
- December 22 -- Construction of the MCWM circuit and modifications to the boiler continued.
- December 23 -- University Holiday
- December 26 -- University Holiday
- December 27 -- University Holiday
- December 28 -- University Holiday
- December 29 -- University Holiday
- December 30 -- University Holiday

January Activities

During the month of January, personnel worked two shifts a day while constructing the MCWM circuit. The circuit was completed and initial slurry-firing commenced by the end of the month. The following reports highlights of the daily activities at the demonstration boiler site. In addition to the highlighted activities, other routine duties were performed to accomplish the program goals. To complete the MCWM circuit, frames, control panels, mezzanines, ladders, etc. were constructed. Systems were fabricated using steel framing, steel piping, copper tubing, electrical conduit, electrical wiring, etc.. Personnel installed equipment (pumps, feeders, valves, sumps, etc.), wired control boxes, tested equipment, installed heat trace and insulation on piping, etc. The weight and size distribution of steel balls in both the 2'x4' and 4'x8' ball mills were adjusted until the proper ratios were obtained. In addition to physical construction, equipment and materials were ordered and picked-up. Changes were also made on the boiler during the month. The door to the fire box was enlarged to 18" x 12 1/2"; two side panels of the boiler were replaced, and larger site ports were installed. A day-by-day synopsis of the activities associated with the boiler is:

- January 2 -- University Holiday
- January 3 -- Construction of the mezzanine around the ball mill began. To accommodate future construction, the mezzanine was designed as a temporary structure. Construction of the MCWM preparation circuit continued.

- January 4 -- Construction of the mezzanine around the ball mill continued. Construction of the MCWM preparation circuit continued.
- January 5 -- Construction of the mezzanine around the ball mill continued. Construction of the MCWM preparation circuit continued.
- January 6 -- Construction of the mezzanine around the ball mill was completed. The Acrison feeder was placed on the mezzanine and positioned in front of the ball mill inlet. Construction of the MCWM preparation circuit continued.
- January 9 -- Construction of the MCWM preparation circuit continued.
- January 10 -- Construction of the MCWM preparation circuit continued.
- January 11 -- Construction of the MCWM preparation circuit continued.
- January 12 -- Construction of the MCWM preparation circuit continued.
- January 13 -- Construction of the MCWM preparation circuit continued.
- January 16 -- Construction of the MCWM preparation circuit continued. Specifically, fabrication of a large flange for the main ball mill entrance was started.
- January 17 -- Construction of the MCWM preparation circuit continued.
- January 18 -- Construction of the MCWM preparation circuit continued.
- January 19 --Construction of the MCWM preparation circuit continued.
- January 20 -- Construction of the MCWM preparation circuit continued. In particular, a purge system for the circuit was constructed and installed. General site maintenance and repair were also conducted.
- January 23 -- Construction of the MCWM preparation circuit continued.
- January 24 -- Construction of the MCWM preparation circuit continued.
- January 25 -- Construction of the MCWM preparation circuit continued.
- January 26 -- Construction of the MCWM preparation circuit continued. The boiler was prepared for MCWM operation. Coal curves were generated for the feeders. General site maintenance and repair were also conducted.
- January 27 -- Construction of the MCWM preparation circuit continued. The boiler was prepared for MCWM operation. Heat tape and insulation were installed on trench piping. An initial test of the slurry circuit was conducted using water. Except for a couple of Moyno pumps wired in reverse, the system was operational.
- January 30 -- An initial shakedown of the MCWM circuit was completed using MCWM. General site maintenance and repair were also conducted.
- January 31 -- An initial shakedown of the rotary-drum vacuum filter was completed. General site maintenance and repair were also conducted. The boiler was fired for 4 hours on coal-slurry with gas support. Data and samples were collected.

February Activities

During the month of February, the boiler was cofired with MCWM and natural gas. A day-by-day synopsis of the activities associated with the boiler is presented:

- February 1 -- The boiler was cofired with MCWM and natural gas. The objective was to purge and clean the day tank. The secondary swirler was repaired because the swirler was not setting properly. Also, general maintenance and repair were performed.

- February 2 -- The boiler was cofired with MCWM and natural gas. The operation was not stable and data and samples were not collected.
- February 3 -- The boiler was cofired with MCWM and natural gas. The operation was not stable and data and samples were not collected.
- February 6 -- The burner/atomizer was modified by replacing the EER atomizer with a fuel oil (Faber) atomizer. General maintenance and repair were performed and damaged site ports on the boiler were repaired.
- February 7 -- A leak on the Faber atomizer was found. The boiler was cofired for 4 hours on MCWM and natural gas. Data and samples were collected.
- February 8 -- The boiler was cofired for 7 hours on MCWM and natural gas. Data and samples were collected.
- February 9 -- No testing was conducted. The cold weather caused many equipment malfunctions. In particular, sample lines for the continuous emissions monitoring system were frozen. While the lines were being unthawed and repaired, general maintenance and repair were performed.
- February 10 -- No testing was conducted. General maintenance and repair were performed.
- February 13 -- The boiler was operated on gas to heat the system and to troubleshoot any particular problems. General maintenance and repair were performed.
- February 14 -- The boiler was cofired for 7 hours on MCWM and natural gas. Data and samples were collected.
- February 15 -- The boiler was cofired for 9 hours on MCWM and natural gas. Data and samples were collected. Several visitors observed the operation. Representatives from DOE, ABB Combustion Engineering, Inc., The World Trade Center, and a polish delegation were on site.
- February 16 -- The boiler was cofired for 7 hours on MCWM and datural gas. Data and samples were collected.
- February 17 -- The boiler was fired for 9 hours on MCWM and natural gas. Data and samples were collected.

- February 20 -- A delivery of coal was received from Bradford. General maintenance and repair were performed. The boiler was entered to get dimensions of the burner and observe and clean out any ash that may have accumulated. The boiler was fired for 2 hours on natural gas and data were collected.
- February 21 -- The boiler was cofired for 2 hours on MCWM and natural gas. Data and samples were collected.
- February 22 -- No testing was conducted. General maintenance and repair were performed. In particular, repairs were made to the MCWM preparation circuit.
- February 23 -- The boiler was cofired for 3 hours on MCWM and natural gas. Data and samples were collected.
- February 24 -- The boiler was cofired for 7 hours on MCWM and natural gas. Data and samples were collected.
- February 27 -- The Faber atomizer was modified by shortening it. The boiler was cofired for 2 hours on MCWM and natural gas. Data and samples were collected. The atomizer tip plugged during operation.
- February 28 -- The boiler was cofired for 4 hours on MCWM and natural gas. Data and samples were collected. During operation the boiler shut down due to a low ultra-violet (U.V.) signal. It was suspected that preheating the MCWM may be causing plugging in a strainer prior to the atomizer. A test was conducted to determine the effect of MCWM temperature on system operation. Initially, the boiler was operated without the MCWM preheat. The MCWM temperature was then incrementally increased and MCWM samples were collected from the burner pump and strainer. The samples were analyzed for particle size, pH, and solids content.

Redesign of Coal Storage and Handling Facilities

One objective of DMC testing is to determine the operating characteristics of a complete, integrated firing system. Although all of the system components (e.g., coal hoppers, crushers, conveyors, and mill) have been used commercially, an integrated system from coal preparation to steam production has not been proved at this scale.

Severe coal handling problems were encountered during DMC testing (DOE program DE-AD22-91PC91160) that was conducted during the previous winter (December 1993 to March 1994). Because of the relatively small quantities of low ash coal required for the testing, the coals were cleaned in a batch mode by heavy media cyclones and stored in a local coal yard. During testing in the winter, snow and ice were included in the shipments. The wet coal (often with moisture content in excess of 12%) tended to bridge and rathole in the hoppers, especially the surge bin. This required constant operator attention and corrective action and resulted in erratic coal feed. This inconsistent coal feed, coupled with the variability introduced by varying coal size

and moisture content, made it difficult to maintain a constant feed to the burner. The moisture content was inconsistent because of drying in the heated building and by the air sparge system in the surge bin.

The operating problems encountered due to high moisture content of the fine coal and fuel transport oscillations led to a reevaluation of the system design and coal storage logistics. For winter testing conducted during this reporting period (December 1994 to March 1995), the moisture content of the coal was limited by storing it in a protected environment after cleaning. Fewer coal handling problems were encountered this winter; however, snowfall was significantly less than that during the previous winter (few inches compared to several feet).

Since most of the coal feed problems occurred in the surge bin, Penn State's Mineral Processing Section evaluated its design and found that the bin outlet dimensions and hopper sidewall angle should be modified to improve coal handling. The current surge bin has a circular opening with a bin angle of 60°. It was recommended that the bin outlet should be pyramidal with a length to width ratio of 3:1 and the sidewall angle should be 70°.

A test hopper was fabricated based on the recommended design criteria and tested with the as-received coal at various moisture levels. This was done to test the flowability of the coal in a new hopper before reengineering the coal handling and feeding system. The pyramidal test hopper was constructed from carbon steel, had a discharge opening of 16 by 48" (3:1 ratio), had sidewall angles of 70°, and was a full-scale model of the bottom portion of a new surge bin. The discharge width (16") was maximized based on the width of candidate weigh-belt feeder belt sizes.

Flowability tests were conducted by first adding water to the coal (- 1/4") at various moisture levels in a barrel. A barrel roller was then used to achieve homogeneous moisture levels. The coal was then transferred into the test hopper and left to settle prior to the flow test. Moisture levels of approximately 8.0, 12.0, 14.1, and 17.8% were tested. The moisture content would vary by 2-4% from the top to the bottom of the hopper. The highest percentage of moisture noted at the bottom of the hopper was approximately 21%. The flow test was conducted by lifting the hopper with a forktruck and allowing the coal to flow from the hopper onto the ground. The test hopper was lifted at a rate of one inch per minute which translates into a coal flow rate of 18.5 lb/min. At each of the conditions tested, there was little or no coal left in the hopper at the end of each test.

As a result of the system design reevaluation and study, a new coal storage and handling system has been engineered. A pyramidal bin with a length to width discharge outlet of 3:1 and a steeper angle (70 vs 60°) was designed and will be installed in April/May, 1995. In addition, the screw feeder will be replaced with a weigh-belt feeder to eliminate fuel feed oscillations. The new surge bin will be constructed out of stainless-steel to eliminate scaling.

DMC Demonstration

During this reporting period, the DMC demonstration was completed. A total of 773.0 hours of operation were accumulated from October through December 1994, of which 189.2 hours were with coal firing (4.2 hours of operation per 1.0 hour of coal firing). For the DMC demonstration, a total of 2,028.5 hours of operation, which is in excess of the proposed 1,000-hour demonstration, were accumulated from May 1994 through December 1994, of which 396.1 hours were with coal firing (5.1 hours of operation per 1.0 hour of coal firing). The DMC demonstration not only included coal firing, but also included baseline testing (natural gas), burner optimization (natural gas and DMC), system modifications, and component repair.

Table 3-2 contains a boiler performance and emissions summary (half hour averages) of the tests performed from October through December 1994. The results from testing conducted from October to December 1994 will be presented in this section. A summary of the entire DMC demonstration will be presented in the Phase I final report which is in preparation. The primary objectives of the testing during the last three months were to continue to improve coal combustion efficiency, examine furnace and convective pass deposition, and establish the extent of deposition during continuous operation.

Combustion and Boiler Performance

The combustion and boiler efficiencies, when firing DMC, ranged from 86 to 95% and from 76 to 83%, respectively (see Table 3-2). Most of the testing was conducted with two shifts/day except for the testing from November 21 to 22, 1994 and from December 5 to 7, 1994. These tests were continuous (24 h/day) but the results have been reported for either 12 or 8 hour periods for the November and December testing, respectively. The combustion and boiler efficiencies ranged from 86 to 94% and from 76 to 83%, respectively for tests conducted with two shifts/day. During continuous testing, the combustion and boiler efficiencies ranged from 92 to 94% and from 80 to 82%, respectively, for the November tests (~16 million Btu/h firing rate) and from 92 to 95% and from 81 to 83%, respectively, for the December tests (~13 million Btu/h firing rate). Most of the DMC operation resulted in combustion efficiencies ranging from 92 to 94% which was below the targeted value of 98%.

Boiler Derating

The rated capacity of a DS-15 package boiler is 15,000 lb saturated steam/h at 300 psig; however, the design capacity was decreased to 14,900 lb steam/h (at a natural gas firing rate of ~19.8 MM Btu/h) when two rows of tubes were removed from the convective pass to accommodate test probes. Natural gas testing that was conducted for the boiler performance guarantees in January 1992 resulted in 14,700 lb steam/h produced when firing at 18.5 MM Btu/h.

Steam production during this reporting period ranged from 9,300 to 15,500 lb/h at firing rates from 12.5 to 16.4 MM Btu/h. Testing was conducted primarily over two ranges of firing

Table 3-2. Summary of Results for the DMC Demonstration

Summary Sheet

TEST/DESCRIPTION:	13-Oct 27	19-Oct 28	20-Oct 29	7-Nov 30 Coal Only	16-Nov 31 Coal Only	17-Nov 32 Coal Only	18-Nov 33 Coal Only	21-Nov 34 AM	21-Nov 35 PM	22-Nov 36 Coal Only	28-Nov 37	30-Nov 38	1-Dec 39
WATER/STEAM SIDE													
Steam flow rate; lb/h	11,835	13,289	15,508	13,167	12,454	13,650	12,748	13,448	14,851	15,027	9,252	10,409	11,052
Water temperature into boiler; °F	209	161	218	195	193	206	209	197	211	214	214	216	217
Drum pressure; psig	209	206	203	212	207	209	207	205	186	184	206	208	188
Calorimeter temperature; °F	161	308	203	305	305	304	303	302	300	302	200	300	278
Steam temperature; °F	385	384	383	382	381	382	381	380	373	373	380	382	374
Steam quality; %	91.31	99.68	93.69	99.56	99.53	99.50	99.42	99.38	99.25	99.38	93.55	99.25	98.01
Blowdown rate; lb/h	3,166	3,142	3,123	3,189	3,156	3,168	3,154	3,134	2,990	2,974	3,148	3,162	3,006
AIR,FUEL, FLUE GAS SIDE													
Coal flow rate; lb/h,MMBtu/h	1,135;16.0	1,102;15.2	1,120;15.4	906;12.5	1,080;14.89	1,147;16.0	1,147;15.8	1,174;15.7	1,174;15.7	1,174;16.4	910;12.81	910;12.81	910;12.81
Air temperature entering air heater; °F	170	155	159	155	161	154	157	144	145	139	167	150	153
Air temperature leaving air heater; °F	422	414	415	399	428	417	416	410	414	408	415	411	413
Air temperature into boiler; °F	388	387	390	365	392	389	391	383	396	390	367	377	383
Furnace outlet temperature; °F	560	593	597	566	573	584	591	602	587	595	549	561	584
Gas temperature leaving air heater; °F	381	397	402	376	393	389	389	391	397	397	370	375	380
Bagfilter inlet temperature; °F	378	389	395	379	389	384	385	389	394	392	371	374	377
Bagfilter outlet temperature; °F	330	345	355	332	332	333	339	338	352	350	308	324	328
Ash content of fly ash; %	34.37	51.10	47.20	41.61	33.59	43.19	51.60	34.37	34.37	53.33	38.55	43.51	43.71
Combustion air flow; lb/h	13,806	14,160	13,759	11,134	13,995	16,783	15,721	14,780	14,359	15,287	11,514	11,841	11,900
Boiler draft; in H2O	0.03	-0.02	0.00	-0.03	-0.10	-0.04	-0.03	-0.02	-0.02	-0.02	-0.01	-0.03	-0.04
Boiler efficiency; %	80.1	81.8	80.7	79.6	76.2	Not Det.(ND)	ND	79.6	79.7	82.1	78.8	79.9	80.5
Mill air flow rate: ACFM;lbs/hr	345;1602	360;1663	365;1677	366;1705	358;1673	353;1630	361;1670	360;1675	349;1613	358;1,658	359;1689	351;1625	357;1639
Mill inlet temperature; °F	83	85	89	81	80	86	85	81	86	84	75	85	89
Mill outlet temperature; °F	194	216	219	207	214	214	207	205	212	210	195	210	217
Burner inlet temperature; °F	162	183	191	174	176	181	175	172	185	183	169	178	179
Natural gas temperature; °F	70	74	82	66	61	68	70	56	67	68	62	69	65
Coal combustion efficiency; %	91.50	93.28	91.71	89.71	86.35	90.48	93.98	91.50	91.50	93.68	88.72	89.70	90.93
EMISSIONS													
O2; %	3.6	4.0	3.3	3.7	4.4	7.0	5.8	4.2	3.7	4.5	4.1	4.4	4.6
CO; ppm	127	164	397	187	1,339	115	274	225	256	301	987	526	782
CO2; %	15.7	15.3	15.8	15.6	14.8	NM	NM	15.0	15.3	14.5	14.8	14.6	14.2
SO2; ppm	Not Measured (NM)	337	334	NM	270	360	311	NM	NM	NM	NM	378	393
NOx; ppm	519	338	364	299	323	312	349	344	403	317	NM	224	242

Portable Land Analyzer (in bold) was used when portions of the continuous emissions monitoring system was not operational.

Table 3-2. Summary of Results for the DMC Demonstration

Summary Sheet

TEST/DESCRIPTION:	2-Dec 40	5-Dec 41 A	5-Dec 42 B	5-Dec 43 C	6-Dec 44 A	6-Dec 45 B	6-Dec 46 C	7-Dec 47 A	7-Dec 48 B
WATER/STEAM SIDE									
Steam flow rate; lb/h	10,639	10,895	11,155	12,148	11,573	11,914	11,855	12,031	11,682
Water temperature into boiler; °F	213	182	206	207	207	207	207	207	207
Drum pressure; psig	204	204	201	194	191	186	188	185	186
Calorimeter temperature; °F	304	304	302	302	301	300	300	301	300
Steam temperature; °F	381	380	378	376	375	373	374	374	373
Steam quality; %	99.48	99.49	99.38	99.37	99.30	99.23	99.27	99.31	99.25
Blowdown rate; lb/h	3,131	3,133	3,104	3,050	3,025	2,989	3,004	2,979	2,985
AIR,FUEL, FLUE GAS SIDE									
Coal flow rate; lb/h,MMBtu/h	904;12.72	904;12.72	904;12.72	904;12.72	904;12.72	904;12.72	904;12.72	904;12.72	904;12.72
Air temperature entering air heater; °F	163	160	165	162	163	162	165	160	156
Air temperature leaving air heater; °F	434	425	425	425	423	421	421	417	413
Air temperature into boiler; °F	402	393	400	399	400	400	402	401	398
Furnace outlet temperature; °F	593	585	582	596	585	583	585	583	579
Gas temperature leaving air heater; °F	394	390	392	398	393	392	392	389	386
Bagfilter inlet temperature; °F	390	386	388	393	389	389	390	388	384
Bagfilter outlet temperature; °F	338	334	342	350	343	342	343	339	335
Ash content of fly ash; %	54.12	54.48	53.97	50.61	53.41	47.67	55.50	58.97	45.85
Combustion air flow; lb/h	11,875	11,692	12,092	12,159	12,423	12,020	12,119	11,974	12,370
Boiler draft; in H2O	-0.03	-0.04	-0.04	-0.08	-0.06	-0.06	-0.06	-0.06	-0.06
Boiler efficiency; %	82.7	82.5	82.1	81.2	82.1	81.0	82.6	83.2	80.9
Mill air flow rate: ACFM;lbs/hr	369;1710	350;1625	358;1657	358;1657	359;1650	350;1610	351;1613	348;1593	350;1611
Mill inlet temperature; °F	84	84	84	86	89	88	89	91	87
Mill outlet temperature; °F	207	212	208	198	209	212	214	215	209
Burner inlet temperature; °F	171	171	171	168	176	178	178	179	172
Natural gas temperature; °F	74	68	71	71	70	66	71	70	72
Coal combustion efficiency; %	94.11	94.11	93.98	93.00	93.92	92.34	94.41	94.84	92.43
EMISSIONS									
O2; %	4.6	4.2	4.8	4.9	5.3	4.8	4.9	4.5	5.3
CO; ppm	5	287	279	183	217	339	240	257	540
CO2; %	14.3	14.4	13.8	13.7	13.7	14.1	13.9	14.1	13.4
SO2; ppm	475	430	375	402	386	391	502	516	480
NOx; ppm	287	304	300	364	354	345	330	327	276

rates, 15.0 to 16.5 MM Btu/h and 12.5 to 13.0 MM Btu/h. Typically, the boiler was not fired over 16 MM Btu/h because increases in the boiler outlet temperature (and hence the baghouse entrance temperature) were observed. At the higher firing rate range, 15.0 to 16.5 MM Btu/h, the mean steam production was 13,600 lb/h or 93% of design capacity and the standard deviation of 1,200 lb steam/h.

Furnace and Convective Pass Deposition

The demonstration boiler was operated on a 2-shift/day and a continuous (24 hour) basis during November and December 1994 to evaluate the effect of ash deposition on boiler performance. Table 3-3 is a summary of the results of the November and December testing. Listed in Table 3-3 are the date of operation, the quantity of coal that was consumed on the date of operation, cumulative coal usage on the date of operation, cumulative coal usage since the last time the boiler was shut down and the ash removed from the system, boiler outlet pressure, ID fan amperage, convective pass temperature (at the location where erosion measurements are made), boiler outlet temperature, steam production, and comments.

The boiler was operated at two firing rates -- approximately 15 and 13 million Btu/h. Prior to testing in November, the boiler was cleaned on November 4, 1994 and ash was removed from the furnace, the entrance to the convective pass, and the breaching (interconnection between the boiler and the heat-pipe heat exchanger). Tests conducted on November 16, 17, and 18, 1994 were performed while operating the boiler on two shifts per day and at 14.9 to 16.0 million Btu/h. The test conducted from November 21 to 22, 1994 was performed while operating the boiler 24-hours/day at a firing rate of 15.7 million Btu/h. The 15.7 firing rate increased from 15.7 (for two twelve hour periods) to 16.4 MM Btu/h (for one twelve hour period) because the feed rate was held constant but the heating value of the coal increased.

The boiler was cleaned on November 23, 1994 and ash was removed from the furnace, entrance to the convective pass, and the breaching. Tests were then conducted on November 28 and 30, 1994 and December 1 and 2, 1994 while operating the boiler on two shifts per day and at 12.8 million Btu/h. A test was conducted from December 5 to 7, 1994 while continuously operating the boiler and firing at a rate of 12.7 million Btu/h.

Figures 3-1 through 3-6 are plots of sootblowing frequency, boiler outlet pressure, ID fan amperage, convective pass temperature, boiler outlet temperature, and steam production as a function of cumulative coal usage when firing the boiler at 15.0 to 16.4 million Btu/h, respectively. (Note that in Figure 3-1 there were no sootblowing events on December 7, 1994 but that the date was included in the legend so that the symbols are consistent between the figures.) The data for Figure 3-1 were obtained from the circular recorder charts, the data for Figures 3-2 through 3-6 were obtained from the operators' data sheets which were manually recorded every 30 minutes.

Table 3-3. Summary of Depostion Analysis

Date	Total Coal Consumed on this Date (lb)	Time	Cumulative Coal Usage on this Date (lb)	Cumulative Coal Usage since Boiler Cleaning; (lb)	Boiler Outlet Pressure (°W.C.)	ID Fan Amp Draw	Convective Pass Probe Temperature (K)	Convective Pass Probe Temperature (F)	Boiler Outlet Temperature (F)	Steam Production (lb/h)	Comments	
11/4/94	Boiler cleaned											
11/7/94	2,652	1230	1,532	1,532	-0.6	31.4	Not Measured	NM	555	12,300		2 shifts
		1300	2,092	2,092	-0.7	31.1	NM	NM	565	12,400		
		1330	2,652	2,652	-0.7	31.2	NM	NM	573	11,400		
11/16/94	4,570	1600	3,425	6,077	-0.5	28.0	NM	NM	560	13,400		2 shifts
		1630	3,998	6,650	-0.5	28.5	NM	NM	590	10,300	Blowdown at 1640	
		1700	4,570	7,222	-0.5	28.4	NM	NM	560	10,210		
11/17/94	5,339	1430	1,323	8,550	-0.8	29.5	NM	NM	579	10,600		2 shifts
		1500	1,897	9,123	-0.9	29.5	NM	NM	588	13,900		
		1530	2,470	9,696	-0.8	29.8	NM	NM	593	13,700		
		1600	3,044	10,269	-0.7	29.6	NM	NM	601	12,700		
		1630	3,617	10,842	-0.6	29.7	NM	NM	572	13,900	Blowdown at 1620	
		1700	4,192	11,415	-0.7	29.6	NM	NM	587	11,500		
		1730	4,765	11,988	-0.6	29.6	NM	NM	598	13,300		
		1800	5,339	12,561	-0.6	29.6	NM	NM	614	14,000		
11/18/94	10,710	1145	2,680	15,249	-0.8	29.7	NM	NM	589	10,900		2 shifts
		1215	3,253	15,822	-0.7	28.0	NM	NM	571	8,315		
		1245	3,827	16,395	-0.7	29.1	NM	NM	612	12,600		
		1315	4,400	16,968	-0.8	29.3	NM	NM	573	11,700	Blowdown at 1300	
		1345	4,974	17,541	-0.8	29.4	NM	NM	587	13,900		
		1415	5,548	18,114	-0.8	29.4	NM	NM	598	10,300		
		1445	6,121	18,687	-0.6	29.4	NM	NM	580	10,700	Blowdown at 1420	
		1515	6,695	19,260	-0.6	29.3	NM	NM	593	13,700		
		1545	7,268	19,833	-0.6	29.5	NM	NM	580	12,900	Blowdown at 1525	
		1615	7,842	20,406	-0.4	29.4	NM	NM	594	13,200		
		1645	8,416	20,979	-0.7	29.6	NM	NM	584	9,500	Blowdown at 1630	
		1715	8,989	21,552	-0.8	29.5	NM	NM	592	11,800		
		1745	9,563	22,125	-0.9	29.2	NM	NM	611	11,300		
		1815	10,136	22,698	-0.9	29.0	NM	NM	591	13,900	Blowdown at 1800	
		1845	10,710	23,271	-0.8	29.4	NM	NM	607	13,000		
11/21 to	37,945	0200	1,209	24,480	-0.8	30.6	NM	NM	577	10,000		Continuous
11/22/1994	noon	0230	1,783	25,054	-0.8	30.4	NM	NM	588	10,300		operation
		0300	2,357	25,628	-0.8	31.1	NM	NM	612	12,800		
		0330	2,931	26,202	-0.8	31.5	NM	NM	596	13,600	Blowdown	
		0400	3,505	26,776	-0.8	31.2	NM	NM	607	11,500		
		0430	4,079	27,350	-0.8	31.5	NM	NM	598	15,300	Blowdown	
		0500	4,653	27,924	-0.8	32.0	NM	NM	616	10,500		
		0530	5,227	28,498	-0.8	31.7	NM	NM	596	12,100	Blowdown	
		0600	5,801	29,072	-1.0	31.0	NM	NM	608	11,700		
		0630	6,375	29,646	-1.0	31.5	NM	NM	603	14,600	Blowdown	
		0700	6,949	30,220	-1.0	31.5	NM	NM	609	12,200		
		0730	7,523	30,794	-1.0	31.0	NM	NM	581	10,900	Blowdown	
		0800	8,097	31,368	-1.0	31.7	NM	NM	608	12,800		
		0830	8,671	31,942	-1.0	31.3	NM	NM	591	10,400	Blowdown	
		0900	9,245	32,516	-1.0	31.2	NM	NM	583	13,000	Blowdown	
		0930	9,819	33,090	-1.0	30.7	NM	NM	593	12,400		
		1000	10,393	33,664	-0.8	30.2	NM	NM	599	12,800		
		1030	10,967	34,238	-0.8	30.0	NM	NM	585	11,000	Blowdown	
		1100	11,541	34,812	-1.0	30.5	NM	NM	615	13,400		
		1130	12,115	35,386	-1.0	30.8	NM	NM	596	13,500	Blowdown	
		1200	12,689	35,960	-1.0	30.6	NM	NM	607	12,600		
		1230	13,263	36,534	-0.8	30.6	961	1,270	617	12,400		
		1300	13,837	37,108	-1.0	30.6	931	1,216	598	13,300	Blowdown	
		1330	14,411	37,682	-0.8	30.5	976	1,297	613	14,200		
		1400	14,985	38,256	-1.0	30.3	932	1,218	599	12,100	Blowdown	
		1430	15,559	38,830	-1.0	30.3	966	1,279	615	13,600		
		1500	16,133	39,404	-1.0	30.6	947	1,245	601	13,800	Blowdown	
		1530	16,707	39,978	-1.0	30.5	955	1,259	612	12,800		
		1600	17,281	40,552	-1.0	30.3	942	1,236	594	13,400	Blowdown	
		1630	17,855	41,126	-1.0	30.6	987	1,317	611			
		1700	18,429	41,700	-1.0	30.4	930	1,214	596	12,200	Blowdown	
		1730	19,003	42,274	-1.0	30.1	964	1,276	606	14,100		
		1800	19,577	42,848	-1.0	30.3	964	1,276	611	13,700		
		1830	20,151	43,422	-1.0	30.8	991	1,324	606	15,600	Blowdown	
		1900	20,725	43,996	-1.0	30.7	973	1,292	606	14,600	Blowdown	
		1930	21,299	44,570	-0.8	30.6	958	1,265	600	13,800		
		2000	21,873	45,144	-0.8	30.4	963	1,274	610	13,700		
		2030	22,447	45,718	-1.0	31.3	1002	1,344	620	15,000		
		2100	23,021	46,292	-1.0	30.2	978	1,301	597	14,200	Blowdown	
		2130	23,595	46,866	-1.0	30.2	963	1,274	589	15,200	Blowdown	
		2200	24,169	47,440	-1.2	31.0	961	1,270	603	15,300		
		2230	24,743	48,014	-1.1	31.0	962	1,272	596	14,900	Blowdown	
		2300	25,317	48,588	-1.2	30.7	964	1,276	610	14,800		
		2330	25,891	49,162	-1.2	31.0	1024	1,384	620	15,100		
11/22/94		0000	26,465	49,736	-1.2	31.5	1003	1,346	613	15,100	Blowdown	
		0030	27,039	50,310	-1.1	31.7	992	1,326	619	13,900		
		0100	27,613	50,884	-1.3	31.4	1013	1,364	623	15,400		
		0130	28,187	51,458	-1.2	31.5	885	1,133	617	15,200	Blowdown	
		0200	28,761	52,032	-1.3	31.6	986	1,315	621	13,900		

Table 3-3. Summary of Depostion Analysis

		0230	29,335	52,606	-1.2	31.5	995	1,331	622	14,000		
		0300	29,909	53,180	-1.3	31.7	968	1,283	611	14,200	Blowdown	
		0330	30,483	53,754	-1.8	31.6	924	1,204	617	14,900		
		0400	31,057	54,328	-1.8	31.7	908	1,175	612	14,900	Blowdown	
		0430	31,631	54,902	-1.9	31.6	921	1,198	623	14,700		
		0500	32,205	55,476	-2.0	32.0	928	1,211	606	16,200	Blowdown	
		0530	32,779	56,050	-2.0	31.9	900	1,160	617	15,400		
		0600	33,353	56,624	-2.0	32.1	900	1,160	593	14,000	Blowdown	
		0630	33,927	57,198	<-2	32.0	902	1,164	615	16,000		
		0700	34,501	57,772	<-2	32.0	901	1,162	618	14,800		
		0730	35,075	58,346	<-2	32.2	832	1,038	591	15,300	Blowdown	
		0800	35,649	58,920	<-2	32.1	841	1,054	603	15,800		
		0830	36,223	59,494	<-2	32.5	854	1,078	607	14,100		
		0900	36,797	60,068	<-2	32.1	828	1,031	606	13,200		
		0930	37,371	60,642	<-2	32.3	863	1,094	617	15,200		
		1000	37,945	61,216	<-2	32.4	806	991	588	15,300	Blowdown	
11/23/94	Boiler Cleaned											
11/28/94	3,645	0930	2,280	2,280	-0.3	26.7	815	1,007	543	9,100		2 shifts
		1000	2,735	2,735	-0.3	26.6	845	1,061	569	8,600		
		1030	3,190	3,190	-0.3	26.7	868	1,103	595	9,100		
		1100	3,645	3,645	-0.3	26.7	808	995	528	8,800	Blowdown	
11/30/94	4,866	1600	1,226	4,871	-0.3	27.7	889	1,141	579	7,500		2 shifts
		1630	1,681	5,326	-0.5	27.3	905	1,169	594	9,700		
		1700	2,136	5,781	-0.5	27.5	835	1,043	523	9800	Blowdown	
		1730	2,591	6,236	-0.5	27.9	867	1,101	549	7,600		
		1800	3,046	6,691	-0.5	28.5	898	1,157	598	8,900		
		1830	3,501	7,146	-0.6	28.9	883	1,130	562	13,000		
		1900	3,956	7,601	-0.5	29.1	899	1,159	573	13,000		
		1930	4,411	8,056	-0.6	30.3	899	1,159	561	8,200	Blowdown	
		2000	4,866	8,511	-0.6	28.9	909	1,177	576	11,100		
12/1/94	7,162	1230	1,247	9,758	-0.5	27.9	887	1,137	561	8,800		2 shifts
		1300	1,702	10,213	-0.4	28.0	909	1,177	580	9,200		
		1330	2,157	10,668	-0.6	27.9	949	1,249	616	10,300		
		1400	2,612	11,123	-0.6	28.8	894	1,150	562	11,000	Blowdown	
		1430	3,067	11,578	-0.6	29.1	924	1,204	593	11,600		
		1500	3,522	12,033	-0.6	27.8	922	1,200	583	9,700		
		1530	3,977	12,488	-0.5	27.8	901	1,162	561	11,300	Blowdown	
		1600	4,432	12,943	-0.6	27.6	898	1,157	593	9,200		
		1630	4,887	13,398	-0.6	28.2	951	1,252	630	12,000		
		1700	5,342	13,853	-0.7	29.8	933	1,220	630	11,900		
		1730	5,797	14,308	-0.7	29.2	886	1,135	571	12,400	Blowdown	
		1800	6,252	14,763	-0.6	29.0	880	1,124	569	11,300		
		1830	6,707	15,218	-0.5	27.3	901	1,162	582	9,300		
		1900	7,162	15,673	-0.5	27.1	861	1,090	538	7,500	Blowdown	
12/2/94	5,457	1300	2,293	17,966	-0.8	29.7	845	1,061	577	11,400		2 shifts
		1330	2,745	18,418	-0.7	28.7	835	1,043	571	10,700	Blowdown	
		1400	3,197	18,870	-0.6	28.5	892	1,146	585	11,200		
		1800	3,649	19,322	-0.7	29.6	858	1,085	594	12,500		
		1830	4,101	19,774	-0.6	29.1	867	1,101	591	7,600	Blowdown	
		1900	4,553	20,226	-0.5	28.9	894	1,150	597	11,700		
		1930	5,005	20,678	-0.6	28.5	913	1,184	610	7,100		
		2000	5,457	21,130	-0.5	28.9	920	1,196	612	9,700		
12/5 thru	53,476	0630	1,496	22,626	-0.6	28.1	NM	NM	587	10,800		Continuous
12/7/94		0700	1,948	23,078	-0.4	27.6	NM	NM	598	8,600		operation
		0730	2,400	23,530	-0.5	27.8	NM	NM	608	10,400		
		0800	2,852	23,982	-0.6	27.9	NM	NM	560	8,800	Blowdown	
		0830	3,304	24,434	-0.8	29.0	NM	NM	613	10,000		
		0900	3,756	24,886	-0.6	28.9	NM	NM	583	10,300	Blowdown	
		0930	4,208	25,338	-0.8	28.5	NM	NM	595	11,800		
		1000	4,660	25,790	-0.6	28.7	NM	NM	605	11,800		
		1030	5,112	26,242	-0.5	28.8	NM	NM	574	8,700	Blowdown	
		1100	5,564	26,694	-0.6	28.7	NM	NM	589	10,100		
		1130	6,016	27,146	-0.8	28.7	NM	NM	608	8,500		
		1200	6,468	27,598	-0.8	28.4	NM	NM	617	7,700		
		1230	6,920	28,050	-0.8	28.4	NM	NM	575	8,200	Blowdown	
		1300	7,372	28,502	-0.7	28.4	NM	NM	593	13,100		
		1330	7,824	28,954	-0.7	28.5	NM	NM	602	10,700		
		1400	8,276	29,406	-0.7	28.4	NM	NM	611	11,700		
		1430	8,728	29,858	-0.6	28.1	NM	NM	574	9,300	Blowdown	
		1500	9,180	30,310	-0.8	28.7	NM	NM	589	10,500		
		1530	9,632	30,762	-0.8	28.3	NM	NM	599	8,500		
		1600	10,084	31,214	-0.5	28.6	NM	NM	578	9,200	Blowdown	
		1630	10,536	31,666	-0.7	28.6	NM	NM	598	11,600		
		1700	10,988	32,118	-0.7	28.3	NM	NM	606	9,700		
		1730	11,440	32,570	-0.6	28.0	NM	NM	610	10,100		
		1800	11,892	33,022	-0.5	28.3	NM	NM	576	10,800	Blowdown	
		2330	12,344	33,474	-0.8	29.3	NM	NM	600	11,900		
		0000	12,796	33,926	-0.7	28.6	NM	NM	598	11,400		
		0030	13,248	34,378	-0.7	28.3	NM	NM	607	11,400		
		0100	13,700	34,830	-0.6	28.6	NM	NM	614	10,500		
		0130	14,152	35,282	-0.8	28.8	NM	NM	579	10,600	Blowdown	
		0200	14,604	35,734	-0.6	28.7	NM	NM	596	10,600		
		0230	15,056	36,186	-0.8	28.5	NM	NM	603	10,500		

Table 3-3. Summary of Depostion Analysis

		0300	15,508	36,638	-0.6	28.5	NM	NM	611	10,500	
		0330	15,960	37,090	-0.6	28.7	NM	NM	577	11,100	Blowdown
		0400	16,412	37,542	-0.6	28.6	NM	NM	599	11,700	
		0430	16,864	37,994	-0.6	28.7	NM	NM	605	10,900	
		0500	17,316	38,446	-0.8	29.0	NM	NM	582	10,400	Blowdown
		0530	17,768	38,898	-0.8	29.0	NM	NM	598	11,200	
		0600	18,220	39,350	-0.7	29.0	NM	NM	608	11,800	
		0630	18,672	39,802	-0.7	28.9	NM	NM	589	11,300	Blowdown
		0700	19,124	40,254	-0.7	29.0	NM	NM	597	11,300	
		0730	19,576	40,706	-0.6	28.6	NM	NM	607	12,400	
		0800	20,028	41,158	-0.8	28.9	NM	NM	573	11,500	Blowdown
		0830	20,480	41,610	-0.8	28.9	NM	NM	587	10,900	
		0900	20,932	42,062	-0.7	28.8	NM	NM	602	11,700	
		0930	21,384	42,514	-0.8	28.6	NM	NM	614	11,600	
		1000	21,836	42,966	-0.8	28.7	NM	NM	585	10,800	Blowdown
		1030	22,288	43,418	-0.8	28.6	NM	NM	595	10,900	
		1100	22,740	43,870	-0.8	28.4	NM	NM	612	12,500	
		1130	23,192	44,322	-1.0	28.5	NM	NM	593	12,200	Blowdown
		1200	23,644	44,774	-1.0	28.5	NM	NM	591	10,900	
		1230	24,096	45,226	-0.8	28.3	NM	NM	572	10,900	Blowdown
		1300	24,548	45,678	-0.8	28.5	NM	NM	603	10,700	
		1330	25,000	46,130	-0.6	28.3	NM	NM	590	11,800	Blowdown
		1400	25,452	46,582	-0.8	28.3	NM	NM	608	11,500	
		1430	25,904	47,034	-0.6	28.1	NM	NM	585	11,500	Blowdown
		1500	26,356	47,486	-0.6	28.2	NM	NM	604	12,600	
		1530	26,808	47,938	-0.8	28.4	NM	NM	593	10,800	Blowdown
		1600	27,260	48,390	-0.8	28.1	NM	NM	610	12,500	
		1630	27,712	48,842	-0.7	28.3	NM	NM	585	11,800	Blowdown
		1700	28,164	49,294	-0.7	28.5	NM	NM	594	11,200	
		1730	28,616	49,746	-0.7	28.3	NM	NM	609	12,400	
		1800	29,068	50,198	-0.6	28.5	NM	NM	587	11,400	Blowdown
		1830	29,520	50,650	-0.8	28.7	NM	NM	598	11,700	
		1900	29,972	51,102	-0.7	28.7	NM	NM	614	11,400	
		1930	30,424	51,554	-0.7	28.5	NM	NM	618	11,200	
		2000	30,876	52,006	-0.6	28.7	NM	NM	593	12,200	Blowdown
		2030	31,328	52,458	-0.7	28.3	NM	NM	594	10,700	
		2100	31,780	52,910	-0.8	28.4	NM	NM	605	11,400	
		2130	32,232	53,362	-0.7	28.2	NM	NM	615	11,600	
		2200	32,684	53,814	-0.8	28.2	NM	NM	588	11,600	Blowdown
		2230	33,136	54,266	-0.8	28.3	NM	NM	598	11,100	
		2300	33,588	54,718	-0.8	28.3	NM	NM	610	12,200	
		2330	34,040	55,170	-0.7	28.4	NM	NM	612	10,600	
		0000	34,492	55,622	-0.8	28.3	NM	NM	593	12,400	Blowdown
		0030	34,944	56,074	-1.0	28.3	NM	NM	610	11,300	
		0100	35,396	56,526	-0.9	28.5	NM	NM	583	10,900	Blowdown
		0130	35,848	56,978	-1.2	28.6	NM	NM	607	12,500	
		0200	36,300	57,430	-1.0	28.6	NM	NM	564	10,100	Blowdown
		0230	36,752	57,882	-1.0	28.4	NM	NM	598	11,600	
		0300	37,204	58,334	-1.2	28.3	NM	NM	609	11,100	
		0330	37,656	58,786	-1.4	28.2	NM	NM	618	11,200	
		0400	38,108	59,238	-1.4	28.4	NM	NM	595	12,300	Blowdown
		0430	38,560	59,690	-1.4	28.5	NM	NM	609	12,100	
		0500	39,012	60,142	-1.2	28.6	NM	NM	574	10,500	Blowdown
		0530	39,464	60,594	-1.5	28.8	NM	NM	597	12,200	
		0600	39,916	61,046	-1.5	28.9	NM	NM	603	11,500	
		0630	40,368	61,498	-1.7	28.8	NM	NM	610	11,800	
		0700	40,820	61,950	-1.8	28.7	NM	NM	581	12,100	Blowdown
		0730	41,272	62,402	-1.9	28.7	NM	NM	607	12,100	
		0800	41,724	62,854	-1.9	28.6	NM	NM	612	12,500	
		0830	42,176	63,306	-2.0	28.6	NM	NM	587	11,200	Blowdown
		0900	42,628	63,758	-2.0	28.7	NM	NM	604	13,000	
		0930	43,080	64,210	<-2	28.4	NM	NM	582	12,500	Blowdown
		1000	43,532	64,662	<-2	28.8	NM	NM	586	11,500	
		1030	43,984	65,114	<-2	28.8	NM	NM	600	11,900	
		1100	44,436	65,566	<-2	28.5	NM	NM	612	12,600	
		1130	44,888	66,018	<-2	28.6	NM	NM	572	11,400	Blowdown
		1200	45,340	66,470	<-2	28.7	NM	NM	574	11,000	
		1230	45,792	66,922	<-2	28.7	NM	NM	588	12,000	
		1300	46,244	67,374	<-2	28.3	NM	NM	598	12,500	
		1330	46,696	67,826	<-2	28.4	NM	NM	608	12,300	
		1400	47,148	68,278	<-2	28.6	NM	NM	581	11,900	Blowdown
		1430	47,600	68,730	<-2	28.8	NM	NM	579	10,400	
		1500	48,052	69,182	<-2	28.6	NM	NM	592	11,200	
		1530	48,504	69,634	<-2	28.6	NM	NM	598	10,900	
		1600	48,956	70,086	<-2	29.3	NM	NM	597	11,100	
		1630	49,408	70,538	<-2	28.7	NM	NM	617	11,300	
		1700	49,860	70,990	<-2	28.9	NM	NM	574	11,200	Blowdown
		1730	50,312	71,442	<-2	28.9	NM	NM	564	10,600	
		1800	50,764	71,894	<-2	28.6	NM	NM	589	12,100	
		1830	51,216	72,346	<-2	28.9	NM	NM	591	10,400	
		1900	51,668	72,798	<-2	28.8	NM	NM	600	11,900	
		1930	52,120	73,250	<-2	28.9	NM	NM	609	11,000	
		2000	52,572	73,702	<-2	29.0	NM	NM	551	11,100	Blowdown
		2030	53,024	74,154	<-2	29.6	NM	NM	568	11,500	
		2100	53,476	74,606	<-2	29.4	NM	NM	574	10,400	

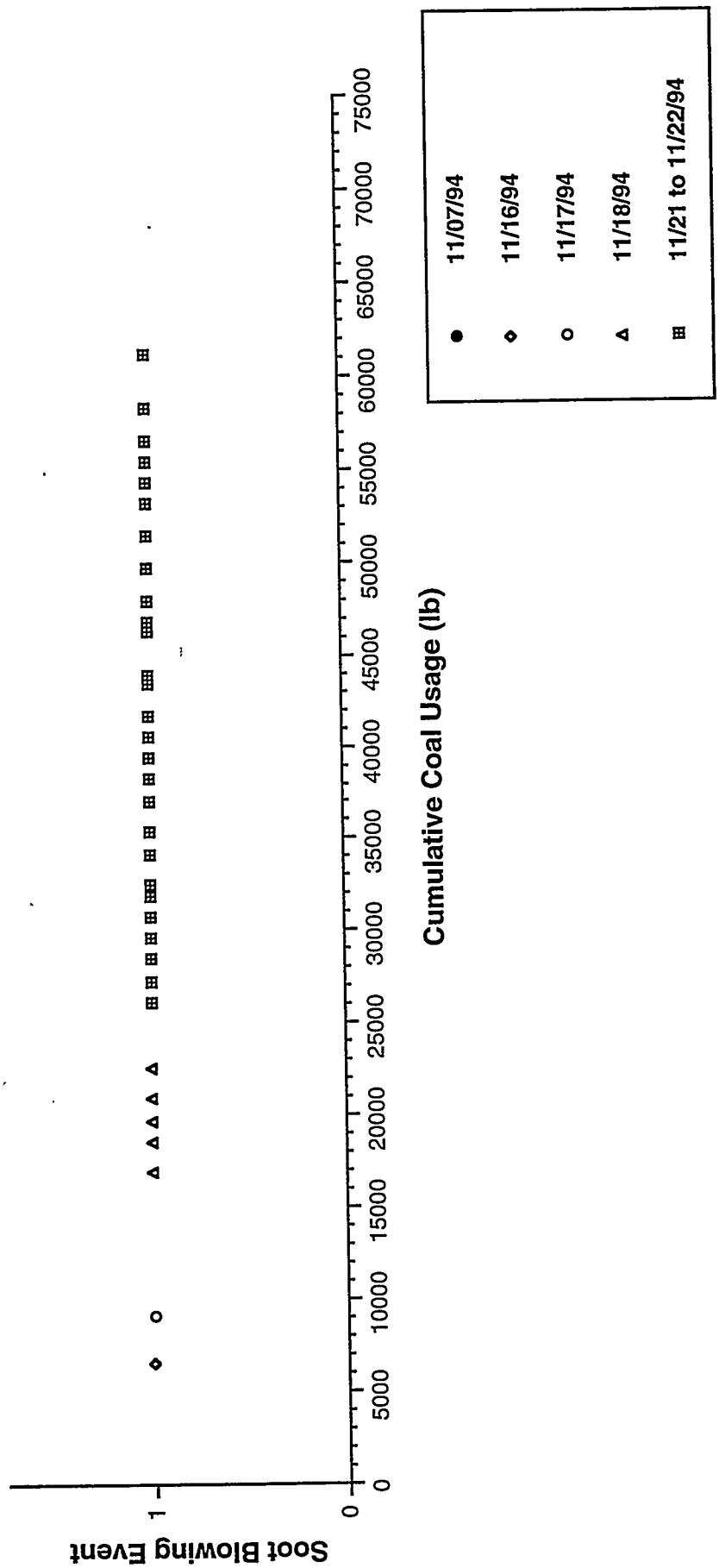

Figure 3-1. SOOT BLOWING FREQUENCY AS A FUNCTION OF COAL CONSUMPTION WHEN FIRING AT 15.0 TO 16.4 MILLION BTU/H

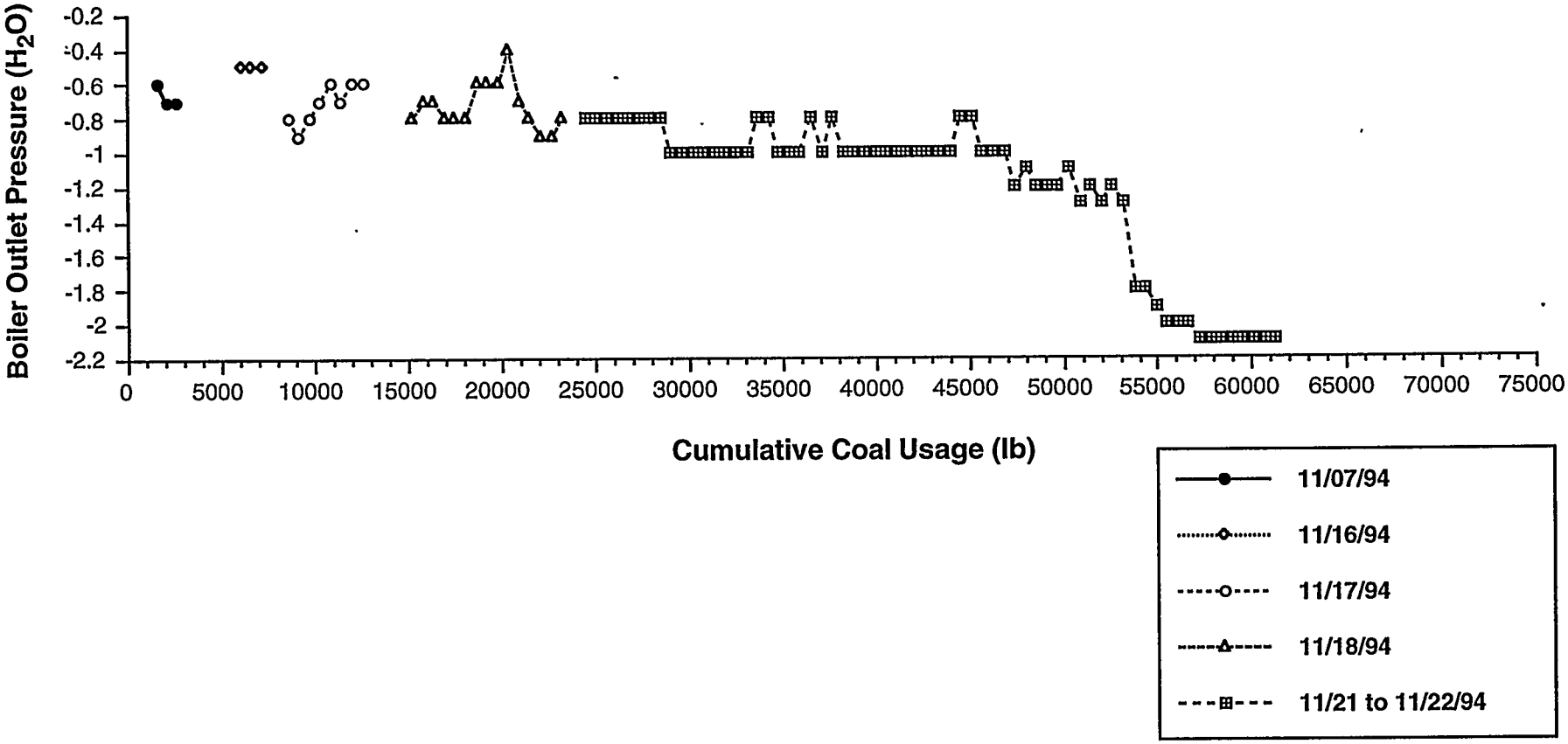

Figure 3-2. BOILER OUTLET PRESSURE AS A FUNCTION OF COAL CONSUMPTION WHEN FIRING AT 15.0 TO 16.4 MILLION BTU/H

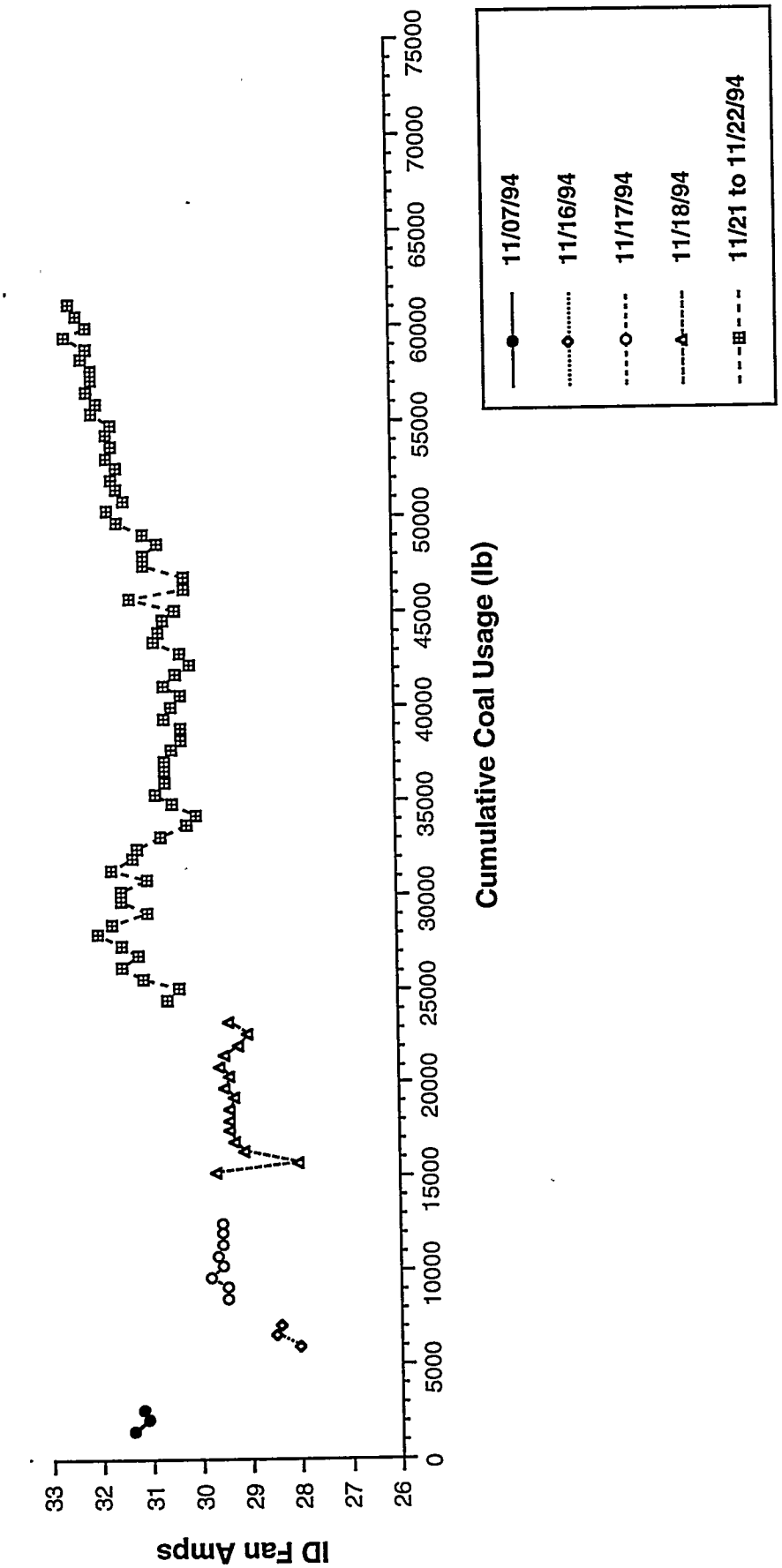

Figure 3-3. ID FAN AMPERAGE AS A FUNCTION OF COAL CONSUMPTION WHEN FIRING AT 15.0 TO 16.4 MILLION BTU/H

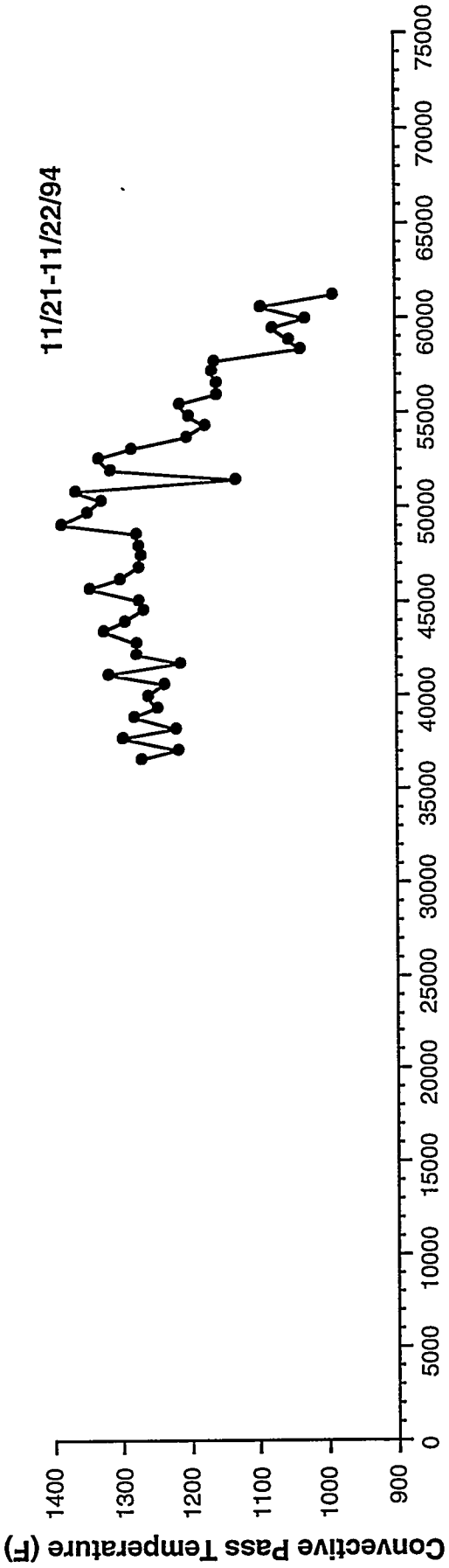

Figure 3-4. CONVECTIVE PASS TEMPERATURE AS A FUNCTION OF COAL CONSUMPTION WHEN FIRING AT 15.0 TO 16.4 MILLION BTU/H

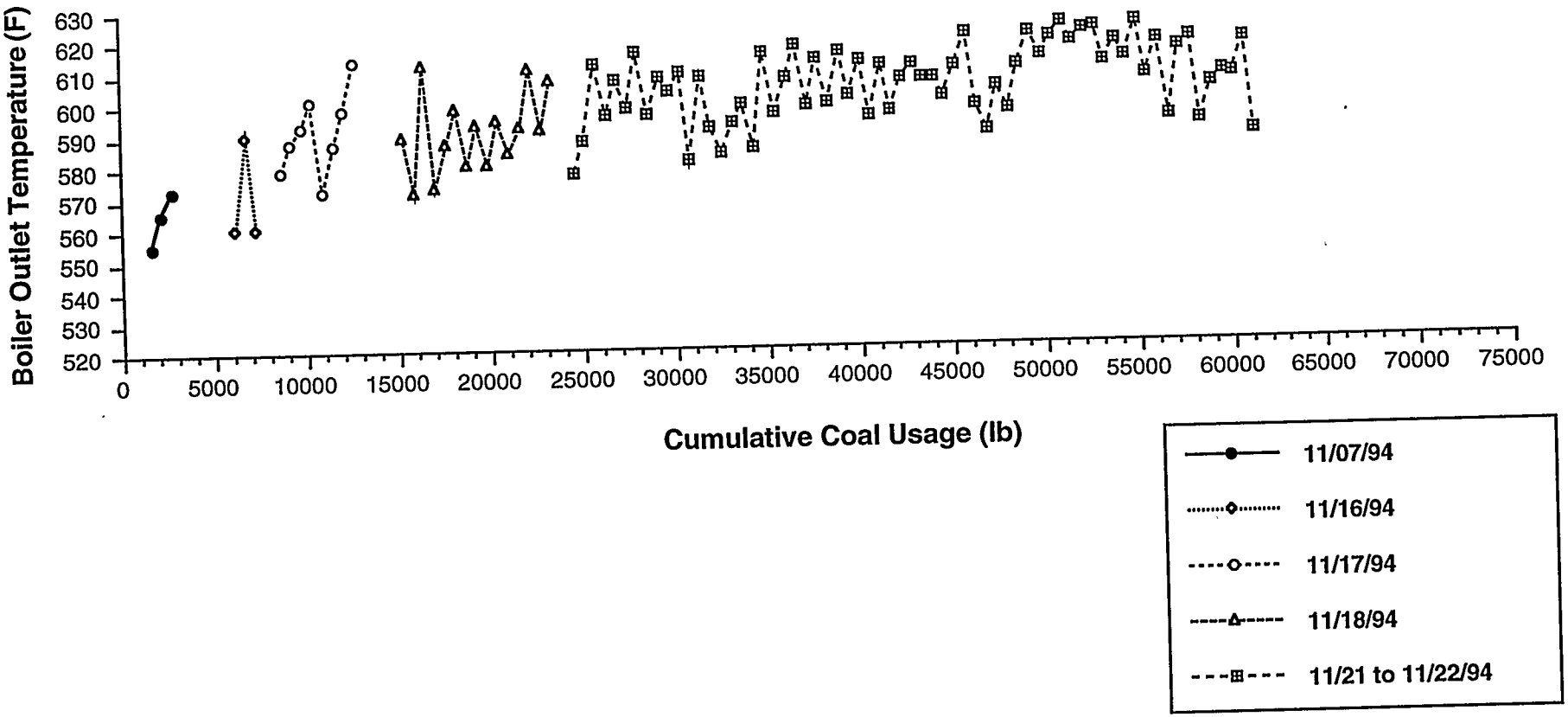

Figure 3-5. BOILER OUTLET TEMPERATURE AS A FUNCTION OF COAL CONSUMPTION WHEN FIRING AT 15.0 TO 16.4 MILLION BTU/H

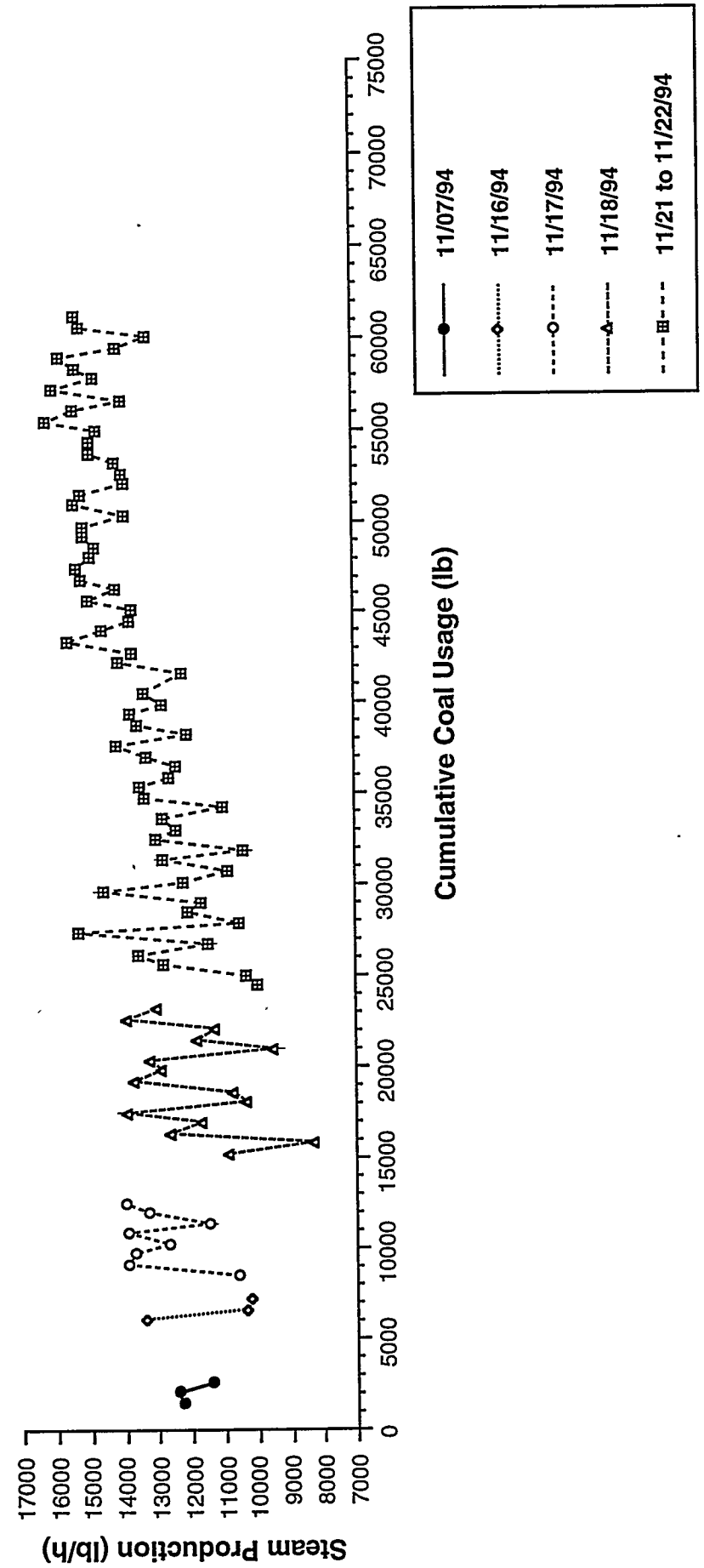

Figure 3-6. STEAM PRODUCTION AS A FUNCTION OF COAL CONSUMPTION WHEN FIRING AT 15.0 TO 16.4 MILLION BTU/H

The minimum pressure indicated on the boiler outlet pressure gauge is -2.0" W.C. (water column). When the gauge went off scale (<2.0" W.C.), the data were plotted (in Figure 3-2) as -2.2" W.C. (for graphing purposes only). The actual pressure was not measured but was probably still decreasing with time of operation. The erosion probe, which contains a thermocouple, was inserted into the convective pass during the test conducted from November 21 to 22, 1994 and the temperature was measured. In addition to the manually recorded steam production and boiler outlet temperature data, the data acquisition system logs these data every 30 seconds.

Figures 3-7 through 3-12 are plots of sootblowing frequency, boiler outlet pressure, ID fan amperage, convective pass temperature, boiler outlet temperature, and steam production as a function of cumulative coal usage when firing the boiler at 12.7 and 12.8 million Btu/h, respectively. Similar to Figure 3-2, the minimum pressure indicated on the boiler outlet pressure gauge is -2.0" W.C. and the data were plotted as -2.2" W.C. (Figure 3-8) when the gauge went off scale (<2.0" W.C.). In Figure 3-10, the convective pass temperature was not manually recorded during the continuous test (12/05 to 12/07/94). In addition, the data were recorded by the data acquisition system in an unreadable format.

Deposition Summary -- Two Firing Rates

Table 3-4 summarizes the results of the tests conducted at the two firing rates. It should be noted that there were no operational problems observed when operating the boiler on a two-shift per day basis. The tests conducted when operating on a continuous basis were terminated when significant deposition was noted in the entrance to the convective pass (when firing at ~15.7 million Btu/h) and when the rear side panels of the boiler warped and discoloration was noted on the back wall (when firing at 12.7 million Btu/h). Many of the results in Table 3-4 are also contained in the Table 3-5 (in the next section summarizing the continuous tests) because most of the system variations occurred during the continuous test. The results are still summarized in Table 3-4 because total coal consumption since the last boiler cleanout is used in this analysis.

Deposition Summary -- Two Continuous Tests

Table 3-5 summarizes the results of the two continuous tests conducted at the two firing rates. As previously mentioned, the tests were terminated when significant deposition was noted in the entrance to the convective pass when firing at ~15.7 million Btu/h (11/21-11/22/94), and when the rear side panels of the boiler warped and discoloration was noted on the back wall when firing at 12.7 million Btu/h (12/05-12/07/94). The boiler was shut down on 11/22/94 because it was the first time that such significant deposition was observed at the entrance into the convective pass. The shutdown on December 7, 1994 was a forced shutdown due to the sidewall (metal) warping allowing burning between the refractory rear wall and the insulation/metal skin interface.

Figures 3-5 and 3-11 do not accurately show the boiler outlet temperature trends because the data are only recorded every 30 minutes and sootblowing affects the appearances of Figures 3-

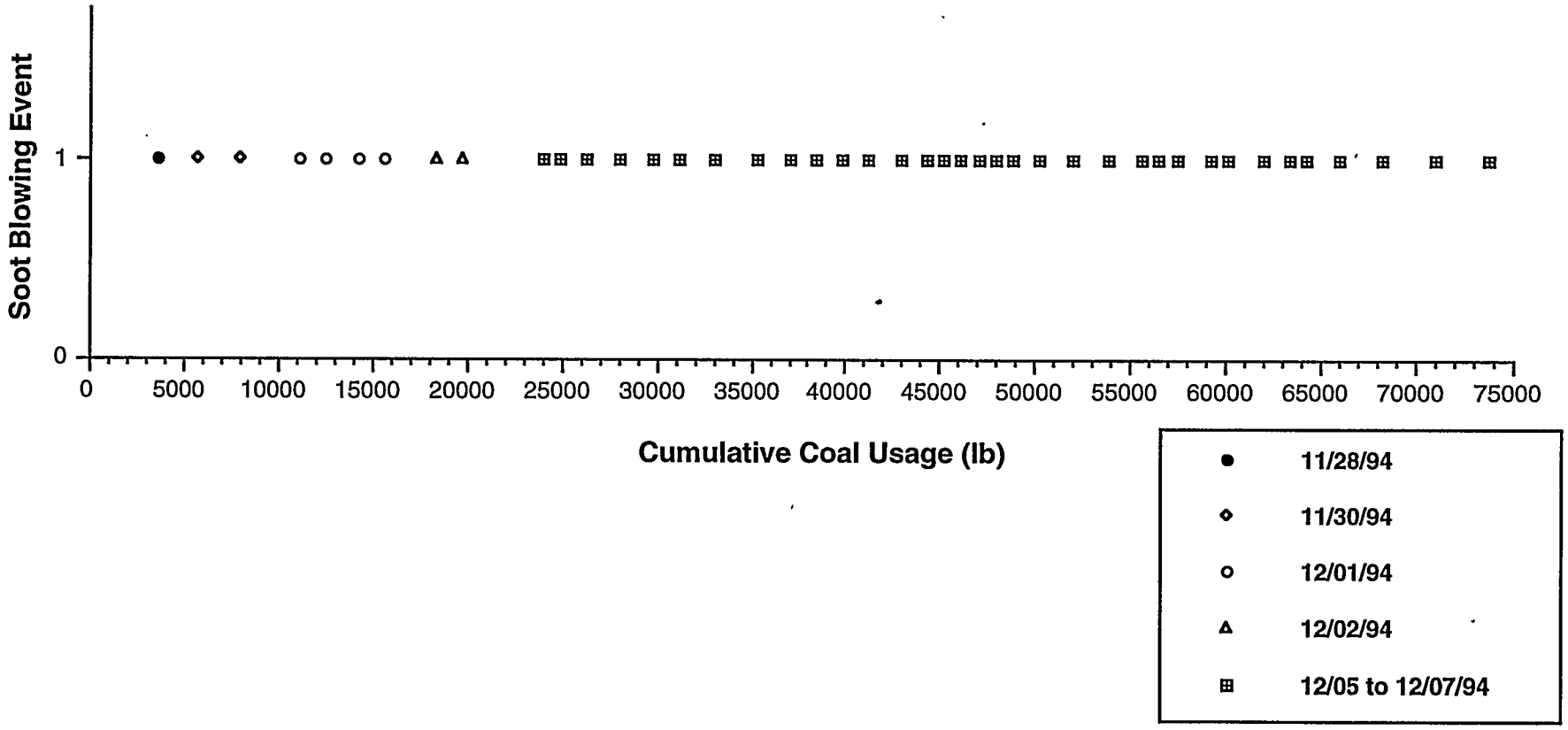

Figure 3-7. SOOT BLOWING FREQUENCY AS A FUNCTION OF COAL CONSUMPTION WHEN FIRING AT 12.7 TO 12.8 MILLION BTU/H

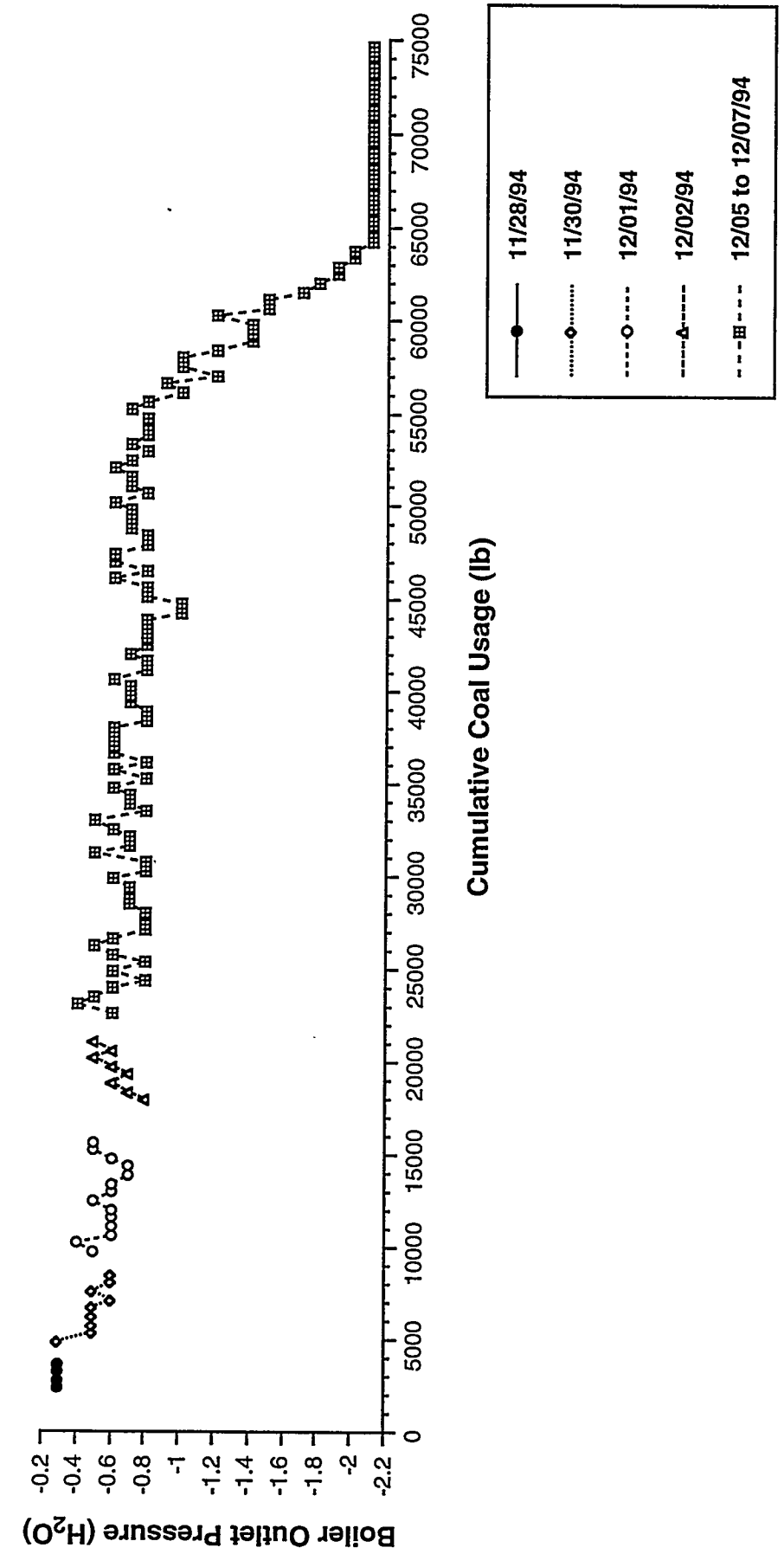

Figure 3-8. BOILER OUTLET PRESSURE AS A FUNCTION OF COAL CONSUMPTION WHEN FIRING AT 12.7 TO 12.8 MILLION BTU/H

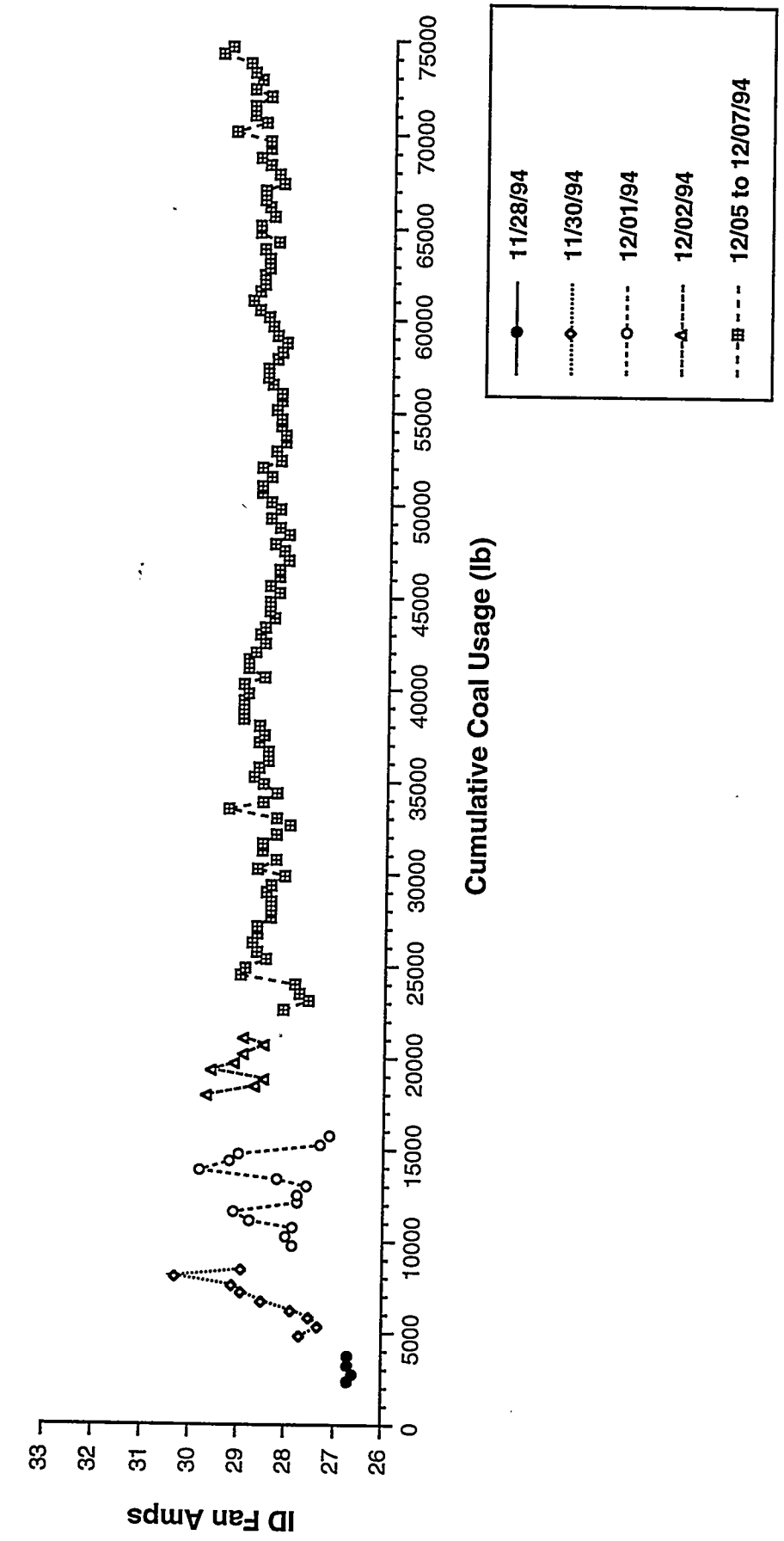

Figure 3-9. ID FAN AMPERAGE AS A FUNCTION OF COAL CONSUMPTION WHEN FIRING AT 12.7 TO 12.8 MILLION BTU/H

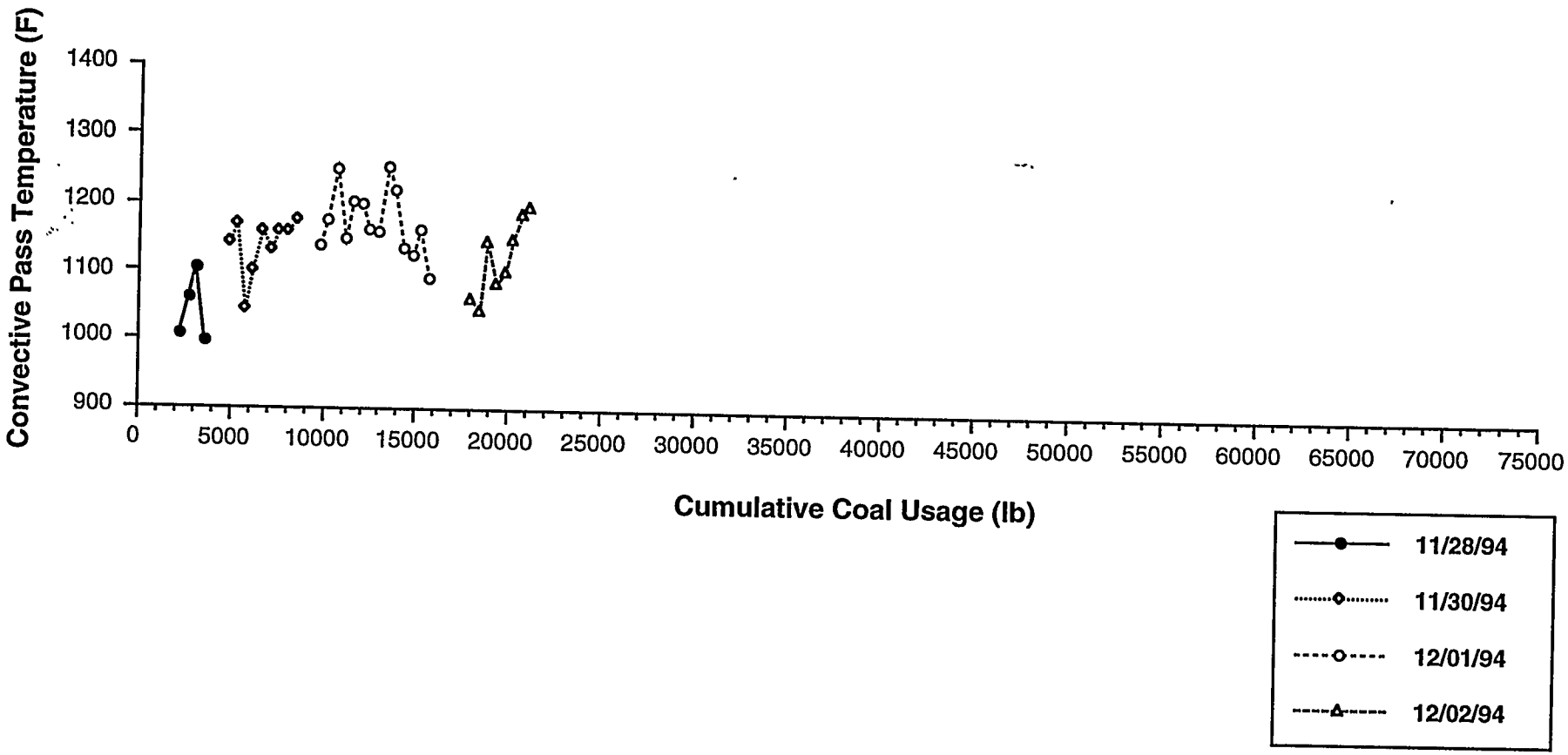

Figure 3-10. CONVECTIVE PASS TEMPERATURE AS A FUNCTION OF COAL CONSUMPTION WHEN FIRING AT 12.7 TO 12.8 MILLION BTU/H

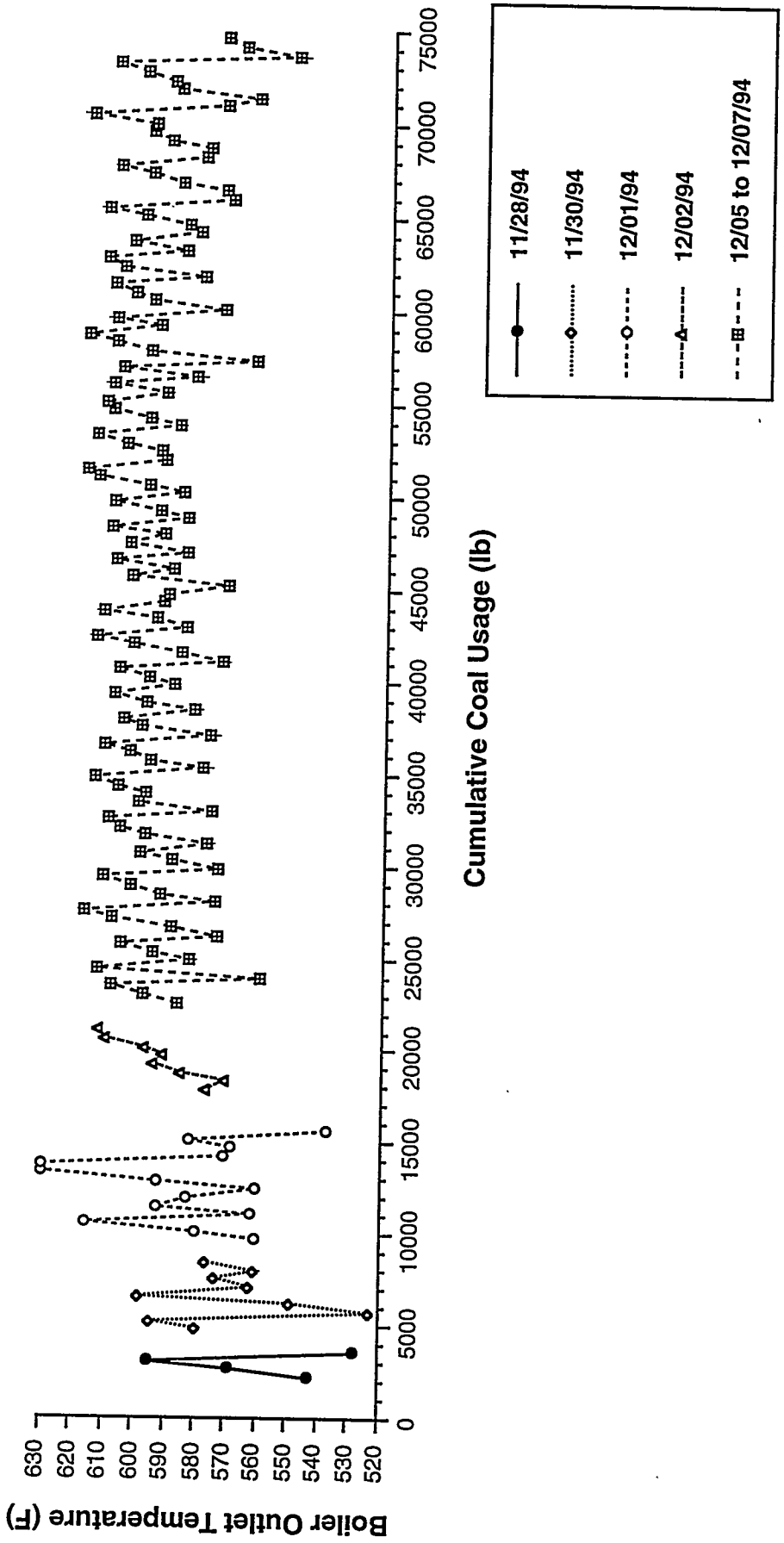

Figure 3-11. BOILER OUTLET TEMPERATURE AS A FUNCTION OF COAL CONSUMPTION WHEN FIRING AT 12.7 TO 12.8 MILLION BTU/H

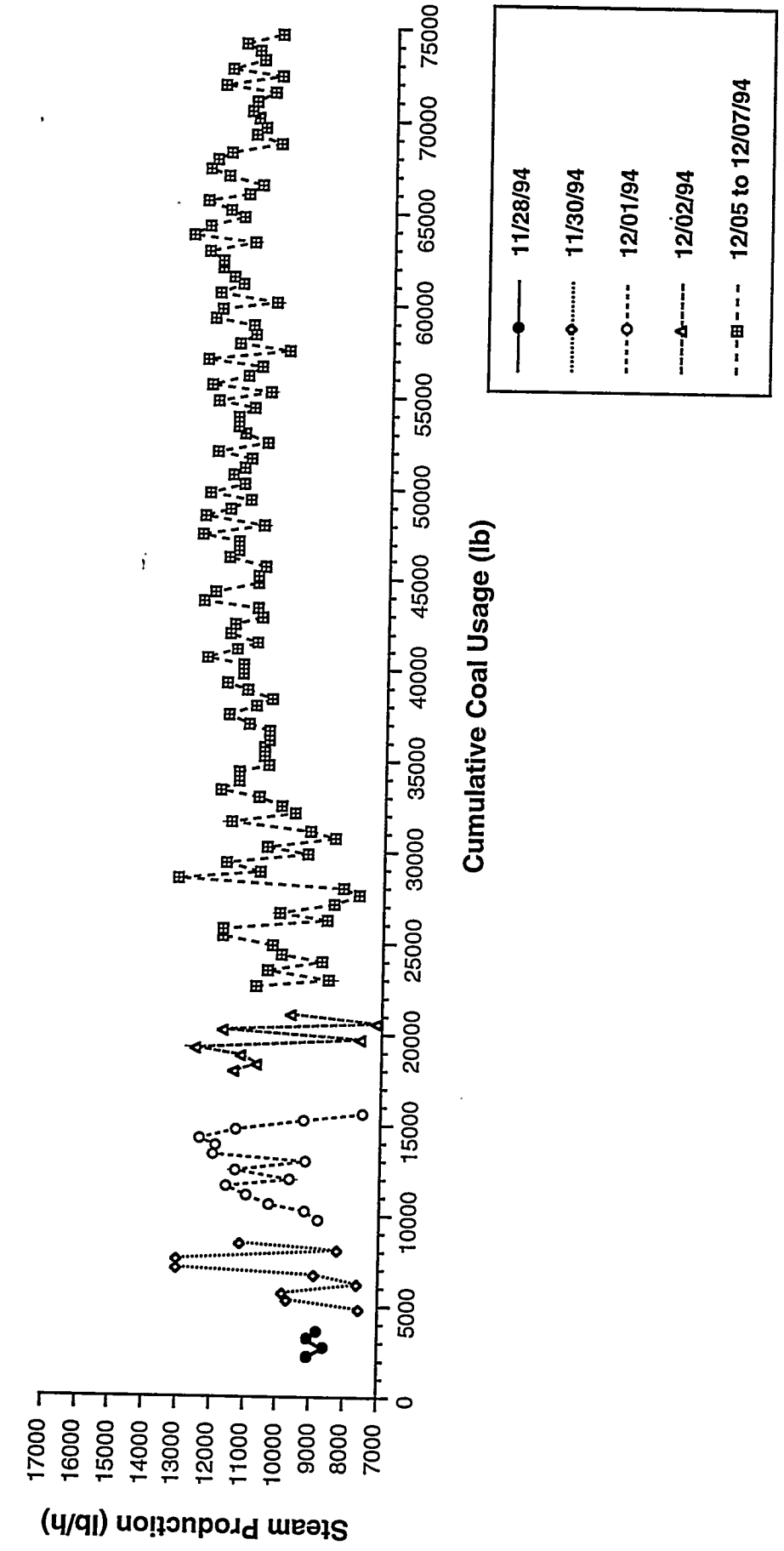

Figure 3-12. STEAM PRODUCTION AS A FUNCTION OF COAL CONSUMPTION WHEN FIRING AT 12.7 TO 12.8 MILLION BTU/H

Table 3-4. Deposition Summary -- Two Firing Rates

15.0 - 16.4 Million Btu/h	12.7 - 12.8 Million Btu/h
• 61,216 lb of coal were consumed at a rate of 1,148 lb/h for 53 h of operation.	• 74,606 lb of coal were consumed at a rate of 904 lb/h for 83 h of operation. (22% more coal was consumed and 57% more operating time was accumulated.)
• The boiler outlet pressure (B.O.P.) maxed out (<-2.2" W.C.) after consuming 57,000 lb of coal.	• The B.O.P. maxed out after consuming 64,000 lb of coal (12% more coal was consumed.).
• The B.O.P. started at -0.8" W.C. and began decreasing at 47,000 lb of coal consumed. There was 10,000 lb of coal consumed between the time the B.O.P. started to decrease and when the gauge maxed out. This is equivalent to 8.7 h of operation.	• The B.O.P. started at -0.8" W.C. and began decreasing at 56,000 lb of coal consumed. There was 8,000 lb of coal consumed between the time the B.O.P. started to decrease and when the gauge maxed out. This is equivalent to 8.9 h of operation.
• The sootblowing frequency was typically every half hour and increased to 1.5 and then 2h before boiler shutdown (during the continuous test).	• After the B.O.P. maxed out, the soot blowing frequency increased to 2, 2.75 2.5, and 2h before the forced shutdown.
• The boiler was cleaned out on 11/23/94 and 855 lb of ash were removed from the furnace/convective pass entrance and 180 lb of ash were removed from the breaching for a total of 1,035 lb. There was 3,979 lb of ash introduced into the boiler (6.50% ash as-rec.; 61,216 lb of coal fired); 26.0% of the ash was retained in the system.	• The boiler was cleaned out on 12/09/94 and 740 lb of ash were removed from the furnace/convective pass entrance and 175 lb of ash were removed from the breaching for a total of 915 lb. There was 4,693 lb of ash introduced into the boiler (6.29% ash as-rec.; 74,606 lb of coal fired); 19.5% of the ash was retained in the system.

Table 3-5. Deposition Summary -- Two Continuous Tests

11/21/-11/22/94 -- 15.0-16.4 Million Btu/h	12/05-12/07/94 -- 12.7-12.8 Million Btu/h
• 37,945 lb of coal were consumed at a rate of 1,148 lb/h for 33 h of operation	• 53,476 lb of coal were consumed at a rate of 904 lb/h for 59 h of operation. (41% more coal was consumed and 79% more operating time was accumulated.)
• The boiler outlet pressure (B.O.P.) maxed out (<-2.2" W.C.) after consuming 33,927 lb of coal	• The B.O.P. maxed out after consuming 43,080 lb of coal (27% more coal was consumed.)
• The B.O.P. started at -0.8" W.C. and began decreasing at 24,000 lb of coal consumed. There was 10,000 lb of coal consumed between the time the B.O.P. started to decrease and when the gauge maxed out. This is equivalent to 8.7 h of operation.	• The B.O.P. started at -0.8" W.C. and began decreasing at 35,000 lb of coal consumed. There was 8,000 lb of coal consumed between the time the B.O.P. started to decrease and when the gauge maxed out. This is equivalent to 8.9 h of operation.
• The sootblowing frequency was typically every half hour and increased to 1.5 and then 2h before boiler shutdown (during the continuous test).	• After the B.O.P. maxed out, the soot blowing frequency increased to 2, 2.75 2.5, and 2h before the forced shutdown.
• The ID fan amperage exhibited a decrease from ~31.5 amps to 30.0 amps after consuming ~1,000 lb of coal. The amperage then slowly increased to ~32.5 over the consumption of ~27,000 lb of coal.	• The ID fan amperage was less than that observed during the 15 million Btu/h tests because of the decreased volume of flue gas and was ~28 amps as compared to 30 to 32.5 amps. The amperage was relatively constant at ~28.5 with an increase to ~29.5 at the time of shut down.
• The convective pass temperature decreased from ~1,300 to 1,000°F while the B.O.P. was decreasing.	• No temperature data was collected.
• Steam production increased as the test progressed.	• Steam production remained relatively constant during the test.

5 and 3-11. Consequently, Figures 3-13 through 3-17 were prepared which show the boiler outlet temperatures, based on a 24-hour clock, for November 21 and 22, 1994, and December 5 through 7, 1994, respectively. Figures 3-13 through 3-17 are traces of only the boiler outlet temperature from the circular charts, which normally contain four temperatures. The decreases in the temperature occur when sootblowing the convective pass. The furnace ash is also blown down after sootblowing the convective pass.

MCWM Demonstration

During this reporting period, the MCWM demonstration was started. A total of 418.5 hours of operation were accumulated during January and February 1995, of which 69.7 hours were with MCWM firing (6.0 hours of operation per 1.0 hour of MCWM firing). To date, the MCWM demonstration includes the completion of the construction of the MCWM preparation circuit, shaking down the circuit, and MCWM firing.

The primary objectives of the testing was to evaluate the burner firing MCWM. The data were still being reduced at the time of report preparation. The results from the MCWM testing will be presented in the Phase I final report to be prepared May/June 1995. Testing for the remainder of the demonstration (March and April 1995) will be to achieve high coal combustion efficiency without natural gas cofiring, examine furnace and convective pass deposition, and determine the extent of deposition during continuous operation.

Reactivity Study of Coal and Char Samples

In an attempt to explain similar maximum carbon burnouts obtained when firing two different micronized coals (Upper Freeport seam and Kentucky (from a previous test program)) in the demonstration boiler, a study of the reactivities of the raw coals and chars/ash samples has been initiated. Char morphology and physical characteristics are also being examined. Coal samples and char samples from three days of testing (March 29, April 8, and July 14, 1994) were selected based on the availability of samples for petrograhic analysis and reactivity studies. The reactivity was determined in a Perkin Elmer Thermogravimetric Analyzer. Isothermal reactivities at 375, 400, 425, and 450°C were determined for all three raw coal samples. Reactivity and burning profiles are being determined currently for char/ash samples. The data are also being reduced.

Evaluate Erosion-Corrosion and Deposition Characteristics

Formation of ash deposits and erosion of tube material by fly ash and unburned char were studied in the convective section of the boiler while firing micronized coal (Brookville Seam coal). Deposition is favored by the relatively low convective section gas velocity and high temperature gradient around a heat exchanger tube. Erosion of tube material by impaction of particles is expected at high convective section gas velocities.

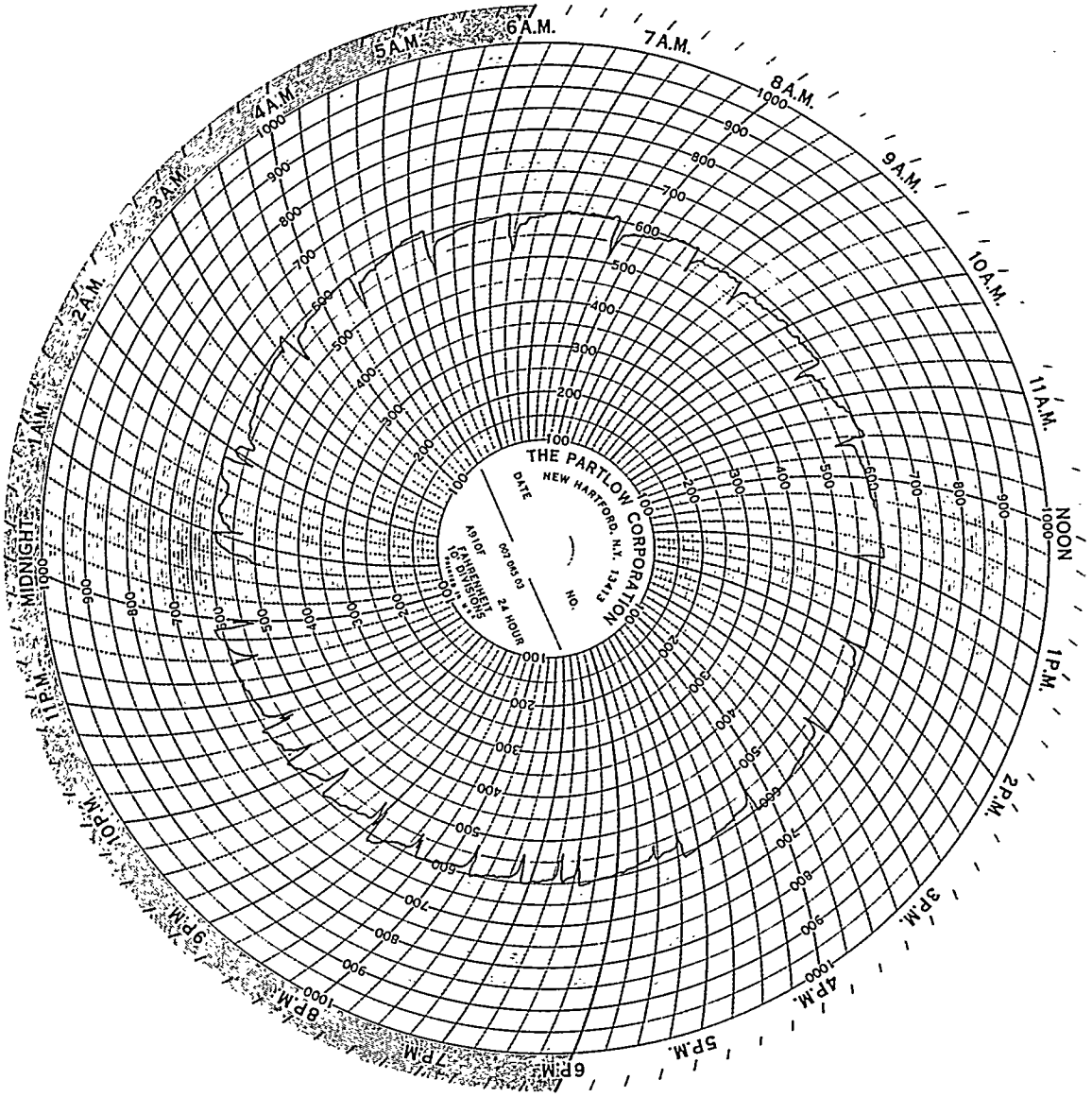

Figure 3-13. BOILER OUTLET TEMPERATURE ON 11/21/94

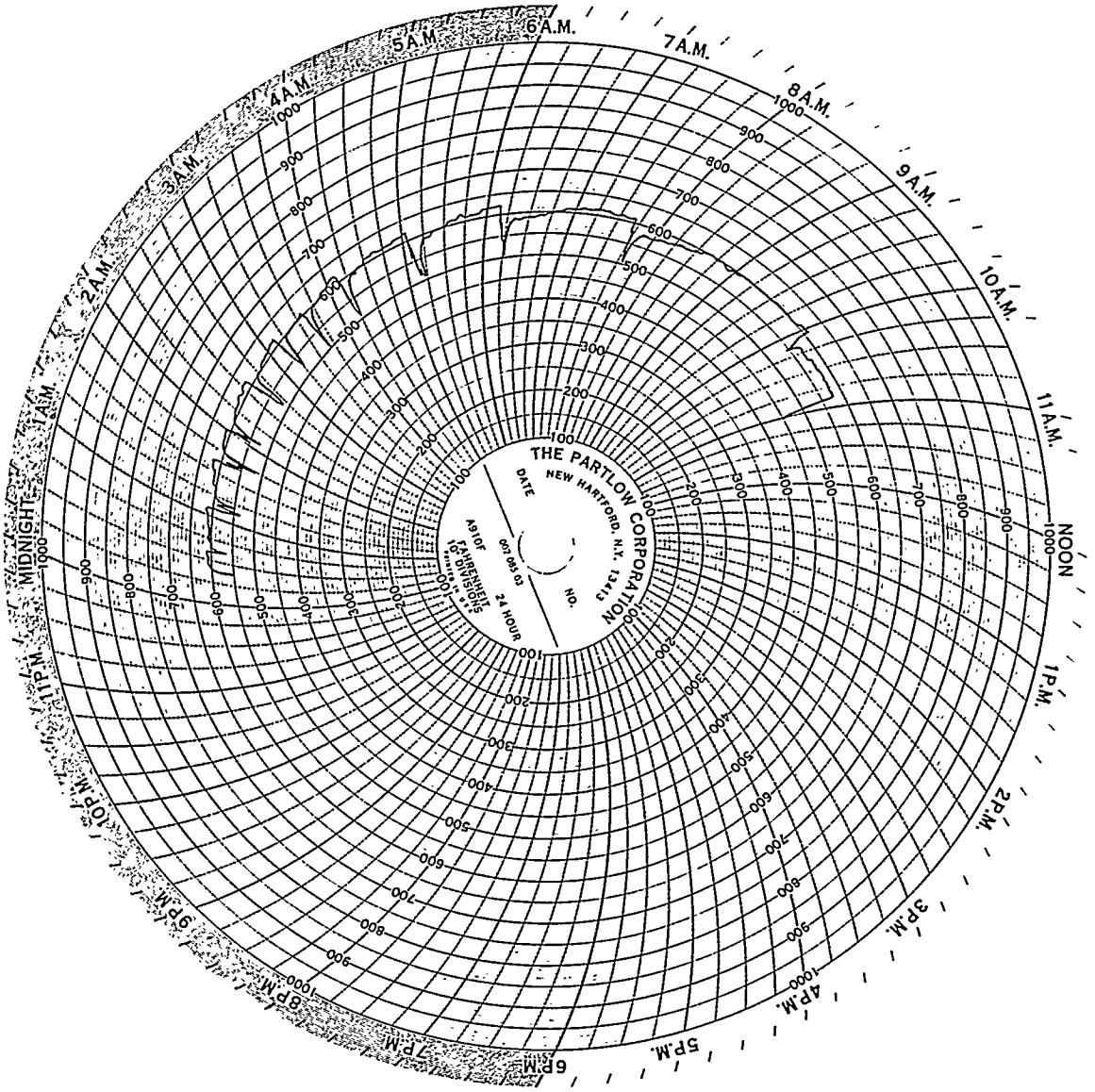

Figure 3-14. BOILER OUTLET TEMPERATURE ON 11/22/94

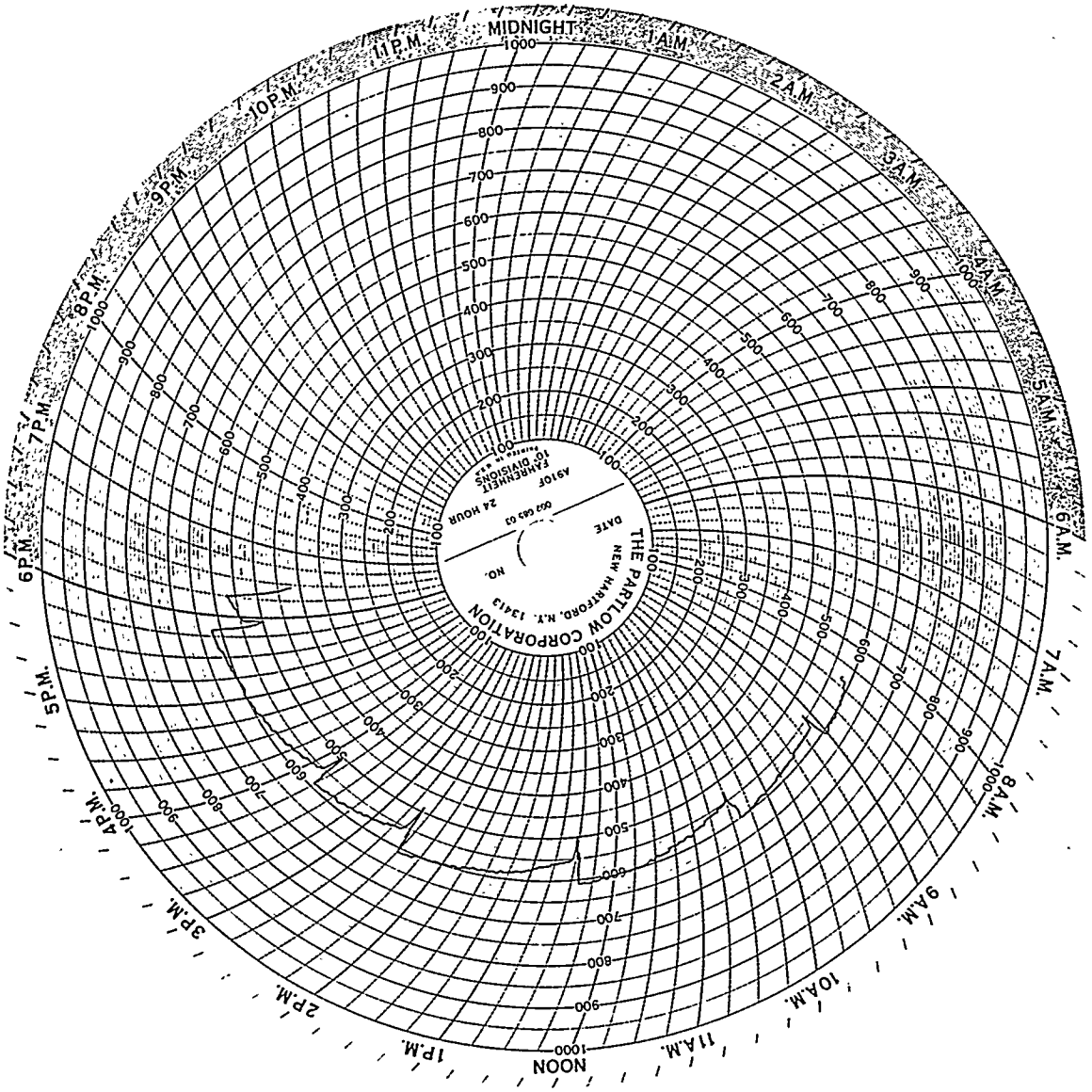

Figure 3-15. BOILER OUTLET TEMPERATURE ON 12/05/94

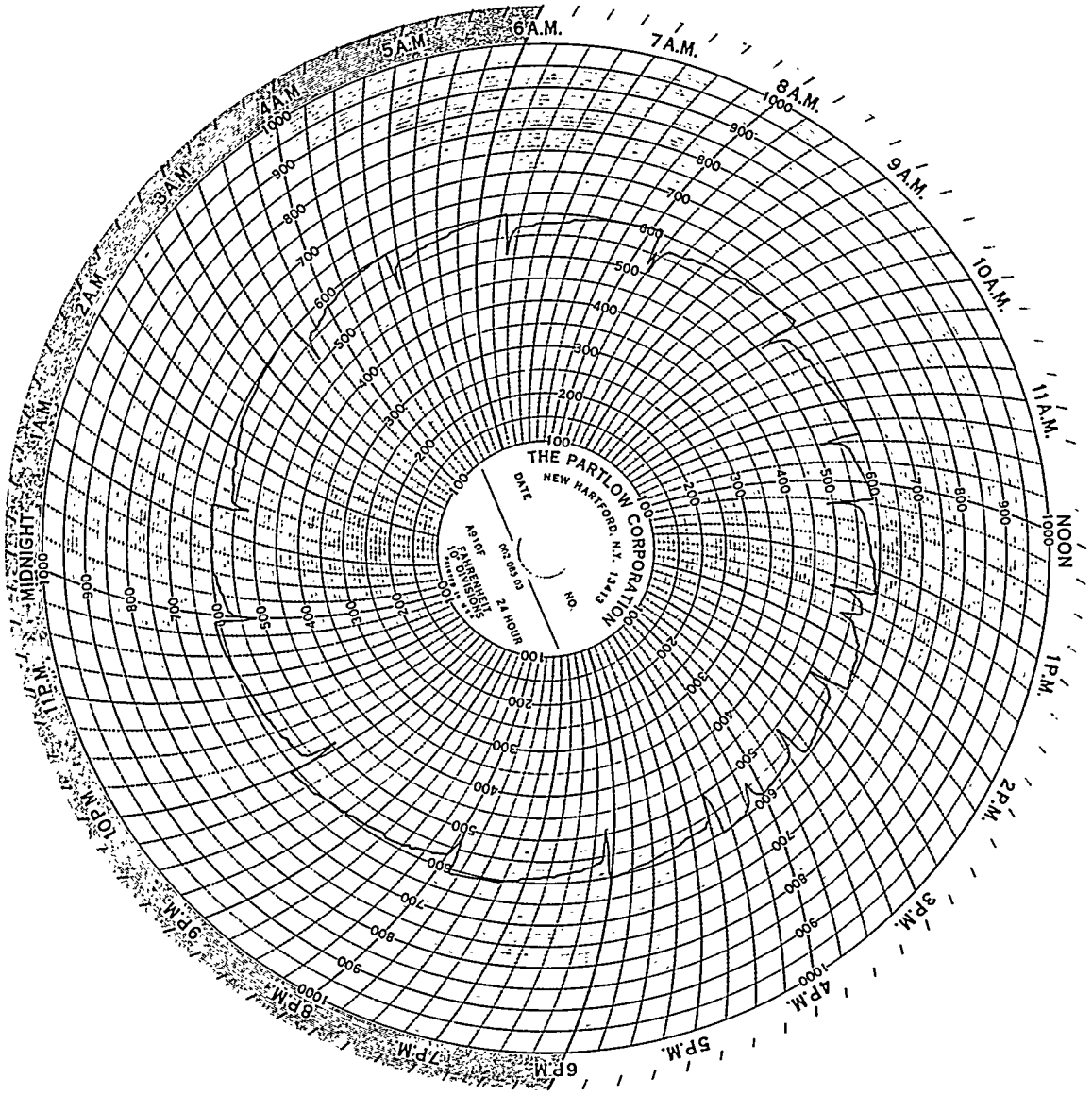

Figure 3-16. BOILER OUTLET TEMPERATURE ON 12/06/94

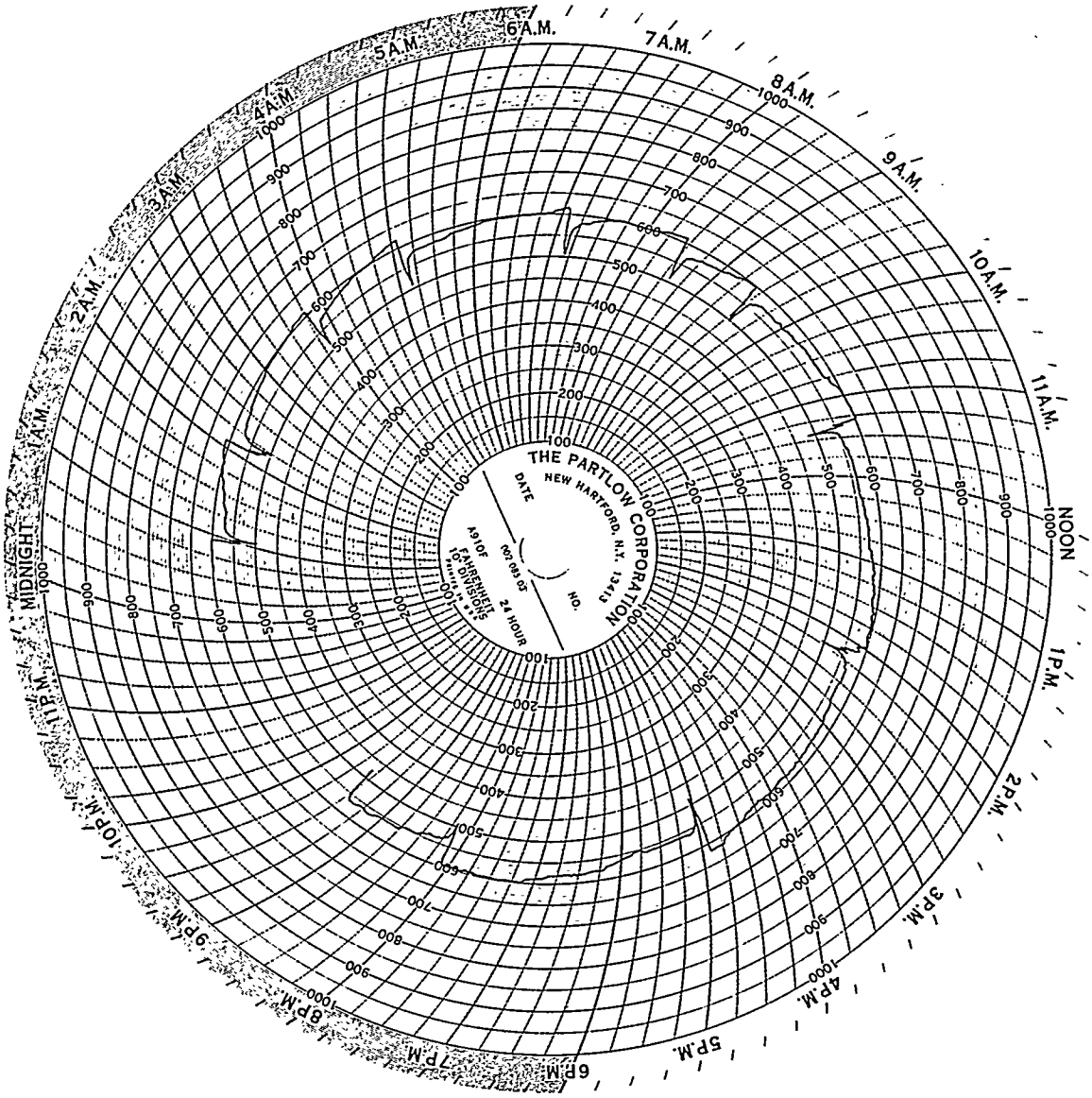

Figure 3-17. BOILER OUTLET TEMPERATURE ON 11/21/94

Deposition of Ash

The trajectories of particles suspended in the gas around a single tube in crossflow, described elsewhere[4], are shown in Figure 3-18. Small particles (10 μm) respond to changes in direction of the gas flow and pass around the tube under the aerodynamic drag on the particles. In the presence of a temperature gradient within the boundary layer around heat exchanger tubes, the thermophoretic force causes diffusion toward the lower temperature region, and deposition occurs on the surface of the tubes.

To evaluate the effect of the temperature gradient on ash deposition, an air-cooled carbon steel tube was used as a probe for measurements when the boiler is firing micronized coal at rate of 4.4 MW_t. The probe was cooled to maintain its temperature at 450, 550, or 650 K and placed in the convective section flow for 2 hours. The flue gas temperature at the location of the probe was 890 K, convective section gas velocity 3.1 m/s, and particle concentration 3.0 g/m^3.

Removal of the accumulated ash covering the circumference of the probe showed patterns of deposition versus angle with respect to the flow direction, as shown in Figure 3-19. The mass of the deposit, collected from 12 sectors at angles from -165° to 165°, was converted to a time-averaged rate, assuming a constant rate of deposition over the 2 hour exposure period. The rate of deposition increases as the temperature gradient within the boundary layer increases by decreasing the probe temperature from 650 to 450 K.

Deposition measurement at a probe temperature of 450 K were repeated 3 times. The pattern of deposition versus angle for 450 K, shown in Figure 3-19, was obtained by averaging the results from the triplicated measurements. The deposit is relative thin on the upstream side at angular positions from -45° to 45°, the region over which impaction of large particles (50 μm) was predicted to occur. The rates of deposition on the probe at temperatures of 550 and 650 K were measured once, and their patterns are shown in Figure 3-19.

Deposits collected on a metal specimen, which was mounted in the opening formed by removing a section from the probe, were observed under scanning electron microscope. The specimen was placed on the upstream stagnation line of the air-cooled support, exposed to the convective section flow at a velocity of 3.1 m/s, and cooled to maintain at temperature of 450 K for 2 hours. The sizes of the particles in the deposits were up to 20 μm. Both ash and unburned char particles occurred in the deposits.

Erosion of Tube Materials

Erosion of carbon steel by particles under the influence of a high velocity gas jet was measured, and the changes in erosion rate with metal temperature and jet gas oxygen concentration were compared with the values calculated by the erosion-oxidation model [5]. Using the model and experimentally determined coefficients for metal and oxide erosion, estimates were made of the erosion rate of a boiler tube for typical conditions in the convective section: gas temperature 890 K,

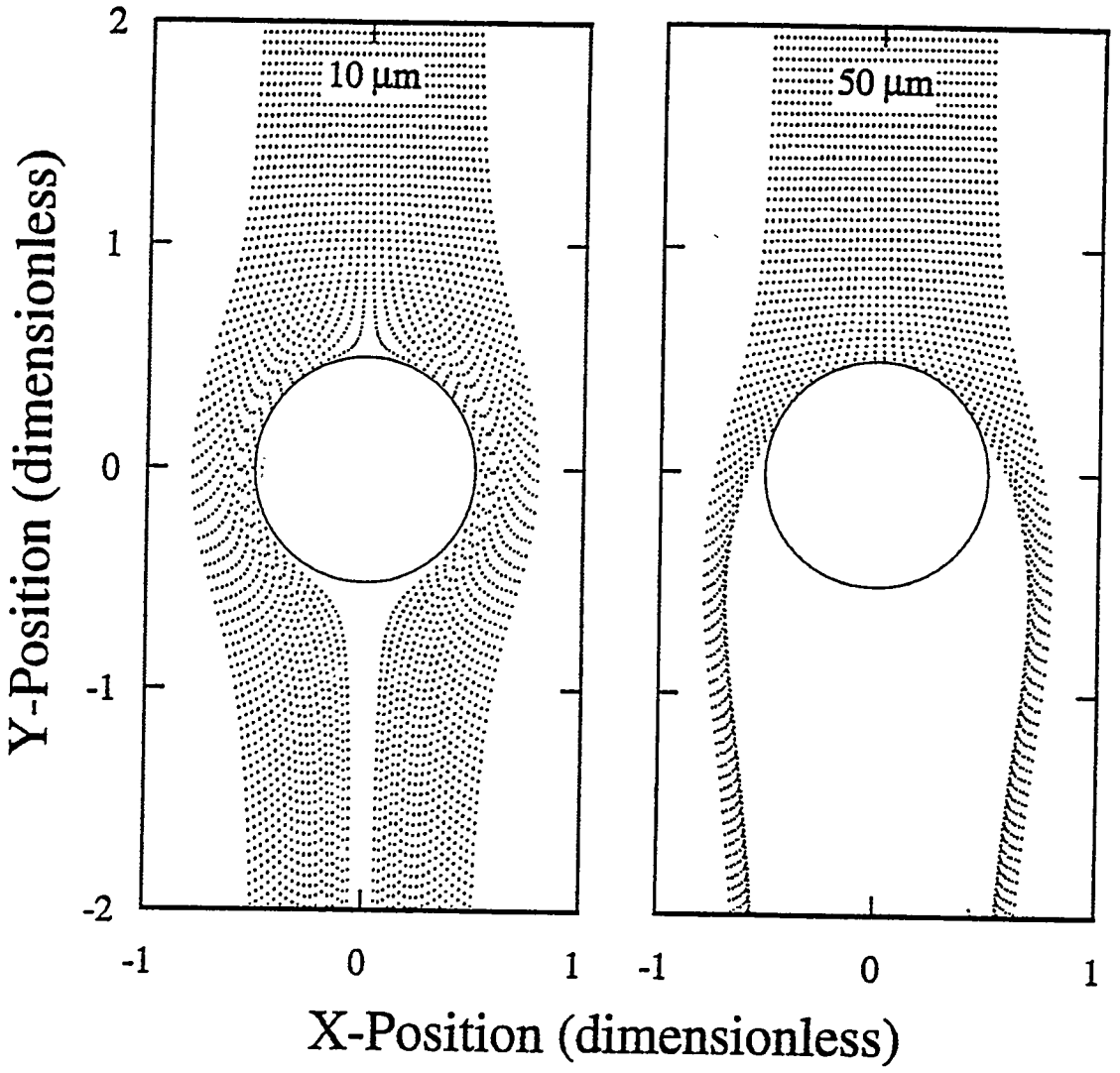

Figure 3-18. TRAJECTORIES OF PARTICLES UNDER THE AERODYNAMIC DRAG AROUND A SINGLE TUBE

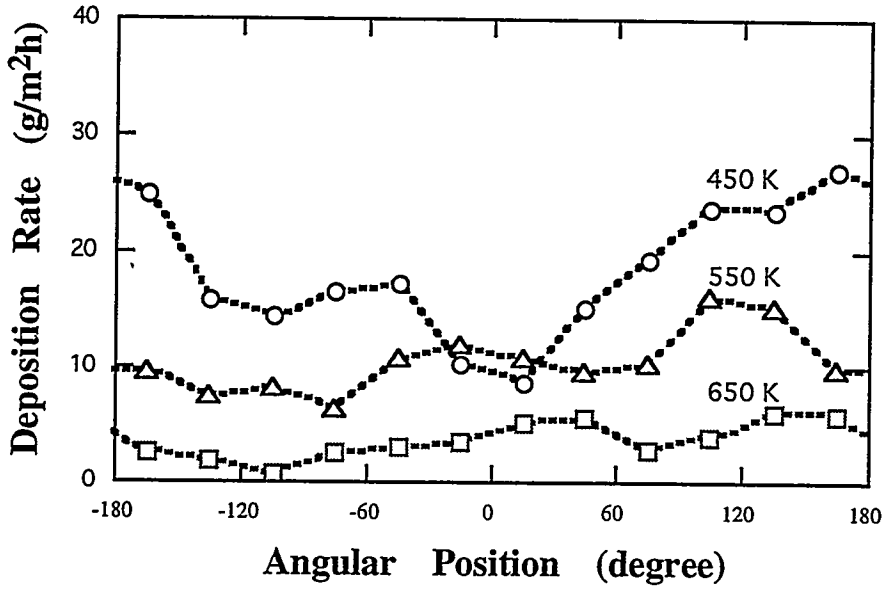

Figure 3-19. DEPOSITION OF ASH ON AN AIR-COOLED TUBE EXPOSED TO THE CONVECTIVE SECTION FLOW AT VELOCITY OF 3.1 m/s

excess oxygen 3.4 vol%, particle loading 3.0 g/m^3, particle density 835 kg/m^3, metal temperature 550 K, tube diameter 51 mm, and the particle size distribution of the baghouse catch[5].

Estimates of the erosion rate as a function of angular position about the circumference of the tube are shown in Figure 3-20. At a relatively low velocity of 5 m/s the erosion rate is low, and erosion occurs only from the oxide layer. A distinguishing feature of oxide erosion is that the rate is greatest at normal incidence, so the maximum erosion occurs at the stagnation line where the impaction energy is also high. Increasing the gas velocity from 10 to 15 m/s icreases the rate of oxide removal and decreases the steady thickness of the scale. At a gas velocity of 20 m/s, the oxide layer becomes thin so that erosion removes both oxide and metal, and the rate begins to increase markedly. With further increase in gas velocity to 25 m/s, the scale becomes even thinner, and erosion tends toward the rate characteristic of bare metal. In competition with these changes, the location of the maximum rate moves toward an angle 20° from the stagnation line, where oblique collision angles of particles favor the ductile erosion of metal.

Raask[6] considered 0.05 μm/hour to be the highest acceptable rate of tube thickness loss. Erosion on the upstream stagnation line of the tube is expected to be less than this rate at flue gas velocities below approximately 9.4 m/s, under the conditions of metal temperature, particle size, particle composition, and particle loading investigated. Velocities higher than this value may be expected in the convective sections of some boilers designed for oil firing. According to the model, erosion at the location near 30° from the stagnation line, where severe erosion is observed at high gas velocities, reaches 0.05 μm/hour at a gas velocity of between 10 and 15 m/s.

Determine Erosion Characteristics of Materials Subjected to Atomized Micronized Coal-Water Mixtures

Background/Introduction

Successful utilization of micronized coal-water mixtures (MCWMs) requires satisfactory atomization of the fuel. In the atomizer, a high pressure air blast (< 200 psig) shears the slurry stream into droplets. Although small in size (~ 20 μm), the large velocities and erosive-corrosive properties of the MCWM result in rapid metal wastage of atomizer components and excessive boiler down time. In order to better understand the erosive processes that occur during MCWM atomization, a fundamental erosion study was conducted.

Experimental Design

Since the last reporting period the experimental procedure has been redesigned to measure erosion of a removable nozzle *orifice disk* (Figures 3-21 and 3-22) instead of a flat material coupon. The new configuration provides a more accurate representation of atomizer erosion and lends itself more easily to recirculation of used slurry. The erosion rate is calculated by measuring the mass lost from the orifice disk and dividing by the total of slurry throughput. Results are expressed in terms of milligrams lost per gram of slurry (i.e., mg/g).

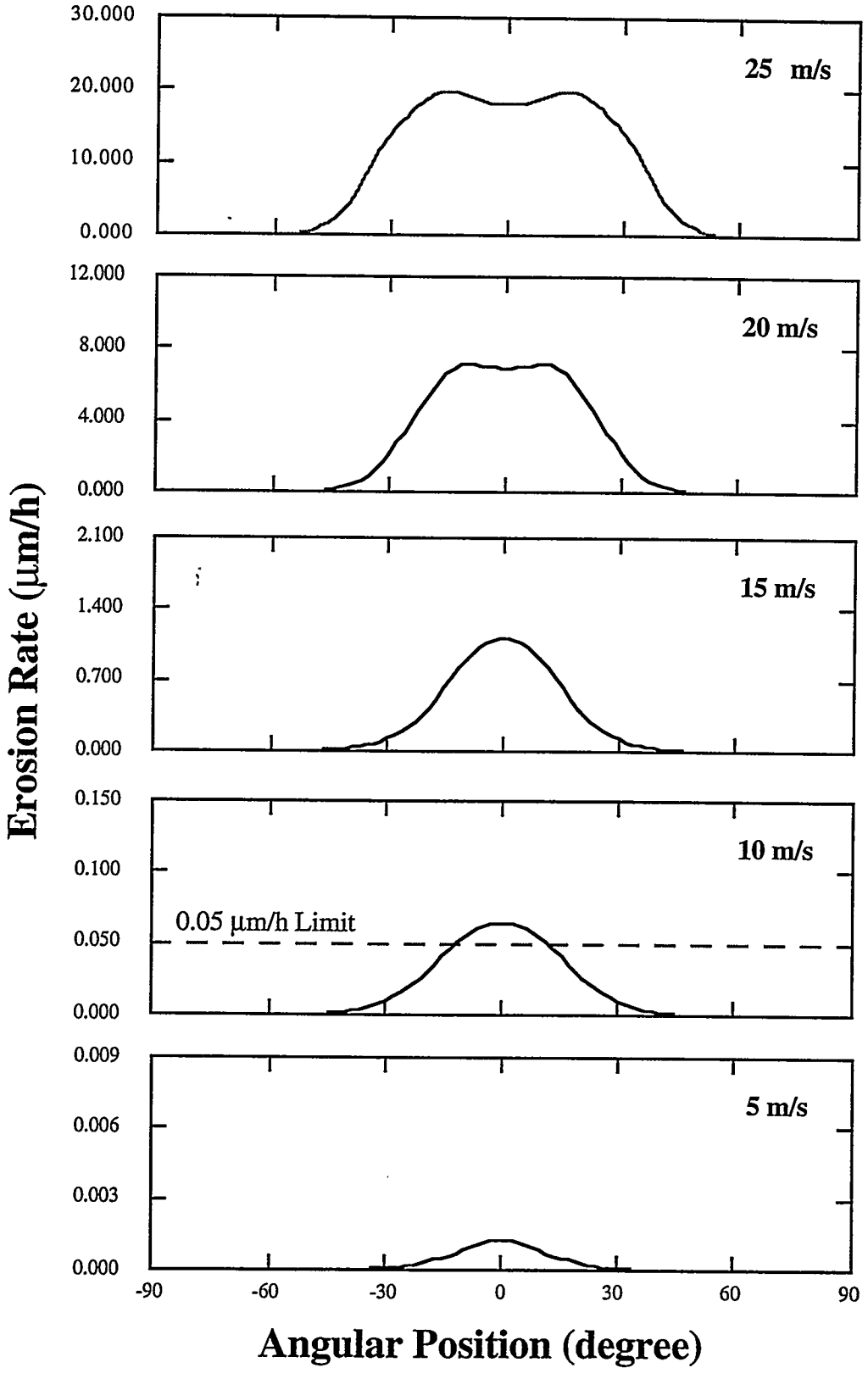

Figure 3-20. ESTIMATES OF THE EROSION RATE AS A FUNCTION OF ANGULAR POSITION ABOUT THE CIRCUMFERENCE OF THE TUBE

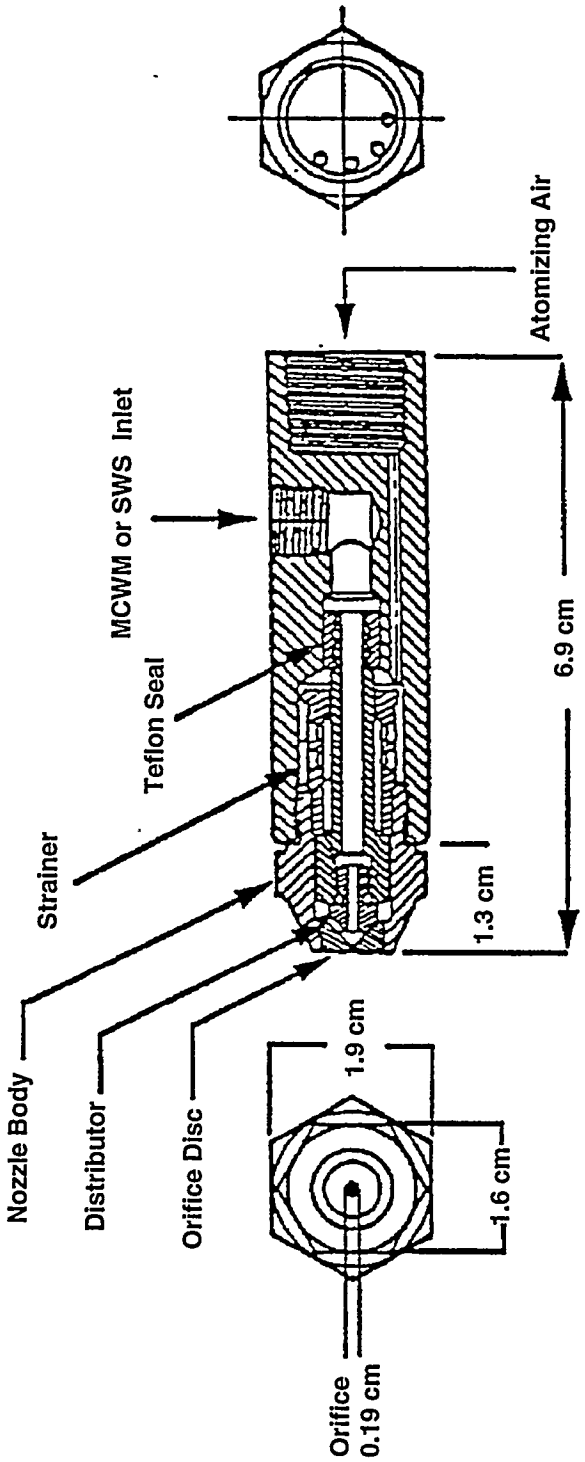

Figure 3-21. SCHEMATIC DIAGRAM OF THE DELAVAN NOZZLE

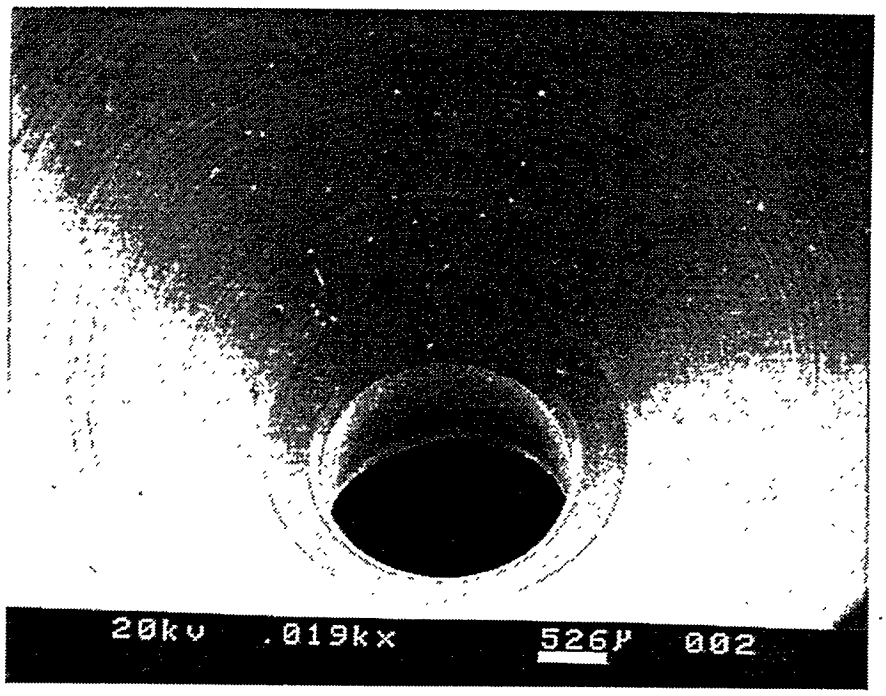

Figure 3-22. PHOTOMICROGRAPH OF THE UNMOLESTED ORIFICE DISK

Description of Apparatus

A closed slurry atomization loop has been designed and constructed around the existing erosion-corrosion testing chamber [5]. Two fluid circuits make up the loop, the fuel train and the atomization air circuit. Both lines are plumbed in series using off-the-self hardware and the component parts are:

- Fuel train
  - 5 gallon steel tank, fabricated from 13" pipe and cap
  - 1HP Robbins and Myers 6P3-CDQ Moyno progressive cavity pump
  - 1/4 HP Reliance mixer
  - 3/8" high pressure hose
  - Micro Motion Model D25 mass flow meter
  - Delevan model 33769-99 variflow nozzle (Figure 3-21), modified for air blast atomization
  - 3/4" tygon tubing return line
- Atomization air circuit
  - Dayton Speedaire 5HP single stage air compressor, model 3Z203B
  - 1/2" Speedaire regulator and filter arrangement
  - Rotometer (100 SCFH capacity)

Shakedown Testing/Preliminary Evaluation

At the end of the last reporting period, atomization erosion testing with MCWM had just started. Two shakedown tests (Tests 1_{CWS} and 2_{CWS}) were performed using MCWM containing cleaned Brookville seam coal at solids loadings of 10 and 50 wt.%, respectively. Each experiment was planned for a 100 hour duration but both were prematurely aborted due to system malfunctions, Tests 1_{CWS} and 2_{CWS} were approximately 63 and 5 h in length, respectively. Neither experiment resulted in a measurable erosion rate and both exposed a weakness (i.e., continuous changes in solids loading, pH, and particle size) in the experimental technique.

Elimination of the experimental uncertainty present in Tests 1_{CWS} and 2_{CWS} was accomplished by designing a new slurry containing silica (SiO_2) and distilled water. Silica-water slurries (SWS) produce no leachate (eliminating possible corrosive species), are more resistant to particle comminution, need no chemical additives (dispersant or pH modifier), and solids loading can be kept under 10 wt.% (important for computational fluid dynamic analysis). Overall, the utilization of SWS instead of MCWM makes identification and interpretation of the mechanisms involved in atomizer erosion more readily attainable and will therefore be used for the remainder of this study.

Experimental Results

Two sets of erosion tests had been conducted (1_{SWS} and 2_{SWS}) using 10 wt.% SWS. The first group of experiments was conducted using only one nozzle orifice disk in an attempt to investigate the variation in erosion rate with time. To clarify the idea, if an erosion test was conducted for *X* hours and at the end of those *X* hours the damaged orifice was weighed, an overall mass loss would be recorded and a single erosion rate would be calculated. Such a

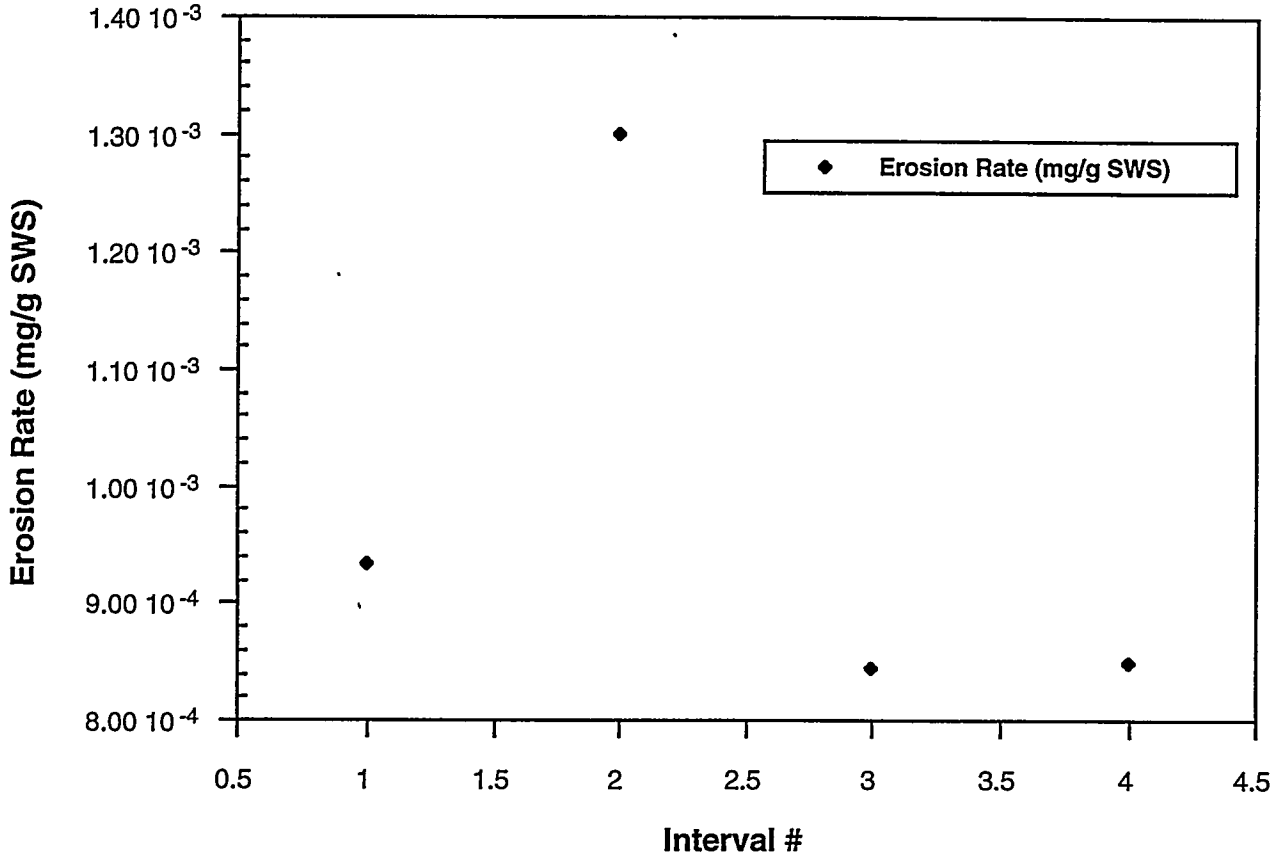

Figure 3-23. TEST 1_{SWS}, EROSION RATE *vs.* TIME INTERVAL

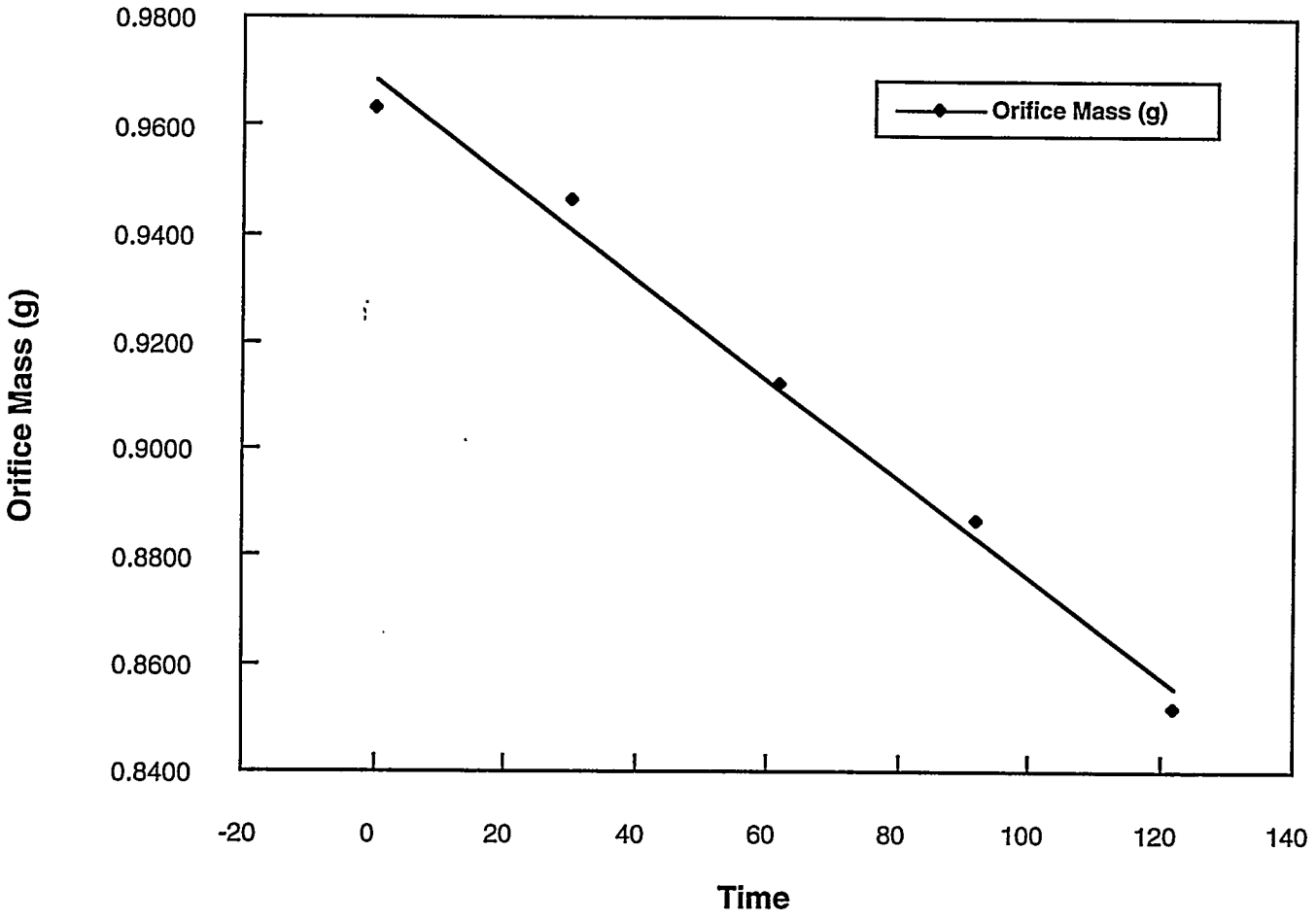

Figure 3-24. TEST 1_{SWS}, ORIFICE MASS *vs.* TIME

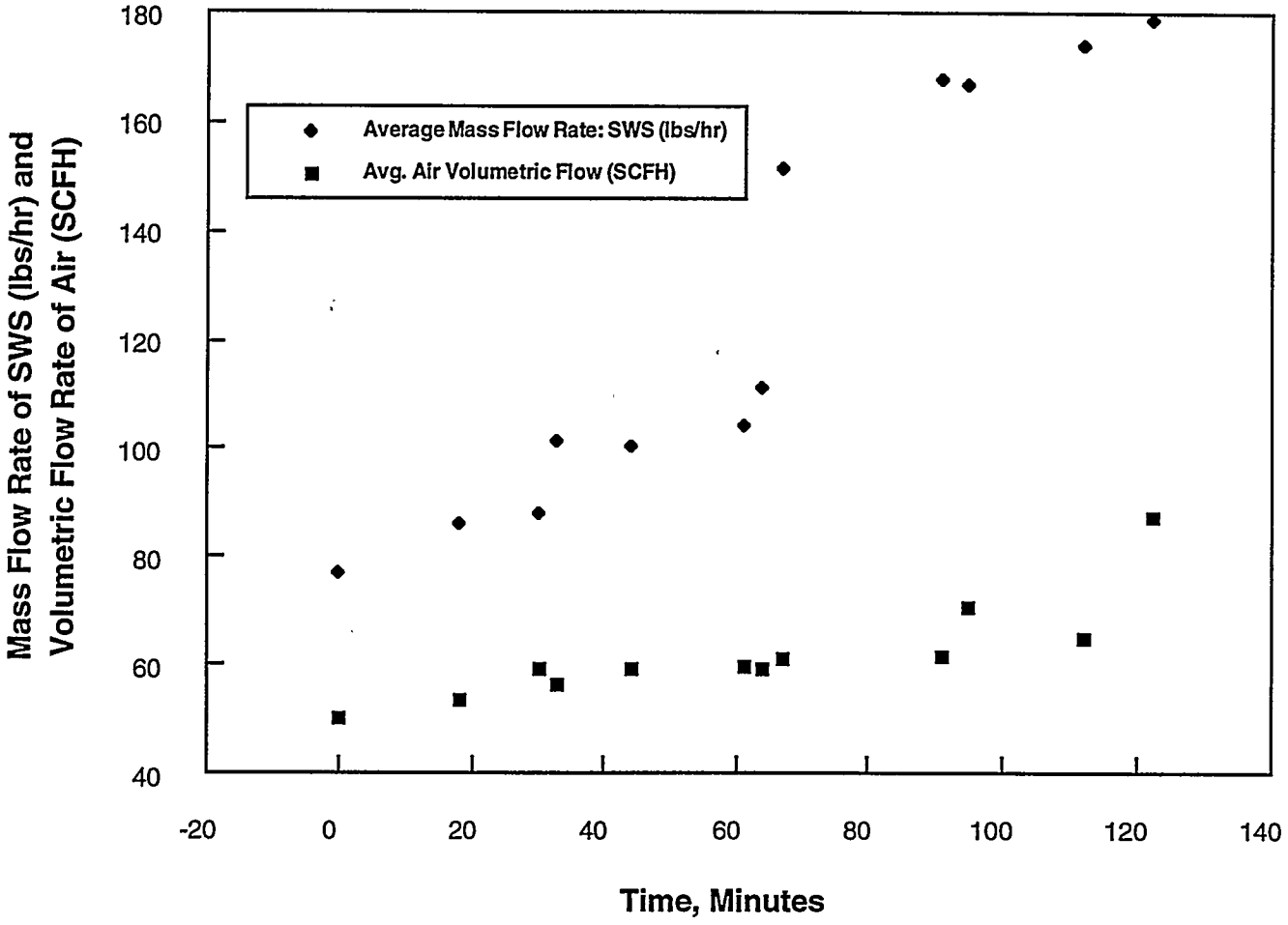

Figure 3-25. TEST 1_{SWS}, FLOW RATES *vs.* TIME

and atomization air pressure was constant at 80 psig. An increase in air flow rate was unavoidable and the influence of such an increase has not yet been evaluated. Ideally, air and slurry flow rates should be held constant, but the testing rig does not have such capability.

Results of the four tests in experiment 2_{SWS} show a trend toward increasing erosion rate as a function of time. Scanning electron micrographs analyzed in chronological order show that areas of extreme material loss are first formed at the air and slurry collision points, then propagate around the circumference of the orifice disk. Comparison of the eroded surface to previously reported topographies does not yield a direct correlation but rather a possible combination of the classic micromachining mechanism (material gouged out of the surface by an impacting "machine tool") observed by Finnie[7] and the platelet mechanism (extrusion and forging of a material lip followed by removal of the "platelet" by subsequent particle impact) proposed by Levy [8]. Figures 3-22 and 3-26 (a & b) show the unmolested orifice and the eroded surface near the air/slurry collision point, respectively.

Measured values of erosion rate for the four intervals in experiment 2_{SWS} range from about 6.5×10^{-4} to about 1.5×10^{-3} g/g SWS. Plots of erosion rate and mass loss vs. time are given in Figures 3-27 and 3-28.

Although more realistic than Test 1_{SWS}, Test 2_{SWS} has two undesirable features which restrict interpretation of the data. Throughout the course of a test, the atomizing air flow rate increased continuously, which may have affected SiO_2 particle velocitles. In addition, the air swirler experienced severe mechanical wear, as shown in Figure 3-29. Swirler degradation undoubtedly alters flow patterns within the mixing region, and this will be eliminated or computationally evaluated before future erosion tests are conducted.

Modeling Efforts and Future Work

In an attempt to match theory with experimental measurements, observed erosion rates will be compared with those calculated using previously published erosion models. Two models have been selected for the analysis, the monolayer energy dissipation model derived by Lyczkowski and Bouillard[9] which emphasizes fluid flow analysis, and the comprehensive model of Sundararajan[10] which focuses on impact dynamics and solid mechanics.

Important to each model are the trajectories and impact velocities of the SiO_2 particles. For that reason, a computational fluid dynamics code (CFD) FLUENT 4.2 is being utilized to provide insight into the flow behavior within the mixing region of the atomizer. Data obtained from the CFD output will then be input into the erosion models and erosion rates calculated. First attempts at such a procedure have been limited by the capabilities of the FLUENT code (three phase system and one phase capability) and yielded erosion rates approximately four orders of magnitude larger than observed values.

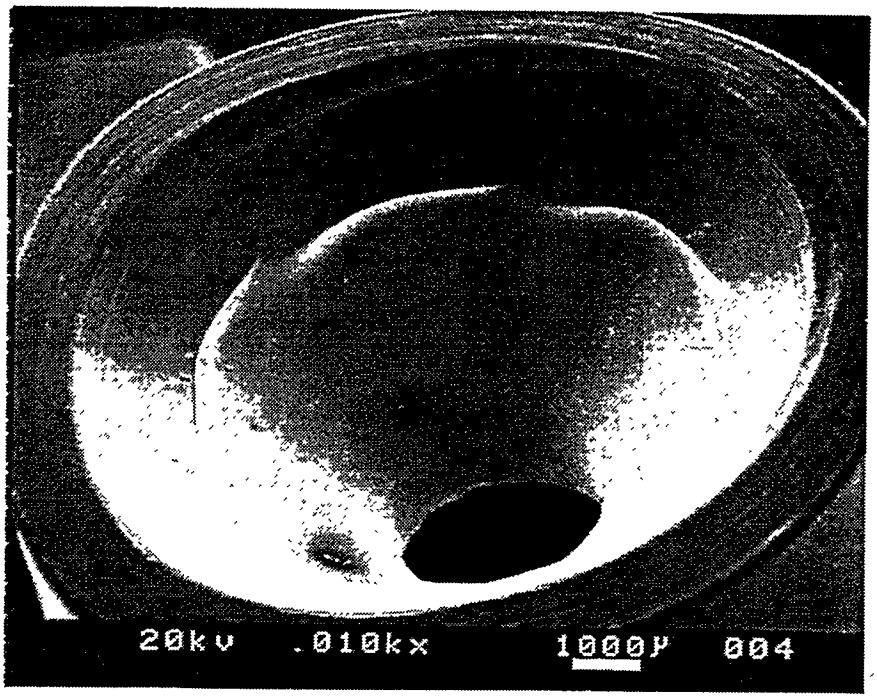

(a)

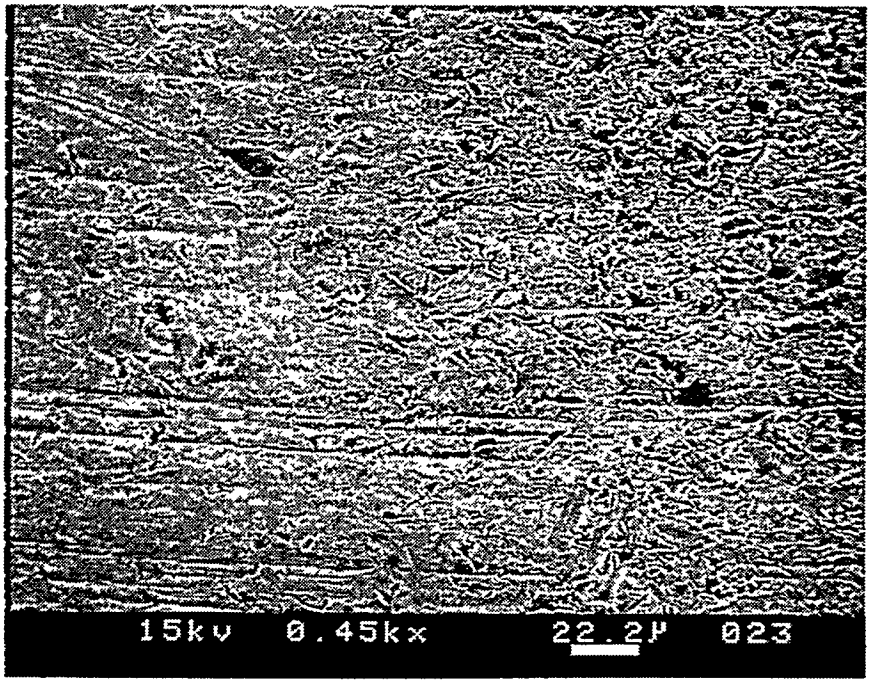

(b)

Figure 3-26. PHOTOMICROGRAPH OF (a) MODEL DISK AND (b) CLOSEUP OF AIR/SLURRY COLLISION POINT

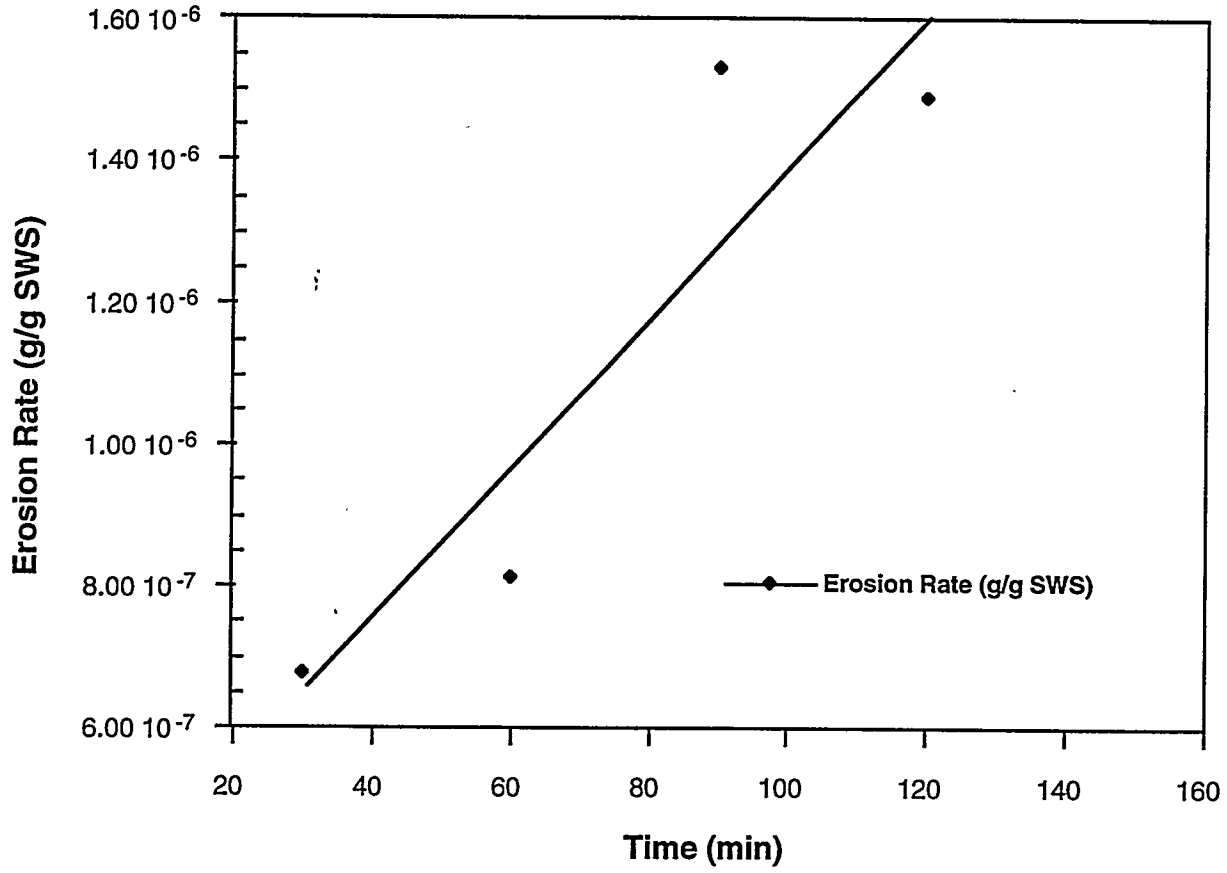

Figure 3-27. TEST 2_{SWS}, EROSION RATE *vs.* TIME

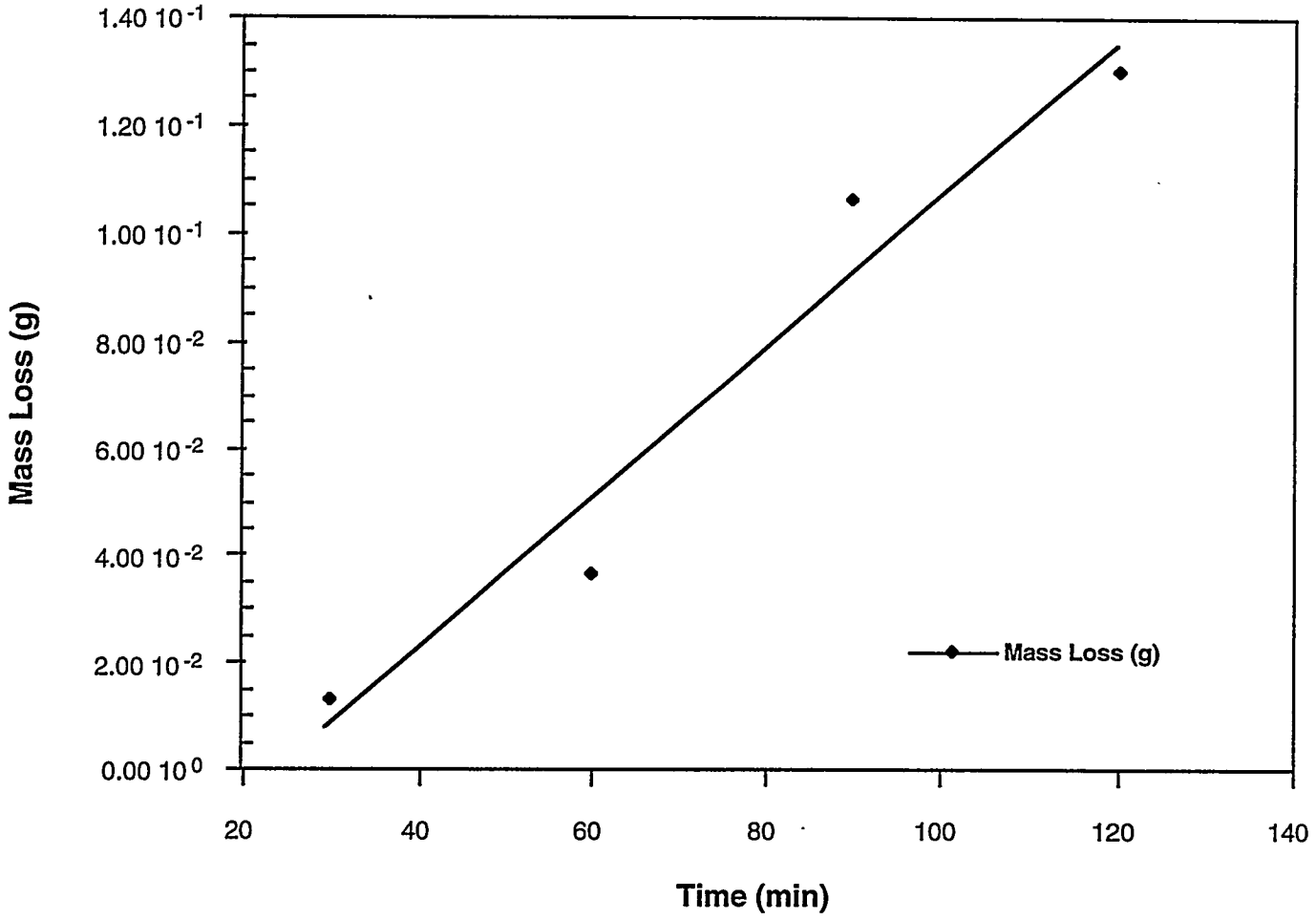

Figure 3-28. TEST 2_{SWS}, MASS LOSS *vs.* TIME

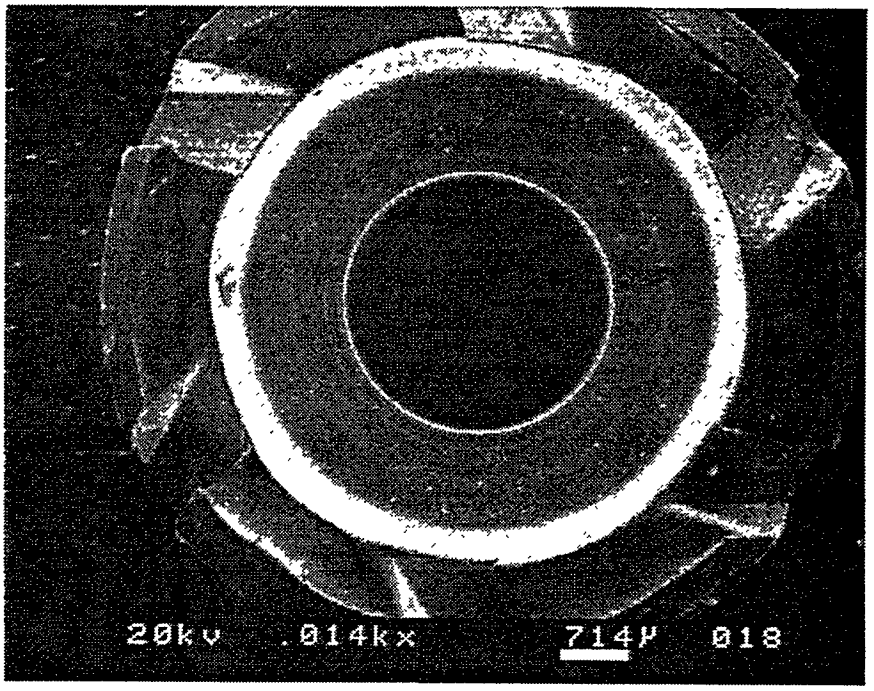

Figure 3-29. PHOTOMICROGRAPH OF THE ERODED SWIRLER

Future experiments will be conducted *without* atomization air. Modification of the investigation in this manner reduces the experimental setup to a laminar single phase system containing a dilute second phase. Such a system is readily analyzed with the FLUENT software and subsequent analyses should yield more acceptable values of orifice erosion rate.

Computer Modeling of the Swirling Turbulent Diffusion Jet of Air and Coal in the Demonstration Boiler

The work discussed in this section is presented in two subsections. In the first subsection, titled "Computer Modeling of Recirculation During Coal Combustion in Boilers", work was performed to model the near burner flow-field and its effect on coal particle trajectories, validate the model, and predict the recirculation in the demonstration boiler using a commercial DMC swirl burner. This burner is then compared to a second commercial burner in the second subsection, Comparative Analysis of Two Commercial, Low-NO_x Pulverized Coal Swirl Burners.

Computer Modeling of Recirculation During Coal Combustion in Boilers

The main objective of this work was to develop an improved understanding of the characteristics of swirling coal-based fuel flames in an oil-designed industrial boiler. The role of numerical modeling in adapting a low-NO_x burner for this retrofit application is described.

In this section, the effects of the near burner flow-field on the coal particle trajectories are discussed. The near burner flow-field can be characterized by the extent and intensity of recirculation. The operating parameters include the positions of secondary/tertiary air nozzles relative to the fuel nozzle, the velocity profiles at the furnace inlet, the ratio of secondary/tertiary air flow, the swirler type, and the swirl number.

Swirling Flow from a Low-NO_x Burner

Most low-NO_x burner technologies are based on the well known principle of internal air staging for NO_x control[11]. In an internally staged flame, a hot fuel-rich primary combustion zone is followed by a fuel lean burnout zone. The primary combustion zone at the exit of the burner contains less air than is required to completely combust the coal (substoichiometric). The purpose of the primary combustion zone is to maximize the evolution of nitrogenous volatile compounds, while simultaneously limiting oxygen availability. As coal is devolatilized in this substoichiometric zone, fuel nitrogen is forced to react to form N_2 rather than NO. When the primary zone stoichiometry is maintained in the range of 0.6-0.7, the conversion of fuel nitrogen to molecular nitrogen is optimized. The coal nozzles are designed to maximize the time and temperature experienced by the coal particles within this zone. Combustion is completed downstream of the burner where stoichiometric ratios of 1.15 to 1.2 exist to maximize carbon burnout.

Burner swirl and mass flow rate control are employed to establish this substoichiometric primary zone. Above a critical swirl number, an internal recirculation zone is formed where a percentage of flow is directed back towards the burner. This zone recirculates hot combustion

products back to the root of the flame promoting flame stability. When the air register is designed properly, this primary zone can be maintained at the correct condition throughout the load range.

The aerodynamics of flows generated by a swirl burner can be described as a fuel laden central primary air jet being mixed with the surrounding co-axial swirling flow. The annular swirling flow contains the main portion of the combustion air. It expands both inside the burner quarl and downstream inside the combustion chamber. The primary fuel containing air jet can be co- or counter-swirling or swirl free.

Inherent to expanding swirling flows is a high degree of turbulence generation. This feature, in connection with reverse flow which carries hot combustion products back towards the burner throat, can lead to very stable ignition and high combustion rates in the near burner field.

Grid Sensitivity in Swirling Flows

Sufficient resolution of grids is needed for the solution of swirling flow. Swirling flows involves steep gradients in the circumferential velocity (e.g., near the centerline of a free-vortex type flow) which will require a fine grid for accurate resolution. Various grids were tried for numerical convergence. A 30x27 grid was used for the modeling of the low NO_x burner. The computational geometry of the combustor is shown in Figure 3-30.

Based on the geometry and grid setup, predictions have been made by solving the finite-difference formulations of the governing equations for the conservation of mass, momentum, energy and chemical species. The governing equations are solved by the finite difference procedure embodied in the Computational Fluid Dynamics code employed (FLUENT).

Swirling Flow Models

Turbulence models have been developed over many years. For strong swirling flow, each of the turbulent shear and normal stresses should be calculated from different eddy viscosities, since the individual stress components may interact and develop quite differently in the flow field. The Reynolds Stress Model (RSM) involves the calculation of the individual Reynolds stresses and is the most suitable turbulent model for the simulation of a swirling flow. In order to utilize the RSM turbulence model, values for each Reynolds stress $\overline{u'^2}$; and for the turbulent dissipation rate, ε, at the furnace inlet are required.

In addition to the choice of a turbulent model, the reproduction of the measured flow field is also strongly dependent upon inclusion of realistic inlet, and boundary conditions. Because the partial differential equations applicable to confined, recirculating jets are elliptic, the solutions are a strong function of the boundary conditions, particularly the inlet profiles. The importance of inlet boundary conditions of numerical simulation of combustor flows has been stated by Sturgess (1983).

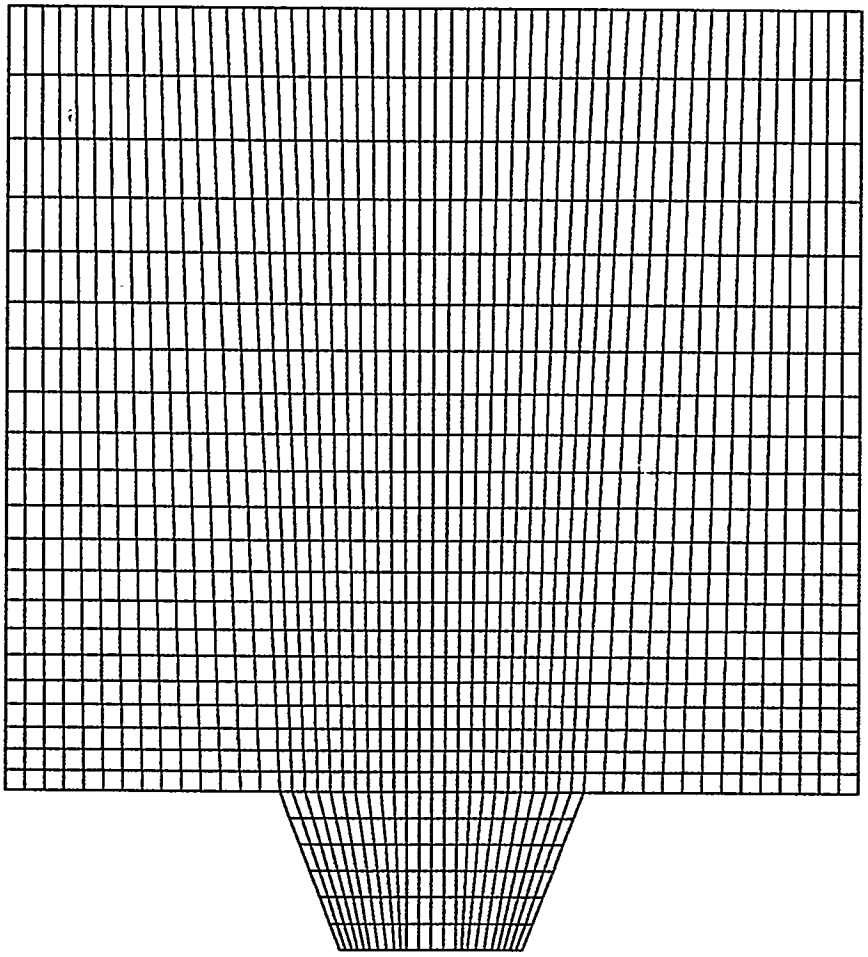

Figure 3-30. GRID PATTERN FOR THE RECIRCULATION STUDY IN THE DEMONSTRATION BOILER

Boundary Conditions

Velocity Components

The commonly used parameter to characterize swirling flows, the swirl number, is defined as the ratio of the axial flux of angular momentum to the axial flux of axial momentum:

$$S = \frac{\int_{R_1}^{R_2} uwr^2 dr}{R_2 \int_{R_1}^{R_2} u^2 r dr}$$

where R1 is the inner radius of the swirl vane (center body radius), R_2 is outer radius of the swirl vane (inside radius of inlet), and u and w are axial and tangential velocity components, respectively. If the axial velocity component is assumed to be constant, the swirl number becomes:

$$S_i = \frac{\int_{R_i}^{R_{i+1}} wr^2 dr}{\frac{R_{i+1}u}{2}(R_{i+1}^2 - R_i^2)}$$

where i is a tunnel number.

The axial velocity component, u, is calculated from

$$u = \frac{\dot{m}}{A_{eq}}$$

where $\dot{m}$ is the fluid mass rate and A_{eq} means the numerical inlet cross sectional area (instead of the actual burner outlet cross sectional area).

The tangential velocity distribution at the inlet depends on the type of swirlers, three of which are specified as follows:

1. Constant Angle: $w_{c1}=C_1$
2. Forced Vortex: $w_{c2}=C_2 \cdot r$
3. Free Vortex: $w_{c3}=C_3 \cdot 1/r$

where w=tangential velocity; C=swirler constant, which is determined for each case; and r=radial position (radius).

In order to provide a basis for comparison, all tangential velocity profiles are measured by a common swirl number, so that, the tangential velocity distributions at the inlet are:

$$w_{c1} = S\,u\,/g_{c1}\ ;\ w_{c2} = \frac{S\,u}{g_{c2}}\,r;\ w_{c3} = \frac{S\,u}{g_{c3}}\,/r$$

where g is the geometry constants:

$$g_{c1} = \frac{2}{3}\frac{1}{R_{i+1}}\frac{R_{i+1}^3 - R_i^3}{R_{i+1}^2 - R_i^2},\ g_{c2} = \frac{R_{i+1}^2 + R_i^2}{2R_{i+1}},\ g_{c3} = \frac{1}{R_{i+1}}$$

Turbulent Kinetic Energy

Often the turbulence quantities at the inlet to the model are uncertain and these quantities are forced to estimate the turbulence intensity, I, which is a measure of the "violence" of the eddies, that is, the time-average fluctuation of the velocity in the fluid. According to the definition of turbulent kinetic energy, k:

$$k = \frac{1}{2}\overline{u_i'^2} = \frac{1}{2}(\overline{u'^2} + \overline{v'^2} + \overline{w'^2})$$

where $\overline{u'^2}$ is the Reynolds stress component in the stream wise direction (normal to the flow inlet). In the modeling calculation, the turbulent kinetic energy at the inlet, K_{in} can be calculated from the turbulence intensity, I_{in}:

$$K_{in} = \frac{1}{2}(u_{in}\frac{I_{in}}{100})^2$$

In Cartesian coordinates, $I_x = 100\,\frac{\sqrt{\overline{u^2}}}{\overline{U}}\,\%;\ I_y = 100\,\frac{\sqrt{\overline{v^2}}}{\overline{U}}\,\%;\ I_z = 100\,\frac{\sqrt{\overline{w^2}}}{\overline{U}}\,\%$,

where $\bar{U} = \sqrt{\bar{u}^2 + \bar{v}^2 + \bar{w}^2}$, so total turbulence intensity at an inlet, I_{in}, is:

$$I_{in} = 100\,\frac{\sqrt{\overline{u_{in}'^2}} + \sqrt{\overline{v_{in}'^2}} + \sqrt{\overline{w_{in}'^2}}}{\overline{U}_{in}}\,\%$$

In general, the inlet turbulence intensity is a function of the flow details upstream. A very quiescent upstream flow might yield an inlet turbulence intensity of 2-3%. If the upstream flow involves flow over rough edges and/or turning and mixing, the inlet intensity might be as large as 10-12%. In engineering, I_{in} is about 10% for free jet, confined jet and flow in pipes; 30-40% for swirling flow [12].

Dissipation Rate

The inlet dissipation rate for swirl is an elusive quantity that is not readily measurable and this is reflected in the disparity among the equations used to calculate it. The dissipation rate is generally given by:

$$\varepsilon = C_{\mu}^{0.75}\frac{k^{1.5}}{\ell_m}$$

$$\text{or } \varepsilon = 8.3\, C_{\mu}\frac{k^{1.5}}{\ell_m}$$

For the case of an annular burner[13]:

$$\varepsilon = C_{\mu}\frac{k^{1.5}}{0.03y_a}$$

where y_a is the width of the annular gap of the burner; C_{μ} is an empirical constant (0.09), and ℓ_m is a length scale characteristic of the turbulence at the inlet. The inlet turbulence length scale, ℓ_m, is calculated by multiplying a radius (or diameter at the inlet) by a constant. For free turbulent jet flow, ℓ_m, is a function of the boundary layer thickness[14]. The inlet turbulence is generated by features in the upstream flow which may possess different characteristic length scales. In such cases, the length scale must be chosen that will yield a realistic value for the turbulence length scale.

In order to make a comparison, the inlet dissipation equation can be simplified to:

$$\varepsilon = \frac{k^{1.5}}{C_{\varepsilon}L_{eq}}$$

where C_{ε} is an empirical constant which ranges from 0.0025 to 1.52[15]. The constants can yield a dissipation rate that ranges over two orders of magnitude. L_{eq} is an equivalent length. For an annular burner, it can be chosen as the annular gap of the burner, equivalent radius, inside radius, or outside radius. Some researchers even use 1/10 of the pipe radius for L_{eq} [16].

In the present work, C_{ε} was taken as 0.426 for the "average" mixing length in turbulent pipe flow[16, 17]. The other computational conditions are the same as those used in the turbulent intensity case.

Validation of the Model

The data used to validate the turbulent model were taken from the Combustion and Carbonization Research Laboratory (CCRL; Canada), tunnel furnace, and include velocity profiles

at the entrance of the furnace, and at several axial locations inside the furnace, for various air flow rates and swirl settings.

The measured and calculated velocity components in axial, radial, and circumferencial directions at the quarl exit are showed in Figures 3-31 through 3-33, respectively; at the second tunnel (1.07 meter away from burner) in Figures 3-34 through 3-36. It is concluded that the swirl flow field can be predicted in a furnace with the modeling method, especially in the quarl downstream of a furnace.

Sensitivity of the Model Constants

Often the turbulence quantities at the inlet are uncertain. The inlet dissipation rate for swirl is an elusive quantity that is not readily measurable; therefore, some sensitivity analysis is needed before any predictions can be made.

The stream functions under different characteristic lengths are shown in Figures 3-37 and 3-38. The characteristic lengths were chosen as $L_m=y_a$ and $L_B=0.43y_a$, where y_a is the width of the annular gap of the burner. There is no difference in stream functions near the quarl under different characteristic lengths. The stream functions were also calculated using different turbulent intensities (from 25%-35%) and the calculated results are shown in Figures 3-39 through 3-41. Slight differences occur away from the quarl.

Prediction and Discussion

Based on the validation of the model, the recirculation in the demonstration boiler was simulated and is shown in Figure 3-42, in which the external and internal recirculation zones are predicted. The effect of the near burner aerodynamics on particle trajectories is as follows:

Tertiary Air Jet Positions

The recirculations at different air ring positions are shown in Figures 3-43 through 3-45.

Swirl Number of Secondary Air

The effect of swirl number on the recirculation in the boiler was determined using the model predictions. The static pressures are shown in Figures 3-46 through 3-48 for swirl numbers 0, of 0.6, and 1.0, respectively.

Secondary/Tertiary Air Distribution

Secondary/tertiary air distribution is another factor which affects recirculation generation. The external and internal recirculation zones are shown in Figures 3-49 and 3-51 for different secondary /tertiary air distributions.

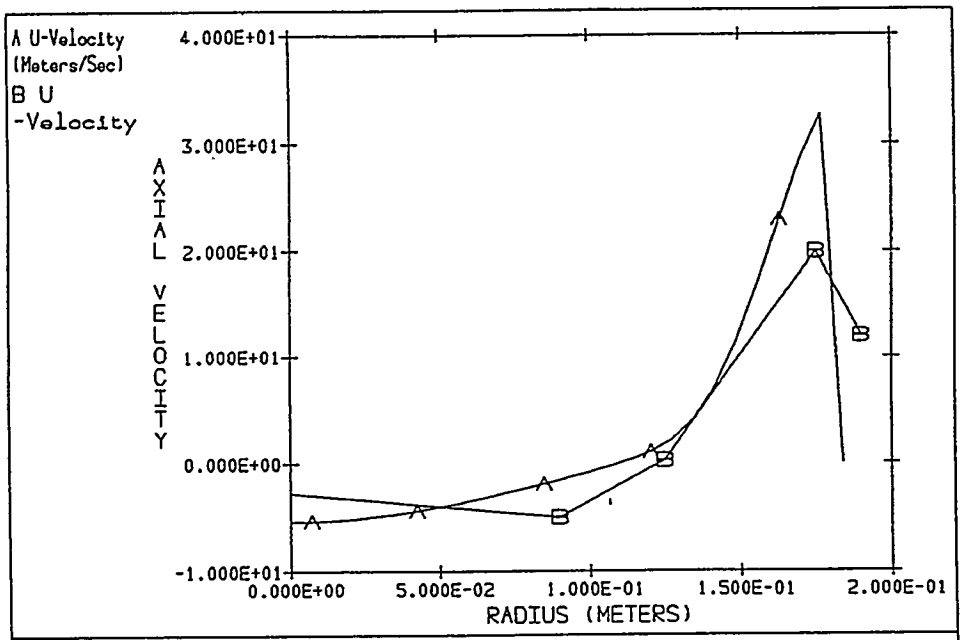

Figure 3-31. MEASURED AND CALCULATED AXIAL VELOCITY COMPONENT AT THE QUARL EXIT OF THE CCRL TUNNEL FURNACE

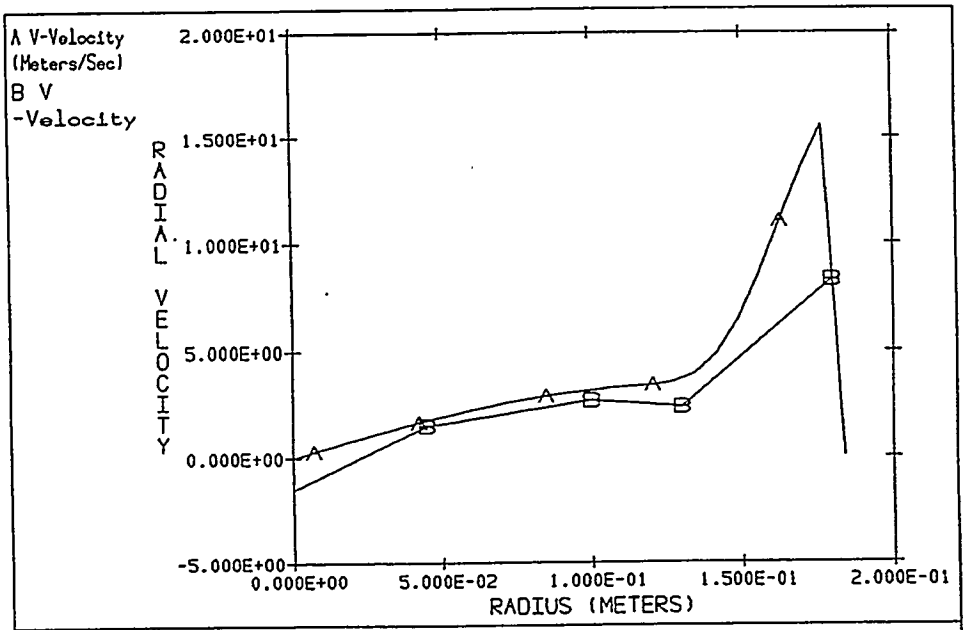

Figure 3-32. MEASURED AND CALCULATED RADIAL VELOCITY COMPONENT AT THE QUARL EXIT OF THE CCRL TUNNEL FURNACE

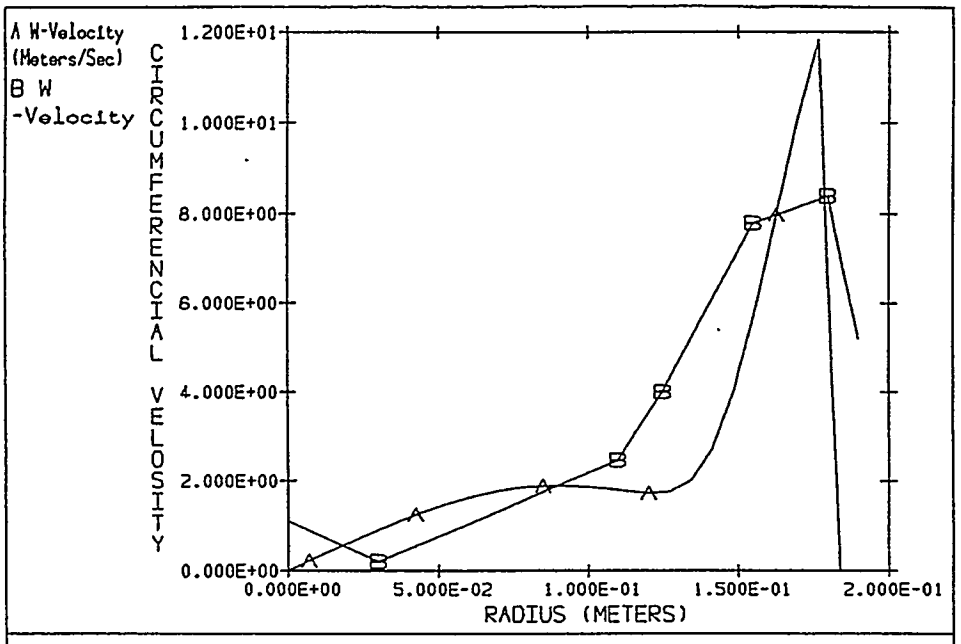

Figure 3-33. MEASURED AND CALCULATED CIRCUMFERENCIAL VELOCITY COMPONENT AT THE QUARL EXIT OF THE CCRL TUNNEL FURNACE

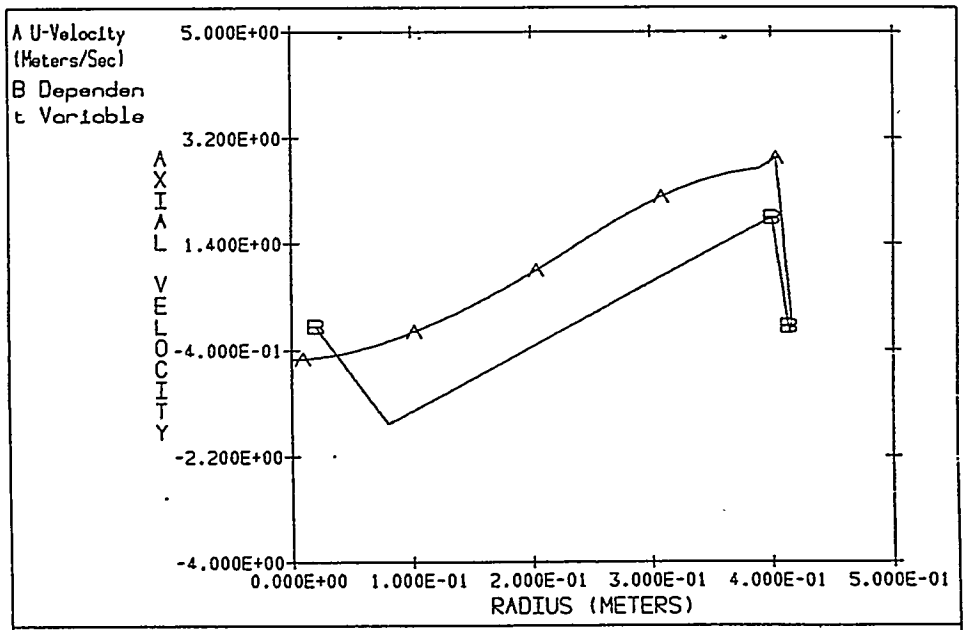

Figure 3-34. MEASURED AND CALCULATED AXIAL VELOCITY COMPONENT 1.07 METERS FROM THE BURNER IN THE CCRL TUNNEL FURNACE

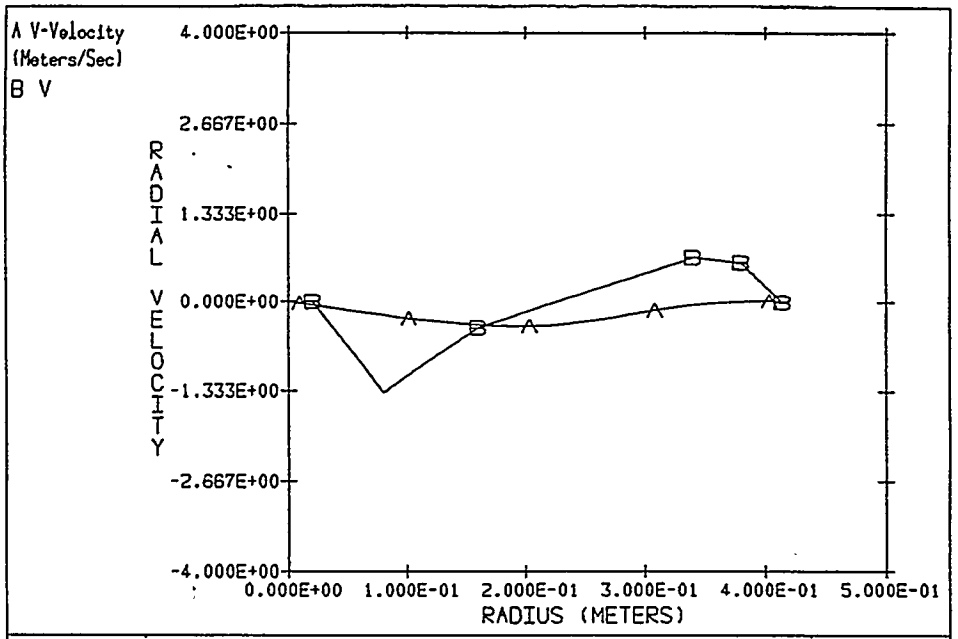

Figure 3-35. MEASURED AND CALCULATED RADIAL VELOCITY COMPONENT 1.07 METERS FROM THE BURNER IN THE CCRL TUNNEL FURNACE

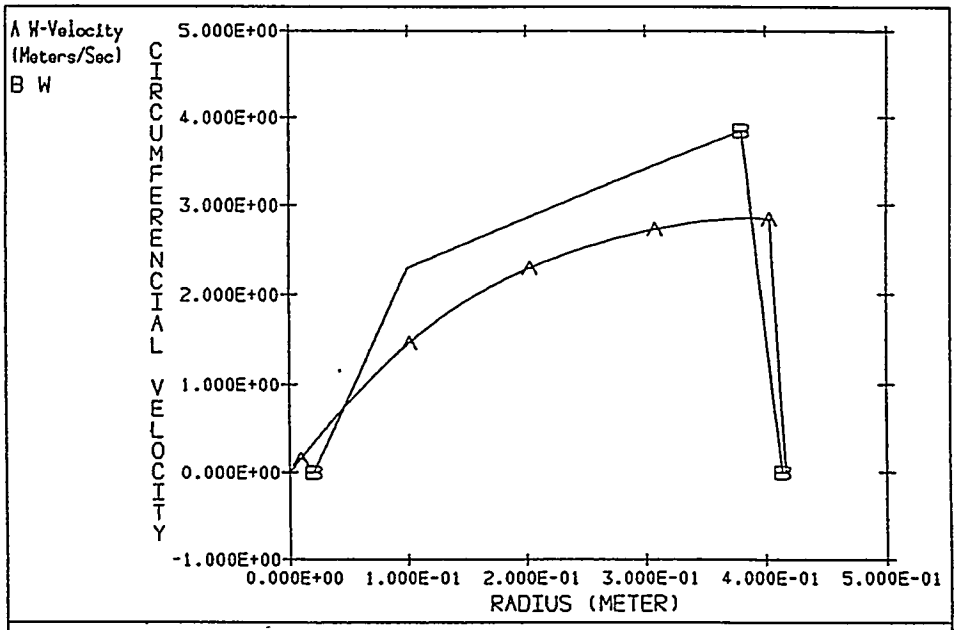

Figure 3-36. MEASURED AND CALCULATED CIRCUMFERENCIAL VELOCITY COMPONENT 1.07 METERS FROM THE BURNER IN THE CCRL TUNNEL FURNACE

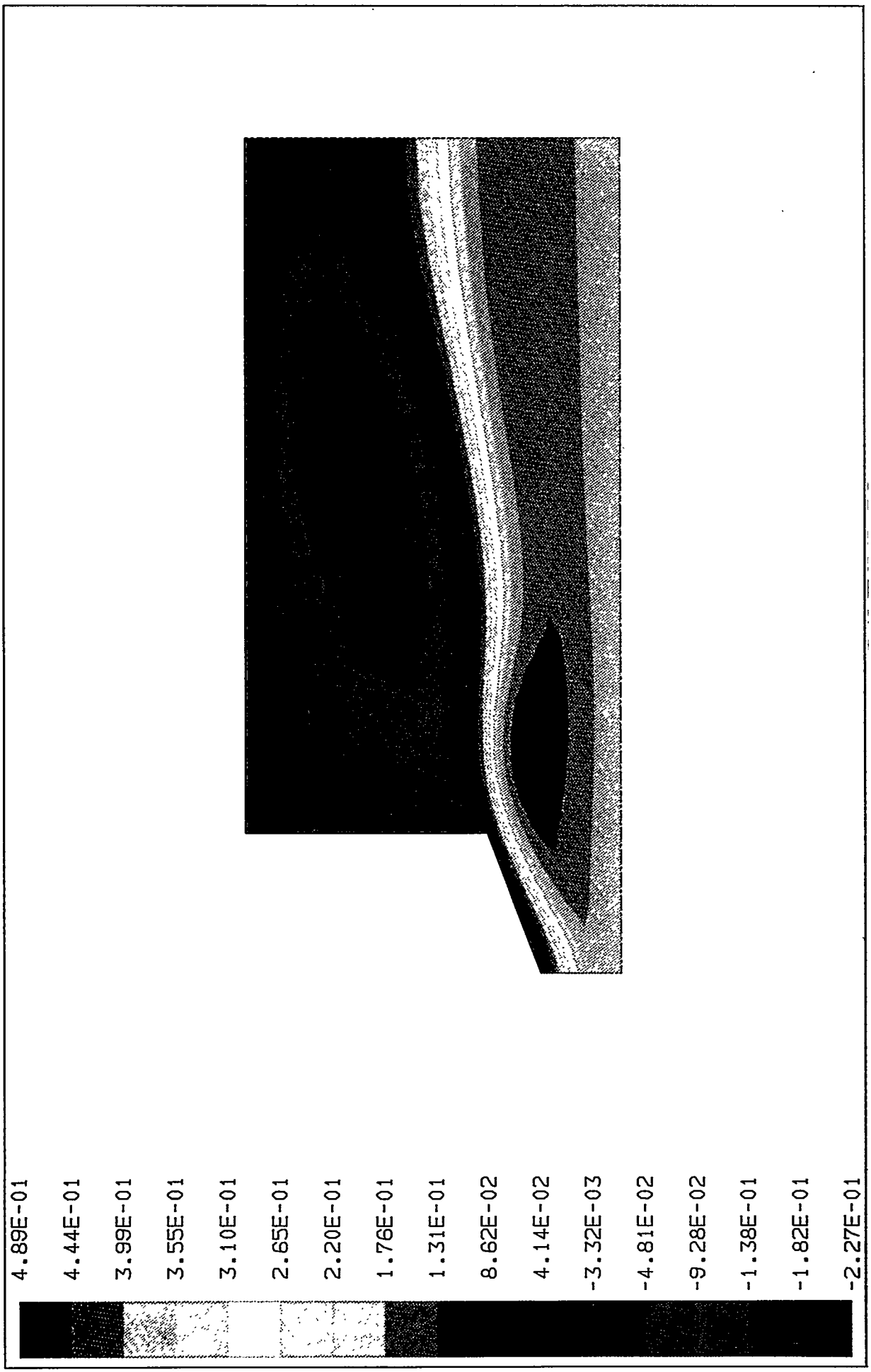

Figure 3-37. STREAM FUNCTION, IN SQUARE METERS/SECOND, IN THE DEMONSTRATION BOILER FOR A CHARACTERISTIC LENGTH OF 0.43 TIMES THE BURNER ANNULAR GAP

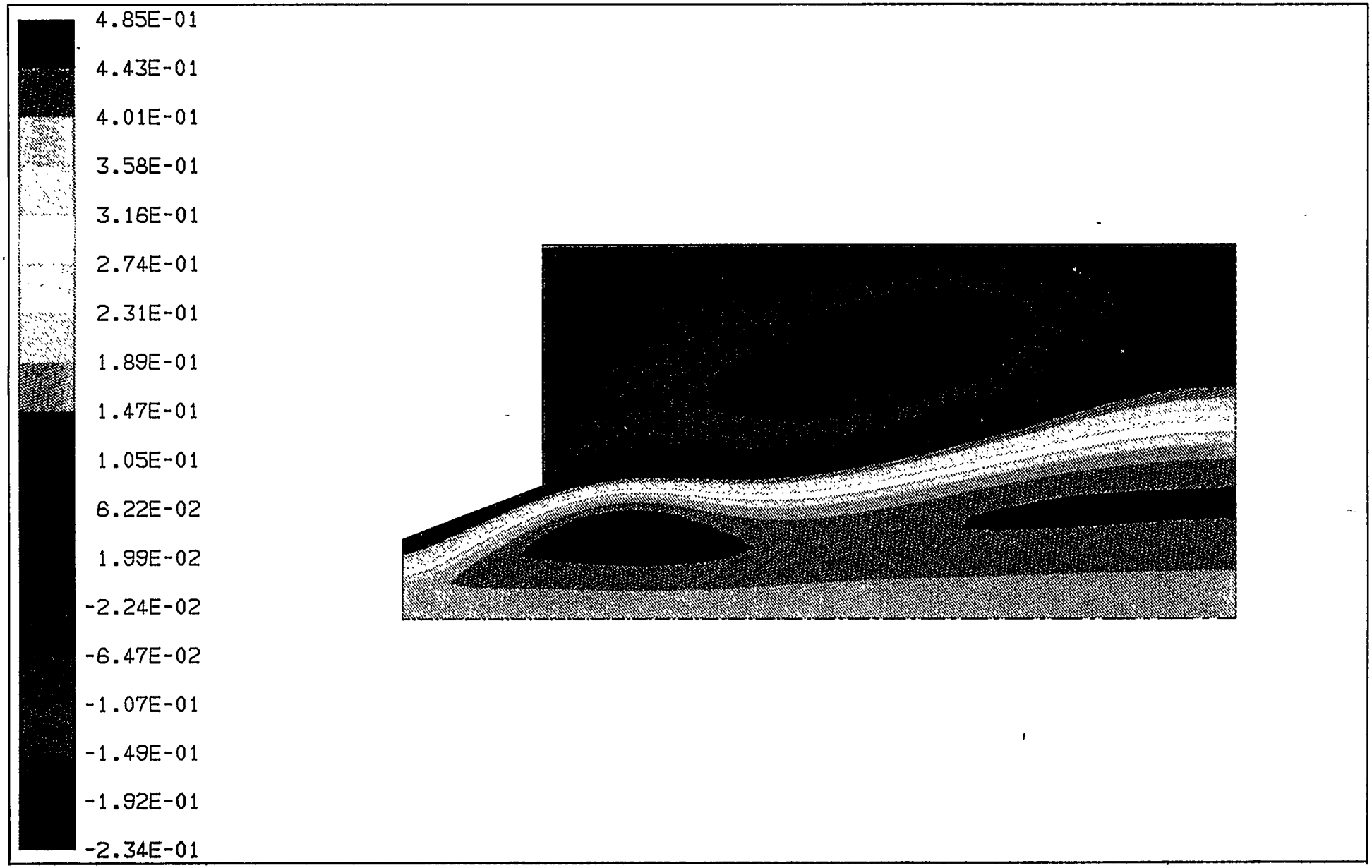

Figure 3-38. STREAM FUNCTION, IN SQUARE METERS/SECOND, IN THE DEMONSTRATION BOILER FOR A CHARACTERISTIC LENGTH EQUAL TO THE BURNER ANNULAR GAP

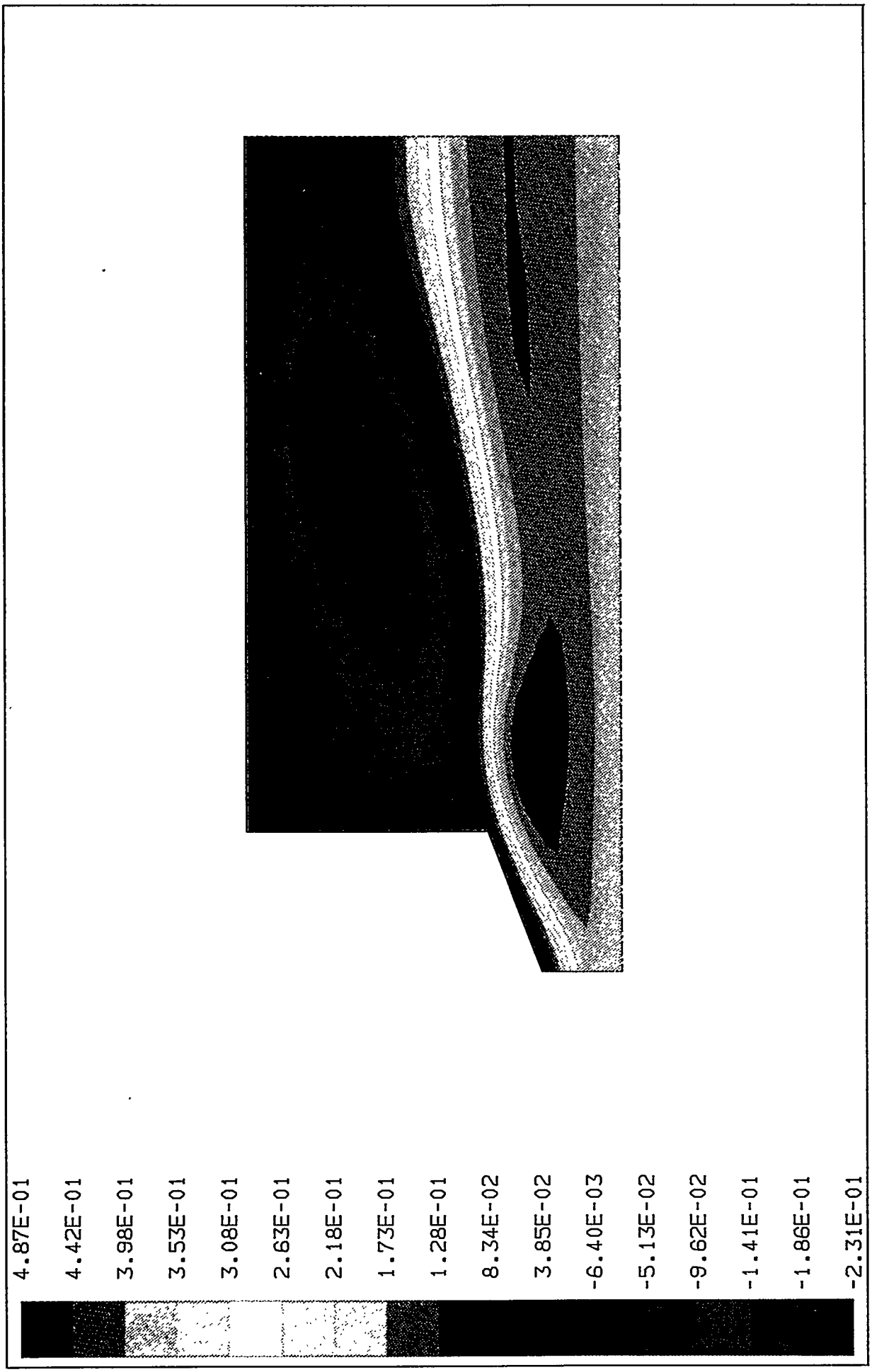

Figure 3-39. STREAM FUNCTION, IN SQUARE METERS/SECOND, IN THE DEMONSTRATION BOILER FOR A TURBULENCE INTENSITY OF 25%

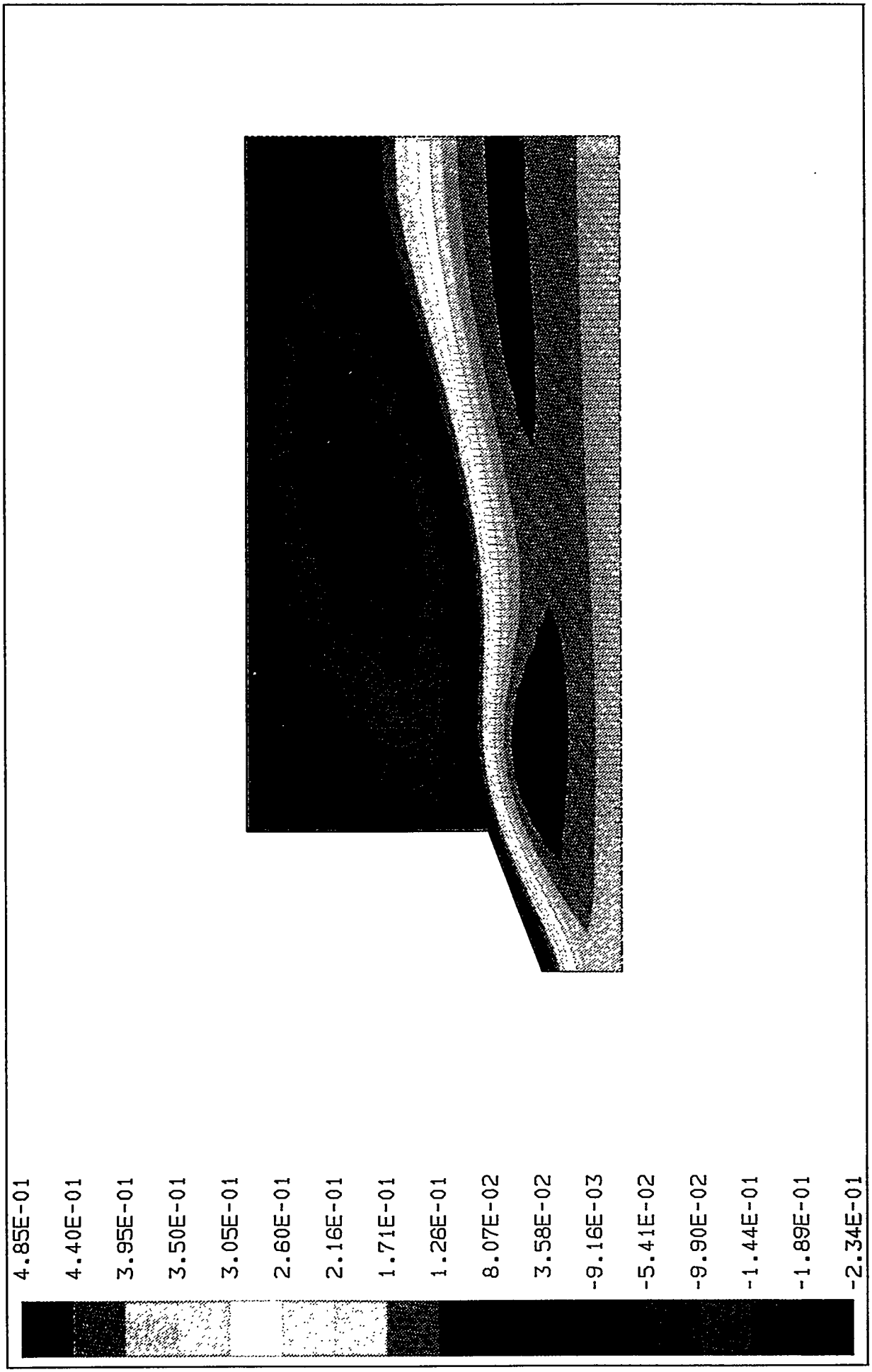

Figure 3-40. STREAM FUNCTION, IN SQUARE METERS/SECOND, IN THE DEMONSTRATION BOILER FOR A TURBULENCE INTENSITY OF 30%

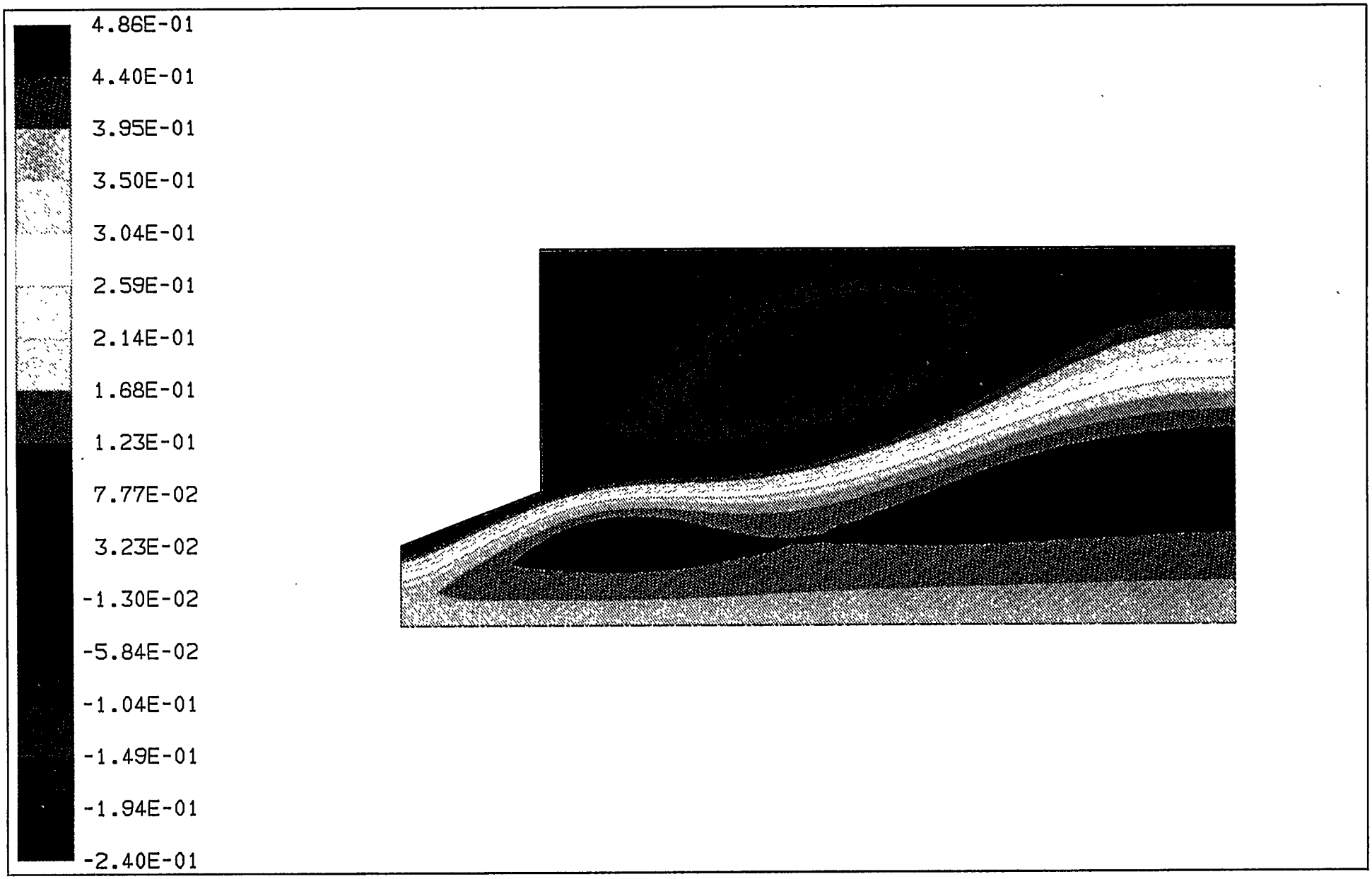

Figure 3-41. STREAM FUNCTION, IN SQUARE METERS/SECOND, IN THE DEMONSTRATION BOILER FOR A TURBULENCE INTENSITY OF 35%

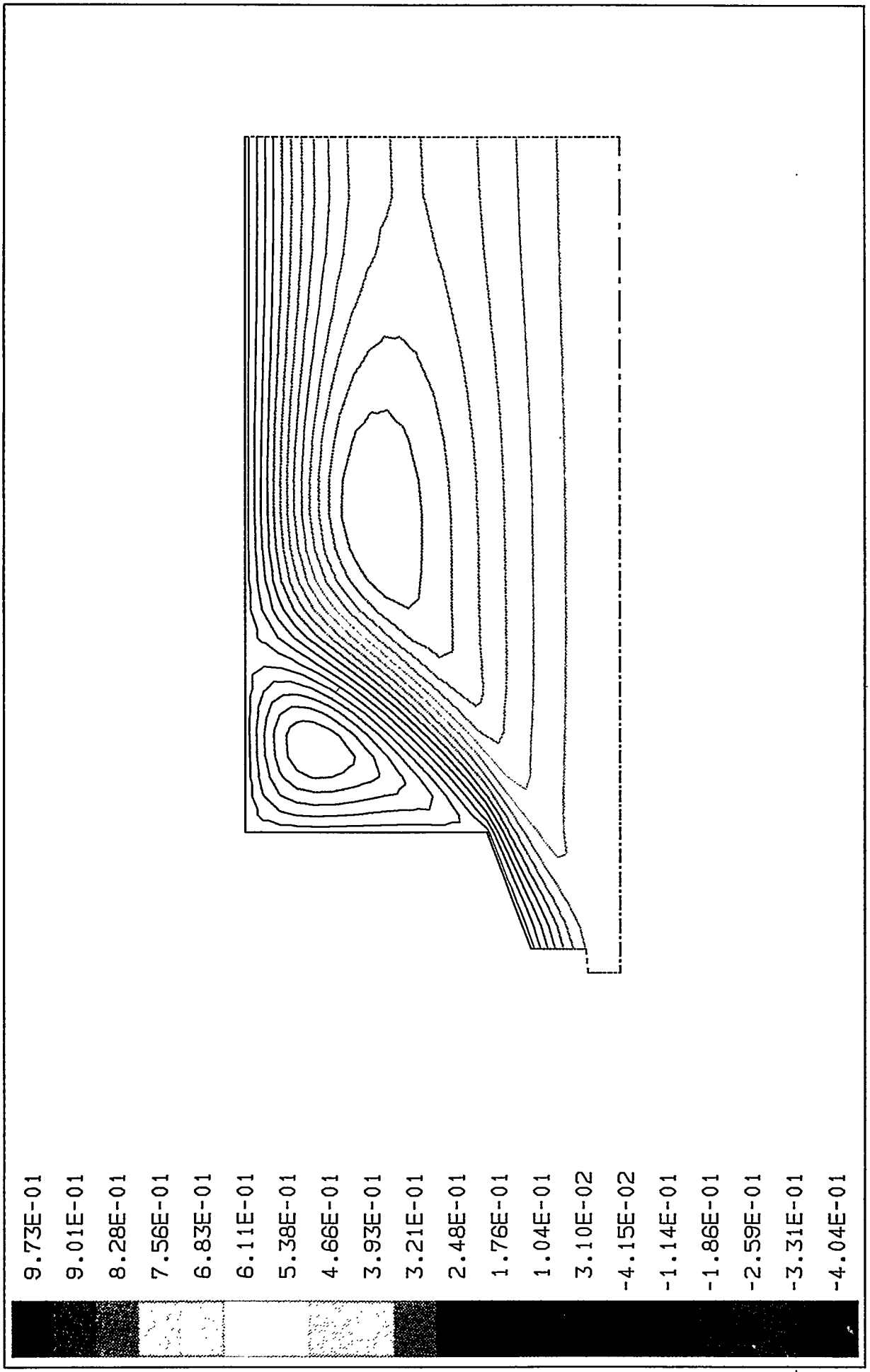

Figure 3-42. STREAM FUNCTION, IN SQUARE METERS/SECOND, IN THE DEMONSTRATION BOILER SHOWING THE RECIRCULATION ZONES

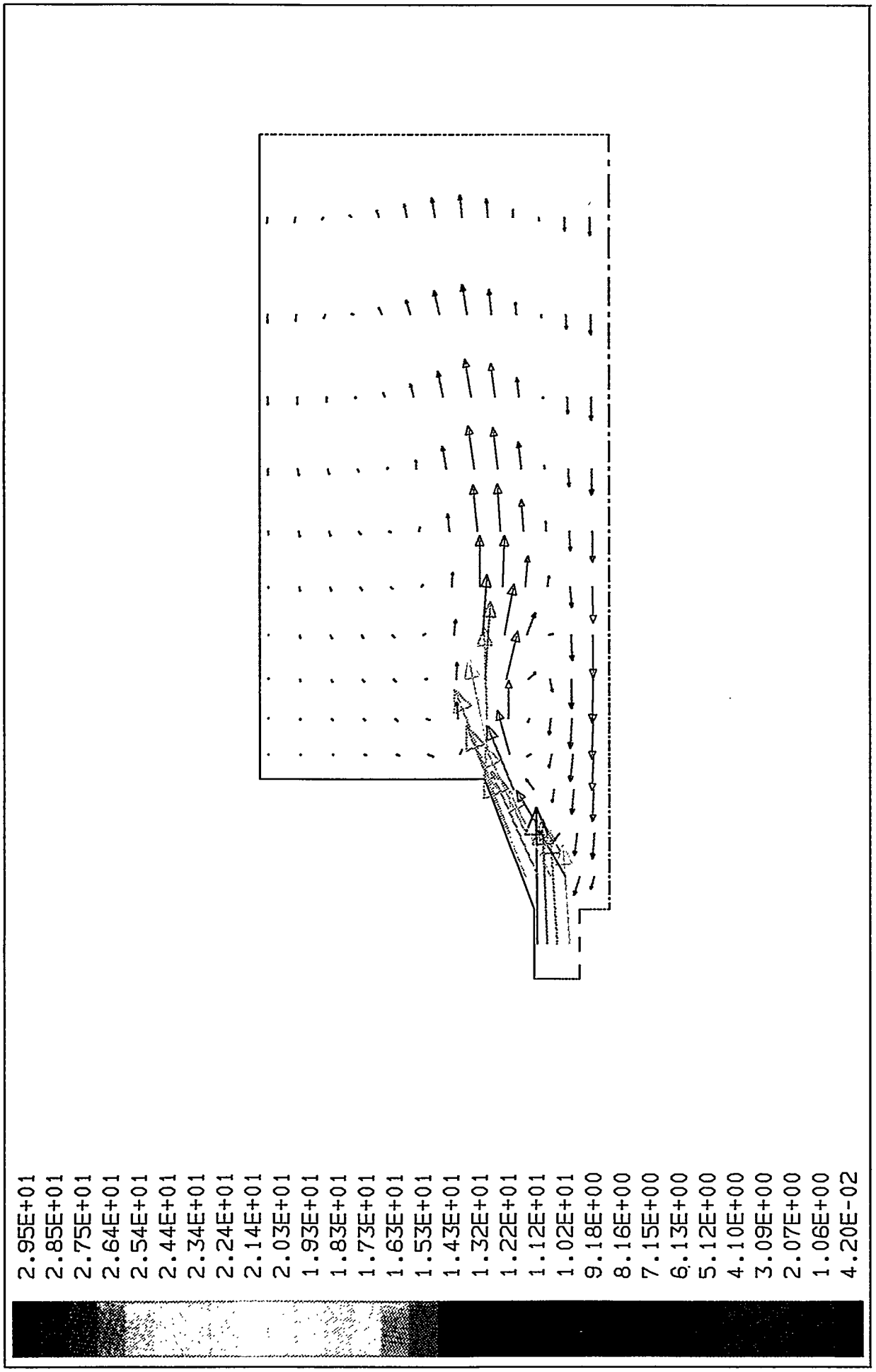

Figure 3-43. VELOCITY VECTORS, IN METERS/SECOND, FOR BURNER CONFIGURATION A

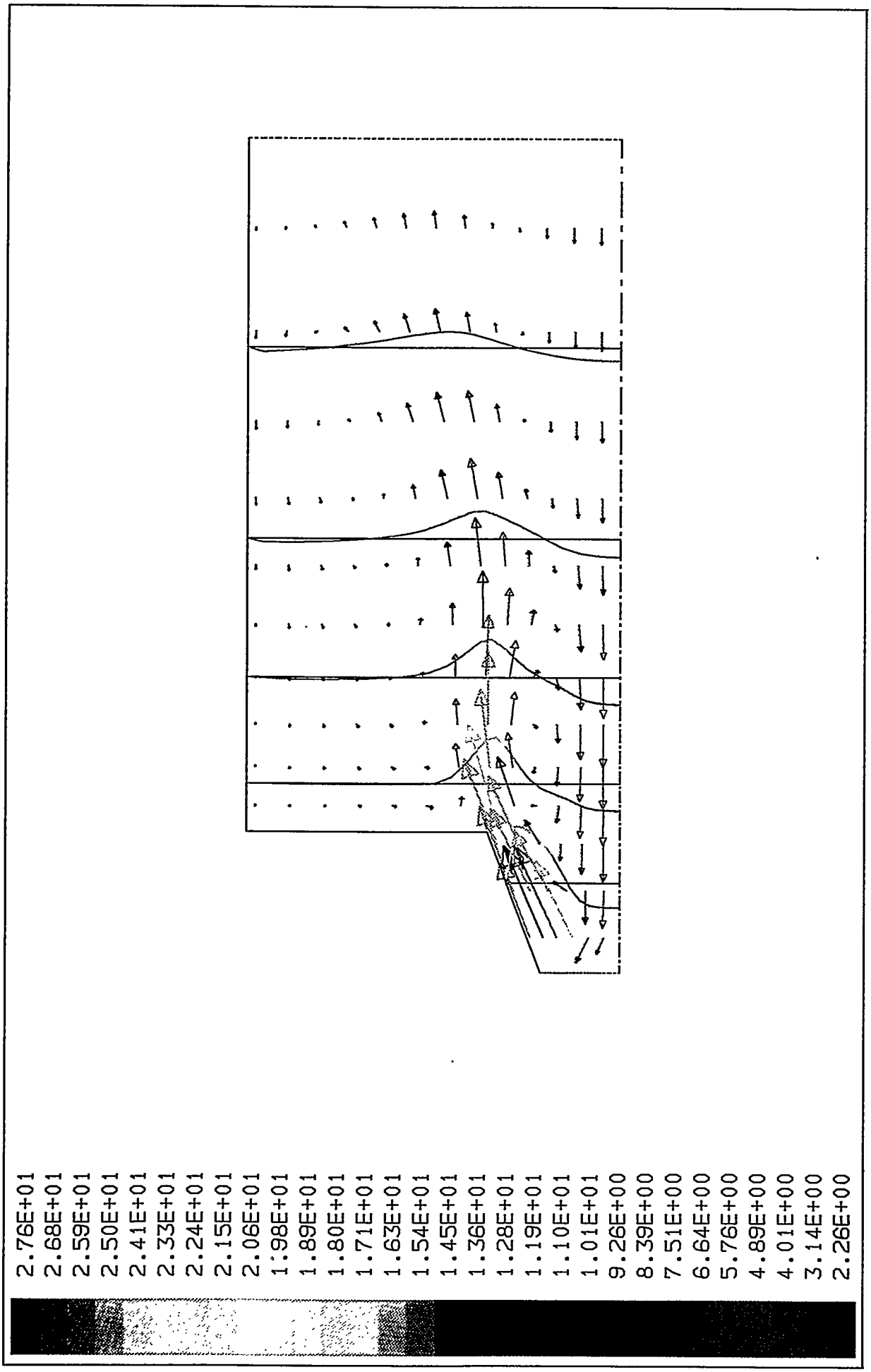

Figure 3-44. VELOCITY VECTORS, IN METERS/SECOND, FOR BURNER CONFIGURATION B

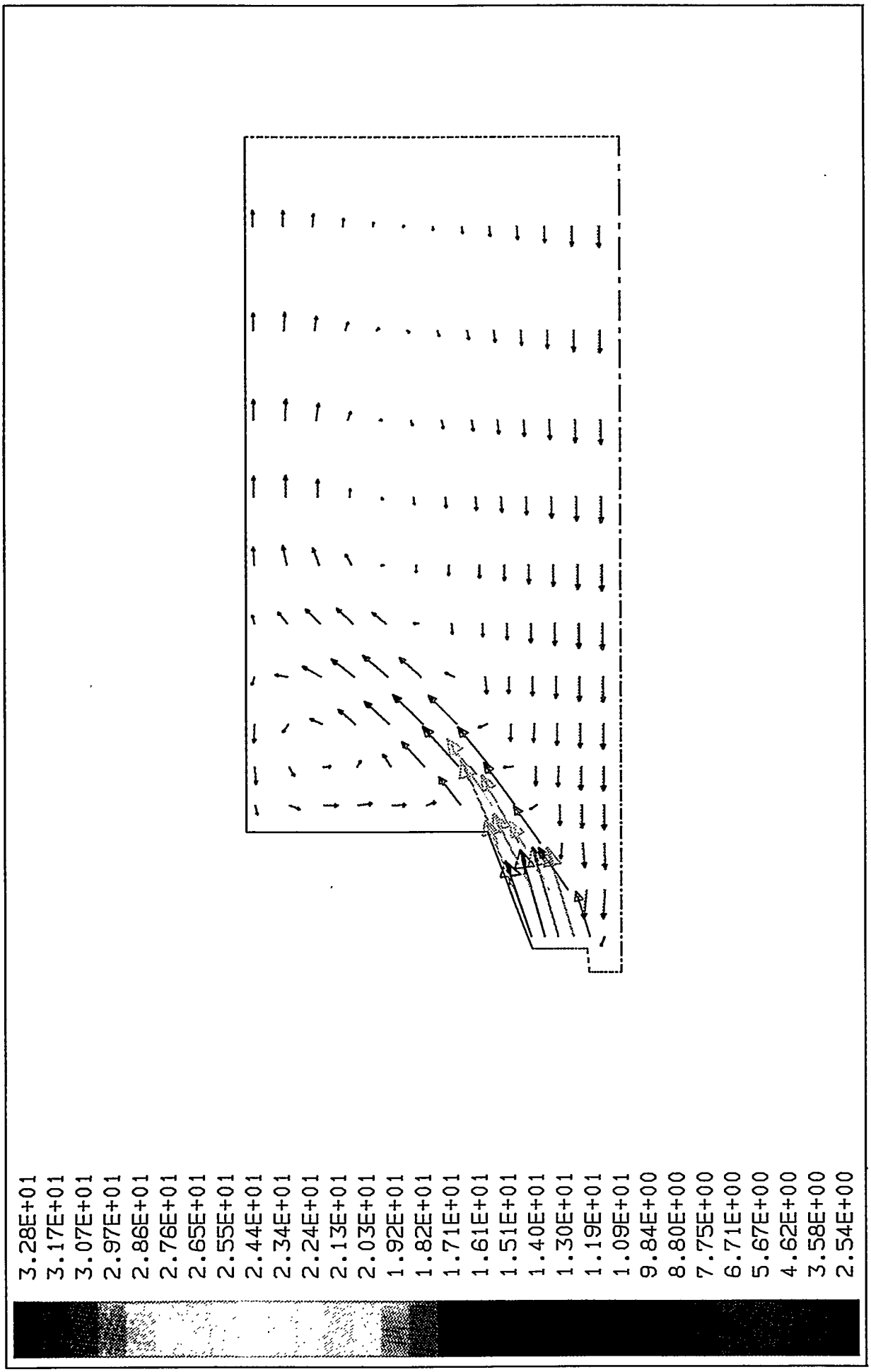

Figure 3-45. VELOCITY VECTORS, IN METERS/SECOND, FOR BURNER CONFIGURATION C

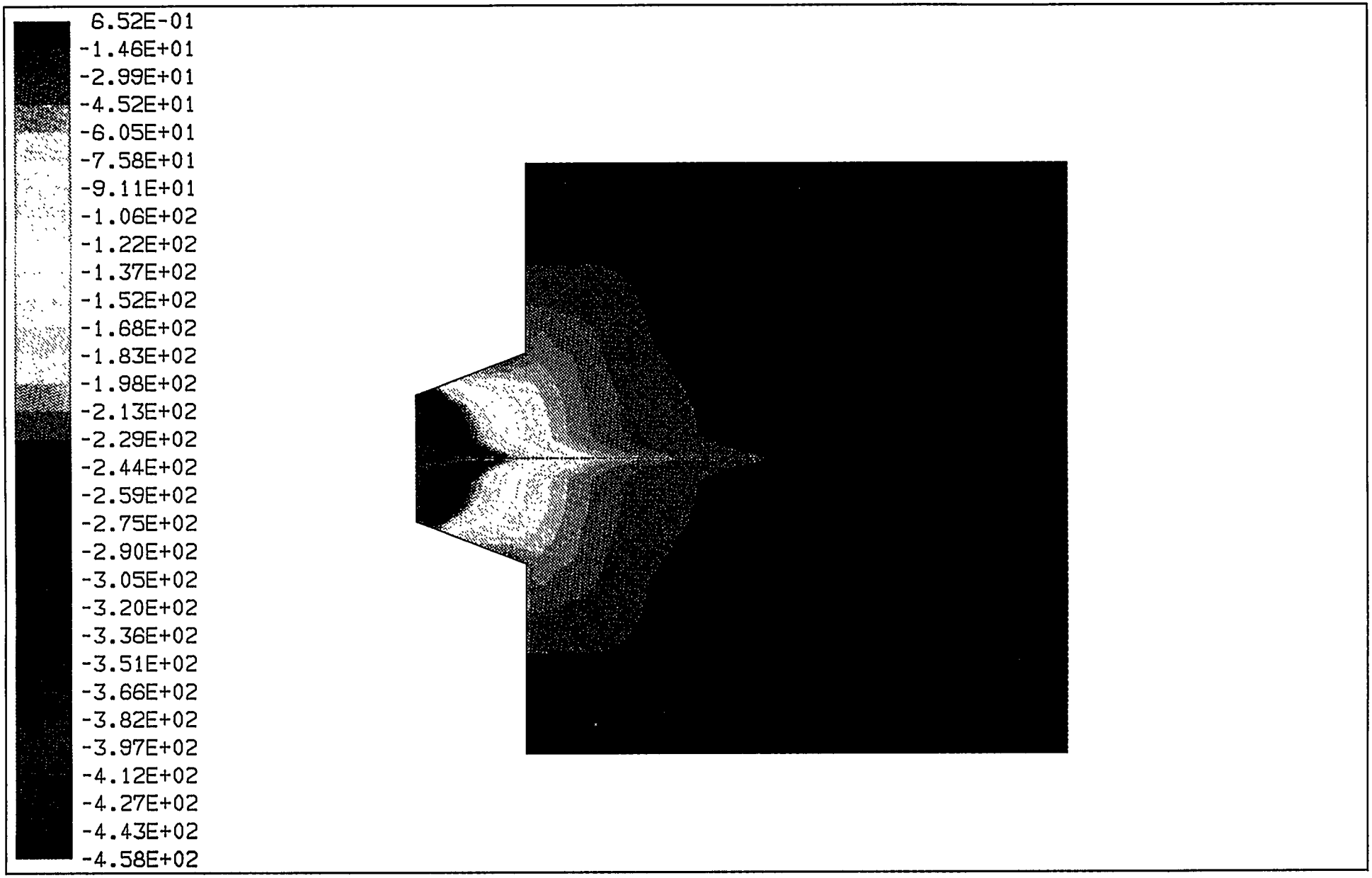

Figure 3-46. STATIC PRESSURE IN THE DEMONSTRATION BOILER WITH A SWIRL NUMBER OF ZERO

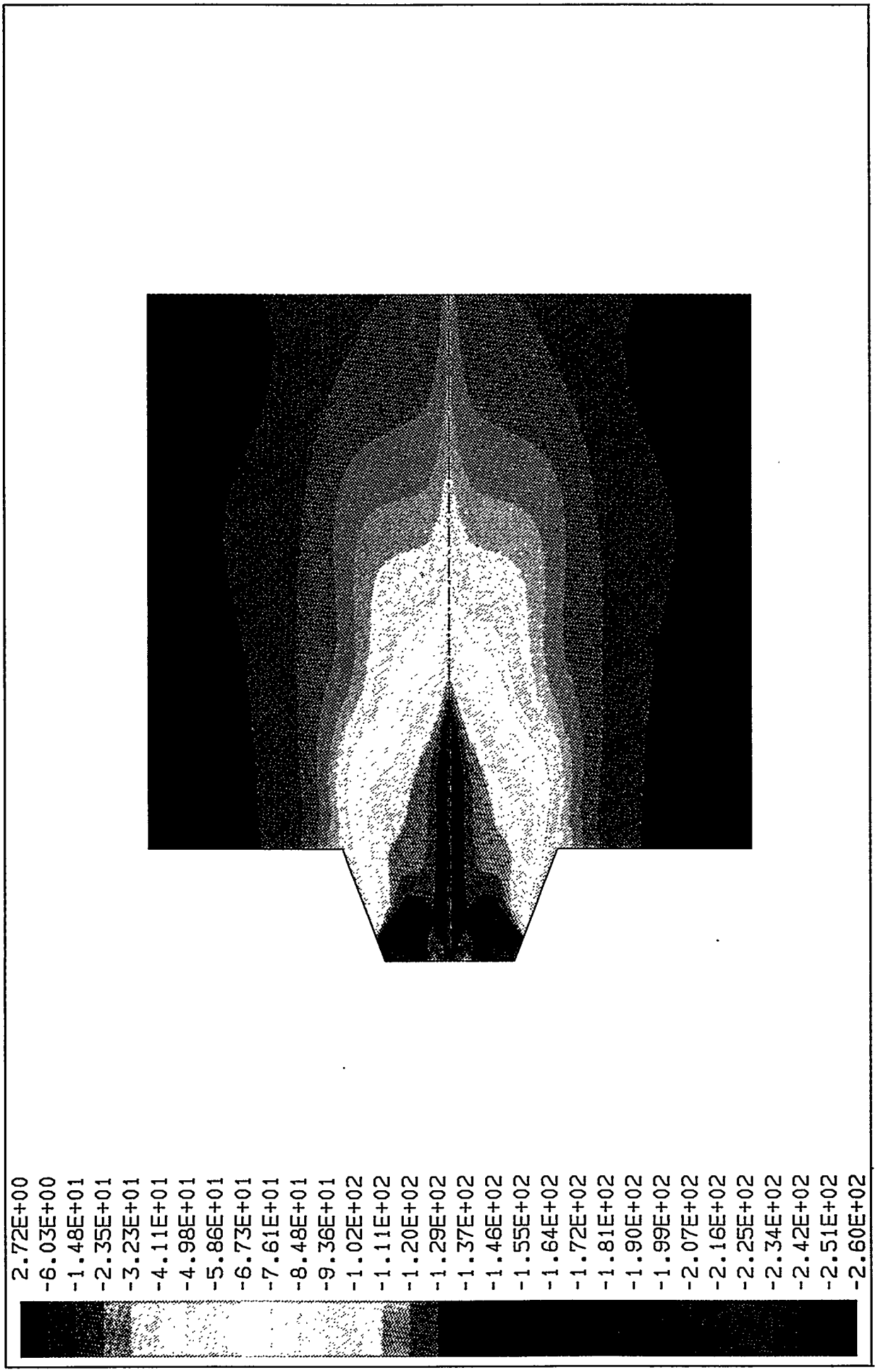

Figure 3-47. STATIC PRESSURE IN THE DEMONSTRATION BOILER WITH A SWIRL NUMBER OF 0.6

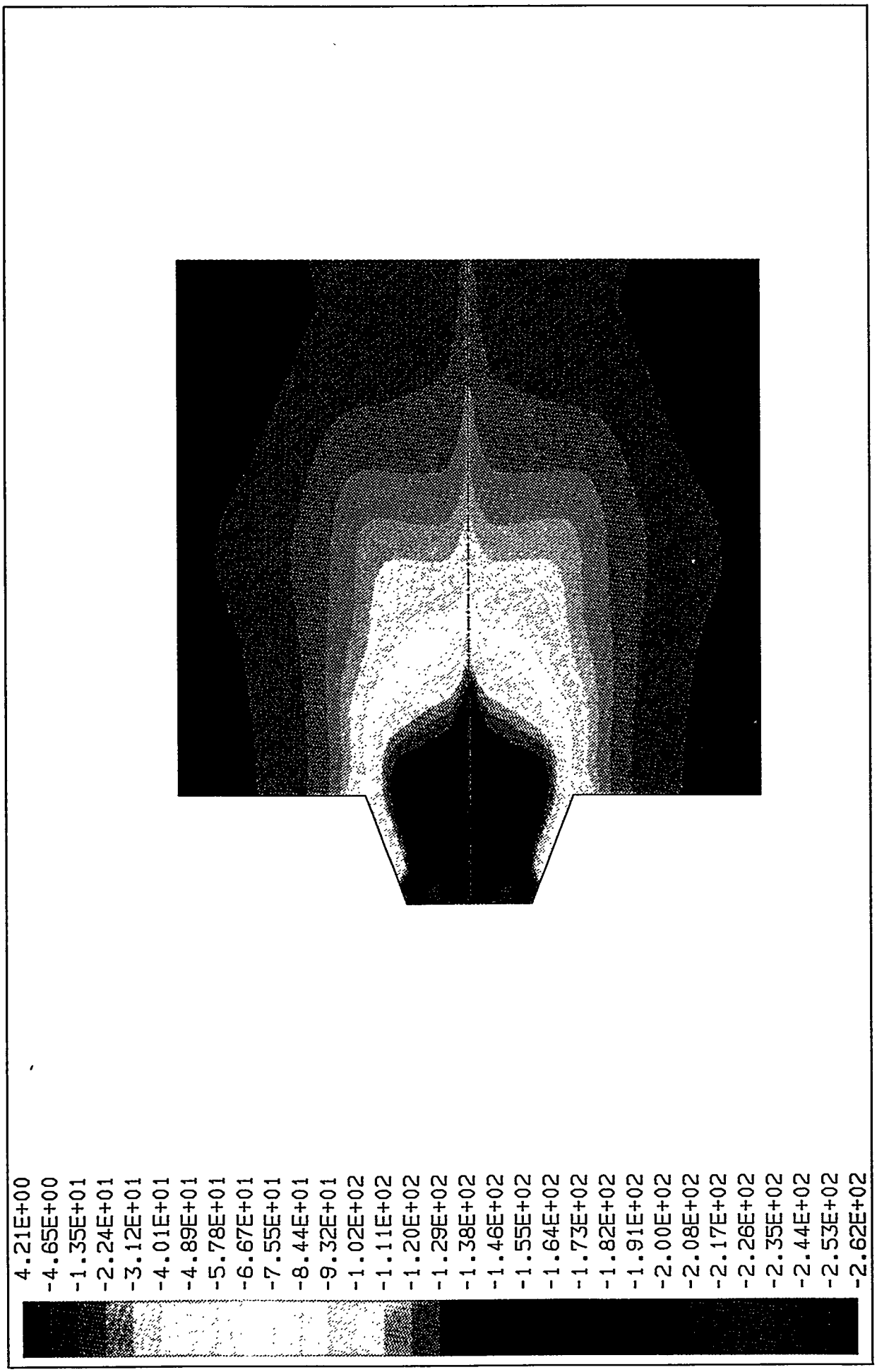

Figure 3-48. STATIC PRESSURE IN THE DEMONSTRATION BOILER WITH A SWIRL NUMBER OF 1.0

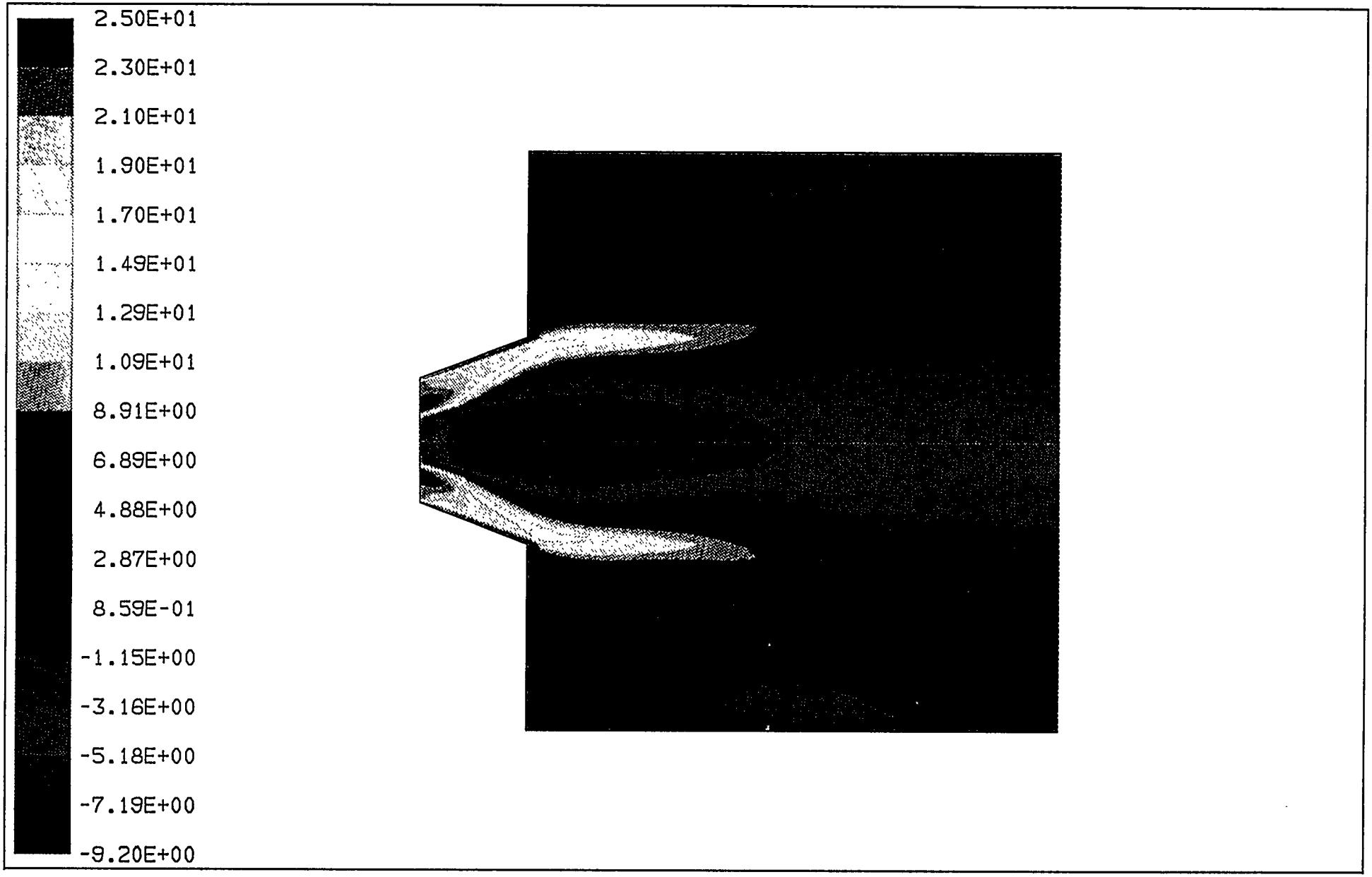

Figure 3-49. RECIRCULATION ZONES, IN METERS/SECOND, IN THE DEMONSTRATION BOILER FOR TERTIARY TO SECONDARY AIR SPLITS OF 65 TO 35%

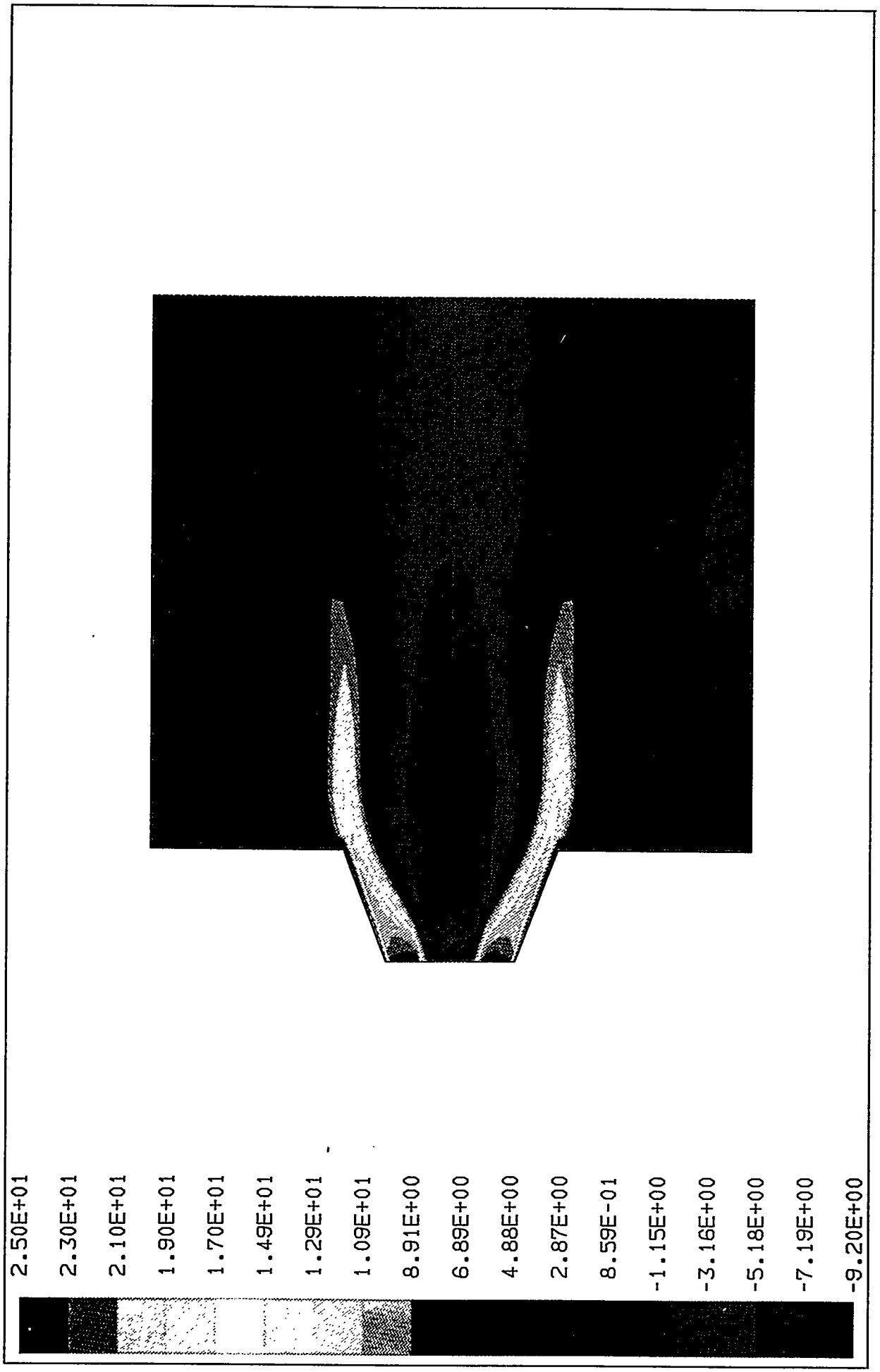

Figure 3-50. RECIRCULATION ZONES, IN METERS/SECOND, IN THE DEMONSTRATION BOILER FOR TERTIARY TO SECONDARY AIR SPLITS OF 70 TO 30%

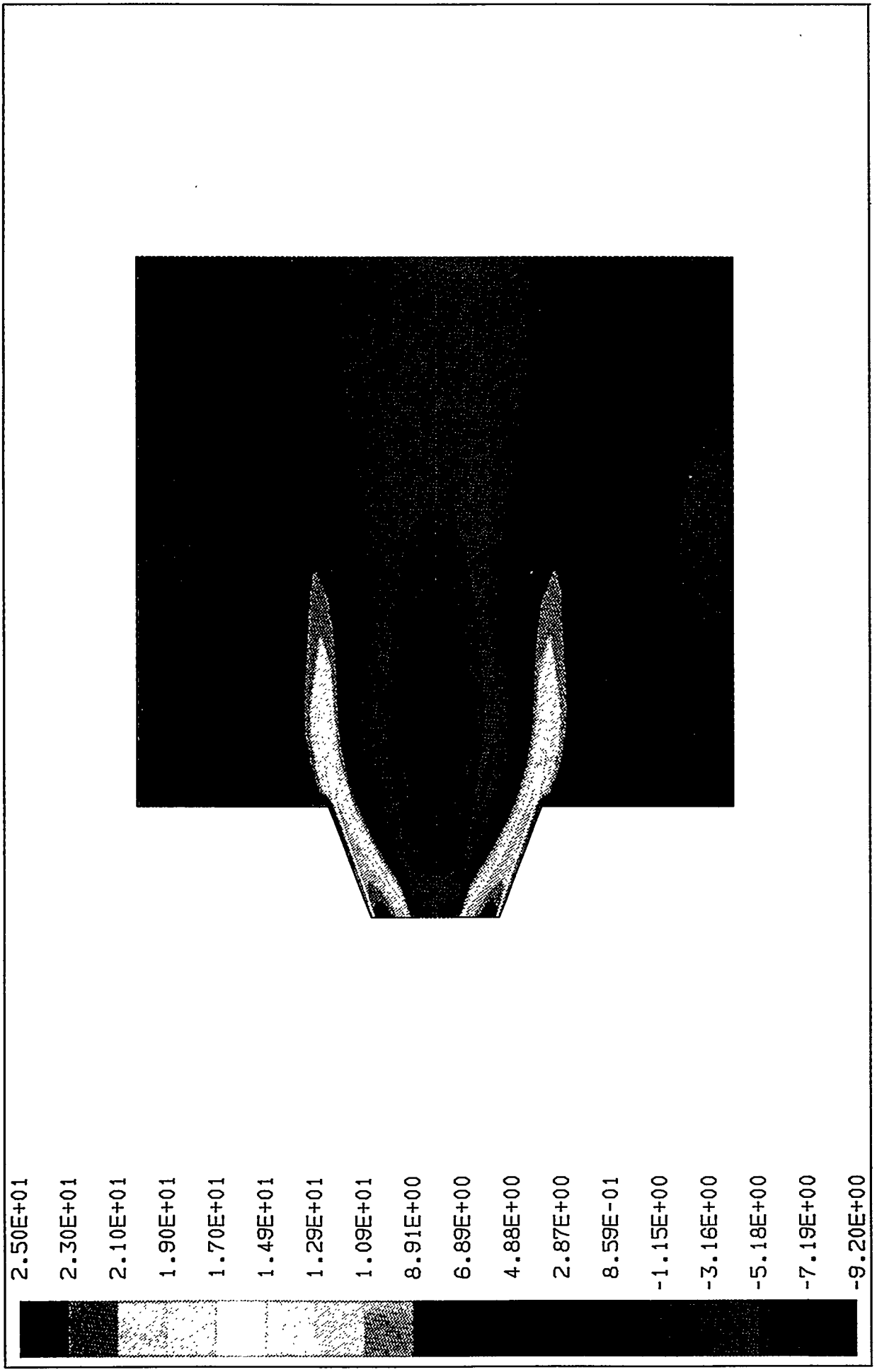

Figure 3-51. RECIRCULATION ZONES, IN METERS/SECOND, IN THE DEMONSTRATION BOILER FOR TERTIARY TO SECONDARY AIR SPLITS OF 75 TO 25%

Swirler Type

Different swirler types result in different vortex forms, which have been simulated by defined tangential velocity profiles at the inlet. The axial velocity contours under free vortex and forced vortex are shown in Figures 3-52 and 3-53.

Particle Trajectories

The particles were injected with the primary air. Stochastic trajectories of the particles are shown in Figure 3-54. The velocity vectors with and without particle injections are shown in Figures 3-55 and 3-56, respectively. The effect of swirl number on particle positions is shown in Figures 3-57 and 3-58.

Particle Velocity

The effect of swirl number on particle velocity is shown in Figures 3-59 through 3-61.

Summary

The aerodynamics of isothermal jets issued from a pulverized coal burner were simulated under different operating conditions.

The model was validated with the experimental data from the CCRL tunnel furnace and included velocity profiles at the entrance of the furnace and at several axial locations inside the furnace, for various air flow rates and swirl settings. The sensitivity analysis was carried out for the uncertain turbulence quantities at the inlet.

The effect of the following operational parameters on the combustion aerodynamics of the burner were investigated and reported:

- Relative positions of the primary, secondary, and tertiary air rings;
- Swirler type;
- Secondary/tertiary air flow rate; and
- Swirl number.

Combustion Aerodynamics of Two DMC Burners

The combustion of natural gas in two burners has been successfully modeled by means of a Computational Fluid Dynamics (CFD) code. The burners that were modeled are the EER low-NOx burner, which is currently being used in this program, and a burner developed by ABB Combustion Engineering for retrofit applications. The burner, called a high efficiency advanced coal combustor (HEACC), has been tested at Penn State as part of another program. The theory and the assumptions employed in the numerical modeling work were described in previous reports and will not be repeated here. However, the most recent results obtained are depicted and these show good agreement with experimental measurements of temperature.

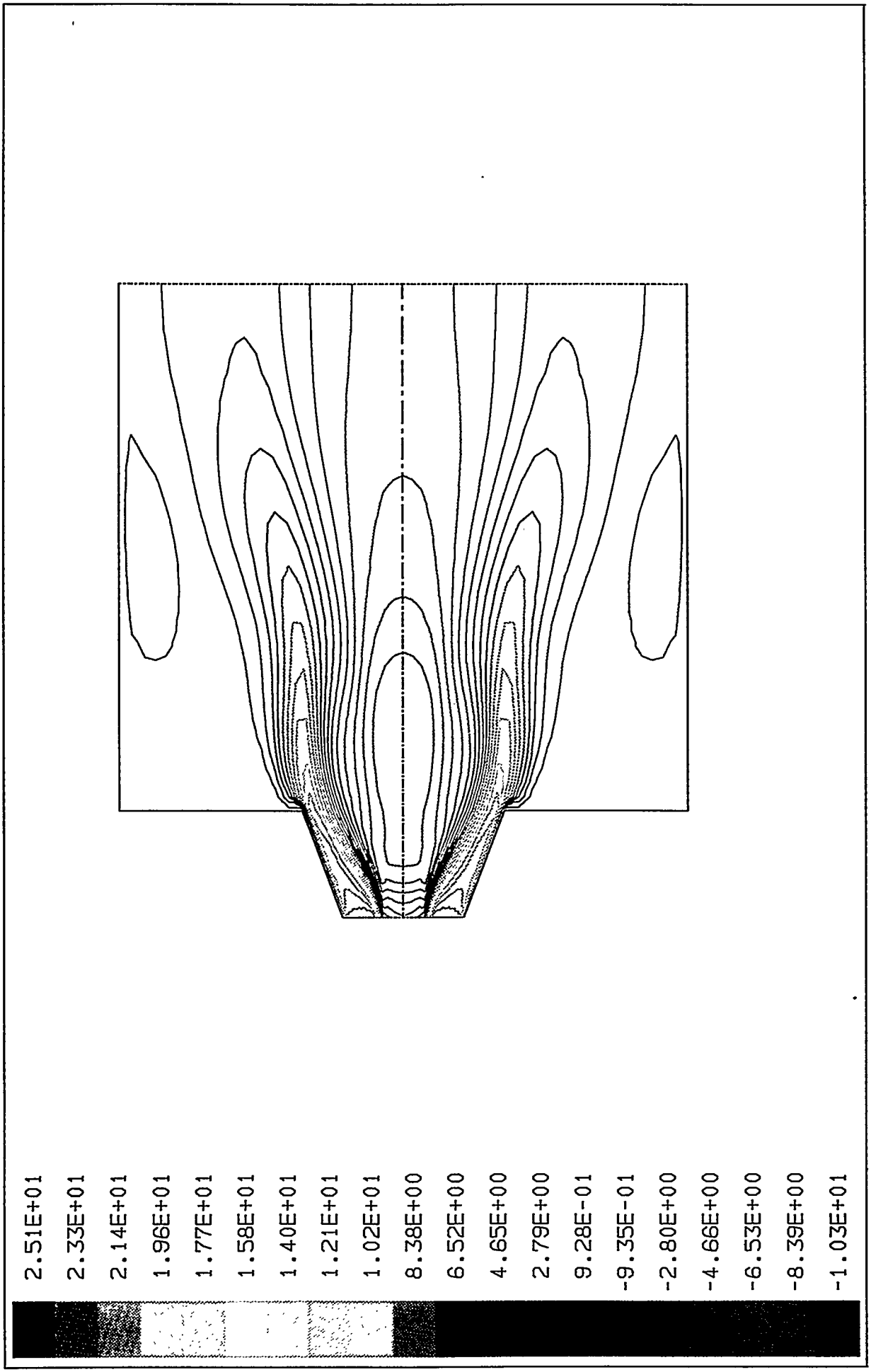

Figure 3-52. AXIAL VELOCITY CONTOURS, IN METERS/SECOND, UNDER FREE VORTEX CONDITIONS

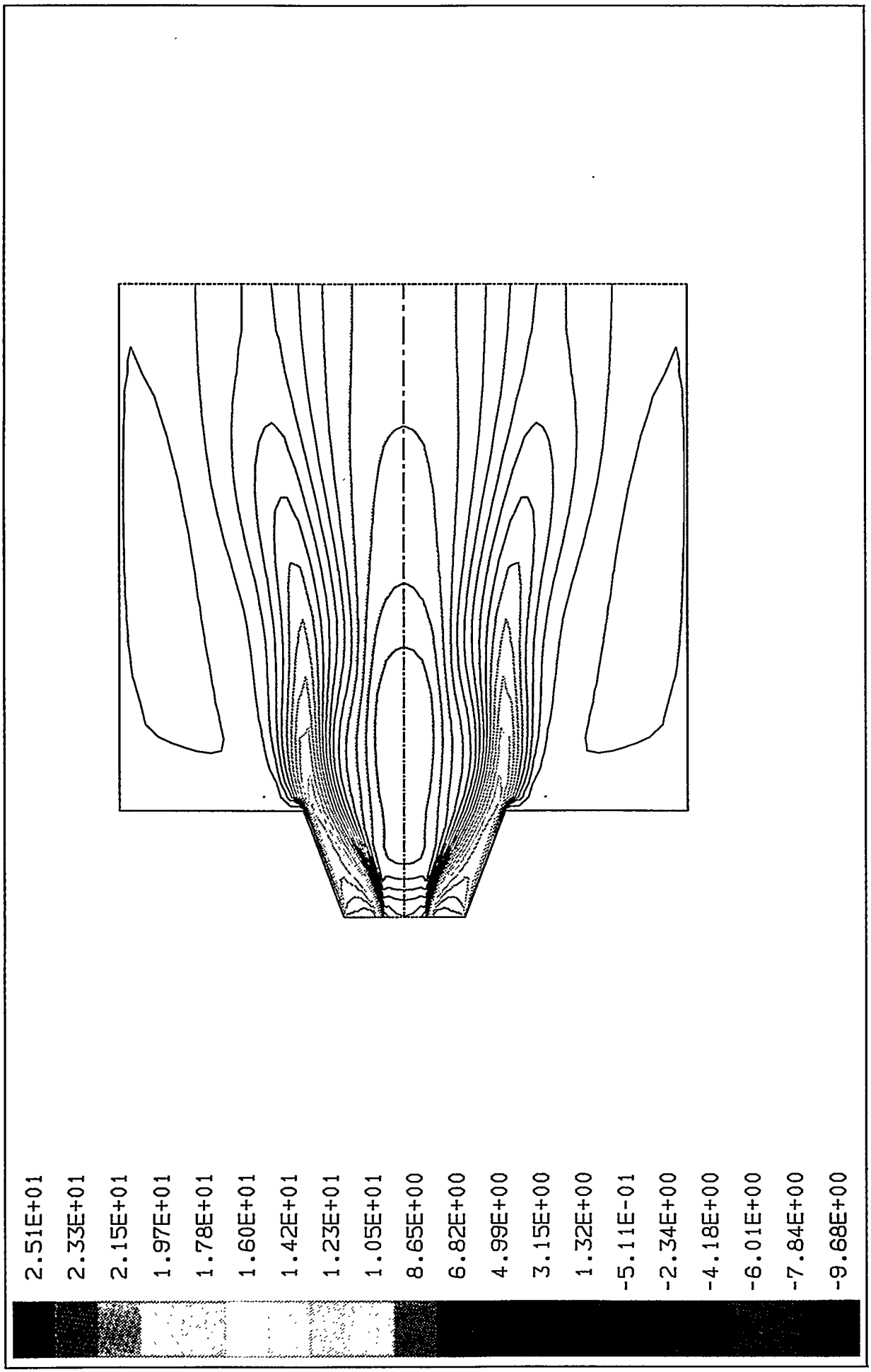

Figure 3-53. AXIAL VELOCITY CONTOURS, IN METERS/SECOND, UNDER FORCED VORTEX CONDITIONS

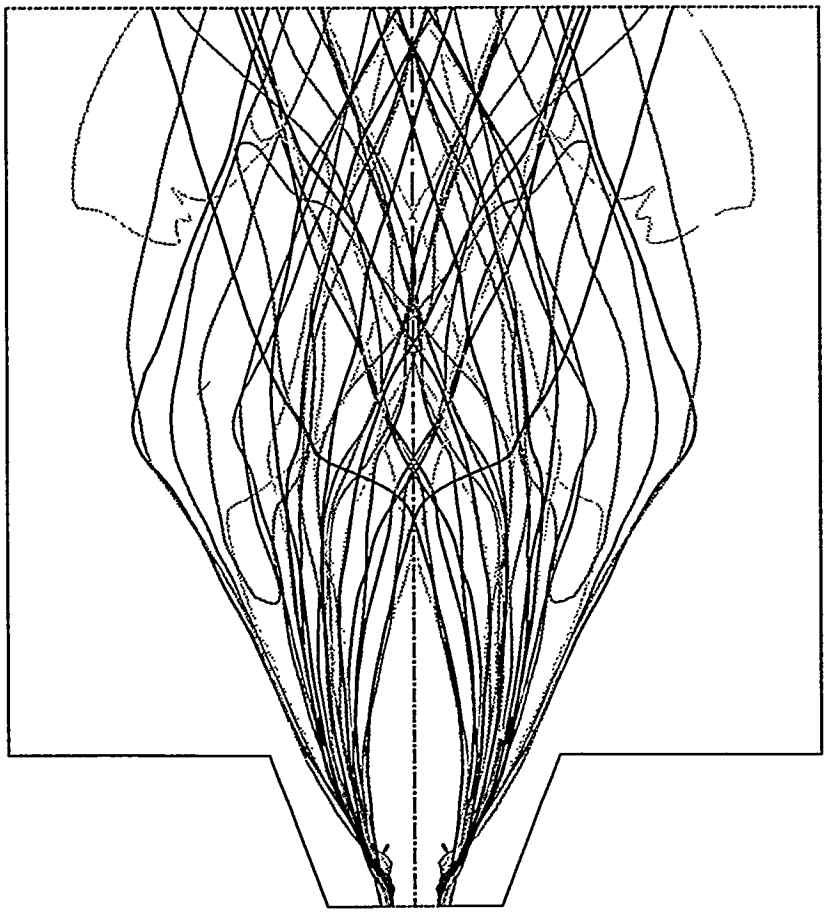

Figure 3-54. STOCHASTIC TRAJECTORIES OF COAL PARTICLES

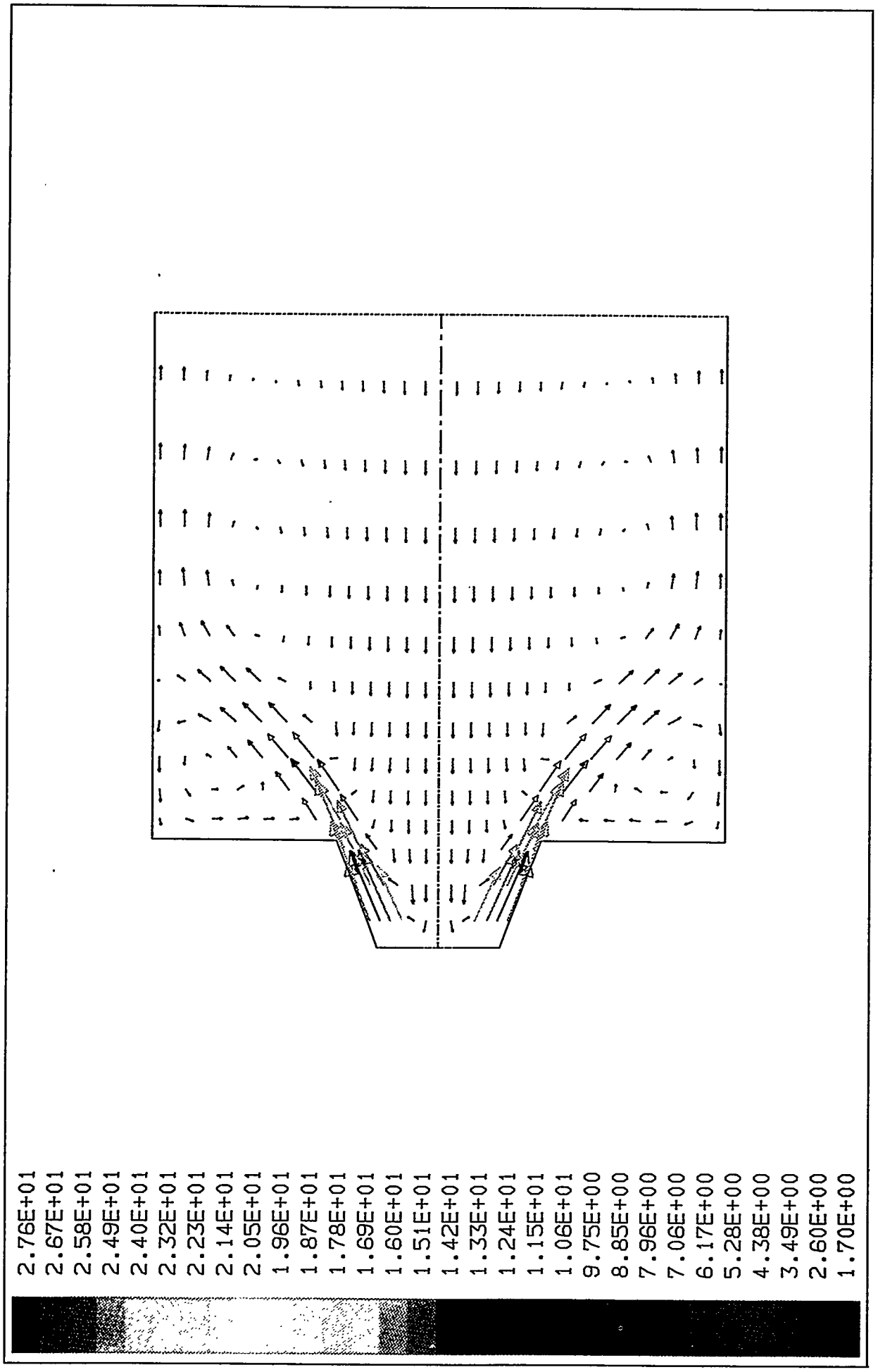

Figure 3-55. GAS VELOCITY VECTORS, IN METERS/SECOND, WITH COAL PARTICLE INJECTION

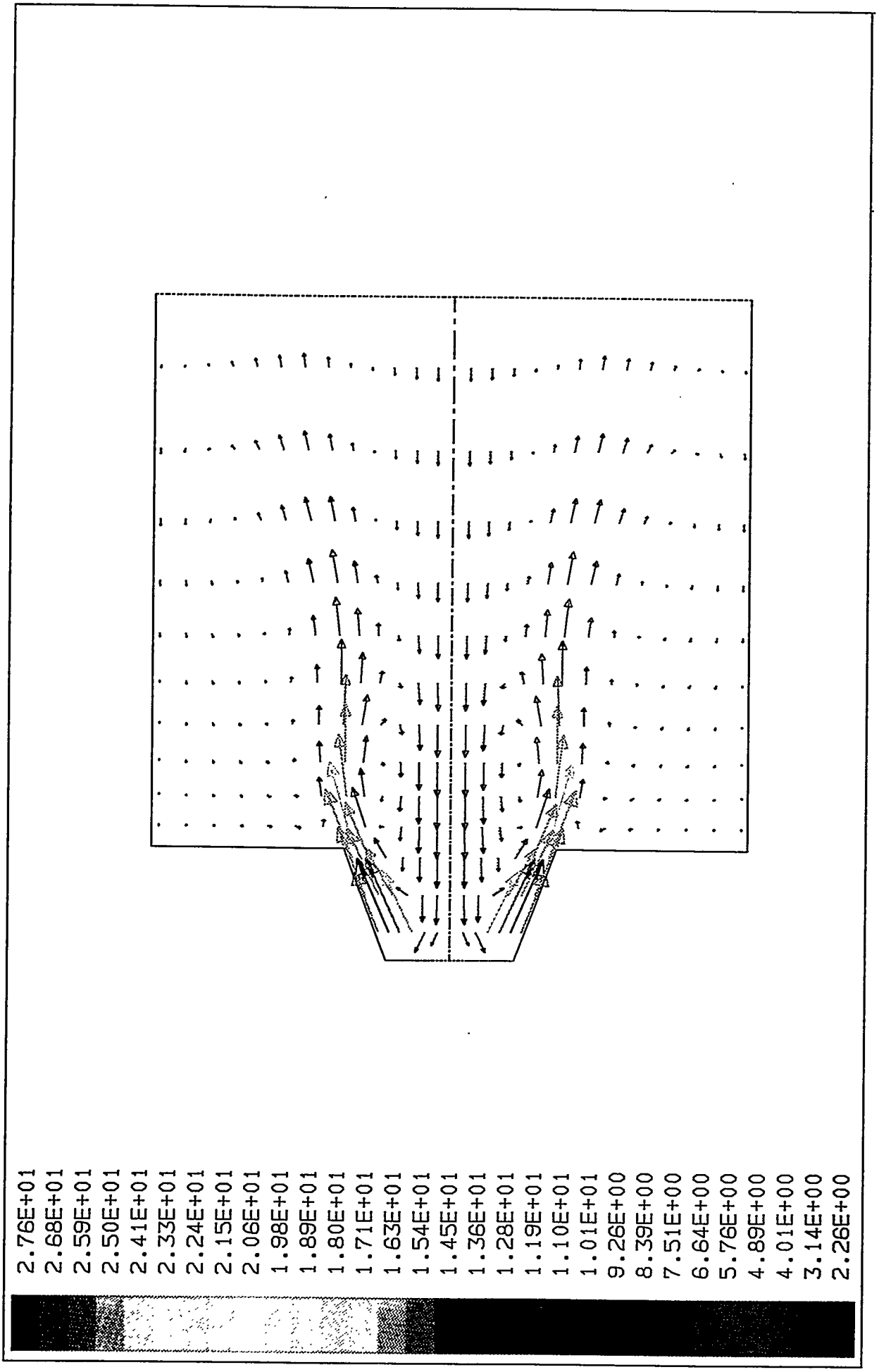

Figure 3-56. GAS VELOCITY VECTORS, IN METERS/SECOND, WITHOUT COAL PARTICLE INJECTION

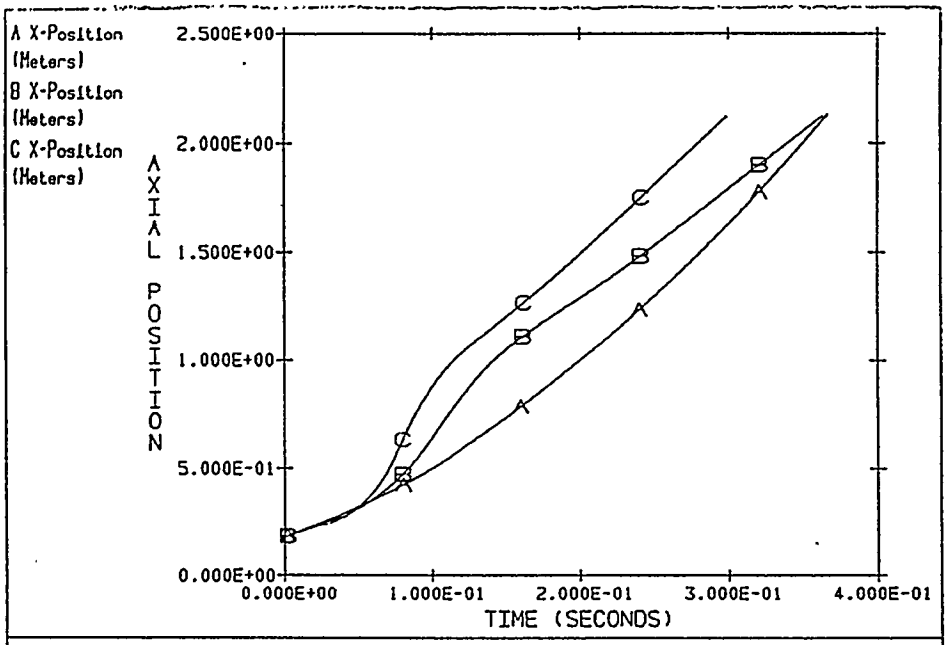

Figure 3-57. THE EFFECT OF SWIRL NUMBER ON THE AXIAL POSITION OF PARTICLE TRAJECTORY; SWIRL NUMBER EQUALS ZERO (A), SWIRL NUMBER EQUALS 0.6 (B), SWIRL NUMBER EQUALS 1.0 (C)

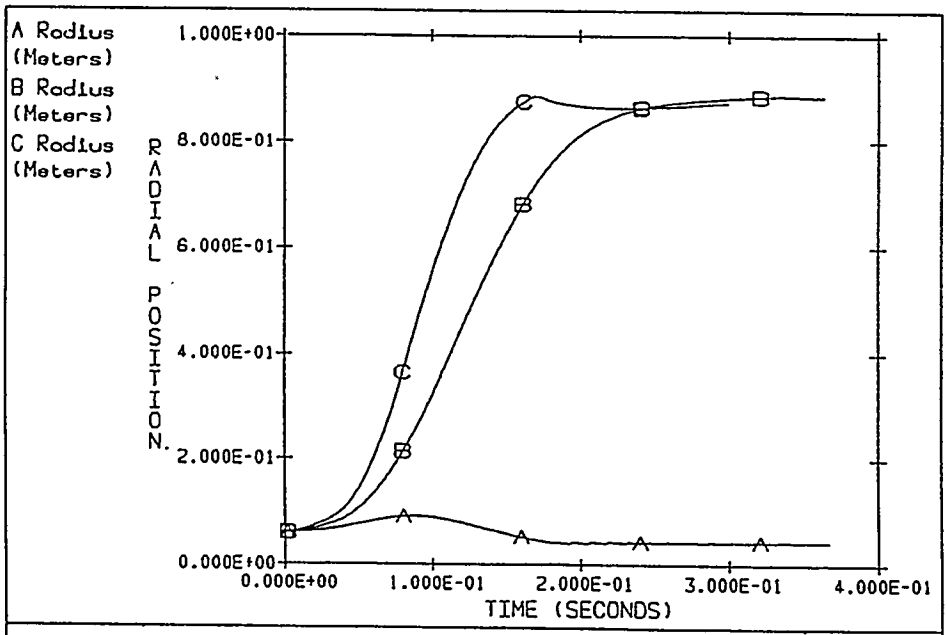

Figure 3-58. THE EFFECT OF SWIRL NUMBER ON THE RADIAL POSITION OF PARTICLE TRAJECTORY; SWIRL NUMBER EQUALS ZERO (A), SWIRL NUMBER EQUALS 0.6 (B), SWIRL NUMBER EQUALS 1.0 (C)

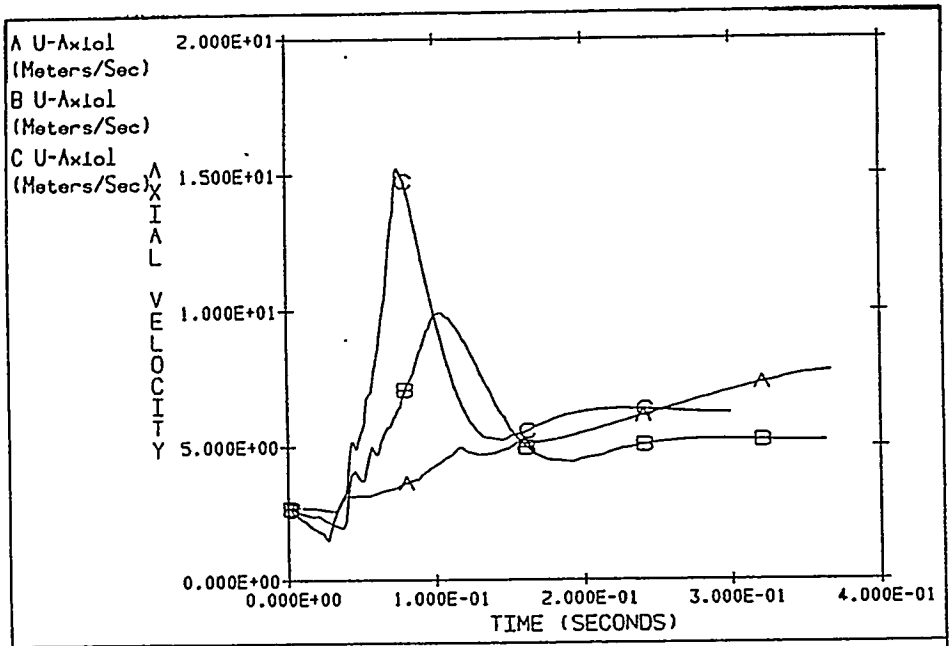

Figure 3-59. THE EFFECT OF SWIRL NUMBER ON THE PARTICLE AXIAL VELOCITY, IN METERS/SECOND; SWIRL NUMBER EQUALS ZERO (A), SWIRL NUMBER EQUALS 0.6 (B), SWIRL NUMBER EQUALS 1.0 (C)

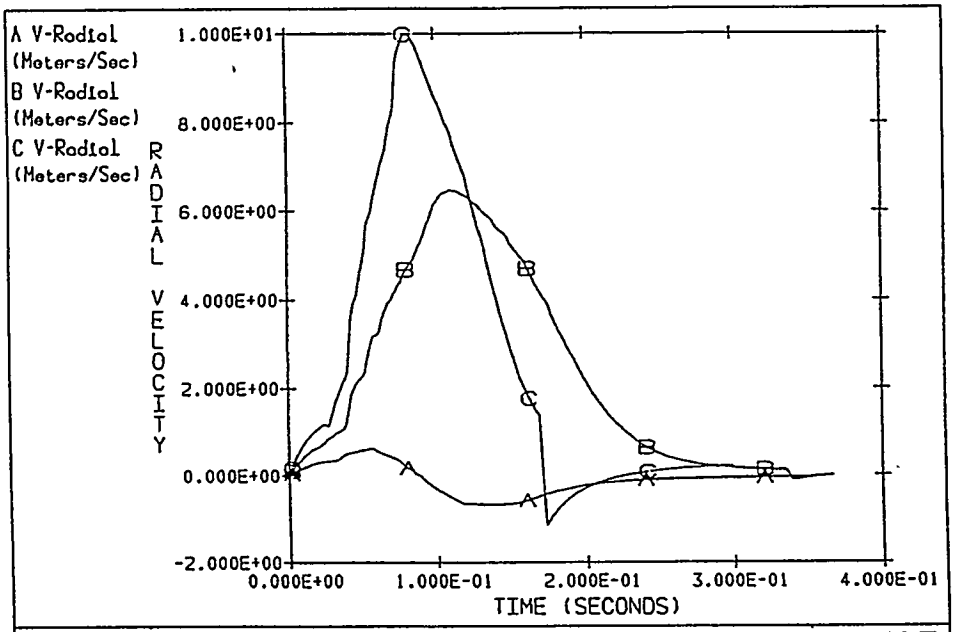

Figure 3-60. THE EFFECT OF SWIRL NUMBER ON THE PARTICLE RADIAL VELOCITY, IN METERS/SECOND; SWIRL NUMBER EQUALS ZERO (A), SWIRL NUMBER EQUALS 0.6 (B), SWIRL NUMBER EQUALS 1.0 (C)

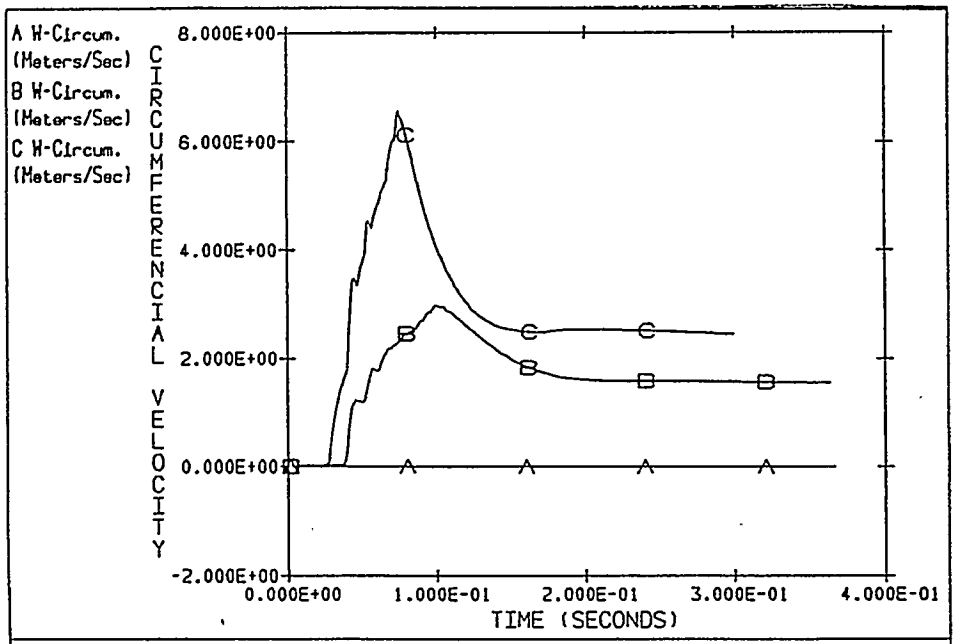

Figure 3-61. THE EFFECT OF SWIRL NUMBER ON THE PARTICLE CIRCUMFERENCIAL VELOCITY, IN METERS/SECOND; SWIRL NUMBER EQUALS ZERO (A), SWIRL NUMBER EQUALS 0.6 (B), SWIRL NUMBER EQUALS 1.0 (C)

Objectives of the New Modeling Effort

The aim of this investigation was to evaluate the combustion aerodynamics of two commercial low-NO_X swirl burners. The influence of burner geometry, swirl number, and flow rates on the performance of each burner was analyzed using a CFD code. For the sake of simplicity, the computations were carried out for isothermal cases. In the absence of any chemical reaction, namely combustion, the aerodynamics of each burner was investigated. It was found that the one burner issued a long (Type III) flame with the potential for undesirable flame impingement on the back wall of the boiler. The other burner is predicted to produce a type II flame. The importance of imparting swirl to the primary air stream was established. Based on the evidence offered by the modeling, recommendations are made for the stable operation of both burners in retrofit applications.

Introduction

The combustion of pulverized coal in utility and industrial boilers is usually achieved through the use of swirl burners[18]. A number of important characteristics of swirl-stabilized pulverized coal flames (i.e., ignition stability, flame temperature and pollutant formation) are strongly influenced by the near burner flow-field[19][20]. Although these influences are understood qualitatively, a more quantitative understanding is required to ensure optimum design of swirl burners[20].

Most commercial swirl burners have several features in common, including: a primary air flow which transports the pulverized coal and a secondary air flow which supplies the main combustion air[18]. Recently, a new design of swirl burners has emerged in which the combustion air is introduced around the centrally injected pulverized coal through secondary and tertiary air streams. The driving force behind the design of such burners is the need to reduce NO_X emissions. In essence, these burners are designed to internally stage the air, and create the fuel-rich and fuel-lean flame zones by aerodynamic means, rather than by physically separated regions of the combustion chamber. The challenge is to produce a fuel-rich, high temperature zone near the burner which will provide sufficient residence time for coal devolatilization, followed by rapid and rigorous mixing of the rest of the combustion air and the remaining char to ensure complete combustion. The overall performance of such burners can be judged by the following criteria: 1) satisfactory levels of combustion efficiency; and 2) satisfactory levels of NO_X emissions. Clearly, both criteria are influenced by the combustion aerodynamics of the burner, which in turn are determined by the burner geometry and the swirl levels for a given fuel.

In this investigation, a CFD code was employed to examine the flow-field issued by two commercial swirl stabilized pulverized coal burners (referred to as the HEACC and the EER burner) in an effort to match the aerodynamics of each burner to those required by the

demonstration boiler in which they were being tested. The objective of this investigation was to compare and contrast the flow-fields issued by the burners and, to predict their performance.

Theory

In the CFD employed, the fundamental equations governing fluid flow (the mass continuity equation, the Navier-Stokes equations, and the energy equation) are solved employing a finite difference numerical procedure. The numerical technique involves the subdivision of the domain of interest into a finite number of control volumes or cells. The partial differential equations are discretized over these cells to obtain sets of simultaneous algebraic relations. Because of the non-linearity and interdependence of the differential equations, an iterative solution has to be adopted [17].

The fluid is regarded as a continuum and is solved in an Eulerian frame of reference in the manner described above. Where a second, disperse phase (such as coal-particles) is present, a Lagrangian approach is preferred. Particles or droplets are followed by means of a particle tracking technique in which the equations of motion, along with any auxiliary relations which may be in effect, are integrated with respect to time. Generally, in turbulent flows in which the swirl number, S, approaches or exceeds unity, the use of the Reynolds Stress Model is recommended. Conservation of angular momentum ($r^2\Omega$ = constant) creates a free-vortex in the fluid. When the forces due to the angular momentum in the fluid are large (i.e., in the cases of flows with swirl numbers equal to or larger than one), the assumption of isotropy used in the calculation of Reynolds stresses is no longer valid. Consequently, the k-ε model was abandoned in favor of the Reynolds Stress Model [17].

The success of any CFD simulation depends upon the correct use of the code and an appreciation of its capabilities and limitations. The modeling of the particulate phase is one area of uncertainty. The heterogeneous reactions of coal combustion are often slow enough to be unaffected by the turbulent fluctuations, but many of the important reactions in the overall combustion process occur in the gas phase. The effect of turbulence on mean chemical properties during coal combustion is often neglected in numerical modeling due to the complexity of the physical models involved. However, two approximate methods have been suggested which attempt to address the impact of turbulent fluctuations on the mean properties of coal combustion. The first method, the volatile reactiveness model, is an extension of an approach for premixed gaseous combustion suggested by Lockwood et. al and Magnussen and Hjertager[21]; [22]. The second approach, the statistical, coal-gas mixture-fraction model, is an extension of gaseous diffusion flame approaches[23]. In the current analysis, the impact of turbulent fluctuations on the mean properties of coal combustion was neglected, which of course will introduce some inaccuracy into the predictions. However, the general trends observed are not expected to change drastically if some of these effects were taken into account. The details of the physical models

employed in the computations are discussed elsewhere [17]. Indeed it is easy to cite many relevant, little-touched and complex physical modeling areas such as the interaction between the turbulence and a particulate phase, the turbulence-chemistry interaction and the turbulence-radiation interaction. It is due to some of these shortcomings of numerical modeling that it is imperative that the predictions be checked against experimental data. Nonetheless, despite some of the above shortcomings the numerical modeling provided insight into the near burner flow field of the two burners.

Simplified Theory of Swirl Flows

To classify the various types of swirling flow, it is convenient and conventional to look specifically at a fluid in cylindrical polar coordinates, rotating about the axis. Axisymmetry is assumed with no radial or axial velocity components: $u = v = 0$. The swirl (or tangential) velocity is hence the only nonzero component and is only a function of the radius r, ($w = f(r)$). In general, vortices can be categorized as free, forced or combined (Rankine). A number of parameters in addition to the tangential or swirl velocity are used to characterize and classify vortices. These include the angular velocity (Ω), the vorticity (ω), and the circulation (Γ). Angular velocity about the central axis Ω, is defined as the number of revolutions per unit time for the fluid as a whole. Vorticity, ω is defined as the curl of the velocity field.

Mathematically, ω can be expressed as:

$$\omega = \text{curl } v$$

$$\omega = \left(\frac{1}{r} \frac{\partial (rw)}{\partial r}, 0\, 0 \right)$$

in the (x, r, θ) directions. Rotating flows with $w = C/r$ are called free or potential vortices. Clearly, the vorticity vanishes ($\omega = 0$) and such flows are called irrotational. On the other hand, flows with solid-body rotation $w = c'r$ are called solid body or forced vortices. Clearly, the vorticity does not vanish ($\omega \neq 0$) and such flows are called rotational. The circulation Γ along one of the concentric paths of rotating motion is defined by $\Gamma = 2\pi rw$ where w is not a function of θ. The general characteristics of vortices are summarized in Table 3-6.

Generation of Swirl Flows

In swirling flows, the fluid emerging from the orifice has a tangential or swirl velocity component in addition to the axial and radial components of velocity encountered in free, axial, non-swirling jets. Because of their wider spread and their faster mixing with the surrounding fluid, swirling jets are frequently applied to coal flames as an effective means of controlling mixing of pulverized coal with the recirculating products of combustion. It is now an established fact that

Table 3-6. General Characteristics of Vortices

	Forced (Free) vortex	Free (Potential) vortex	Combined (Rankine) vortex
Tangential velocity, w	$w = c' r$	$w = \frac{C}{r}$	$w = \frac{C'}{r}\left[1 - \exp\left(-\frac{r^2}{r_0^2}\right)\right]$
Angular velocity, Ω	$\Omega = c'$	$\Omega = \frac{C}{r} = f(r)$	$\Omega = f(r)$
Circulation, Γ	$\Gamma = 2\pi\,\Omega\, r^2$	$\Gamma = 2\pi\, C$	$\Gamma = 2\pi\, C'\left[1 - \exp\left(-\frac{r^2}{r_0^2}\right)\right]$
Vorticity, ω	$\omega = 4\pi\Omega$	$\omega = 0$	$\omega = \frac{4\pi\, C'}{r_0^2}\left[\exp\left(-\frac{r^2}{r_0^2}\right)\right]$

for strongly swirling jets there exists a central or Internal Recirculation Zone (IRZ) which may be used to stabilize the coal flames on burners and further more reduce the formation of NO_X. Swirl flows are generated by three principal methods:

1) tangential entry of the fluid stream, or a part of it, into a cylindrical duct;
2) the use of guided vanes in axial tube flow; and
3) rotation of mechanical devices which impart swirling motion to the fluid passing through them. This includes rotating vanes or grids and rotating tubes.

Industrial pulverized coal swirl burners typically employ a combination of the above methods to generate flows with swirl numbers of 0.6. Hence, establishing the recirculating aerodynamic regimes which greatly enhance burner flame stability, and general burner performance. In the absence of fundamental and practical data on the use of pulverized coal swirl burners, the manufacturers employ a wide variety of swirl generation devices. Several manufacturers have centered on the use of swirl generation concepts which employ multi-vaned tangential inlet devices. For example, some manufacturers have successfully employed optimized versions of vaned tangential swirlers into the coal-water fuel burners that they have developed. These devises are relatively inexpensive to construct and are capable of generating swirl numbers of 0.6 or greater. A major drawback to most vaned tangential swirler designs is that they tend to operate with relatively high pressure losses. These losses translate directly into an increase in burner fan head requirements. An increase in required fan head negatively impacts on the overall efficiency of the power system and can increase plant capital equipment cost as well.

In swirling free jets or flames, both axial flux of the angular momentum and the axial thrust are conserved[24];[25]. These can be written as:

$$G_\phi = \int_0^R \rho u\, w\, r\, 2\pi r\, dr = \text{constant} \qquad (1)$$

$$G_x = \int_0^R \rho u\, u\, 2\pi r\, dr + \int_0^R p\, 2\pi r\, dr = \text{const} \qquad (2)$$

where u, w and p are the axial and tangential components of the velocity and static pressure, respectively, in any cross section of the jet. Since both of these momentum fluxes can be considered to be characteristic of the aerodynamic behavior of the jet, a non-dimensional criterion based on these quantities can be set up as:

$$S = \frac{G_\phi}{G_x R} \qquad (3)$$

where R is the exit radius of the burner nozzle. Experiments have shown that the swirl number is the significant similarity criterion of swirling jets produced by geometrically similar swirl generators[25, 26]. The calculation of swirl number using equations (1-3) requires accurate measurements of velocity and of static pressure distributions to be made in the cross-section of the swirling jet. The designer may not always have access to experimental data and there is interest in determining the swirl number directly from air register design data. The angular momentum and the velocity term in the expression for the axial momentum can be predicted with reasonable accuracy [18]. However, it is more difficult to predict the value of the static pressure integral because it undergoes changes along the flow in the swirl generator, depending upon the geometry of the burner nozzle[19, 27, 28]. When the swirl number is calculated from input velocity distributions in the swirl generator rather than from the velocity distributions in the jet, the static pressure term can be omitted and the swirl number can be given with good approximation as[25]:

$$S' = \frac{G_\phi}{G'_x R} \tag{4}$$

where

$$G'_x = \int_0^R \rho u\, u\, 2\pi r\, dr \tag{5}$$

Several different versions of the swirl number are found in the literature depending on the inclusion or otherwise of the pressure term in the axial thrust [26]. However, the swirl number most commonly used, S' neglects the pressure term. This parameter is commonly used to define the relative effectiveness of swirl generation devices and was used in this investigation to determine some of the boundary conditions for the computations. It is also important to emphasize the fact that the variation of the tangential velocity with the radius of each burner was considered to be constant. In other words, the assumption of a forced vortex was used to define the boundary conditions for each burner.

Although swirl levels can affect flow patterns, geometric features characteristic of swirl burners for coal (quarl angle and length, blockage ratio, the presence of an oil gun) can also determine the flow type. In general there is a lack of information on swirling flows from double concentric jets typical of coal burners, and for jets containing solids[19-21, 27, 29-33].

Specifications of the Two Burners

The HEACC employed a staggered configuration and was designed around the use of axial flow vane type swirlers, with their characteristically low pressure drop for swirl generation. The secondary air swirl was controlled by interchangeable swirler assemblies with the mass flow rate of the secondary air being equal to 25% of the total register air flow. The tertiary air swirl could be generated from either the tangential inlet configuration, the blades located within the register or a

combination of the two. The mass flow rate of the tertiary air was designed to be 75% of the total register air flow. The primary air swirl was also generated by a series of blades. The generic geometry depicted in Figure 3-62 illustrates the main dimensions of both burners. The diameters of the primary, secondary and tertiary air streams referred to as D1, D2, and D3 were different for the two burners and the respective diameters were used the actual computational models for each burner. The main purpose of Figure 3-62 is therefore to illustrate the simplifications made to the geometry of each burner during the modeling effort.

The EER burner was designed as a telescopic configuration with both the secondary and tertiary air streams being introduced tangentially and then going through a series of swirler assemblies. The secondary air flow provided 30% of the total combustion air with the remaining 70% being made up by the tertiary air flow. Unlike the HEACC, the primary air stream was not swirled.

Both burners contained an internal gun similar to the traditional oil guns in the double concentric, pulverized coal swirl burners. The function of this gun was to allow an atomizer tip access to the center of the burner to allow the firing of the coal water slurry fuel. Both burners are capable of firing natural gas, pulverized coal, and MCWM. The swirling mechanisms utilized in each burner are summarized in Table 3-7.

The operating conditions for each burner were used as the boundary conditions for the CFD code and were summarized in Table 3-8. It is important to point out that as each burner can be operated over a range of air and fuel mass flow rates, inlet velocities, and swirl numbers, the computations were not limited to what is reported. In fact a wide range of operational parameters were varied and modeled for each burner and the reported conditions simply show a set of typical conditions for each burner for comparative purposes.

Discussion

The first objective was to predict theoretically the near burner flow-field issued by each burner into the boiler. The computational domain was composed of the inlet of each burner, the burner quarl, the front wall of the boiler and the side wall of the boiler (with a length equal to half of the total length of the wall). The effect of a central MCWM gun was simulated by adding a bluff body on the axis of the primary nozzle to give blockage ratios typical of the actual geometries of the two burners.

The computations were carried out on a nonuniform grid with a concentration of nodes within and near the quarl. The results were checked for grid independence, within reasonable limits. The results from computations carried out on four different grids (25x25, 30x30, 40x40 and 50x50) were checked. The differences in the calculated velocities were typically less than five percent of the maximum velocity for the 30x30, 40x40 and 50x50 grids. Consequently, a compromise was made between the grid fineness and the Central Processing Unit time of the workstation by choosing a 41x41 grid. The computational domain, hence set up, was assumed to

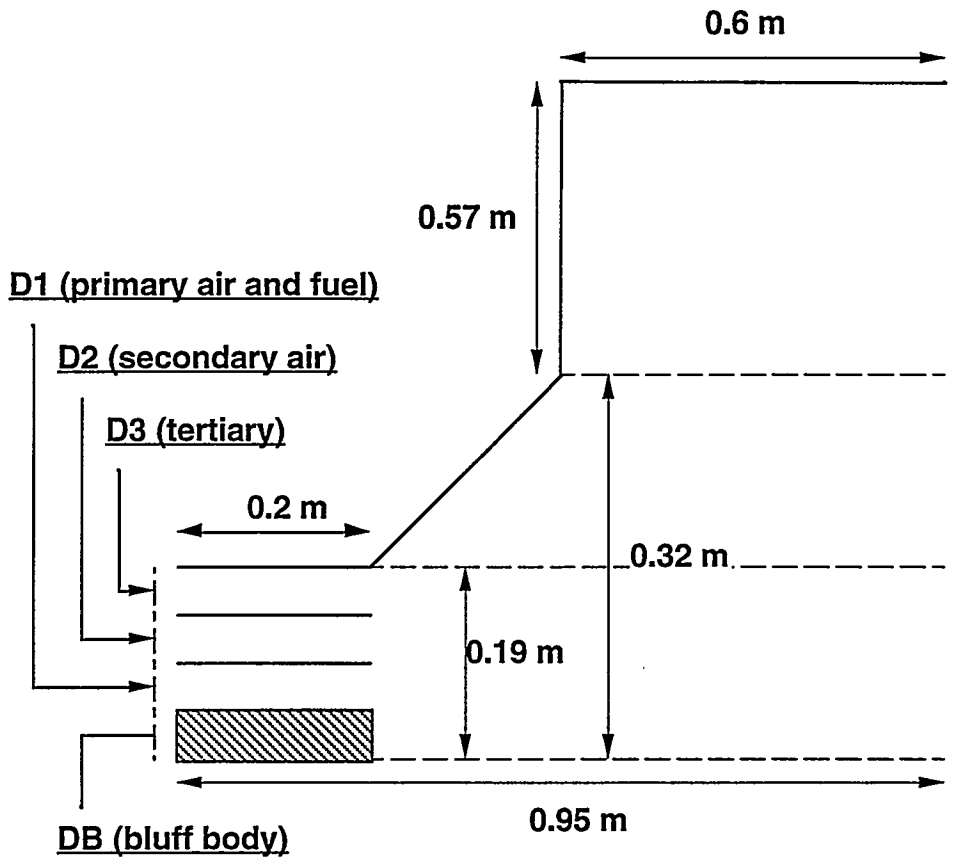

Figure 3-62. THE GENERIC GEOMETRY OF THE BURNERS AS MODELED IN THIS INVESTIGATION

Table 3-7. Summary of the Swirling Mechanisms for the Two Burners

Swirling Mechanism:	HEACC	EER Burner
Primary air	Guide vanes	Not swirled
Secondary air	Guide vanes	Tangential entry/Guide vanes
Tertiary air	Tangential entry/Guide vanes	Tangential entry/Guide vanes

Table 3-8. Operating Conditions for the Two Burners

	HEACC	EER Burner
Coal flow rate (kg/s)	0.17	0.17
Total combustion air (kg/s)	1.99	1.99
Excess air (%)	20	20
Primary air velocity (m/s)	26	28
Primary air temperature (K)	400	400
Primary air swirl number	1.2	0.0
Secondary air velocity (m/s)	26	28
Secondary air temperature (K)	1,000	1,000
Secondary swirl number	1.2	0.4
Tertiary air velocity (m/s)	26	28
Tertiary air temperature (K)	1,000	1,000
Tertiary air swirl number	1.0	1.0

be realistic, accurate and still allow the computations to be carried out for an axis-symmetrical two-dimensional geometry.

It is now well established that at sufficiently high swirl numbers, an IRZ is formed in both cold and combusting flows[31]. However, the size of this IRZ is dependent on whether the flow is cold or combusting[20, 31]. Recent efforts have demonstrated that combustion can have a significant and dominant effect on the flame aerodynamics.

For highly-swirled natural gas flames, two main flame types (Types I and II) have been reported. The same classification was later applied to highly-swirled pulverized coal flames [20]. Type I flames are usually observed at relatively high primary air velocities and as a result of the large momentum associated with the primary air jet, the internal recirculation zone is penetrated by the primary air jet. Consequently, the primary air jet and the pulverized coal particles carried with it divide the IRZ into smaller segments which may, or may not, be equal in size, depending on the symmetry of the flow filed. Type II flames are observed at relatively low primary air velocities and allow the formation of a larger IRZ since, in this case the primary air jet no longer carries adequate momentum to penetrate the IRZ. Other researchers have identified a third type of flame referred to as Type III in which the degree of penetration of the IRZ by the primary jet differs from that of Type I and hence the need for a third category (Figure 3-63) [19, 21, 27].

In this investigation the same three flame types will be employed to classify the flames issued by the two burners. It is important to point out that all of the reported results are for isothermal cases. At present, the physical models utilized in the CFD code employed remain inaccessible and consequently the mathematical modeling of coal combustion did not meet the expectations of the users and was not reported. This situation is being remedied and mathematical modeling of coal combustion will be undertaken in the near future.

Figure 3-64 illustrates the near burner flow-field for the HEACC. The velocity vectors clearly depict the regions of reverse flow. The overall impact of the tangential velocity components of the primary, secondary and tertiary air streams was to create the aforementioned IRZ. The boundary of the IRZ was of course defined by a velocity contour in the x direction with its magnitude equal to zero. This was illustrated graphically by Figure 3-65 where filled contours of u-velocity (i.e. the component of velocity in the x-direction) were used to define the boundary of the IRZ by assigning a negative value to the filled contours within the IRZ. In order to characterize the IRZ the volume and the mass flow rate of the gases in the IRZ should be used. The volume of the gases in the IRZ is self evident from Figure 3-65. The mass flow rate of the gases in the IRZ can be determined by integrating the area encompassed by a u-velocity contour put equal to zero. For the HEACC the mass flow rate in the IRZ was calculated to be 0.0035 kg/s. This mass flow rate corresponds to a total mass flow rate of 0.18 kg/s. Figure 3-66 illustrates the amount of mass flow rate recirculated by the IRZ for burner (a). In further reference to the flame classification recommended by the

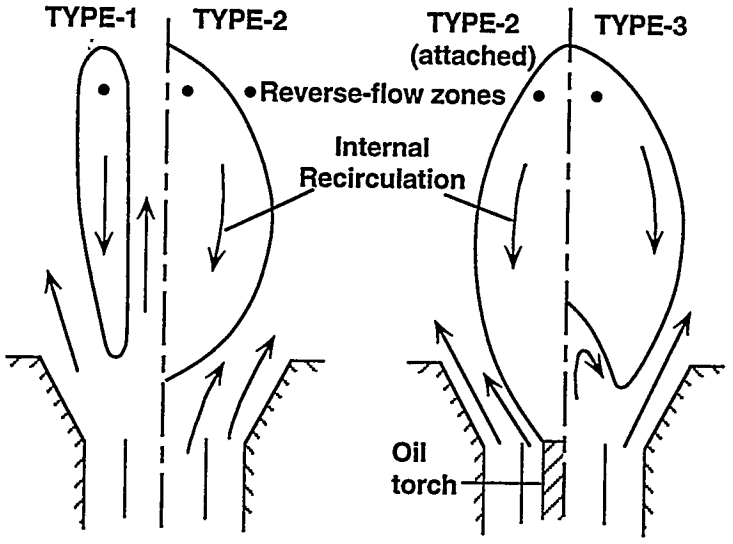

Figure 3-63. FLAME TYPES ISSUED FROM SWIRL BURNERS

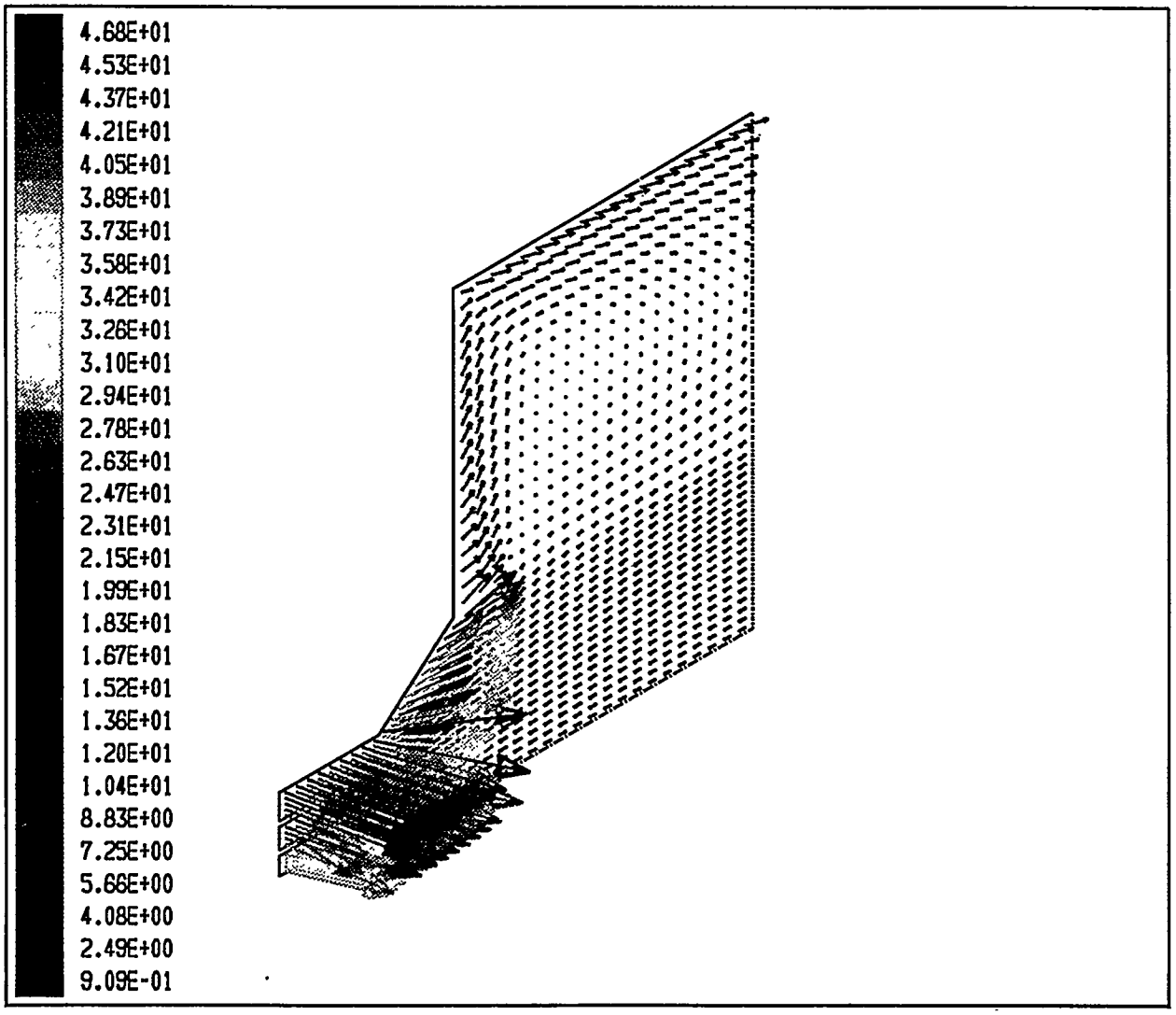

Figure 3-64. VELOCITY VECTORS FOR THE HEACC S1=1.2, S=1.2, S3=1.2

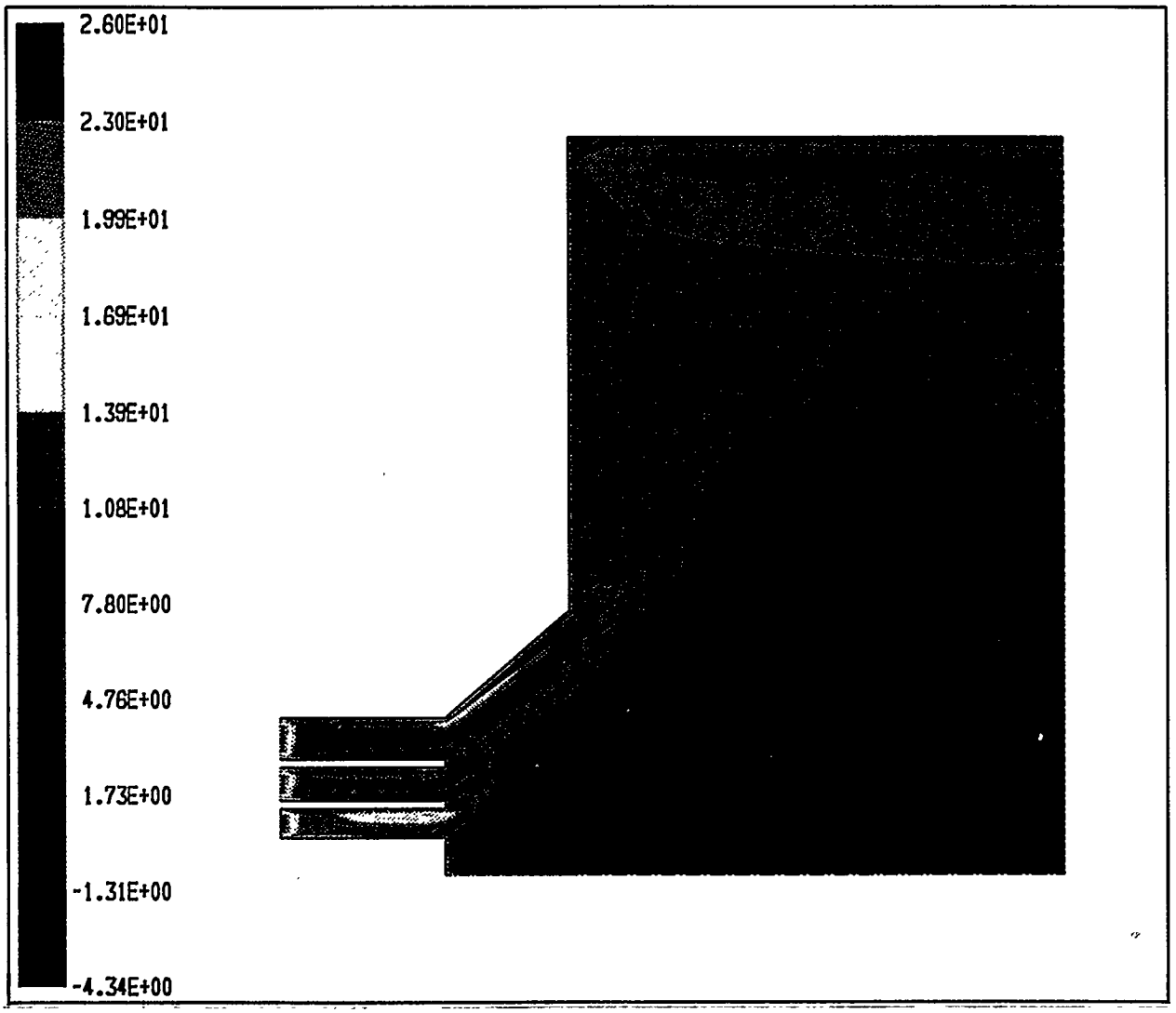

Figure 3-65. FILLED CONTOURS OF U-VELOCITY FOR THE HEACC S1=1.2, S=1.2, S3=1.2

International Flame Research Foundation (Ijmuiden, Netherlands), the flame issued by burner (a) was classified as a type II flame as the primary flow did not penetrate the IRZ.

Figure 3-67 illustrates the near burner flow field for the EER burner. The IRZ as formed by this burner was smaller than the IRZ formed by the HEACC by 12.5% (on a volume basis) for the same flow rate of air and fuel (Figures 3-67 and 3-68). Further more, the IRZ of the EER burner is completely penetrated by the primary air jet. The reason being the absence of swirl in the primary air jet of the EER burner. The flame issued by the EER burner can be classified as a type I if the IRZ is completely penetrated by the primary air jet. It was also found that under certain operating conditions the flame issued by the burner could be classified as Type III due to the partial penetration of the IRZ by the primary flow. For the EER burner the mass flow rate in the IRZ was calculated to be 0.00206 kg/s. This mass flow rate corresponds to a total mass flow rate of 0.1952 kg/s (Figure 3-69).

An overall comparison between the results of the computations for the burners reveals the following:

1) average jet velocities in the x-direction (i.e. the u-velocity of the jet) for the EER burner are higher than those for the HEACC as shown in Figures 3-65 and 3-68;
2) the degree of swirl imparted to the primary, secondary and tertiary air streams in the HEACC is considerably higher than the degree of swirl imparted to the secondary and tertiary air streams in the EER burner. Consequently, the profiles of tangential velocity are more developed in the computational domain for the HEACC burner. The parameters affecting the aerodynamics of each burner include; the swirl number, the quarl angle and the burner geometry. The quarl angle was kept constant foe both burners and therefore the predicted differences can only be due to the differences in the geometry of each burner and their respective swirl numbers;
3) The above discussion forms the logical basis of the differences in the intensity of the IRZs formed by each burner. The HEACC has the potential to create a more intense IRZ than the EER burner. Based on these findings the flame issued by the EER burner is expected to be longer with the potential for some impingement on the backwall of the boiler. The HEACC on the other hand produces a shorter flame; and
4) The results also offer strong evidence that imparting swirl to the primary jet of a burner can enhance the rate of mixing of the primary jet with the secondary and tertiary jets. This finding is in agreement with the experimental findings of other research groups [19, 21, 27].

In the absence of measurements, the analysis of coal combustion in swirling jets can only be made with the assumption that coal flows with the gas and within the streamlines as it enters the burner. The possibility of some of the coal separating from its stream-tube and being injected into

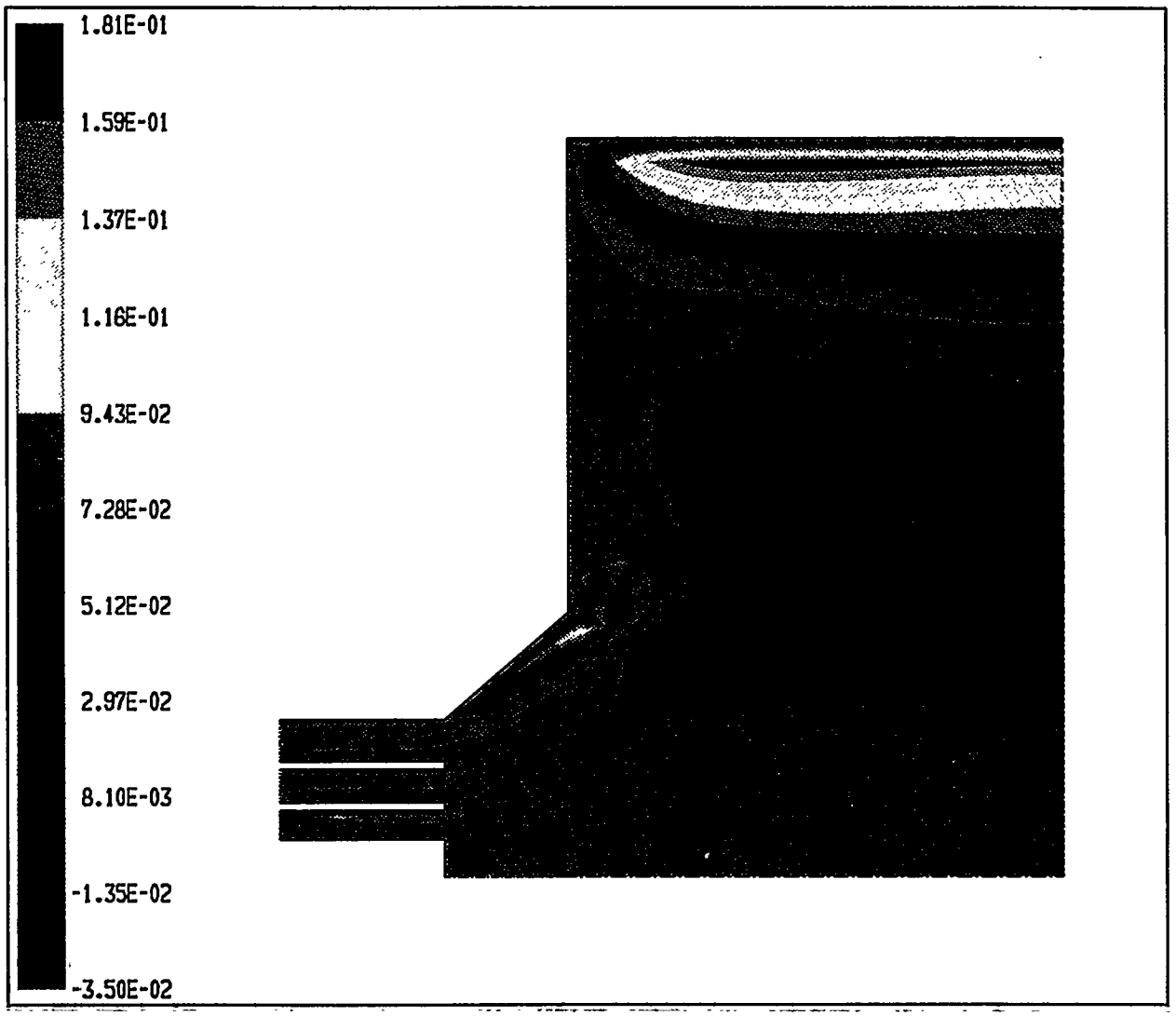

Figure 3-66. FILLED CONTOURS OF THE MASS FLOW RATE FOR THE HEACC S1=1.2, S=1.2, S3=1.2

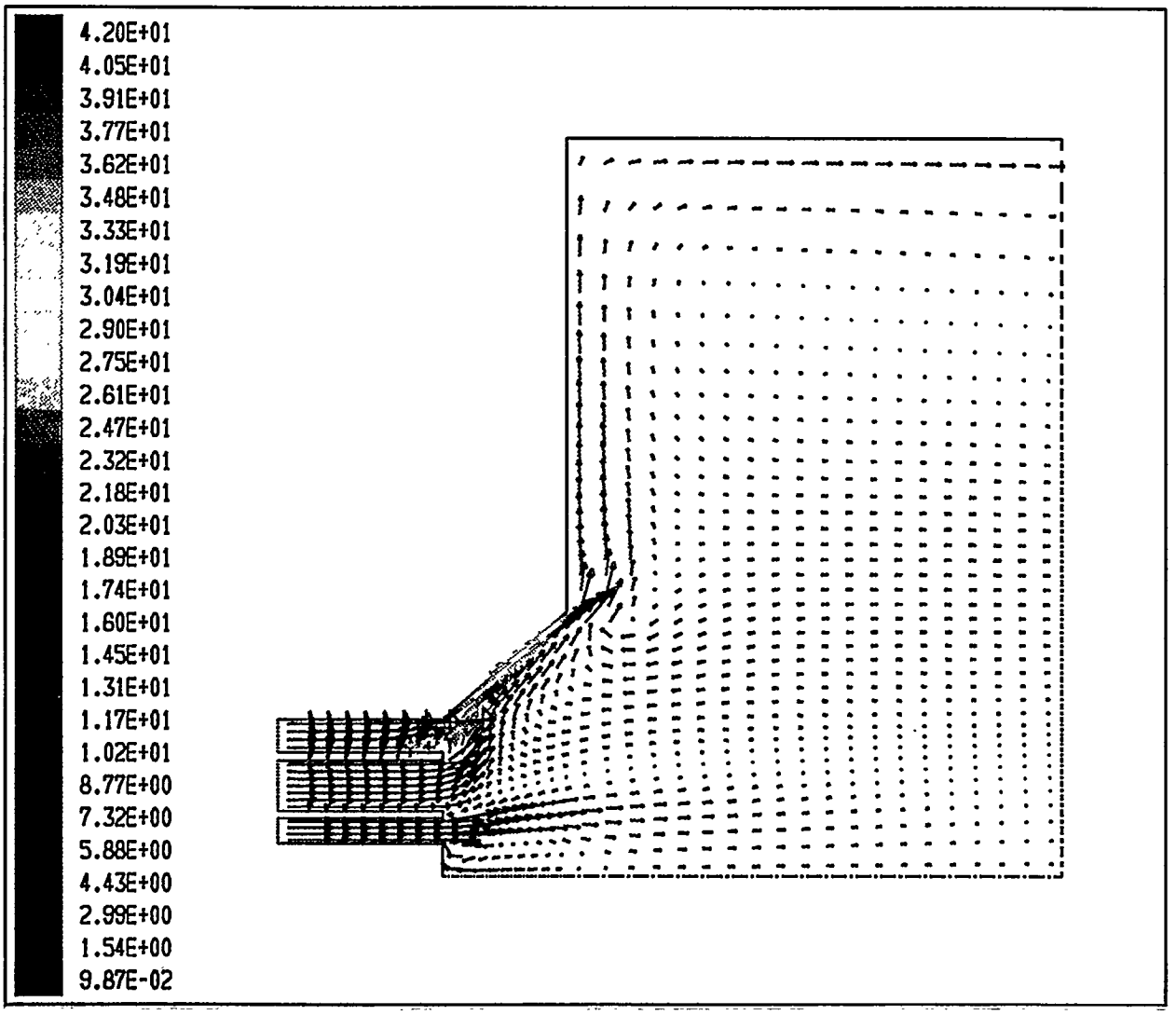

Figure 3-67. VELOCITY VECTORS FOR THE EER BURNER S1=0.0, S2=0.4, S3=1.0

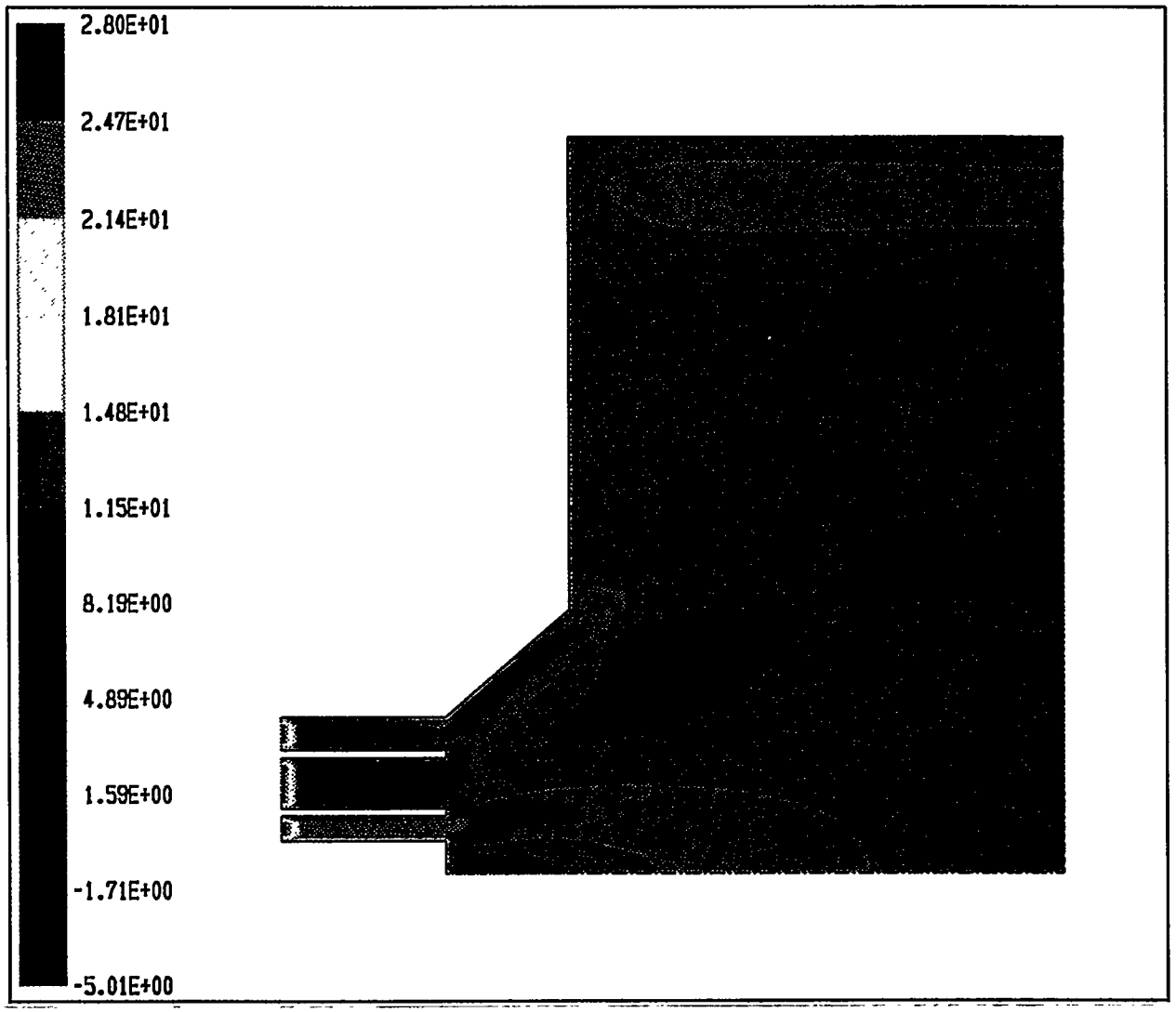

Figure 3-68. FILLED CONTOURS OF U-VELOCITY FOR THE EER BURNER S1=0.0, S2=0.4, S3=1.0

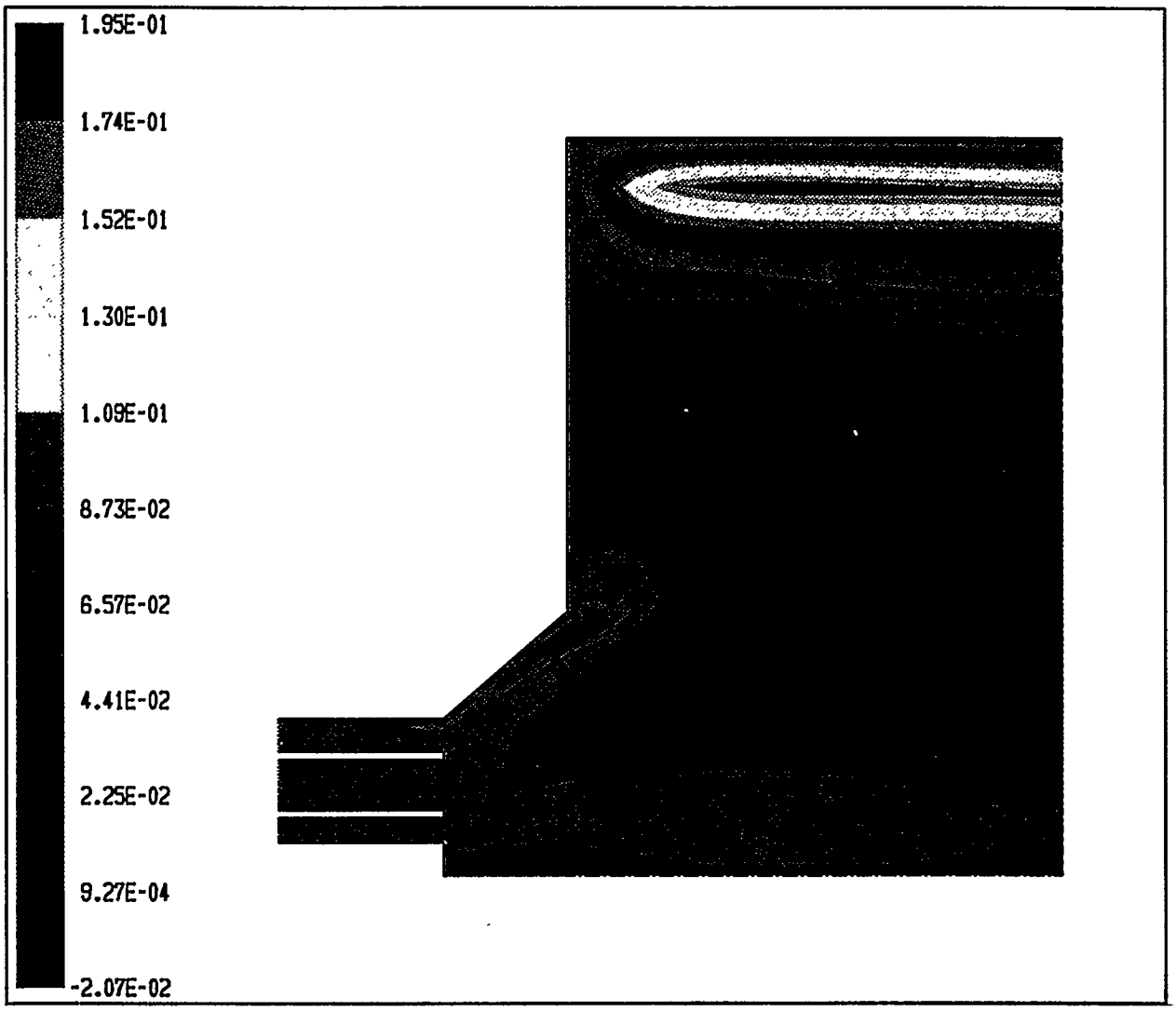

Figure 3-69. FILLED CONTOURS OF THE MASS FLOW RATE FOR THE EER BURNER S1=0.0, S2=0.4, S3=1.0

the hot IRZ is suggested in the literature. Indeed, the turbulent diffusion of coal necessary for such an effect is implied by the gas turbulent exchange coefficients measured by Truelove at al [34, 35] . However, its extent and relevance remains to be quantified. Future work will address some of the above issues.

Concluding Statements

1. For the same flow rates of air and fuel and for the same quarl angle, the shape and intensity of the jets issued by the two burners differ significantly. A Type II flame was issued from the HEACC and Types I and III from the EER Burner.
2. Without primary swirl in the EER burner a portion of the primary flow penetrated the IRZ partially before being deflected radially, resulting in Type III flow, or completely resulting in a Type I flame Complete penetration of the IRZ - (Type I flow) was expected for the higher velocities employed for the primary air stream in the EER burner.
3. Given the existing geometry of the demonstration boiler the flame issued by the EER burner may impinge on the back wall of the boiler. A potential solution is to impart swirl to the primary flow of the EER Burner.

3.4 Subtask 2.4 Evaluate Emissions Reductions Strategies

In Subtask 2.4, the emissions from MCWM and DMC testing are to be determined. During this reporting period, the DMC demonstration was completed and the results from emissions testing is presented.

DMC EMISSIONS

The SO_2, NO_x, and CO emissions (lb/MM Btu corrected to 3% O_2) during testing from October through December 1994 are given in Figures 3-70 and 3-71 as a function of test number and coal combustion efficiency, respectively. The SO_2, NO_x, and CO emissions ranged from 0.59 to 1.14, from 0.48 to 1.01, and from 0.25 to 2.91 lb/MM Btu, respectively.

Targeted NO_x emissions of <0.6 lb/MM Btu were achieved when firing DMC at 12.5 to 12.8 MM Btu/h with 90 to 92% combustion efficiency. For the most part however, the NO_x emissions were greater than the targeted value. NO_x emissions ranged from 0.48 to 0.84 lb/ MM Btu when firing DMC at 12.5 to 12.8 MM Btu/h with a mean of 0.65 lb/MM Btu. When firing DMC at 15-16 MM Btu/h, the NOx emissions ranged from 0.67 to 1.01 lb/MM Btu with a mean of 0.80 lb/MM Btu.

The CO emissions varied considerable during the testing. This may be a function of variable coal feed and burner operation. Very high CO emissions (sometimes >4,000 ppm) were observed during the natural gas/coal cofiring period when transiting to 100% coal firing.

4.0 PHASE I, TASK 3: ENGINEERING DESIGN

During this reporting period, Task 3 was completed except for the design of the MCWM preparation facility. The two retrofit designs for a boiler located at the Naval Surface Warfare

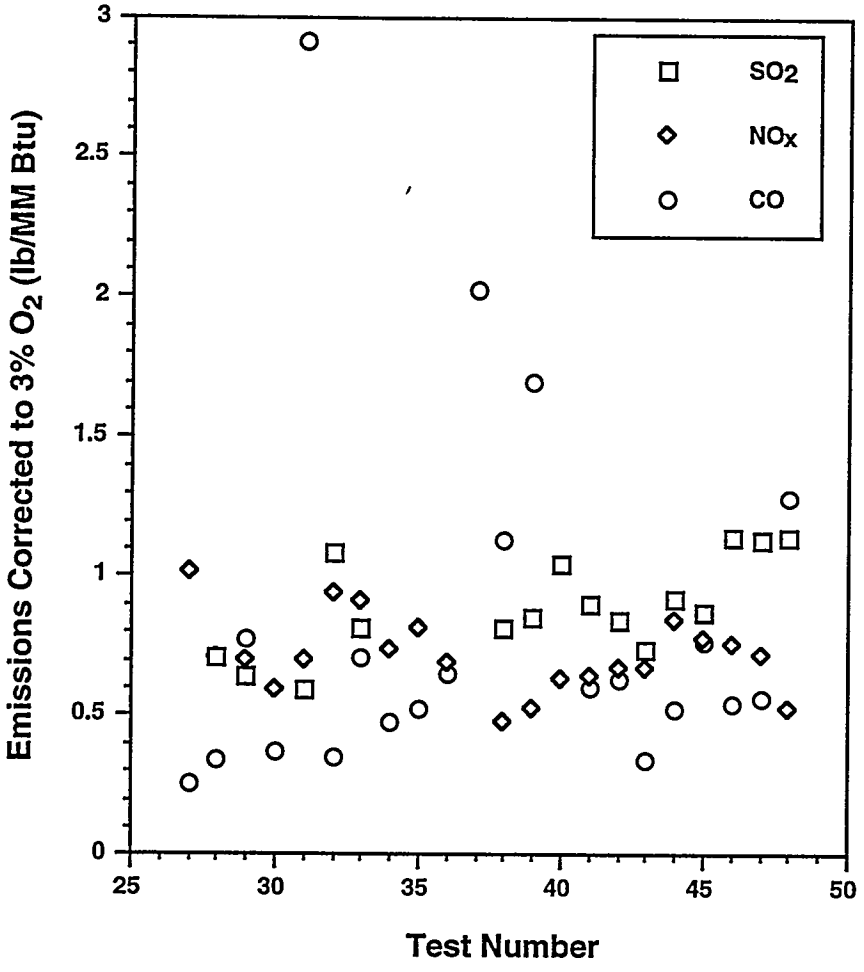

Figure 3-70. SO_2, NO_X AND CO EMISSIONS DURING DMC TESTING CONDUCTED FROM OCTOBER TO DECEMBER 1994

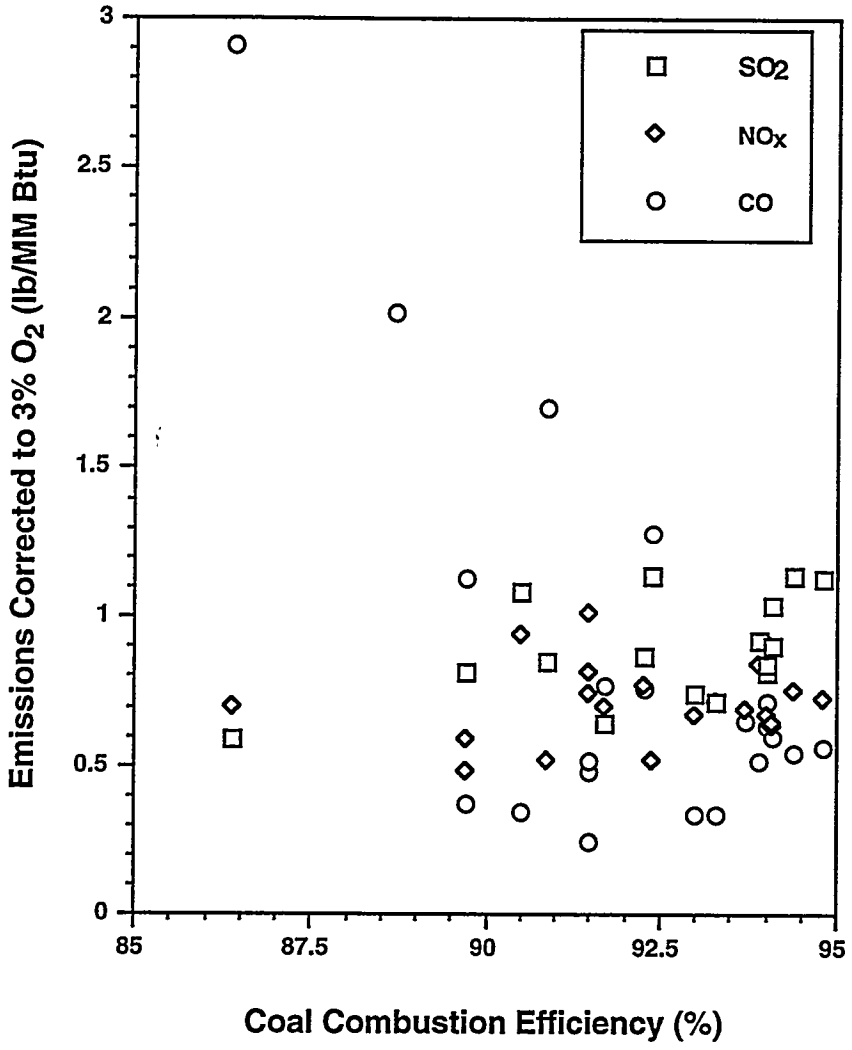

Figure 3-71. SO_2, NO_X AND CO EMISSIONS AS A FUNCTION OF COAL COMBUSTION EFFICIENCY DURING DMC TESTING CONDUCTED FROM OCTOBER TO DECEMBER 1994

Center at Crane, Indiana were completed. The designs were for the conversion of a boiler that currently fires natural gas or fuel oil to fire either DMC or MCWM. The designs include the following systems: coal or MCWM unloading, DMC preparation, burner supply, burner and burner front piping, combustion air preheat, flue gas particulate removal, and associated controls. For each of the designs, the following engineering documents have been prepared: system description, mass and energy balances, instrument list, major equipment list, electrical equipment list, building list, compressed air consumption, construction cost estimate, and a drawing package comprised of a process flow diagram, piping and instrumentation diagram, mechanical equipment arrangements, control logic diagrams, and electrical one line.

The complete design packages will be provided in the Phase I final report. A summary of the design activities of the subsystems is given in the following sections.

4.1 Subtask 3.1 MCWM/DMC Preparation Facilities

No work was conducted on the MCWM preparation facility. The DMC preparation facility was incorporated into Subtask 3.2.

4.2 Subtask 3.2 Fuel Handling

Subtask 3.2 was completed in July 1994.

4.3 Subtask 3.3 Burner System

Subtask 3.3 was completed in July 1994.

4.4 Subtask 3.4 Ash Removal, Handling, and Disposal

Subtask 3.4 was completed in July 1994.

4.5 Subtask 3.5 Air Pollution Control

Work consisted of revising the major equipment list.

4.6 Subtask 3.6 Integrate Engineering Design

Work consisted of reviewing the design packages and revising the major equipment and instrument lists, and the cost for the equipment. Work also consisted of engineering revisions to the drawings.

5.0 PHASE I, TASK 4: ENGINEERING AND COST ANALYSIS

5.1 Subtask 4.1 Survey Boiler Population/Identify Boilers for Conversion

This subtask is complete, and the results are contained in the Phase I Final Report which is under preparation.

5.2 Subtask 4.2 Identify Appropriate Cost Estimating Methodologies

This task is complete and reported in the previous semiannual technical progress report [5].

5.3 Subtask 4.3 Estimate Basic Costs of New Technologies

This subtask is complete, and the results are contained in the Phase I Final Report which is under preparation.

5.4 Subtask 4.4 Process Analysis of MCWM and Dry, Micronized Coal

DMC RETROFIT EVALUATION

This subsection presents an evaluation of the profitability of retrofitting the existing Crane gas/oil-fired boilers to fire Dry Micronized Coal (DMC), and a comparison with retrofitting to fire micronized coal water mixture (MCWM). The profitability of retrofitting the boilers to fire MCWM was previously completed. The analysis is based on cost information provided by Energy and Environmental Research Corporation (EER), and on work done by Science Applications International Corporation (SAIC). Particular attention is given to showing the sensitivity of profitability to critical influences such as fuel prices, less boiler derating when using DMC, utilization rates, boiler life, and the cost of capital

The total capital required to retrofit to fire DMC includes provision for a fuel preparation facility on site, whereas in the case of MCWM, it was assumed that the MCWM was delivered to the site. This means retrofitting to fire DMC has higher total capital requirement (TCR) than for the case of MCWM. The critical piece of equipment is the mill since this is the devie that produces the fuel. Conveyors and other equipment for handling the fuel are also required. DMC preparation on site is necessary because of the hazards of transporting fine coal, especially for the DMC required in this case. It is important to note that the mill will more often than not be operating below rated capacity. Typically, the size of mill required is obtained by considering the size reduction to be performed and the desired rate of fuel production. This yields the power consumption of the mill which is linked to mill size by factors which are available in engineering and manufacturers' publications. The desired mill size is determined with all this knowledge and an allowance for safety in design, down time, etc. Except for custom made mills, mills come in certain standard sizes and a mill just bigger than desired is often selected. All this suggests that a mill will more often than not be operating under capacity, and can therefore be used to provide DMC for different boiler plant sizes.

EER's cost estimate may be on the high side because it uses quotes which already have contingencies allowed for, in addition to high management and engineering fees, and overall contingencies. To get around this, the sensitivity analyses include TCR variation. In general, however, the TCR for DMC retrofitting is believed to be higher than for MCWM retrofitting. Reasons for this are that:

1. No coal storage space or handling equipment are required in the case of MCWM.
2. The MCWM supply system is considerably simpler because MCWM is pumpable and therefore existing oil supply systems can be utilized with little modification.
3. The cost of boiler modifications for MCWM can be much less than for DMC especially when a cleaned coal is used.

The variables that influence the economic feasibility of retrofitting to fire DMC are the differential fuel cost (DFC), the expected life of the boiler plant, TCR, boiler derated capacity (BDC), boiler use, and the discount rate. The coal used is assumed to have the same characteristics as that used for preparing the MCWM. In this evaluation, a 20% derating is assumed as a base case. That is, the boiler will operate at a BDC of 80%. EERC's TCR estimate of $5.215 million is taken as a base. A base 4% discount rate, and a 50% boiler use are assumed. A base case expected boiler life of 20 years is used. In addition, a sensitivity analysis varying all the variables was performed.

The results show that:

- NPV increases with increasing differential fuel cost (DFC).
- NPV increases with boiler derated capacity (BDC).
- NPV increases with increasing expected boiler life.
- NPV decreases with increasing discount rate.
- NPV decreases with increasing total capital requirement (TCR).
- NPV increases with increasing boiler use.

The main conclusion is that retrofitting the Crane boiler to fire DMC is not economically viable. Only at low TCRs does the retrofit show viability. Therefore, MCWM retrofitting seems to be more economical and is recommended for the Crane boiler.

5.5 Subtask 4.5 Analyze/Identify Transportation Cost of Commercial Sources of MCWM and Cleaned Coal for Dry, Micronized Coal Production

This subtask is complete, and the results are contained in the Phase I Final Report which is under preparation.

5.6 Subtask 4.6 Community Spillovers

This subtask is complete, and the results are contained in the Phase I Final Report which is under preparation.

5.7 Subtask 4.7 Regional Market Considerations and Impacts

This subtask is complete, and the results are contained in the Phase I Final Report which is under preparation.

5.8 Subtask 4.8 Integrate the Analysis

This subtask is complete, and the results are contained in the Phase I Final Report which is under preparation.

6.0 PHASE I, TASK 5: FINAL REPORT/SUBMISSION OF DESIGN PACKAGE

The Phase I final report is under preparation and will be completed on June 1, 1995. Tasks 3 and 4 have been completed, and work on Tasks 1 and 2 is underway.

7.0 PHASE II, TASK 1: EMISSIONS REDUCTION

The objectives of this task are to develop strategies to provide for ultra-low emissions when firing coal-based fuels in industrial-scale boilers. Emissions to be addressed include SO_2, NO_x, fine particulate matter (<10 μm), and air toxics (volatile organic compounds and trace metals).

7.1 Subtask 1.1. Evaluation of Emissions Reduction Strategies

It is the objective of this subtask to evaluate emissions reduction strategies for the installation of commercial NO_x and SO_2 systems on the boiler. This effort is being conducted in conjunction with another DOE program (Cooperative Agreement No. DE-FC22-89PC88697). The work in this subtask is being conducted primarily by literature searches and discussions with manufacturers of flue gas cleanup equipment and with other researchers in the field.

Literature searches were conducted on NO_x, SO_2, volatile organic compounds, and trace metals removal systems. Each of these is presented in the following subsections. The literature searches are for all coal-fired boilers and are not limited to industrial-size boilers. The information from the literature searches will be used with that received from the vendors and engineering firms to select appropriate control systems for installation on the demonstration boiler (Section 7.3).

NO_x CONTROL STRATEGIES

Introduction

Nitrogen oxides (NO_x) are formed during the combustion of fossil fuels such as natural gas, oil or coal. NO_x refers to nitric oxide (NO) and nitrogen dioxide (NO_2). NO_x emitted from combustion processes is typically 90-95% NO and the balance NO_2. As a pollutant, NO_x is thought to be harmful in several ways: it is a contributor to acid rain, it destroys the ozone layer, and it is a heat-trapping compound suspected of increasing atmospheric temperatures (i.e., global warming[36]). At low elevations, NO can also react with sunlight to create photochemical smog. As the U.S. Environmental Protection Agency (EPA) and several states implement strict rules to curb NO_x emissions, more and more boilers are subjected to tighter emission limits.

NO_x emissions can be controlled either during the combustion process or after combustion is complete. Combustion control techniques depend on air or fuel staging techniques to take advantage of the reaction kinetics to reduce the NO_x formed. Post-combustion control techniques generally rely on the introduction of reagents which, at specified temperatures, destroy the NO_x either with or without the use of a catalyst.

This section details the current conventional as well as experimental NO_x control strategies. The information is presented as:

- Combustion Modifications/Strategies and
- Post Combustion Strategies
  - A: NO_x Control
  - B: Combined NO_x/SO_2 Control

Emphasis is placed on post combustion control but combustion modifications are briefly examined as some post combustion strategies involve a combination of the two. Combined NO_X/SO_2 techniques are covered as well, since this is the area where most of the current research is being done.

Combustion Modifications/Strategies

The first actions usually taken to control NO_X emissions, also known as primary measures, take the form of combustion modifications. This section will briefly describe general combustion control measures followed by options to control NO_X for different types of combustors and boilers. The emphasis in this section is on commercially used combustion systems for NO_X control.

The NO_X concentration in the flue gas from coal combustion is affected by many factors, such as coal characteristics, burner characteristics, furnace chamber construction and size, and operating conditions.

Options to control NO_X during combustion and the effects thereof are different for new and existing boilers. For new boilers, combustion modifications can be easily made during construction. For existing boilers, the situation is different and the viable alternatives are limited. Modifications can be complicated and cause unforeseen problems. In most cases, these problems can only be solved after a considerable amount of time (and quite possibly, money) is spent.

When combustion modifications are made, it is very important to avoid adverse impacts on boiler operation (i.e., efficiency) and also the formation of other pollutants (such as N_2O, or CO). Criteria for low NO_X operation are as follows[37]:

- Operational safety (stable ignition over the desired load range);
- Operational reliability (prevent corrosion, erosion, fouling, slagging, overheating of tubes, etc.);
- Complete combustion (to avoid producing high emissions of CO)
- Lowest possible pollutant emissions, avoiding formation of other pollutants such as polyorganic matter (POM), or N_2O;
- Minimal adverse impact on the flue gas cleaning equipment; and
- Low maintenance costs.

Regardless of whether the technique is called low excess air (LEA), burners-out-of-service (BOOS), overfire air (OFA), low-NO_X burners (LNB), flue gas recirculation (FGR), or fuel reburning, all redistribute the fuel and air so that mixing is slowed, the availability of O_2 in critical NO_X formation zones is reduced, and the amount of fuel burned at peak flame temperatures is lowered.

The simplest of the combustion control strategies is low-excess air (LEA) operation. Essentially, this means reducing the excess air level to some constraint point (carbon monoxide formation, flame length, flames stability, etc.). LEA has had limited success so far (1-15% NO_X reduction).

Staged combustion involves modifying the primary combustion zone stoichiometry, i.e., the air/fuel ratio. This can be done operationally or by equipment modifications.

An operational technique that can be used is burners out of service (BOOS). In this technique, the fuel flow to selected burners is terminated while leaving the air registers open. The remaining burners operate fuel-rich, which limits oxygen availability, lowering peak flame temperatures, and reducing NO_X formation. The unreacted products combine with the air from the "off" burners to complete burnout before exiting the combustor. This technique has been successful on gas-fired units, but has had poor results on coal[38].

Another way to achieve staged combustion is by installing secondary and even tertiary overfire air (OFA) ports located above the main combustion zone. The installation of OFA ports may require modifications to furnace parts, if air ports were not provided originally. OFA may also require the routing of large ductwork in places which might not have adequate space. Both of these factors may severely affect the cost of this control strategy.

Low-NO_X burners (LNB) are designed to achieve the staging effect internally. The air and fuel flow fields are partitioned and controlled to achieve the desired air/fuel ratio, which reduces NO_X formation. Low-NO_X burners are applicable to virtually all combustion devices with circular burners. An LNB replacement may or may not involve modifications to pressure-parts, or additional fans or ducts. This could possibly affect the economics of an LNB replacement.

Combustion temperature reduction is an effective way to reduce thermal NO_X emissions. One way to reduce combustion temperature is by adding a dilutent. This is the technique employed by flue gas recirculation (FGR). In FGR, a portion of flue gas leaving the combustion process, is recirculated back into the windbox. Generally, 10-20% of the combustion air is effective in reducing the combustion temperature. Because FGR beneficial effects are limited to reduction of thermal NO_X, the technique is applied primarily to natural gas or distillate oil combustion. In fact, this technique suffered difficulties on coal and was withdrawn from the market[38].

Reburning, commonly called "fuel staging" or "in-furnace reduction" involves diverting up to 20% of the furnace's total fuel input to create a second substoichiometric combustion zone downstream of the primary zone. Hydrocarbon radicals from the secondary fuel reduce the NO_X produced in the primary zone.

Different fuels can be used as the secondary or reburning fuel. The fuel must be easy to ignite and have a low nitrogen content. Various fuels that have been tested including natural gas, oil, peat, coal, and wood. The solid fuels must have a light volatile content and be finely ground. Natural gas has shown to give the best results due to its low nitrogen content, high energy intensity, ease of ignition, and the fact there is no need for a carrier gas[37].

Demonstrations of gas reburning on coal-fired boilers around 100 MW in size have accomplished NO_X reductions of between 40-65% with a total gas/coal displacement of 10-20%.

OFA and FGR are often used in conjunction with gas reburning schemes. To succeed with reburning, it is important that the operational parameters be optimized. The optimal conditions for reburning have been defined through pilot-plant operations and research. Published results vary but a general summary is[39-43]:

- Minimize excess air in the primary zone;
- Separate the secondary & primary zones so combustion is complete;
- Inject secondary (reburning) fuel in as high a temperature zone as possible (>1,200°C) to avoid competing reactions and to obtain sufficient reaction time;
- Good entrainment, mixing and dispersion of the reburning fuel is critical for success. (Recirculated flue gas used as a carrier gas for the secondary fuel, i.e., coal, can aid in mixing.);
- The stoichiometry in the reburn zone should be 0.65-0.9 and the residence time 0.05-1.5 seconds. (Here lies a major discrepancy); and
- Burnout air should be injected so that rapid mixing is obtained. A residence time of 0.7-0.9 seconds is needed to complete the burnout.

Combustion modifications/strategies can be used to achieve modest NO_X reductions. However, they eventually "butt heads" with the fragile balance among CO and unburned hydrocarbon emissions, unburned carbon in the bottom ash and fly ash, the avoidance of reducing zones in the combustor which may cause corrosion.

It is also important to realize that NO_X emissions might not remain constant even after combustion modifications. Several factors such as operators experience, the amount of automated controls, load variability, changes in pulverizers, etc. can cause baseline NO_X emissions to fluctuate within a large range of values.

Other important performance impacts include: (1) slagging and fouling characteristics of the boiler, (2) different ash characteristics and higher or lower fly ash loadings, (3) corrosion of tubes in reducing zones, (4) higher fan power consumption, and (5) pulverizer constraints.

These fluctuations and performance impacts, as well as increasingly tighter emissions limits, force consideration of post combustion strategies.

Post Combustion/Strategies:

NO_X Control

There are generally two strategies for controlling NO_X formation after combustion: selective catalytic reduction (SCR) and selective non-catalytic reduction (SNCR). In SCR, ammonia is injected into the flue gas upstream of a catalytic reactor. The catalyst used is usually TiO_2 or Al_2O_3 based, but can be made of other materials including activated carbon or iron oxide. The ammonia reacts with NO_X forming elemental nitrogen and water. In SNCR, a reagent (usually ammonia or urea), is injected into the furnace exit region where temperatures are sufficiently high to promote the reaction of the reagent with NO_X, thereby forming elemental nitrogen and water.

Recently, new experimental post combustion methods to treat NO_X have surfaced. These will be addressed further at the end of this section.

Selective Catalytic Reduction (SCR)

In the SCR method, the NO_X in the flue gas is reduced through injection of ammonia in the presence of a catalyst. The reaction products are nitrogen and water. The reaction is selective, therefore oxidization of ammonia and sulfur dioxide (SO_2) should not occur.

The most common mechanisms are listed below, with (1) being the dominant reaction.

$$4\,NO + 4\,NH_3 + O_2 \text{ ---------> } 4\,N_2 + 6\,H_2O \quad (7\text{-}1)$$
$$NO + NO_2 + 2\,NH_3 \text{ ---------> } 2\,N_2 + 3\,H_2O \quad (7\text{-}2)$$
$$6\,NO + 4\,NH_3 \text{ ----------> } 5\,N_2 + 6\,H_2O \quad (7\text{-}3)$$
$$2\,NO_2 + 4\,NH_3 + O_2 \text{ -------> } 3\,N_2 + 6\,H_2O \quad (7\text{-}4)$$

The temperature of the flue gas at the catalyst is the most important parameter. The optimum temperature is between 300 - 400°C for most commercial catalysts. At lower temperatures, sulfur trioxide (SO_3) in the presence of water reacts with ammonia and forms ammonium bisulfate (NH_4HSO_4) and ammonium sulfate $(NH_4)_2SO_4$. Ammonium sulfate is a powdery substance that can add to the particulate level in the flue gas. Ammonium bisulfate (ABS) is a sticky material that can clog the catalyst pores or deposit downstream and cause equipment deterioration. The amount formed depends on the SO_3 and NH_3 concentrations as well as the temperature. Figure 7-1 (adapted from[44]) shows the deposition temperature of ABS as a function of both NH_3 and SO_3 concentrations.

Many different types of catalysts can be used. The activity of a catalyst is important for the level of NO_X conversion as well as other reactions such as the oxidation of SO_2 to SO_3. Usually, the more active a catalyst is, the less selective it is. The activity of the catalyst is mainly dependent upon the catalyst composition and flue gas temperature.

NO_X removal efficiency is dependent upon several factors including inlet NO_X concentration, flue gas temperature, ammonia injection ratio, oxygen concentration, catalyst properties (space velocity (SV), active area, and geometry) and SO_2 and SO_3 concentrations.

The space velocity is considered to be a critical design parameter in SCR operation. It is a ratio of the volumetric flow of flue gas to the volume of the reactor. It is inversely proportional to residence time in the SCR unit. The calculation of the space velocity takes the following factors into account: required NO_X removal efficiency, temperature, permissible ammonia slip, and flue and dust gas analysis. In coal-fired power plants the space velocity is normally between 1,000 and 3,000 h^{-1} [37]. Space velocities above 5000 h^{-1} should be avoided[45].

An increase in the ammonia ratio promotes higher NO_X reduction, but quite possibly could lead to increased ammonia emissions from the stack. The unreacted ammonia leaving the stack is called ammonia slip.

The SCR system consists of three main parts: the catalyst, the flue gas section, and the ammonia supply/injection system. These are discussed further in the following sections.

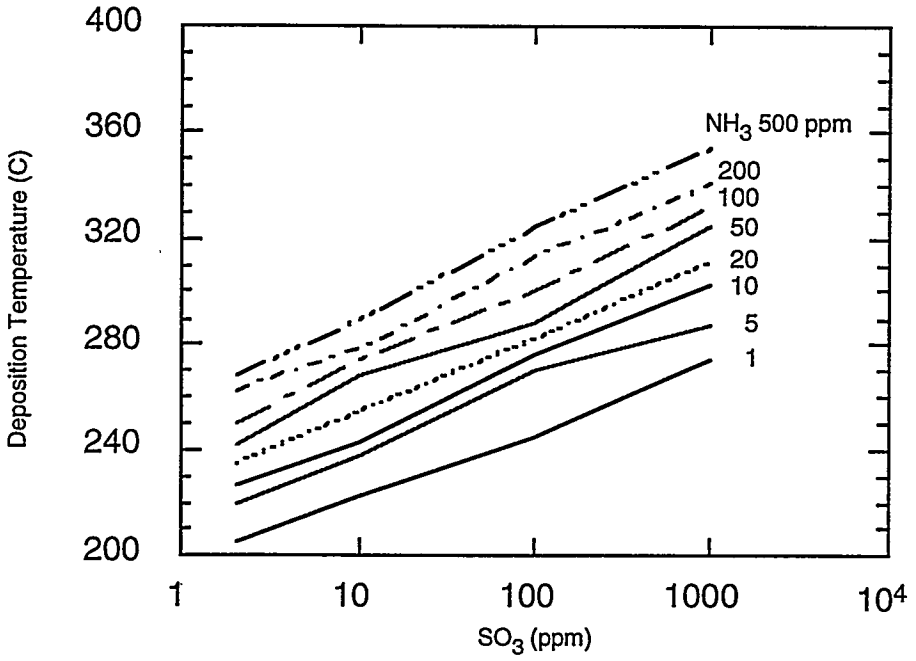

Figure 7-1. DEPOSITION TEMPERATURE OF AMMONIUM BISULFATE (NH_4HSO_4)

Catalyst

The catalyst for SCR can be placed in different positions in the gas flow, the main consideration being the flue gas temperature. The different positions used, as shown in Figure 7-2 are described as high dust, low dust, and tail end[37].

High Dust

In high dust applications, the catalyst is placed between the economizer and the air preheater at the location of the optimum flue gas temperature range for commercially available catalysts. The flue gases passing through the catalyst contain all the fly ash and sulfur oxides from combustion. This can cause degradation of the catalyst, leading to decreased NO_X removal efficiency.

When installing a high dust SCR system on an existing plant, there may be difficulties in finding space for the equipment. The existing equipment may also need to be modified for various reasons such as; maintaining optimum flue gas temperature during the entire load span and during start-up and stoppages, and to adjust equipment for optimal gas flow.

At the Chamber Works Cogeneration Plant, Carneys Point, New Jersey, which was the first U.S. pulverized coal plant to be equipped with an SCR unit, several design modifications were incorporated[46]. Modifications made included: addition of an economizer bypass duct, turning vanes, flow rectifier, and soot blowers.

Economizer Bypass Duct. Flue gas conditions will vary with load requirements. At 35-50% load, part of the flue gas is bypassed around a section of the economizer, thus keeping the flue gas above the critical ammonium sulfate formation temperature of 320°C.

Turning Vanes. Turning vanes provide uniform gas flow and also minimize gas-side pressure drop. Extensive scale-model flow testing was done to simulate the flow from the economizer exit to the air heater inlet in order to determine the exact geometry of the vanes.

Flow Rectifier. The linear velocity of loading the gas stream was limited to approximately 6 m/s to prevent catalyst erosion due to the high dust associated with the location of the catalyst. A flow rectifier made of square pipes, straightens out the gas and provides an inlet velocity profile that is in conjunction with the catalyst flow path. This tends to decrease erosion potential.

Soot Blowers. Due to the high dust loading, soot blowers were added upstream of the catalyst to occasionally clean the catalyst surface.

Other structural changes may be needed when retrofitting an existing plant[37]. These include (but are not limited to):

- Reinforcing the boiler structure as well as the boiler building;
- Reinforcing the electrostatic precipitator; and
- Changing the metal sheets in the air preheater to an enameled form which will allow for easier cleaning of ammonium bisulfate deposits.

All of these changes may lead to a long boiler down time.

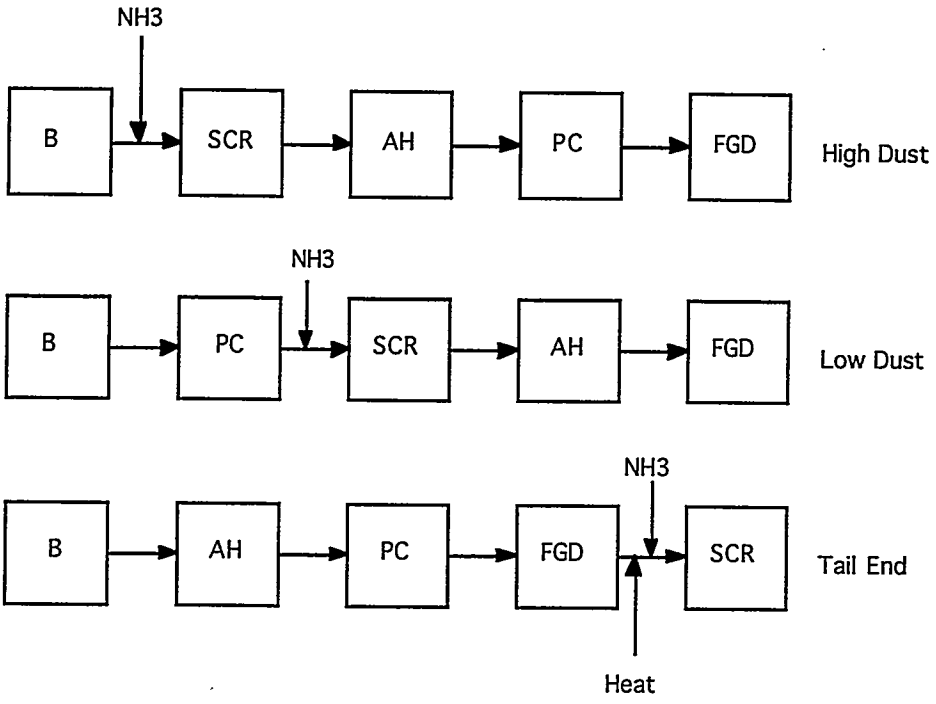

AH = Air Heater; B = Boiler; FGD = Flue gas desulphurization unit; PC = Particulate collector (baghouse or ESP); SCR

Figure 7-2. CATALYST PLACEMENT POSITIONS

Low Dust

In this situation, the catalyst is placed after a hot gas electrostatic precipitator and before the air preheater. The flue gas reaching the catalyst is virtually dust free but will contain sulfur oxides. This particular catalyst location is not common in an industrial setting.

Tail End

In the tail end system, the catalyst is placed at the end of the flue gas cleaning equipment chain, after the desulfurization unit. Therefore, the flue gases reaching the catalyst contain only small amounts of sulfur oxides and particulates. The only problem with this catalyst location is that the flue gas temperatures are too low for most industrial types of catalysts, so reheating is required. The flue gases are usually heated by first utilizing excess (waste) heat from the cleaned gases after the catalyst. But even this is usually not sufficient.

Extra heat (30-50°C) is also needed by direct or indirect heating. To reheat the flue gas through 50 C will require the energy equivalent to about 2-3 % of boiler capacity. For direct heating, duct burners, are used with high value fuels such as gas or oil. The combustion must be free of soot to prevent any additional loadings to the clean flue gas or degradation of the catalyst. The alternative is to use a regenerative heat exchanger utilizing high pressure steam or some type of synthetic heat transfer medium (i.e., DowTherm^{TM}). No contamination of the flue gas is caused by this alternative.

The tail end location has many benefits:

- Longer catalyst life (less risk of degradation);
- Optimum flue gas temperature can be maintained regardless of boiler load;
- A high activity catalyst can be used, therefore lowering catalyst volumes; and
- No fly ash to mix with unreacted ammonia.

The biggest disadvantage is reheating the flue gas.

With regards to retrofit applications, the tail end location is probably the easiest to find sufficient space for installation. Other benefits of retrofitting at the tail end location are that there is no need to reinforce the boiler or other parts of the plant, and boiler down time is minimal.

Catalyst Geometry

For a coal-fired boiler, there are two main types of catalyst geometry - plate or extruded. The notable exceptions include zeolite and activated carbon which can be granulated and used in the form of a bed.

Plate type catalysts have a metal net which acts as a support onto which active substance is applied. The plates can be a mixture of plane level and corrugated plates or all be corrugated as shown in Figure 7-3. The main geometric specifications used is the distance between plates and specific surface area.

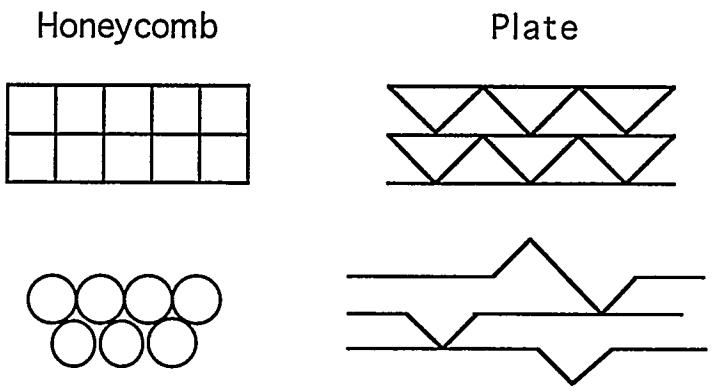

Figure 7-3: CATALYST GEOMETRY CONFIGURATIONS

Extruded types of catalysts, often called honeycombs, are self-supporting and usually formed square or as a honeycomb. The pitch and wall thickness are usually used when characterizing honeycomb catalysts. Since the conversion of SO_2 to SO_3 is a volumetric reaction, catalyst manufacturers tend to decrease catalyst wall thickness in order to achieve higher surface area and lower the conversion rate.

For high dust purposes, honeycomb catalysts are primarily produced with a specific surface area between 420 - 490 m^2/m^3. Plate type catalysts posses a surface area of around 330 -350 m^2/m^3[47]. Because of the smaller void fraction, the differential pressure loss of a honeycomb catalyst is higher than for a plate with the same catalyst volume. For an SCR system in a coal fired-boiler designed for 80% NO_x reduction with a maximum 5 ppm NH_3 slip, the range of pressure drop (over the catalyst layers only, excluding ducting to and from the reactor and the reactor inlet and outlet flanges) is 60 - 100 mm H_2O[45].

Configuration of the Catalyst

Two types of reactors are used in an SCR installation.

Horizontal Flow Fixed Bed

This type of reactor is generally used for flue gas with relatively low dust concentration, since high concentrations of dust tend to form precipitates which will settle out of the flow. These types of units are mainly installed in oil and gas-fired boilers.

Vertical Flow Fixed Bed

This is the type of reactor which is generally used in coal-fired boilers, where the gas has a high dust concentration. Important design features include:

- Flue gas flows downward through the reactor, preventing dust deposits;
- Less floor space (compared to horizontal) is required which is important in retrofit applications; and
- Catalyst replacement is from the side.

The catalyst in the honeycomb does not allow fabrication of elements longer than 1 meter. Therefore, in an SCR unit designed for 80 % removal of NO_x with a maximum 5 ppm NH_3 slip in coal-fired boilers, the amount of catalyst most often has to be distributed over 3 layers and a fourth layer may be installed without catalyst (a so called "dummy-layer" to help gas flow distribution)[45].

Types of Catalysts

The catalysts that are used today can have different chemical compositions as well as different geometrical form. The following is a list of catalyst types currently in operation (or research stages) and their working temperatures:

Titanium oxide (TiO_2) supported:	275 - 400°C
Zeolite:	380 - 600°C
Nickel sulfate ($NiSO_4$):	50 - 250°C
Activated carbon/coke	90 - 200°C
Pillared clays	250 - 450°C

Titanium Oxide Supported Catalyst

Titanium oxide (TiO_2) based catalysts now completely dominate the SCR market[37]. They were developed in Japan and are now also used in Europe.

The base material consists of activated TiO_2. Vanadium and tungsten oxides as V_2O_5 and WO_3, respectively, are usually added as further active components. The concentrations depend on the flue gas composition and operating conditions. V_2O_5 is added to enhance catalyst activity [48], but this increase in activity can lead to a decrease in selectivity, so WO_3 is added to reduce the SO_2 oxidation activity. The addition of WO_3 also broadens the temperature window by 186°C (from 233 to 419°C) for the same NO_X concentration levels[49]. This allows greater flexibility in operation.

Additional work has been done on other metal supports (ZrO_2, Al_2O_3) for V_2O_5 - WO_3 catalysts, but TiO_2 supported catalysts are still the catalyst of choice.

Zeolite

A zeolite is a porous crystalline solid which has a well defined pore system and a large internal surface area, consisting mainly of different aluminum silicates. The zeolite is primarily manufactured in a granular form and used in a bed type catalyst but can also be manufactured in monolithic layers in an extruded form.

The primary advantage of zeolite catalysts is their high temperature tolerance. At some plants, flue gas exit temperatures may exceed the maximum temperature limitation for SCR, thereby incurring the cost of an additional heat exchanger. Fresh SCR activity was found significantly enhanced when zeolites were promoted with either Fe or Cu[50].

Nickel Sulfate ($NiSO_4$) Catalysts

Recently, significant SCR activities have been measured for $NiSO_4$ catalysts at temperatures as low as 30°C (Chen et. al., 1990). In this work, researchers simulated a flue gas and passed it over a bed of $NiSO_4$ catalyst. This catalyst exhibited a 95% conversion of the NOx at a temperature range of 50 - 120°C and exhibited another conversion peak (70%) at a temperature range of 220 - 250°C.

Promising as though this research looks, there are a few drawbacks:

- With as little as 2.2% H_2O in the inlet gas, NO_X conversion decreased to a steady level of 30% within 30 minutes;
- The effect of SO_2 on SCR activity is unclear: While the addition of SO_2 clearly enhanced NO_X reduction, the formation of $(NH_4)_2SO_4$ occurred. After some time, this may cause the catalyst performance to decrease;
- SO_3 was not used in any of the experiments. Typical flue gas SO_3 concentrations are on the order of 2 - 5% of the total SO_X (sulfur dioxide (SO_2) and sulfur trioxide (SO_3)) concentrations[51]. SO_3 may react with ammonia and form ABS, thus causing corrosion and flow blockage problems; and

- Nickel sulfate (as well as other transition metal sulfates) are still in the preliminary research stages.

Activated carbon

In this process, activated carbon or coke is used as the catalyst. The activated carbon can be used for flue gas desulfurization and denitrification, separately or in combination. (The combination method will be discussed later in the section on Combined NO_X/SO_2 Control.)

In the denitrification only process, the plant is placed in a tail end position, after the flue gas desulfurization plant. The reaction is carried out at temperatures above 90 C. At lower temperatures, an undesired parallel reaction to ammonia nitrate, which is very explosive, can occur [52]. Particulates have to be removed from the flue gases prior to entering the activated carbon reactor to avoid build up and an increase in pressure drop over the reactor. The particulate concentration should be kept below 50 mg/m^3. The SO_2 concentration should also be kept below 50 mg/m^3 to avoid the risk that $(NH4)2SO4$ or $NH4HSO4$ may be formed which could destroy the grains of the adsorbent and/or cause clogging of the reactor[37].

A process modification is currently being developed for NO_X reduction using activated carbon produced from brown coal[37]. This process is being developed in Germany where pilot-plant experience indicated that SO_2, fly ash, and heavy metals were causing the deactivation of the catalyst and chemical and mechanical losses were experienced during regeneration. The advantage of using activated carbon from brown coal instead of bituminous coal or anthracites is that it is cheaper (10% of the cost) and therefore reactivation would not be necessary and the spent carbon could simply be burned in the furnace. The impurities would be again released and collected in downstream collection devices[53].

A NO_X removal rate of greater than 80% has been achieved with the activated carbon process[52, 54]. The reaction depends on flue gas temperature (optimum 100 C) and on the moisture content of the flue gases. Efficiency starts to decrease when the moisture content exceeds 7.5% and strongly decreases when over 12%.

Pillared Clays

Pillared clays (PILC) have been recently examined as possible SCR catalysts[55]. Researchers tested five PILCs in the temperature range of 250 - 450 C. They all showed considerable activity in the decreasing order:

$Cr2O3$-PILC > $Fe2O3$-PILC > $TiO2$-PILC > $ZrO2$-PILC > $Al2O3$-PILC

$Cr2O3$-PILC exhibited higher activities than a "commercial" $WO3$-$V2O5/TiO2$ catalyst but was severely affected by SO_2. $Fe2O3$-PILC showed good activities and was also SO_2 resistant.

Further pillared clay research is currently being done in the area of catalyst preparation (PILC calcination and dopant type and amount). Proponents, feel that pillared clay catalysts will be superior to commercial TiO_2 based SCR catalysts.

Catalyst Degradation

The catalyst lifetime is limited by different forms of degradation, which cause loss of activity and conversion efficiency. The main causes of degradation are:

- Formation or deposition of solids;
- Alkali metal poisoning;
- Erosion; and
- Sintering.

Formation or Deposition of Solids

The pores of a catalyst can be blocked by deposition of solids through condensation or by small particles of fly ash. Ammonium bisulfate can condense in the pores depending on flue gas temperature and concentration of SO_3 and NH_3 (see Figure 7-1). Calcium, present in the fly ash, can react with SO_3 to form $CaSO_4$ causing the catalyst to become clogged. In wet-bottom boilers with fly ash recirculation, volatile arsenic may deposit in the catalyst, blocking the active surface area.

Alkali Metal Poisoning

Current research has found that the strength of the alkali oxide poison follows the order of basicity[56]:

$$Cs_2O > Rb_2O > K_2O > Na_2O > Li_2O$$

The poisoning occurs when alkali metals attack the -OH functional groups on the catalyst surface, thereby decreasing the available active sites. This is generally the cause of the deactivation for high dust catalyst locations in coal-fired boilers[45].

Erosion

Solids and particulates can cause physical damage to the catalyst. A high fly ash content as well as uneven particle concentration and size distribution can lead to erosion.

Sintering

Heating the catalyst to too high a temperature can cause sintering. This leads to the destruction of the pore structure and decreased catalyst activity.

Replacement of Catalyst

The catalyst activity will decrease over time due to the various forms of degradation. Therefore the catalyst to be periodically replaced.

There are several ways to measure decrease in catalyst activity. One method is to compare the catalyst activity to a fresh sample. Another method is to measure ammonia slip. An increase in ammonia in the flue gas is a sign of loss of activity or problems with the catalyst. The washing frequency of the air preheater can also be used, since the decreased activity will lead to increased ammonia slip and sulfate formation. One common catalyst management plan consists of changing a catalyst layer after NO_x removal efficiency falls below target removal levels. This strategy is shown in Figure 7-4.

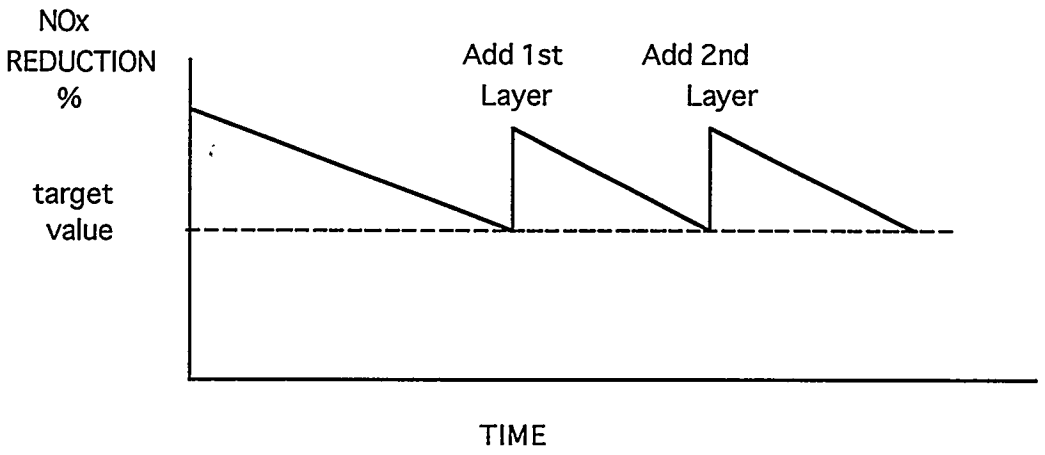

Figure 7-4: CATALYST MANAGEMENT PLAN

The used catalyst has to be disposed of. This may cause an additional expense unless an exchange program has been worked out between the catalyst supplier and the plant. The amount of catalyst used varies according to conditions. For a 300 MW coal burning power plant, the average amount of waste catalyst can be 40 m^3/yr.[37].

Ammonia Supply/Injection System

The ammonia supply system consists of equipment for storage, vaporization, air mixing, and injection of ammonia. Anhydrous ammonia (99.5% pure) and aqueous ammonia (a solution of 25 - 30% ammonia) normally are stored in liquid form. Ammonia in concentrated form is usually stored in pressurized tanks or in cooled tanks. Aqueous ammonia is much safer to handle, store and transport than anhydrous ammonia.

Before the ammonia is injected into the flue gas, it is vaporized by hot water or steam. The evaporated ammonia is mixed with air in a mixer to not more than 5% ammonia. This is important, as the NH_3/air mixture is explosive under favorable conditions in the region of 15 - 30% NH_3.

Injection is carried out through nozzles arranged in a grid covering the whole flue gas duct. The NO_X/NH_3 ratio must be as even as possible to avoid sulfate formation and excess ammonia slip. The ammonia injection grid (AIG) is one of the most important design aspects of an SCR unit. Proper AIG design reduces cost in several ways[57]:

- Less ammonia is used;
- Reduced catalyst volume;
- Extended catalyst lifetime;
- Reactor can be smaller because less catalyst is required; and
- With less catalyst, pressure loss is reduced.

Flue Gas Section

The most important aspect of the flue gas section is to maintain optimal flue gas conditions at the inlet to the catalyst. It is essential to have a uniform distribution of flue gas flow as well as a matching NH_3 distribution. The temperature, velocity, and NO_X concentration of the inlet gas need to be as uniform as possible. A uniform particulate distribution in terms of size and concentration is also desired.

Homogeneous gas flow into the catalytic reactor is achieved by the use of guide vanes and rectifiers. Nets or "dummy" layers can be used before the catalyst to protect the catalyst from erosion. Soot blowers are often installed to periodically remove ash build up from the catalyst.

Controlling the temperature of the catalyst is very important to prevent the formation of ammonia sulfates at temperatures too low and the oxidation of SO_2 at temperatures too high. Different means of controlling the temperature in a the catalytic reactor are available depending on catalyst location, operating conditions, as well as design. Shut-off valves are often installed at the catalyst reactor inlet and outlet. The use of efficient insulation ensures that the catalyst temperature

does not significantly decrease during shut down periods. An economizer bypass can be added to maintain optimum flue gas temperature during part load operation.

SCR Systems

In this section, some of the different SCR systems are summarized for NO_X control for coal combustion. For each system process details, status, and reduction capabilities are presented.

System Name:	**Selective Catalytic Reduction**
Company:	Babcock & Wilcox
Address:	1562 Beeson St. Alliance, OH, 44601, U.S.A.
Telephone:	(216) 860-6762
Contact:	Campobenedetto, E.
Reagent:	Ammonia
End Products:	Nitrogen, Water
Flue Gas Temp:	245 - 400 C (Depending on sulfur level)
Catalyst Type:	Norton NC-300, zeolite based
NO_X Reduction:	> 90%
Reference: [58]	

System Name:	**AIT Selective Catalytic NO_X Reduction (SCNR)**
Company:	Advanced Industrial Technologies
Address:	P.O. Box 493 Paramus, NJ, 07653, U.S.A.
Telephone:	(201) 265-1414
Contact:	Wang, J.
Reagent:	Ammonia
End Product:	Nitrogen, Water
Flue Gas Temp:	250 - 550 C
Catalyst Type:	AIT proprietary, zeolite based
NO_X Reduction:	see notes
Notes:	AIT claims that their catalyst, unlike precious metal catalysts, is inexpensive and is not poisoned by sulfur compounds, chlorides, and other contaminants, usually found in flue gases. The catalyst bed also offers low pressure drop and good resistance to surface fouling. AIT claims that SNCR can be designed to meet any outlet NO_X and ammonia slip limit specification.
Reference: [59]	

System Name:	**Selective Catalytic Reduction**
Company:	Johnson Mathey CSD
Address:	436 Devon Park Dr. Wayne, PA, 19087, U.S.A.
Telephone:	(610) 971-3104
Contact:	Sczudlo, G.
Reagent:	Ammonia
End Products:	Nitrogen, Water

Flue Gas Temp: 300 - 400 C
NO_X Reduction: > 90%
Reference: [60]

System Name: Selective Catalytic Reduction
Company: KVB, Inc.
Address: 9342 Jetonimo
Irvine, CA, 92718, U.S.A.
Telephone: (714) 587-2350
Contact: Reed, C.
Reagent: Ammonia
End Products: Nitrogen, Water
Flue Gas Temp: 280 - 400 C
NO_X Reduction: > 90%
Reference: [61]

System Name: $DENO_X$ (Selective Catalytic Reduction)
Company: Haldor Topsoe AS
Address: Nymollevej 55, DK-2800 Lyngby, Denmark
Reagent: Ammonia
End Products: Nitrogen, Water
Flue Gas Temp: 310 - 400 C
Catalyst Type: TiO2 based
Catalyst Location: All
NO_X Reduction: 80 - 95%
Reference: [37]

System Name: Activated Carbon SCR
Company: Hugo Petersen

Reagent: Ammonia
End Products: Nitrogen, Water
Catalyst Type: Activated carbon pellets
Catalyst Location: Tail End
Notes: Activated carbon from brown coal is used. Residual flue gas SO_2 leaving the desulfurization plant is removed by activated carbon before entering the catalytic reactor. This company was one of the first to use activated carbon from brown coal instead of hard coal.
Reference: [37]

Selective Non-Catalytic Reduction (SNCR)

Description

NO_X emissions can be controlled through thermal reactions by using appropriate reducing chemicals in a process called selective non-catalytic reduction (SNCR). SNCR is an attractive

control strategy in that no catalyst is required, thereby alleviating the problem of disposing of spent catalyst.

There are many methods using different chemicals, all requiring a specific temperature window to allow the desired reactions to occur. The temperature window is generally between 900 - 1,100°C. Ammonia can be formed below the temperature window and the reducing chemicals can actually form more NO_X above the temperature window. The most commonly used chemicals are ammonia or urea ($CO(NH_2)_2$). Other chemicals which have been tested in research work include, amines, amides, and amine salts, and cyanuric acid for which the reaction can proceed at temperatures as low as 400°C[62].

Good mixing of chemicals and NO_X in the flue gas at the optimum temperature is key to high NO_X reduction. This can be a problem through, because of the high viscosity of flue gas and a lack of available injection points. Figure 7-5 shows different levels for injection that can be used to meet temperature constraints.

There are several alternative carriers for the reducing chemicals, such as steam, pressurized air, water, and when in combination with combustion modifications, overfire air or recirculated flue gas.

The key problem is finding an injection point where the temperature is right under all operating conditions and boiler loads for the chemicals used. The chemicals then have to be adequately mixed with the flue gases to ensure maximum NO_X reduction without producing too much NH_3. NH_3 slip from SNCR can affect downstream equipment by forming ammonium sulfates. The effect of these ammonium sulfates has been discussed previously.

Chemicals

As stated earlier, the main reducing agents used in large-scale operations are ammonia, concentrated or in solution (NH_4OH), as well as urea with or without the addition of chemicals. Urea is dissolved in water to form a solution that will not clog the injection system. Cyanuric acid has also been tested as a possible NO_X reducing chemical.

Basically, NH_3 has a lower operating temperature window than urea, 850 - 1,050°C compared to 1,000 - 1,150°C respectively. Enhancers (additives) such as hydrogen (H_2), carbon monoxide (CO), hydrogen peroxide (H_2O_2), ethane (C_2H_6), light alkanes, and alcohols have used in addition to urea in order to reduce the temperature window[63]. The NOxOUT™ process uses urea with additives. Processes using NH_3 as the reducing chemical are patented in several countries as the Exxon Process named Thermal De-NO_X in the USA and Thermal NO_X in Germany, but there are countries such as Austria and Denmark where there is no patent for this process[37]. The cyanuric acid process is marketed under the name RAPRENOX™. These processes are discussed further in the SNCR systems section.

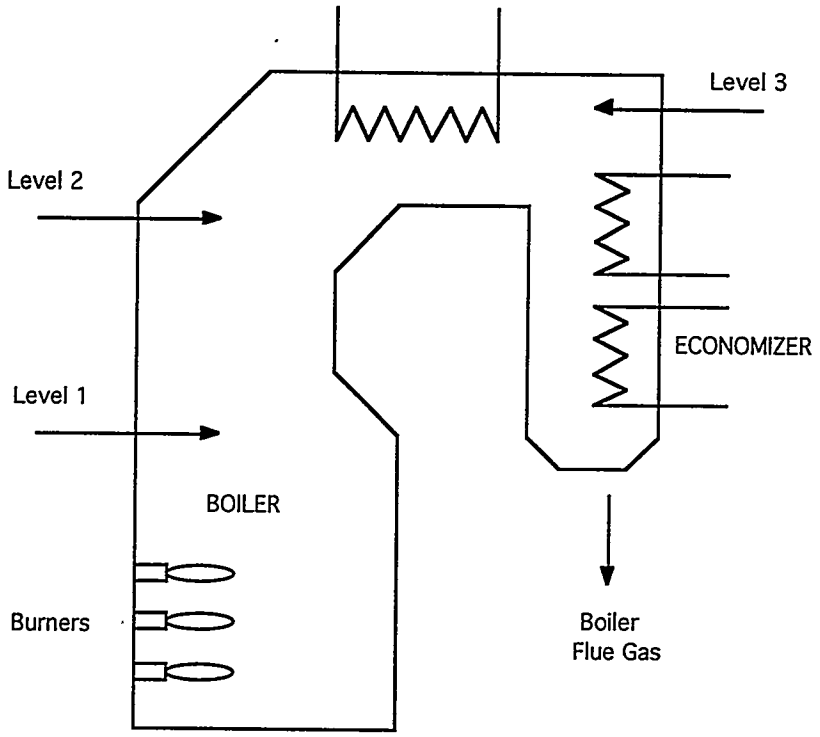

Figure 7-5. SNCR INJECTION LEVELS

Design

An SNCR system consists of storage and handling equipment for the chemicals used, equipment for mixing chemicals with the carrier, and the injection system. The injection system consists of nozzles installed in the furnace wall to achieve the best distribution over the furnace area. It is important to have the nozzles produce fine droplets as this will help promote mixing. Injection into the furnace can be achieved by either placing several nozzles on each side of the boiler or by locating a few nozzles on wall. The injection rate is usually controlled by the boiler load.

Performance/Experience

The common view is that SNCR processes are generally capable of reducing NO_X by 25 - 50% [64]. Further NOx reductions can be obtained on specific boilers where operational conditions are favorable. Normally, stoichiometric ratios of 1.0 - 2.0 are used for optimal NO_X reduction.

The addition of natural gas in a molar ratio to NO_X of about 1.0 has been shown to minimize ammonia slip, increase NO_X reduction, and widen the temperature window[65]. Figure 7-6a shows the effect on NO_X reduction of varying CH_4:NH_3 ratios while Figure 7-6b shows the effect of methane on the temperature window.

One possible drawback in using SNCR is the production of nitrous oxide (N_2O). In the troposphere, N_2O is a relatively strong absorber of infrared radiation and, therefore, has been implicated as a contributor to the "Greenhouse Effect"[66].

Recent research has shown that the urea SNCR process produces the most N_2O, followed by cyanuric acid and ammonia in that order[67]. Figures 7-7a and 7-7b show NO_X reduction and N_2O production respectively as a function of temperature for the three different processes. The best NO_X reductions were achieved when the stoichiometric ratio was 2.0.

SNCR Design Systems

In this section, some of the different SNCR systems are outlined. For each system process, details, status, and reduction capabilities are presented. A process diagram is also presented when applicable.

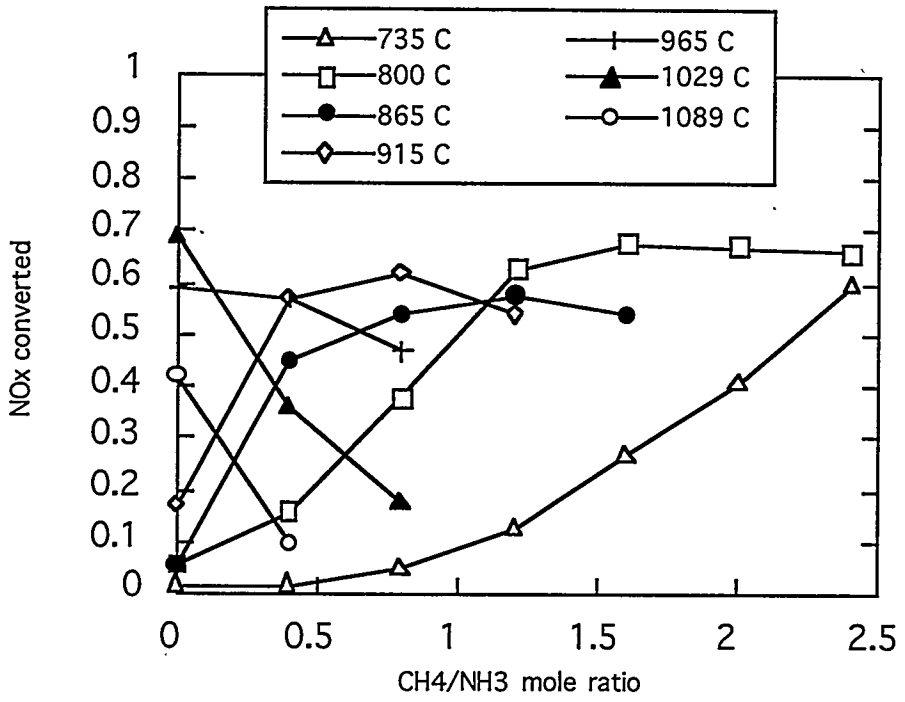

a) Effect of CH_4:NH_3 Ratio on NOx for Different Temperatures

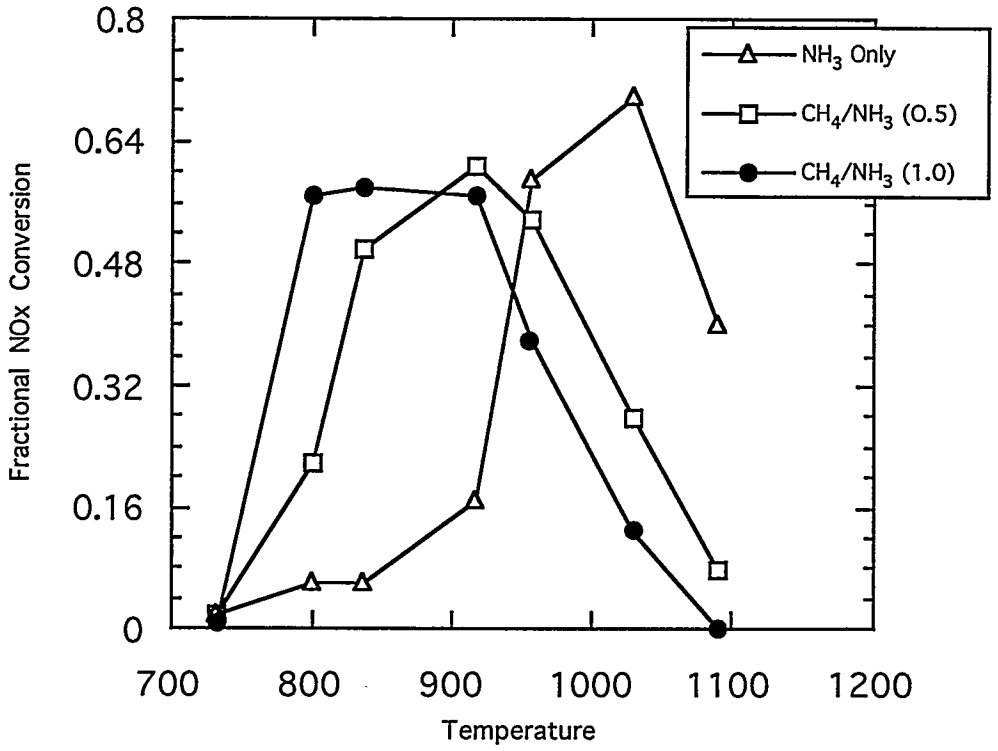

b) Effect of Methane on Temperature Window

Figure 7-6. METHANE EFFECTS ON SNCR

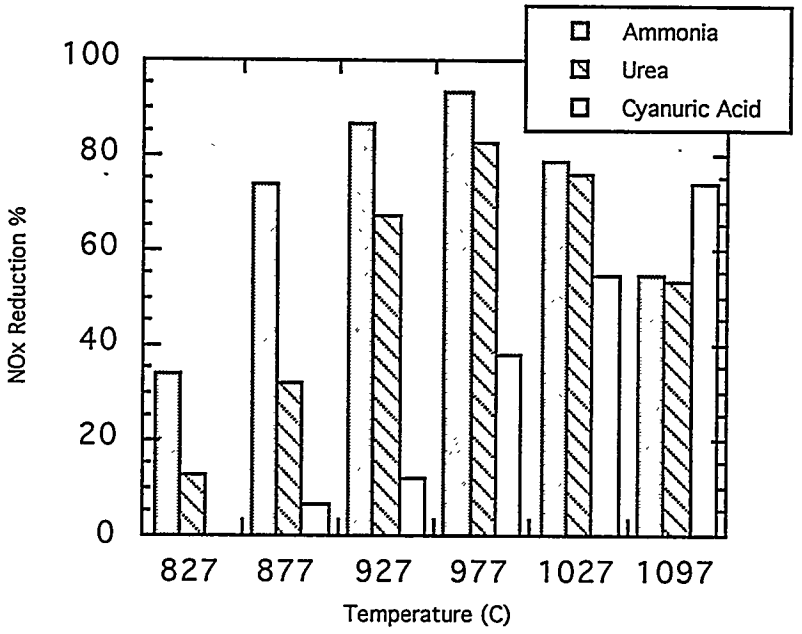

a) NO_X Reduction vs. Temperature

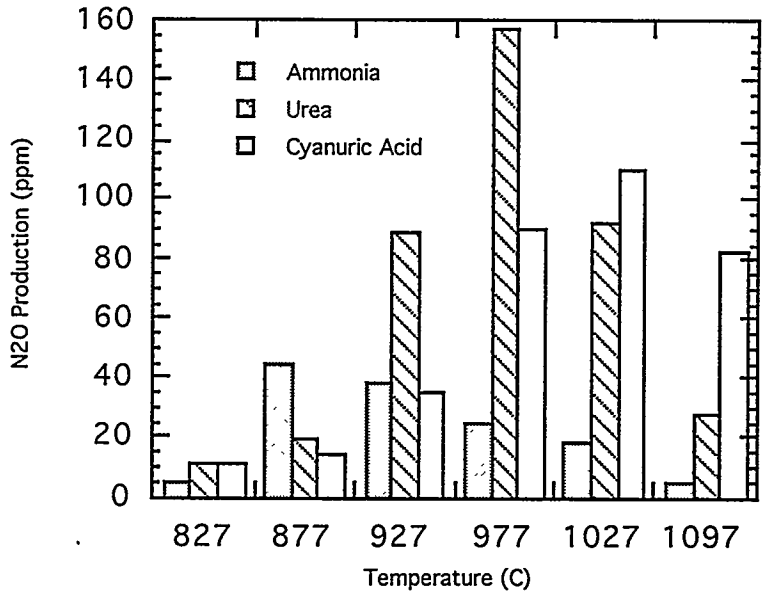

b) N_2O Production vs. Temperature

Figure 7-7. NO_X REDUCTION AND N_2O PRODUCTION
NO_i = 700 ppm; N/NO = 2.0

System Name: **AB-SNR-deNO$_x$**
Company: Aalborg Boilers A/S
Address: Gasvaerksvej 24 DK - 9100
Aalborg, Denmark

Reagent: Ammonia
Additives: Hydrocarbons (natural gas)
End Product: Nitrogen, Water
Flue Gas Temp: 850 - 1050 C, optimum 950 C

Scale of Operation: Commercial
Largest Capacity Treated: 135 MW

NO_X Reduction: 50 - 70%

Notes:

In order to minimize the emission of unreacted NH_3, natural gas is added in a molar ratio to NO_X of about 1.0 in part of the load range. This plant met a demand of no greater than 15 ppm NH_3 in the flue gas.

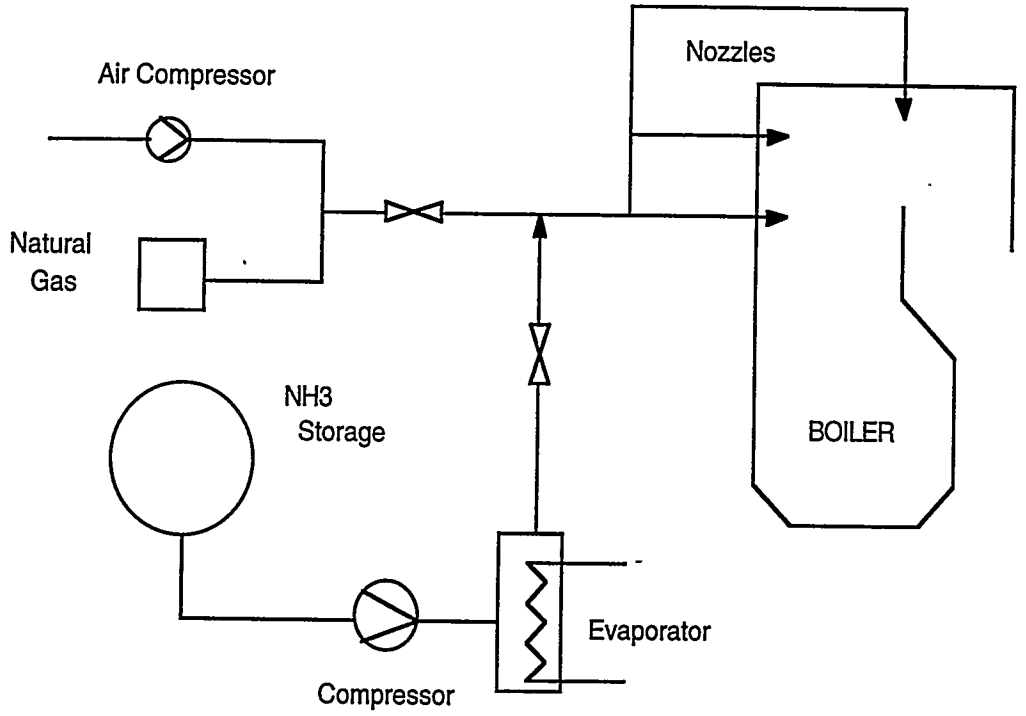

Reference: [37, 68]

System Name: **Thermal De-NO_X**

Company: Exxon Research & Energy Corporation
Address: P.O. Box 101
Florham Park, NJ, 09732, U.S.A.

Telephone:
Contact:

Reagent: Ammonia
Additives: Hydrogen at low temperatures
End Product: Nitrogen, Water
Flue Gas Temp: 900 - 1050 C, optimum 1000 C

Scale of Operation: Commercial
Largest Capacity Treated: 500 MW

NO_X Reduction < 80%

Notes:
Additives are not usually used, but hydrogen can be used at low temperatures to further enhance NO_X reduction.

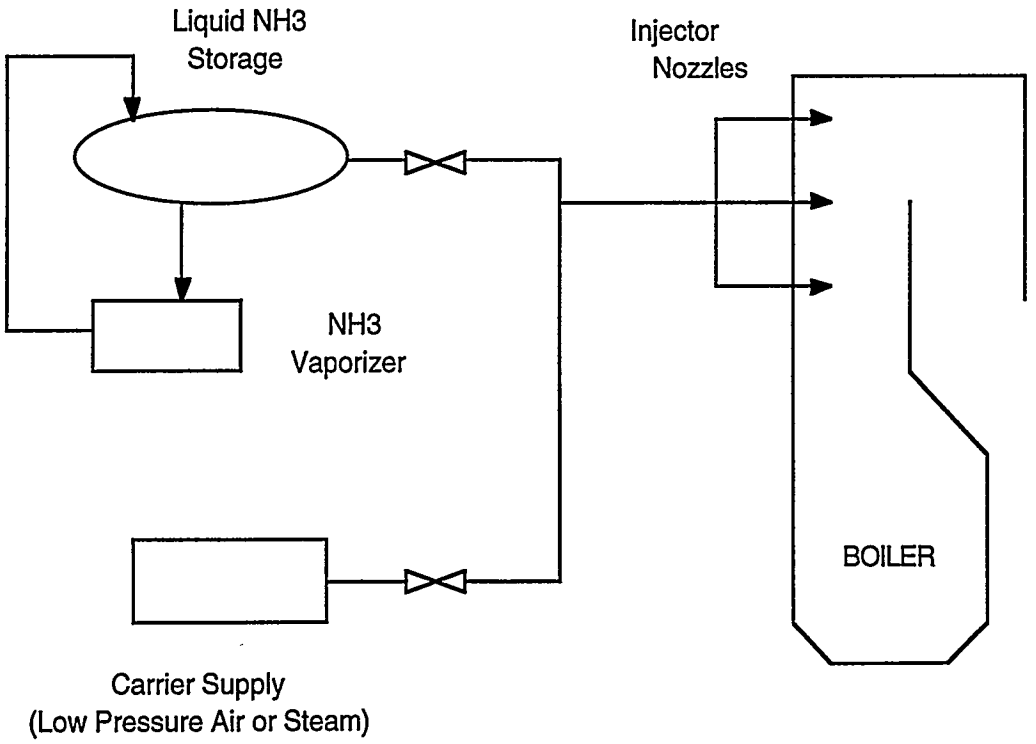

Reference: [37, 68]

System Name: NO_XOUT^{TM}

Company:	Nalco Fuel Tech
Address:	P.O. Box 3031 Naperville, IL, 60566, U.S.A.
Telephone:	(708) 983 -3241
Contact:	Grisko, S.
Reagent:	Urea
Additives:	Proprietary enhancing chemicals
End Product:	Carbon dioxide, Nitrogen, Water
Flue Gas Temp:	700 - 1100 C
Scale of Operation:	Commercial
Largest Capacity Treated:	700,000 lb steam/hr @ 510 C Boiler
NO_X reduction:	30 - 70%

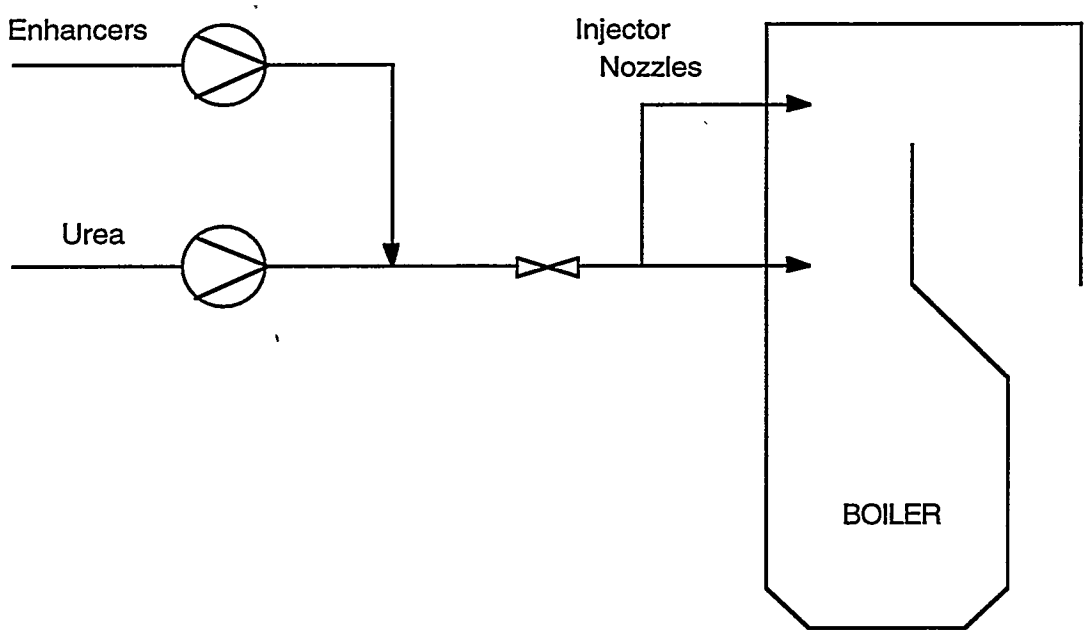

Reference: [69-71]

System Name:	**Two stage DeNO$_X$ process**
Company:	Noell - KRC
Address:	2420 East Hillcrest Ave. Visalia, CA 93277, U.S.A.
Reagent:	Urea, Methanol
End Product:	Nitrogen, Water
Flue Gas Temp:	750 - 1,050°C
Scale of Operation:	Commercial
Largest Capacity Treated:	325 MW
NO$_X$ Reduction:	50 - 70%

Notes:

This process was tested on a large scale waste incinerator plant in Switzerland in 1988 with results of 65 - 80% NO$_X$ reduction and NH3 slip of 1 ppm at 65% reduction. Two boiler zones are used for chemical injection. Urea is added in the first zone to reduce NO$_X$ and methanol is then added to reduce NH3 slip in the second zone. The injection system is key in this process.

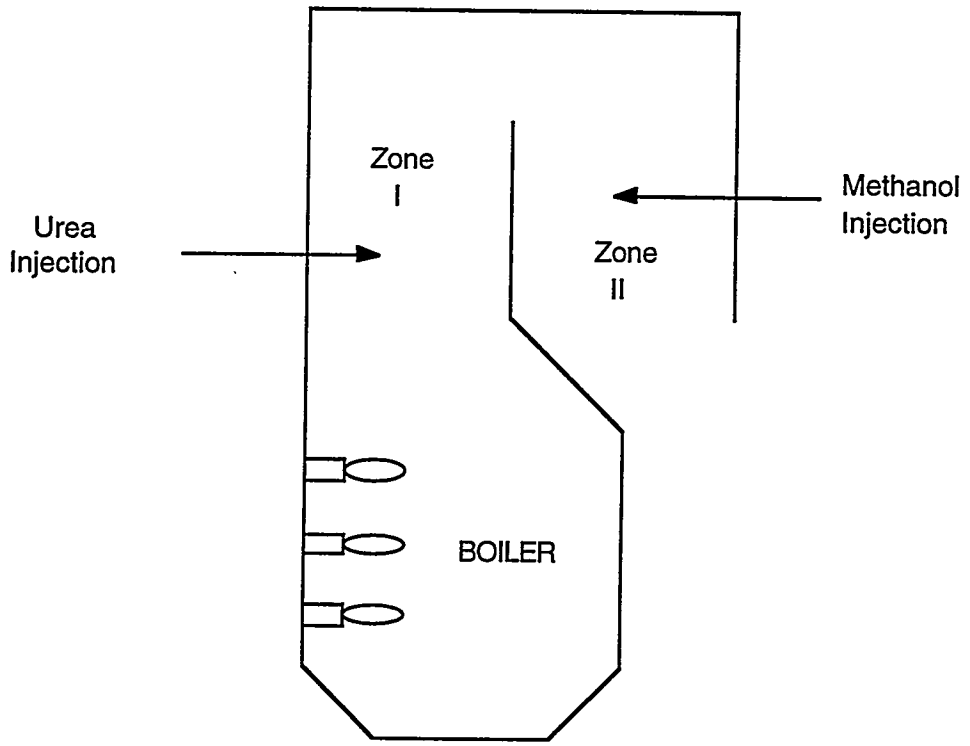

Reference: [37]

System Name: **RAPRENOX**
Company: Technor, Inc.

Reagent: Cyanuric acid
Additives: Radical enhancers
End Product: Carbon dioxide, Carbon monoxide, Nitrogen, Water
Flue Gas Temp: 400 - 1,200°C (*)

Scale of Operation: Research (1992)
NO_X Reduction: 95%

Notes:

In the RAPRENOX process, exhaust gas is used to heat the cyanuric acid ($C_3H_3N_3O_3$) which causes it to sublime and transform into isocyanic acid (HNCO). HNCO then reacts with NO_X by a series of complex reactions forming CO_2, CO, N_2, and H_2O.

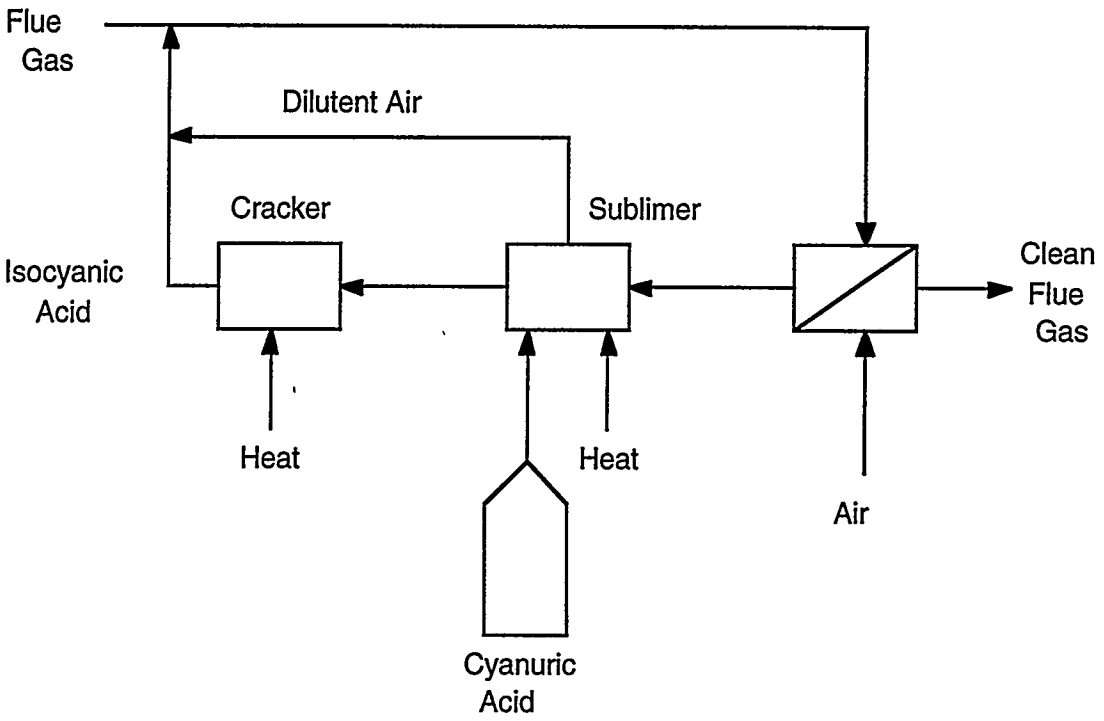

* Follow up work has shown that at low temperatures (400 - 800°C), the reaction will not proceed in the absence of catalysts (Lyon & Cole, 1990). The original work was done in a stainless-steel flow reactor and it was found that the surface decomposition of HNCO initiates the RAPRENOX process. The reaction does not occur at low temperatures in the absence of such surfaces. More experimental research is being done in this area.

Reference: [62, 72]

Other NO_X Post Combustion Control Strategies

This section outlines a few systems that could not be classified under SCR or SNCR. The majority of the systems in this section are in the research stage.

NO_X Wet Scrubbing

Like SO_2, NO_X can be removed by chemical absorption using a redox couple. The chemical active species will be regenerated at an electrode surface, and several redox couples can be considered for this purpose[73]. In such a process, the flue gas is continuously scrubbed in the absorption tower, whereas the aqueous phase is circulated batchwise in both the absorption tower and the electrochemical cell. Continuous scrubbing of the gas results in the regular increase of acid concentration in the liquid phase. These produced acids can be removed at concentrations as high as 40%. A complete study of NO_X scrubbing into a ceric solution (Ce(IV)) is presently under investigation [74].

Advance Industrial Technology (AIT) has developed the Promosorb Promoted Chemicosorption^{TM} Process, a wet scrubbing method employing an alkalinic scrubbing medium containing a proprietary promoter agent which makes possible the neutralization of NO_X, (including the inactive nitric oxide (NO)), by alkalis[59]. This system is used very effectively when treating flue gases containing some other acid gases like HCl, HF, or SO_2 in addition to NO_X. Promosorb systems can remove NO_X and all the acidic contaminants in a single operation.

Wet scrubbing is discussed further in the combined NO_X/SO_2 section.

CombiNO$_X$

The CombiNO$_X$ process is an integration of advanced reburning and NO_X scrubbing to reduce NO_X emissions from a coal-fired boiler flue gas[75]. Advanced Reburning is an Energy and Environmental Research (EER) patented technology which consists of injecting an SNCR reducing agent (urea), into the fuel rich zone generated by reburning fuel injection. Overfire air is injected downstream of the fuel rich zone to complete combustion of the reburn fuel. Finally, methanol is injected downstream of the advanced reburning section to convert NO to NO_2. Figure 7-8 shows the Advanced Reburning system. The NO_2 is then removed in a "liquor - modified" SO_2 scrubber. Pilot-plant data, from EER's 10 MM Btu/hr (2.93 MW) Reburn Tower Furnace, demonstrated that an overall NO_X reduction of 89% is feasible[76].

The temperature at which urea and methanol are injected is very important for high NO_X reduction levels. Better than 75% NO_X reduction was achieved at a urea injection temperature of 900 - 1,121°C, with the optimum (82% reduction) at 1,010°C. 80% of the NO was converted to NO_2 at a methanol injection temperature of 715°C. Also key to NO_X reduction is the composition of the scrubbing solution. A solution consisting of 8 percent limestone ($CaCO_3$), 8 percent sodium carbonate (Na_2CO_3), and 1 percent sodium thiosulfate ($Na_2S_2O_3$) was found to yield satisfactory (90% NO_2 capture) results[76].

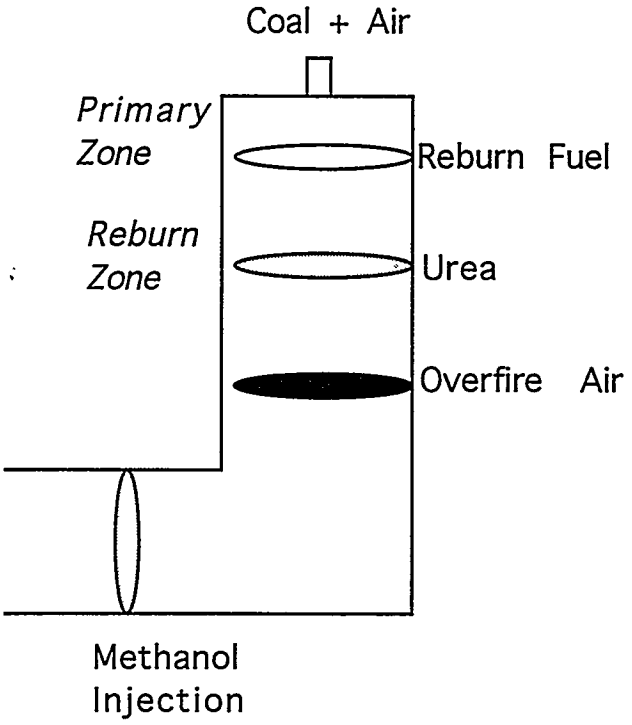

Figure 7-8. ADVANCE BURNING SYSTEM (CombiNO$_X$)

AquaNO$_X$

AquaNOx^{TM}, developed by AIT, removes NO$_X$ by contacting the NO$_X$ containing waste gases with an aqueous solution of catalytic reagent, AR-35, which catalyzes the conversion of NO$_X$ to an activated complex which it subsequently hydrolyzed[59]. AquaNO$_X$ systems are operated at temperatures ranging from ambient up to about 70°C.

Microbial

Recent research has examined the possibility of removing NO2 from flue gases with the use of denitrifying bacteria[77, 78]. Two strains, *Pseudomonas denitrificans* ATCC 13867 and *Paracoccus denitrificans* ATCC 17741, exhibited the highest reduction rates of the bacteria tested. However, additional work is needed on the biological removal of nitric oxide and nitrogen dioxide since these gases constitute a significant fraction of NO$_X$ found in combustion gases.

Ultraviolet Light

A novel, ultraviolet (UV) light in a photo-catalytic process to remove NO$_X$ from flue gases has recently been reported[79]. Flue gas at between 15 - 80°C is passed through a fixed bed of commercial titanium oxide (TiO2), which contains an embedded UV lamp. The UV light initiates and then catalyzed the breakdown of NO$_X$ into N2 and O2 in the presence of TiO2. The average catalyst grain size is about 200 μm and the lamp intensity is 150 W. Degradation rates of 50 - 70% have been achieved in a residence time of 34 s for inlet NO$_X$ concentrations of 1,400 ppm. Catalyst poisoning can be prevented with the addition of O2 and propane (C3H8), while degradation rates of up to 100% are achievable by adding ammonia.

Microwaves

Dow Chemical Co. (Freeport, Tex.) has recently unveiled a two step process that utilized simple chemistry in destroying NO$_X$ from flue gases[80]. Based on technology patented by CHA Corp. (Laramie, Wyoming), it has demonstrated the ability to remove greater than 99% of NO$_X$ via adsorption and chemisorption on char (heat-treated and devolatilized coal). The loaded char is then regenerated by microwave energy, which reduces the absorbed NO$_X$ to N2 and CO2. This process is not hindered by the presence of O2, H2O, or VOC's.

Plants could use different process configurations, depending on NO$_X$ load ranges. For facilities producing less than 50 tons NO$_X$/year, Dow recommends the use of batch char canisters with central regeneration. Plants producing NO$_X$ in excess of 50 tons/y could use dual stationary beds or moving beds with continuous regeneration, depending on NO$_X$ load range. The required microwave energy is approximately 1,000 - 1,500 kW/ton NO$_X$.

Combined NO$_X$/SO$_2$ Removal Strategies

The combined control of NO$_X$ and SO2 emissions continues to be an active area of research. Conceptually, removing both NO$_X$ and SO2 in one process should be more advantageous than using two individual processes in series. However, the combined systems have been and are still

considered to be complex (if not expensive, also). This opinion is changing, however, possibly due to the anticipation of more stringent emission standards for both nitrogen and sulfur oxides.

Basically, there are three categories that combined NO_X/SO_2 control systems fall under: downstream post combustion processes, in-boiler processes, and techniques which are primarily modifications made to existing flue gas desulfurization (FGD) systems.

Downstream Post Combustion Processes

NOXSO

The NOXSO process, developed by the Noxso Corporation (Library, PA), is a dry, regenerable flue gas cleaning system, designed to simultaneously remove more than 90% SO_2 and 70-90% of the NO_X from the flue gas. The SO_2 is concentrated to salable sulfur, sulfuric acid or liquid SO_2 and the NO_X is reduced to elemental nitrogen with no wastes produced. The NOXSO process is shown in Figure 7-9.

The flue gas is first cooled to 160°C by either spraying water into the flue duct or directly into the sorbent bed. The gas is cleaned as it passes through a fluidized bed of sodium-impregnated alumina sorbent at 160°C. Removal of particulate matter can be accomplished either before or after the process.

The saturated sorbent in the adsorber is air lifted to the top of the sorbent heater. A natural gas fired air heater provides the hot air to heat the sorbent to 620°C. During this heating all of the NO_X and a small portion of the SO_2 desorbs. The concentrated stream of NO_X is recycled back to the boiler at a temperature of 230°C.

A portion of NO_X returned to the combustion air stream is destroyed in the boiler. This is achieved by two mechanisms. The first takes advantage of reaction equilibrium. By injecting NO_X into the boiler, the NO_X concentration is higher than the equilibrium value, thereby suppressing NO_X formation by the reverse of the following reaction:

$$N_2 + O_2 \text{ <------> } 2NO \qquad (7\text{-}5)$$

Reduction by the second mechanism takes place by free radicals, present in the fuel rich portion of the flame, which reduces NO_X to N_2 and H_2O. Boiler destruction efficiencies, tested on three different coal combustors (pulverized coal, tunnel furnace, and cyclone), have been measured from 57 - 75%[81].

The sorbent, now NO_X free, is carried by either steam or N_2 from the sorbent heater to the moving-bed regenerator. The hot sorbent is first treated with natural gas which reduces the sulfate on the sorbent to SO_2, H_2S, and NaS. The remaining sulfide is further treated with steam to hydrolyze it to H_2S. These species are converted in a Claus reactor to elemental sulfur that can be sold as a by-product. The regenerated sorbent is cooled and returned to the fluidized-bed adsorber.

A study was recently completed in a 5 MW pilot plant at Ohio Edison's Toronto Power Plant[82]. From November 1991 to December 1992, the pilot plant processed flue gas for a total of

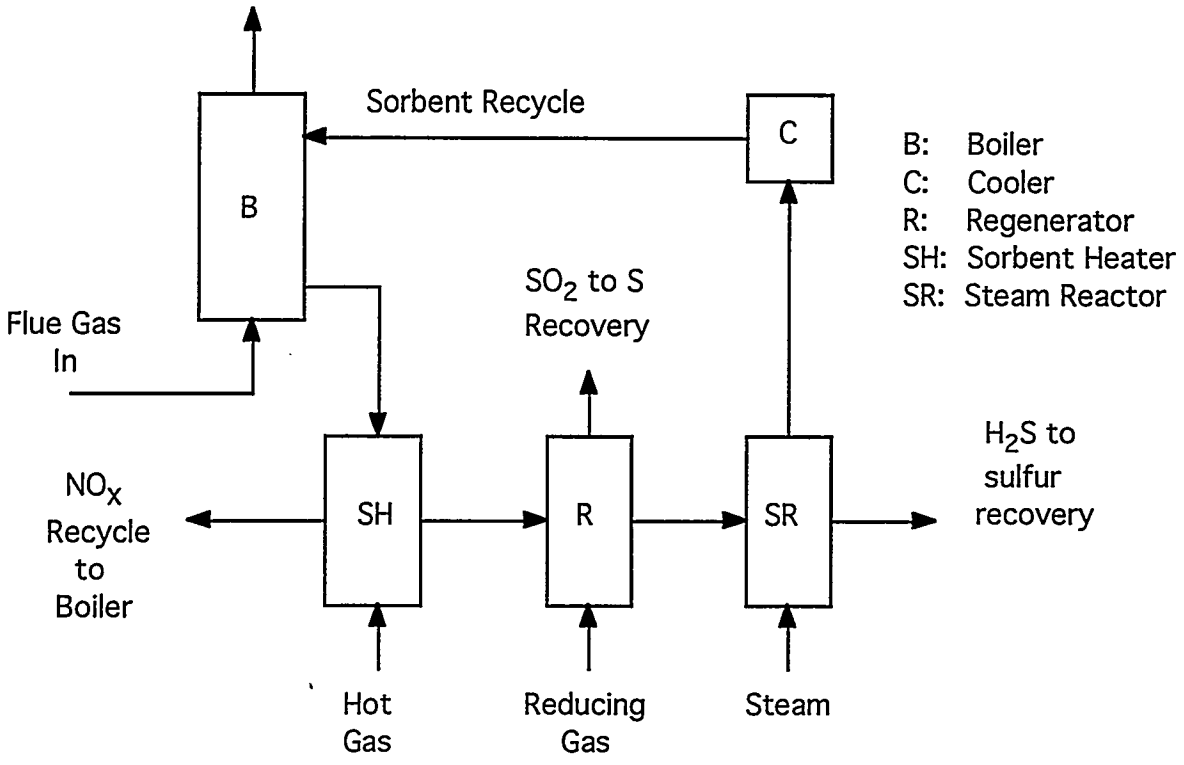

Figure 7-9. NOXSO PROCESS

5,213 hours. Once the initial shakedown problems were solved, the pilot plant availability averaged 76% from April to December 1992.

The following is a summary of the pilot plant results:

- Removal efficiencies of 95% SO_2 and 92% NO_X were measured at a sorbent recirculation rate of 8,000 lb/hr, a flue gas flow rate of 5,800 scfm, and an adsorber bed temperature of 160°C. Average pollutant removal efficiencies during various operating conditions were 95% SO_2 and 80% NO_X at typical inlet SO_2 and NO_X flue gas concentrations of 2,000 ppm and 350 ppm respectively.
- Sorbent makeup was 2.5 lb/hr over the 6,000 hours of operation at a constant set of operating conditions. This rate was measured on both the amount of sorbent makeup required to maintain steady system inventory and the amount of sorbent fines collected from the process off gas streams in the baghouse.
- Mass and energy balances were continuously monitored to assess the process performance. The sulfur balance between the adsorber and regenerator, the NO_X balance between the adsorber and the sorbent heater, and the carbon balance in and out of the regenerator all closed to within ± 15%. The sorbent heater, air heater, and sorbent cooler energy balances were typically 85%, 98%, and 85%, (with 100% equal to perfect closure), respectively.

A 115 MW demonstration of the process will be conducted under the third round of the DOE Clean Coal Technology Program. Process concerns have primarily been in the area of NO_X recycle in a large-scale test[83].

SO_X-RO_X-NO_X-BO_X

The SO_X-RO_X-NO_X-BO_X ($SNRB^{TM}$) process is a combined SO_X, NO_X, and particulate (RO_X) emission control technology developed by Babcock & Wilcox (Alliance, OH) in which high removal efficiencies for all three pollutants are achieved in a high temperature baghouse. The SNRB process is shown in Figure 7-10.

A 5 MW process demonstration, co-sponsored by DOE, the Ohio Department of Development/Ohio Coal Development Office, and the Electric Power Research Institute was completed in May 1993 at Ohio Edison's R.E. Burger Plant under the second round of the DOE CCT[84].

The $SNRB^{TM}$ process incorporates dry sorbent injection for SO_X emission control, selective catalytic reduction for NO_X emissions, and a pulse-jet baghouse operating at 230-450°C for controlling particulate emissions. Low exit SO_2 and SO_3 levels, thereby reducing the risk of ammonium sulfates, may allow lower air preheater exit temperatures and greater system efficiency. The unique features of the process provide several distinct advantages in comparison with other control technologies[84]. These include:

- Multiple emission control in a single unit;
- Low area space requirements;
- Operating simplicity;
- Flexible;
- Enhanced SCR operating conditions;
- Improved SO_2 sorbent utilization; and
- Dry materials handling.

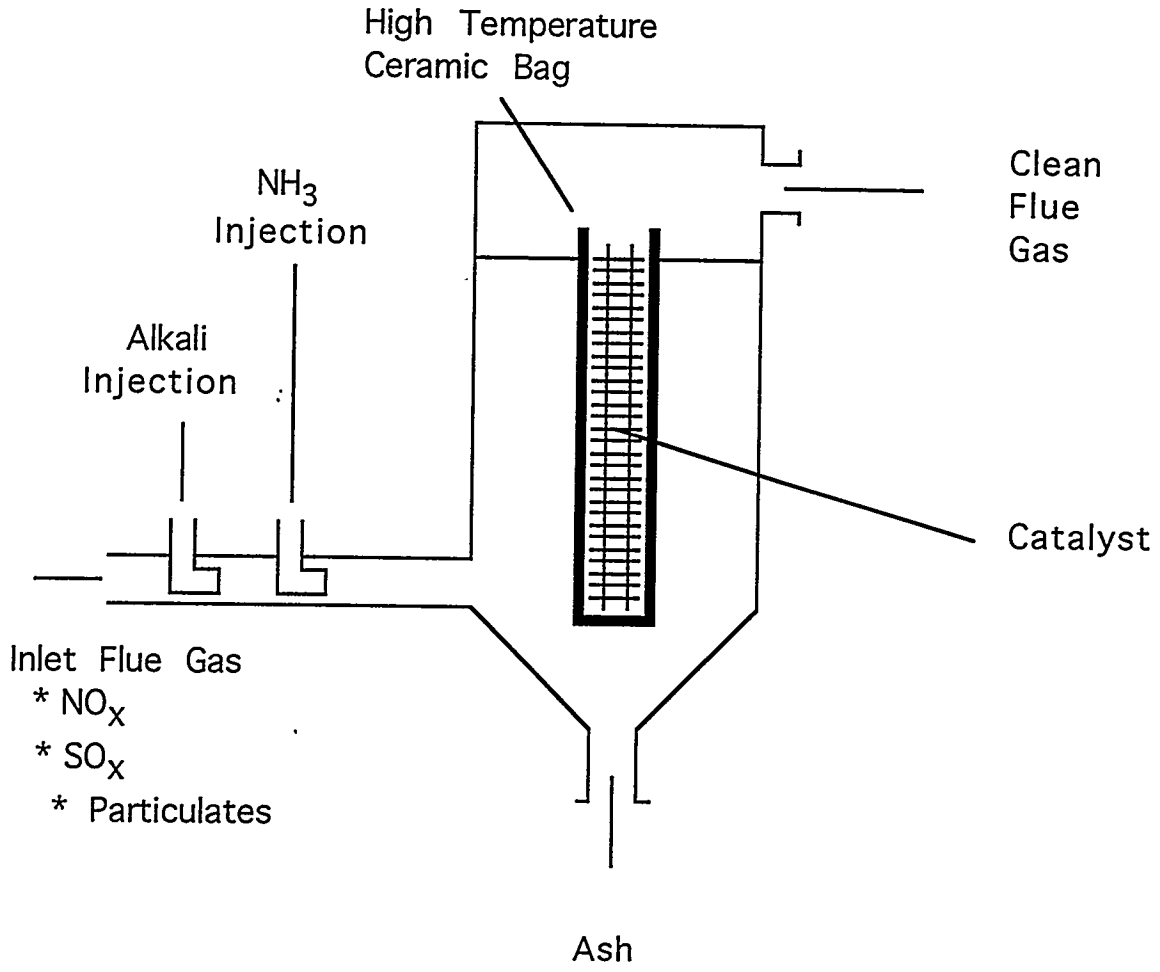

Figure 7-10. SNRB™ PROCESS

The components and the design characteristics of the 5 MW pilot plant are summarized below[84, 85]:

- Six compartment pulse-jet baghouse

Flue gas flow	30,000 ACFM @ 425°C
Air to cloth ratio	4:1
Operating temperatures	230 - 480°C
Filter bags	20' long x 6" diameter.
Number of Filter bags	252 (6 x 42)
Bag material	
3M	Nextel ceramic fibers
Owens Corning fiberglass	S2-Glass fiberglass
Cleaning air pressure	30 - 40 psig
Cleaning air pulse	80 - 100 ms
Catalyst	
Norton	NC-300 series zeolite

- Commercial scale bag/catalyst assemblies
- Independent injection/baghouse operation temperature control
- Pneumatic materials handling
- Dry sorbent storage and injection

Storage	2,350 ft^3
Hydrated lime	300 - 700 lb/hr
Sodium bicarbonate	300 - 1,300 lb/hr

- Anhydrous NH_3 storage and injection

Storage	1,000 gallons
Dilution	19:1
Flow rate	3 - 30 lb/hr

During the one year demonstration program, SO_2 removal efficiencies of greater than 80% were achieved using commercially hydrated lime (Dravo Lime Co., Pittsburgh, PA) at Ca/S stoichiometries of 1.8 - 2.0. The addition of sodium bicarbonate allowed for greater SO_2 removal (> 90%) over a wide range of baghouse temperatures from 220 - 470 C[86].

NO_X reductions greater than 90% were achieved at NH_3/NO_X molar ratios of 0.85 - 0.90 while NH_3 slip was kept below 5 ppm[84].

SNOX & DESONOX

The SNOX (WSA-SNOX) process developed by Haldor Tospsoe A/S, is designed to catalytically remove 95% or more of the SO_2 and NO_X in the flue gas. The process produces a salable by-product of concentrated sulfuric acid. The WSA-SNOX process is outlined in Figure 7-11.

As shown in Figure 7-11, flue gas leaving the boiler is cooled in the air heater by air exiting the WSA-2 tower. The flue gas is further cooled in a trim cooler, where the heat from the cooling of the flue gas is used to produce low pressure process steam.

The flue gases pass through a baghouse or ESP for particulate removal to minimize catalyst degradation. Next, a gas heat exchanger is used to heat the flue gas entering the NO_X reactor and cool the gas exiting the SO_2 reactor. The heated incoming flue gas is mixed with NH_3 prior to

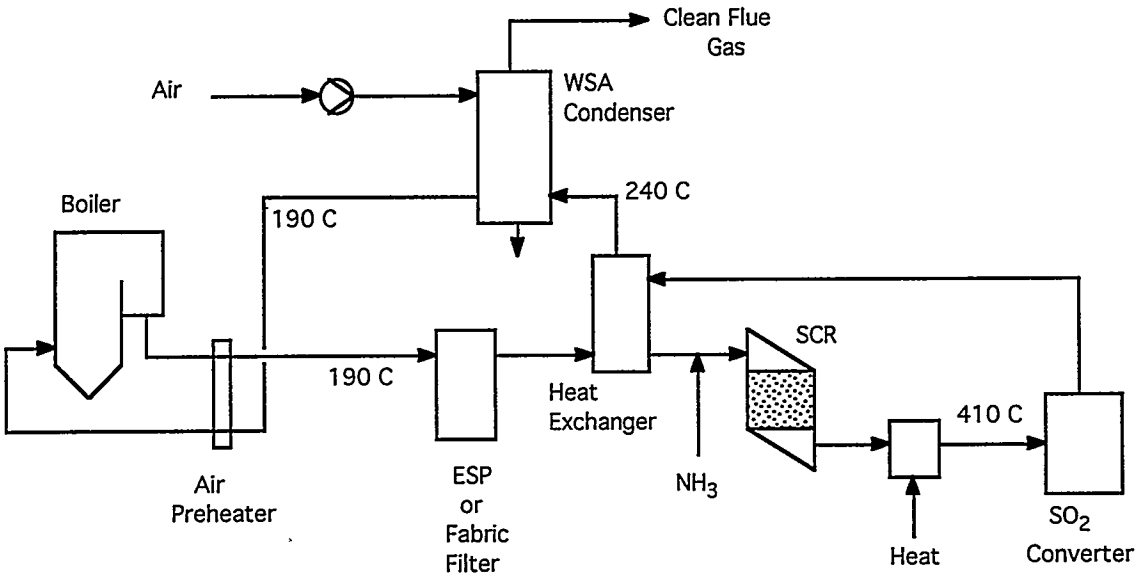

Figure 7-11. WSA-SNOX PROCESS

entering the SCR reactor where the NO_x is converted to N_2 and H_2O. After NO_x conversion, the flue gas is heated by a burner prior to entering the SO_2 reactor where SO_2 is oxidized to SO_3. This processed gas is then cooled against incoming gas in the gas heat exchanger. This cooling process allows the SO_3 to hydrolyze to sulfuric acid gas. The gas then passes through the WSA-2 tower prior to discharge to the atmosphere. In the WSA-2 tower, the vapor is condensed, concentrated to 95% H_2SO_4, and then pumped to a storage tank. The SO_2 reactor removes trace ammonia that might have formed ammonium sulfate in the tower[87].

Although the process consumes an extensive amount of energy, significant energy recovery within the process is claimed to give net energy savings of 1 -4% (1% for each percent of sulfur in the fuel) for the plant[83]. Unlike most processes, the operating costs are assumed to decrease with increasing sulfur content in the flue gases. This is due to the increased production of salable H_2SO_4 and the possibility of increased heat recovery from the formation of H_2SO_4.

In Denmark, a 3 MW process demonstration unit operated on a low sulfur flue gas stream from 1987 - 1991 and a 300 MW full scale SNOX plant began operation in November 1991 on a boiler firing medium sulfur (1.6%) coal[83].

In the U.S., a 35 MW demonstration of the technology is being conducted at Ohio Edison's Niles Station Boiler No. 2 using bituminous coal from southeastern Ohio and western Pennsylvania (3.76% sulfur) under the second round of the DOE CCT program[87]. The unit is a pre-NSPS 100 MW cyclone coal fired utility boiler. The tests were scheduled for completion in December 1993 but no results have been published thus far.

Some advantages of the system are:

- No alkali reagent required for SO_2 removal as in most wet scrubber systems.
- No waste products to deal with such as calcium sulfate.
- Sulfuric acid produced can be sold, which can offset costs of SO_2 removal.
- The process uses fewer moving components than most other scrubber. This lowers operational and maintenance costs, and increases availability.

A similar process called DESONOX was conceived by the firm Degussa (South Plainfield, NJ) and is being developed jointly with Stadtwerke Munster, Lentjes, and Lurgi[88]. A single reactor tower containing reduction and oxidation catalysts is used. The sulfuric acid by-product created is of sufficient purity to be used in producing fertilizer (70%). The DESONOX process is shown in Figure 7-12.

In this process, ammonia is added to the flue gases after a hot ESP and the flue gases then are passed through a selective catalyst (zeolite), to reduce NO to N_2 at 450°C. The flue gas temperature is reduced in two air preheaters from 460 to 140°C. In the last preheater, the SO_3 is partly condensed to H_2SO_4. In a two step washing unit, the flue gases are further chilled as well as the rest of the H_2SO_4. A wet ESP, separates the acid mist and the clean gas is reheated by direct exchange with the hot sulfur acid in the condensation unit.

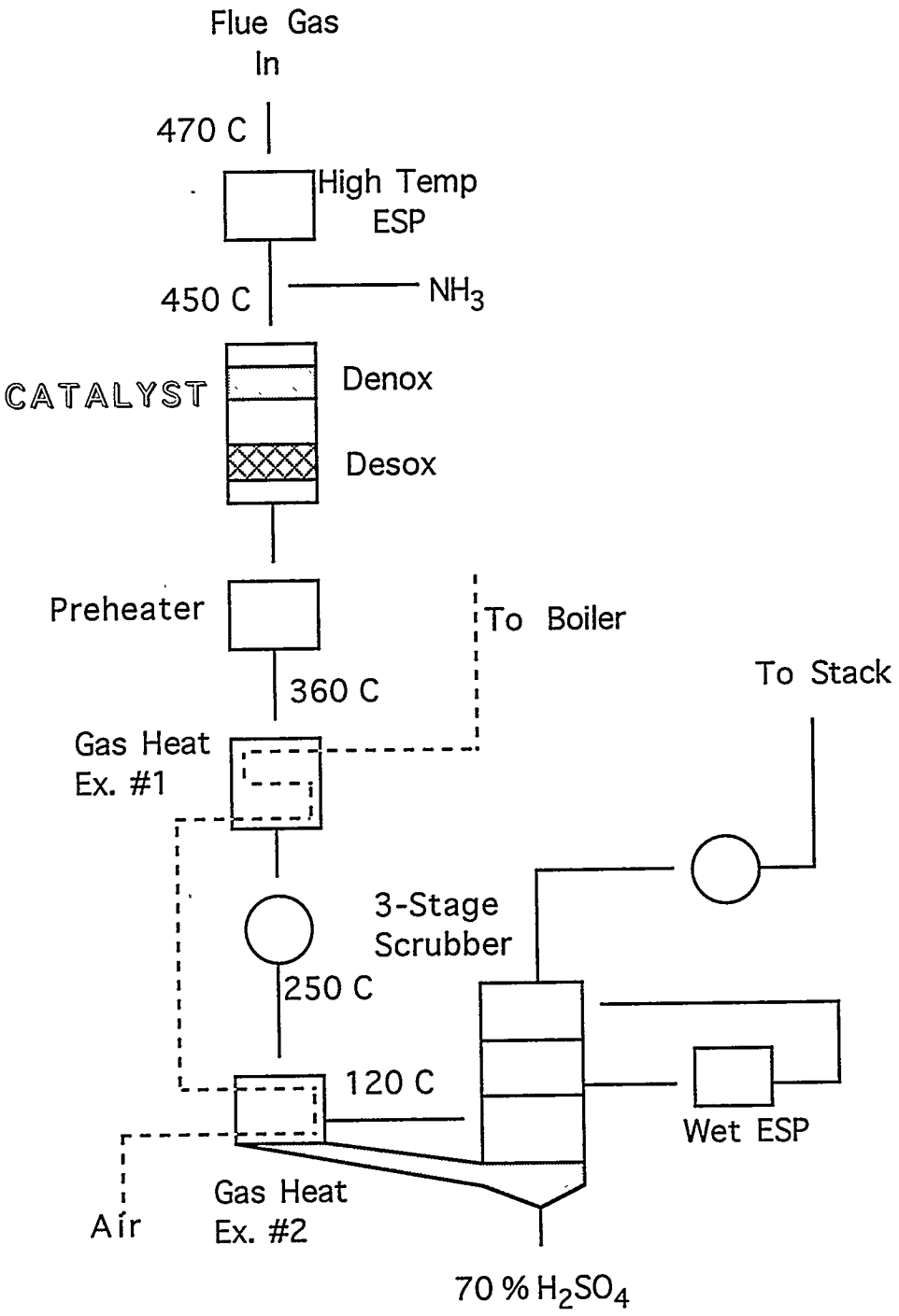

Figure 7-12. DESONOX PROCESS

This process has been demonstrated on a 75,000 scfm (98 MW) demonstration boiler at the Hafen cogeneration plant in Munster since November 1988. Removals for low-sulfur coal operation have been approximately 80% for NOx and 90% for SO_2.

One possible design modification involves the addition of hydrogen peroxide (H_2O_2) to allow DESONOX to operate on systems firing high sulfur coal. During the final scrubbing step, H_2O_2 is added in order to oxidize residual SO_2 to SO_3 [89]. This is claimed to permit compliance with federal emission standards, even when high sulfur coals are used.

Copper Oxide Process

The copper oxide (CuO) process combines SO_2 capture with catalytic reduction of NO_x using NH_3 in an absorber containing CuO impregnated alumina sorbent. Regeneration of the sorbent via reducing gas produces a concentrated SO_2 stream that can be processed into a salable by-product (elemental sulfur or sulfuric acid). Figure 7-13 shows the basic schematic of this system.

In the 1970's Shell (Houston, TX), developed a parallel passage (fixed bed) reactor system and conducted full-scale tests on an oil-fired boiler at the Showa Yokkaichi Sekiyn refinery in Japan [83]. UOP (Des Plaines, IL), licensed the Shell technology and completed a 0.5 MW pilot plant demonstration on a coal-fired unit at Tampa Electric Co.'s Big Bend station in 1980[90]. Average removals for SO_2 and NO_x were 90% and 70% respectively. A proof-of-concept demonstration unit is under development at the Commonwealth Edison power plant in Kincaid, IL. The plant burns high sulfur Illinois coal. Commercialization of the process depends on the results of this test, and is not expected for at least 10 years[37].

Concurrent with the work done at Shell, DOE's Pittsburgh Energy Technology Center (PETC) independently developed a fluidized-bed reactor system. Small scale tests have shown 90% reduction for both NO_x and SO_2. Under DOE contract, a conceptual design and cost estimate for a 500 MW commercial scale unit is being developed by A.E. Roberts & Assoc., Inc. (AER) as a subcontractor to UOP[91].

Rockwell International (Canoga Park, CA) is currently working on a variation of the above PETC process[37]. In this process, particulates as well as NO_x and SO_2 are removed in a single unit. The moving bed absorber serves as a high efficiency collection device as well as catalyzing NO_x reduction and removing SO_2. This process is undergoing tests at PETC in their Life Cycle Test Facility[92]. Optimum conditions for sorbent regeneration are currently being examined.

Electron Beam

An electron beam (E-Beam) process developed by the Ebara Corporation has removed 90% of SO_2 and 80% of NO_x in a 5 MW pilot plant at Chubu Electric's Shinnagoya Thermal Power Plant in Japan[93]. Using NH_3 as a base, ammonium sulfate and ammonium nitrate by-products were produced from flue gas containing inlet concentrations of 800 ppm SO_2 and 225 ppm NO_x.

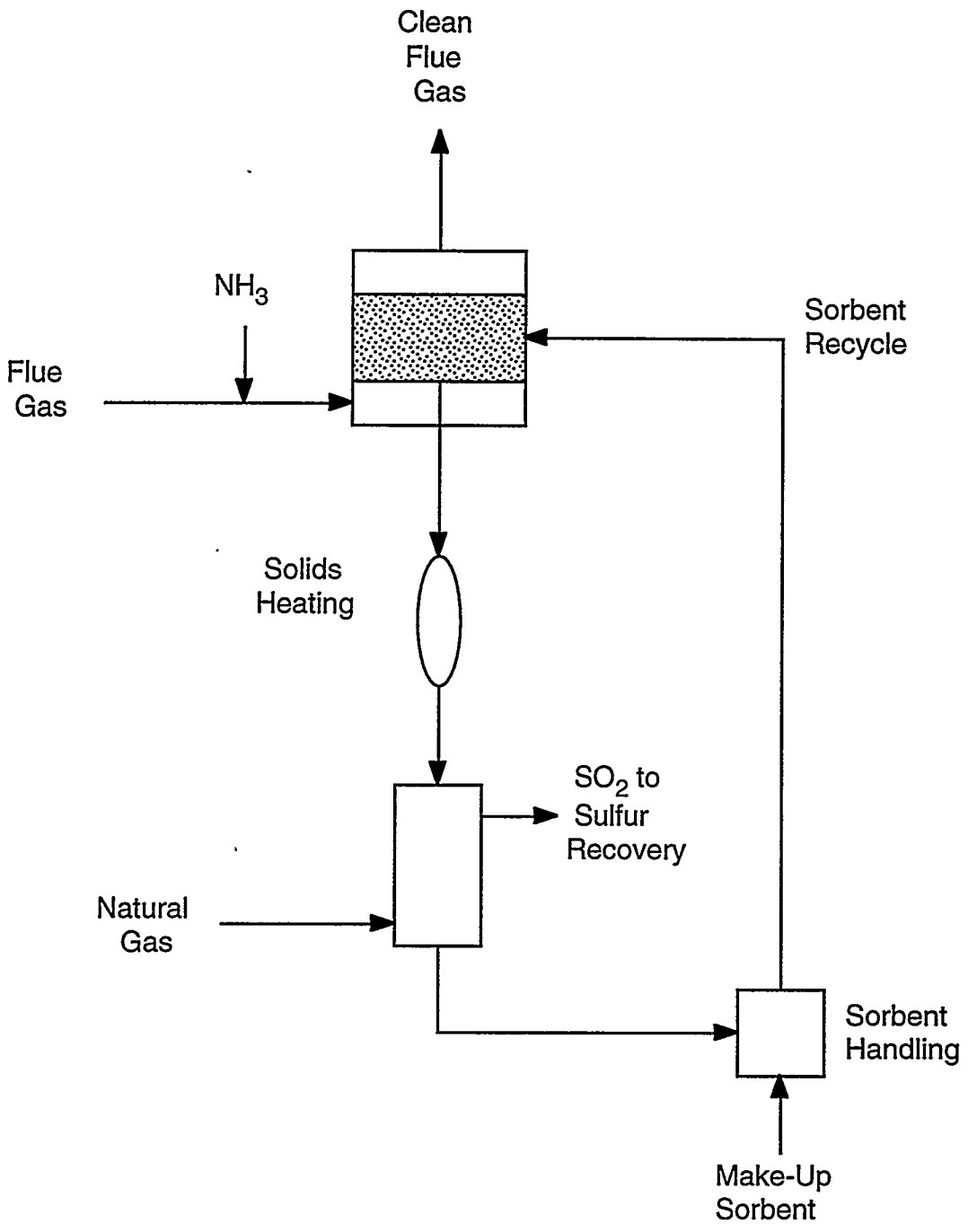

Figure 7-13. CuO PROCESS

These by-products have the potential value as an agricultural fertilizer. The E-Beam process is shown in Figure 7-14.

Before entering the E-Beam reactor, the flue gas is cooled with water to a temperature of about 60 - 80°C. In the E-Beam reactor, a beam of high energy electrons is fired into the flue gas in the presence of near stoichiometric amounts of NH_3 which is added upstream of the E-Beam reactor. NO_X and SO_2 are oxidized, which react with the NH_3 to form ammonium sulfate and ammonium nitrate which is collected downstream in an ESP or baghouse.

The Ebara Corporation is currently investigating zone irradiation (triple stage) to achieve high efficiencies at lower total dose rates. This is intended to reduce the process energy use by one-third or to no more than 2% of the plants total output.

Research Cottrell (Sommerville, NJ) has developed a similar process which uses lime as the base rather than NH_3. This process removed 90% of SO_2 and 60% of NO_X in a pilot-plant test[83].

The process can be carried out with almost complete utilization of secondary products in the form of valuable mineral fertilizer. The high 90% efficiency of cleaning the gases does not depend on the initial SO_2 and NOx concentrations within a wide range of flue gas flowrates[94]. The process is dry so there is no need to treat waste water. Other advantages include the compactness of the system, no need to heat the gases or to have a catalyst, and high reliability has been shown in studies[94]. The process has some favorable economics when compared with more conventional methods of eliminating NOx and SO_2[95].

The disadvantage of the system include the complexity of releasing the beam from a vacuum to the atmosphere. Also, protection against radiation is needed while the accelerator (used for radiation) is operating.

Commercial issues include economic scale-up of the E-Beam guns, and uncertainties regarding by product utilization. Research is also being done on the angle of electron beam injection. It has been shown that for certain angles of injection, plant efficiencies increased by 30% [96].

Activated Carbon Process

Activated carbon can adsorb SO_2 as well as catalyze the reduction of NO_X in the presence of NH_3. This process uses two sorbent beds for optimum removal for each species, as shown in Figure 7-15.

In this process the SO_2 is removed in the first adsorber at temperatures ranging form 90 - 150°C. SO_2 reacts with the moisture in the flue gas to form H_2SO_4 through catalytic oxidation, and the H_2SO_4 is adsorbed onto the activated carbon. Prior to the second stage, NH_3 is injected into the flue gases in a mixing chamber. In the second stage, NH_3 reacts catalytically with NO to form N_2 and H_2O. The activated carbon is transported from top to bottom of the reactor while the flue gas flow across each layer enters the first and lowest part of the bed. The SO_2 rich gas

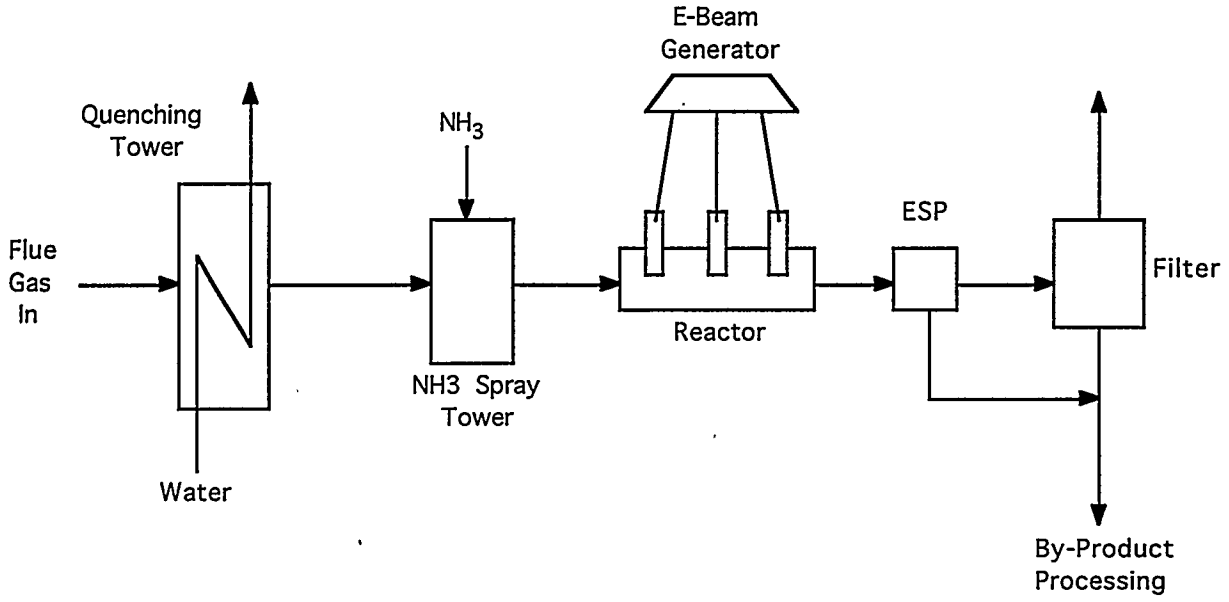

Figure 7-14. E-BEAM PROCESS

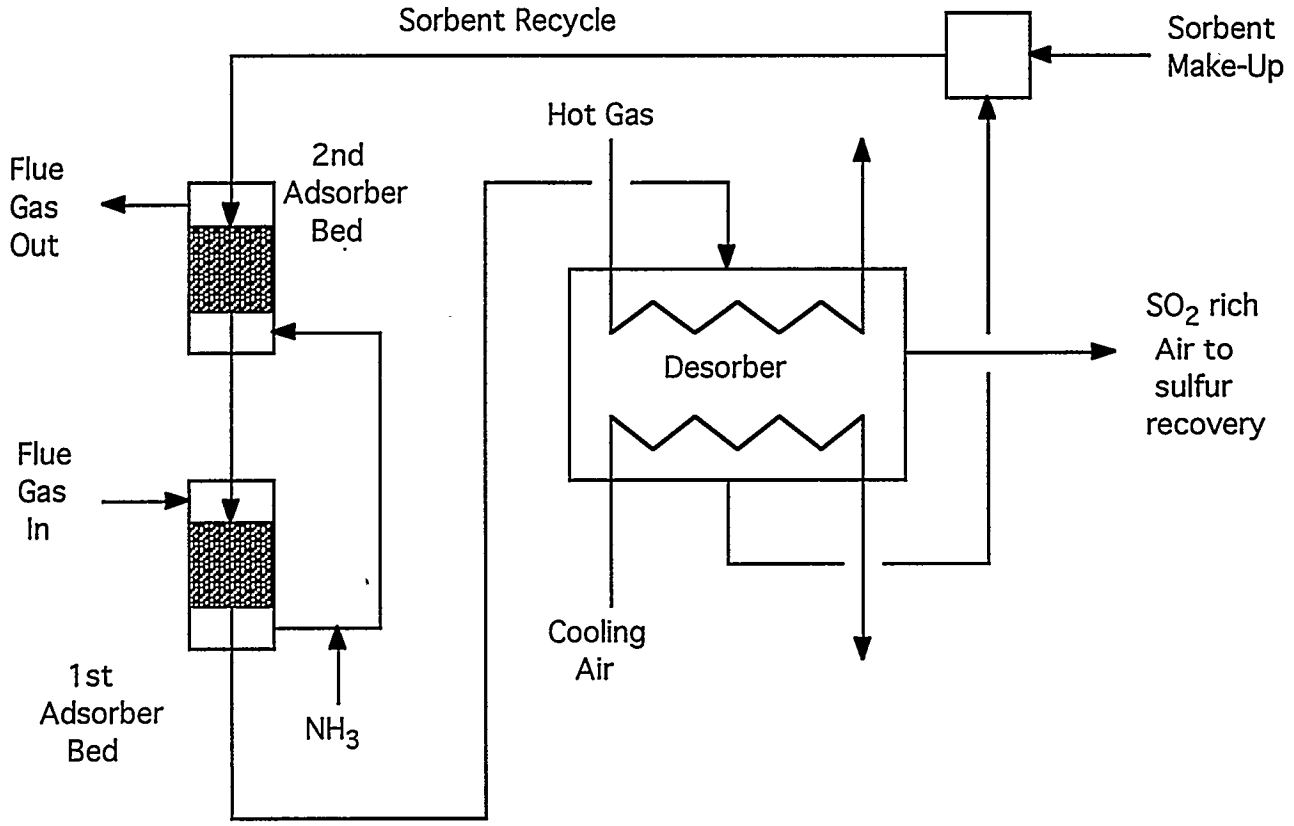

Figure 7-15. ACTIVATED CARBON PROCESS

obtained through desorption at 400 -450°C can be further processed to elemental sulfur, H_2SO_4 or liquid SO_2[52].

Some properties of the activated carbon used in the BF-process (below) include[52]:

Shape:	Cylindrical
Diameter:	4 mm
Length:	4 - 8 mm
Bulk density:	470 ± 20 kg/m^3
BET-N_2 surface:	1,000 m^3/g
Specific pore volume:	77 cm^3 / 100 g

Activated carbon systems have been applied commercially by BF-GmbH and others in Japan (Sumitomo Heavy Industries/EPDC) and Germany (Hugo Petersen). Such systems have reported 90 - 99.9% SO_2 removal and 50 - 80% NO_x removals. Most experience however, has been with low to medium sulfur systems and there is some concern regarding process suitability for high sulfur systems because of high carbon consumption[83].

Some problems of the process include the high cost of activated char and plugging and corrosion in the char regenerator. Also, the temperature of the adsorption tower must be closely controlled as well as the thermal regeneration of the char.

However, Research Triangle Institute (RTI) and the University of Waterloo are currently working on an activated carbon process which has shown the ability to remove 95% SO_2 and 75% NO_x from coal combustion flue gas[97]. This process is shown in Figure 7-16.

The flue gas leaving the ESP is first cooled to approximately 100 C. The SO_2 is then catalytically oxidized to SO_3 which is removed as medium strength H_2SO_4 in a series of periodically flushed trickle bed reactors containing activated carbon as catalyst. The SO_2 free gas is reheated to approximately 150 C and NH_3 is injected into the flue gas. The gas is passed over a bed of activated carbon catalyst to reduce NO_x to N_2 and H_2O. The clean gas is vented to the stack.

A preliminary engineering and economic evaluation of the RTI-Waterloo process has recently been completed for a 100 MW electric power plant burning 2.8% sulfur coal[97]. Capital costs reported were $162 - 188/kW (1991 dollars) with a levelized cost of 6.4 - 9.0 mils/kWh.

Parsons

The Parsons process developed by Ralph M. Parsons Co. (Pasadena, CA) is designed to remove very high levels of SO_2 and NO_x (up to 99%). As shown in Figure 7-17, simultaneous catalytic reduction of SO_2 to H_2S and NO_x to N_2 occurs in a hydrogenation reactor using steam/methane reformer gas. The H_2S is recovered and processed to elemental sulfur, which is a salable by-product.

Performance of the hydrogenation reactor was tested with high sulfur coal in a 10 MW demonstration pilot plant at the St. Mary's Municipal power plant in Ohio[83]. Results showed 98%

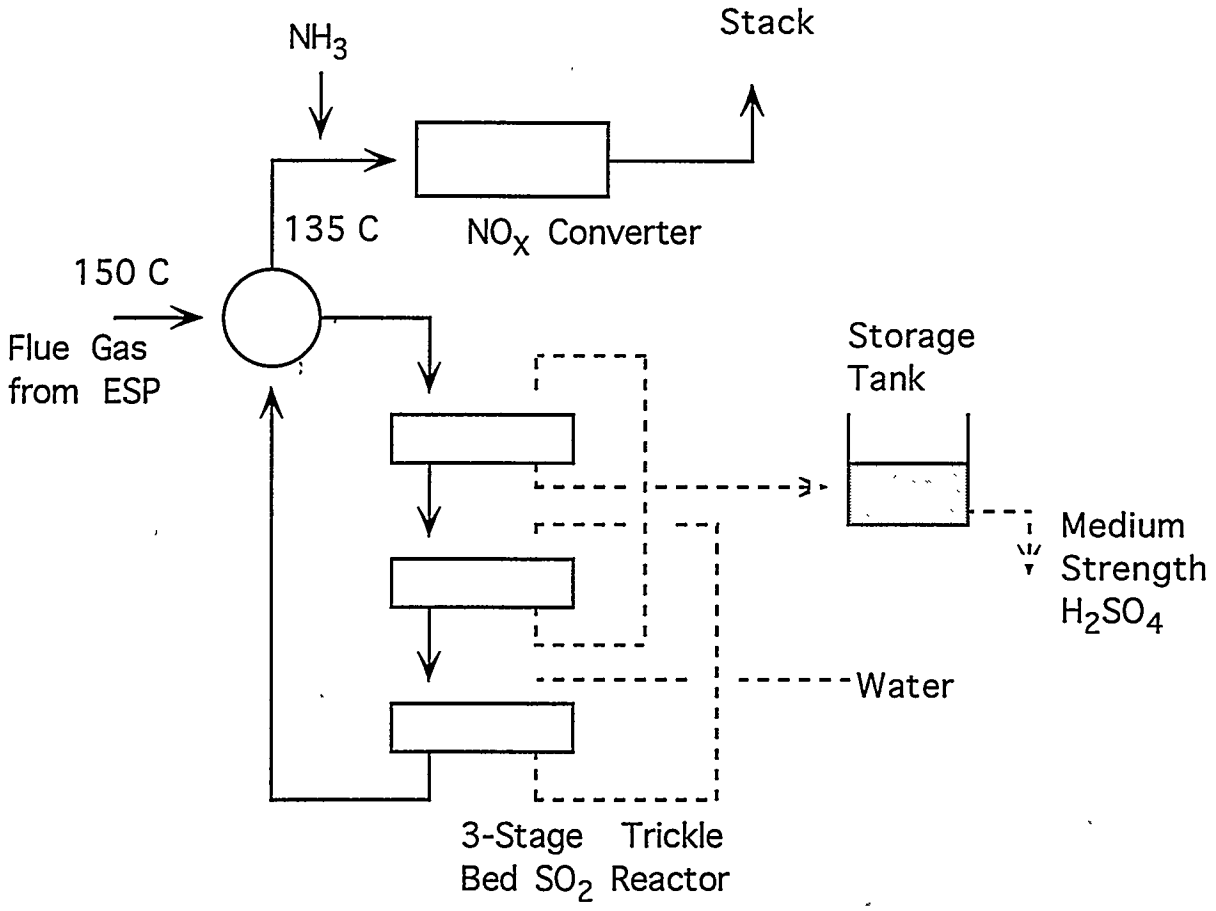

Figure 7-16. RTI-WATERLOO PROCESS

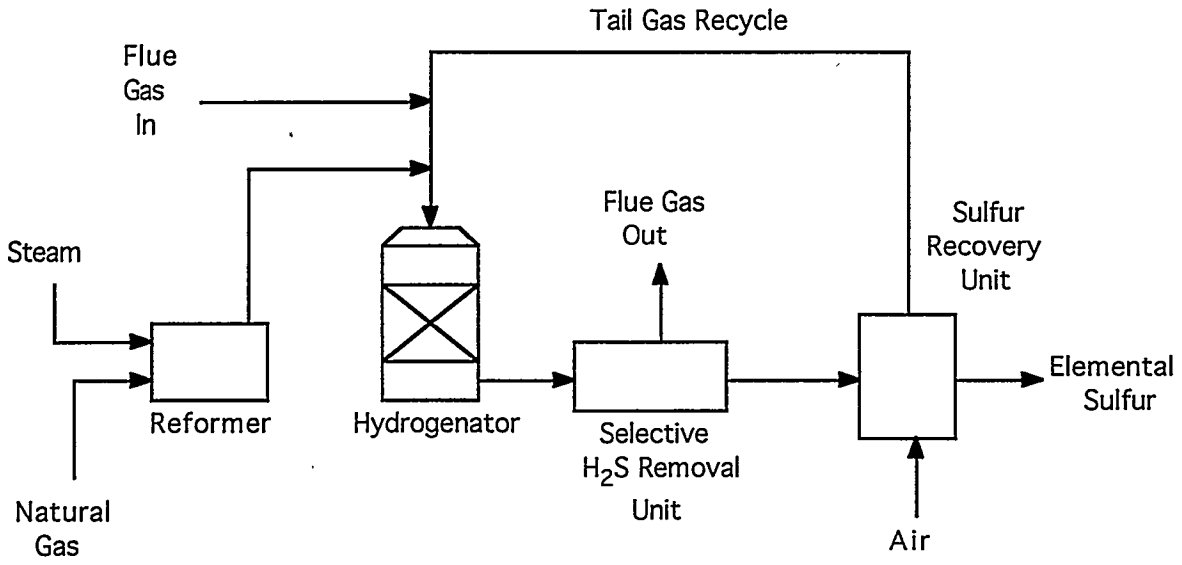

Figure 7-17. PARSONS PROCESS

SO_2 reduction and 92 - 96% NO_X reduction were achievable. A two day test with high dust loading, showed no change in the NO_X and SO_2 reduction performance of the catalyst, and no plugging of the honeycomb openings. The long term effect of high dust loading is not known at this time however.

Corona Discharge

The means of cleaning gases to remove sulfur and nitrogen oxides in a corona or arc discharge is based on accelerating the NO_X and SO_2 oxidation processes[98]. The essence of this method is that a corona or arc discharge is set off in a reactor which contains a mixture of flue gases and ammonia. In the reactor, processes of dissociation, ionization, and excitation of molecules increases with decrease in temperature of the gaseous mixture. The final product consists of ammonium salts.

The potential advantages of this process are :

- Simultaneous removal of SO_2 and NOx;
- The process is dry, thus no requirement to treat waste water;
- No need for a catalyst; and
- More economically attractive than many conventional FGD methods.

The RIACE process by ENEL-CRTN, Italy, is currently in the bench-scale testing stage[37]. Figure 7-18 shows this bench scales process. Tests have been carried out with a 1,000 m^3/hr flue gas at ENEL's plant in Marghera. A pilot plant of 10,000 m^3/hr has also been planned. This process is expected to reduce NO_X by 70% and SO_2 by 90%.

Another corona discharge method, CORONOX, is currently under development by FLS Miljo A/S, Denmark[37]. Bench-scale tests (2,000 m^3/hr) started in 1988. These test confirmed that the process was feasible and could produce ammonium nitrate and ammonium sulfate by-products, with little N_2O production (about 10 ppm). The CORONOX process is shown below in Figure 7-19.

Ultraviolet

A patented bench scale ultraviolet process designed for 80 - 90% reduction of NO_X and SO_2 is currently being developed by Concord Scientific Corp., Canada[37]. As shown in Figure 7-20, NO_X and SO_2 in the flue gases are reduced by irradiating the flue gases with ultraviolet light (at a wavelength between 170 - 200 nm) in the presence of ammonia.

System 99

The System "99", developed by RCM Technology Inc. (Los Angeles, CA), is similar to the CuO process. In this system, flue gases are cooled to 30 - 80 C before entering the reactor. Ammonia is injected into the fluidized reactor containing the RCM proprietary adsorbent media and ammonium sulfite ($(NH4)2SO3$) is formed. This can be further processed to ammonium sulfate or elemental sulfur if desired. The catalyst used is an extremely porous, proprietary and patented, highly calcined mineral material which is said to be key to the process[99]. A 12,000 scfm pilot

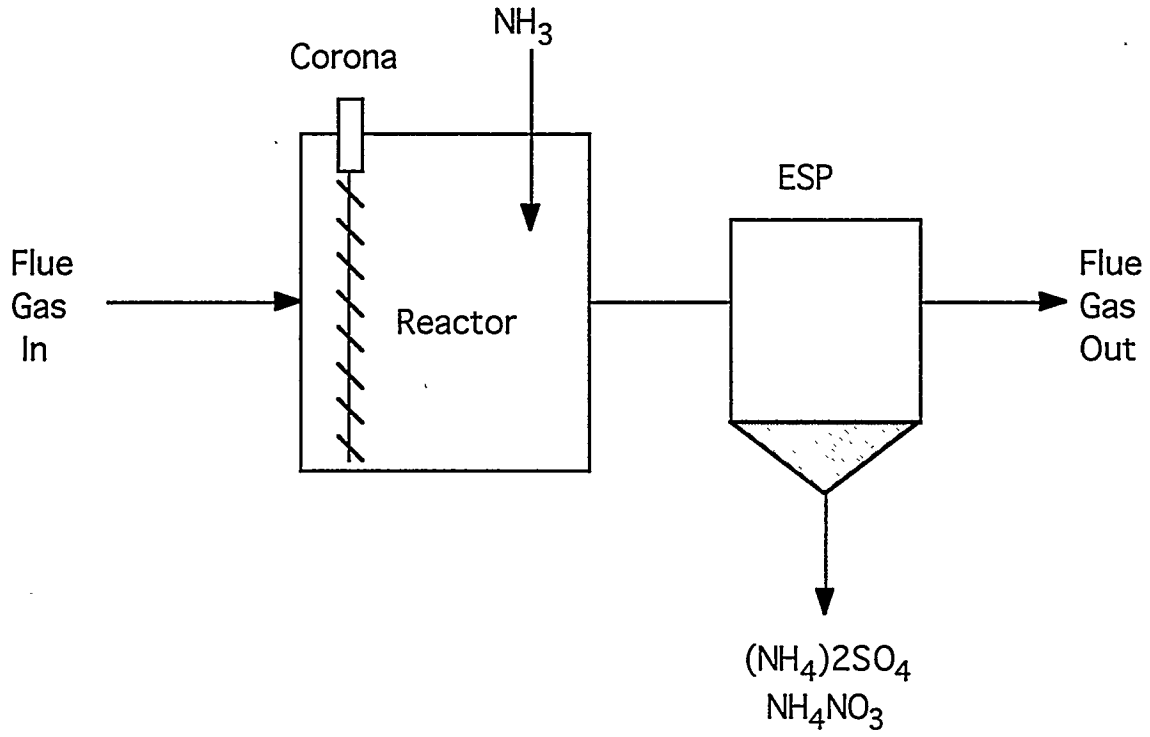

Figure 7-18. RIACE PROCESS

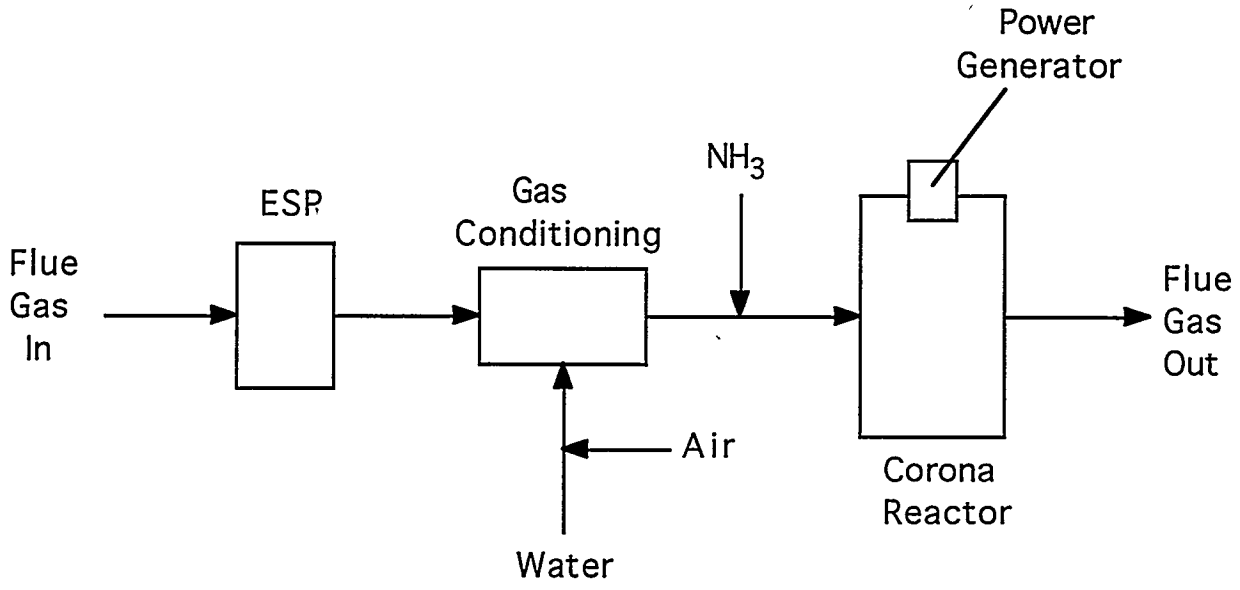

Figure 7-19. CORONOX PROCESS

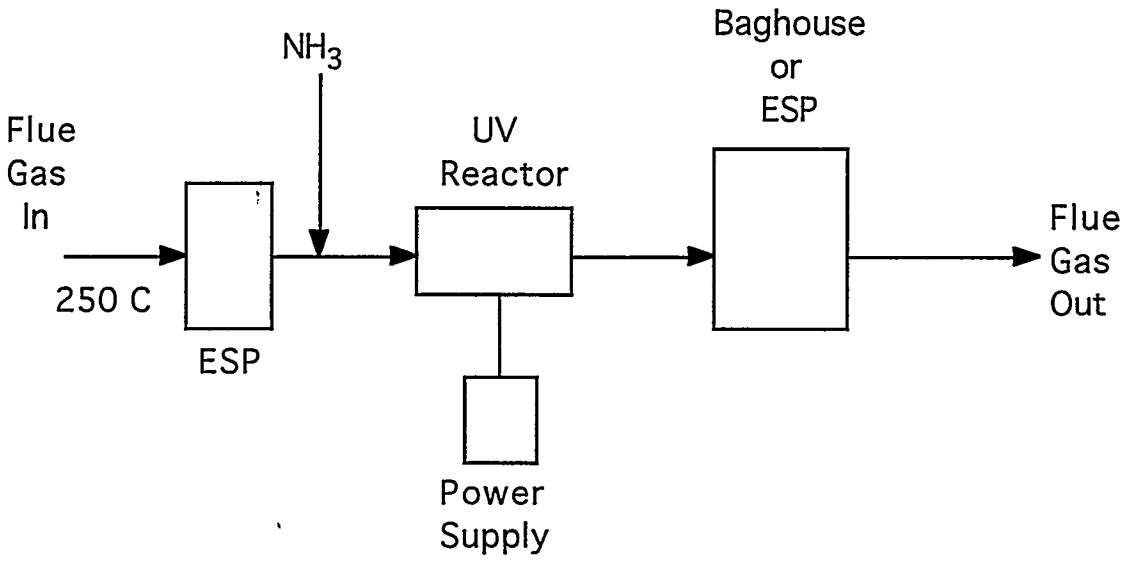

Figure 7-20. UV PROCESS

plant is operating with expected removal rates of 95% for SO_2 and 75 - 95% for NO_X. The process is shown in Figure 7-21.

Ozone

The ozone method of removing SO_2 and NO_X from flue gases consists of introducing a strong oxidizing agent, ozone, to the gases. It oxidizes SO_2 and NO_X to SO_2 and N_2O_5, which are readily dissolved in water and in aqueous solutions. The acid solution obtained in the process of treating the gases is then neutralized by an aqueous solution of ammonia[100].

Kammang Engineering Co., Austria, is said to be developing the NONOX process which expects SO_2 and NO_X removal rates of 95% or greater[99]. The primary process concern is the cost of the ozone generator, but developers are working to alter the process to avoid the need.

In-Boiler Processes

SONOX

Ontario Hydro and R-C Environmental Services have developed an in-furnace slurry injection process for the simultaneous control of SO_2 and NO_X from power plant flue gases. The process is shown in Figure 7-22.

In the SONOX process, an aqueous slurry consisting of a calcium-based sorbent such as limestone, dolomite, hydrated lime, etc. and a nitrogen based additive, are injected into the furnace at temperatures ranging between 900 -1,350°C[101]. In a 0.6 MBtu/hr combustor, under optimum operating conditions, the SONOX process has shown the ability to remove 85% of the SO_2 and 90% of the NO_X. However, the NO_X removal rate is effectively 63 - 80% since 11 -27% of the NO_X removed forms N_2O. The specific removal rates depend on the coal used, type of sorbent and nitrogen additive, temperature and stoichiometry. The optimum temperature was approximately 1,200°C and the optimum Ca/S and Additive/NO ratios were 2.5 - 3.0 and 1.5 - 1.7, respectively.

The SONOX process has been demonstrated on a pilot-plant (0.6 MM Btu/hr) level but the following questions need to be answered before full-scale commercialization[101]:

- Optimum nozzle array configuration and slurry size distribution to assure good gas-slurry contact,
- Optimum sulfation and NO_X removal temperature window in upper furnace,
- Effect of increased solids loading on boiler tube erosion,
- Effect of increased loading and resistivity on ESP performance, and
- Solids handling of the calcium-rich ash.

Integrated Dry Sorbent Injection

Research Cottrell (Sommerville, NJ) and Riley Stoker (Worcester, MA) are jointly conducting proof-of-concept demonstrations of an integrated dry sorbent injection process for coal fired boiler SO_2 and NO_X control, under a DOE contract with co-funding by EPRI. The process

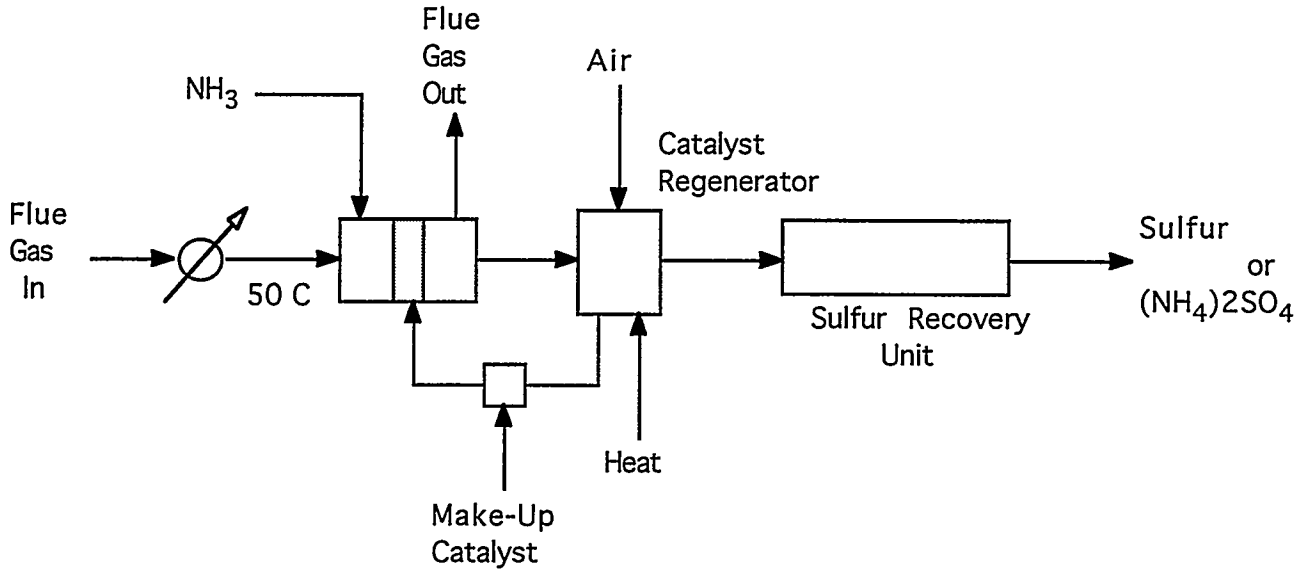

Figure 7-21. SYSTEM "99" PROCESS

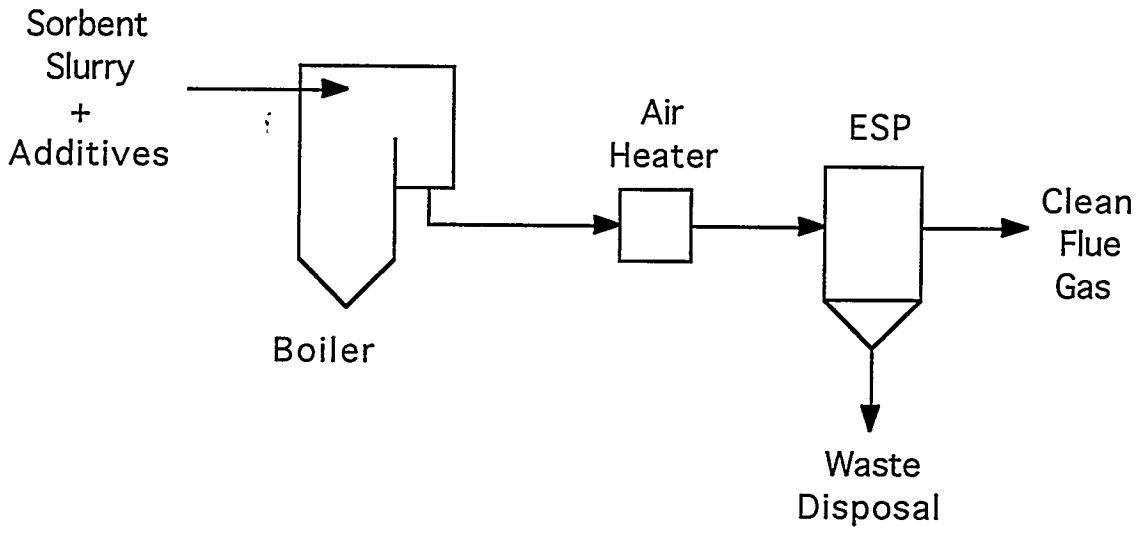

Figure 7-22. SONOX PROCESS

consists of combustion modification using low-NO_X burners to reduce NO_X emissions, dry injection of hydrated lime at the economizer for primary capture of SO_2; dry injection of a commercial grade sodium bicarbonate at the air heater for additional SO_2 and NO_X removal, and flue gas humidification for precipitator conditioning[102]. This concept, which is illustrated in Figure 7-23, offers the potential to remove 90+% of the SO_2 and 75+% of the NO_X.

Gas Reburning/Sorbent Injection

Evaluation of Gas Reburning/Sorbent Injection (GR-SI) technology is being carried out by Energy and Environmental Research Corporation as part of DOE's CCT. Process specifications studies have confirmed that GR-SI technology is capable of achieving 60% reduction of NO_X and 50% reduction of SO_2. NO_X emissions are reduced by staged fuel addition using natural gas as the reburn fuel, while SO_2 emissions are reduced by capturing sulfur by dry, calcium based sorbent injection which will be augmented by the displacement of about 15 - 20% of the coal input by natural gas firing[103]. Figure 7-24 shows the application of gas reburning-sorbent injection (GR-SI) to a commercial wall-fired utility boiler.

The primary disadvantage of sorbent injection is that the sorbent is not utilized effectively. Under optimum conditions, only 20 - 30% of the sorbent is reacted with SO_2. The remainder exits the boiler as unreacted calcium oxide. Thus, high sorbent injection rates are required to achieve significant SO_2 emission reductions. This results in high sorbent cost and poses an extensive load on the ESP[103]. Current economic projections indicate that the combined technology may have broad applicability to older, relatively small boiler units requiring emission reduction as a result of the Clean Air Act Amendments of 1990. The projected capital cost of this type of installation is about $90/kW for GR-SI, $30/kW for GR with operating costs of 6 - 9 mills/kWh[104].

Other In-Boiler Processes

The combination of sorbent injection and SNCR technologies has been investigated for simultaneous SO_2/NO_X removal. A slurry consisting of a urea based solution and various Ca-based sorbents was injected into a pilot-scale natural gas reactor with doped pollutants. This process achieved up to 80% reduction of SO_2 and NO_X at reactant/pollutant stoichiometries of 2 and 1, respectively[105]. Further full-scale studies to assess this combined sorbent/urea-based slurry injection technology are needed.

Dry sodium bicarbonate injection has been tested at five coal-fired utility boilers by NaTec Resources Inc. (Dallas, TX). Removal values have reached 75% for SO_2 and have ranged from 0 - 40% for NO_X on systems equipped with ESPs[99]. SO_2 removals up to 90%, with 25% NO_X removal, were obtained in small-scale tests with injection upstream of a baghouse [83].

Retrofit Flue Gas Desulfurization Systems

The dominant flue gas desulfurization (FGD) technology today is wet scrubbing with sodium carbonate, lime, or limestone. These processes can remove over 90% of the SO_2, but are

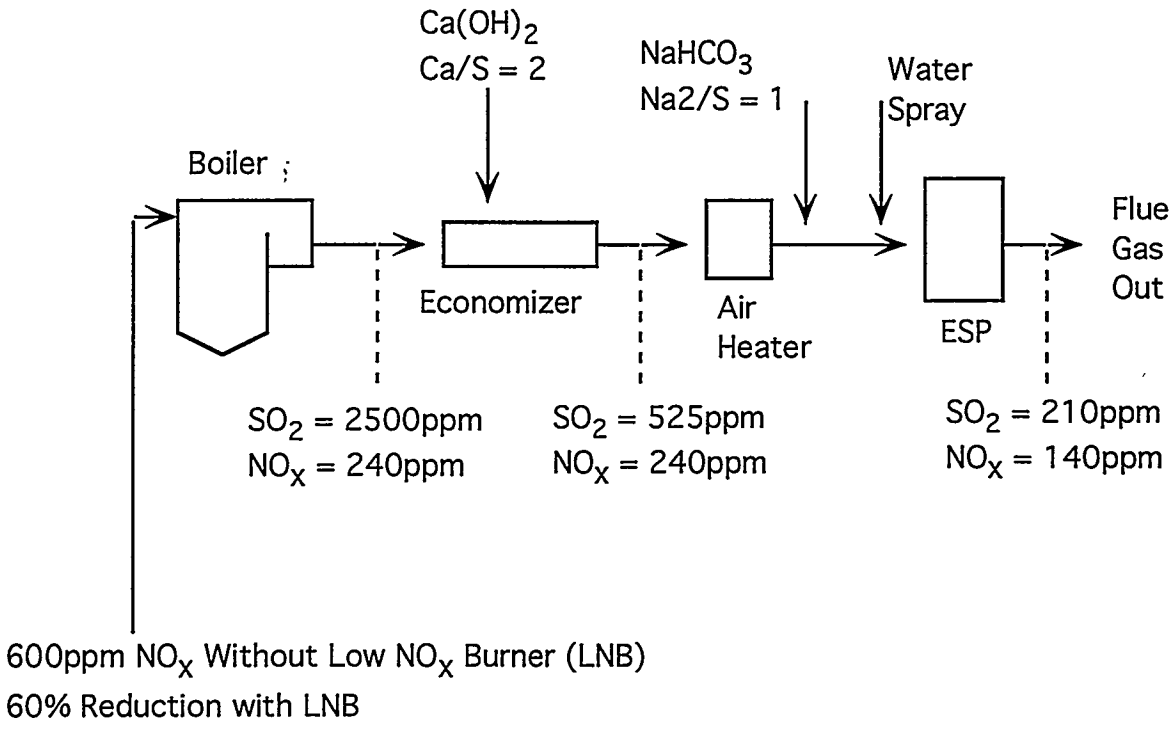

Figure 7-23. DRY SORBENT INJECTION PROCESS

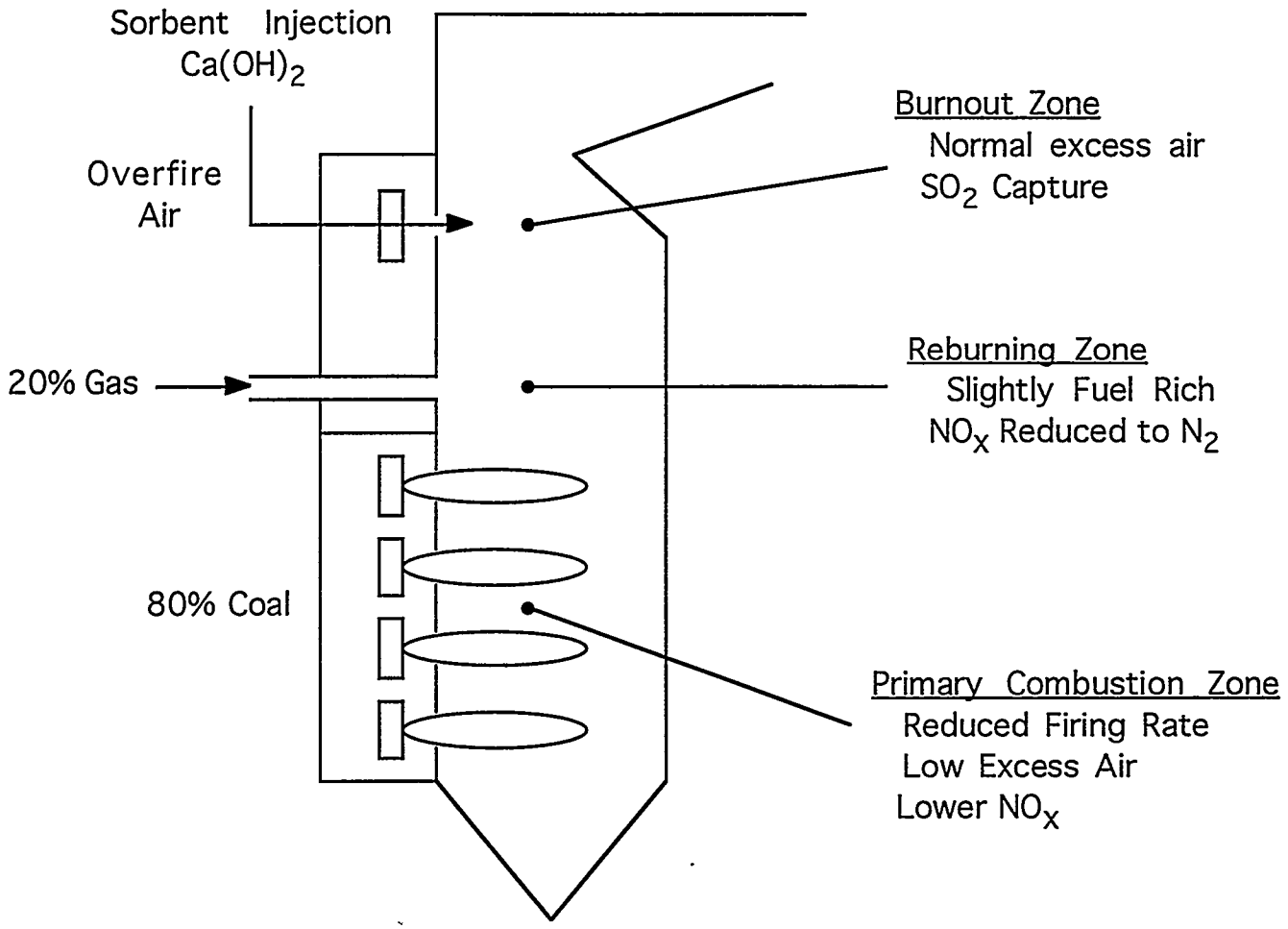

Figure 7-24. GR-SI FOR A WALL-FIRED UTILITY BOILER

largely ineffective for NO_X removal because of the low solubility of NO. There is a large number of scrubbers in place now or planned for the future, therefore, a process which could remove NO_X simply by using chemical additives could have a significant impact on control strategies[83]. Figure 7-25 shows the basics of a retrofit FGD system.

Ferrous Chelate Addition

The addition of metal chelates, such as ferrous ethylenediaminetetraacetic acid ($Fe(II)*EDTA^{2-}$) promotes NO_X removal because they quickly extract any absorbed NO from solution. This chelating agent forms a strong complex with NO:

$$NO + Fe(II)EDTA \text{ ---------> } Fe(II)EDTA*NO \qquad (7\text{-}6)$$

When SO_2 is absorbed, reaction of the complex with SO_3^{2-} leads to a number of nitrogen-sulfur compounds, including hydroxylamine disulfonate, and eventual regeneration of the Fe(II)EDTA [106].

$$Fe(II)EDTA*NO + SO_3^{2-} \text{ ----------> } Fe^{2+}EDTA + \text{N-S compounds} \qquad (7\text{-}7)$$

The chemistry of these subsequent reactions is not completely known, but most of the NO that is absorbed forms anionic compounds that are removed in solution entrained with the precipitated calcium sulfite and calcium sulfate.

Pilot-scale tests of the technology were conducted during 1991 by the Dravo Lime Company (Pittsburgh, Pa) at the Miami Fort station of Cincinnati Gas and Electric Company. Tests were sponsored by the U.S. DOE PETC. The pilot unit took a slip stream of flue gas from Unit 7, a 530 MW coal fired boiler. Flue gas NO_X levels were 400 - 700 ppm and SO_2 was added to give 2,500 ppm SO_2. The scrubber tower was 3 ft in diameter, 40 ft tall, equipped with a quench header, with either sieve trays or 6-12 ft of packing, headers for spray nozzles, and one or two mist eliminators [107].

Nitrogen oxide removals of up to 60% were obtained using Munters PN Fill packing in the scrubber tower. SO_2 removals were nearly 100%.

An estimate of the design requirements for a commercial scale scrubber has been made from the pilot-plant results. The design is determined by NO removal since the height of a transfer unit for NO is about 30 times that for SO_2 (Harriot et. al., 1993). Figure 7-26 shows the predicted NO removal as a function of packing height for an L/G ratio of 5.8 L/m^3 (43 gal/1,000 acfm). Operating at a higher liquid rate would reduce the packing height needed and could be used even though the ratio of 5.8 L/m^3 is already fairly large.

A variation of the above mentioned process is being developed by Dow Chemical Co., (Midland, MI). The process is based on liquid phase absorption of NO and electrochemical regeneration of the circulating iron chelate solution. The problem with using Fe(II)EDTA is that it reacts with dissolved O_2 to form Fe(III)EDTA, which is ineffective for NO removal. The Dow process claims to reduce the total iron concentration by controlling the ionic state in the active Fe(II)

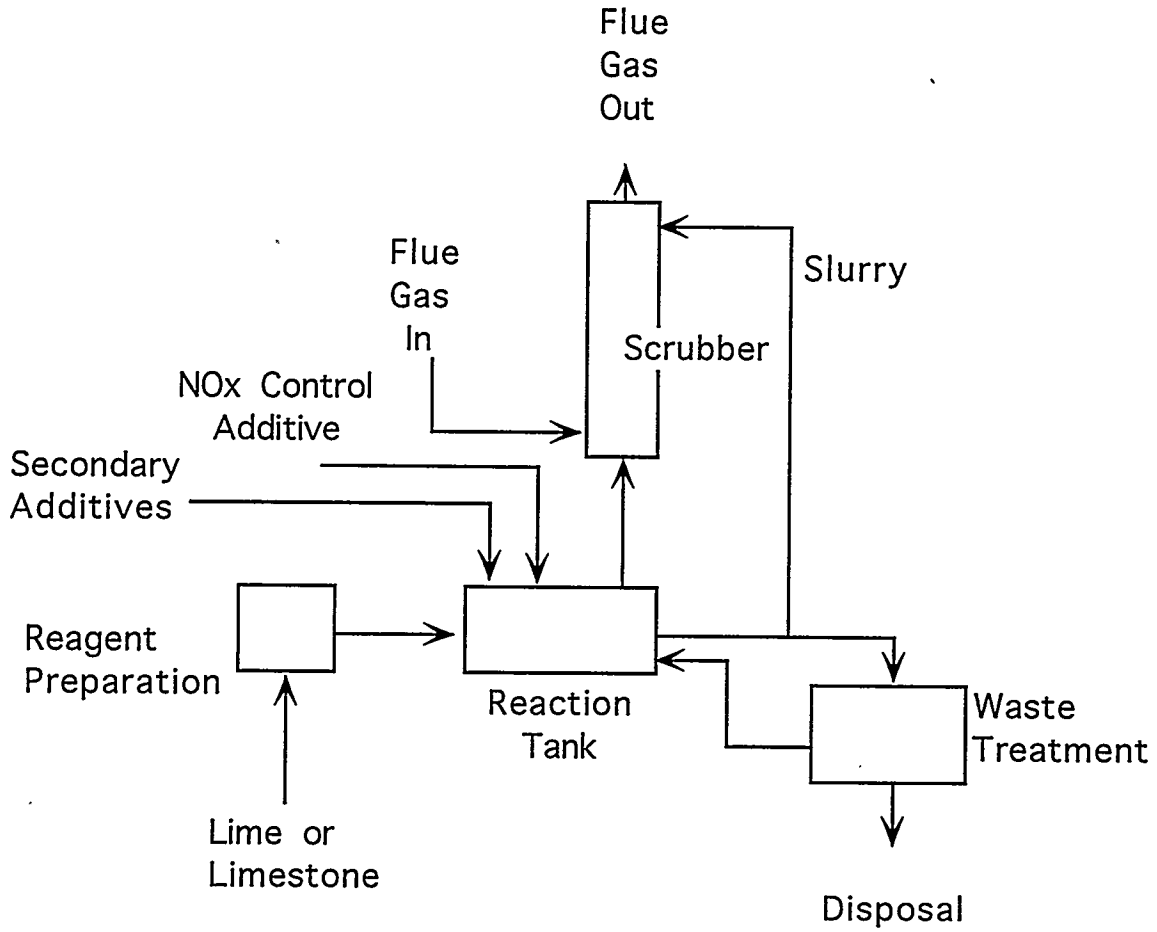

Figure 7-25. RETROFIT FGD SYSTEM

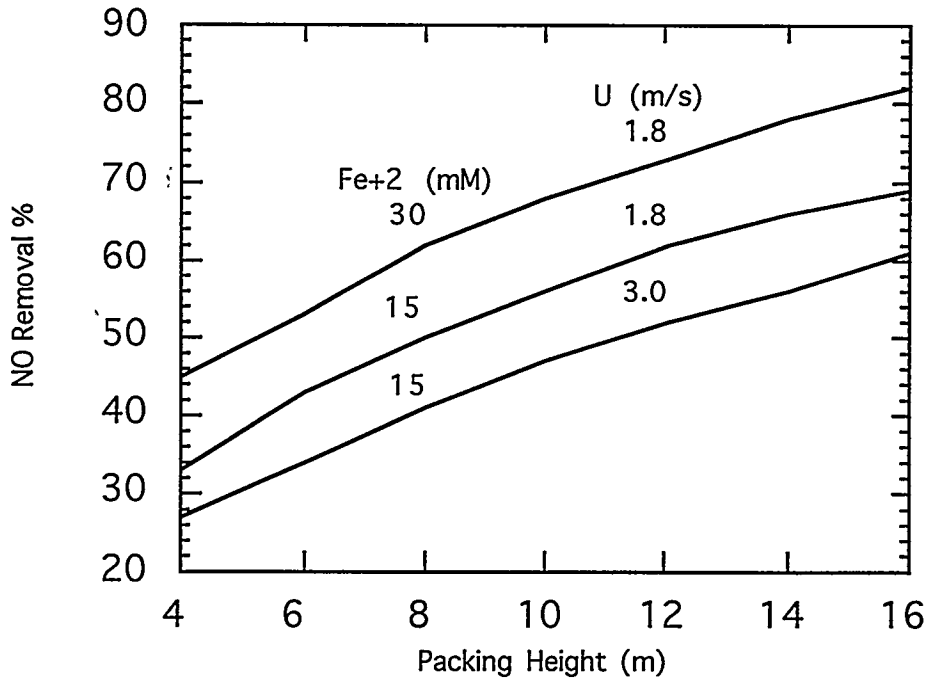

Figure 7-26. PREDICTED NO REMOVAL FOR MUNTERS PN FILL PACKING @ L/G = 5.8 L/m^3

form and unburdening the scrubber solution of the inactive Fe(III) load (Sloss et. al., 1992). The enhanced Fe(III) reduction method is accomplished using an electrochemical cell consisting of cathode and anode compartments separated by membranes. When current is applied to the cell, the majority of the ferric chelate is reduced to ferrous chelate at the cathode and water is electrolyzed to O_2 and H_2 at the anode[108]. Expected NO_X removal is 60 - 80%. The Dow process is illustrated in Figure 7-27.

An additional metal chelate process is the ARGONOX process. The ARGONOX process, developed at Argonne National Laboratory (Argonne, IL), is suitable for retrofitting existing wet SO_2 scrubbers and capable of 50 -70% NO_X reduction and 90% SO_2 reduction. Tests have shown that EDTA can be effectively replaced by hexamethylenetetraamine (HMTA)[109]. HMTA is a bulk petrochemical used in resin manufacture and to treat urinary infections in humans and animals. HMTA costs only a fifth of EDTA. The ARGONOX process, which is still in development, is shown in Figure 7-28.

Phosphorus Addition to Wet Scrubbers

The addition of yellow phosphorus in wet scrubbing systems can result in the high efficiency simultaneous removal of SO_2 and NO_X from combustion flue gas. Yellow phosphorus reacts with O_2 to produce O_3 which oxidizes NO_X to NO_2. NO_2, which is much more soluble in water than NO, and SO_2 are removed from the flue gas by dissolution into an aqueous solution, where they are converted to ammonium sulfate and gypsum. Yellow phosphorus is oxidized to yield a salable by-product, phosphoric acid.

This technology, jointly developed by Lawerence Berkeley Laboratory (LBL) and Bechtel, Co. (San Francisco, CA), was capable of 90% NO_X removal at an L/G > 60 gal/1000 cfm in bench-scale testing[110]. The LBL-PhoSNOX process is illustrated in Figure 7-29.
A pilot plant testing program for the LBL-PhoSNOX process has been planned to verify the process performance and feasibility, and to obtain process data for scale up to commercial demonstration units.

Concluding Statements

The emissions from coal-fired plants contain nitrogen and sulfur oxides which may pose a health hazard. Some sulfur can be removed from coal prior to burning, but nitrogen proves to be very difficult to remove. Therefore, some type of NO_X control strategy will need to be implemented if coal is to be the fuel of choice for the future.

Through combinations of advanced combustion measures, it is possible to reduce NO_X emissions by up to 50% under favorable conditions. Pre-combustion measures are usually the most cost effective way to reduce NO_X emissions and therefore lower the reduction rate required for flue gas treatment.

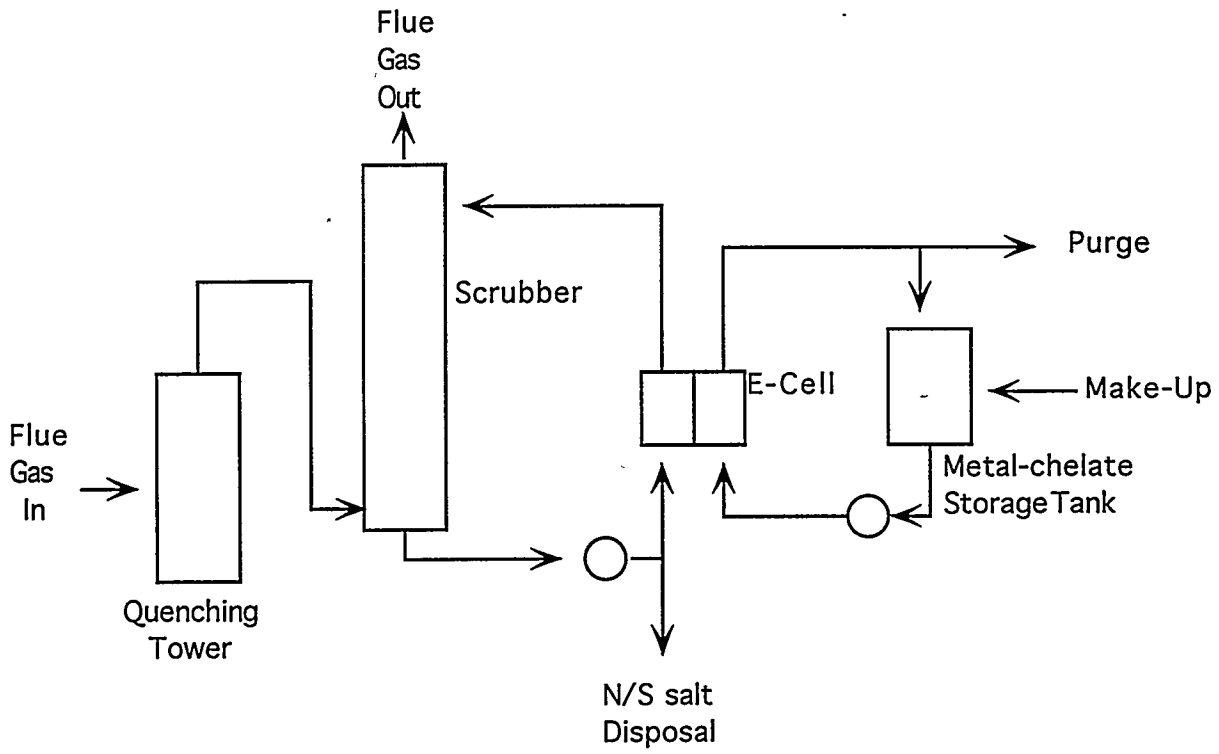

Figure 7-27. DOW PROCESS

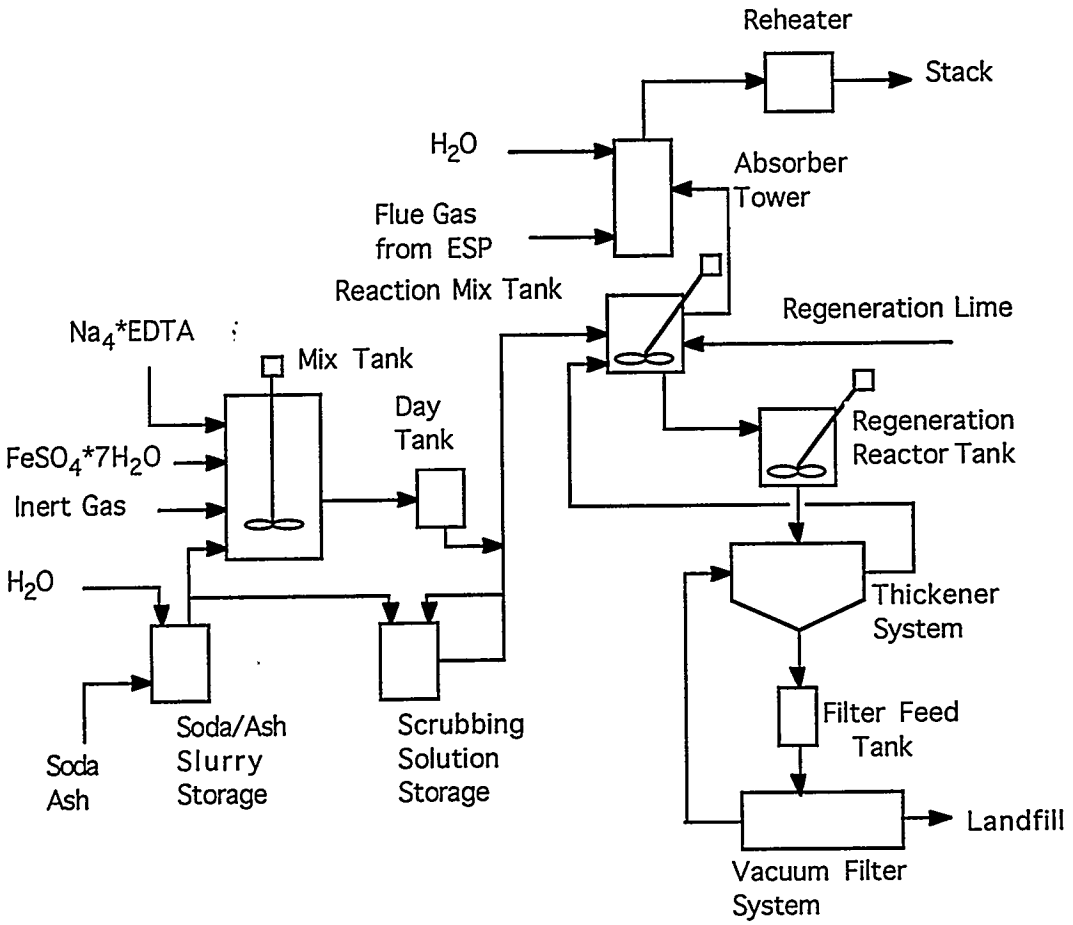

Figure 7-28. ARGONOX PROCESS

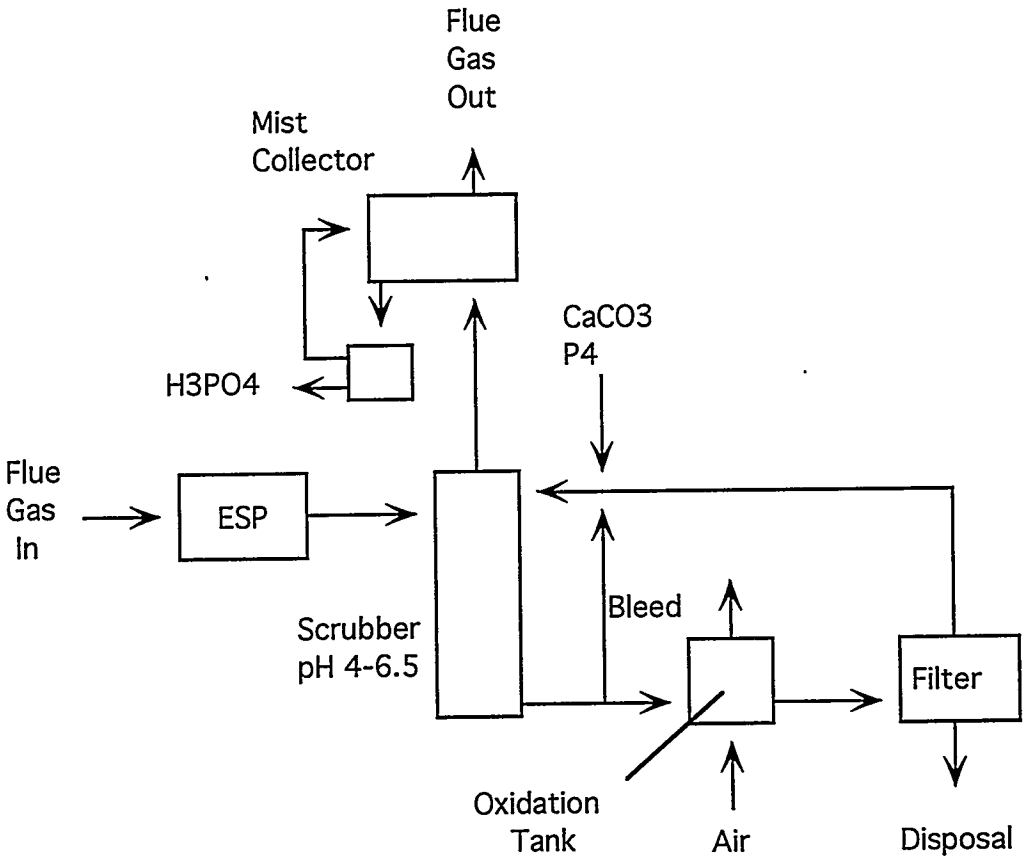

Figure 7-29. LBL-PhoSNOX PROCESS

Selective catalytic reduction (SCR) has proved to be an effective technology, capable of removing 80 - 90% of the NO_X in the flue gas. This is not without some sacrifices though. Usually, reheating the flue gas is needed, thereby compromising boiler efficiency. Also, SCR is relatively unproven on high sulfur U.S. coals. Selective non-catalytic reduction (SNCR) can be installed where temperatures are suitable, to reduce NO_X emissions by 50 - 60%. Several new NO_X control strategies are currently being developed, however, most are only in the research stage.

The new field of research seems to be in the area of combined NO_X/SO_2 control. Integrated systems that combine control functions in a single process offer a number of advantages for retrofit and new plants. In recent years, considerable progress has been made in developing such systems, and new concepts continue to emerge from the laboratory.

It is important, when considering an emission control strategy, to avoid the production of new pollutants, either by depositing wastes that have a potential to leach, producing contaminated waste water, or by generating additional atmospheric pollutants (N_2O, NH_3). It is also important to consider increased CO_2 emissions due to high energy use in operating the flue gas treatment plant (i.e., reheating the flue gas). Therefore, in the future, plant efficiency as well as emission control will have to be taken into account when developing an emission control strategy.

SO_2 CONTROL STRATEGIES

Introduction

In recent years, the demand for reducing pollutants in the air from industrial sources has grown excessively. With strict Clean Air legislation demanding that utilities cut sulfur dioxide (SO_2) and nitrogen oxides (NOx) emissions by 10 million tons a year by the year 2000, an influx of research and development has led to a number of emission control systems[111]. It has been estimated that there are more than 200 flue gas desulfurization (FGD) processes currently on the market or under development[111]. Within recent times, the dominant commercial technology has been scrubbing with lime or limestone slurries. As previously discussed, there is also fast moving advancement of integrated flue gas cleanup (FGC) systems where SO_2 and NO_X are both removed in the system.

Worldwide, there are currently 581 flue-gas desulfurization systems operating on a total capacity of about 150 GW[112]. Approximately 70% of the units are based on lime or limestone wet scrubbing. About 20% of the units utilize either sodium-based or lime slurry (spray) dry scrubbing. The remaining 10% use various regenerable processes or sorbent injection technologies of one form or another[112].

These FGD processes can be categorized by reagent chemistry; form of product; equipment; chronology of development, country of development, degree of development, or commercial operation. In this subsection, SO_2 removal processes are summarized. They are categorized by those that produce wet products (wet process) or dry products (dry process).

Wet Scrubbing Flue Gas Desulfurization Processes

Wet scrubbing with lime and limestone has been the most popular commercial FGD systems. The inherent simplicity, the availability of limestone, and the high removal efficiencies obtained are the main reasons for this popularity. Wet scrubbing processes may use either an aqueous slurry or an aqueous.solution. When scrubbing with an aqueous slurry, some of the absorbent and the reaction products are present as suspensions of solids in water. During the adsorption step of the scrubbing process, the suspended alkali dissolves to react with the adsorbed SO_2. Limestone with forced oxidation as been used as a reference process in the following review. This process is one of the most popular in the commercial market.

Limestone with Forced Oxidation (LSFO)

Process Outline

A limestone slurry is used in an open spray tower with in-situ oxidation to remove SO_2 and form a gypsum sludge. The major advantages of this process relative to a conventional limestone FGD system are easier dewatering, more economical disposal of the scrubber product solids, and decreased scaling on tower walls. LSFO is capable of greater than 90% SO_2 removal and has over 20 full-scale, operating facilities in the U.S.[113].

System Description

The hot flue gas exits an electrostatic precipitator (ESP) and enters a spray tower where it comes into contact with a sprayed dilute limestone ($CaCO_3$) slurry (see Figure 7-30). The SO_2 in the flue gas reacts with the $CaCO_3$ in the slurry to form hydrated calcium sulfite ($CaSO_3 \cdot 1/2 H_2O$). Compressed air is bubbled through the slurry which causes this sulfite to be naturally oxidized and hydrated to form calcium sulfate ($CaSO_4 \cdot 2H_2O$). The $CaSO_4$ (gypsum) can first be dewatered using a thickener or hydroclones then dewatered again using a rotary drum or horizontal belt filters. This gypsum is then transported to a landfill for disposal. The formation of the calcium sulfate (gypsum) crystals in a recirculation tank slurry also helps to reduce the chance of scaling.

The absorbing reagent, limestone, is normally fed to the open spray tower in an aqueous slurry at a molar feed rate of 1.1 moles of $CaCO_3$/mole of SO_2 removed. This process is capable of removing more than 90% of the SO_2 present in the inlet flue gas[113].

Evaluation

Limestone with forced oxidation is one of the most dominant processes in the industry at this present time. The main reasons for this attraction is the high reliability of the system and the ease of removing the gypsum by-product.

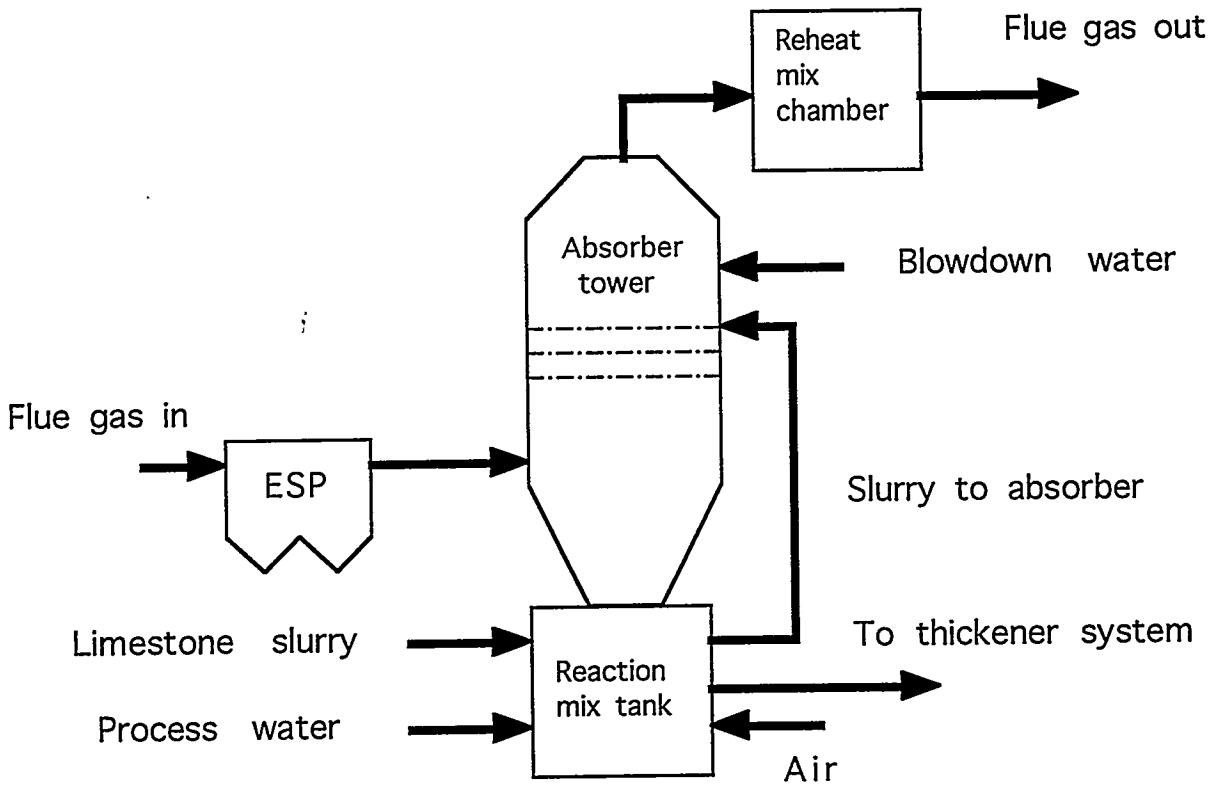

Figure 7-30. LIMESTONE WITH FORCED OXIDATION PROCESS [3]

The advantages of the LSFO systems are:

- Lower scaling potential on tower internal surfaces due to the presence of gypsum seed crystals and reduced calcium sulfate saturation levels. This in turn allows a greater reliability of the system;
- Gypsum product is filtered easier than the $CaSO_3$ produced with conventional limestone systems;
- A lower chemical oxygen demand in the final disposed product;
- The final product can be safely and easily disposed of in a landfill;
- The forced oxidation allows the limestone utilization to be greater than conventional systems;
- Low cost of raw material (limestone) used as absorbent; and
- LSFO is an easier retrofit than natural oxidation systems since the process uses smaller dewatering equipment.

A disadvantage of this system is the high energy demand due to the relatively higher liquid to gas ratio necessary to achieve the required SO_2 removal efficiencies.

Limestone with Forced Oxidation Producing a Wallboard Gypsum By-Product (LS/WB)

Process Outline

A limestone slurry is used in an open spray tower with in-situ oxidation to remove SO_2 and form a gypsum by-product. The solids from the recycle tank are washed to yield a salable wallboard quality gypsum material. Disadvantages are high corrosion potential and limits on system chloride content.

System Description

As in the LSFO system, the limestone/wallboard gypsum (LS/WB) FGD process uses a sprayed limestone slurry to remove the SO_2 from the flue gas. The flue gas enters the spray tower where the SO_2 reacts with the $CaCO_3$ in the slurry to form calcium sulfite ($CaSO_3$). This calcium sulfite is then oxidized to calcium sulfate in the absorber recirculation tank. The calcium sulfate produced with this process is of a high quality so that it may be used in wallboard manufacture.

There are a few differences with this process in order to achieve a high quality gypsum. The LS/WB system uses horizontal belt filters to produce a drier product and provides enough cake washing to remove residual chlorides. Since the by-product is a higher quality, the use of the product handling system is replaced with by-product conveying and temporary storage equipment. Sulfuric acid addition is used in systems with an external oxidation tank. The acid is used to control the pH of the slurry and neutralizes unreacted $CaCO_3$.

The limestone feed rate is 1.05 moles of $CaCO_3$/moles of SO_2 removed which is slightly lower than the feed rate for the LSFO system[113].

Evaluation

Advantages of the LS/WB process are:

- The disposal area is kept at a minimum since most of the by-product is reusable. Some provisions should be for off-specification gypsum;
- Money can be made from the sale of gypsum to cement plants and agricultural users; and
- SO_2 removal is slightly enhanced because of the high sulfite to sulfate conversion.

There are some disadvantages of the system. At present, there are few full-scale operating systems in the United States. To produce quality gypsum, specific process control and tight operator attention are consistently needed. If this is not the case, such things as chemical impurities can lead to off-specification gypsum. Another disadvantage is the inability to use cooling tower blowdown as system make-up water due to chloride limits in the gypsum by-product. In certain plants, a prescrubber may be needed in order to remove chlorides from the flue gas upstream of the scrubber to prevent a buildup of chloride concentration in the gypsum product.

Lime Dual Alkali (LDA)

Process Outline

A sodium sulfite solution is used in an open spray tower to remove SO_2. Lime is added to a slip stream product solution to simultaneously regenerate the sodium sulfite and form a sludge high in calcium sulfite. Major advantages of this process are higher availability due to reduced scaling in the absorber and increased reagent reactivity. A disadvantage is that the use of a lined landfill may be required because of the soluble sodium salts entrained in the solid product.

System Description

In this process, the hot flue gas exits the ESP and then enters into an open spray tower. The gas comes into contact with a sodium sulfite solution that is sprayed in the tower. An initial charge of sodium carbonate reacts directly with SO_2 to form sodium sulfite (Na_2SO_3) and CO_2. The sulfite then reacts with more SO_2 and water to form sodium bisulfite ($NaHSO_3$). Some of the sodium sulfite is oxidized by excess oxygen in the flue gases to form sodium sulfate. This does not react with SO_2 and can not be reformed by the addition of lime to form calcium sulfate. The above process can be shown in the following reactions :

$$Na_2CO_3 + SO_2 \rightarrow Na_2SO_3 + CO_2 \quad (7\text{-}8)$$

$$Na_2SO_3 + SO_2 + H_2O \rightarrow 2NaHSO_3 \quad (7\text{-}9)$$

$$Na_2SO_3 + 1/2\ O_2 \rightarrow Na_2SO_4 \quad (7\text{-}10)$$

$$2NaOH + SO_2 \rightarrow Na_2SO_3 + H_2O \text{ (minor reaction)} \quad (7\text{-}11)$$

The calcium sulfites and sulfates are reformed in a separate regeneration reaction tank. They are formed by mixing of the soluble sodium salts (bisulfate and sulfate) and slaked lime. The calcium sulfites and sulfates precipitate from the solution in the regeneration tank. The scrubber

liquor then has a pH of 6 to 7 and consists of a mixture of sodium sulfite, sodium bisulfite, sodium sulfate, sodium hydroxide, sodium carbonate, and sodium bicarbonate[113].

Evaluation

The lime dual alkali process has considerable advantages over the LSFO process. The system has a higher availability since there is less potential for scaling and plugging of the soluble absorption reagents and reaction products. Corrosion and erosion is prevented with the use of a relatively high pH solution. Some other worthwhile advantages are:

- A low maintenance labor and materials usage because of the high reliability of the system;
- The main recirculation pumps are smaller since the absorber liquid/gas feed rate is less. This feed rate is smaller due to the high reactivity of the sodium-based reagent;
- A lower power consumption is achieved due to the smaller pump requirements;
- There is no need for a process blowdown water discharge stream; and
- The highly reactive alkaline compounds in the concentrated absorbing solution allow for better turndown and load following capabilities.

Two disadvantages of the system are the higher costs for the reagent (sodium carbonate) and the need for a lined landfill for the disposal of the sodium contaminated calcium sulfite/sulfate sludge.

Limestone with Dibasic Acid (LS/DBA)

Process Outline

Dibasic Acid (DBA) is added to act as a buffer/catalyst in the open spray tower where a limestone slurry absorbs the SO_2 and forms a calcium sulfite/sulfate sludge. The major advantage of this process are increased SO_2 removal efficiency and decreased liquid to gas ratio.

System Description

The dibasic acid enhanced limestone process is very much like the LSFO process. The hot flue gas exits an ESP and enters a spray tower where it comes into contact with a diluted limestone ($CaCO_3$) slurry. The SO_2 in the flue gas reacts with the limestone and water to form hydrated calcium sulfite.

$$CaCO_3(s) + SO_2(g) + 1/2\ H_2O \text{ ---> } CaSO_3 \cdot 1/2H_2O(s) + CO_2(g) \qquad (7\text{-}12)$$

This equation is rate limited by the absorption of SO_2 into the scrubbing liquor.

$$SO_2(g) + H_2O \text{ --> } H^+ + HSO_3^- \qquad (7\text{-}13)$$

The dissolved SO_2 ions then react with the calcium ions to form calcium sulfite. The hydrogen ions in solution are partly responsible for the back pressure needed to reform SO_2.

After absorbing the SO_2, the slurry drains down to a recirculation tank at the bottom of the tower. Here the calcium sulfite is oxidized to calcium sulfate dihydrate using oxygen.

$$CaSO_3 \cdot 1/2H_2O(s) + 1/2\ O_2 + 3/2H_2O \text{ --> } CaSO_4 \cdot 2H_2O \qquad (7\text{-}14)$$

Dibasic acid acts as a buffer by absorbing free hydrogen ions formed by Equation (7-13). This then shifts the reaction to the right to form more sulfite ions, thus removing more SO_2 ions.

Alkaline limestone is added to replace the buffering capabilities of the acid, therefore there is no net consumption of the DBA during SO_2 absorption.

The limestone dissolution rate is increased by increasing the SO_2 removal efficiency at a low slurry pH. This may result in a lower reagent consumption due to an increase in $CaCO_3$ availability in the recirculation tank.

Evaluation

The process offers some advantages compared to the LSFO process:

- Increased SO_2 removal efficiency;
- Reduced liquid/gas ratio and the potential to decrease the reagent feed rate. This will lower capital and operating costs for the limestone grinding equipment, slurry handling and landfill requirements;
- The low pH and reduced gypsum relative saturation levels lessen the chance of scaling; and
- By reducing the maintenance requirements and increasing the flexibility of the system, the system reliability also increases.

The disadvantages of the system include:

- More process capital is needed for DBA feed equipment;
- Potential for corrosion and erosion due to the low system pH;
- Odorous by-products produced by DBA degradation. Although the SO_2 absorption reactions do not consume the DBA, the acid does degrade by carboxylic oxidation into many short chains. One of these chains is valeric acid which has a musty odor; and
- Control problems may be caused by foaming in the recirculation and oxidation tanks due to the presence of the DBA.

Limestone with Inhibited Oxidation (LS/Inhibit)

Process Outline

A limestone slurry is used in an open spray tower to remove SO_2. Emulsified sulfur is added to the limestone slurry, which forms thiosulfate thus inhibiting the oxidation of sulfite. Thiosulfate can reduce scaling and enhance dewatering properties of the sulfite sludge although its effectiveness is somewhat site specific.

System Description

In the inhibited oxidation process, the hot flue gas exists the ESP and enters an open spray tower where it come into contact with a dilute calcium carbonate ($CaCO_3$) slurry. This slurry contains thiosulfate which inhibits natural oxidation of the calcium sulfite. The calcium sulfite is formed from the reaction with SO_2 in the flue gas and the $CaCO_3$ slurry. The slurry absorbs the SO_2, then drains down to a recirculation tank below the tower. By inhibiting natural oxidation of the sulfite, gypsum scaling on process equipment is reduced along with gypsum relative saturation. The gypsum relative saturation is reduced below 1.0. Thiosulfate is either added directly as $Na_2S_2O_3$ to the feed tank or is generated in situ by the addition of emulsified sulfur. In some cases, thiosulfate has the ability to increase the dissolution of calcium carbonate and enlarge the size of the sulfite crystals to improve solids dewatering[113].

The process is capable of removing more than 90% of the SO_2 in the flue gas. The calcium sulfite slurry product is thickened, stabilized with fly ash and lime, and then transported to a landfill. The $CaCO_3$ feed rate is 1.10 mole of Ca / mole of SO_2 removed.

Evaluation

The effectiveness of thiosulfate is site specific since the amount of thiosulfate needed to inhibit oxidation strongly depends on the chemistry and operating conditions of each FGD system. Variables such as saturation temperature, dissolved magnesium, chlorides, flue gas inlet SO_2 and O_2 levels, and the slurry pH all affect the thiosulfate effectiveness.

Very high oxygen concentrations have a direct impact on the natural oxidation rates in scrubbers. Higher O_2 concentrations in the flue gas can occur during low load operation. In this case, thiosulfate levels over 1,000 ppm may be required and inhibition of oxidation below 15% may not be possible[113].

Decreasing the pH increases limestone dissolution, however it also increases the solubility of the metal ion catalyst. This in turn increases the initiation reaction thus increasing sulfite oxidation. Higher saturation temperature also increases the oxidation rate. By increasing the oxidation rate, the effectiveness of the thiosulfate is decreased.

High concentrations of magnesium increase the sulfite concentration in the slurry which increases the oxidation rate. Therefore, the concentration of the sulfite in the solution directly affects the effectiveness of the thiosulfate. Strong salts in the system do not appear to affect the ability of the thiosulfate to inhibit oxidation.

In some instances, when thiosulfate was added to the system an increase in limestone utilization was recorded. This occurred due to the thiosulfate reducing the gypsum relative saturation level which in turn reduced the level of calcium dissolved in the liquor. The dissolution rate is increased by lowering the calcium concentration in the slurry.

Thiosulfate also improves the dewatering characteristics of the sulfite product. By preventing the high concentrations of sulfate, the thiosulfate allows the calcium sulfite to form larger, single crystals. This increases the crystals' settling velocity and improves the filtering characteristics which causes a more solid content of dewatered product.

There are a few disadvantages of the process. The thiosulfate/sulfur reagent requires additional process equipment and storage facilities. Also, the reagent has be known to cause corrosion of many stainless steels under scrubber conditions. Another disadvantage is that thiosulfate is fairly temperature dependent. This limits its application to sites which operate within a particular temperature range.

Magnesium Enhanced Lime (MagLime)

Process Outline

A magnesium and calcium sulfite solution is used in an open spray tower to remove SO_2 and form a calcium sulfite rich sludge. The magnesium sulfite is regenerated in the reaction tank liquor forming the calcium sulfite. The makeup for magnesium lost with the solid product is supplied with the reagent lime (5-8% MgO). This process is effective at achieving high SO_2 removal efficiency while reducing scale formation[113].

System Description

In the magnesium enhanced lime, the hot flue gas exits the ESP then enters a spray tower where it comes into contact with a magnesium sulfite/lime slurry. Magnesium lime is fed to the open spray tower in an aqueous slurry at a molar feed rate of 1.1 moles CaO/mole SO_2 removed. The SO_2 is absorbed by the reaction with magnesium sulfite, forming magnesium bisulfite. This occurs through the following reactions :

$$SO_2 + H_2O \rightarrow H_2SO_3 \rightarrow H^+ + HSO_3^- \quad (7\text{-}15)$$

$$H^+ + MgSO_3 \rightarrow HSO_3^- + Mg^{2+} \quad (7\text{-}16)$$

The magnesium sulfite absorbs the H^+ and increases the HSO_3^- concentration in Equation (7-16). This allows the scrubber liquor to absorb more of the SO_2. This absorbed SO_2 reacts with hydrated lime to form solid-phase calcium sulfite. The magnesium sulfite is reformed by the following reactions :

$$Ca(OH)_2 + 2HSO_3^- + Mg^{2+} \rightarrow Ca^{2+} + SO_3^{2-} + 2H_2O + MgSO_3 \quad (7\text{-}17)$$

$$Ca^{2+}\ SO_3^{2-} + 1/2H_2O \rightarrow CaSO_3 \cdot 1/2H_2O\ (solid) \quad (7\text{-}18)$$

Inside the absorber, some magnesium sulfite present in the solution is oxidized to sulfate. This sulfate then reacts with the lime to form calcium sulfate solids. Calcium sulfite and sulfate solids are the main products of the Maglime process. The calcium sulfite sludge is first dewatered using a thickener and vacuum filter systems, and then is fixated using fly ash and lime prior to transportation to a lined landfill for disposal.

The magnesium remains dissolved in the liquid phase. Magnesium is only lost when it is removed with the scrubber liquid entrained in the product solids or blowdown streams.

Evaluation

It should be noted that there are several different types of lime that contain magnesium oxide. Thiosorbic lime is a popular one on the market. It naturally contains 4 to 8% MgO [113]. Some advantages of this process compared to the LSFO process are :

- At low liquid-to-gas ratios there is a high SO_2 removal efficiency;
- The lower gas-side pressure drop due to lower liquid-to-gas ratios;
- Reduced potential for scaling, which improves the reliability of the system;
- A lower slurry recycle rate allows for lower power consumption;
- A lower capital investment due to smaller reagent handling equipment and no oxidation air compressor; and

- A reduction in fresh water use since the process water may be recycled for the mist eliminator wash.

The two major disadvantages are the expense of the lime reagent compared to limestone and the difficult dewatering characteristics of the calcium sulfite/sulfate sludge. The sulfite can be oxidized to produce gypsum, but will require extensive equipment and process control for this to occur. A small disadvantage is that the lime slaking requires fresh water.

Pure Air

Process Outline

A limestone slurry is sprayed into a co-current, downflow, grid packed absorber to remove SO_2. An Air Rotary Sparger system is employed to provide agitation as well as forced oxidation to yield a gypsum sludge. The co-current absorber decreases space requirements and pressure drop, and the grid packing enhances SO_2 removal efficiency.

System Description

In the Pure Air process, SO_2 absorption and oxidation of $CaSO_3$ to $CaSO_4$ occur in a single vessel (single loop, in situ oxidation). Booster fans move the flue gas through a co-current grid packed tower. Slurry that is recycled constantly is used to quench the hot gas and to provide available alkali for the collection of SO_2 in the grid stage. Also, natural oxidation is enhanced by the contact between slurry and the flue gas in the grid stage. The integral tower sump is utilized as the in-situ oxidation tank, the recycle reservoir, and the reaction vessel for limestone dissolution. The following reactions take place in this tower :

$$SO_2 + H_2O \rightarrow H_2SO_3 \qquad (7\text{-}19)$$

$$H_2SO_3 \rightarrow H^+ + HSO_3 \qquad (7\text{-}20)$$

$$H^+ + HSO_3 + 1/2\ O_2 \rightarrow 2H^+ + SO_4^{2-} \text{ (natural oxidation)} \qquad (7\text{-}21)$$

$$2H^+ + SO_4^{2-} + CaCO_3 + H_2O \rightarrow CaSO_4 \cdot 2H_2O + CO_2 \qquad (7\text{-}22)$$

An Air Rotary Sparger (ARS) system is used to blow air into the integral sump to completely oxidize the sulfite to sulfate. Gypsum slurry is drawn from the integral sump to maintain a 20-25 weight per cent slurry content. This stream is collected in a surge tank for further processing.

The gas/slurry mixture is separated by gravity after leaving the grid stage. The slurry falls to the sump while flue gas passes through a multi-stage mist eliminator that is washed intermittently. The clean gas flows to the stack while collected entrainment is returned to the sump. Dry powdered limestone is pneumatically conveyed and injected directly into the integral sump. Make-up water is reclaimed from the gypsum dewatering section.

Pure Air is also unique in its marketing approach. The company will build, own, and operate its FGD facility on a utility site under a long term contract.

Evaluation

The Pure Air process offers many advantages over the LSFO process. Some of these advantages are as follows[113]:

- The absorber is a more compact size and has less of a pressure drop. The reason is that the design allows for a high gas velocity;
- By combining advanced technology with a new business approach, capital and operating costs can be reduced by about 50% compared to conventional FGD systems;
- SO_2 removal efficiency is increased due to the increase of liquid/gas contact in the grid packing;
- Complex air oxidizing system piping is eliminated due to the combined tank agitation and oxidation;
- 100% of the calcium sulfite is oxidized to calcium sulfate;
- It is estimated that only one 100% module for SO_2 removal/oxidation is needed for plants up to 1000 MW; and
- Wallboard or landfill grade gypsum can be produced using this system.

A disadvantage of the Pure Air system compared to the LSFO system is that there is the potential for plugging due to scaling. This occurs when the system is operated using a open grid packing with natural oxidation. This can be prevented if the system is operated in a forced oxidation or inhibited oxidation mode.

Chiyoda Thoroughbred 121 (CT-121)

Process Outline

The process is a second generation limestone slurry process in which SO_2 absorption, sulfite/bisulfite oxidation, and precipitation of calcium sulfate all take place in a single reaction vessel called the jet bubbling reactor (JBR). The CT-121 process offers better limestone utilization, easier solids dewatering, and simpler operation relative to the limestone forced oxidation process.

System Description

In the JBR, the flue gas is injected beneath the slurry typically at a depth of 10 to 16 inches. The gas creates a froth zone as it rises in discrete bubbles. The froth zone provides the gas-liquid interfacial area where the SO_2 in the flue gas dissolves in the liquid film on the surface of the bubbles. The gas bubbles are continually collapsing and reforming to generate new and fresh interfacial areas and to transport reaction products away from the froth zone[113].

The JBR process also operates at a lower pH (3.5 to 4.5) than other limestone systems. The advantage of this is that complete dissolution of limestone occurs at a pH of 3.5 to 4.5, which prevents a large amount of limestone to leave the system with the waste solids and minimizes the chance of gypsum scaling. In industrial tests, limestone utilization decreased rapidly at a pH greater than 5.2. A lower pH also allows a higher concentration of transition metal catalysts which in turn increases the tendency for oxidation of absorbed SO_2 to occur[114].

Air is added to the slurry at the bottom of the JBR in order to completely oxidize the sulfite to sulfate immediately (see Figure 7-31). By doing this, the vapor pressure of SO_2 is eliminated since the salt of a strong acid (sulfate) has negligible vapor pressure. Since the sulfite ion is continually being removed through precipitation as gypsum, SO_2 adsorption proceeds at a rapid pace in spite of the fact that there is essentially no liquid phase buffering capacity.

Evaluation

The Chiyoda Thoroughbred 121 process offers many advantages compared to the LSFO process. Some of these advantages include:

- The gypsum crystals produced from the process are larger than conventional methods. This allows for an easier dewatering operation. The crystals are larger because all the reactions occur in a single tank designed more like a crystallizer than a typical reaction tank;
- A reduction in dewatering equipment compared to the LSFO system. This is due to the easier dewatering characteristics of the gypsum by-product;
- The elimination of recycle pumping which results in less crystal attrition and lower power consumption;
- Complete use of limestone feed reagent due to the low operating pH;
- The simplicity of the system allows for an easier operation. This results in a higher reliability of the system operation;
- A high removal efficiency during wide swings in boiler load. This is due to the absorption reaction occurring over a wider range of pH and slurry solids concentration;
- A lower overall operation and maintenance costs in the SO_2 absorption and solids handling areas. The reason for this is the elimination of the large slurry pumps, spray nozzles and associate piping, and less dewatering equipment;
- The elimination of plugging and scaling in the absorber and in piping. Complete limestone dissolution and utilization removes the possibility of scaling. Also, all the absorbed SO_2 is completely oxidized to sulfate and crystal formation occurs on the crystals suspended and recirculated in the JBR slurry, instead of on equipment surfaces; and
- The achievement of high desulfurization (95% and higher) without using excess limestone and without the use of buffering agents such as adipic or dibasic acid [113].

There are only two main disadvantages of the system. One is that the system has a higher gas side pressure drop than spray towers. This increases the costs since ID/booster fans are needed to provide sufficient flue gas pressure to overcome the flow resistance of the JBR. The other disadvantage is that some systems may require a prescrubber if wallboard gypsum production is to be achieved. However, the 100 MW demonstration of the system at Yates, GA has produced quality gypsum without a prescrubber.

Wellman-Lord Process

The Wellman-Lord Process uses sodium sulfite to absorb SO_2 which is then regenerated to release a concentrated stream of SO_2. Most of the sodium sulfite is converted to sodium bisulfite by reaction with SO_2 as in the dual alkali process. Some of the sodium sulfite is oxidized to sodium sulfate. Prescrubbing of the flue gases is necessary to saturate and cool the flue gas to about 55°C[115]. This removes chlorides and remaining fly ash, and avoids excessive evaporation

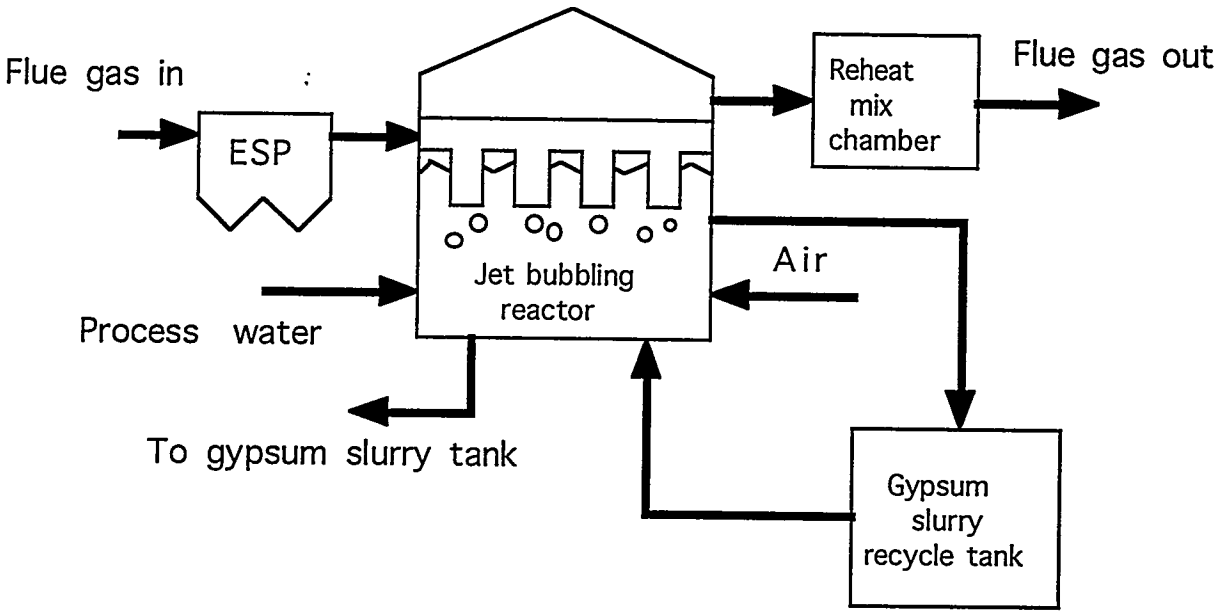

Figure 7-31. CHIYODA THOROUGHBRED 121 PROCESS [3]

in the absorber. The advantages of this process is that a slurry is used rather than a solution, thus prevents scaling and allows the production of a marketable material. The disadvantage of the process is the high energy consumption and maintenance due to the complexity of the process. Another disadvantage of the process is that a purge stream of about 15% of the scrubbing solution is required to prevent the buildup of sodium sulfate[115]. Regeneration of the remaining scrubbing solution takes place in a two stage evaporator. Thiosulphate must be purged from the regenerated sodium sulfite. The concentrated SO_2 stream may be compressed, liquefied and catalytically oxidized to produce sulfuric acid or reduced to elemental sulfur.

Saarberg-Hoelter Process

The Saarberg-Hoelter Process is based on the reaction between SO_2 and calcium compounds. The main difference between this process and conventional lime/limestone processes is that the SO_2 is removed by a solution containing no suspended solids. The solution is made up of slaked lime ($Ca(OH)_2$) with small amounts of formic acid (HCOOH) and hydrochloric acid (HCl). The chloride ions form calcium chloride ($CaCl_2$). The high rate of dissolution increases the concentration of available calcium ions in the scrubber solution. This reduces the chance of scaling and deposition within the absorber. It also allows a relatively low liquid to gas ratio to be used and recycle of the solution is unnecessary.

Calcium bisulfite ($Ca(HSO_3)_2$) is produced by reducing the pH value within the scrubber. Calcium bisulfite is the only calcium-sulfur compound with significant solubility in water. At pH values between 8 and 11 the following reaction scheme takes place [116]:

$$Ca^{2+} + 2OH^- + 2SO_2 + 2Cl^- \text{---> } Ca^{2+} + SO_3^{2-} + HSO_3^- + H^+ + 2Cl^- \quad (7\text{-}23)$$

As the above reaction occurs the concentration of the OH^- ions decreases as the H^+ ions increase. This causes the pH of the solution to fall to a value between 5 and 4.5[115]. The formic acid acts like a buffering agent by absorbing the H^+ ions to form HCOOH as in the following equation.

$$COOH^- + H^+ \text{---> } HCOOH \quad (7\text{-}24)$$

Acceptable SO_2 removal rates as well as formation of calcium bisulfite are promoted by the value of the above pH. The buffering effect is removed when the formate ions are used up, therefore causing the pH to fall again to a value of about 4, which is the optimum pH for the oxidation of calcium bisulfite to gypsum[115].

$$Ca(HSO_3)_2 + O_2 + 2H_2O \text{---> } CaSO_2 \cdot 2H_2O + H_2SO_4 \quad (7\text{-}25)$$

A separate oxidation vessel is used for oxidation. The calcium ions used up in the formation of gypsum are replenished by adding lime to the scrubber solution. This also has the effect of adjusting the pH to a value acceptable for SO_2 absorption. Additional gypsum is produced by neutralizing the sulfuric acid formed in the oxidizer by the above reaction.

$$H_2SO_4 + Ca(OH)_2 \text{---> } CaSO_4 \cdot 2H_2O \quad (7\text{-}26)$$

The concentration of formic acid is adjusted prior to the separation of the gypsum in a thickener. The scrubbing solution is returned to the absorber.

Other advantages of the system include no prescrubbing of flue gas is necessary and the presence of HCl in the flue gas reduces the requirement for the addition of hydrochloric acid. Chloride corrosion is prevented by using the chlorides in solution instead of suspensions. SO_2 removal efficiencies of 90 to 95 % have been reported with this process[115, 117].

Citrate Process

In this FGD process, an aqueous solution of sodium citrate is used to absorb sulfur dioxide from the flue gas. A prescrubber is used to remove fly ash and chlorides from the flue gas before scrubbing with the citrate solution. The adsorbent is stripped with steam to recover concentrated SO_2 then a purge stream of the absorbent is passed to a crystallizer[118]. In this crystallizer the sodium sulfate is removed as $Na_2SO_4 \cdot 10H_2O$.

Sodium citrate acts as a buffering agent to improve the solubility of SO_2 in water. Sulfur dioxide dissociates into HSO_3^- and H^+ ions as it is dissolved in water.

$$SO_2 + 2H_2O \rightarrow HSO_3^{2-} + H_3O^+ \qquad (7\text{-}27)$$

The above reaction moves to the right since the sodium citrate removes the H^+ ions by reacting with them. SO_2 is distilled out of solution by passing the absorbent solution through a heat exchanger then to a heated stripping tower. The mixture of water vapor and SO_2 is condensed which forms two immiscible liquid phases. The water phase is returned to the stripping tower. The SO_2 phase may either be contacted with H_2S in a separate reactor to form sulfur by a liquid phase Claus reaction or by using a Resox™ unit[119]. An SO_2 removal efficiency of 90% has been reported[120].

Dry Scrubbing Flue Gas Desulfurization Processes

Dry scrubbing refers to processes in which the product of the reaction between sulfur dioxide and the reagent is a solid. This can be achieved by injecting a dry sorbent into the flue gas where it absorbs the sulfur dioxide. The spent sorbent and fly ash are collected in an integrated particular removal step using a baghouse or ESP. Another method of adsorbing SO_2 from the gas is by spraying (fine droplets) of an aqueous solution or suspension of reagent. The droplets are dried by the heat of the flue gas and collected with the fly ash using an ESP or baghouse as above. One final method for dry scrubbing is use of a reagent bed where the SO_2 can be adsorbed. The sorbent in this method is normally regenerated. The following systems give a more detailed description of some dry FGD processes.

Tampella LIFAC

Process Outline

Limestone is injected into the upper part of the boiler where the initial stage of SO_2 removal occurs. An activation reactor is needed between the air heater and particulate collector. Water is

sprayed into the flue gas at the reactor inlet to humidify the gas for additional SO_2 removal. This yields a dry solid which is captured downstream in the existing ESP. Tampella can achieve 80% SO_2 removal efficiency and is suitable for retrofit installations due to its elimination of large diameter spray tower absorbers[121].

System Description

The LIFAC (Limestone Injection into the Furnace and Activation of unreacted Calcium) process reduces SO_2 emissions by 75 to 85 % utilizing commercially available pulverized limestone as a sorbent[121]. The limestone is injected into the upper furnace of the boiler. Here, the hot flue gas decomposes the calcium carbonate to form calcium oxide and carbon dioxide. The calcium oxide formed reacts with some of the SO_2 in the flue gas to produce calcium sulfite. Some of these sulfite ions react with the calcium oxide to form calcium sulfate.

Humidification is carried out in an activation chamber formed by a vertical elongation of the ductwork between the air preheater and the ESP. The humidification is carried out by injecting water to convert any unreacted calcium oxide to calcium hydroxide and to hydrate the calcium salt reaction products. More SO_2 reacts with calcium hydroxide to form $CaSO_3$ and $CaSO_4$. The calcium hydroxide also reacts with CO_2 in the flue gas to form calcium carbonate.

The absorption reactions produce a dry solid which, along with fly ash, is collected downstream in the ESP. Some of the scrubbed flue gas is extracted, heated and recycled back to the outlet of the activation chamber. This gas is used to reheat the humidified flue gas stream before it enters the ESP. The by-products of the process are placed in an unlined landfill for disposal.

Evaluation

The Tampella LIFAC system is a dry, throwaway system evaluated as a retrofit process. The Tampella LIFAC offers some advantages over wet FGD systems. The process does not require any dewatering and sludge handling equipment. This reduces the maintenance requirements and costs of the system, especially compared to wet systems. The elimination of the wet FGD equipment used for slurry allows the LIFAC process to have a smaller space requirement. This is useful for retrofit installations.

There are also advantages by injecting the limestone in a dry form. The reagent handling system is less complex than wet systems. This will also reduce the manpower requirements for operation. Less power is needed since there are fewer pumping requirements, that is, no slurry handling and recycle is needed. The dry limestone form allows a lower flue gas pressure drop in the system.

The disadvantages of the LIFAC system are common to dry processes. Since there is an increase in particulate loading and changes in ash resistivity, the ESP performance is inhibited. This increase can also affect the performance of the boiler. The larger quantity of dry solids

produced is due to a higher feed rate. The process requires more than twice the reagent feed needed for conventional wet systems and is also higher than other dry systems.

LIFAC operates at a closer approach to adiabatic saturation temperature to facilitate flue gas humidification. This may cause some duct deposition problems and corrosion. Corrosion is a main concern at the humidification area and the down stream ductwork. The humidification area is problematic due to operation below the acid dewpoint and the downstream ductwork is susceptible due to the high moisture content. There is also possible plugging of the activation reactors which can cause negative pressure transients because of the ID fans location downstream.

The system uses gas reheat which tends to increase the steam consumption to a higher level compared to other dry process. The system also uses a large amount of stainless steel which is considered to be an expensive construction material. A final disadvantage of this process is that the system has not been shown to achieve over 90% SO_2 removal[113].

Lime spray dryer (LSD)

Process Outline

In this semidry process, the flue gas is contacted with lime slurry in a spray dryer absorber. The slurry reacts with SO_2 to form a solid which is collected in a baghouse (or ESP) along with fly ash. Relative to the limestone forced oxidation process, the major advantages of the LSD process are dry solids handling, and possibly lower operating and maintenance costs for certain applications. Some disadvantages are the possibility of "blinding" the fabric filter bags, greater potential for solids buildup on internal duct surfaces, and a more costly reagent.

System Description

In this process, the hot flue gas exits the boiler air heater and then enters a spray dryer vessel. The flue gas comes into contact with an atomized slurry of lime and recycled solids. The slurry is formed by the reaction :

$$CaO + H_2O \rightarrow Ca(OH)_2 \qquad (7\text{-}28)$$

The SO_2 in the gas is absorbed into the slurry and react with the lime and fly ash alkali to form calcium salts. This is shown in the following equations:

$$Ca(OH)_2 + SO_2 \rightarrow CaSO_3 \cdot 1/2H_2O + 1/2H_2O \qquad (7\text{-}29)$$

$$Ca(OH)_2 + SO_3 + H_2O \rightarrow CaSO_4 \cdot 2H_2O \qquad (7\text{-}30)$$

HCl present in the flue gas is also absorbed into the slurry and reacts with the slaked lime. The water that enters with the slurry is vaporized, thus lowering the temperature and raising the moisture content of the scrubbed gas. Before the scrubbed gas is released from the atmosphere, it passes through a particulate control device downstream of the spray dryer. Some of collected reaction product and fly ash is recycled to the slurry feed system. The rest is sent to a landfill for disposal.

Evaluation

- The LSD process offers a few advantages over the LSFO process. Only a small alkaline stream of scrubbing slurry is needed to be pumped into the spray dryer. This stream contacts the gas entering the dryer instead of the walls of the system. This prevents corrosion of the walls and pipes in the absorber system. Since the pH of the slurry and dry solids is high then mild steel materials can be used for construction instead of expensive alloys;
- The spray dryer's product is a dry solid that is handled by conventional dry fly ash handling systems. This eliminates the need for dewatering solids handling equipment. This also reduces associated maintenance and operating requirements;
- The system requires less pumping power, thus reducing the overall power requirement;
- Capital costs and steam consumption is reduced since a flue gas reheat system is not needed. The gas is not saturated when it exits the absorber therefore reheat is not necessary;
- Chloride concentrations increase the SO_2 removal efficiencies. This is an advantage since in wet systems, chlorides reduce the efficiency. This also allows the use of cooling tower blowdown for slurry dilution after completing the slaking of the lime reagent; and
- Manpower requirements such as operating, laboratory and maintenance, are less for the LSD process compared to the LSFO process. The is due to the less complex absorption system.

A major product of the lime spray dryer process is calcium sulfite (25% or less oxidizes to calcium sulfate). The solids handling equipment for the particulate control device has to have a greater capacity than conventional fly ash removal applications[113]. Also, higher quality insulation is needed to prevent condensation and corrosion since the temperature of the scrubbed gas is lower and the moisture content is less.

For the LSD process, fresh water is needed in the lime slaking system. This fresh water represents almost half of the system's water requirement. This differs from the wet scrubbers where cooling tower water can be used for limestone grinding circuits and most other makeup water applications.

To achieve a high removal efficiency, the LSD process requires a higher reagent feed ratio than conventional wet systems. Approximately 1.5 moles of CaO/mole of SO_2 removed is needed for 90% removal efficiency[113]. Lime is also more expensive than limestone, therefore the operating cost is increased. This costs can be reduced if higher coal chloride levels and/or calcium chloride spiking is implemented. Chlorides have the effect of improving removal efficiency and reducing reagent consumption.

A higher inlet flue gas temperature is needed when a higher sulfur coal content is used. If the air heater outlet temperature is raised to facilitate an improvement in the spray dryer system, then a reduction of the overall boiler efficiency occurs.

These advantages and disadvantages can be weighed for specific site applications.

Lurgi Circulating Fluid Bed (CFB)

Process Outline

Hydrated lime is injected into a circulating fluid bed (CFB) reactor to remove SO_2. Water is also injected into the reactor to humidify the gas and increase SO_2 removal efficiency. Solids are captured downstream in a mechanical dust curtain and the existing ESP, and a portion is recycled to the reactor. The long retention time of the solids can yield greater than 90% SO_2 removal efficiency[113].

System Description

The Lurgi Circulating Fluid Bed (CFB) FGD process is a dry, throwaway system. A fluid bed is created by flue gas flowing upward through a suspended bed of fine grain solids in a reactor. The fluid bed level is increased as the velocity of the flue gas is increased. At the top of the reactor, some solids are discharged to be collected by the downstream particulate collector. The circulating fluidized bed is created by recirculating these solids back to the reactor.

Hot flue gas enters a venturi-shaped entrance of a reactor where it is mixed with powdered hydrated lime, recycled solids and water. The water is injected to humidify the flue gas and aid in SO_2 removal. The hydrated lime reagent reacts with the SO_2 in the flue gas to form $CaSO_3$ and $CaSO_4$ salts. The main reaction in the process is :

$$2\ Ca(OH)_2 + 2\ SO_2 \text{ ---> } 2\ CaSO_3 \cdot 1/2H_2O + H_2O \qquad (7\text{-}31)$$

As the sorbent moves through the system, a portion of the unreacted lime reacts with the CO_2 in the flue gas to form calcium carbonate. The spent solids and fly ash are removed from the top of the absorber and captured by a mechanical curtain installed upstream of an ESP's first field.

Evaluation

The circulating fluid bed has several process parameters which promote high desulfurization efficiencies. One is the long time the flue gas has contact with the reagent solids. This occurs since the lime is passed through the circulating bed many times. The process also exhibits good SO_2 mass transfer from the flue gas to the solid reagent due to the use of fine grain, porous reagent. The solids mixing in the bed abrades the particle surfaces which exposes more fresh alkali surfaces to the flue gas. Another reason for the good mass transfer is the constant mixing that occurs due to a high slip velocity and high turbulent flow between the gas and solids.

Some other advantages of the system are:

- A lower maintenance costs is achieved since the chance of scaling and corrosion is less compared to wet systems;
- Operating and maintenance requirements are less. This is due to the elimination of dewatering equipment that is necessary for wet systems. The dry solids formed can be handled by conventional fly ash systems. Also, since the lime is injected in dry form, the reagent handling is simpler;
- Less power is used since fewer pumps are needed due to the absence of slurry; and

- Lower capital costs since no reheat is used, therefore less steam consumption. The operating and maintenance is also less since no recycle pumps and dewatering equipment is used.

Some disadvantages compared to the LSFO process are:

- A higher feed ratio is used in the CFB process. This is significant since lime is more expensive than limestone;
- The humidification of the solids and flue gas may cause some duct deposition and plugging problems. Plugging problems can cause negative pressure transients since the I.D. fans are located downstream of the absorber;
- The ESP performance may be inhibited because of the increased particulate loading and changes in the ash resistivity. Additional removal equipment may be needed to maintain particulate emission levels at or below required limits; and
- The solids recycle rate is higher than most other dry processes. This may cause a strain on the recycle pumps.

The LURGI CFB process can be used in new plants and as a retrofit. However, if it is used as a retrofit, some space limitation may be encountered with the installation of the mechanical collector.

Duct Spray Drying (DSD)

Process Outline

A slaked lime slurry is sprayed directly into the ductwork to remove SO_2. The reaction products and fly ash are captured downstream in the ESP. A portion of these solids is recycled and reinjected upstream of the fresh sorbent. Duct Spray Drying (DSD) is a relatively simple retrofit process capable of 50% SO_2 removal[113].

System Description

The DSD system is a dry FGD process. The process involves spraying of a slaked lime slurry directly into the ductwork upstream of the existing ESP. The slurry can be sprayed by using a rotary atomizer or a dual fluid atomizer. The slaked lime is produced by hydrating raw lime to form calcium hydroxide ($Ca(OH)_2$). This slaked lime is atomized and absorbs the SO_2 in the flue gas. The SO_2 reacts with the slurry droplets as they dry to form equimolar amounts of calcium sulfite and calcium sulfate. The water in the lime slurry improves SO_2 absorption by humidifying the gas. The reaction products, unreacted sorbent, and fly ash are collected in the ESP located downstream. Some of the unreacted sorbent may react with some of the CO_2 in the flue gas to form $CaCO_3$. Also, a little more SO_2 removal is achieved in the ESP.

As stated above, there are two different methods for atomizing the slurry. One is the rotary atomizer, where the ductwork provides the short gas residence time (1-2 sec). When using this device, the ductwork must be long enough for one or two residence times to allow for drying of the slurry droplets. There must also be no flow obstructions in the duct[113].

The other method is using the dual fluid atomizers, where compressed air and water are used to atomize the slurry. This is called the Confined Zone Dispersion (CZD) process. The dual

fluid atomizer has shown to be more controllable due to the adjustable water flow rate. They also are relatively inexpensive and have a long and reliable operational life with little maintenance. The spray is confined in the duct which allows better mixing with the flue gas rather impinging on the walls.

Evaluation

The DSD process is still under development to improve its capabilities. As of present, the advantages displayed by the process compared to the LSFO process are:

- The simplicity of the process. The dry reagent is injected directly into the flow path of the flue gas. A separate SO_2 absorption vessel is not required since the SO_2 is removed in the duct itself;
- The injection of lime in a dry form allows a less complex reagent handling. Slurry pumps are not needed as in wet systems. This elimination in slurry recycle and handling systems lowers operational labor and maintenance, and removes the problems of pluggage, scaling, and corrosion found in slurry handling;
- Lower power requirements since less equipment is needed;
- No usage of steam for reheat. Most LSFO systems require some form of reheat to prevent corrosion of downstream equipment; and
- The elimination of a sludge dewatering system. The FSI process produces a dry solid which can be removed by conventional fly ash removal systems.

Some of the problems encountered by the DSD system is also common to other dry processes. The disadvantages of the DSD system compared to the LSFO system are:

- The limitation of the SO_2 removal efficiency. At present, the highest achieved is 50% [122].
- The higher cost of quicklime compared to limestone. Also, the utilization of the reagent is less in the dry system;
- The possible reduced efficiency of the ESP due to the changes in ash resistivity and the increased grain loading in the flue gas. Some additional collection device may be required. Humidification does help the ESP collection efficiency;
- The difficulty of making the droplet vaporized between the water injection system and the ESP. The injection point of the ductwork must be long enough to ensure a residence time of 1 to 2 seconds in a straight, unrestricted duct path; and
- The pluggage of the ducts which can cause negative pressure transients due to the I.D. fans location downstream. This pluggage and dust deposition occurs if the residence time in the duct is insufficient for droplet vaporization.

Duct Sorbent Injection (DSI)

Process Outline

Hydrated lime is injected into the ductwork to remove SO_2. Water is injected upstream of the lime injection point to cool and humidify the flue gas. The solids are collected in the ESP and a portion is recycled and re-injected with fresh sorbent to increase reagent utilization. This process has low space requirements and can achieve 50% SO_2 removal efficiency[113]. A major concern of the DSI process is the long term effects of wall wetting and the potential for solids deposition.

System Description

In this dry FGD process, hydrated lime (calcium hydroxide) is injected either upstream or downstream of a flue gas humidification zone. In this humidification zone, the flue gas is humidified to within 20°F of the adiabatic saturation temperature by injecting water into the duct downstream of the air preheaters. The SO_2 in the flue gas reacts with the calcium hydroxide to form calcium sulfate and calcium sulfite as follows [122]:

$$Ca(OH)_2 + SO_2 + 1/2\ O_2 + H_2O \text{ ---> } CaSO_4 \cdot 2H_2O \qquad (7\text{-}32)$$

$$2\ Ca(OH)_2 + 2\ SO_2 \text{ ---> } 2\ CaSO_3 \cdot 1/2\ H_2O + H_2O \qquad (7\text{-}33)$$

To avoid solids deposition on the ductwork and in the ESP, the water droplets are vaporized before they strike the surface of the wall or enter the ESP.

The unused sorbent along with the products and fly ash are all collected in the ESP. About 50% of the collected result is shipped to a landfill. The other 50% is recycled to be injected back with fresh sorbent into the ducts[113].

Evaluation

The duct sorbent injection system offers many of the same advantages and disadvantages that other dry systems offer. Some of these advantages are :

- The simplicity of the process compared to a LSFO system. The humidification water and hydrated lime are injected directly into the existing flue gas path. No separate SO_2 absorption vessel is necessary. The handling of the reagent is also simpler than the wet systems since there is no need for slurry pumps;
- The cost reductions found in most dry systems. Operational labor and maintenance costs are less since there is less equipment. There is no need for equipment such as slurry recycle and handling. Slurry handling also tends to cause pluggage, scaling and corrosion of wet systems. This problem is eliminated in dry systems;
- The lower power requirements due to less equipment. The process does not require reheat, therefore the steam usage is also reduced; and
- The elimination of a sludge dewatering system since, as in most dry systems, the products are dry and can be handled by conventional fly ash handling systems.

Some of the problems encountered by the DSI system is also common to other dry processes. The disadvantages of the DSI system compared to the LSFO system are:

- The limitation of the SO_2 removal efficiency. At present, the highest achieved is 80% [113].
- The higher cost of quicklime compared to limestone. Also, the utilization of the reagent is less in the dry system;
- The possible reduced efficiency of the ESP due to the changes in ash resistivity and the increased grain loading in the flue gas. Additional collection devices may be required. Humidification does help the ESP collection efficiency;
- The difficulty of making the droplet vaporize between the water injection system and the ESP. The injection point of the ductwork must be long enough to ensure a residence time of 1 to 2 seconds in a straight, unrestricted duct path; and
- The plugging of the duct which can cause negative pressure transients due to the I.D. fan located downstream. This plugging and dust deposition occurs if the residence time in the duct is insufficient for droplet vaporization.

Economizer Injection (EI)

Process Outline

The hydrated lime is injected into economizer inlet of the boiler. An optimum temperature range (900 - 1,000°F) for SO_2 removal occurs near this location. Economizer Injection (EI) also achieves 50% SO_2 removal efficiency. The advantages of this process are its simplicity and low capital cost[113].

System Description

The Economizer Injection system is a dry FGD process. In this process, quicklime is hydrated and then injected directly into the inlet of the economizer section of the boiler to react with SO_2 in the flue gas. The temperature of the gas entering the economizer can be about 1,000°F. Some of the hydrated quicklime ($Ca(OH)_2$) reacts with SO_2 to form calcium sulfite ($CaSO_3$). About 10% of the calcium hydroxide dehydrates to form a porous lime particle with a high surface area which makes the lime more reactive[113].

$$Ca(OH)_2 \text{ ---> } CaO + H_2O \qquad (7\text{-}34)$$

This reactive lime formed then reacts with more SO_2 to form calcium sulfite and calcium sulfate.

The rest of the calcium hydroxide that is not dehydrated reacts with even more SO_2 to form calcium sulfite:

$$Ca(OH)_2 + SO_2 \text{ ---> } CaSO_3 + H_2O \qquad (7\text{-}35)$$

This reaction occurs best at a temperature between 950-1,050°F [122]. The rest of process provides humidification for any unreacted lime and products in a humidification section. The final product is mixed with fly ash and removed in the ESP located downstream.

Evaluation

The EI system is best suited for older units in need of a retrofit process. The main factors that affect the operating process are sorbent injection temperature, initial SO_2 concentration, Ca/S stoichiometric feed rate, the sorbent/gas mixing rate, and the sorbent particle size[113]. Sorbent utilization in the system can be improved by the use of additives in the hydration step.

The system offers some advantages over the LSFO process:

- The simplicity of the process. The dry reagent is injected directly into the economizer and duct work. No separate SO_2 absorption vessel is necessary. The handling of the reagent is also simpler than the wet systems since there is no need for slurry pumps;
- The cost reductions found in most dry systems. Operational labor and maintenance costs are less since there is less equipment. There is no need for equipment for slurry recycle and handling. Slurry handling also tends to cause plugging, scaling and corrosion of wet systems. This problem is eliminated in dry systems. The dry sorbent injection does not inject sufficient water to cause duct corrosion problems and scaling. This is prevented by monitoring the approach to saturation temperature so that it is above the adiabatic saturation temperature;
- The lower power requirements due to less equipment. The process does not require reheat, therefore the steam usage is also reduced; and

- The elimination of a sludge dewatering system since, as in most dry systems, the products are dry and can be handled by conventional fly ash handling systems.

The process does have its disadvantages compared to a LSFO system. Some of the major ones are:

- The limitation of the SO_2 removal efficiency. At present, the highest achieved is 80% [113].
- The higher cost of quicklime compared to limestone. Also, the utilization of the reagent is less in the dry system;
- The potential for corrosion at the point of humidification, the ESP, the downstream ductwork, and the stack. The corrosion at the humidification point is caused by operation below the acid dewpoint, but the rest of the corrosion is caused by the humidified gas temperature being close to the water saturation temperature. It is also possible for plugging to occur. If the duct and boiler gas path is plugged, negative pressure transients can occur due to the I.D. fan; and
- The possible reduced efficiency of the ESP due to the changes in ash resistivity and the increased grain loading in the flue gas. Additional collection device may be required. Humidification does help the ESP collection efficiency.

The Economizer Injection process is under further development. At present, the process can be used for either low sulfur or high sulfur coals.

Furnace Sorbent Injection (FSI)

Process Outline

Hydrated lime is injected into the furnace cavity of the boiler to react with SO_2. Water is injected into the ductwork downstream of the air heater for flue gas conditioning. The reaction products and fly ash are collected in the existing ESP. This retrofit process achieves a maximum of 50% SO_2 removal efficiency[113]. The advantages of the FSI are primarily the simplicity of the process and its low capital cost.

System Description

The Furnace Sorbent Injection (FSI) system is a dry FGD process. This process encompasses the Limestone Injection Multistage Burner (LIMB) system which is another popular dry sorbent injection process. In the FSI system, hydrated lime or limestone is injected directly into the furnace cavity. This differs from the LIMB process where the hydrated lime is injected through a coal burner or alternate coal burners in the burner array.

The reagent is exposed to gas temperature as high as 1,600°F in the furnace. At this temperature, the hydrated lime quickly decomposes to form highly reactive, porous lime particles with a high surface area. The reactions are:

$CaO + H_2O \rightarrow Ca(OH)_2$ (hydrated lime) (7-36)

$Ca(OH)_2 \rightarrow CaO + H_2O$ (7-37)

Some of this lime (CaO) reacts with the SO_2 in the flue gas to generate solid calcium sulfate. A portion of the unreacted lime reacts with CO_2 in the gas to form $CaCO_3$. The remainder of the unreacted CaO, along with the $CaSO_4$ is partially humidified (hydrated) in a flue gas

humidification section of the ductwork. This finally product is mixed with the fly ash in the flue gas, then removed in the downstream ESP.

Evaluation

The FSI can be applied to boilers burning low sulfur or high sulfur coals. The parameters that affect the efficiency of the FSI system are the flue gas humidification, type of sorbent, efficiency of ESP particulate removal device, and the temperature and location of the sorbent injection. The process is better applicable for large furnaces with lower heat released rates. Systems that use hydrated calcium salts sometimes have problems with scaling. However, in the FSI process this can be prevented by keeping the approach to adiabatic saturation temperature above a minimum threshold value.

The major advantages of the FSI system are:

- The simplicity of the process. The dry reagent is injected directly into the flow path of the flue gas. A separate SO_2 absorption vessel is not required since the SO_2 is removed in the furnace;
- The injection of lime in a dry form allows a less complex reagent handling. Slurry pumps are not needed as in wet systems. This elimination in slurry recycle and handling systems lowers operational labor and maintenance, and removes the problems of plugging, scaling, and corrosion found in slurry handling;
- Lower power requirements since less equipment is needed;
- No usage of steam for reheat. Most LSFO systems require some form of reheat to prevent corrosion of downstream equipment; and
- The elimination of a sludge dewatering system. The FSI process produces a dry solid which can be removed by conventional fly ash removal systems.

The FSI process also has a few disadvantages when compared to the LSFO process. One major disadvantage is that the process can only remove 55% to 72% of SO_2 at a calcium-to-sulfur ratios of 2.0[113]. Some other disadvantages compared to the LSFO process are:

- The lower utilization of the lime reagent. The lime is also more expensive than limestone. It was found that the lime works better than the limestone[113];
- The potential for solids deposition and boiler convective pass fouling. Solid deposition occurs during the humidification step through the impact of solid-droplets or by operating below the solid dew-point;
- The potential for corrosion at the point of humidification, the ESP, the downstream ductwork, and the stack. The corrosion at the humidification point is caused by operating below the acid dewpoint, but the rest of the corrosion is caused by the humidified gas temperature being close to the water saturation temperature. It is also possible for plugging to occur. If the duct and boiler gas path is plugged, negative pressure transients can occur;
- The possible reduced efficiency of the ESP due to the changes in ash resistivity and the increased grain loading in the flue gas. Additional collection devices may be required. Humidification does help the ESP collection efficiency;
- The danger of injecting the hydrated lime at a temperature higher than the optimum high temperature (~2300 °F)[113]. If this occurs, the calcium sulfate reaction product becomes unstable and the sorbent eventually is deactivated because of sintering. Multiple injection ports in the wall of the furnace may be needed to allow for the

injection of lime into an appropriate flue gas environment. The injection point of the boiler then changes with load swings to avoid impacts on the temperature profile; and

- The need for further hydration of the free lime in the product. This free lime is very reactive when exposed to water and poses many safety hazards for disposal areas. If the lime is not hydrated, then special handling and disposal equipment will be needed to remove it.

Concluding Statements

The importance of flue gas desulfurization systems is eminent. Emissions regulations are predicted to become even more stringent in the future. The challenge is to find efficient, reliable, cost effective FGD processes for retrofit and construction in old and new coal fired plants respectively. Thus far, wet scrubbers are the most popular units on the market, the prinicpal reason being the vast research and experience associated with these systems. Second to wet scrubbers are dry scrubbers. These processes are mostly found in smaller plants that have smaller load restrictions and are more attuned to a lower cost compliance. The combined SO_2 and NO_x processes are developing rapidly and are showing promise as alternatives for emissions control in the future.

CONTROL STRATEGIES FOR PM10 AND AIR TOXICS

Introduction

The control and mitigation of fine particulate matter (PM10) and air toxics (volatile organic compounds and trace metals) has received an increased amount of attention in recent years as a result of the 1990 Clean Air Act Amendments[123]. This subsection reviews a number of commercially available technologies capable of meeting federal emissions regulations. The discussion is divided into two separate sections, the first deals with PM10 and the second, air toxics. Due to a lack of detailed study on the respective subjects, information will be provided in tabulated format and whenever possible generalized schematics are used to illustrate the device of interest.

PM10

Fine particulate matter or more commonly, PM10, is defined as particles which posses an aerodynamic diameter of less than 10 μm. Numerous technologies exist which effectively mitigate PM10 from process gases. They differ with respect to capture efficiency, operating temperature, energy requirements, and the necessary capital outlay. Table 7-1 lists four of the more common particulate control systems in conjunction with some of the operational capabilities and requirements of each. The systems are shown schematically in Figures 7-32 through 7-35 with their respective PM10 removal efficiencies illustrated in Figure 7-36.

Air Toxics

Trace Metals

In conventional solid fuels (coal, wood, agricultural wastes), trace metals exist within the porous particles, either as discrete inorganic minerals, or bonded to the overall carbon skeleton-

Table 7-1. Common Control Methods for PM10

Device	PM10 Removal Efficiency, %, [2], (Figure 7-36)	Comments
Fabric Filter, Figure 7-32	> 99.99	Large space requirement and low efficiencies while filter cake builds up. Filter material selected on basis of particle abrasivity, operational temperture, and gas velocity.
Cyclones, Figure 7-33	80 - 95.5	Efficiency may be increased to 90 - 97% for particle sizes of 5 - 10 μm but much larger operational costs are imposed due to the larger pressure drop required.
Wet Scrubber, Figure 7-34	> 99.5	Capable of collecting dust, mist, fumes (air toxic removal). Increase in operational costs resulting from wastewater removal.
Electrostatic Precipitators, Figure 7-35	> 99.9	Wet or dry capabilities, low pressure drops. Temperature dependent, particle resistivities may limit efficiencies, large space requirements.

- temperature
- particle size
- abrasiveness of the dust
- gas face velocity (through the bag)

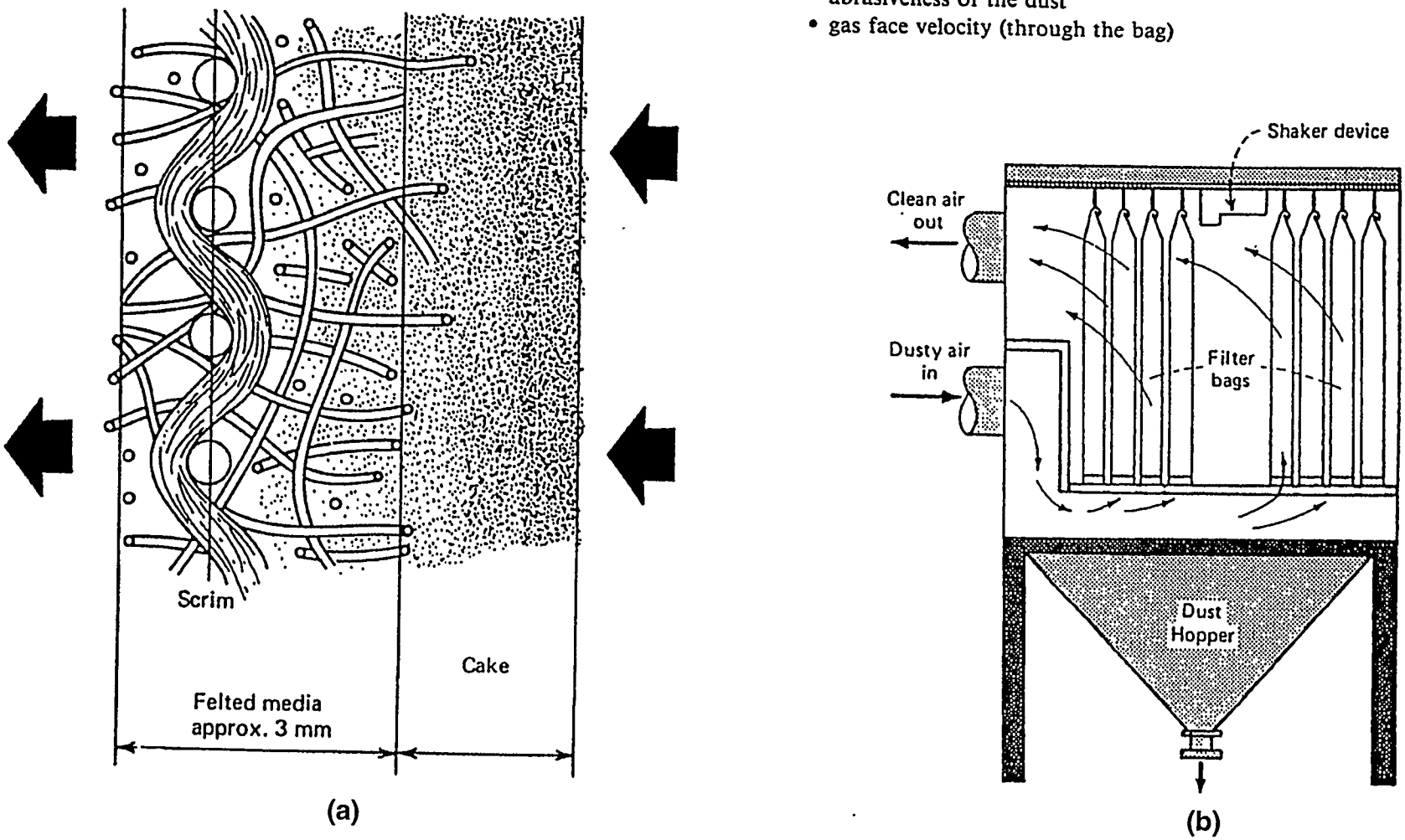

Figure 7-32. FELTED MEDIA SHOWING DISTRIBUTION OF DUST (a) AND SINGLE-COMPARTMENT BAGHOUSE FILTER WITH SHAKER (b)

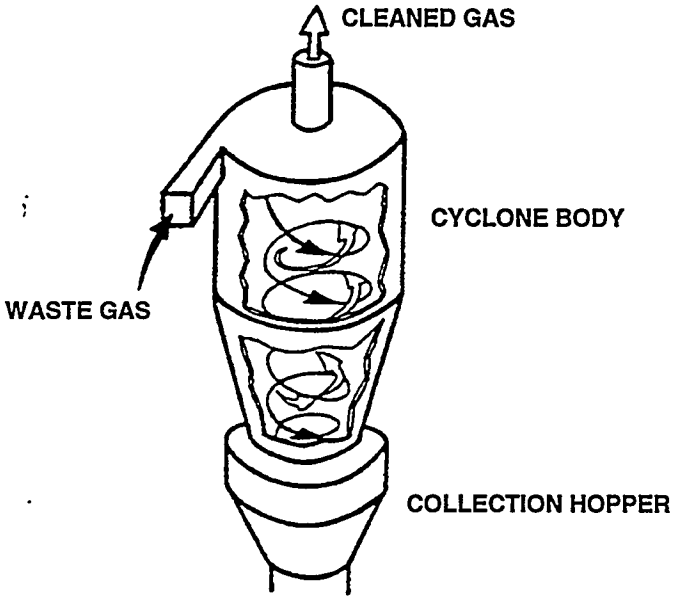

Figure 7-33. COMMON CYCLONE DUST COLLECTOR

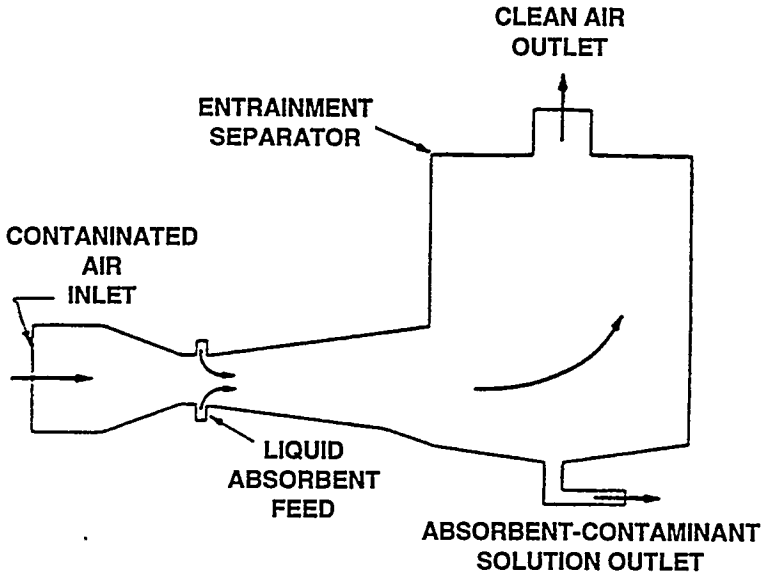

Figure 7-34. VENTURI SCRUBBER

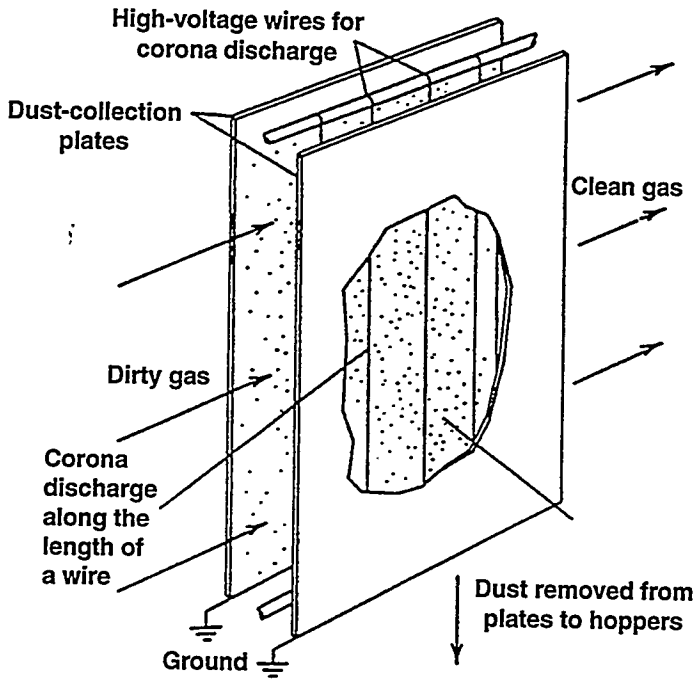

Figure 7-35. DIAGRAMMATIC SKETCH OF A SINGLE-STAGE PRECIPITATOR

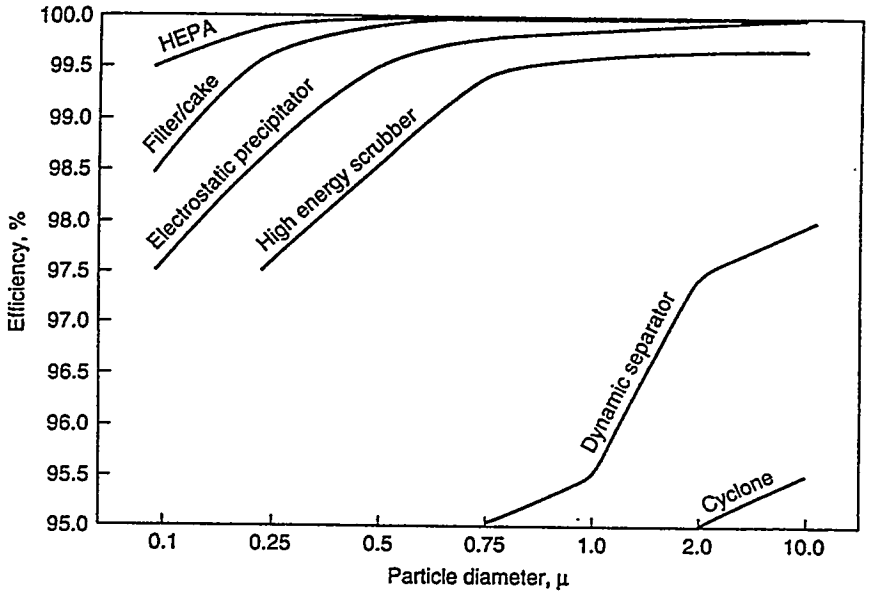

Figure 7-36. COLLECTION EFFICIENCY VERSUS PARTICLE SIZE BY TYPE OF COLLECTOR

based fuel structure. The fate of the metal depends primarily upon its' volatilization temperature which is found to be a function of the local chorine and sulfur concentrations (see Table 7-2). Metals with low volatilization temperatures, e.g., lead and mercury, are difficult to remove because they remain in gaseous form throughout the combustion system. Conversely, metals with high volatilization temperatures will tend to heterogeneously nucleate on the surface of small fly ash particles after exiting the combustion environment (see Figure 7-37[124]), and may be removed to a large extent by the conventional control technologies cited above (see Tables 7-3 through 7-5).

Coal cleaning technologies provide another mechanism for trace metal control. Past analysis suggest that to a large extent arsenic, barium, lead, and manganese (and to a lesser extent cadmium, chromium, nickel, and selenium) are associated with inorganic materials. If those materials are removed so then are the metals. The study of Akers and Dospoy [125], Tables 7-6 through 7-11, and the data provided by Tillman, Table 7-12, lend support to this theory.

Volatile Organic Compounds

Volatile organic compounds (VOCs) are compounds of carbon that combine with nitrogen oxides in the presence of sunlight to form ozone, a criteria air pollutant subject to federally mandated concentration limits[123]. All VOC's have boiling points below 212°F and semivolatile organic compounds have boiling points between 212 and 572°F. Although some adsorption onto fly ash may occur in combustion systems, the high vapor pressure of VOCs result in their emission from the stack in gaseous form.

The most common strategies for VOC control are incineration (thermal and catalytic), activated carbon adsorption, combined absorption/incineration, and absorption. The control efficiency of each technique is a function of VOC concentration and device selection is therefore commonly decided by VOC content (See Figure 7-38[126-128]. Table 7-13 provides an outline of the common control techniques used.

Concluding Remarks

Possible control strategies for the capture and mitigation of PM10 and air toxics (trace metals and VOCs) have received increased attention in recent years as a result of the Clean Air Act Amendments requirements of 1990. Numerous techniques commonly employed and commercially available which provide industry with viable options for fugitive emissions control have been provided. [129-132]

DISCUSSIONS WITH VENDORS AND ENGINEERING FIRMS

Vendors and engineering firms were contacted to identify appropriate emissions control technologies for retrofited undustrial boilers. Information has not been received from several of the companies contacted; therefore, a summary of the contacts and information received will be presented in the next semiannual report. From this information, appropriate NO_x and SO_2

Table 7-2. Metal Volatility Temperatures for Free Metal in Systems With and Without Chlorine

Metal	Volatility Temperature Without Chlorine in System		Volatility Temperature With Chlorine in System	
	°F	°C	°F	°C
Antimony	1,219	660	1,219	660
Arsenic	89	32	89	32
Barium	1,560	849	1,659	904
Beryllium	1,929	1,054	1,929	1,054
Cadmium	417	214	417	214
Chromium	2,935	1,613	2,931	1,611
Lead	1,160	627	4.4	-15
Mercury	57	14	57	14
Nickel	2,209	1,210	1,279	693
Selenium	604	318	604	318
Silver	1,659	904	1,160	627
Thallium	1,329	721	1,329	721

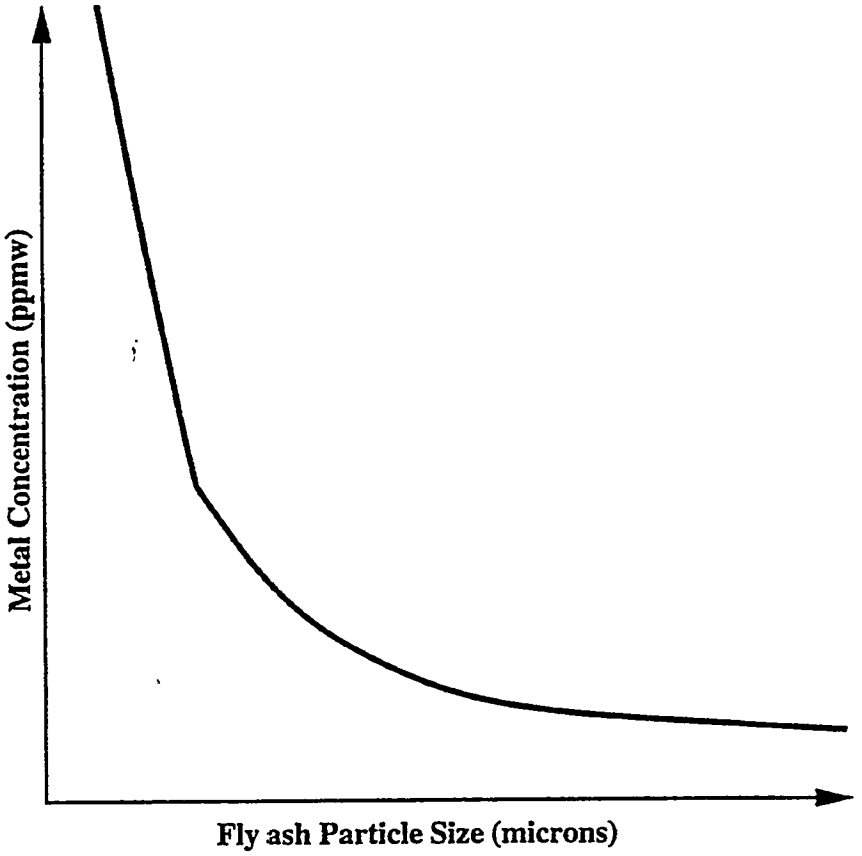

Figure 7-37. REPRESENTATIVE METAL ENRICHMENT CURVE FOR FLY ASH, SHOWING THE HIGHEST CONCENTRATIONS OF METALS IN SUBMICRON PARTICLES

Table 7-3. Typical Particulate Matter Trace Element Removal Efficiencies of Various Control Technologies

	Average Trace Elements Removal Efficiencies (%)					
				SO_2 Scrubber[a]		
Trace Elements	Cyclone Separator	Electrostatic Precipitator	Venturi Scrubber	Coal-fired Boiler	Oil-fired Boiler	Baghouse
Aluminum	66.0	99.2	99.6	99.0	92.0	~100
Arsenic	75.3	95.3	94.2	97.0	81.0	ND
Beryllium	84.3	98.4	99.2	98.0	ND	ND
Cadmium	44.0	95.6	92.3	99.0	77.0	ND
Chromium	27.7	95.1	92.5	95.0	90.0	ND
Iron	54.2	99.1	>99.5[a]	99.0	95.0	~99.9[a]
Lead	30.0	95.5	98.0[a]	99.0	94.0	~100
Mercury	3.2	0.0[a]	12.6[a]	55.0	87.0	ND
Nickel	18.6	52.5	95.0	95.0	83.0	~100
Selenium	33.1	86.0	91.4	87.0	97.0	ND
Titanium	74.4	98.9	99.8	ND	ND	~100
Zinc	39.4	97.0	98.4	98.0	90.0	~!00

[a]Does not represent an average value, since only one data point was available.
ND-No data available.

Table 7-4. Conservatively Estimated "Wet" Air Quality Control System Efficiencies Associated with Trace Metal Capture (Values in Mass %)

Metal	Control System			
	Packed Tower Scrubber	Venturi Scrubber 20" H_2O Pressure Drop	Venturi Scrubber 60" H_2O Pressure Drop	Wet ESP Scrubber
Antimony	40	85	97	95
Arsenic	40	85	97	95
Barium	50	90	98	97
Beryllium	50	90	98	97
Cadmium	40	85	97	95
Chromium	50	90	98	96
Lead	40	85	97	95
Mercury	30	60	90	60
Silver	50	90	98	97

Table 7-5. conservatively Estimated "Dry" Air Quality Control System Efficiencies Associated with Trace Metal Capture (values in mass %)

Metal	Control System			
	ESP, 2-Fields	ESP, 4-Fields	Fabric Filter (baghouse)	Dry Scrubber Fabric Filter
Antimony	85	85	90	95
Arsenic	85	85	90	95
Barium	97	90	99	99
Beryllium	97	90	99	99
Cadmium	85	85	90	95
Chromium	97	90	99	99
Lead	85	85	90	95
Mercury	10	60	10	90
Silver	97	90	99	99

Table 7-6. Conventional Coal Cleaning, Upper Freeport Seam Coal

Test 1 (80% Energy Recovery)

	Raw		Clean		
Elements	ppm[a]	grams/ BBtu[b]	ppm	grams/ BBtu	Reduction (%)
Ash	44.0%		12.2%		72
Arsenic	66	3,619	18	600	83
Barium	254	13,926	62	2,068	85
Cadmium	5	274	3	100	63
Chromium	50	2,741	25	834	69
Fluorine	670	36,735	136	4,536	87
Lead	12	658	11	367	44
Mercury	0.7	38	0.25	8	78
Nickel	27	1,480	23	767	48
Selenium	1.1	60	1.89	63	-4
Zinc	73	4,002	35	1,167	71

Test 2 (56% Energy Recovery)

	Raw		Clean		
Elements	ppm	grams/ BBtu	ppm	grams/ BBtu	Reduction (%)
Ash	43.8%		10.2%		
Arsenic	73	4,002	19	618	84
Barium	276	15,133	54	1,757	88
Cadmium	6	329	3.5	114	65
Chromium	51	2,796	28	911	67
Fluorine	550	30,155	137	4,457	85
Lead	18	987	7	228	76
Mercury	0.7	38	0.28	9	76
Nickel	30	1,645	21	683	58
Selenium	1.6	88	1.65	54	38
Zinc	75	4,112	29	943	77

[a]parts per million grams
[b]grams per billion Btu

Table 7-7. Conventional Coal Cleaning, Rosebud/McKay Seam Coal

Test 1 (99% Energy Recovery)

	Raw		Clean		
Elements	ppm[a]	grams/ BBtu[b]	ppm	grams/ BBtu	Reduction (%)
Ash	10.9%		8.6%		21
Arsenic	2	117	2	77	34
Barium	284	16,676	118	4,567	73
Cadmium	0.8	47	0.5	19	60
Chromium	5	294	11	426	-45
Fluorine	50	2,936	30	1,161	60
Lead	0.7	41	4	155	-277
Mercury	0.12	7	0.1	4	45
Nickel	15	881	11	426	52
Selenium	0.51	30	0.67	26	13
Zinc	6	352	5	194	45

Test 2 (90% Energy Recovery)

	Raw		Clean		
Elements	ppm	grams/ BBtu	ppm	grams/ BBtu	Reduction (%)
Ash	11.4%		8.1%		29
Arsenic	3	165	2	78	53
Barium	320	17,581	117	4,560	74
Cadmium	0.8	44	0.8	31	29
Chromium	6	330	10	390	-18
Fluorine	50	2,747	50	1,949	29
Lead	4	220	4	156	29
Mercury	0.14	8	0.12	5	39
Nickel	14	769	10	390	49
Selenium	1.87	103	0.78	30	70
Zinc	7	385	6	234	39

[a]parts per million grams
[b]grams per billion Btu

Table 7-8. Conventional Coal Cleaning, Croweburg Seam Coal

Test 1 (91% Energy Recovery)

	Raw		Clean		
Elements	ppm[a]	grams/ BBtu[b]	ppm	grams/ BBtu	Reduction (%)
Ash	13.89%		6.63%		53
Arsenic	6.8	268	4	115	57
Barium	69.4	2,733	10	315	88
Cadmium	0.4	16	0.1	1	92
Chromium	29.0	1,140	7.7	252	78
Fluorine	35.4	1,394	50	1,650	-18
Lead	10.0	393	8	270	31
Mercury	0.1	5	0.06	2	58
Nickel	33.0	1,298	27	899	31
Selenium	1.0	39	1.6	51	-31
Zinc	79.9	3,146	20	638	80

Test 2 (90% Energy Recovery)

	Raw		Clean		
Elements	ppm	grams/ BBtu	ppm	grams/ BBtu	Reduction (%)
Ash	13.13%		4.84%		63
Arsenic	4.8	187	3.6	116	38
Barium	29.5	1,151	3.4	109	91
Cadmium	0.3	12	0.0	1	91
Chromium	3.0	115	10.2	328	-184
Fluorine	36.4	1,421	46.2	1,479	4
Lead	7.7	299	7.1	227	24
Mercury	0.09	3	0.12	4	-16
Nickel	26.5	1,035	28.4	910	12
Selenium	0.6	23	1.3	41	-79
Zinc	70.8	2,761	17.3	555	80

Test 3 (95% Energy Recovery)

	Raw		Clean		
Elements	ppm	grams/ BBtu	ppm	grams/ BBtu	Reduction (%)
Ash	13.57%		6.74%		50
Arsenic	5.5	217	2.5	83	62
Barium	47.1	1,861	13.3	441	76
Cadmium	0.3	13	0.1	3	80
Chromium	28.9	1,141	9.9	328	71
Florine	56.5	2,231	41.3	1,365	39
Lead	10.1	397	6.2	205	48
Mercury	0.1	5	0.2	6	-33
Nickel	28.9	1,141	27.9	923	19
Selenium	1.0	39	0.8	28	30
Zinc	75.4	2,978	25.8	818	73

[a]parts per million grams
[b]grams per billion Btu

Table 7-9. Conventional Coal Cleaning, Kentucky No. 71 Seam Coal

Test 2 (73% Energy Recovery)	Raw		Clean		
Elements	ppm[a]	grams/ BBtu[b]	ppm	grams/ BBtu	Reduction (%)
Ash	34.5%		5.21%		85
Arsenic	1.8	88	1.5	51	43
Barium	98.6	4,929	11.9	392	92
Chromium	41.2	2,060	12.9	425	79
Fluorine	717	35,841	59.4	1,956	95
Lead	21.4	1,070	3.5	116	89
Mercury	0.15	8	0.12	4	48
Nickel	42.9	2,144	11.7	385	82
Selenium	1.5	77	0.9	29	62
Zinc	96.7	4,834	13.1	431	91

[a]parts per million grams
[b]grams per billion Btu

Table 7-10. Conventional and Advanced Physical Cleaning, Sewickley Seam coal (ppm except where noted)

	Raw	Conventional cleaning	Custom coal advanced process
Ash content	29.2%	15.2%	14.0%
Antimony	0.80	0.48	0.26
Arsenic	14.0	7.2	3.5
Cadmium	0.20	0.63	0.34
Chromium	16.07	8.35	8.22
Cobalt	0.27	0.24	0.22
Lean	14.73	6.96	6.16
Mercury	0.16	0.14	0.14
Nickel	13.39	9.13	8.21
Selenium	1.14	1.54	1.24

Table 7-11. Chemical/Physical Coal Cleaning, Pittsburgh Seam Coal (ppm except where noted)

	Raw coal	Conventional cleaning	Midwest ore process
Antimony	<0.5	<0.5	<0.5
Arsenic	7.0	4.4	2.0
Baryllium	1.1	0.8	0.7
Cadmium	<0.1	<0.1	<0.1
Chromium	37.8	12.5	11.7
Lead	13.1	4.4	1.8
Mercury (ppb)	31.1	193	106
Nickel	32.2	12.7	9.3
Selenium	1.8	0.4	0.5

Table 7-12. Typical Reduction in the Trace Metal Content of Coal as a Function of Coal Cleaning Systems (values in wt %)

Metal	Coal Cleaning System		
	Commercial Coal Prep. Plants	Advanced Physical Cleaning	Advanced Chemical Cleaning
Arsenic	26 - 50	71 - 90	51 - 70
Cadmium	26 - 50	51 - 70	51 - 70
Copper	26 - 50	11 - 25	71 - 90
Lead	51 - 70	71 - 90	91 - 98
Manganese	51 - 70	91 - 98	>98
Mercury	11 - 25	---	---
Nickel	26 - 50	51 - 70	26 - 50
Selenium	11 - 25	---	51 - 70
Zinc	26 - 50	51 - 70	>98

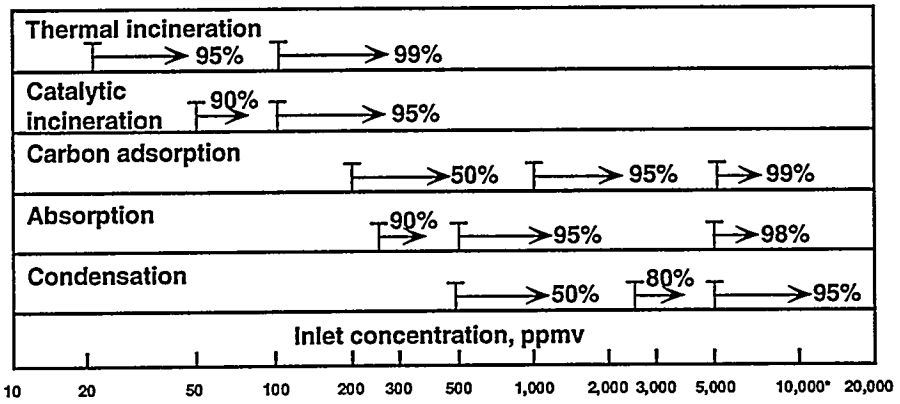

*Beyond 10,000 ppmv, explosiveness and other safety considerations are of concern.

Figure 7-38. CONTROL EFFICIENCY IS A FUNCTION IN INLET-VOC CONCENTRATION

Table 7-13. Common VOC control techniques

Technique	Efficiency, %, [6]	Comments
Thermal incineration, Figure 7-39	> 95	Converting gaseous organic-vapor emissions to carbon dioxide and water through combustion. If VOC concentration is too low for self sustaining combustion, supplemental fuel is needed and translates to additional cost. Operating temperatures of 1200 - 1600°F
Catalytic incineration, Figure 7-40	> 95	Similar to thermal incineration but catalyst lowers the oxidation temperature allowing combustion to occur around 600°F. Lower cost than thermal incineration resulting from less support fuel.
Carbon adsorption, Figure 7-41	> 95, at 1000 ppmv	Organics are retained on the surface of highly porous activated carbon. Adsorption cycles may be operated in two modes, regenerative and nonregenerative.
Adsorption/incineration, Figure 7-42	> 95	Adsorber concentrates the organic-laden air before treatment by incineration, very useful for low concentration high volume feed streams.
Condensation	50 - 95, fct. of type of organic and concentration.	Contaminated gas stream is cooled to saturation thereby condensing contaminants to a liquid. Limited however, to streams with relatively high organic concentrations, > 5000 ppmv.
Absorption	> 98 at 5000 ppmv > 90 at 300 ppmv	Mass transfer of selected components from gas stream into nonvolatile liquid. Choice of absorbent depends on the solubility of the gaseous organic compounds and cost.

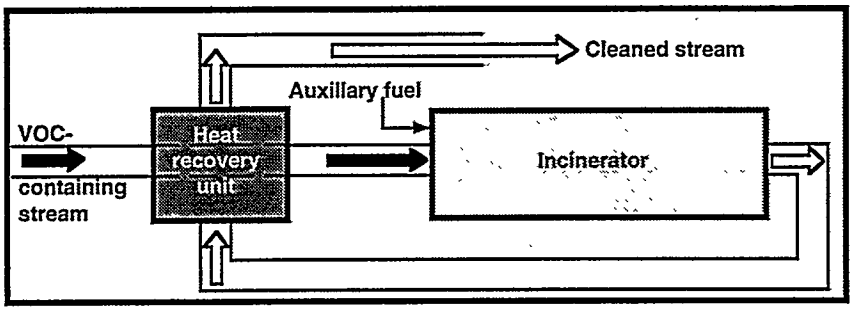

Figure 7-39. THERMAL INCINERATION SYSTEM FOR DESTRUCTION OF ORGANIC POLLUTANTS

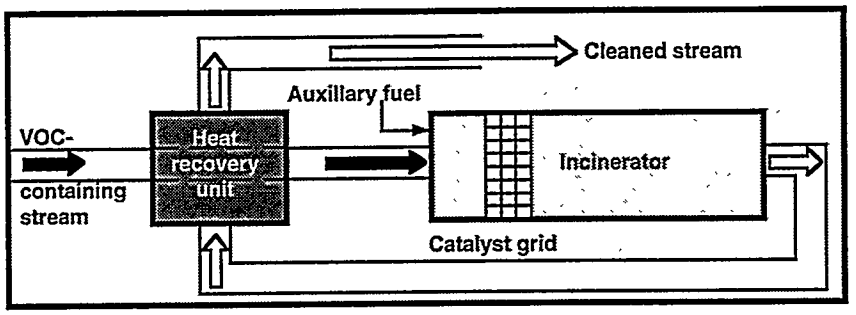

Figure 7-40. CATALYTIC INCINERATION SYSTEM

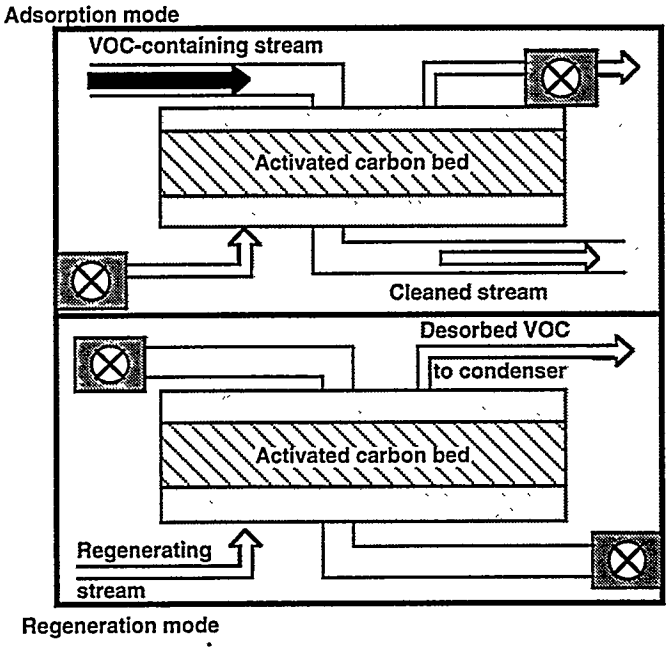

Figure 7-41. REGENERATIVE ADSORBERS USED FOR VOC DESTRUCTION

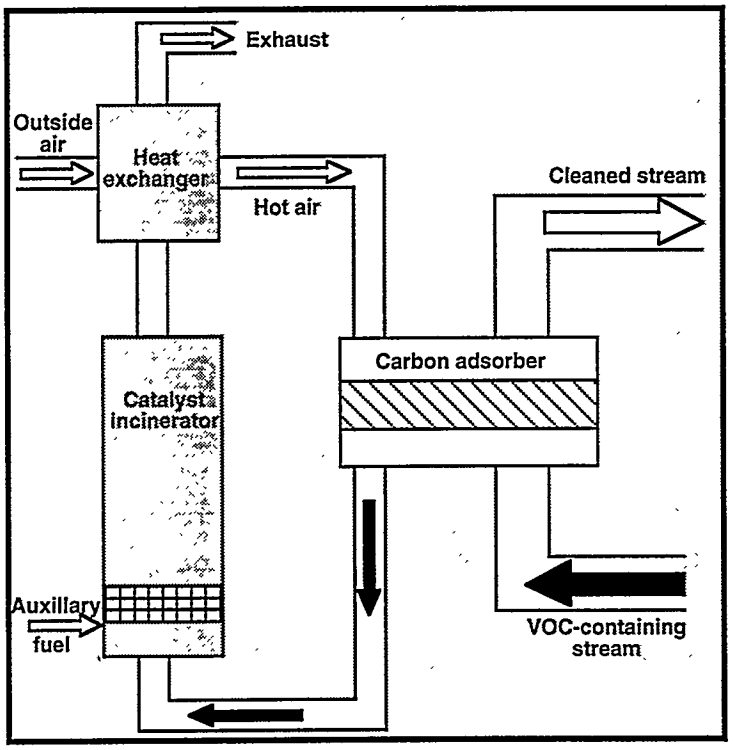

Figure 7-42. COMBINED ADSORPTION AND INCINERATION PROCESS

technologies will be identified, the systems will be designed, and component procurement will begin during the next reporting period.

7.2 Subtask 1.2 Conduct Fundamental Emissions Reduction Studies

No work was conducted on this subtask.

7.3 Subtask 1.3. Install System on the Demonstration Boiler

No work was conducted on this subtask.

7.4 Subtask 1.4 Evaluate Emissions Reduction System

No work was conducted on this subtask.

8.0 PHASE II, TASK 2: COAL PREPARATION/UTILIZATION

The long-term objectives of this task are:

- to establish more precise criteria for the formulation of MCWM.
- to develop improved cleaning procedures in order to increase the yield of usable coal from any given source and to expand the reserve base of candidate coals for retrofitted boilers.
- to develop optimized procedures for low-cost production of MCWM.

8.1 Subtask 2.1 Optimization of Particle Size Consist for MCWM Formulation

The particle size distribution is an important factor for determining the coal loading and subsequent viscosity. It is constrained by the maximum particle size for proper combustion and the optimum size consist for high solids loading with low viscosity. It is generally considered that either a bimodal or a broad size distribution is required. The advantage for having a bimodal distribution can be understood in the sense that the small particles fit into the interstices between the larger particles so that higher packing densities can be achieved. However, the optimum blending and size ratios have not been clearly defined for real systems. Also, the term "broad size distribution" is ambiguously used in the industry. Sometimes, it is used interchangeably with bimodal distribution; at other times, it is applied to a distribution covering a wide range of particle sizes without a clear definition. Since there is no technique for predicting the optimum size distribution *a priori*, the size distribution required for low viscosity slurry is generally obtained by trial-and-error, and is not necessarily optimum. Without a clear understanding of the optimum size distribution, processes for slurry production can not be optimized.

The rheological properties of coal slurry are determined by the degree of the dispersion, particle size distribution, and concentration. Many workers have attempted to produce theoretical or experimental relationships for effect of concentration on the dispersion rheology. While variabilities exist in experimental results, in most cases the critical packing volume fraction f_c is incorporated in the relationships. This is because, as the concentration increases, the particles come closer and closer together, until finally they are too close together to be able to move. At this

point, the concentration has reached ϕ_c and the dispersion has become solid. The viscosity of the suspension increases very sharply in the region of the concentration close to ϕ_c.

The precise value of ϕ_c is closely related to particle packing. For a randomly distributed bed of uniform size spheres, the packing density is about 60%. Therefore, it can be expected that the viscosity of a suspension should increase rapidly as the concentration approaches 60%. The packing density can be increased by inserting small particles in the interstices between larger particles. This shifts the critical packing volume fraction to a higher value, and hence the viscosity is lower than that of the monodisperse system at the same concentration. This was verified experimentally by Chong[133] who observed that the viscosity decreased markedly as the particle size ratio between the large and small particles decreased. However, when the particle size ratio was less than 1:10, no appreciable further decrease in viscosity was observed. At this size ratio, the small particles pass easily between the larger particles. The fine-particle suspension behaves as a fluid towards the larger particles.

For the condition where the size ratio is sufficiently small such that there is no appreciable interaction between the small and large particles,Farris[134] developed the blending ratio that produces the lowest possible viscosity. For an N component system, this is given by

$$\phi_1 = \phi_2 = \phi_3 = \cdots\cdots = \phi_N \qquad (8\text{-}1)$$

such that

$$(1-\phi_T)=(1-\phi_i)^N \qquad (8\text{-}2)$$

where $\phi_i = V_i / (V_o + V_1 + V_2 + V_3 + \cdots + V_i)$, V_i is the volume of the i^{th} component, V_o is the volume of liquid, and ϕ_T is the total solids concentration.

As Henderson and Scheffee[135] showed, this relationship yields a particle size distribution given by:

$$F_i = \frac{\theta^i - 1}{\theta^N - 1} \qquad (8\text{-}3)$$

where F_i is the cumulative fraction of particles smaller than or equal to the i^{th} component and

$$\theta = (1-\phi_T)^{-1/N} \qquad (8\text{-}4)$$

For a system of particles with a geometric progression of sizes, the particle size distribution transforms to[46]:

$$F_i = \frac{D_i^n\theta - D_S^n}{D_L^n\theta - D_S^n} \qquad (8\text{-}5)$$

where D_i is the particle size of the i^{th} component, D_L is the largest particle size, D_S is the smallest particle size, and $n = \log\left(\frac{1}{1-\phi_T}\right)^{\frac{1}{N}} / \log\left(\frac{D_L}{D_S}\right)^{\frac{1}{(N-1)}}$. This equation is strictly applicable for discrete sizes of successive size ratio greater than 10:1. This limits the number of sizes in a multi-component system to 3 or 4 at the most (e.g., 1, 10, 100, and 1000 μm).

Furnas[136] obtained a similar expression for the particle size distribution to obtain maximum packing. He assumed that there would be a constant ratio, r, between the amounts of consecutive sizes for maximum packing. For a particle system of N size intervals, the cumulative size distribution for maximum packing is given by:

$$F_i = \frac{r^i - 1}{r^N - 1} \qquad (8\text{-}6)$$

For a system of particles with a geometric progression of sizes of ratio q, the particle size distribution transforms to:

$$F_i = \frac{D_i^m r - D_S^m}{D_L^m r - D_S^m} \qquad (8\text{-}7)$$

where $m = \log(r)/\log(q)$. This equation is very similar to the Farris equation (Equation 8-5) with q being replaced by r. In fact, it can be shown that θ is also the constant ratio of volumes between successive sizes, i.e., r and θ are equivalent. Also, m equals n since $D_L = q^{N-1}D_S$, giving $\log q = \log(D_L/D_S)^{1/(N-1)}$. Therefore, Equations 8-5 and 8-7 have exactly the same form but with different definitions of the constant ratio of volumes between consecutive sizes (r is empirical and θ is theoretical). This indicates that a particle size distribution that gives maximum packing should also give the minimum viscosity as indicated by Skolnik et al.[3]. However, it should be emphasized that the packing density of a particulate system based on the composition from

Equation 8-7 with a low value of q can be much less than that of a bimodal system with a size ratio greater than 10:1.

Unfortunately, these equations have been widely misinterpreted and have often been applied to continuous distribution of sizes arbitrarily divided into discrete size classes. The idealized size distribution, calculated using Equation 8-5 with a size ratio (large:small) of 10:1, is shown Figure 8-1 (labeled 1) for a system with a maximum size of 100 μm and a minimum of 1 μm. The continuous distribution (labeled 2) does not represent an appropriate approximation despite having the "correct" values of F_1, F_2 and F_3 at 1, 10 and 100 μm, respectively. The presence of intermediate sizes leads to a crowding effect which violates the no-interaction requirement. Slurries prepared using the continuous distribution would have substantially higher viscosity. In many cases, in fact, it may even be impossible to produce a slurry at the specified concentration ϕ_T. The nearest, practical approach would be the bimodal distribution labeled 3 on Figure 8-1. A distribution of this type can easily be prepared by blending two ground products. While such a distribution would probably have a higher viscosity than the idealized mixture of 3 discrete sizes, many of the attributes of the latter would be preserved.

The rheological characteristics of practical bimodal distributions such as that described by curve 3 in Figure 8-1, have not been fully established. For example, it is inevitable that some of the intermediate sizes will be present. The degree to which these can be compensated for by increasing the ratio of median sizes to 15:1, say has not been delineated. Therefore, investigation of the effect of size ratio for practical, bimodal systems will be a significant part of the future work.

Equation 8-5 can be used to predict the optimum composition to give maximum flowability of a slurry. The actual flow behavior, however, depends on the rheological character of the individual components and their interaction in the mixture. For simple Newtonian systems with a single solid component, it is generally assumed that the viscosity is given by:

$$\mu = \mu_o f(\phi) \qquad (8\text{-}8)$$

where μ_o is the viscosity of the medium and $f(\phi)$ describes the effect of solids concentration. If the idealized, no-interaction condition is satisfied, this can be extended to binary mixtures by considering the system as a suspension of the coarse component in a "medium" consisting of the fine-particle slurry. Formulation of rheological models using this approach was discussed in a previous report[137]. Extension to non-Newtonian slurries will be included in the Phase III research.

Experimental studies of the rheological character of slurries prepared from the Taggart seam coal are in progress. Shear stress-shear rate measurements are being made as a function of solids

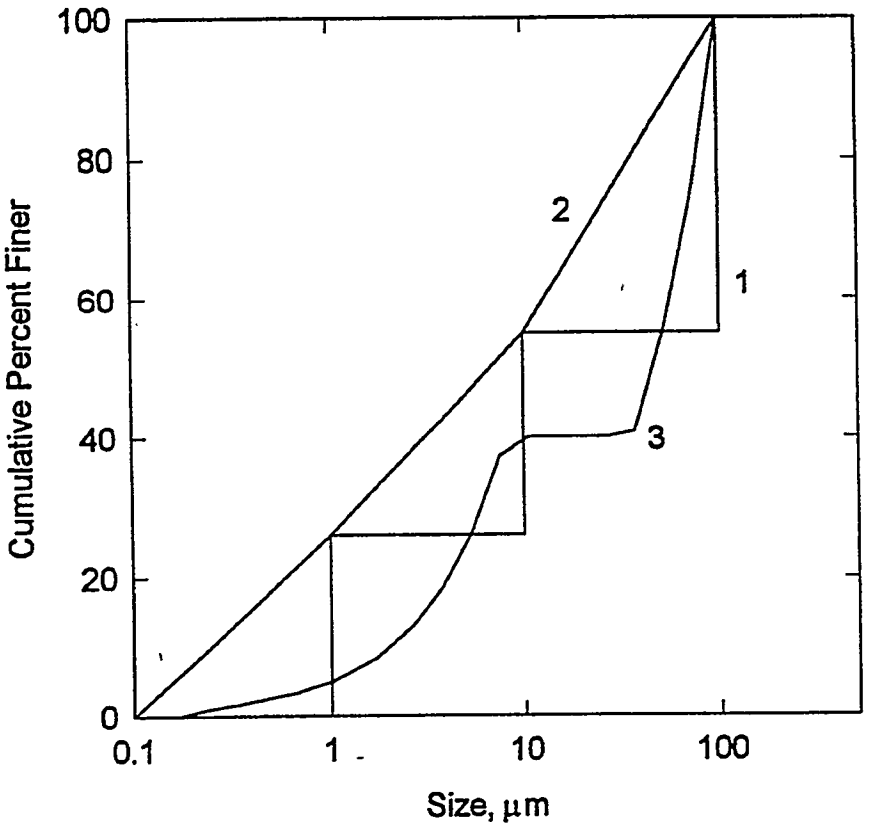

Figure 8-1. PARTICLE SIZE DISTRIBUTION FOR DENSE SLURRY FORMULATION:
1. Idealized trimodal distribution
2. "Equivalent" continuous distribution
3. Practical, bimodal approximation

concentration using a Haake Rotovisco RV3. For each slurry, measurements are being carried out for both increasing and decreasing shear rates and at different rates of increase or decrease. Some typical results are shown in Figure 8-2. It can be seen that the rheological behavior follows a typical, plastic-type pattern. At high shear rates, the slurries exhibit Bingham plastic characteristics with an apparent yield value. Deviation from the Bingham type occurs at low shear rates and the stress decreases to a "true" yield value lower than the apparent, Bingham yield value. Slight hysteresis in the curves suggests that there is some time-dependency of the rheological behavior but that this is generally small.

8.2 Subtask 2.2 Fine Grinding/Classification/Liberation

GRINDING KINETICS

Mathematical modeling of the size-reduction process is being carried out using the size-mass balance approach[138]. In this way, the process is characterized in terms of the sets of breakage rates S_i and primary breakage distributions B_{ij}. Experimental measurements of these parameters for the Taggart seam coal ground in a conventional ball mill and a stirred-media mill were described in a previous report[5].

To compare the shape of the product size distributions at various solids concentrations for the Taggart seam coal, simulations were conducted using the back-calculated breakage parameters. Grinding times were selected that gave a product size of 80% passing 200 mesh, and the results are plotted in Figure 8-3. It can be seen that the size distributions fall into three distinct groups: one for slurry densities of 50% and less, one for slurry densities of 60-65%, and one for the slurry density of 70%. The higher density slurries produce comparatively more fines. The variation in the shape of the size distribution suggests the mechanism of fracture changes when going from low to high pulp densities. This is more evident in Figure 8-4 which shows that the higher density slurries give flatter breakage distributions, which affects the shape of the product size distribution accordingly. These results agree with the findings noted previously [139]. Similar trends were observed for the other coals.

Figure 8-5 shows the size distributions for the five coals ground at 65% solids with 0.5% dispersant. Typically, the softer (higher HGI) coals produce a flatter size distribution, containing a larger portion of fines. However, this trend is not observed for this high solids loading. It seems that in addition to the solids content, the coal surface properties play a important role in determining the viscosity of the coal slurry, which in turn affects the shape of the size distribution. The solid line represents the optimum size distribution calculated by Equation 8-5 with a maximum particle size of 200 μm and a minimum particle size of 0.1 μm. It can be seen that the size distributions for all coals do not follow the optimum size distribution. Generally, a natural breakdown of the particles does not produce the shape of the optimum size distribution under a simple grinding process. Therefore, a circuit arrangement involving staged grinding will be needed.

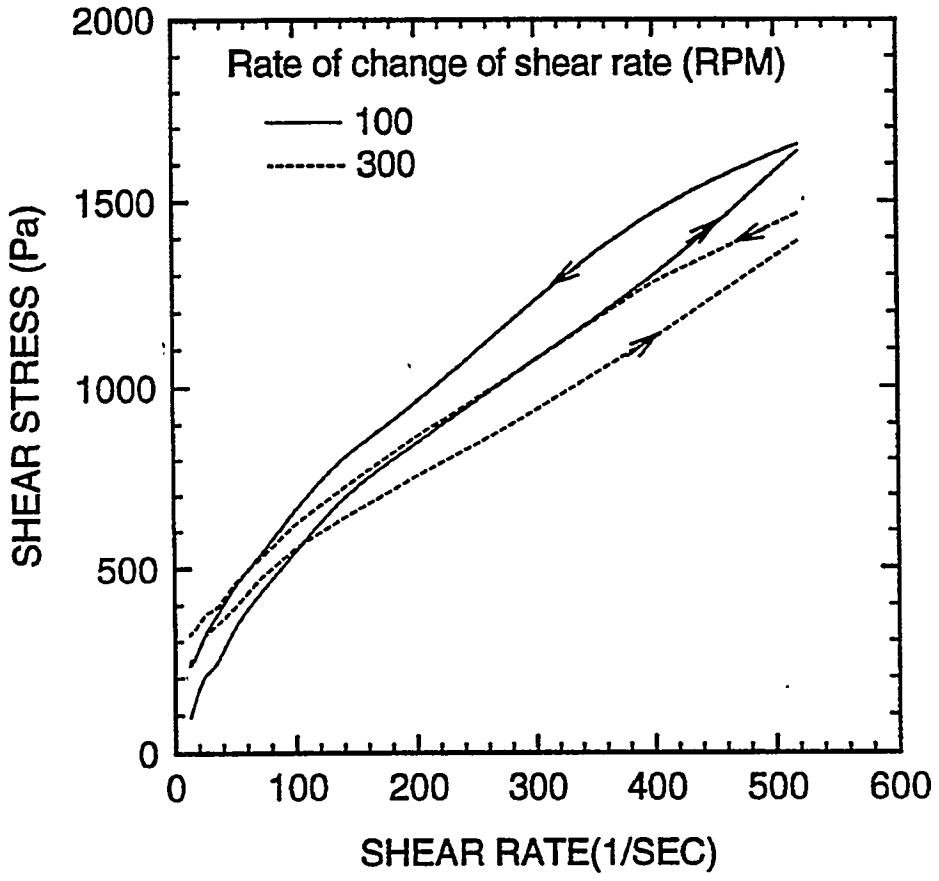

Figure 8-2. PLOTS FOR INCREASING AND DECREASING SHEAR RATES AT DIFFERENT RATES OF CHANGE OF SHEAR RATE

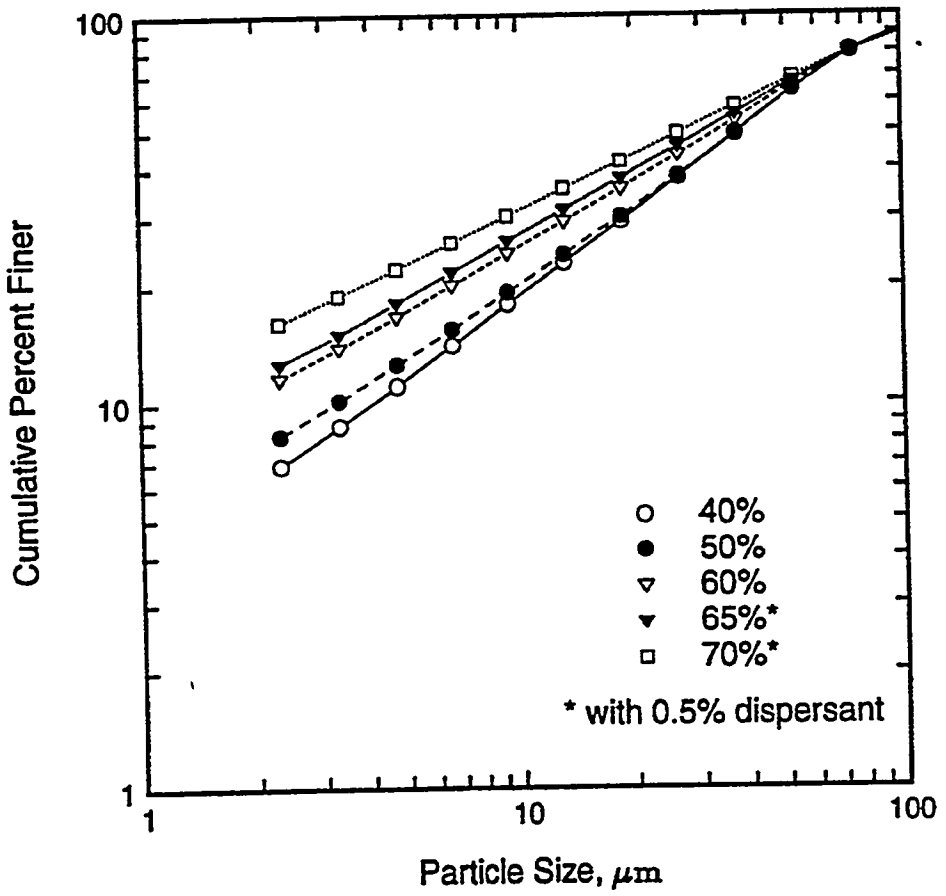

Figure 8-3. SIMULATED SIZE DISTRIBUTIONS FOR THE TAGGART SEAM COAL TO GIVE 80% PASSING 200 MESH

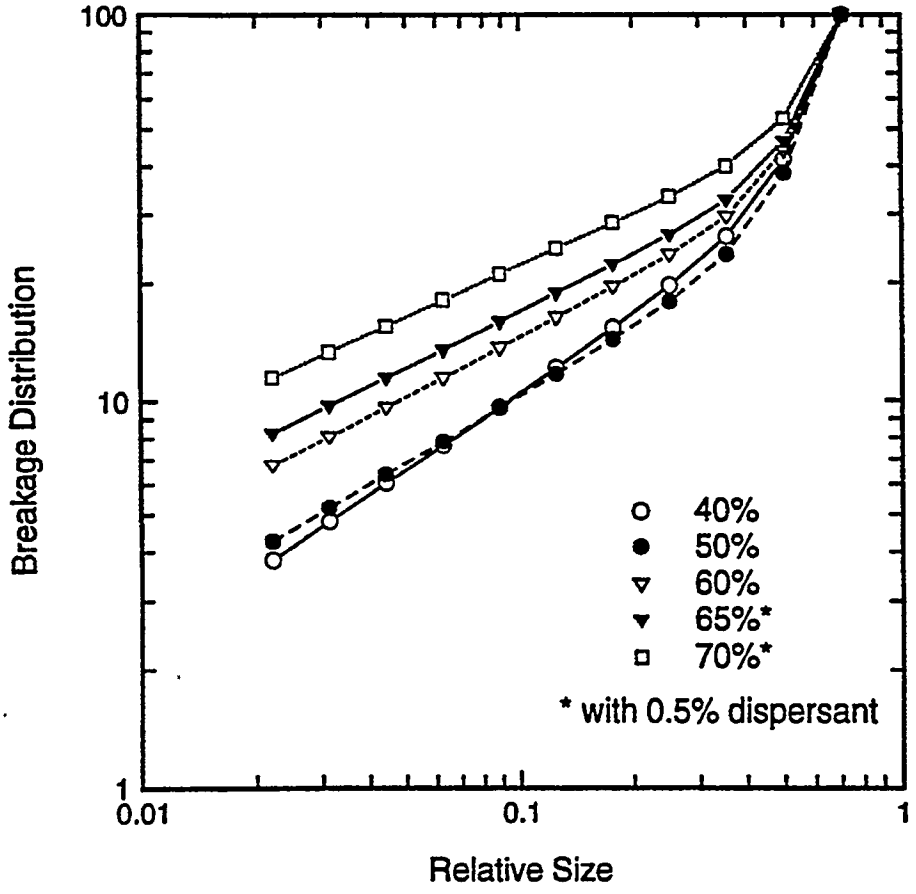

Figure 8-4. BACK-CALCULATED CUMULATIVE B-VALUES FOR VARIOUS SOLIDS CONCENTRATIONS OF THE TAGGART SEAM COAL

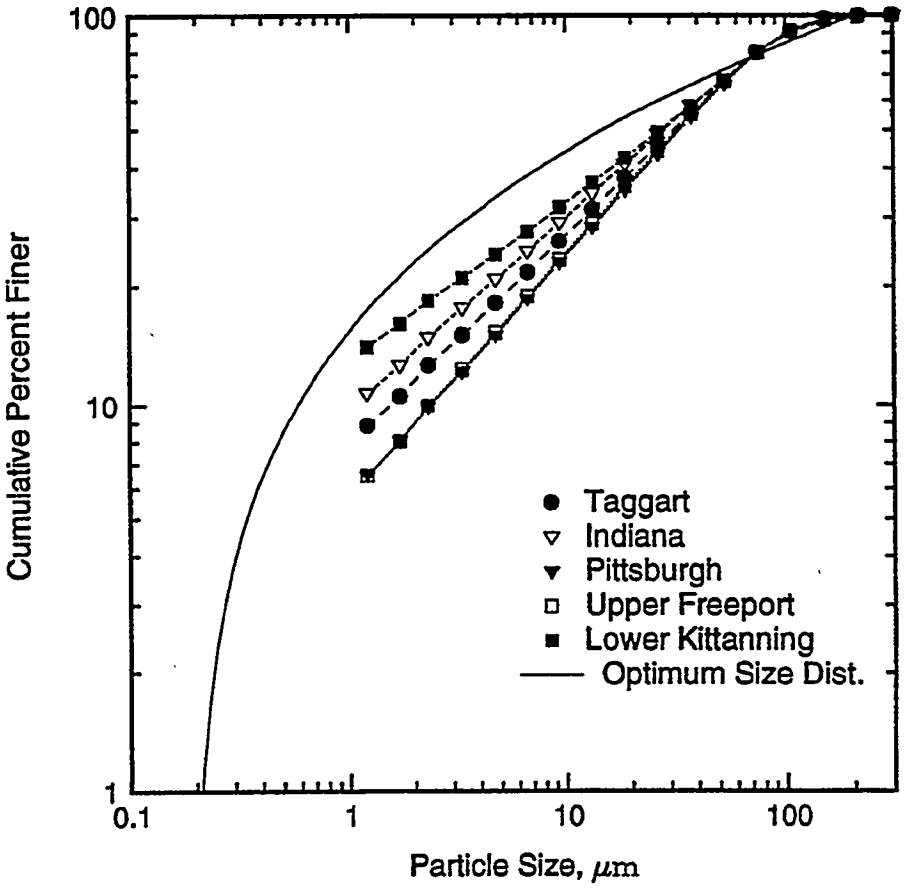

Figure 8-5. SIZE DISTRIBUTIONS FOR ALL COALS AFTER GRINDING AT 65% SOLIDS WITH 0.5% DISPERSANT TO OBTAIN 80% PASSING 200 MESH, ALONG WITH THE OPTIMUM SIZE DISTRIBUTION AS DETERMINED BY EQUATION 8-5

The simplest way to obtain the desired size distribution is by blending products from two mills. For this purpose, stirred ball milling can be used to produce the finer stream, which can be mixed with the ball mill product to obtain the required size distribution. One such circuit arrangement is shown in Figure 8-6. In this case, the coal is ground in a ball mill and some fraction is split out for further grinding in a stirred ball mill. The fractions are then blended to produce the proper size distribution.

Figure 8-7 shows the product size distributions after 16 minutes in the stirred ball mill and the ball mill products at various slurry conditions giving 70% passing 200 mesh. Since the calculated limiting size distribution of 80% passing 200 mesh lies between the two mill products, blending of the products should produce the desired size distribution. Table 8-1 shows the proportions required to produce the calculated size distribution. It can be seen that the lower the slurry density, the higher the proportion of the stirred ball mill products needed to compensate for the steeper size distribution of the ball mill products.

Table 8-1 also gives the specific energy requirement for each grinding scenario. The overall specific energy decreases as the slurry density increases because less of the grinding is performed in the energy-intensive stirred ball mill. Therefore, to obtain a flatter size distribution at the minimum energy use, the ball mill should be operated at higher slurry densities to reduce the amount of stirred ball milling required.

As noted before, this "optimum" size distribution is actually far from ideal since Equation 8-5 requires discrete particle sizes with a size ratio greater than 10:1. As experimentally shown by Farris[134], the viscosity becomes increasingly higher as the size ratio of particles decreases. Therefore, a suspension with the limiting size distribution will be more viscous than a binary mixture of particles of size ratio greater than 10:1. Practically, a true binary system of two discrete sizes cannot be produced by grinding, but it can be closely imitated using a size distribution having two modes.

For the circuit illustrated in Figure 8-6, a classifier can be used instead of a splitter in order to produce a bimodal size distribution using two mills. The product from the first mill (ball mill) is separated into coarse and fine streams. Then the fine stream is further ground in the second mill (stirred ball mill) to obtain an ultrafine product with an average size that is ten times smaller than the coarse fraction. The ideal mixing ratio of coarse and fine particles for a bed porosity of 0.4 is 60:40. Therefore, a simple grinding strategy would be to produce a product of 40% passing 400 mesh for ball milling, with the -400 mesh material being sent to the stirred ball mill.

Figure 8-8 compares the final size distribution when the two streams are mixed together. It can be seen that the frequency distribution for the coarse size fraction (ball mill product) becomes broader, containing a higher proportion of particles greater than 200 μm as the slurry concentration increases. This indicates that an additional classifier may be necessary to control the

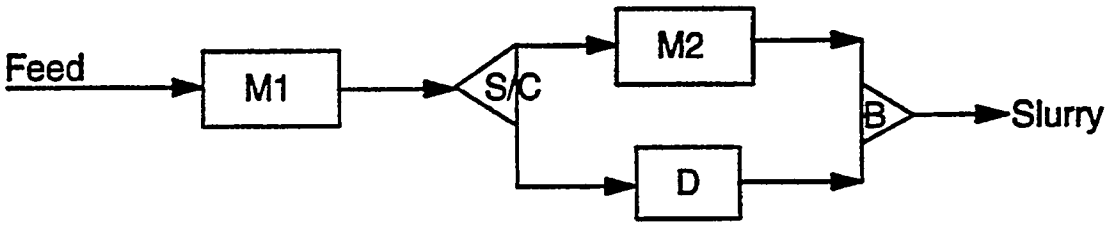

M1 = Grinding Mill - Coarse Component
M2 = Grinding Mill - Fine Component
S = Splitter - Coarse Component
C = Classifier - Coarse Component
D = Dewatering System - Coarse Component
B = Blender - Final Slurry

Figure 8-6. TWO-STAGE GRINDING CIRCUIT FOR PRODUCING COAL-WATER MIXTURES WITH THE APPROPRIATE SIZE DISTRIBUTION

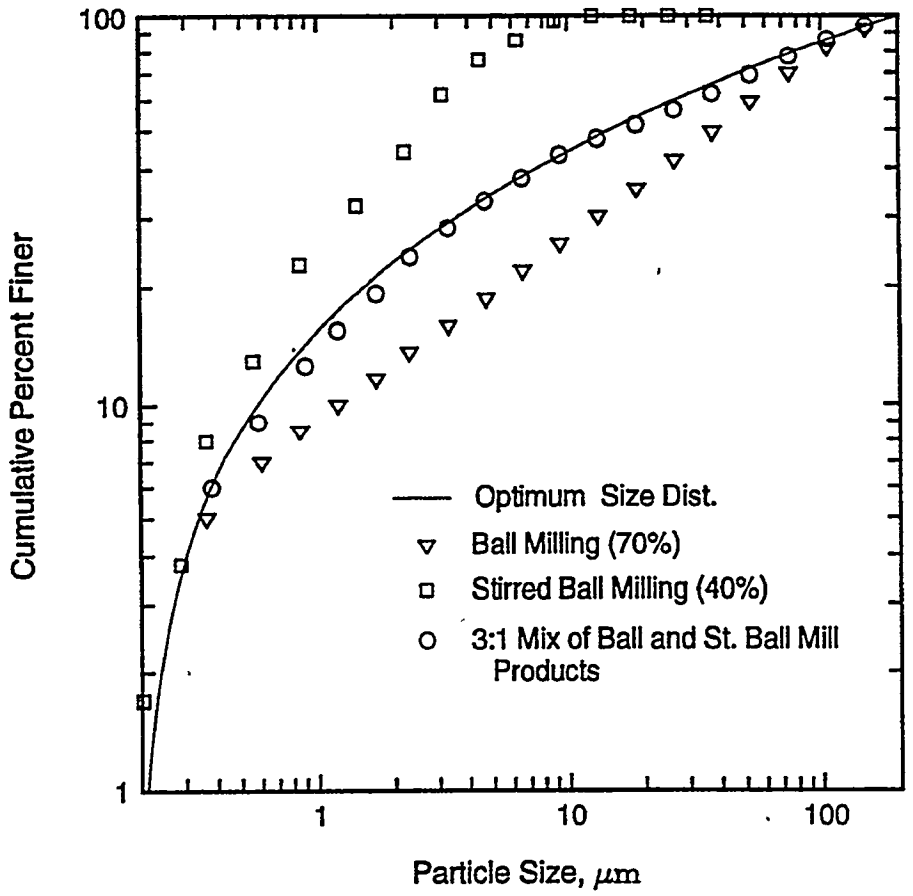

Figure 8-7. SIZE DISTRIBUTIONS FOR THE FOLLOWING CONDITIONS:
a) after 16 minutes in a stirred ball mill
b) after 30 minutes in a conventional ball mill
c) 3-to-1 mixture of the conventional and stirred ball mill products
d) optimum size distribution as determined by equation 8-5

Table 8-1. Specific Energy Requirements to Obtain the Optimum Size Distribution Calculated by Equation 8-5 for Different Ratios of the Conventional and Stirred Ball Mill Ground Taggart Seam coal.

Solids Conc.	Specific Grinding Energy kwh/t		Mixing Ratio BM/SBM	Overall Grinding Energy, kwh/t
	Ball Mill	S. B. Mill		
40%	5.8	308.8	65/35	111.8
50%	4.1		65/35	110.8
60%	7.6		70/30	98.0
65%	4.5		70/30	95.8
70%	7.2		75/25	82.6

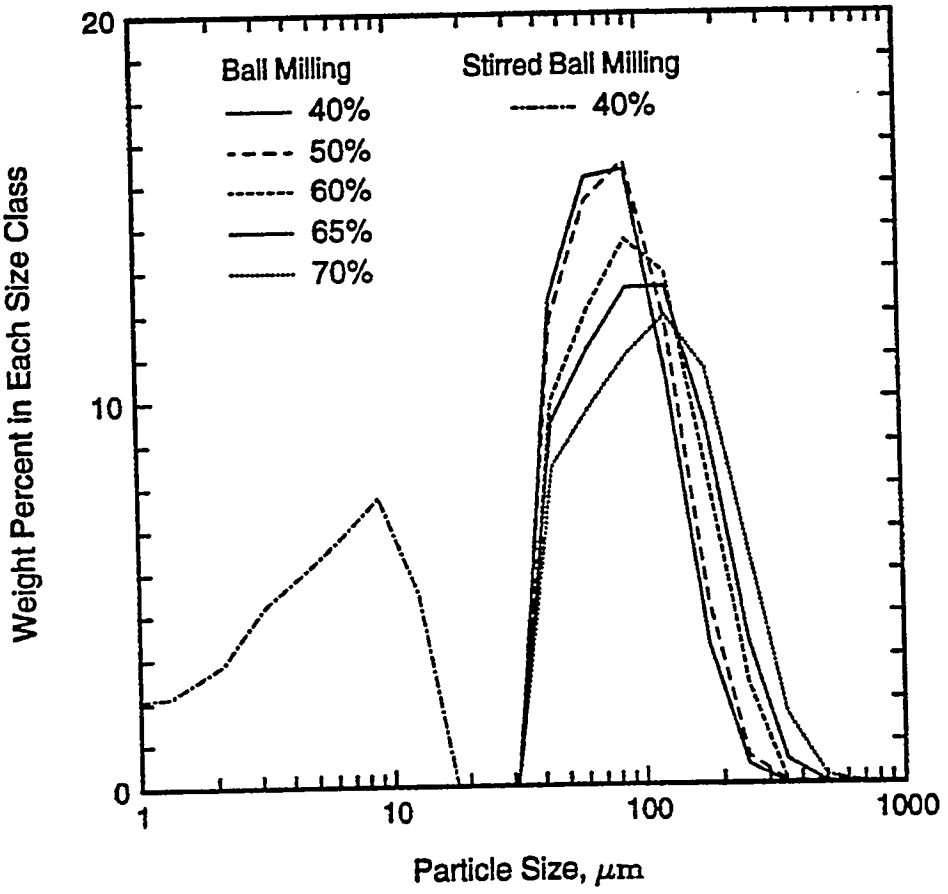

Figure 8-8. FREQUENCY DISTRIBUTION OF THE FINAL PRODUCT AFTER THE COARSE STREAM FROM BALL MILLING AND THE FINE STREAM FROM STIRRED BALL MILLING ARE MIXED

maximum particle size at a high slurry loading (>60% solids) in the ball mill circuit. At a solids loading of 40-50%, a reasonable approximation to a binary mixture was produced, with the two modes at 100 μm and 10 μm, giving a size ratio of 10:1. The grinding time required for this product was 20 minutes for ball milling and 8 minutes for stirred ball milling, giving a specific grinding energy of 66.4 kwh/t, which is much less than the energy needed to produce the "optimum" size distribution.

In summary, the specific rate of breakage decreases as the solids concentration increases from 40% to 70%. For a given coal, the grinding rate decreases as the solids concentration increases. The addition of a dispersant improves the breakage rate. The shape of the size distribution also changes as a functions of solids concentration, with more fines being produced at higher solids loadings. The result is that the net production rate of fines passes through a maximum. However, single-stage grinding in a conventional ball mill is unlikely to produce the shape of the size distribution (i.e., broad) required for a stable coal-water mixture. Stirred ball milling alone also does not produce the shape of size distribution needed for coal-water mixtures. A combination of the ball mill and stirred ball mill products can be used to obtain the desired size distribution.

CLASSIFICATION

Separations based primarily on differences in particle size can be characterized using size selectivity curves. These curves, which show the fraction of feed material of a given size that reports to the coarse particle stream, are analogous to the fractional recovery curves used to characterize density separations.

The size selectivity value for size interval i is defined as

$$s(x_i) = \frac{t(x_i)T}{f(x_i)F}$$

where $t(x_i)$ and $f(x_i)$ are the weight fractions of the coarse and feed material, respectively, in size interval i. T and F are the mass flow rates of the coarse and feed streams, respectively. Thus by knowing the size distributions and the coarse product yield (T/F), the size selectivity values can be calculated. A plot of $s(x_i)$ versus the log of the top size of size interval i produces the familiar S-shaped curve shown in Figure 8-9.

In many cases, the size selectivity values do not reach zero at the fine sizes but parallel the abscissa. This can be represented mathematically as an apparent bypass, which is defined as the fraction of the feed material that bypasses to the coarse stream. In these cases, the size selectivity values are related to the classification or corrected values, $c(x_i)$, by:

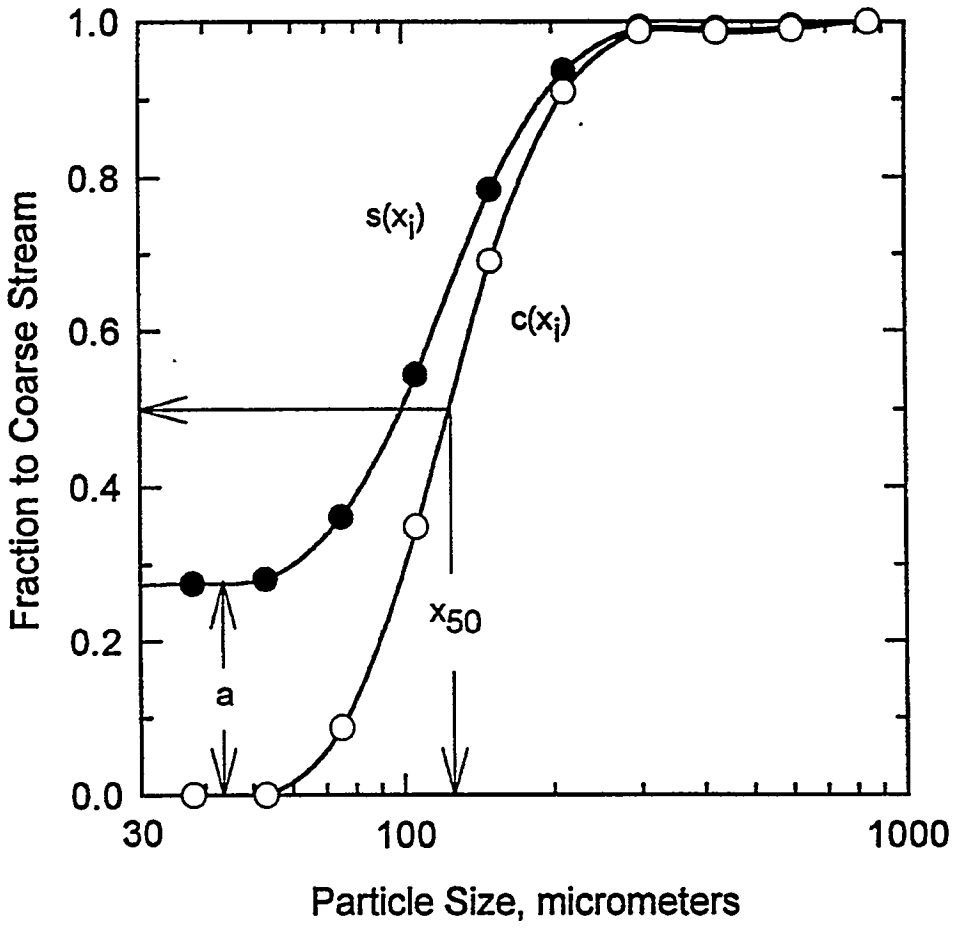

Figure 8-9. TYPICAL SIZE SELECTIVITY AND SIZE CLASSIFICATION CURVES

$$s(x_i) = (1-a)c(x_i) + a \qquad (8\text{-}10)$$

where a is defined as the apparent bypass (see Figure 8-9).

Various mathematical functions can be used to fit the classification values. One such function is the log-logistic, which is given by

$$c(x_i) = \frac{1}{1+\exp\left[\left(\frac{2.1972}{\ln k}\right)\ln\left(\frac{x_i}{x_{50}}\right)\right]} \qquad (8\text{-}11)$$

where k is the sharpness index defined as the size at which $c(x_i)= 0.25$ divided by the size at which $c(x_i) = 0.75$, i.e., $k=x_{25}/x_{75}$. The cut size, x_{50}, is defined as the particle size that has an equal probability of reporting to the coarse or the fine stream, i.e., the size at which $c(x_i) = 0.5$. Thus the entire size selectivity curve can be described by x_{50}, k, and a, all of which can be determined by nonlinear optimization.

Size classification tests will be performed using 50 and 76 mm diameter classifying cyclones. These units will be installed in closed circuit to allow for recycling of the product streams. Separations of the -100 mesh Type III coal will be made for different cyclone geometries. Simultaneous samples will be taken of the cyclone overflow (fine product) and cyclone underflow (coarse product) streams. Size analyses will be conducted using a combination of screening and/or Microtrac analysis. The size selectivity curves will be constructed and the corresponding parameters will be determined to describe the separation at each condition.

8.3 Subtask 2.3 Fine Gravity Concentration

DENSE-MEDIUM SEPARATION

The investigation of centrifugal dense-medium separation continued. Baseline testing was carried out using the continuous, solid-bowl centrifuge to determine the effect of operating conditions on magnetite classification. This information is important as it determines the magnitude of the relative density differential, which is defined as the difference in the relative densities between the underflow and the overflow streams. Large differentials, for example, greater than 0.4, are indicative of significant solids classification. This effect is usually associated with poor separator performance.

A schematic of the solid-bowl centrifuge is shown in Figure 8-10. The coal/magnetite/ water slurry is pumped into the feed port of the centrifuge. As the bowl rotates, the slurry is thrown against the outer wall. Differential settling occurs between the coal and the magnetite particles. The dense refuse particles settle the fastest and report to the bowl wall. Because of the

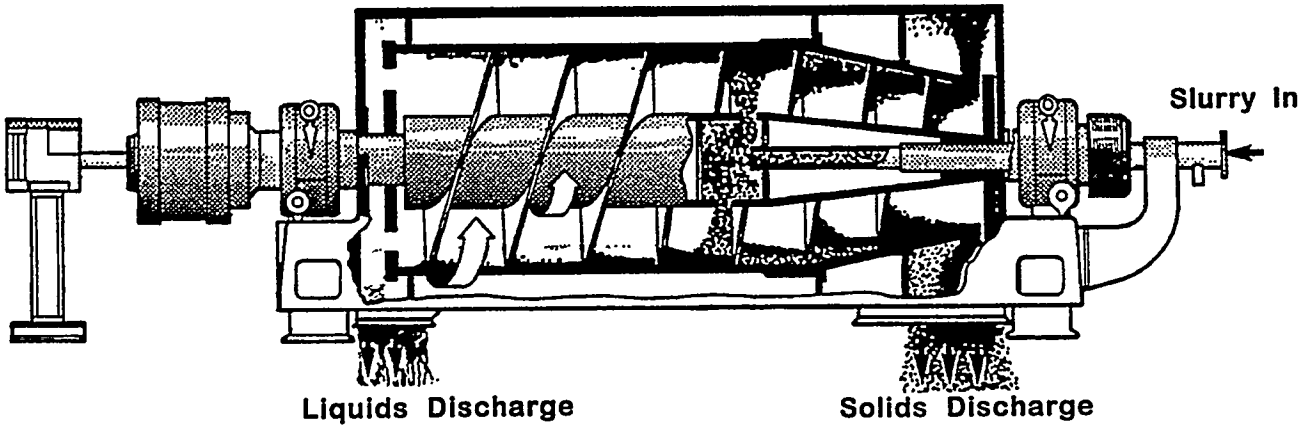

Figure 8-10. SCHEMATIC DIAGRAM OF THE SOLID-BOWL CENTRIFUGE

density gradient created by the settling of the magnetite, the light coal particles do not settle or settle at a much slower rate compared to the refuse particles. As such, the clean coal and a portion of the dense medium are discharged through the weir openings located opposite of the feed end. The settled refuse particles and the remaining portion of the dense-medium slurry are conveyed by the scroll to the conical section of the bowl where they are discharged.

The separation can be changed by varying the bowl and scroll speeds, the feed rate, and the weir height. In order to minimize the extent of magnetite classification in the centrifuge, it is necessary to operate the centrifuge at a lower bowl speed and hence, lower number of g's than would be used for solid-bowl dewatering applications. Varying the scroll speed independent of the bowl speed changes the differential speed between the two. This allows a slower or faster rate of discharge of the settled solids. Variations in the feed rate and weir height also can be made to control the volume of the dense medium that reports to the discharge ports.

A series of tests was run at different centrifuge settings to determine an operating range for the centrifuge. It was found that a bowl speed of 800 rpm, which translated to 55 g's, a differential (between the bowl and scroll speeds) of 5.3, a feed rate of 3 gpm, and a weir setting to give the maximum pond depth were appropriate for producing a dense-medium slurry discharge at both ends of the centrifuge.

Samples were taken of the overflow and underflow streams and the relative density of the slurry was calculated for each. These results are shown in Table 8-2. It can be seen that the relative density differential was approximately 0.2 in each case. Furthermore, the calculated feed relative density was the same as that being pumped to the centrifuge. This indicates that the centrifuge was operating under steady-state conditions. Testing was initiated to separate the -100 mesh Upper Freeport seam coal (Type III) under similar operating conditions.

MAGNETIC FLUID SEPARATION

Testing of a magnetic-fluid based separator, which consisted of a modified Franz magnetic separator with the machined pole pieces as described in a previous report[5], was initiated. A mapping of the magnetic field was conducted using a Gauss meter and an appropriate probe. The variation of the field intensity at a fixed current as a function of the height in the gap region is shown in Figure 8-11. As can be seen, the rate of decrease in the magnetic field intensity was nearly constant from the bottom to the top of the gap area. Hence, the magnetic field gradient, which is defined by the slope of the curve, is approximately uniform with a magnitude of 593 Gauss/cm. This gradient is required to produce the buoyant force (i.e., apparent density) needed to separate the particles. The apparent density of the fluid, ρ_a, is given by

$$\rho_a = \rho_f + \frac{\mu |\nabla H|}{4\pi g} \qquad (8\text{-}12)$$

Table 8-2 Relative Densities of Product Streams from the Solid-Bowl Centrifuge (measured feed relative density =1.30).

Product	Relative Density	Feed Relative Density (Calculated)
Overflow 1	1.21	1.30
Underflow 1	1.41	
Overflow 2	1.24	1.30
Underflow 2	1.40	
Overflow 3	1.24	1.30
Underflow 3	1.41	

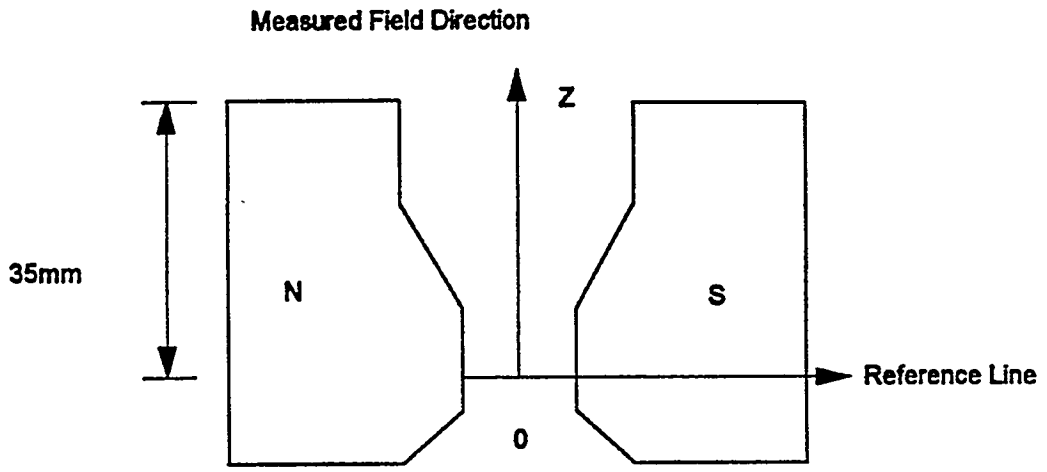

SIDE VIEW OF THE MAGNET

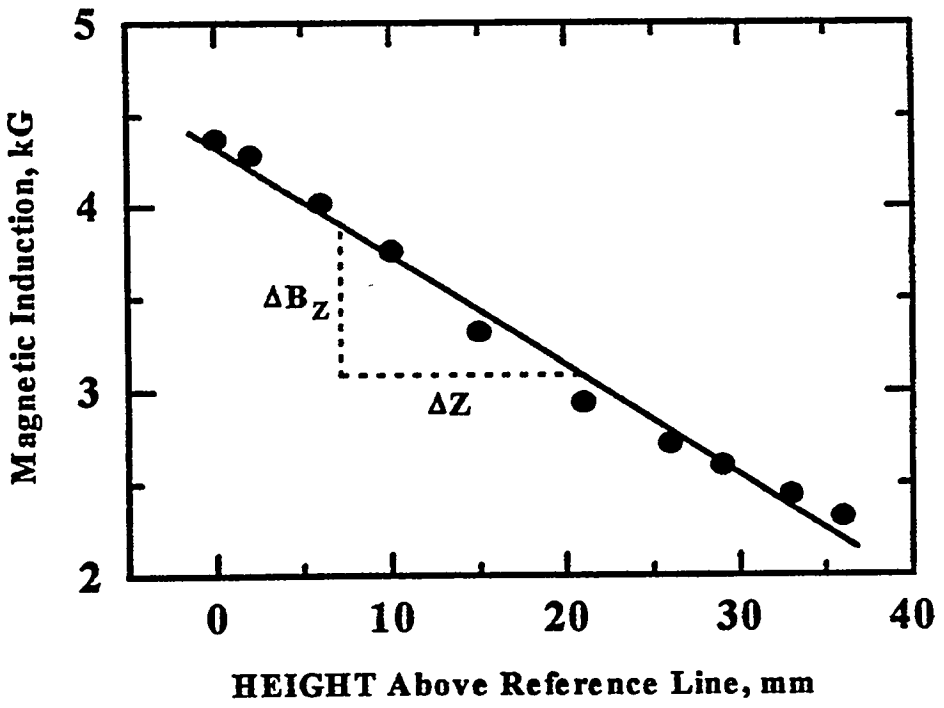

Figure 8-11. VARIATION OF THE MAGNETIC FIELD BETWEEN THE POLE PIECES AS A FUNCTION OF THE HEIGHT FOR A GAP SETTING OF 24 mm

where ρ_f is the true density of the fluid, μ is the fluid magnetization, ∇H is the magnetic field gradient, and g is the gravitational acceleration. Measurements also showed that the design of the pole pieces produced a uniform magnetic field along the length of the device as desired. Separations using the Upper Freeport seam coal were initiated. These will be described in more detail under Phase III.

8.4 Subtask 2.4 Agglomeration/Flotation Studies

DEVICE TO SIZE SEPARATE FLOTATION PRODUCTS

To evaluate the kinetics of fine coal cleaning, size separation of flotation products in the range of 10 to 74 μm is desired. For such purposes, a Cyclosizer has been used in the past by many investigators. A Warman cyclosizer, which is a five product particulate separation system, was used in this part of the investigation. Particle sizing is accomplished in a series of inverted cyclones whereby the apex discharge is allowed to collect in an enclosed apex chamber. The device was first calibrated with fine particles of silica. Several problems were encountered when attempts were made to separated coal samples. To remove the very fine particles, the material was decanted prior to the analysis by the cyclosizer. Most of the -10 μm particles were separated in this manner. The size distributions of the 5 cyclosizer products are given in Figure 8-12. Even though the sample had been decanted, about 30 % of the material was lost as carry over with water. The weights recovered in various cyclones are given in Table 8-3 for two repeat tests. Cylones 1 and 2 captured smaller but denser particles as can be seen from the ash analysis results in Table 8-4. The use of micromesh sieves to classify the products was also explored but the method was much too laborious. Therefore, a Donaldson air classifier was used and the results are presented in Table 8-5 It can be seen that the ash and sulfur values of various products did not vary considerably and one can assume that the separation is primarily based on particle size. The method is being used to fractionate coal flotation products. From the results, we plan to determine flotation kinetics as a function of particle size.

AGGLOMERATION FLOTATION

Agglomerate flotation of Lower Kittanning (Type II) and Upper Freeport (Type III) coals was not very successful, probably due to inadequate liberation. To improve the coal quality, alternate circuit configurations were considered and the results are presented in the paragraphs that follow.

In this study, four different grinding-flotation circuits, as shown in Figure 8-13, were investigated for various coals to establish the role of circuit configuration on efficiency of coal cleaning.

Circuit 1: Coarse grinding to -600 μm and flotation

Circuit 2: Fine grinding to -65 μm and flotation

Circuit 3: Fine grinding with 2 stages of flotation

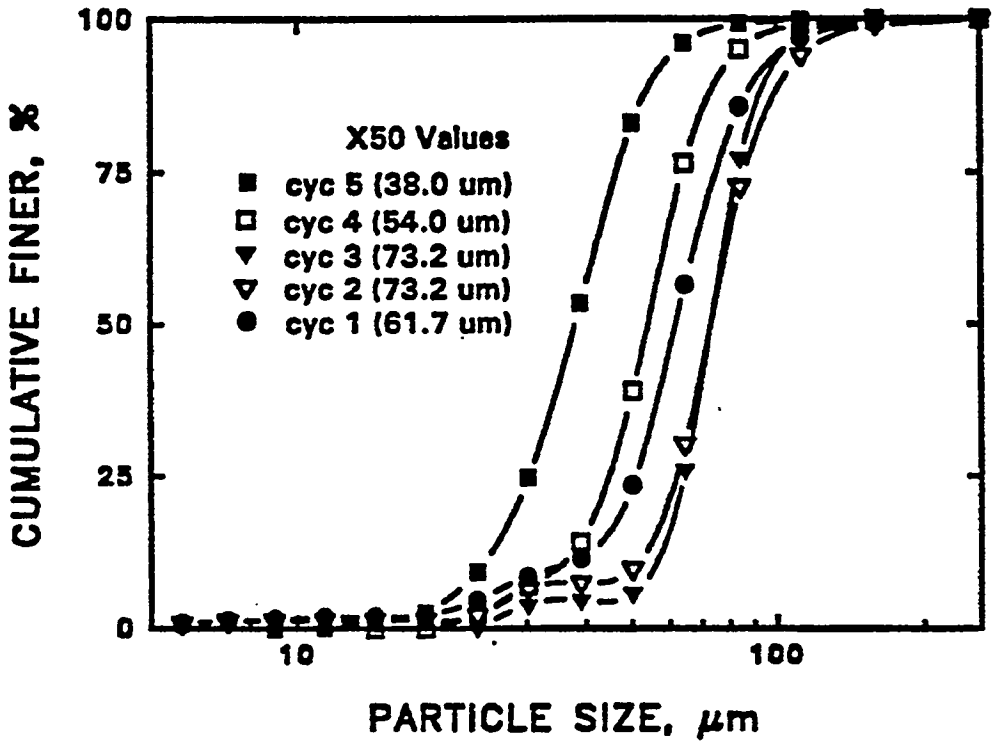

Figure 8-12. CYCLOSIZER PRODUCT SIZE DISTRIBUTIONS USING COAL (Repeat test 0207)

Table 8-3. Cyclosizer Weights and Recovery Percents for Replicate Tests.

	Test #: 0207		Test #: 0217	
	Weight, g	Weight, %	Weight, g	Weight, %
Feed Weight	48.35		27.25	
cyclone 1	0.7	1.4	0.9	3.3
cyclone 2	1	2.1	0.75	2.8
cyclone 3	10.7	22.1	7.15	26.2
cyclone 4	13.8	28.5	8.8	32.3
cyclone 5	4.8	9.9	3.1	11.4
recovery		64.1		76.0

Table 8-4. Material Balance for Cyclosizer Products.

Product	Wt., %	Assay Ash, %	Recovery Ash, %
cyclone 1	1.90	69.00	13.68
cyclone 2	2.50	42.99	11.21
cyclone 3	34.78	7.19	26.06
cyclone 4	39.29	6.81	27.88
cyclone 5	17.02	8.06	14.29
decant	4.50	14.64	6.87
	100.00	100.00	100.00

Table 8-5. Attribute Tracking in Donaldson Products.

Product	Wt., (%)	Assay, (%)		Recovery, (%)	
		Ash	Sulfur	Ash	Sulfur
74 µm	1.14	7.4	1.60	1.23	1.17
63 µm	3.85	7.2	1.32	4.06	3.26
49 µm	2.93	5.8	1.46	2.49	2.74
40 µm	3.42	5.8	1.45	2.91	3.18
33.3 µm	17.38	6.7	2.14	17.06	23.84
21.9 µm	15.96	6.9	1.65	16.13	16.88
12.5 µm	39.69	6.7	1.38	38.95	35.10
4.4 µm	15.63	7.5	1.38	17.17	13.83
Total	100.00	6.83	1.56	100.00	100.00

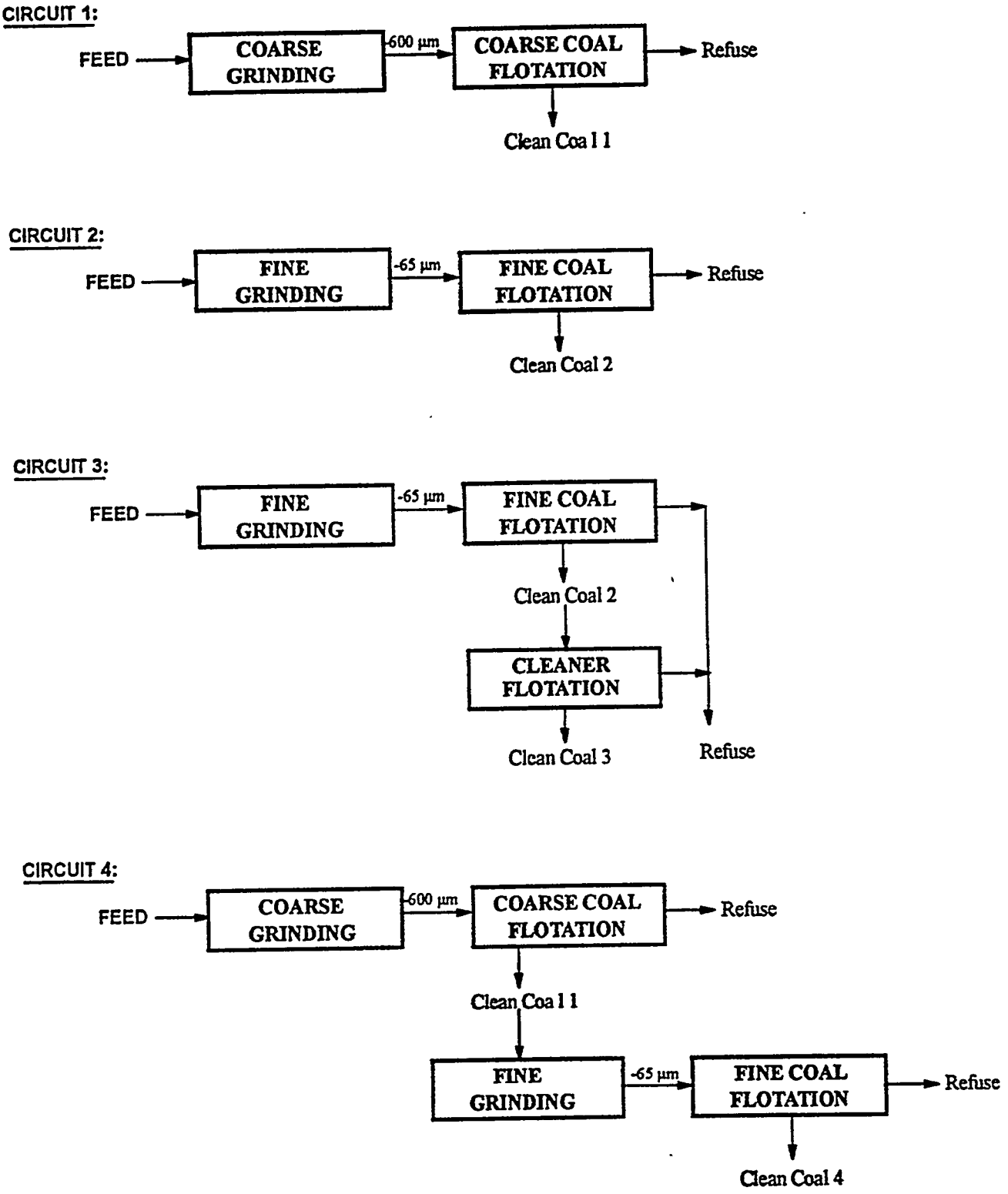

Figure 8-13. VARIOUS GRINDING-FLOTATION CIRCUIT CONFIGURATIONS

Circuit 4: Coarse grinding and flotation followed to a regrinding of the froth product and flotation of fine coal

For the ease of comparison, the results obtained from each circuit are presented in Figures 8-14 to 8-17 for Pittsburgh, Indiana, Lower Kittanning and Upper Freeport coal, respectively. In these figures, the symbol □ is used for Circuit 1, Δ is used for Circuit 2, ◊ is used for circuit 3, and ▼ is used for Circuit 4.

Circuit 1: Coarse Grinding and Flotation

Flotation studies were performed for the coal ground to -600 μm using 0.28 kg/T of dodecane as collector and 0.5 kg/T of MIBC as frother. A clean coal product of about 5.5% ash for Pittsburgh, 6.7% ash for Lower Kittanning and 6.7% ash for Upper Freeport were obtained with a combustible matter recovery of 80%. In the case of Indiana VI coal, the ash content was high (5.8%) and the combustible matter recovery was low (50%). In this approach, the decrease in ash content was not satisfactory.

Circuit 2: Fine Grinding and Flotation

In this scheme, the feed was ground to -65 μm in order to increase the degree of liberation. Based on preliminary tests, the amount of collector was varied with coal type as follows: 0.07 kg/T for Pittsburgh, Lower Kittanning and Upper Freeport coal samples and 11.2 kg/T for Indiana VI coal. With the exception of Indiana VII (Type II coal), the selectivity improved with a decrease in particle size probably due to better liberation. For Indiana VII coal, on the other hand, the ash content of clean coal was much greater with even lower combustible matter recovery (25%). In order to further decrease ash content of the clean coal products, a block copolymer was employed. This reagent increases the hydrophobicity of coal and therefore enhances the separation. Aliquots of aqueous solution of the Pluronic L-64 and the collector were added to the flotation cell. The effect of surfactant on the flotation efficiency was found to be a function of surfactant concentration. Selected results are given in Figures 8-14 to 8-17 with dashed lines through the data points. It can be seen that the presence of the polymeric surfactant substantially enhanced the ash rejection for Pittsburgh and Indiana VII coals. The ash rejection was more and the combustible matter recovery was higher. For Lower Kittanning and Upper Freeport coals, on the other hand, the influence of surfactant was relatively small.

Circuit 3: Fine Grinding-Rougher and Cleaner Flotation

This circuit was tested only for the Lower Kittanning coal sample. A cleaner flotation stage was added after fine grinding and flotation. The quantities of the collector, frother and surfactant were the same as in circuit 2. In the cleaner stage, only frother was used. The results are added to Figure 8-16. It can be seen that a cleaner flotation stage increased the ash rejection considerably. A clean coal product of 5.4% ash with 80% combustible matter recovery was obtained. This

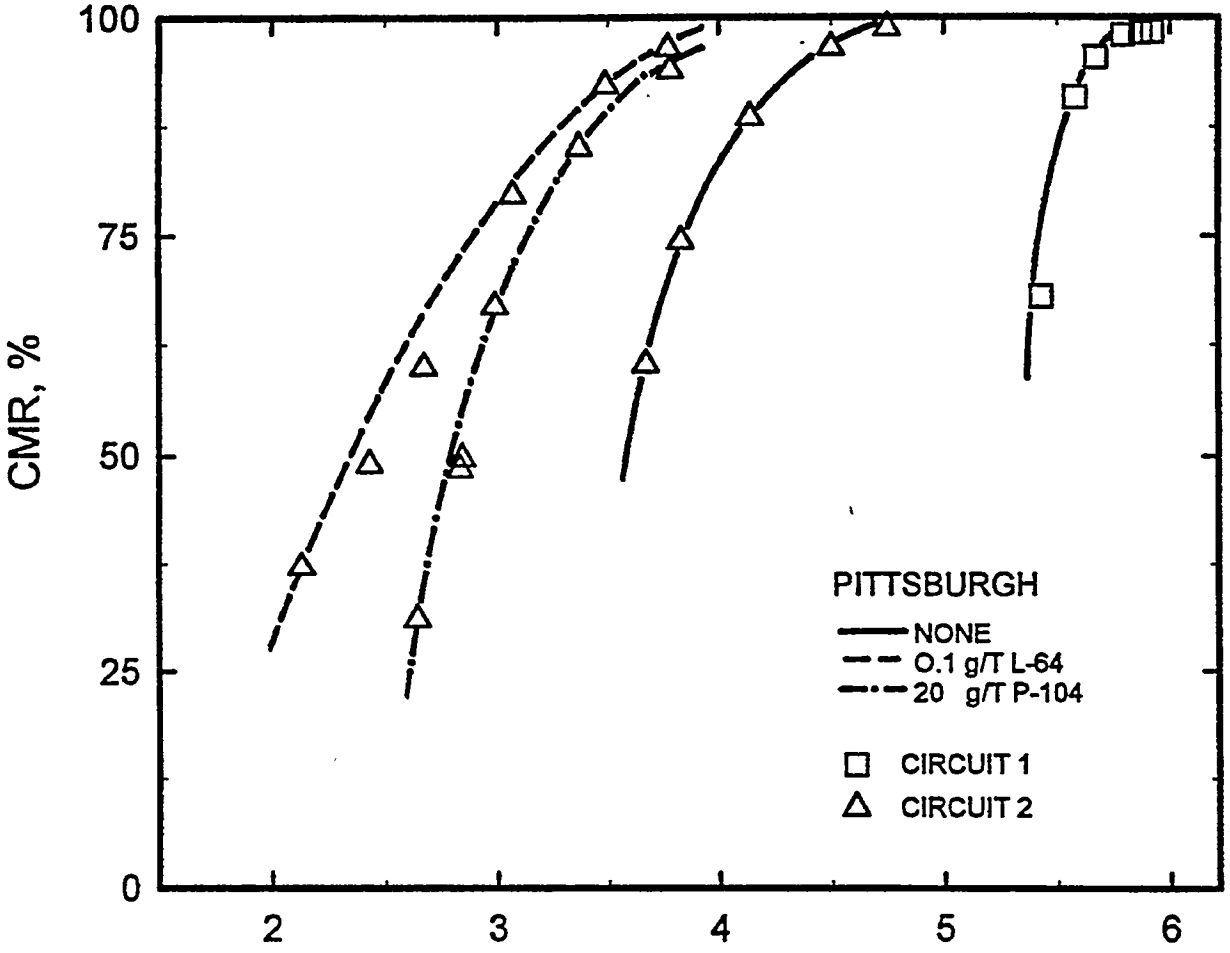

Figure 8-14. EFFECT OF VARIOUS GRINDING-FLOTATION CIRCUITS ON FLOTATION OF PITTSBURGH SEAM COAL

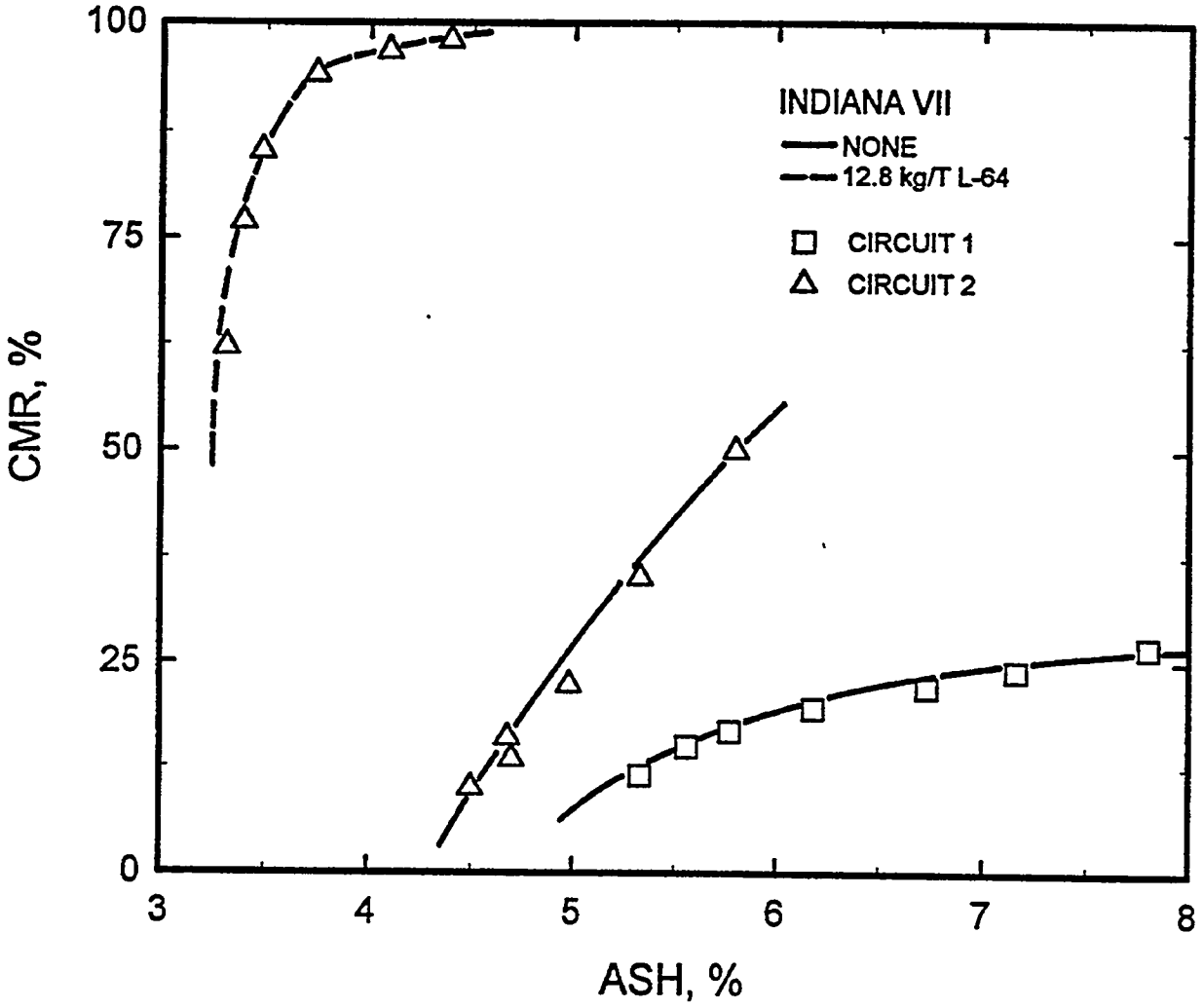

Figure 8-15. EFFECT OF VARIOUS GRINDING-FLOTATION CIRCUITS ON FLOTATION OF INDIANA VII SEAM COAL

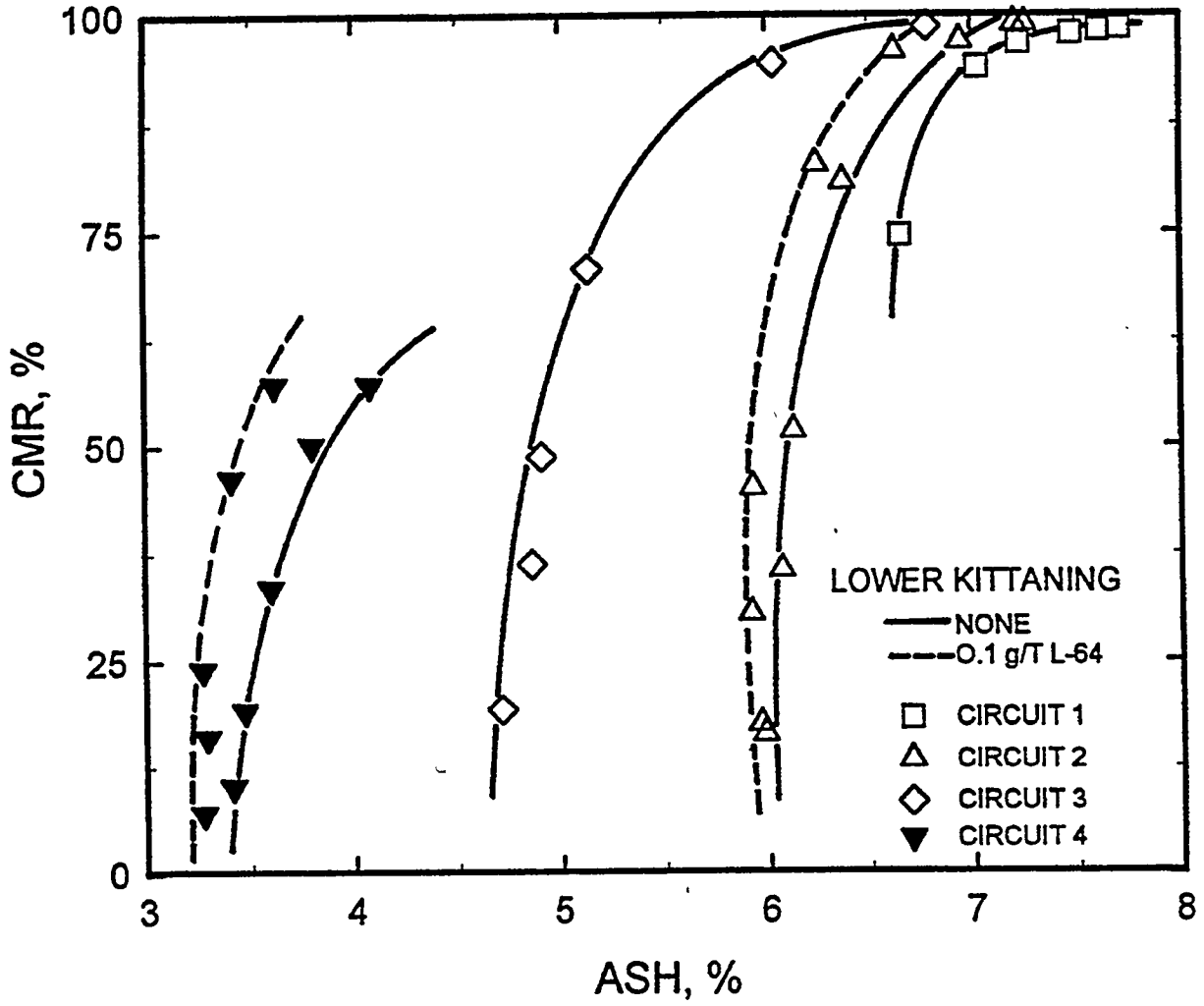

Figure 8-16. EFFECT OF VARIOUS GRINDING-FLOTATION CIRCUITS ON FLOTATION OF LOWER KITTANNING COAL

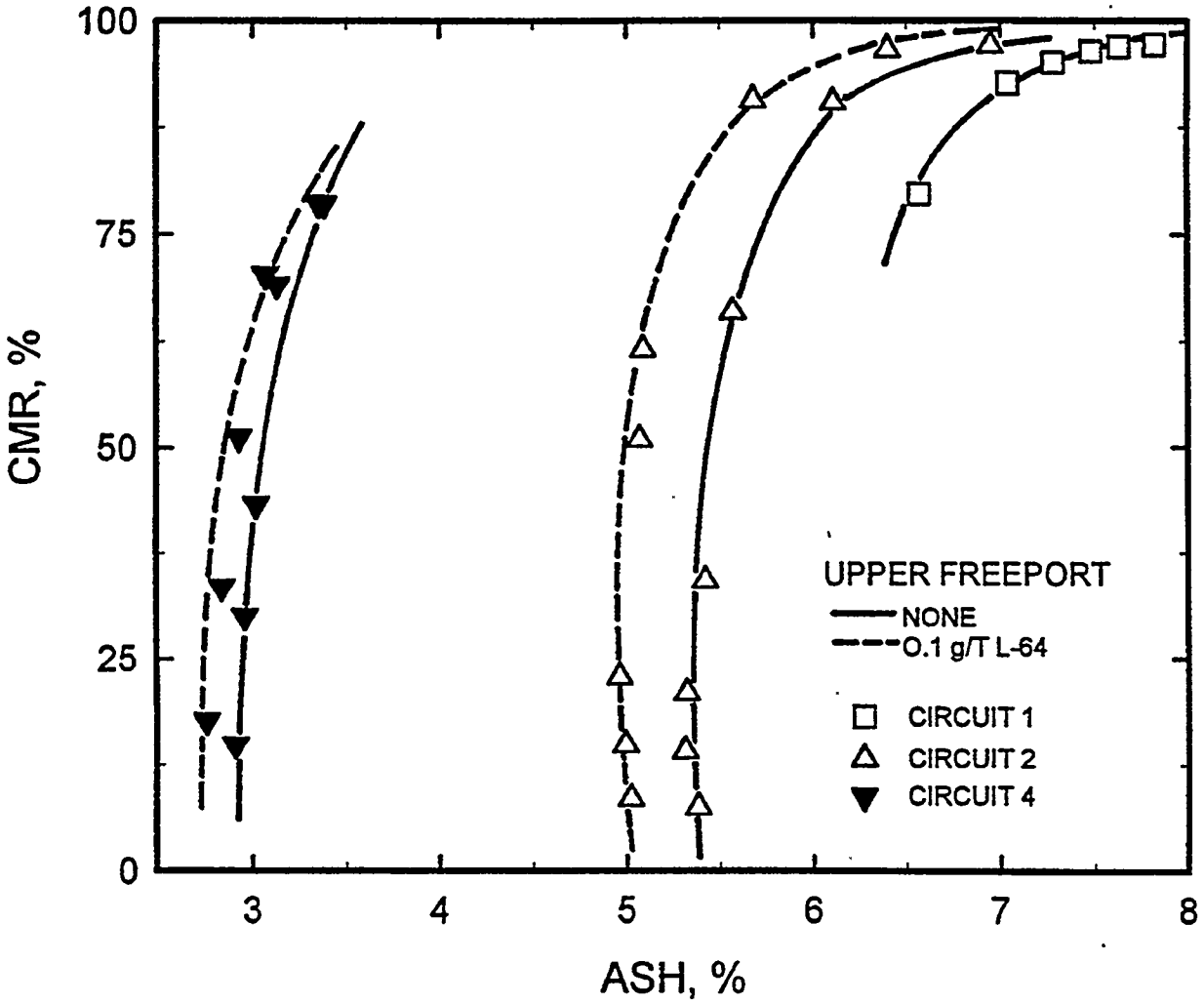

Figure 8-17. EFFECT OF VARIOUS GRINDING-FLOTATION CIRCUITS ON FLOTATION OF UPPER FREEPORT COAL

improvement can be explained by successive cleaning of the entrained ash material and locked coal particles from clean coal product of the rougher flotation stage.

Circuit 4: Coarse Grinding-Rougher Flotation-Re Grinding-Cleaner Flotation

This circuit was tested for Lower Kittanning and Upper Freeport coals due to lack of satisfactory flotation response observed with these coals in the other three process circuits. In the rougher stage, flotation was carried out using coarse feed (-600 μm) and 0.5 kg/T of MIBC. The froth product collected for one minute contained 6% ash for Lower Kittanning and 5.8% ash for Upper Freeport. These products were ground further to obtain finer feed material (-65 μm) for the cleaner flotation stage. In the cleaner stage, dodecane (0.07 kg/T) and MIBC (0.5 kg/T) were used as collector and frother, respectively and the results are presented in Figures 8-16 and 8-17 for the two coals. The results show that the efficiency of coal cleaning was improved by this circuit configuration. For the Lower Kittanning coal (Type II), a clean coal product with an ash content of 4.2% at a combustible matter recovery of 60% was obtained in the absence of the surfactant. The corresponding ash was 3.6% when the block copolymer was used as a promoter (dashed line, filled triangle in Figure 8-16). For the Upper Freeport coal, a clean coal product of about 3.2% ash was obtained with a combustible matter recovery of 75%. Even though the product ash was less, the effect of the block copolymer reagent was less dramatic.

Based on these results, one can conclude that the selection of the most effective grinding-flotation circuit depends on coal type. In some coals (coals with feed ash content less than 8%), application of Type II circuit in the presence of surfactant is sufficient to obtain a clean coal product with a satisfactory quality and acceptable recovery. In other coals (coals with high feed ash), the Type II circuit and the use of surfactant might not be enough and the use of circuits III or IV would become necessary.

8.5 Subtask 2.5 Fundamental Studies of Surface-Based Processes

SURFACE TENSION

Studies were continued to determine the surface tension of the block copolymer reagents which increase the separation efficiency of coal flotation. The values of CMC published in the literature vary over a large magnitude and there is no general agreement[140-142].

Surface tension measurements were made for PEO/PPO/PEO block co-polymer solutions with a Kruss Digital Tensiometer K10T using Wilhelmy Plate method. To prepare the surfactant solutions, double distilled water with a resistivity of at least 1.5 Mohm was used in all the experiments. The distillation equipment was a Barnstead 210 Biopure Distilled Water System which was equipped with a Q baffle system to produce pyrogen free water. Solutions were prepared at room temperature and stirred before each measurement. The pH was not adjusted. The glassware was cleaned with a chromic acid solution before usage.

It was found at concentrations less than CMC (~$1x10^{-6}$ M), the surface tension varied with time, the volume of liquid in the measurement vessel and the number of these molecules in the system. Therefore, these measurements were done as a function time at varying concentrations using 50 ml of solution in a vessel 4.5 cm in diameter. At these concentrations, the solutions were gently stirred to enhance diffusion. In the absence of stirring, the time of equilibration was very long and the reproducibility of measurement was poor. The results are presented in Figure 8-18 for the reagent, Pluronic L-64. At very low concentrations of 10^{-9}, 10^{-8} M and $2x10^{-8}$ M, one hour was not enough for diffusion of surfactant molecules to the surface. The time needed to reach a constant value of surface tension decreased with increasing concentration of the reagent.

The equilibrium surface tension values are presented in Figure 8-19 as a function of surfactant concentration. The surface tension decreased from 72 dynes/cm with increasing concentration and reached a minimum value of about 33 dynes/cm. The shape of the surface tension versus concentration plot is quite complex and is difficult to interpret at this stage. Recently, similar results were reported by Hecht and Hoffmann,[140-142] for a different reagent, Pluronic F127. These studies are being continued because the surface tension effects both contact angle and flotation of coal. Mechanism of adsorption will be established after completion of the studies.

CONTACT ANGLE

Captive bubble method was used to measure contact angles on a polished coal substrate. Coal samples were selected by avoiding those with cracks, locked particles of pyrite, mineral occlusions, etc. The polishing procedure consisted of rough polish on a series of emery papers followed by wet polishing for about 20 minutes each on rotating laps using, successively, 1.0, 0.3 and 0.05 μm alumina suspension. The samples were washed thoroughly with distilled water to remove any adhering alumina particles and stored under nitrogen. Prior to a measurement the sample was polished again with 0.05 μm alumina for 10 minutes. Powder free vinyl gloves or glass forceps were used for all specimen handling to avoid contamination. For measurements, the substrate with an area of about 1 square inch was divided into about 40 imaginary subsections. Independent contact angle measurements, each corresponding to a separate sub-section, were carried out, resulting in a total of 40 contact angle measurements for a given set of conditions. An air bubble generated by a Gilmont micro syringe was brought in contact with the polished surface. Once the three phase contact had occurred, the air bubble was released from the syringe by moving the syringe assembly slowly to a side. The angles were measured with a Goniometer attached to a microscope used for observing the air bubble or the oil droplet.

Extra polishing was needed once the samples were exposed to the oil. In this case, repolishing with 0.05 μm alumina was not enough to regenerate the original. A complete polishing procedure was required to obtain oil-free surface. For example, in the case of Pittsburgh coal, the

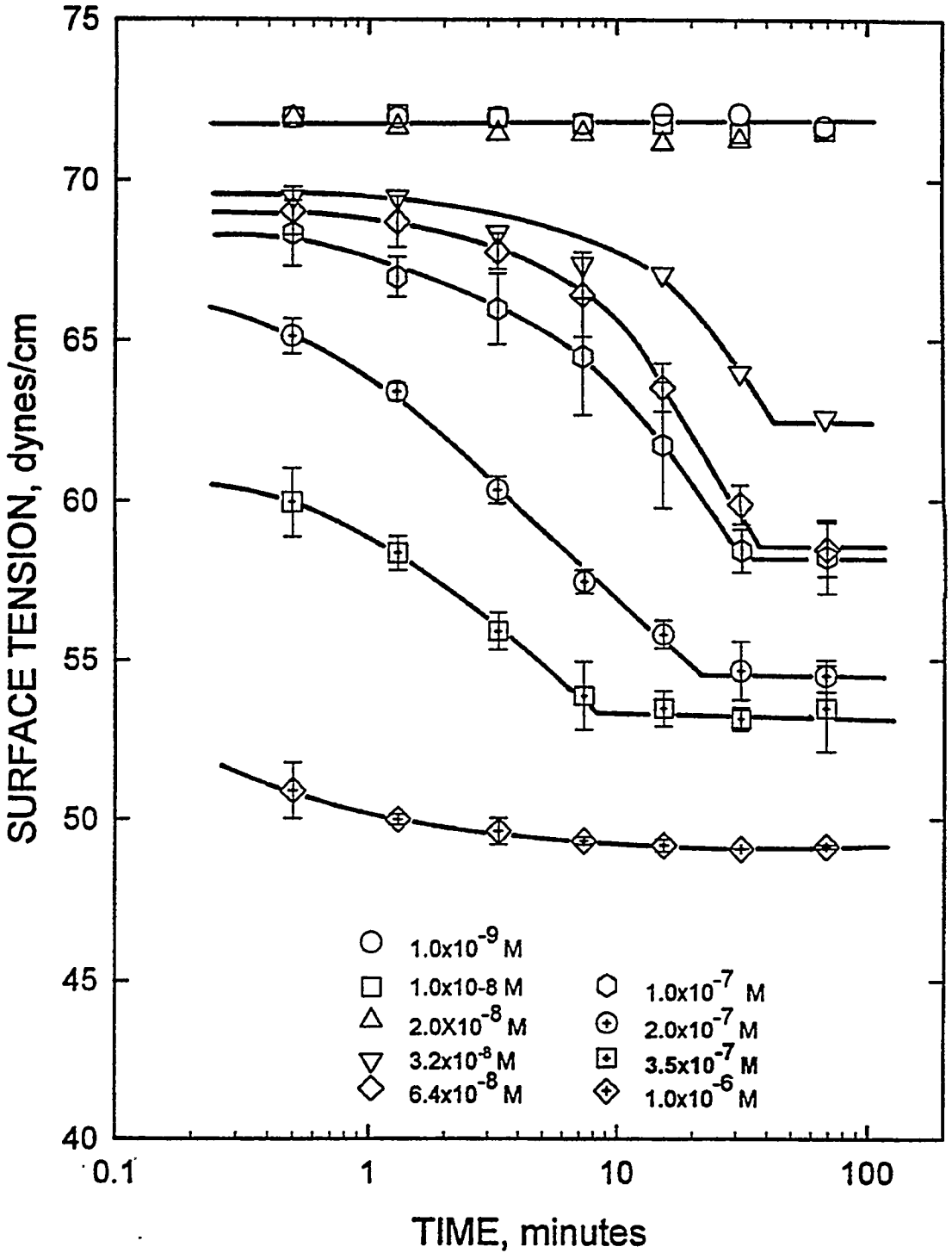

Figure 8-18. SURFACE TENSION AT VARIOUS PLURONIC L-64 CONCENTRATIONS AS A FUNCTION OF TIME

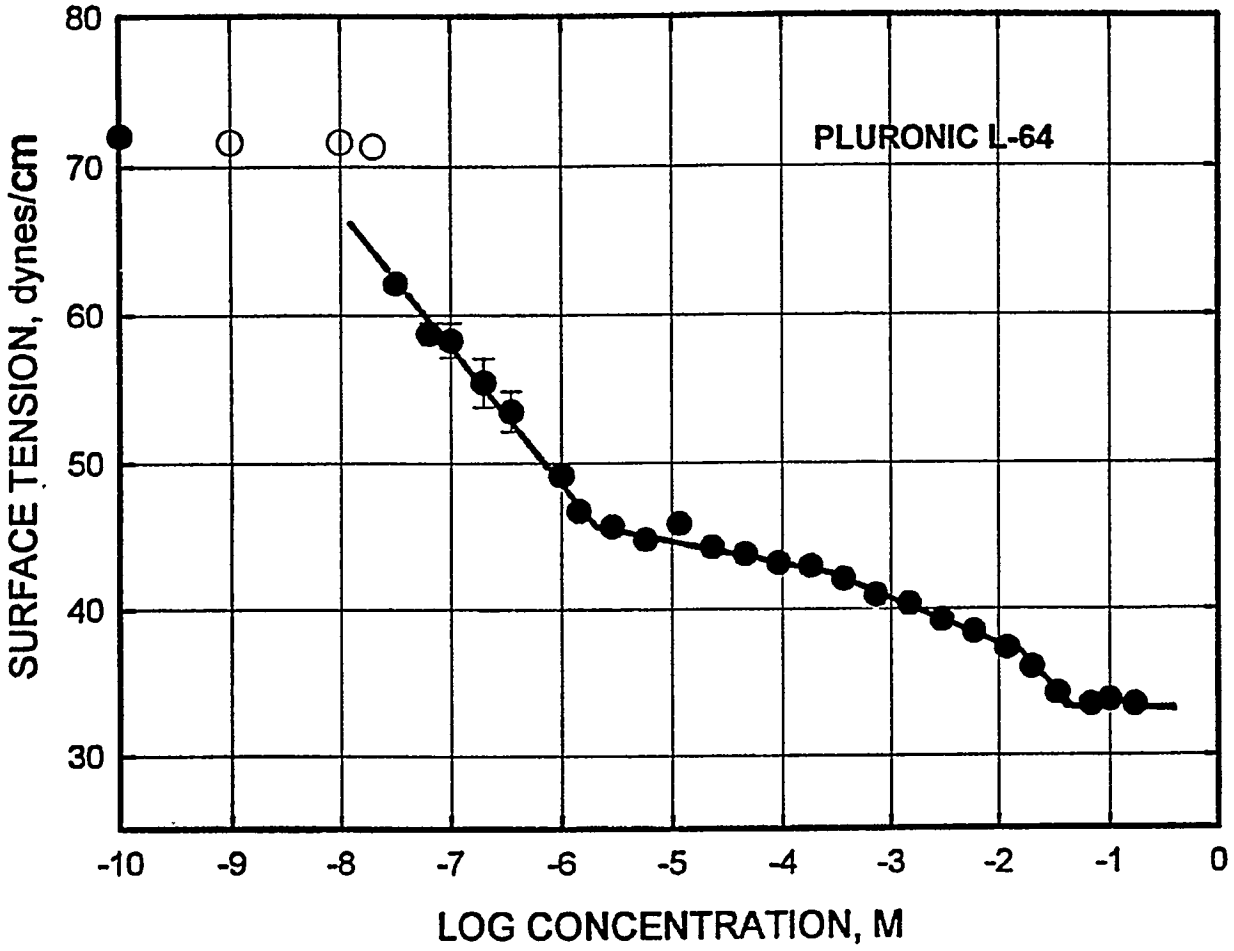

Figure 8-19. SURFACE TENSION AS A FUNCTION OF PLURONIC L-64 CONCENTRATIONS

average contact angle was found to be 47.3 and 67 degrees for coal/air/water and coal/dodecane/water systems, respectively. When the sample was polished only with 0.05 μm alumina after exposing the hydrocarbon, these values increased to 54.5 and 89.9 degrees, respectively.

The average contact angle values obtained for coal/air/water and coal/dodecane/water systems are given in Table 8-6. It includes the contact angles of three type of coals under various conditions. It can be seen that three samples of the Upper Freeport coal, UFA, UFB and UFC gave very different values of the average contact angle (47.5, 51.6 and 32.1). Close examinations revealed that the UFC sample contained a substantial portion of a more hydrophilic maceral and consist of vary narrow bands (< 1 mm in thickness) of unidentified macerals. In contrast, the UFA sample consisted of broad maceral bands, most likely vitrinite. No clear bands were seen in sample UFB.

Effect of Block Co-Polymers:

In a separate study, it was observed that block co-polymers of PEO/PPO/PEO rendered the surface of coal more hydrophobic and the contact angle was a strong function of surfactant concentration and type. For the three coals, the contact angle increased with an increase in concentration and reached a maximum at a concentration between $1x10^{-7}$ M and $1x10^{-6}$ M for all the surfactants tested. It can be seen from Figure 8-20 that the effect of surfactant on contact angle was also a function of coal type. However, the surfactant concentration for the maximum contact angle was about the same (~10^{-6} M) for all the coals tested. The contact angle decreased as the concentration approached the critical micelle concentration (CMC) most probably due to the formation of surface micelles. In Table 8-6, selected contact angles are given for both the coal/air/water and coal/dodecane/water systems.

8.6 Subtask 2.6 Column Flotation

Test work on Type II-1 (Lower Kittanning) and Type III-1 (Upper Freeport) coals has been carried out in Phase II of the project. The washabilities of these coals were given in a previous report [137]. The flotation experiments were carried out in a 0.063 m diameter flotation column equipped with a Mott Metallurgical bubble generator. The column had an overall height of 1.5 m and was operated in a semi-batch mode with tailing recirculation[143]. Provision was made for the recycle stream to be introduced at elevations of 0.33 m, 0.64 m, 0.89 m and 1.14 m from the base of the column. Except where indicated, counter-current flow of air and tailings slurry was maintained with the tailings stream entering at a height of 0.89 m from the base of the column. A schematic of the experimental set-up is shown in Figure 8-21.

The raw coal was ground in a disc pulverizer, and sieved through a -100 mesh screen. A coal slurry was prepared using a weighed amount of the - 100 mesh fraction and transferred into the column using a peristaltic pump. The required dosage of methyl iso-butyl carbinol (MIBC)

Table 8-6. Contact Angle Values of Three Coals Under Various Conditions.

Coal	Sample	Coal/Air/Water	Coal/Dodecane/Water
		θ_A	θ_D
Pittsburgh Coal	PA1	47.3[a]	67.0[a]
	PA2	54.5[b]	89.9[b]
	PA3	47.2[a]	-
Upper Freeport Coal	UFA1	47.5[a]	79.7[b]
	UFA2	-	81.1[b]
	UFA3	-	72.5[b]
	UFB1	51.63[b]	91.8[b]
	UFC1	32.10[b]	77.9[b]
Lower Kittanning	LKA1	45.1[a]	-
	LKA2	47.0[b]	88.0[b]
Coal/surfactant (10^{-7} M L-64)		θ_A	θ_D
Pittsburgh	PA1	57.0[a]	77.0[a]
Upper Freeport	UFA1	58.0[a]	-
Lower Kittanning	LKA1	52.5[a]	-

[a] Angles are average of about 30-50 measurements.
[b] Angles are average of about 20-40 measurements.

The last digit in the sample code refers to:
1 = Measurements were done on an original, well polished sample.
2 = Measurements were done on a sample which exposed to oil after polishing with 0.05 μm alumina.
3 = Measurements were done on a sample which exposed to oil after polishing with 1.0, 0.3 and 0.05 μm alumina.

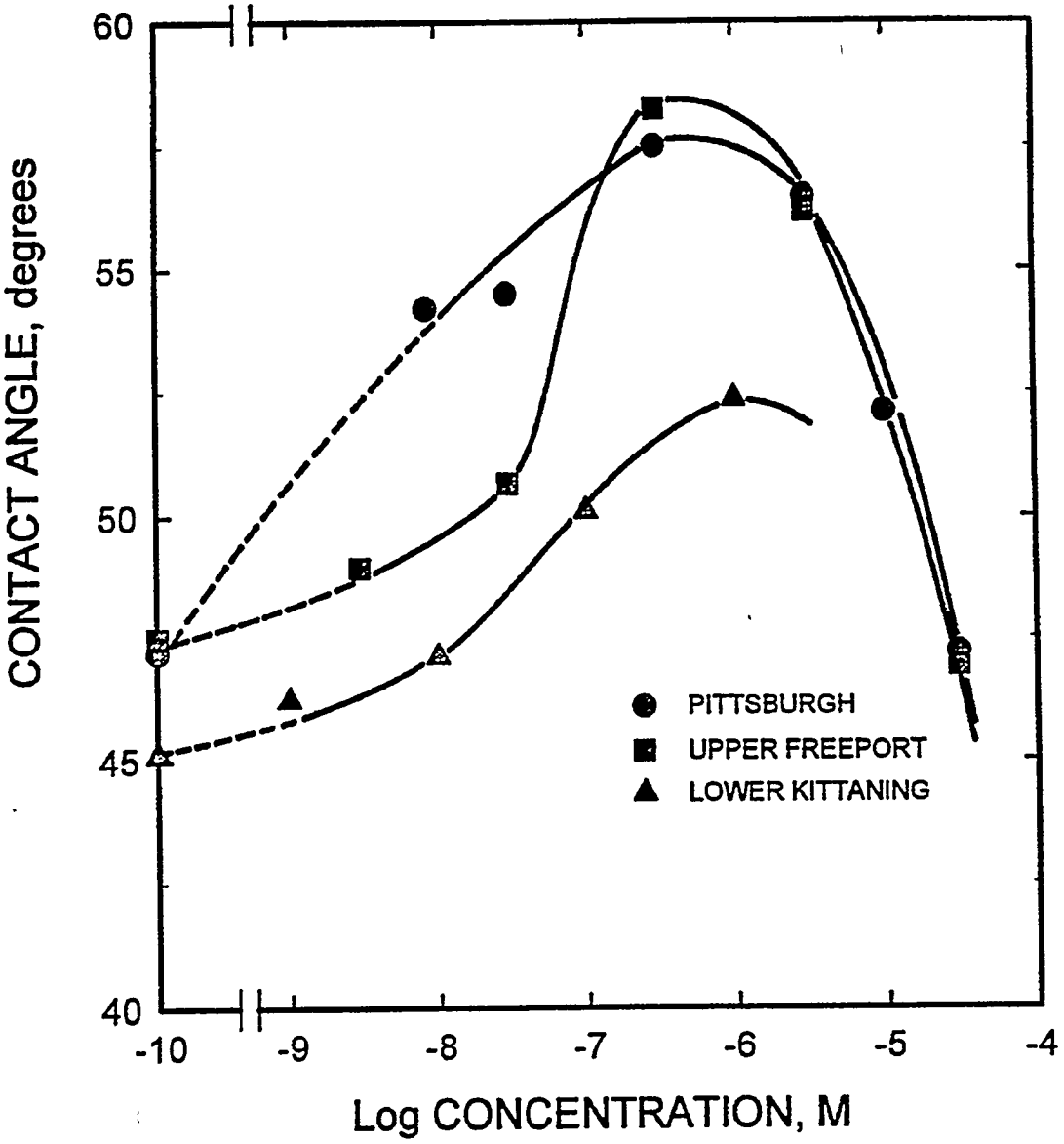

Figure 8-20. CONTACT ANGLES FOR THREE COAL SAMPLES AS A FUNCTION OF PLURONIC L-64 CONCENTRATION

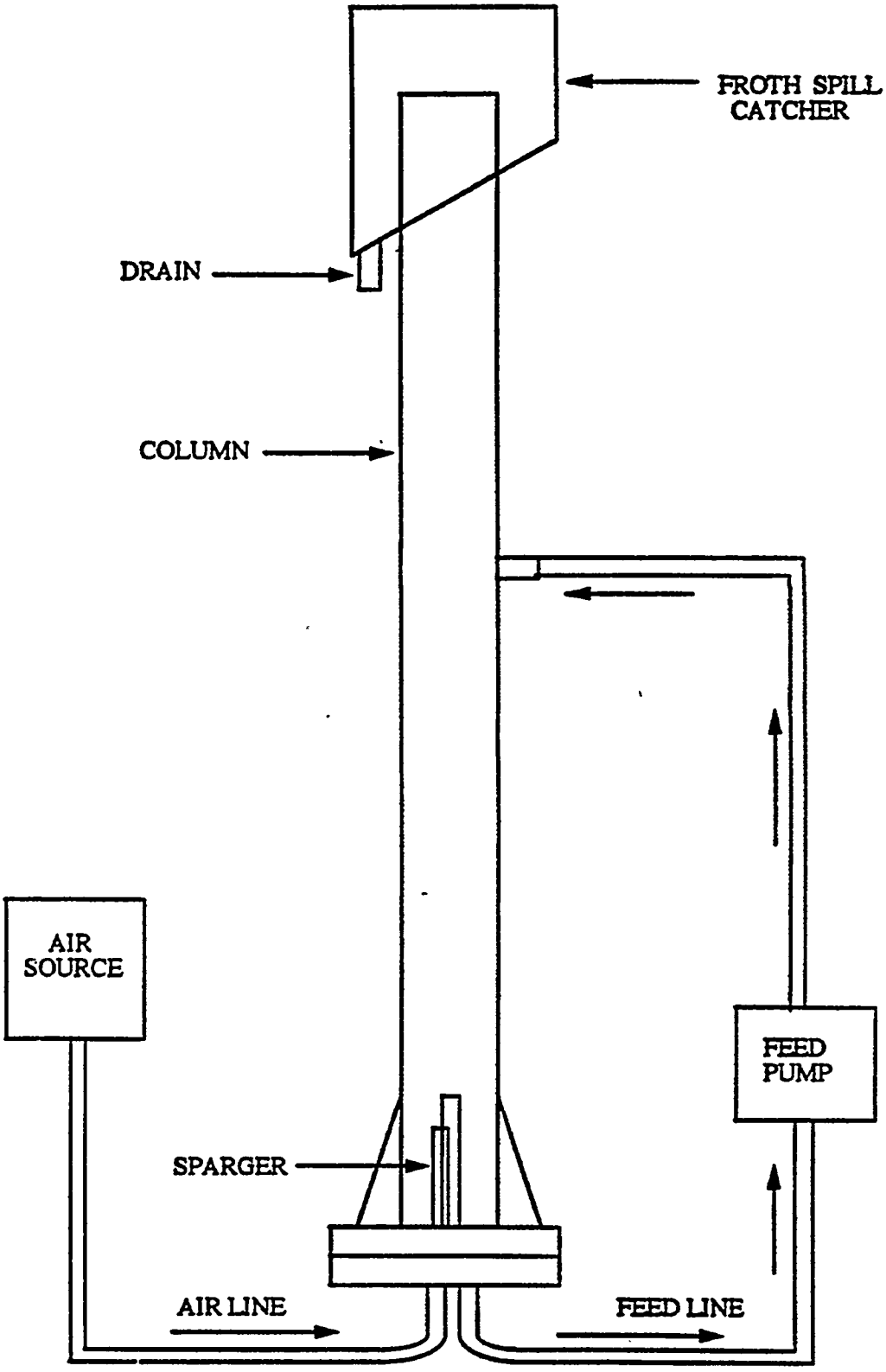

Figure 8-21. SCHEMATIC DIAGRAM OF THE EXPERIMENTAL SET-UP

frother was added using a hypodermic syringe. The tailings were recirculated at a fixed rate of 0.072 m^3/h. After allowing for the frother to be properly mixed with the slurry, the air was turned on to the desired value and the froth overflowing the cell lip was collected as a function of time. The froth product was filtered, dried and weighed. The clean coal fractions recovered at the different time intervals were analyzed for sulfur and ash contents. Sulfur was determined using a LECO model SC-432 analyzer. Initially, the ash content was determined by ASTM method employing a Fisher Coal Analyzer (Model 490). However, with the commissioning of our new LECO thermogravimetric analyzer (Model TGA-501), the ash analysis is currently being repeated. From the composition and mass of feed and concentrate, the yield, ash and sulfur rejections (ash/sulfur rejection is defined as the fraction of ash/sulfur recovered in the tailings stream) were calculated. The variables investigated were: gas velocity, feed solids concentration (5%, 10% and 15%), collector and wash water addition. In the case of Upper Freeport coal, the effects of frother concentration and ground coal storage under argon were also investigated. In the aging experiments, the ground coal samples were stored under argon for approximately one month prior to flotation.

UPPER FREEPORT COAL

The effect of frother concentration on yield is shown in Figure 8-22. At the three levels tested, the highest yield was obtained at a concentration of 50 ppm (v/v). Thus, the frother concentration was fixed at this level for the subsequent experiments.

The variation of clean coal yield with grade is shown in Figure 8-23. In general, the results show that the clean coal ash and sulfur contents increase with yield. However, slightly better *grade-yield* curves were obtained with freshly ground coal, with the effect being more pronounced with ash content. Thus, the subsequent experiments were carried out on freshly ground samples. The results obtained in this study are consistent with those reported earlier by Huettanhain [144] for single-stage microbubble flotation of an Upper Freeport seam coal. They also show that a clean coal product with an ash content of 5% may be obtained at yields lower than 45%. However, the target objective of 1% sulfur was not attained in any of these experiments.

The effects of wash water (273 ml/m) and collector (0.4 kg/T dodecane) addition on the grade-yield curve are shown in Figure 8-24. The results obtained are similar to those observed with freshly ground coal. However, the yield of clean coal with ash content less than 5% increased by about 11% (to 56%) with the use of dodecane. These results also show that the addition of collector (0.4 kg/T dodecane) had negligible effects on the initial rates of flotation (see Figure 8-25). However, there was a 15% drop in the terminal yield with collector addition. This observation (i.e. reduced yield with dodecane addition) may be related to changes in froth characteristics (e.g. water content, mobility, etc.). For example, there was a considerable amount

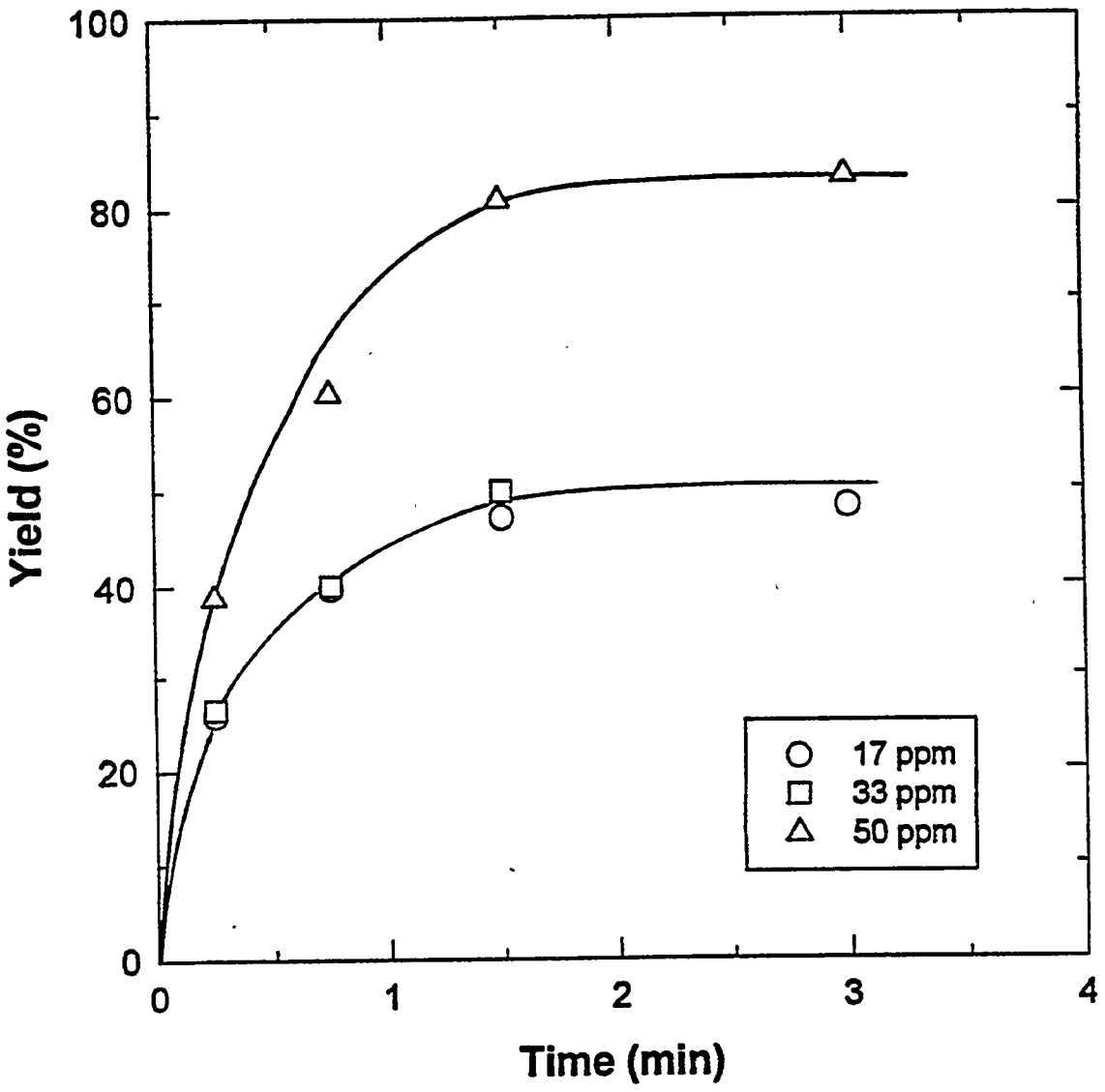

Figure 8-22. EFFECT OF FROTHER CONCENTRATION ON CLEAN COAL YIELD

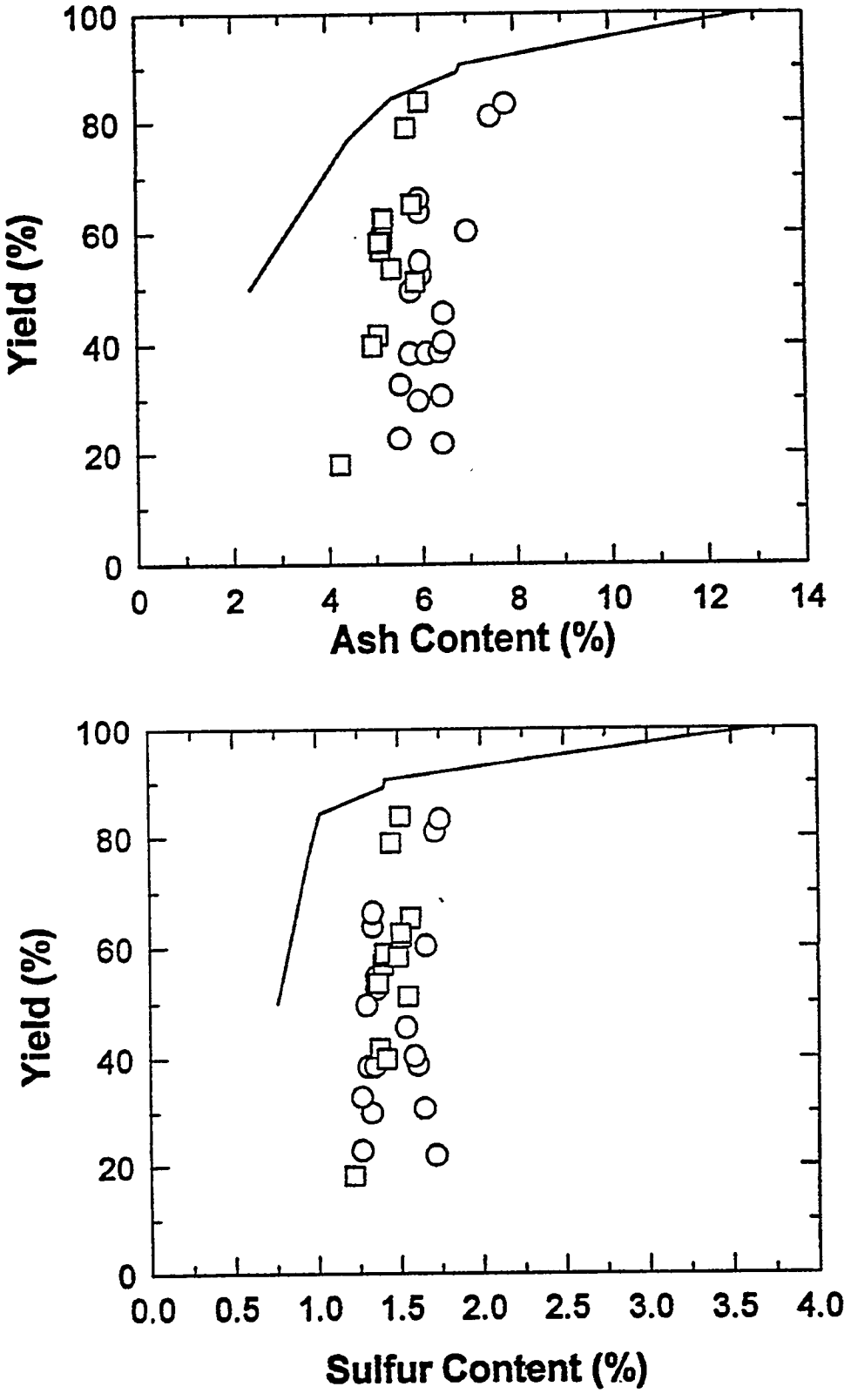

Figure 8-23. EFFECT OF COAL AGING ON GRADE-YIELD CURVE
(○) aged (□) fresh coal (-) washability

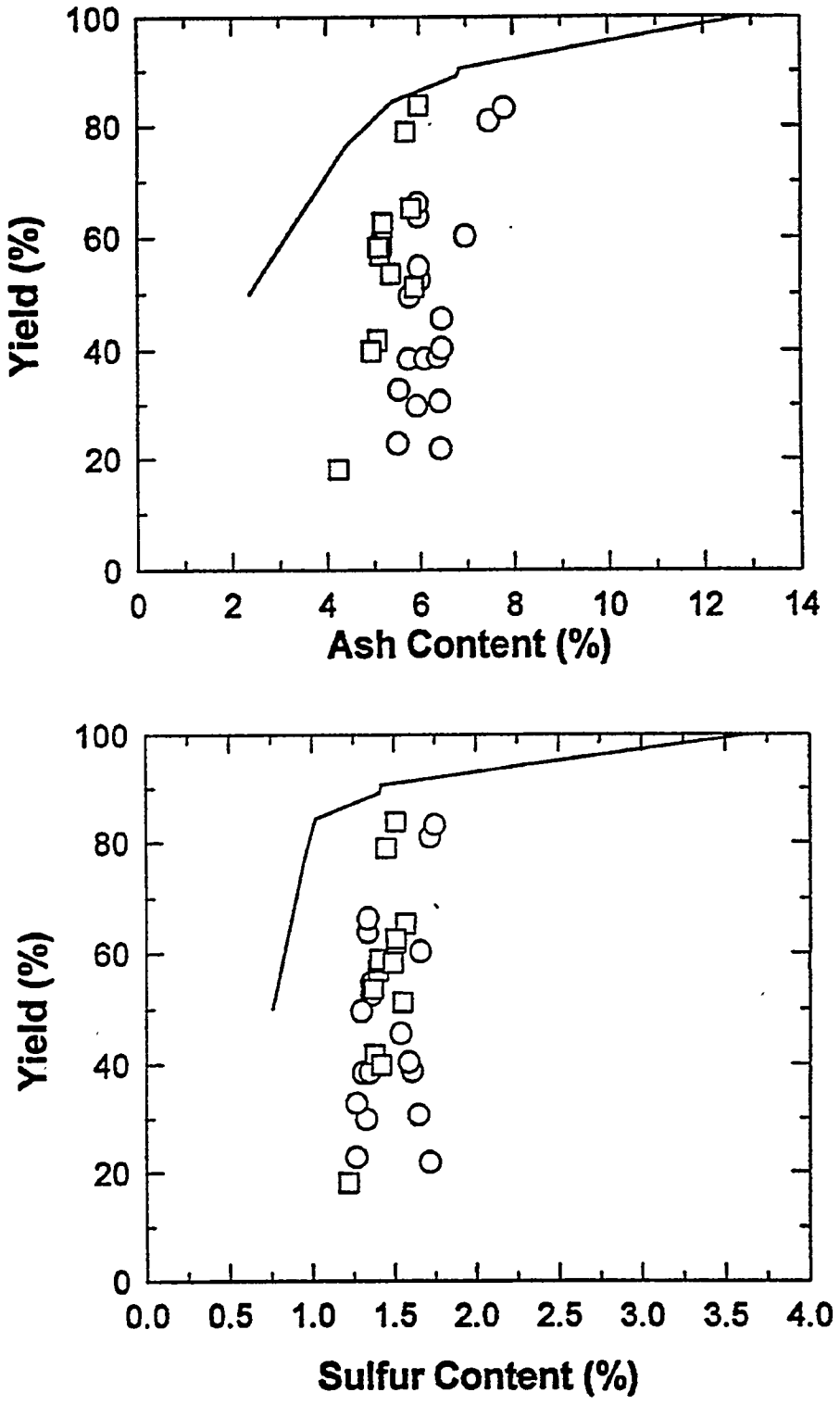

Figure 8-24. EFFECT OF TREATMENT CONDITIONS ON GRADE-YIELD CURVE
(○) fresh coal (□) fresh coal/washwater (△) fresh coal/collector (▽) fresh coal/collector/washwater (-) washability

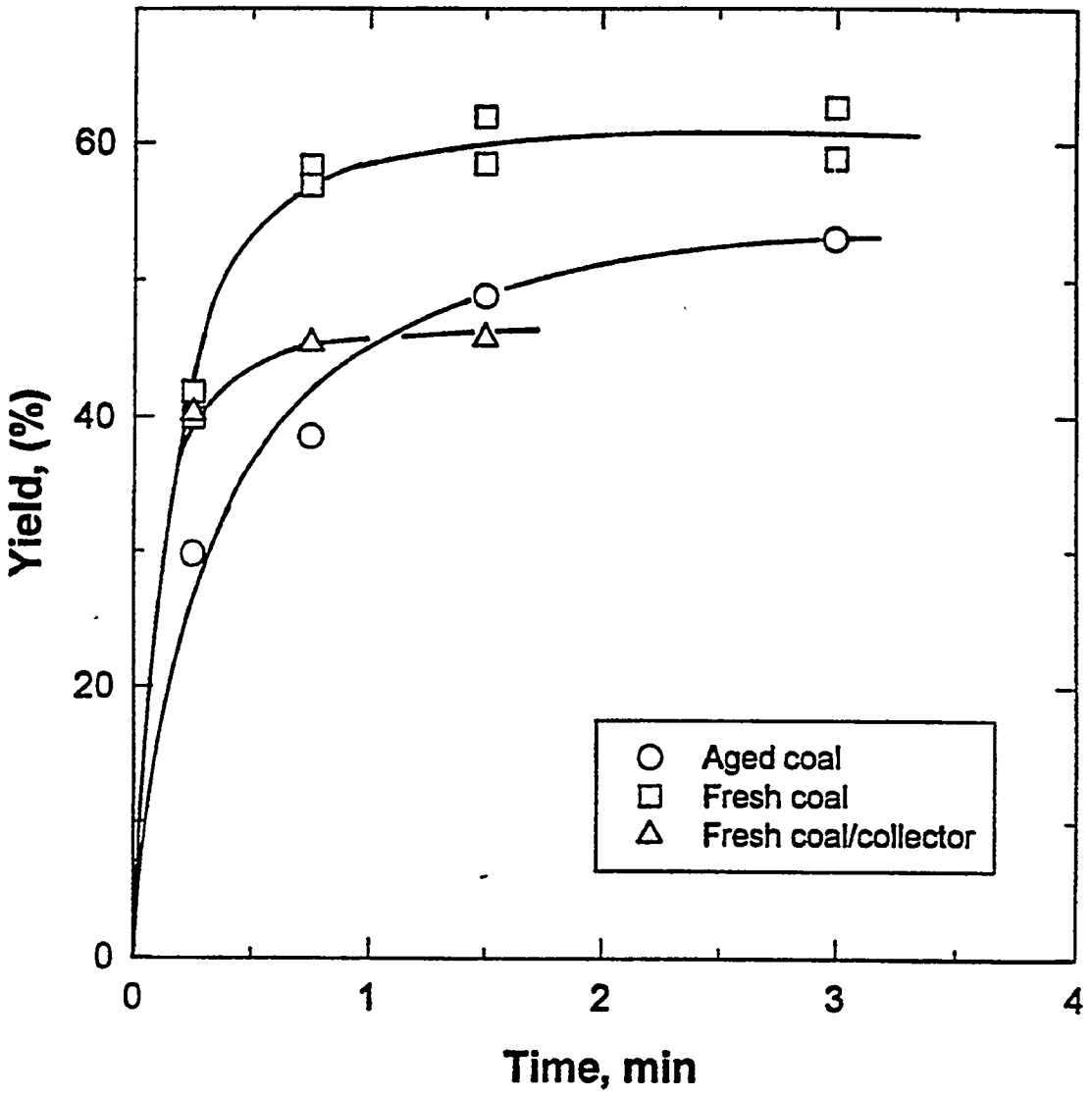

Figure 8-25. EFFECT OF COAL TREATMENT ON INITIAL RATE OF FLOTATION

of froth left in the column that could not reach the cell lip. This is considered to be an artifact of the batch flotation experiment as will be discussed later.

The effect of gas velocity on the rate of flotation and grade-yield curve is shown in Figure 8-26. The results show that the terminal recoveries increased with gas velocity. However, in the analysis of batch flotation data, it is the initial recovery rates that are more useful (The initial recovery rates are determined when the conditions in the flotation cell may be taken to be fairly constant. Thus, they are more representative of continuous operation data. By contrast, the terminal recoveries are determined over longer periods of time, and may include the effects of changing flotation conditions.). For the freshly ground coal, the initial recovery rates decreased with increasing gas velocity. The best grade-yield relationships were obtained at a superficial gas velocity of 1.16 cm/s. Duplicate experiments carried out at this gas velocity confirmed that clean coal with less than 5% ash content can be obtained at yields of 58-63%. Above this value, the product grade deteriorates. For the aged samples, the initial recovery rates increased with gas velocity. However, it is interesting to note that the best grade-yield curves were also observed at the same gas velocity (1.16 cm/s) even though the clean coal ash contents were higher (see Figure 8-27). The higher ash content of the product may be suggestive of a less selective separation with coal aging. These results suggest that the optimum gas velocity for column flotation of minus 100 mesh Upper Freeport coal is 1.16 cm/s.

Ityokumbul[145] has suggested that the maximum gas velocity for column flotation is related to the diameter by the relationship:

$$U_{g,max} = 0.11 D_c^{0.5} \qquad (8\text{-}13)$$

It was shown that for air sparging through porous media, the values predicted by Equation 8-13 agreed rather well with experimental observations. However, for coal flotation the detrimental effect of using higher gas velocities was less pronounced as the results in this study also show. For example, while the maximum gas velocity predicted for the 6.4 cm column used in the present study is 2.8 cm/s, relatively good grade-yield curves were obtained at a higher gas velocity (3.77 cm/s).

In order to determine the column carrying capacity, the variation of clean coal recovery and grade-yield curve with initial solid concentration were determined and the results are shown in Figure 8-28. The results show that the initial rates of clean coal production increased with solid concentration up to a maximum of 10%. Above this value, the changes were marginal. Indeed, the same trends are observed with the grade-yield curve. This would suggest that the optimum solid concentration for the flotation of Upper Freeport coal is 10%. On the basis of the results obtained here, the maximum carrying capacity at a gas velocity of 1.74 cm/s is estimated to be in the range

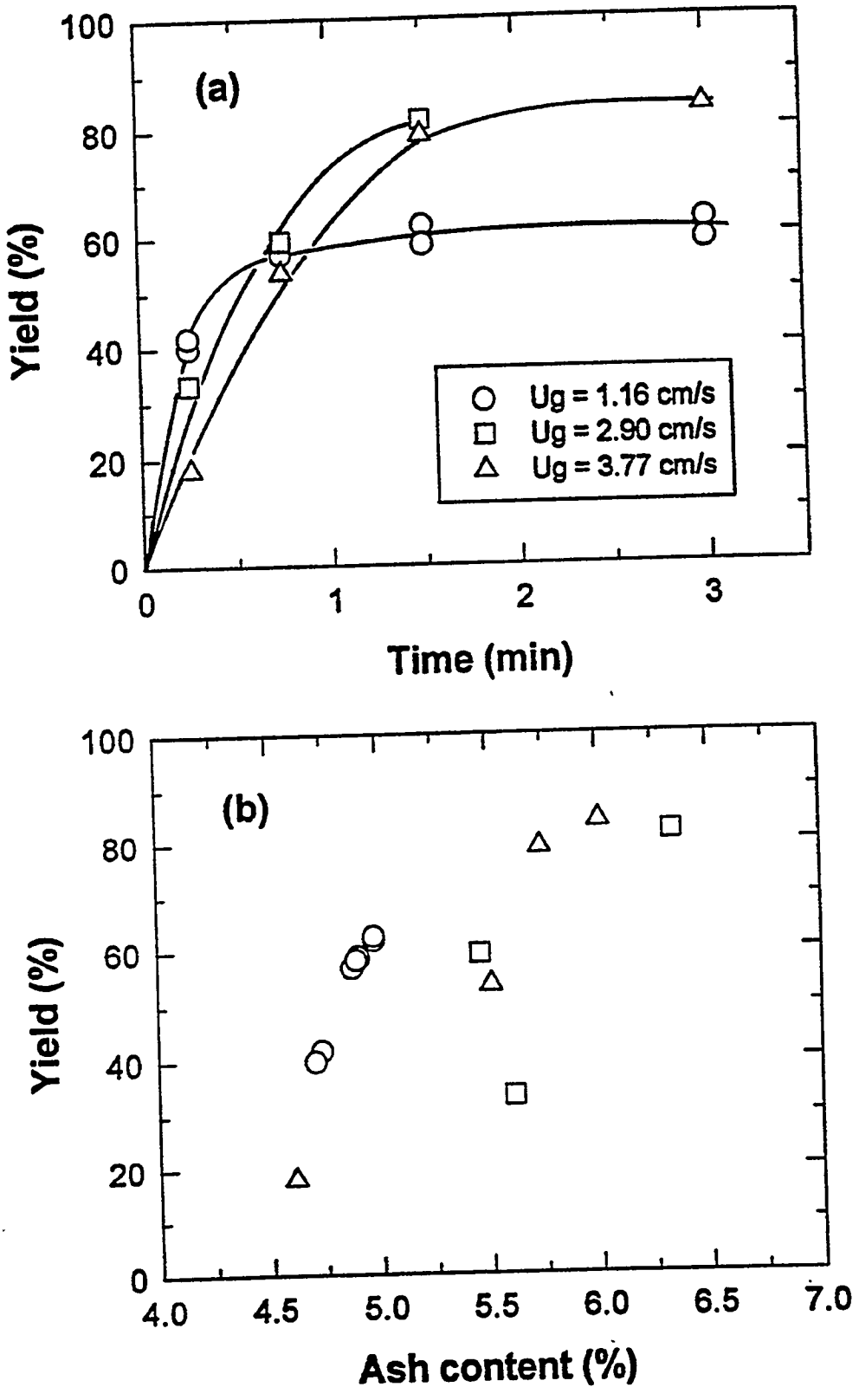

Figure 8-26. EFFECT OF GAS VELOCITY ON (a) RATE OF FLOTATION (b) GRADE-YIELD [same symbols as in (a)]

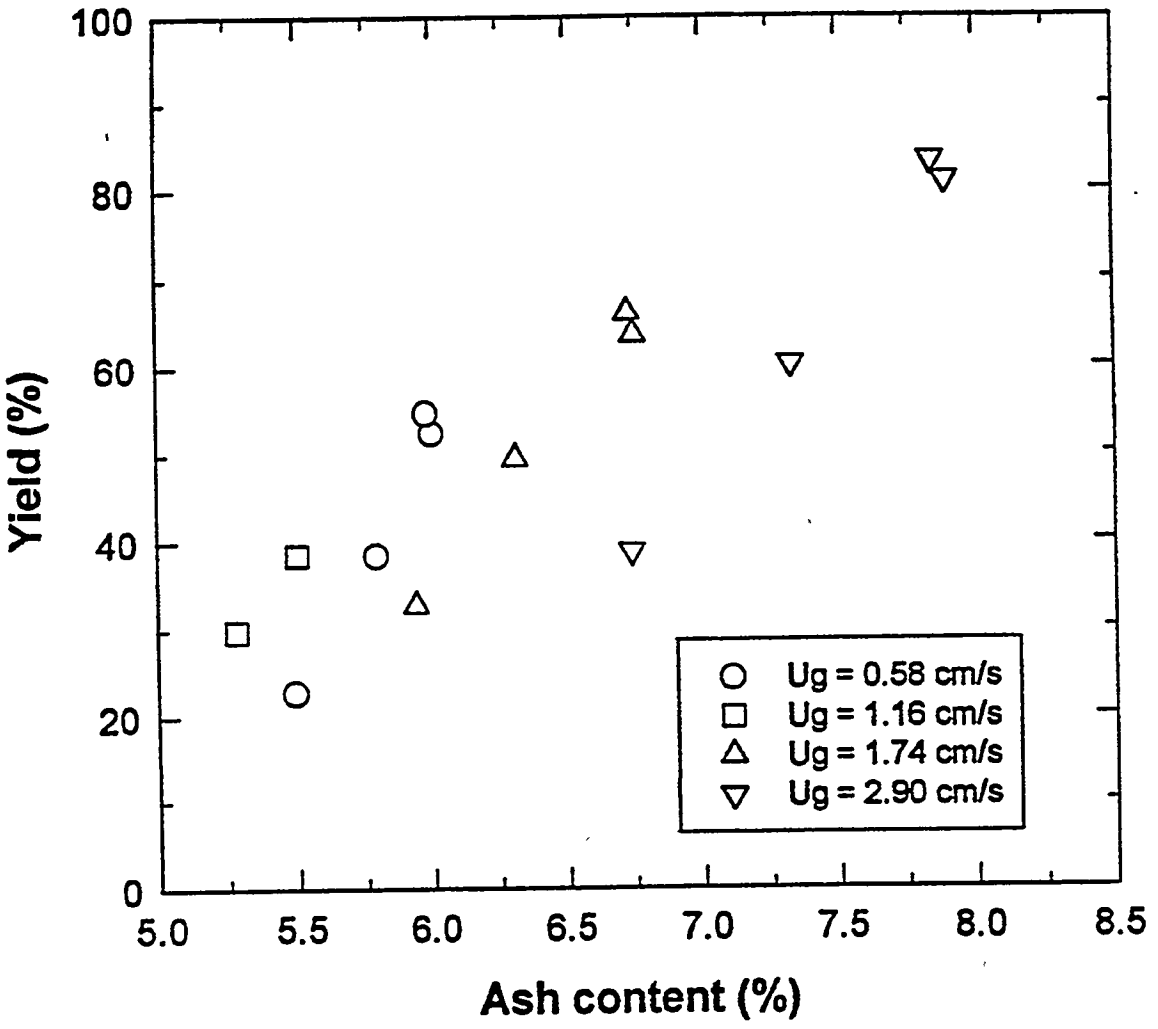

Figure 8-27. EFFECT OF GAS VELOCITY ON GRADE-YIELD CURVE FOR AGED COAL SAMPLES

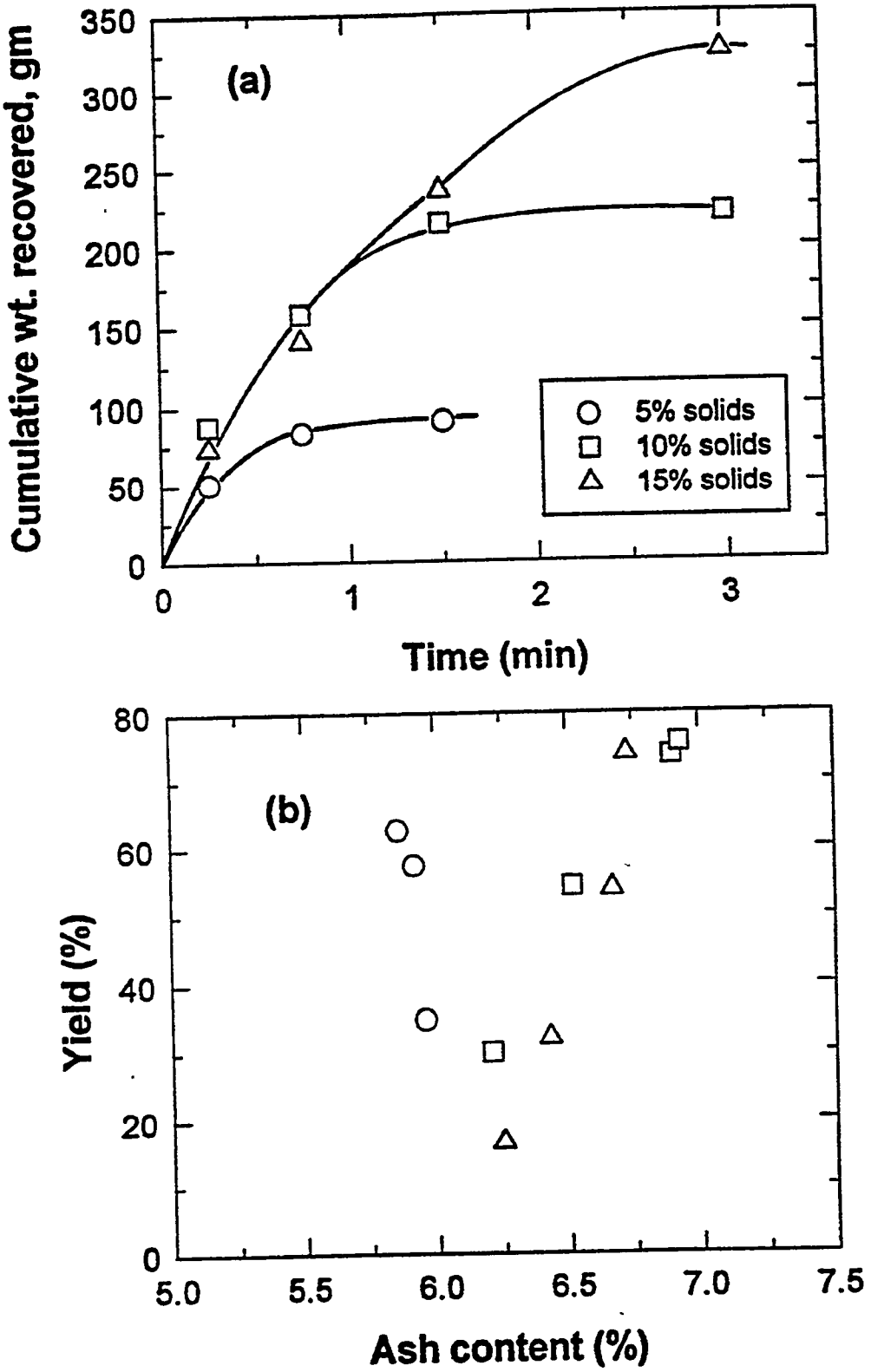

Figure 8-28. EFFECT OF FEED SOLID CONCENTRATION (a) RATE OF FLOTATION (b) GRADE-YIELD [same symbols as in (a)]

150 - 200 g/min. We note that similar results were reported by Bensley [146] for column flotation of fine coal.

As indicated earlier, the project objective of 5% ash was only met at low yields, while the sulfur objective (1%) was not met in any of the tests. We therefore carried out a series of flotation tests to simulate a two-stage (rougher and cleaner) operation. In these tests, a fresh feed containing 10% solids was floated in the unit (rougher) at a gas velocity of 1.76 cm/s and the material overflowing the cell lip (rougher concentrate) in the first minute collected. The rougher concentrate was diluted to approximately 5% solids with water, and refloated (cleaner) with frother addition. The results obtained are shown in Table 8-7. Coincidentally, we observed that the cleaner tailings had approximately the same composition as the feed material. Thus, in a continuous operation, it can be recycled to this unit with out loss of efficiency. With this arrangement, we were able to produce a final concentrate (clean coal) with 4.87% ash and 1.32% sulfur at an overall yield of about 40%. For the Upper Freeport, no scavenger flotation was carried out on the rougher tailings. If this is done, the overall yield will be considerably higher as the results of[144] suggest. Even with a cleaner operation, the target sulfur content was exceeded. This may be attributed to the relatively high organic sulfur and/or unliberated pyrite in the coal.

Figure 8-29 shows the overall variation of clean coal yield with ash rejection. Similar trends were observed with sulfur rejection. As expected, the results show that with cleaner flotation of rougher concentrate, the rejection curves shift towards the limiting separation for locked particles. In general, the yield of clean coal decreases with increasing ash and sulfur rejections. Similar results have been reported by[147] for the chemical desulfurization of oil sand coke residues. For maximum benefits, it is desirable to concurrently maximize the yield, sulfur and ash rejections. In order to determine the optimum flotation results, we have defined a yield index (The yield index is defined as the product of the yield and the variable that is being maximized (e.g., sulfur rejection, ash rejection, etc.). Traditionally, the separation efficiency (difference between the valuable and refuse recovery) has been used in optimizing flotation data. While both of these indices predict a maximum, the nature of the relationship between them is largely unknown at the present time. However, it is noted that the yield index seeks to concurrently maximize the yield and the variable of interest. For this reason, the yield index will be used in the present work.) similar to the desulfurization index used by Ityokumbul[147]. Intuitively, the yield index should exhibit a maximum; at both 0% and 100% yields, the index is zero. Since the index is a non-zero, non-negative function, it must exhibit a maximum. Figures 8-30 and 8-31 show the variation of yield indices with ash and sulfur rejections. For clarity, the fresh coal samples were combined in Figure 8-31. As expected, the yield indices exhibit a maximum of 40-45% for both ash and sulfur rejections in the range 55-65%. Figure 8-32 shows a comparison of the yield indices determined in the present study with those calculated from the

Table 8-7. Selected Process Conditions for Two-Stage (rougher/cleaner) Flotation of Upper Freeport Coal.

	% Solids	Yield (wt %)	% Ash	% Sulfur
Feed	10	100	11.4	2.9
Rougher Concentrate[a]	4.8	49.6	6.31	1.81
Rougher Tailings	ND	50.4	15.8	3.21
Cleaner Concentrate	ND	77.9	4.87	1.32
Cleaner tailings	1.06[b]	22.1	11.4	2.65

[a] The rougher concentrate was diluted with water to yield feed material with 4.8% solids

[b] Estimated quantity

ND - Not determined

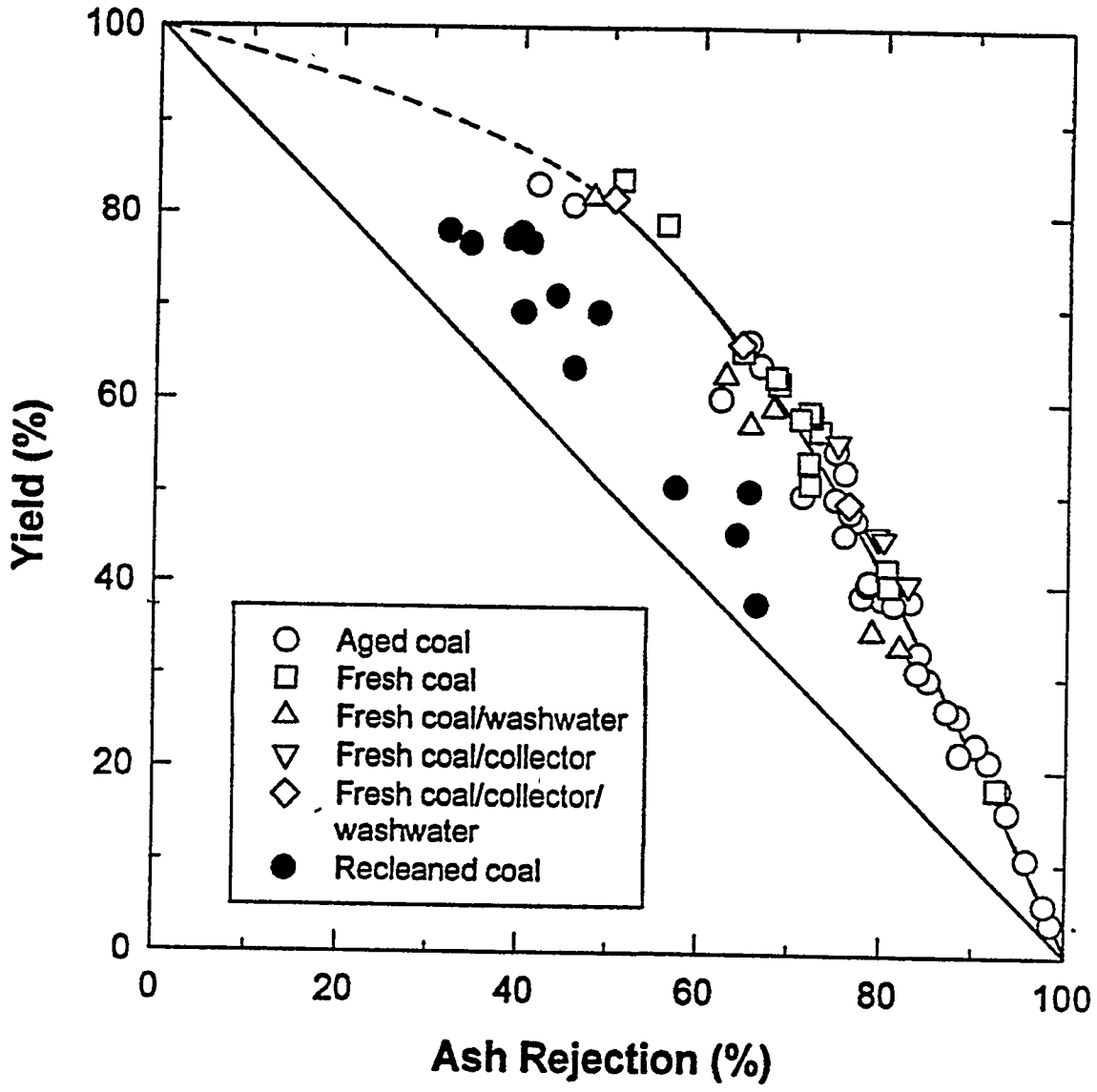

Figure 8-29. VARIATION OF CLEAN COAL YIELD WITH ASH REJECTION

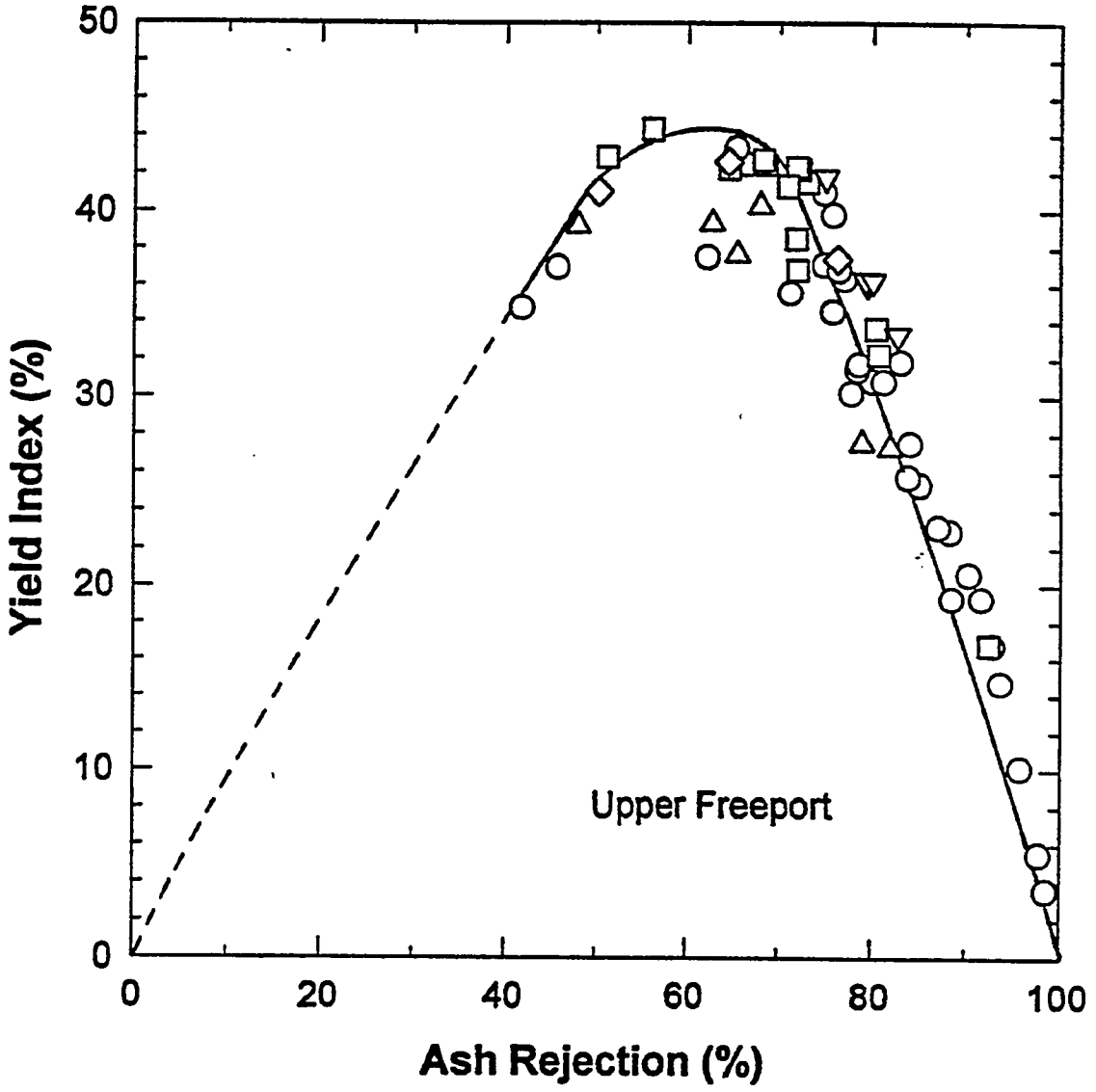

Figure 8-30. VARIATION IN YIELD INDEX WITH ASH REJECTION (symbols same as in Figure 8-29)

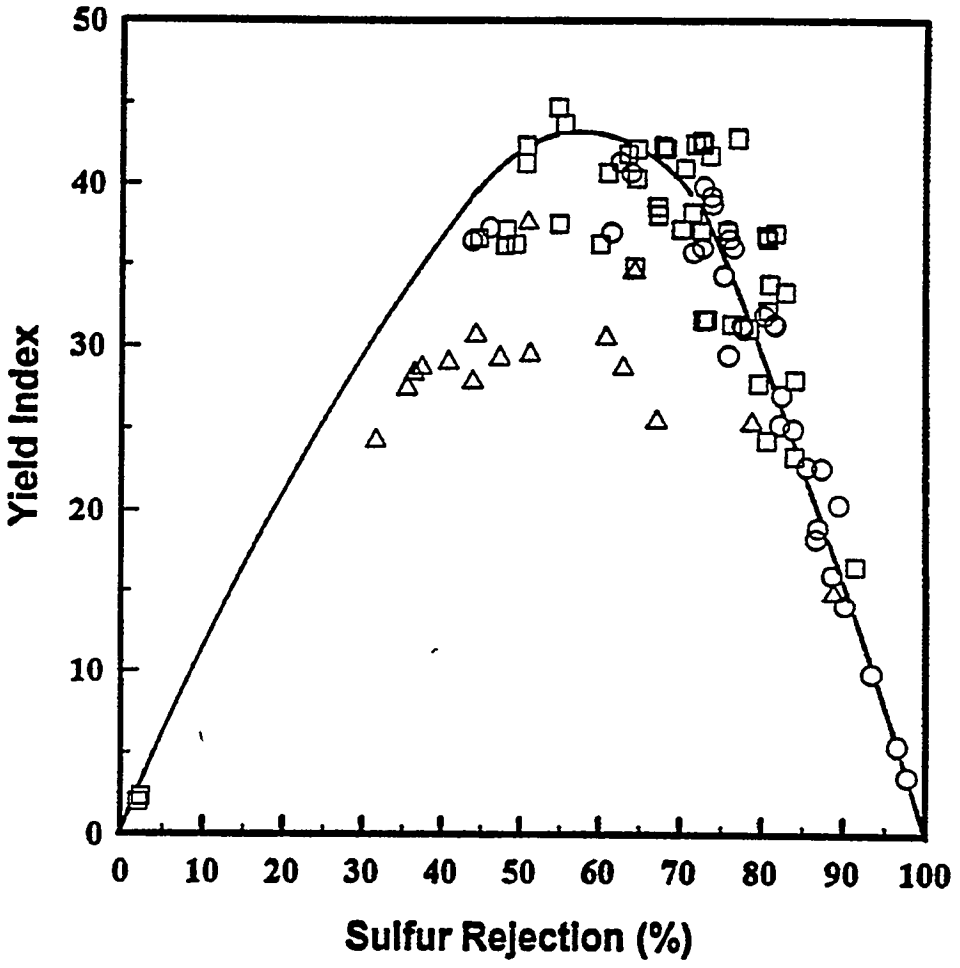

Figure 8-31. VARIATION OF YIELD INDEX WITH ASH REJECTION
(○) aged coal (□) fresh coal (△) rewashed coal

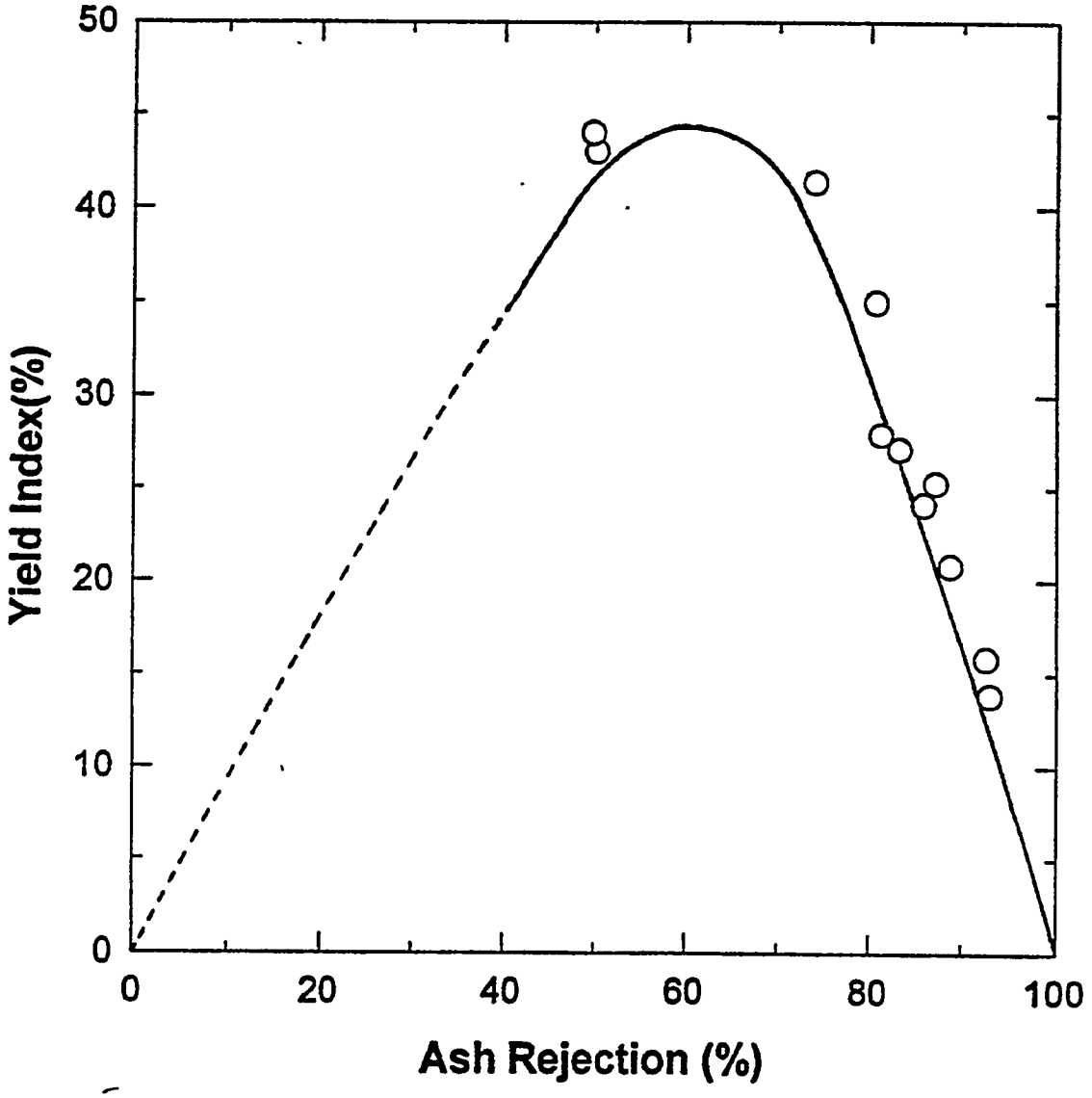

Figure 8-32. COMPARISON OF PRESENT RESULTS WITH THOSE OF HUETENNHAIN et al. (1990)
(O) experimental data (-) present study

work of[144]. In general, the agreement is quite good. In both cases, the coal samples were ground to -100 mesh (with d50 > 40 mm). [144] reported that better grade-yield response were obtained with coarse grinding of an Upper Freeport coal. This would suggest that fine grinding (d50 < 10 mm) may not be necessary for column flotation of Upper Freeport seam coal with feed ash content in the range 10 - 18%. However, confirmation of this effect may require additional work. The results also show that with additional stages of cleaning, the maximum shifts to lower ash and sulfur rejections. This observation is consistent with the expected lowering of the fraction of liberated ash and pyrite particles in the rougher concentrate.

LOWER KITTANNING

The effect of gas velocity on the rate of flotation and the grade yield curve is shown in Figure 8-33. As with the Upper Freeport coal, the optimum gas velocity appears to be 1.16 cm/s. However, the initial rates of clean coal recovery were higher with the Lower Kittanning seam coal. The grade-yield curve obtained at this gas velocity was significantly different from those at lower and higher gas velocities. For example, no other gas velocity produced a clean coal with 5% ash content.

The variation of clean coal yield and grade-yield curve with initial solid concentration are given in Figure 8-34. As with the Upper Freeport coal, the initial rates of clean coal production increases with initial solid concentration to a maximum of 10%. Similarly, the maximum carrying capacity is estimated to be in the range 150 - 200 g/min. The results also show that the grade-yield data changes marginally with initial solid concentration up to 10%. Above this value, it deteriorates rapidly. Thus, it is concluded that the maximum initial solid concentration for column flotation of Lower Kittanning coal is 10%.

The results of this investigation show that at a gas velocity of 1.74 cm/s, column flotation did not produce clean coal with a 5% ash content. Thus, a series of flotation tests were conducted to simulate a three-stage (rougher, cleaner and scavenger) operation. A fresh feed containing 10% solids was floated in the unit (rougher) and the material overflowing the cell lip (rougher concentrate) in the first minute collected. The rougher concentrate was diluted to approximately 5% solids with water, and refloated with frother addition to give a final concentrate. For the scavenger flotation, tailings from three different runs were combined, and reprocessed in the unit with frother addition. The results obtained are shown in Table 8-8. Coincidentally, we observed that the cleaner tailings, and the scavenger concentrates had approximately the same composition as the feed material. Thus, in a continuous operation, they may be combined with fresh feed and processed in the rougher unit. With this arrangement, we were able to produce a cleaner concentrate with 4.91% ash and a scavenger tailings (refuse) with 23.4% ash.

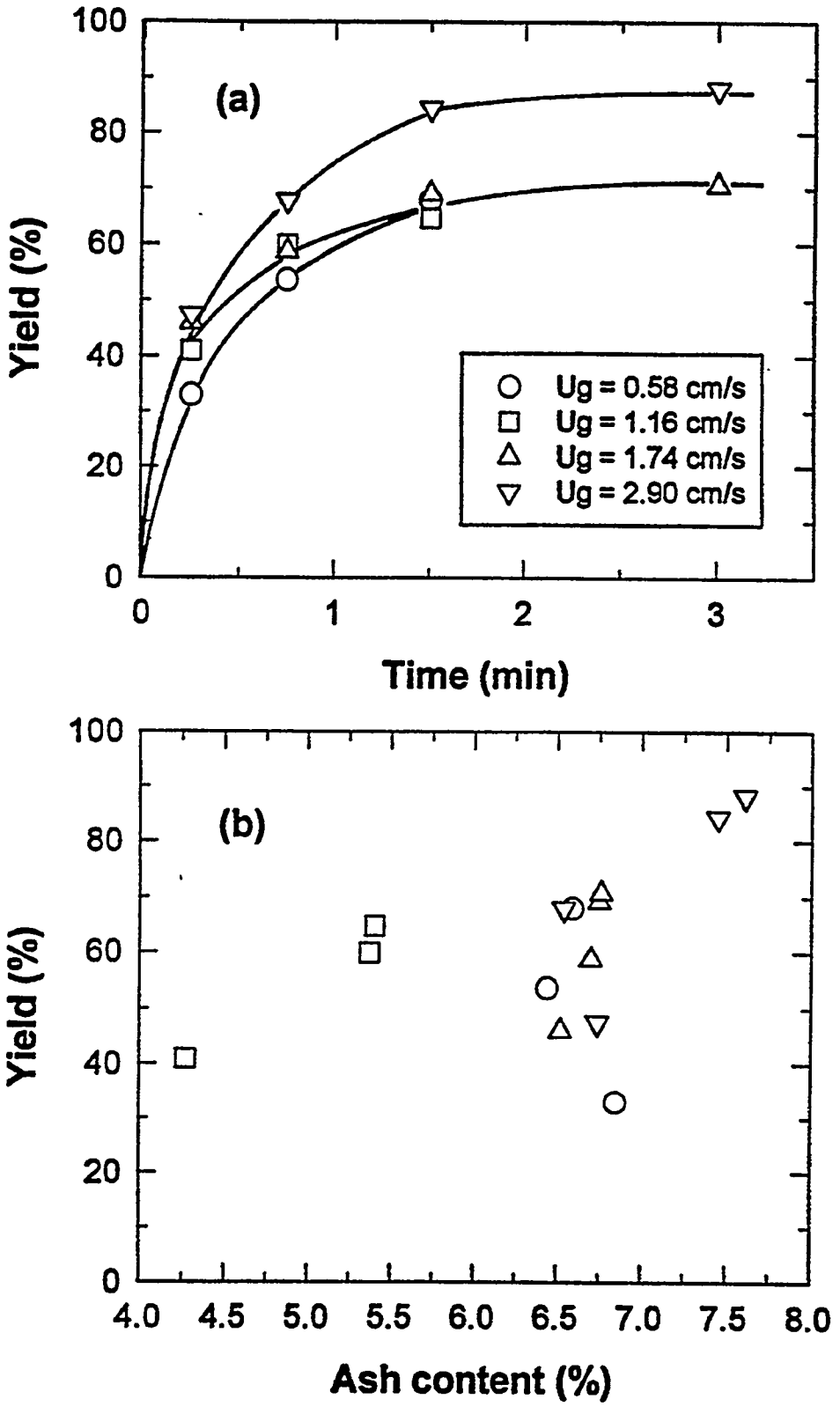

Figure 8-33. EFFECT OF GAS VELOCITY ON (a) RATE OF FLOTATION (b) GRADE YIELD CURVE [symbols same as in (a)]

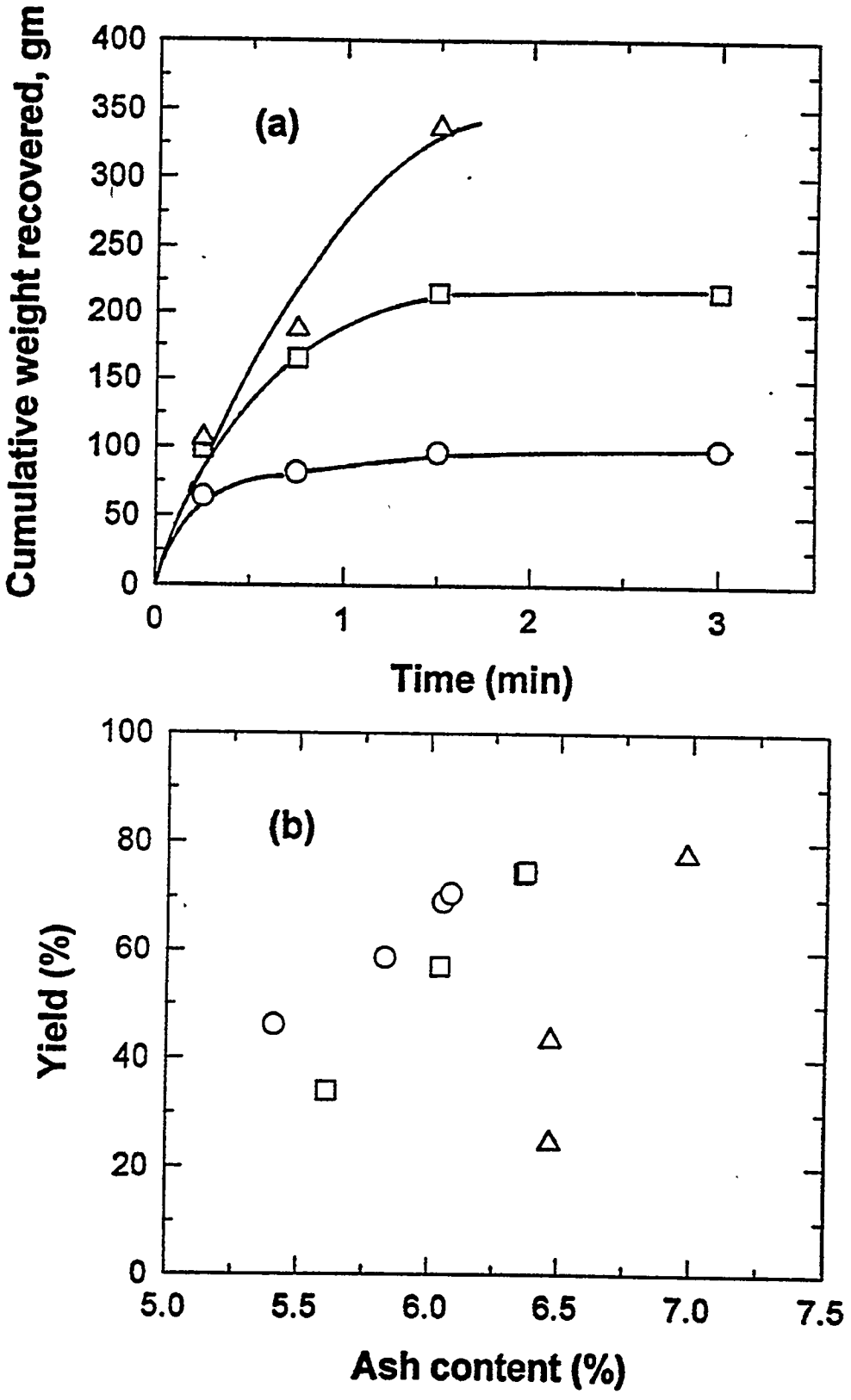

Figure 8-34. EFFECT OF FEED SOLID CONCENTRATION ON (a) RATE OF FLOTATION (b) GRADE YIELD CURVE
(○) 5% solids (□) 10% solids (△) solids

Table 8-8. Selected Process Conditions for Three-Stage (Rougher/Cleaner/Scavenger) Flotation of Lower Kittanning Coal.

	% solids	Yield wt. %	% Ash
Feed	10	100	9.73
Rougher Concentrate[a]	5.05	51.8	6.19
Rougher Tailings	5	48.2	12.4
Cleaner Concentrate	ND	69.7	4.91
Cleaner tailings	1.5[a]	30.3	9.13
Scavenger Concentrate	ND	44.8	9.31
Final Tailings	2.76[b]	55.2	23.4

[a] The rougher concentrate was diluted with water to yield feed material with 4.8% solids

[b] Estimated quantity

ND - Not determined

As indicated earlier, column flotation was not effective in the removal of the sulfur from the coal. Our results show that sulfur rejection is directly related to the yield of clean coal (see Figure 8-35). Moreover, the sulfur content of the raw coal met the project specifications. Thus, only optimization of the yield and ash rejection is required. In order to determine the optimum results from column flotation of Lower Kittanning coal, the yield index was plotted as a function of ash rejection (see Figure 8-36). The yield index for rougher flotation exhibits a maximum of 40% at ash rejections of 55-65%. It is noted that similar results were obtained with Upper Freeport coal.

FLOTATION COLUMN SIMULATION

On the basis of the results obtained in this study, a flotation column circuit simulation was conducted using experimentally observed separation factors for mass, ash and sulfur. The circuit tested for the Upper Freeport and Lower Kittanning samples are shown in Figure 8-37. As indicated earlier, tailings scavenging operation were not carried on the Upper Freeport sample. The results of these simulations, together with the separation factors used are shown are shown in Tables 8-9 and 8-10. These results show that with a feed containing 10% solids, the Upper Freeport and Lower Kittanning seam coals will produce clean coal having the following composition:

	Upper Freeport	Lower Kittanning
Yield (wt. %)	45	64
Ash content (%)	4.94	4.85
Sulfur content (%)	1.48	0.78

It is noted that with scavenger flotation of the Upper Freeport rougher tailings, the yields may be raised to 55-60% without significant loss of grade.

CONCLUSION

The results obtained here show that for column flotation of - 100 mesh Upper Freeport and Lower Kittanning seam coals:

(i) The optimum gas velocity is 1.16 cm/s.

(ii) The maximum initial solid concentration is 10%.

(iii) The optimum flotation results are obtained at ash rejections in the range 55-65%.

(iv) The variation of ash rejection with yield was independent of the type of coal. Our results agreed rather well with those reported by Huettenhain et al.[144] for microbubble flotation of a similar Upper Freeport seam coal.

(v) The simulation results show that a three-stage (rougher, cleaner and scavenger) flotation is required for the production of clean coal with ash content less than 5%. However, only the Lower Kittanning sample will concurrently meet the project objective of 1% total sulfur.

(vi) Fine grinding of the coal may not offer significant improvements in the grade-yield curve. However, confirmation of this may require additional test work.

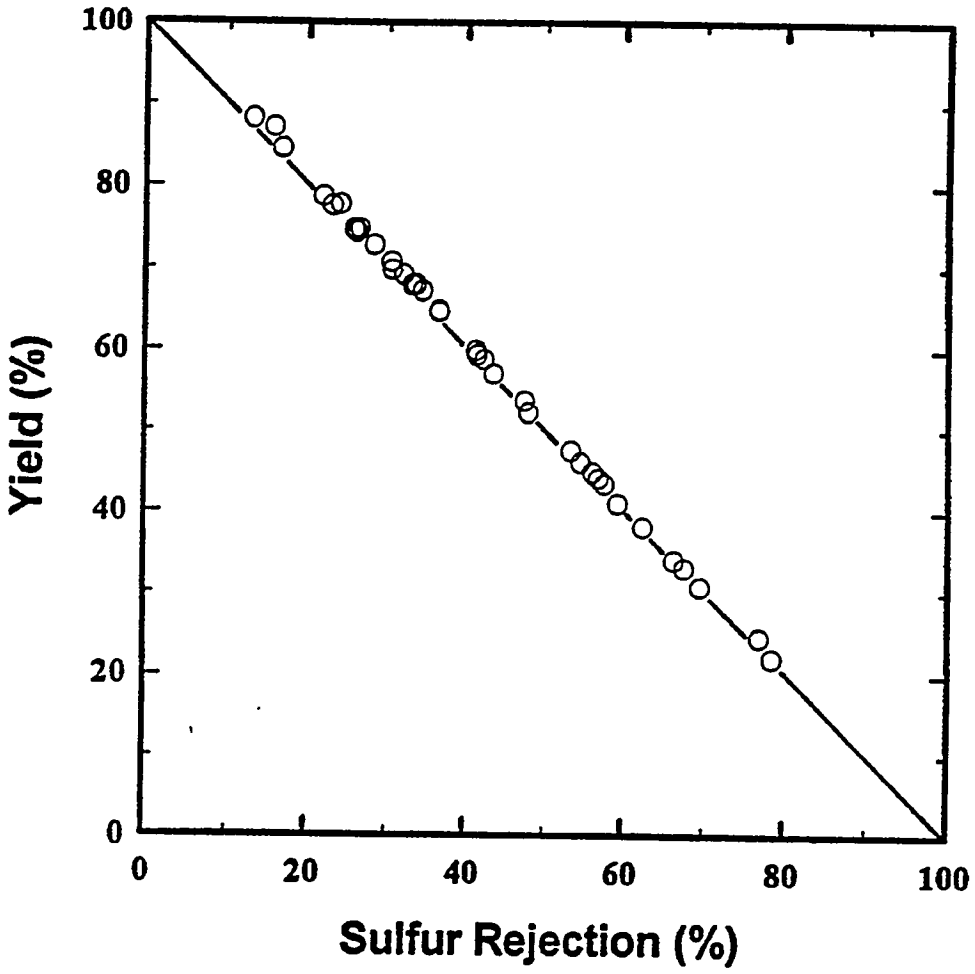

Figure 8-35. RELATIONSHIP BETWEEN CLEAN COAL YIELD AND SULFUR REJECTION (-) LIMIT FOR LOCKED PARTICLES

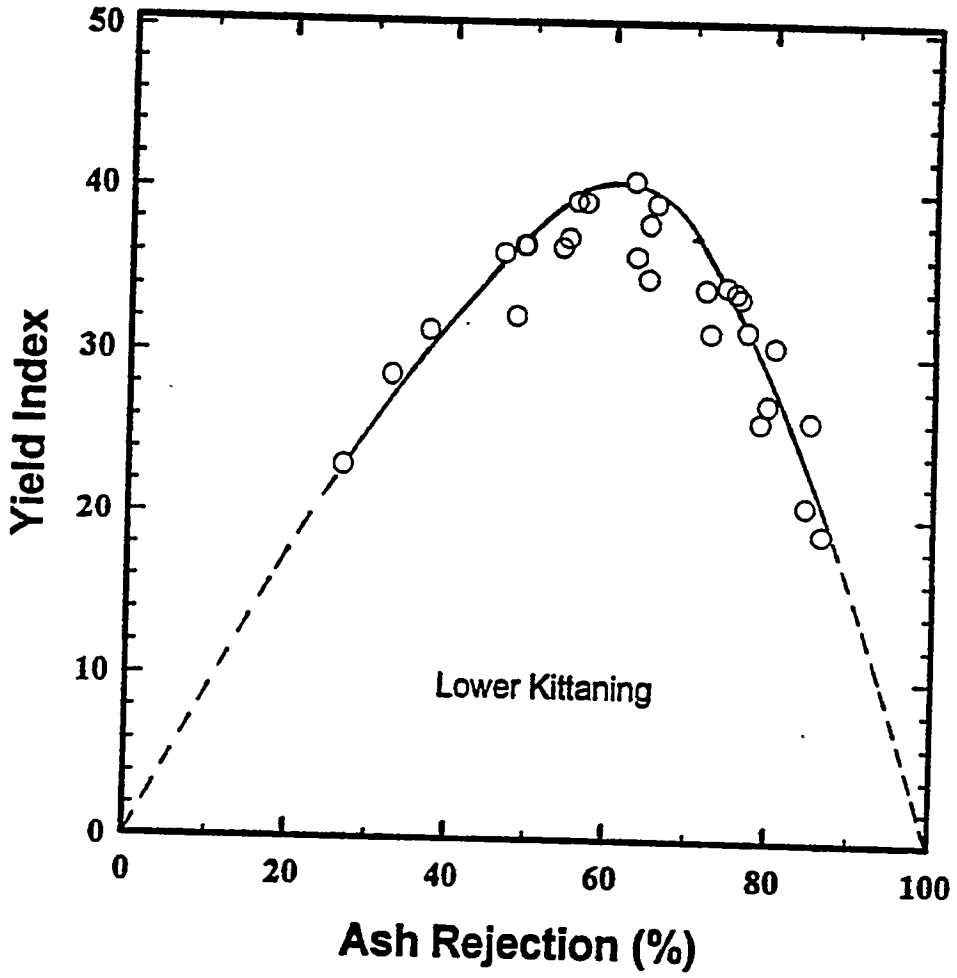

Figure 8-36. VARIATION OF YIELD INDEX WITH ASH REJECTION

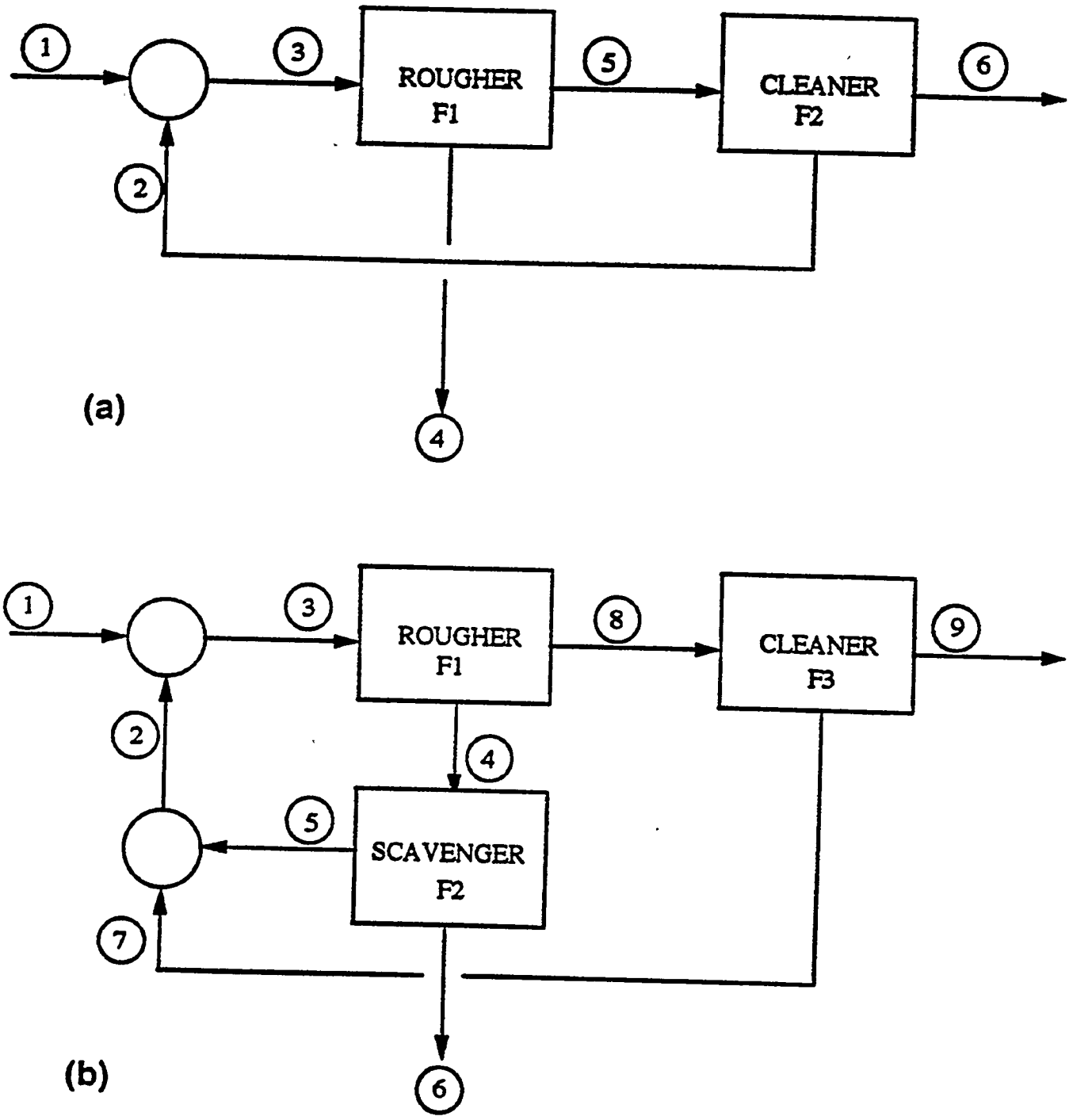

Figure 8-37. SIMULATION CIRCUITS TESTED FOR COLUMN FLOTATION OF (a) UPPER FREEPORT COAL (b) LOWER KITTANNING COAL

Table 8-9 Simulation Results from Two Stage (Rougher, Cleaner) Flotation of Upper Freeport Coal (Feed: 10% Solids).

Separation Factor[a]	Mass	Ash	Sulfur		
f1	0.54	0.33	0.36		
f2	0.694	0.513	0.558		
				Composition of stream	
Stream #	Weight	Weight	Weight	% Ash	% Sulfur
1	300.00	33.00	8.40	11.00	2.80
2	59.38	6.32	1.59	10.64	2.68
3	359.38	39.32	9.99	10.94	2.78
4	165.32	26.34	6.39	15.94	3.87
5	194.07	12.98	3.60	6.69	1.85
6	134.68	6.66	2.01	4.94	1.49
Solver[b]	-2.84E-14	-8.88E-16	0		

[a] Separation factor is the fraction of feed material responding to the overflow
[b] Overall material balance for the circuit

Table 8-10. Simulation Results from Three Stage (Rougher, Cleaner, Scavenger) Flotation of Lower Kittanning Coal (Feed: 10% Solids).

Separation Factor[a]	Weight	Ash	Sulfur		
f1	0.57	0.369	0.565		
f2	0.448	0.245	0.439		
f3	0.747	0.583	0.735		
				Composition of stream	
Stream #	Weight	Weight	Weight	% Ash	% Sulfur
1	300.00	30.00	2.40	10.00	0.80
2	152.39	13.38	1.24	8.78	0.81
3	452.39	43.38	3.64	9.59	0.80
4	194.53	27.37	1.58	14.07	0.81
5	87.15	6.71	0.70	7.70	0.80
6	107.38	20.67	0.89	19.25	0.83
7	65.24	6.68	0.55	10.23	0.84
8	257.86	16.01	2.06	6.21	0.80
9	192.62	9.33	1.51	4.85	0.78
Solver[b]	1.218E-08	6.288E-10	1.447E-10		

[a] Separation factor is the fraction of feed material responding to the overflow
[b] Overall material balance for the circuit

8.7 Subtask 2.7 Dry Cleaning of Fine Coal

Previous testing has shown that clean coal containing less than 5% ash and approximately 1% sulfur can be produced when processing -100 mesh Type II and Type III coals in the batch triboelectrostatic separator. In these cases, the results were presented as grade-recovery curves. Comparison of the actual curves with the washability (float-sink) curves provides an estimate of the separation efficiency. Although such comparisons are valid when the same coal is used, different coals cannot be compared with each other, because the grade-recovery curves will change depending on the coal being separated.

As noted in a previous report, fractional recovery curves are used to characterize gravity-based separations (e.g., cyclones, tables, spirals). These curves show the fraction of or the probability of feed coal of a particular relative density for a given size interval reporting to the clean coal. Since these curves are relatively independent of the type of coal being treated in the separator, they provide a consistent measure of separator performance.

The performance of the batch triboelectrostatic separator was also evaluated using fractional recovery curves. Samples were taken at selected increments along both collecting plates. This material was then subjected to centrifugal float-sink separation at 1.30, 1.35, 1.40, and 1.50 relative densities. The resulting fractional recovery curves obtained at different distances along the plates for two of the test coals are shown in Figure 8-38.

For the Upper Freeport seam coal, it can be seen that most of the low relative density material (below ~1.35 relative density) reported to the clean coal plate, however, a small percentage (~10%) was lost to the refuse plate. At the higher relative densities, misplacement of the particles to the clean coal occurred only at the farthest distance down the plate. This misplacement may be the result of charge dissipation or agglomeration of the particles.

For the Pittsburgh seam coal, less than 5% of the low relative density material was lost to the refuse plate, while over 20% of the higher relative material contaminated the clean coal plate. Comparison of the two plots shows that the separations were similar, at least in terms of the relative densities of separation. Additional testing will be necessary to determine if this technique can be used to provide an independent measure of triboelectrostatic separator performance.

8.8 Subtask 2.8 MCWM Density Control

The stability of suspensions of nominally -10 mm Taggart coal has been investigated. The surface charging behavior determined by Microelectrophoresis (Laser Zee) is illustrated in Figure 8-39. The results indicate that this coal is uncharged at about pH 4.5. The effects of pH on stability of suspensions of the coal are entirely consistent with the electrokinetics result. Coagulation and rapid settling (about 2 cm/min.) were observed at pH 5.4; the result is shown in Figure 8-40. At pH 6.5, there was sufficient coagulation to provide significant settling and

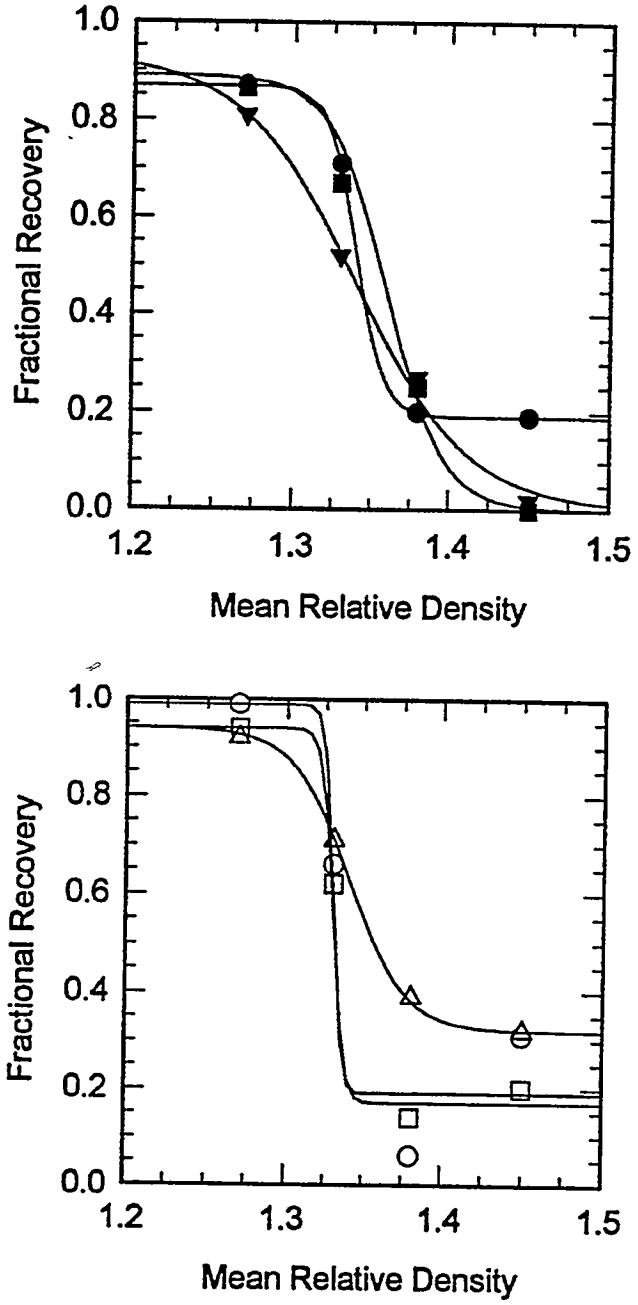

Figure 8-38. FRACTIONAL RECOVERY CURVES AS A FUNCTION OF DISTANCE FOR THE BATCH TRIBOELECTROSTATIC SEPARATOR:
(a) Upper Freeport seam coal: ▼ 2-4 cm, ■ 4-6 cm, ● 6-8 cm;
(b) Pittsburgh seam coal: ▽ 2-4 cm, □ 4-6 cm, ○ 6-8 cm

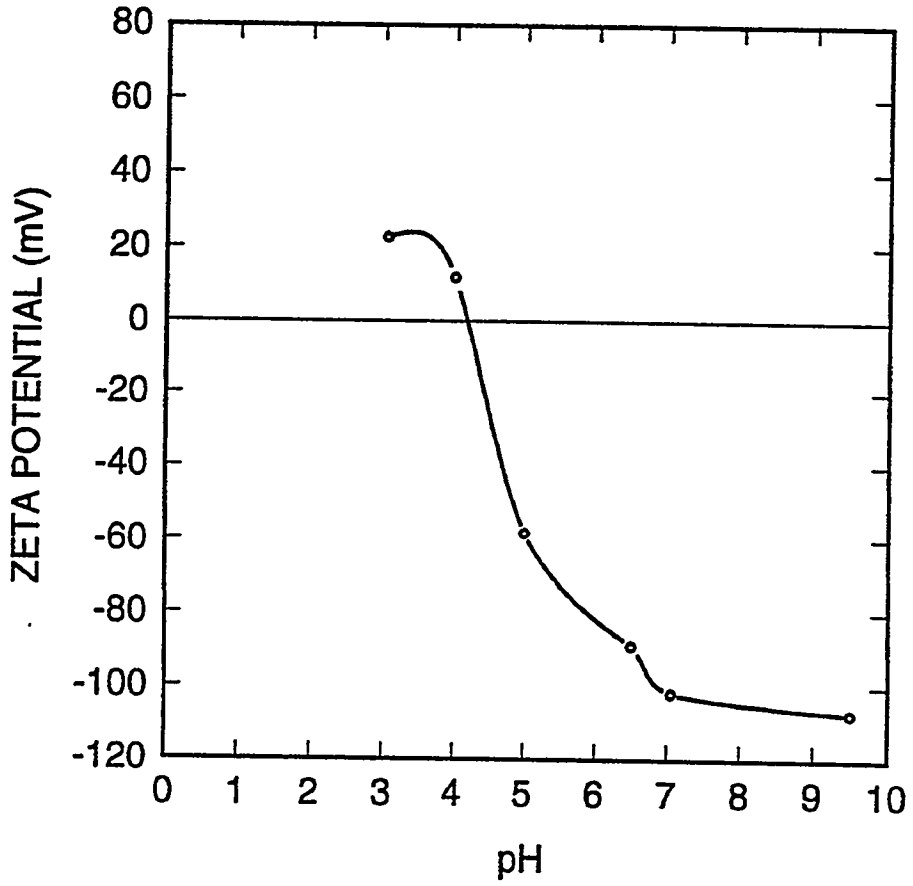

Figure 8-39. PLOT OF LASER ZEE MEASUREMENTS ON -10 μm TAGGART COAL

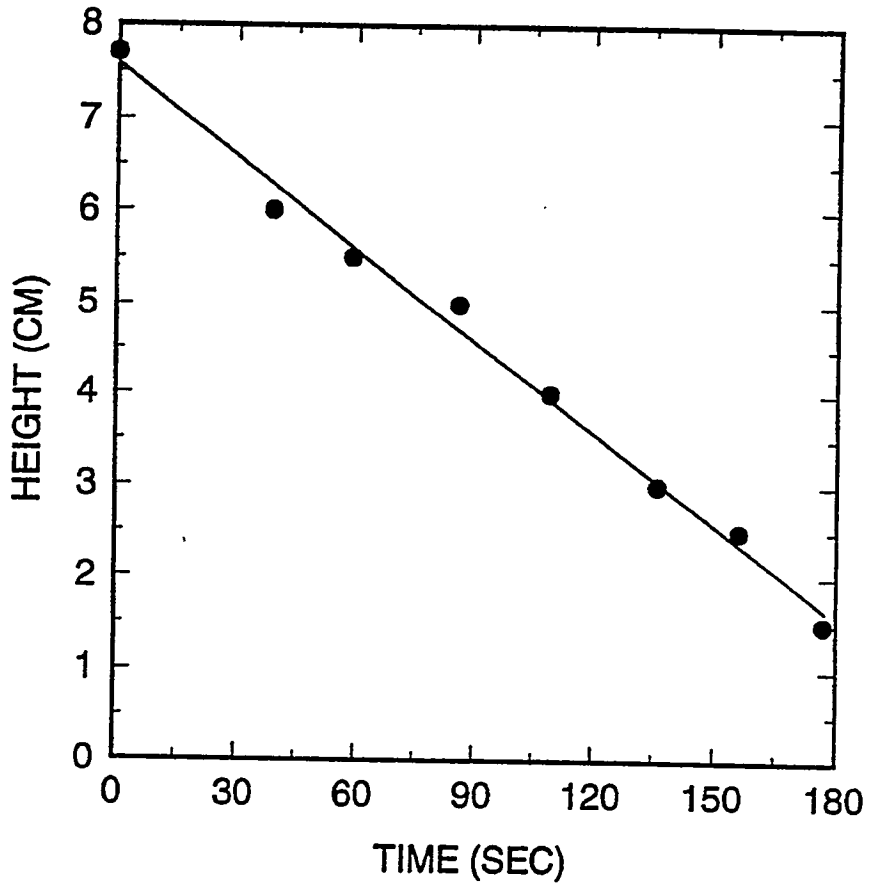

Figure 8-40. SETTLING CURVE FOR TAGGART COAL AT pH 5.4

clarification over a 24 hour period. When the pH was increased to 8 or more, there was no visible clarification even after 2 days.

The slurry stability tests described above indicate that simple sedimentation/thickening processes can be used to increase slurry density for the -10 μm Taggart coal. The result illustrated in Figure 8-40 for settling at pH 5.4 demonstrates that the original 5 wt% slurry could be thickened to about 22% by sedimentation for only three minutes. Further thickening, e.g., to 50% solids may, however, take considerably longer times. At high concentrations, structure in the flocculated suspension opposes sedimentation and the thickening process becomes dominated by slow breakdown of the structure under the self-weight of the sediment.

The hydrodynamic forces in sedimentation depend on concentration, while structure breakdown can be expected to depend on both concentration (which largely determined the strength of the structure) and sediment depth (which determines the structure-breaking stress acting any particular location). It follows that sedimentation rates should depend on depth as well as concentration, especially for flocculated suspensions. Unfortunately, this adds significantly to the complexity of the problem. A rigorous analysis of continuous thickening processes would required detailed knowledge of the constitutive relationships for the particular system being thickened. Several authors[148-150] have outline such analyses. However, because of the mathematical complexity and the need for experimental permeability/compressibility parameters these have seen rather limited application to practical systems.

Experimental studies of long-time sediment consolidation under gravity or centrifugal forces indicate that there is a compressive yield stress which must be overcome before consolidation can occur[148, 151]. The compressive yield stress generally increases with solids concentration.[148, 151], investigating flocculated kaolin suspensions, obtained an empirical expression for the relationship between solids concentration and the compressive yield stress. The relationship was found to be relatively insensitive to the extent of flocculation - provided that the suspension was flocculated.

In batch sedimentation processes, sediment compression at any given location ceases when the concentration reaches the value for which the yield stress is equal to the buoyant weight of the overlying sediment. The yield stress defines the concentration profile would in the final sediment. The same concentration profile would exist in a continuous thickener if the time required for consolidation were less than the retention time in the device. This concept has been used as the basis for a simplified thickener model[152]. The model uses batch sedimentation data to predict continuous thickener performance.

Measured relationships between sediment self-weight and the extent of consolidation are used to establish underflow densities. Supernatant turbidity data provide the information necessary to predict overflow clarity. The work has shown that thickener depth can play a role in

determining solids-handling capacity as well as dewatering performance. The use of this model in the design and simulation of dewatering systems for slurry density control in micronized coal-water slurry preparation will be evaluated in Phase III of this project.

8.9 Subtask 2.9 Stabilization of MCWM

Subtask 2.9 has been completed and the results are being incorporated into the Phase II final report.

9.0 PHASE II, TASK 3 ENGINEERING DESIGN AND COST; AND ECONOMIC ANALYSIS

9.1 Subtask 3.1 Basic Cost Estimation of Boiler Retrofits

Subtask 3.1 has been completed. Work on this subtask began with a review of efforts since the early 1980s that have been directed towards the development and utilization of coal-based fuels, predominantly slurries. In the process of reviewing the type and number of projects it becomes apparent that the fortunes of the research and application of coal-water mixtures (MCWMs) varies inversely to the contemporary price of oil. Having made that observation, option valuation techniques that have been developed by financial analysts, and recently begun to be applied to capital project analyses, are proposed as a means to account for oil-price volatility in boiler retrofit economic analysis. Two option valuations are performed, the first is an ex ante estimate of the premium for acquiring the option to retrofit a boiler. The second option pricing estimation technique evaluates the value for having a fuel switching capability as an embedded recurring call option on the minimum price of two fuels, with extensions to three or more fuels. These option pricing techniques are presented for the illustrative purposes of describing their relative merits and demonstrating their shortcomings.

BACKGROUND

During this century, the United States has ceded its position as major producer and exporter of crude oil to other countries that are endowed with more massive and easily exploited oil reserves. Over the same time period, the quality of life United States citizens has also dramatically improved with the advent and incorporation into the economy of a whole host of technologies, many of which rely upon this easily utilized source of energy. The problem, as illuminated by the 'energy crisis,' is that future access to oil apparently is not guaranteed, resulting in a threat to this improved quality of life.

The United States is awash in coal and a plethora of technologies have been proposed to promote coal utilization as a means to avoid the perceived dire consequences of dependence upon a foreign-controlled fuel source. The main problem is that, in many applications, coal-based fuels are simply not as easy or economical to use as oil-based fuels. The result is that the promise of these technologies has remained only that, a promise. Beginning in the 1970s, the promise seemed to become closer to realization with expectations of oil prices rising to the margin of coal-based fuel

technology viability. When oil prices did not achieve or maintain these levels, and coal-based technology research indicated higher than expected costs, many technology developers refocused their attention on attaining economic viability through lowering costs.

A motivation for developing boiler retrofit technologies, therefore, stems from this desire to decrease dependence on foreign sources of energy. Dependence upon imported energy sources makes the United States vulnerable to an "oil price shock," such as that experienced from 1973 to 1974 and later during 1979 to 1980. Another goal of policy makers is to improve the competitive position of coal, and thereby the United States, through promoting the development of technologies that improve upon the economics of its use.

THE CONTEXT FOR MCWM PROJECT DEVELOPMENT

This section briefly reviews a sampling of technologies using MCWMs that have been investigated. This review was conducted by examining past DOE MCWM projects described in the National Technical Information Service's (NTIS) database[153]. All references in the following are to this database unless otherwise noted. This review includes projects dating from 1970 to the present and is not intended to be comprehensive but only to illustrate some of the different projects attempted and ongoing.

Coal-Fueled Diesel Systems for Stationary Power Applications

In this technology development effort, 0.5% ash, 1% sulfur high volatile micronized bituminous coal slurry is combusted in a 3 to 6 MW, 360 to 400 rpm engine. The potential market being pursued for with this technology is the small-scale, 10 to 100 MW cogeneration and modular electric generation markets that are not easily served economically by scaling-down other coal-based fuel technologies and would otherwise require a turbine. The project developer's forecast is for a potential market that would consume 3 to 6 million tons per year (tpy) of coal.

Coal-Fueled Diesels for Modular Power Generation

Interest in this technology was revived in the 1970s with the sudden upward swings in oil prices. With successful technology demonstrations during the 1980s by Cooper-Bessemer and Arthur D. Little, the DOE's Morgantown Energy Technology Center (METC) has continued development of this technology. The technology is expected to be ready for deployment during the late 1990s when oil and gas prices are expected to escalate much more rapidly than the price of coal.

CWM-Fired Residential Warm-Air Heating System

This technology involves the development of a warm-air heating system for residential use that would be competitive with similar oil and natural gas-fired systems. This effort has progressed from developing the combustor and reactor components necessary to fire MCWMs to a "manufacturing prototype" package unit that contains all the necessary items needed for residential use.

Coal-Fueled Diesel Technology Development

This work, performed primarily by General Electric, focuses on the technical development and economic assessment of a MCWM-fire diesel engine for locomotive. This research started in 1984 and, in 1992, successfully demonstrated a medium speed diesel engine.

Coal-Fired Gas Turbine

The DOE has funded work on the retrofitting of gas turbine that initially used MCWM. An Allison 501-KM engine was fired using MCWM instead of a dry coal fuel mainly for safety and convenience considerations. Further use of MCWM on this project was curtailed due to the relative cost advantage of using a dry coal fuel instead.

Conversion of Large DOD Gas- and Oil-Fired Heating Plants to Coal

M.C. Lin reviewed the near-term economic viability for retrofitting DOD boilers from non-coal to coal-based fuels, including MCWMs, in 88 large heating plants located at 55 army installations in the continental U.S. His analysis showed that cost savings could be potentially be achieved at 38 of these heating plants. The calculated life-cycle cost savings were estimated at $8 million to $239 million.

Factors Affecting MCWM Economics

Rolf Manfred[154] summarized the technical and other factors that are relevant to MCWM economics. His review mainly addressed the potential utility retrofit market but his comments are germane to the current EFRC development effort. The factors effecting MCWM project economics that Manfred identified are:

- Oil price growth
- MCWM cost reduction
- Reduction of boiler derating
- Establishment of domestic and export market clusters
- Reduction of conversion risks

The growth in oil prices, and the resulting growth in the differential between oil and MCWM prices, greatly determines the potential extent of MCWM market penetration in the United States. Manfred reviews the potential for the displacement of No. 6 fuel oil in utility boilers by MCWM. At a No. 6 fuel oil price of $4.6/MM Btu ($29/bbl), providing a differential fuel cost (DFC) of $1.4/MM Btu, the potential utility retrofit market for MCWM as of 1985 was estimated to be about 3,000 MWe. This level of market penetration consists only of coal-design boilers that now burn oil and cannot otherwise easily reconvert to pulverized coal-firing. He then speculates that for a No. 6 fuel oil price of $5.3/MM Btu the potential utility market would climb to 40,000 MWe. This level of market penetration in utility boiler retrofits represents 59,000,000 tpy of coal.

Further MCWM cost reduction is cited by Manfred as an another means to improve the potential market for utility boiler retrofits. He suggests that site-specific studies should identify cost reductions in the MCWM supply system including: determination of optimal process plant

location, selecting the optimal mode of MCWM transport, decreasing coal cost, and minimizing the cost of required additives.

The economic loss associated with the reduction of boiler capacity when using MCWMs can be mitigated by a variety of methods. Manfred notes that these methods to reduce the amount that the boiler must be derated include: use of finer coal sizes, reduction in the ash and sulfur content, and improved MCWM atomization in the boiler.

Manfred maintained that the scale up of MCWM production from the pilot to commercial-scale levels to take advantage of economies of scale is hampered primarily by the uncertainty in future of energy supply and demand levels. He asserted that a consistent DFC of $1.7/MM Btu to $2.0/MM Btu must be achieved before the market for MCWM can begin to grow. The uncertainty associated with achieving and maintaining this DFC level leads to a "chicken-and-egg" situation. Potential MCWM producers require long-term supply contracts to recover their necessary capital investments at a reasonable return, while potential MCWM consumers are loath to assume the risks inherent in signing such contracts. If oil prices drop, consumers who signed such would be at a significant disadvantage in competing with others in their own market due to having to pay comparatively higher energy costs. Manfred stated that the deployment of MCWMs , as of 1985, have been slowed by: 1) the change of oil consumers perceptions from a shortage in world oil supplies to a glut; 2) a reduction in oil consumption; and 3) falling oil prices.

Manfred's circa 1985 measures listed above for improving the marketability of MCWMs provides a blueprint upon which related development programs, such as the current DOD/DOE effort being pursued by the EFRC, should be structured. Those factors that effect the economic viability of retrofit and are under the control of the current project team, such as reducing costs, reducing boiler derating, improving coal quality, identifying markets and reducing conversion risks, are systematically being addressed in this program.

The importance of oil prices in setting MCWM economic viability noted by Manfred and others, however, makes a brief review of oil price trends worthwhile. This review provides the necessary context within which to evaluate the past, present and future of viability of MCWM projects and assess the emerging analytic tools being developed to perform these evaluations.

A Review of Oil Price Trends

Oil price trends in the twenty-one years since 1972 can be best summarized as volatile. This volatility in oil prices can be seen in Figure 9-1, which shows the prices of the Arabian Light and Dubai crudes from 1972 to 1993. As the figure shows, the prices of these crudes began at $1.90/bbl, climbed to a high of $36/bbl by 1980, receded to $13/bbl in 1986, and has since varied between $13/bbl to $20/bbl. In addition, it can be seen that these price trends do not follow a smooth path but are punctuated by sudden changes in the trend slopes in the years prior to 1986.

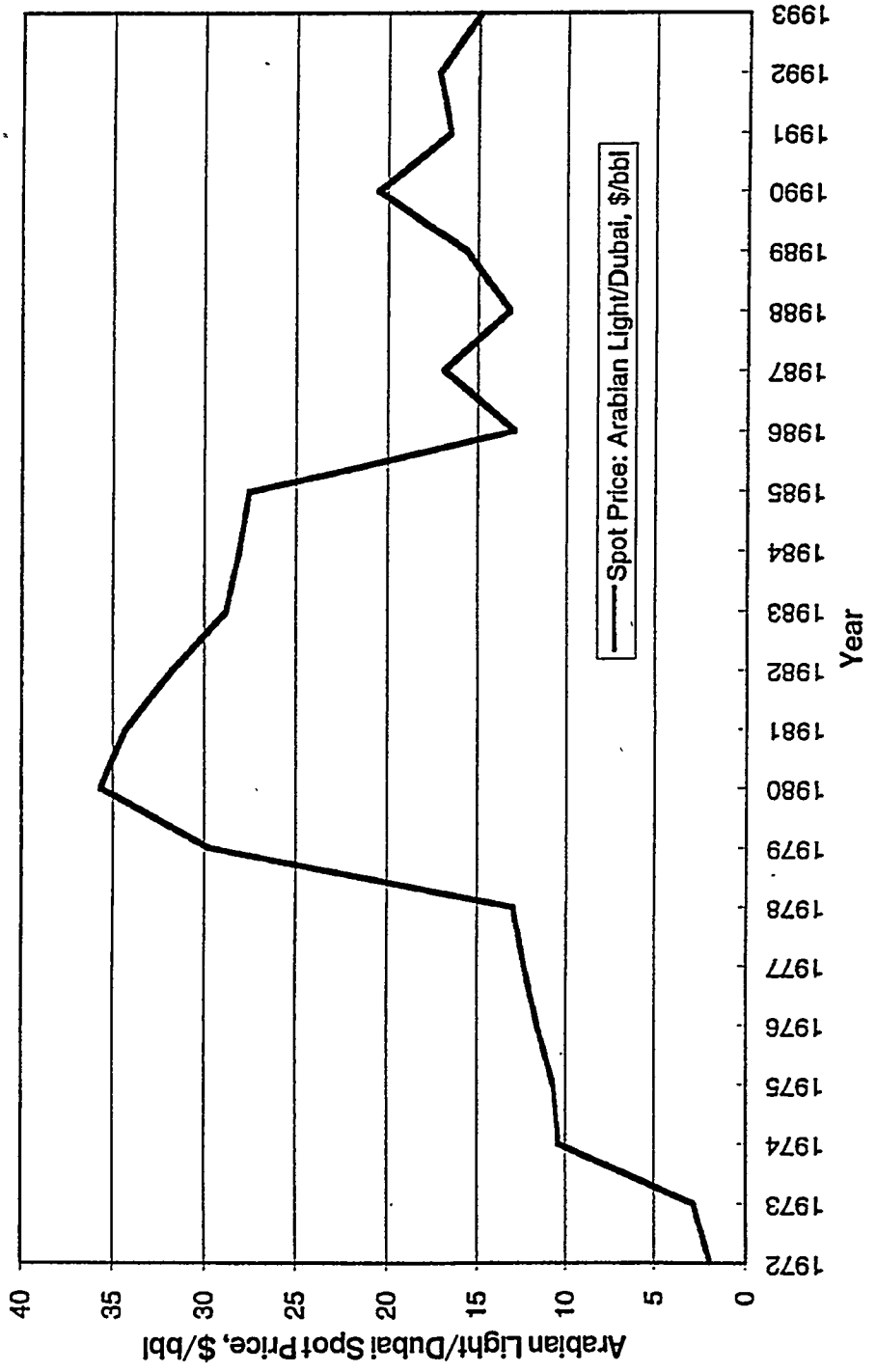

Figure 9-1. YEAR-END SPOT OIL PRICES (1972-1993)

After 1986 oil prices begin to more closely resemble a random walk and it becomes more difficult to identify any type of upward or downward trend in oil prices.

Explanations for these variations in oil prices have been documented, investigated, and reported upon by many. One common theme that recurs is that the sudden price changes are unrelated to the actual costs of lifting crude but upon other issues. A succinct and cogent review of the past, present and probable future of the world oil market is presented by Adelman[155]. It is clear that even at the 'low' 1972 oil price levels, oil producers realized profits of well over 100 percent per year. Most of this low-cost and highly profitable oil production originated from the Organization of Petroleum Exporting Countries (OPEC) where, by the beginning of the 1970s, the oil companies were "in the saddle" only as well paid jockeys. In the intervening years OPEC attempted to raise world oil prices by a variety of means, some planned, others opportunistic, that was in turn alternatively reviled or supported (sometimes both) by the oil-consuming countries. OPEC's goal was to suppress oil-on-oil competition and raise the oil-prices to the projected cost of synthetic liquid hydrocarbons (estimated to be $60 to $100/bbl). This goal, while resulting in spectacular upward price increases, was thwarted by excess supply and a real, if somewhat slow, response by consumers to higher prices. While oil industry forecasters continue to issue prophesies regarding oil prices it is difficult to believe any that project even moderate upward trends in oil prices over the next decade.

Effects of Divergent Cost Estimates on MCWM Project Economics

One of the major hurdles that MCWM technology developers face is lowering the costs necessary to implement a boiler retrofit. Any confusion and uncertainty regarding capital requirements raise the hurdle for project developers, since this uncertainty is magnified at the 250 MM Btu/hr or less boiler size. Potential boiler retrofit investors and customers are motivated to avoid risk and uncertainty regarding the basic question of, "How much?"

Addy[156] Schaal[157] found that boiler retrofit cost estimates for units scaled to or directed at the Crane boiler diverged widely. Using data from the EFRC's own Coal-Water Fuel Demonstration Facility, whose boiler is slightly smaller than the Crane boiler, Addy and Schaal determined that the Crane boiler could be retrofitted to fire MCWM at a lower life-cycle cost than continuing to fire natural gas and fuel oil. The EER conceptual design cost estimate for Crane was 2.9 times greater than that anticipated by the EFRC experience, resulting in the viability of retrofitting the Crane boiler varying from possibly above breakeven to being unprofitable. The project developers will have to address what costs are actually necessary and those that can be pared down if economic viability of the retrofitting boilers of this size is to be achieved. Economic viability, however, could be achieved by considering boilers larger than Crane.

The EFRC experience with widely divergent cost estimates for industrial coal boilers is not unique. In 1979, the DOE's Energy Information Agency (EIA) compared cost estimates for new

coal-fired industrial boilers compared to equivalent oil-fired units using a 175 MM Btu/hr size as a basis[158]. The study investigators found that cost estimates for the coal-fired units varied from 2.5 to 5 times that of an oil-fired unit. The EIA chose to review these particular coal-fired cost estimates since one or another had been used by the Congressional Budget Office (CBO), the DOE's EIA, and the Environmental Protection Agency as the basis for drafting laws and developing regulations directed at boilers of this size. They concluded that variations of cost of this magnitude could have serious implications in the development of benefit-cost analyses that are used as the basis for setting laws and regulations. The likely result are laws and regulations that work at cross purposes to promoting industrial coal use and regulating their emissions.

The EFRC effort differs from the context that prompted the EIA study, however, since the current concern is to make each potential boiler retrofit be economical on its own merits in the current and near term era of energy prices and environmental regulations. The EFRC and EIA's experiences underscore the sensitivity of capital costs on coal-based fuel use, the absolute necessity to pare down these capital costs to allow coal use if coal is to be economical relative to other fuel forms, and the uncertainty that has permeated the estimates for the capital costs.

Speculative Coal-Water Slurry Utilization Efforts

Some of the more speculative technologies involving MCWMs include Magneto Hydro Dynamics (MHD), MCWMs produced from anthracite, and "flame-free" coal gasification. MHD involves the extraction of electric energy from an extremely fast moving stream of combustion gases, followed by successive heat recovery and more conventional power production technologies. The MHD technology demonstration program has been completed recently with key technologies, such as suitable high temperature heat exchangers, not yet developed.

An effort has been undertaken to develop a MCWM derived from anthracite as a means for the DOD to increase its use of anthracite at its steam generating facilities. This project involved the use of a technology developed and owned by Otisca Industries, Ltd. to produce MCWMs for combustion. This effort has not been altogether successful to date as the anthracite-base MCWM required substantial gas cofiring to burn well. The project developers have suggested a number of areas for research and development directed at reducing the amount of gas cofiring required in order to meet legislated anthracite purchase and consumption targets.

"Flame-free" coal gasification is a euphemism for coal gasification using a nuclear fission heat source. A brief review of work using this approach is presented by[159]. Green's review begins with a synopsis of a National Research Council (NRC) study that was undertaken as a result of the 1991 U.S. Energy Policy's emphasis upon reducing the nation's dependence on imported sources of energy. This NRC study looked at direct and indirect conversion processes using coal in particular. A conclusion of the NRC study was that conversion processes using coal combustion for process heat were unattractive due to the production of greenhouse gasses. A

recommendation of the NRC was that non-fossil heat sources be investigated for these conversion processes, notably coal gasification integrated with a nuclear heat source.

Green reports that in the early 1980s the West German Protoptypanlage Nukleare Prozesswarme (PNP) project pursued steam gasification of bituminous coal, ideally in a micronized and cleaned slurry form, and hydro-gasification of lignite using 950 °C heat from a 40 MW nuclear reactor. The PNP program was halted due to unfavorable economics when the world price of oil dropped during the middle part of the decade.

Green also reports on the current efforts in Japan to develop a nuclear process heat capability, primarily for steelmaking, that could be adapted to flame-free coal gasification. He bemoans the Clinton administration's 1993 decision to terminate funding for the Modular Helium Reactor (MHR), the United State's equivalent program in high-temperature reactor technology, concluding with, "...pollution-free nuclear process heat would be deployed first by Japan to the economic disadvantage of the United States."

Unfortunately, casual reference to Japan's, or any other countries', efforts towards a particular technology development or policy does not itself constitute proof of its economic viability and provide a justification to pursue international competition in industrial research. For example, the Japanese government and Japanese corporations, in spite of their renowned prowess for dominating many of the world's high technology industries, have a rather poor record of acquiring access to low-cost energy sources. Japanese steel companies have in the past signed long-term coal contracts at premium prices, only to have those prices plunge on the world's coal markets shortly thereafter, resulting in an economic disadvantage to the Japanese relative to other steel producers.

A recent example of Japanese involvement in marginal or non-economic endeavors in energy to secure their own sources of energy is Abu Dhabi's Upper Zakum offshore oil field. This oil field required a $6 billion capital investment and has yet to pay off this investment despite steadily increasing production from 310,000 barrels per day (bpd) in 1990 to 450,000 bpd expected by the end of 1994. By comparison, most OPEC oil fields lift crude at such low costs that they easily recover their capital costs within a single year.

The Upper Zakum project is a joint venture involving Abu Dhabi, whose Zakum Development Company owns 88 percent with the Japanese government's Japan Oil Company and nine Japanese oil firms own the other 12 percent. The project owners admit to having much higher costs than the other OPEC producers but are yet seeking to increase their output (at the expense of other OPEC members) in order to recoup their very large investment. The supposition is that low-cost oil field output should be restrained in favor of their own high-cost output! Ironically, even though the Japanese are part owners in the Upper Zakum project they do not value its crude very

highly compared to crudes from other oil fields since it yields relatively little of the gasoline that is in high demand and comparatively more of the lower-value fuel oils.

The point to be made here is that the decision to embark upon a research intended to directly provide an 'economic advantage' should be based review of the projects' own merits; not alone upon looking at "what the other guy is, or seems to be, doing."

Recommendations for Future Economic Analysis of MCWM Projects

Once it is recognized that MCWM projects are attempting to replace other fossil fuels, predominantly oil, and that the price of oil has been very volatile since the early 1970s, it becomes obvious that any project that relies upon long term oil prices levels can be considered speculative. The crux of the problem lays with the discounted cash flow (DCF) analysis that have been used by project developers and forms the core analysis tool for the economic evaluation of most projects. The primary problem is projecting oil prices out into the future, sometimes out as far as 25 years, in order to derive the net benefits (or cash flows) of using the coal-based fuel.

The development of quantitative methods to value financial instruments in an environment where fluctuations in the price of stocks and commodities are normal may provide some relief to this problem. The next two sections perform pricing of the project from two different viewpoints based upon the distribution of price changes, termed volatility or risk, in the price of oil and not on forecasts as to those oil price levels.

AN OPTION PRICING MODEL APPROACH FOR EX ANTE EVALUATION OF RETROFITTING OIL-FIRED BOILERS TO COAL-FIRING

This section describes an option pricing model (OPM) approach to evaluating investments in new, innovative technologies based upon the market conditions of existing goods. The option pricing model can be used to evaluate the value of investing to improve the efficiency of those technologies that offer the potential to make use of lower priced resources to perform the same function as provided by existing technologies. The value of using option pricing theory stems from its efficient use of market information while also minimizing the reliance upon subjective and arbitrary inputs, such as determining the "correct" discount rate or engaging upon the often hazardous practice of forecasting future oil price levels.

The specific case studied here is an evaluation of retrofitting an oil-fired boiler to coal firing. Here, the option to expend capital and retrofit a boiler is evaluated relative to continuing to fire the boiler with fuel oil. This paper represents a first attempt at using option pricing theory to value the retrofit development effort by EFRC relative to the market price for fuel oil.

A spreadsheet-based binomial option pricing model is developed that allows a limited evaluation of the value of an option to retrofit oil-fired boilers to coal firing. The model shows that the price of the call option on retrofitting boilers is 65.6 ¢/MM Btu and can vary between 15 and

An economic evaluation of retrofitting oil-fired boilers has been conducted by [156]. They recognized that, in determining the economic viability of switching an existing boiler to firing MCWM, the cost of the retrofit would need to be compared to the current cost of oil-firing. Addy and Considine term this the differential fuel cost. The differential fuel cost is a recognition of the per unit premium in capital and operation costs of retrofitting as opposed to continuing oil-firing. It can be thought of as a price discount for MCWM that must be given to boiler owners to encourage them to invest the necessary capital to switch from using fuel oil.

Addy and Considine found that a differential fuel cost of about 1.50 $/MM Btu is required in order for retrofitting to be an economically viable alternative to firing fuel oil. In addition, they found that boiler retrofit economics are more sensitive to differential fuel costs than any to other variable with the exception of retrofit capital costs. This last observation underlines the need to better connect the analysis to market pricing data.

[157] provides a speculative estimate of likely MCWM production costs of 3.23 $/MM Btu, f.o.b. slurry preparation plant This cost for MCWM includes recovery of capital. With truck transportation charges of 0.90 $/MM Btu, the delivered cost of slurry fuel to the Crane site is 4.13 $/MM Btu. However, this analysis was based on supplying just one relatively small boiler. Schaal extended his analysis to consider that the MCWM production facility would supply multiple boilers in a given market area. If retrofitting is an economically viable option, then other boilers should be expected to retrofit as well. At a production level equivalent to ten Crane boilers, the delivered cost of MCWM falls to 1.90 $/MM Btu. It is reasonable to assume that average costs are still decreasing at this level of production since it would still be a small fraction of the total production at an existing coal preparation facility.

Binomial Option Pricing Model Description

This section presents the option pricing model to be used to evaluate the value of the option to retrofit oil-fired boilers to firing MCWM. First, the structure of the model as given by Pickles and Smith is described. Second, the parameters of the model relevant to the current case study are presented and discussed. Finally, the fuel oil price volatility estimator is discussed.

It should be noted that the economic analyses presented in the previous section are speculative in nature. That is, they represent an estimate of costs that have a rather large variance. The value to acquire the option to retrofit can be thought of, in this case, as the amount that can be spent in research, development and engineering efforts to further define (reduce the variance of) and lower the costs of retrofitting.

Model Structure

Pickles and Smith use a multi-period multiplicative binomial option pricing model in their analysis. A two period model is shown in Figure 9-2. As can be seen from the figure, the price of a stock, S, can take only one of two possible changes in any one subsequent time period. There

An economic evaluation of retrofitting oil-fired boilers has been conducted by [156]. They recognized that, in determining the economic viability of switching an existing boiler to firing MCWM, the cost of the retrofit would need to be compared to the current cost of oil-firing. Addy and Considine term this the differential fuel cost. The differential fuel cost is a recognition of the per unit premium in capital and operation costs of retrofitting as opposed to continuing oil-firing. It can be thought of as a price discount for MCWM that must be given to boiler owners to encourage them to invest the necessary capital to switch from using fuel oil.

Addy and Considine found that a differential fuel cost of about 1.50 $/MM Btu is required in order for retrofitting to be an economically viable alternative to firing fuel oil. In addition, they found that boiler retrofit economics are more sensitive to differential fuel costs than any to other variable with the exception of retrofit capital costs. This last observation underlines the need to better connect the analysis to market pricing data.

[157] provides a speculative estimate of likely MCWM production costs of 3.23 $/MM Btu, f.o.b. slurry preparation plant This cost for MCWM includes recovery of capital. With truck transportation charges of 0.90 $/MM Btu, the delivered cost of slurry fuel to the Crane site is 4.13 $/MM Btu. However, this analysis was based on supplying just one relatively small boiler. Schaal extended his analysis to consider that the MCWM production facility would supply multiple boilers in a given market area. If retrofitting is an economically viable option, then other boilers should be expected to retrofit as well. At a production level equivalent to ten Crane boilers, the delivered cost of MCWM falls to 1.90 $/MM Btu. It is reasonable to assume that average costs are still decreasing at this level of production since it would still be a small fraction of the total production at an existing coal preparation facility.

Binomial Option Pricing Model Description

This section presents the option pricing model to be used to evaluate the value of the option to retrofit oil-fired boilers to firing MCWM. First, the structure of the model as given by Pickles and Smith is described. Second, the parameters of the model relevant to the current case study are presented and discussed. Finally, the fuel oil price volatility estimator is discussed.

It should be noted that the economic analyses presented in the previous section are speculative in nature. That is, they represent an estimate of costs that have a rather large variance. The value to acquire the option to retrofit can be thought of, in this case, as the amount that can be spent in research, development and engineering efforts to further define (reduce the variance of) and lower the costs of retrofitting.

Model Structure

Pickles and Smith use a multi-period multiplicative binomial option pricing model in their analysis. A two period model is shown in Figure 9-2. As can be seen from the figure, the price of a stock, S, can take only one of two possible changes in any one subsequent time period. There

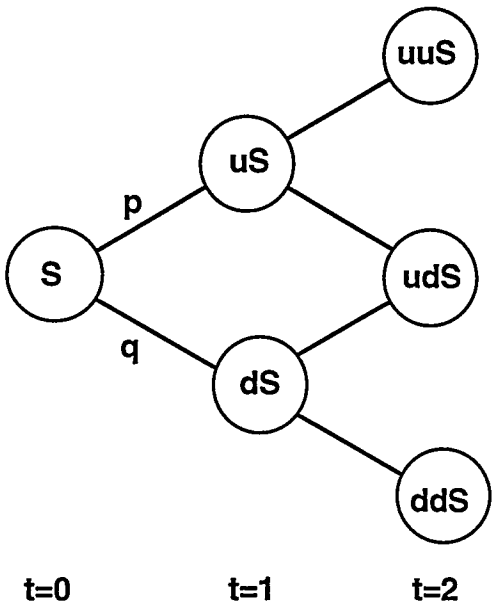

Figure 9-2. TWO PERIOD BINOMIAL OPTION PRICING MODEL

exists the probability, p, that the stock price will increase by the up factor, u, from its current value. Likewise, the variable q represent the probability that the stock price will decrease by the down factor, d, from its current value.

Evaluating the present value of a call option on the asset S at the terminal period, as depicted in Figure 9-2, requires some knowledge about the project. Specifically, the initial stock price, stock price volatility, strike price, the length of time the option exists, the number of time periods in the model, the risk-free interest rate, and the payout rate all work to determine the model structure.

In the current case, the stock price, S, is taken as the market price of No. 2 fuel oil as is fired in the Crane boiler. This is a simplification since the Crane boiler, as it is currently configured, is capable of switching between No. 2 fuel oil and natural gas within a matter of hours. This aspect of the current operation is not addressed here. Fuel oil price volatility is further described below. The initial stock price is taken then as the 1992 year end price of 3.15 $/MM Btu (Initial price No.2 fuel oil is taken as 54.25 cents per gallon.). Fuel oil pricing is also discussed below.

The exercise price of the option, the amount to be spent to actually realize the benefits of firing coal water slurry, is taken as the sum of the delivered cost of fuel plus the required differential fuel cost required by the boiler owner to undertake the retrofit. Using information supplied above, the exercise price, X, has a value of 3.40 $/MM Btu. Therefore, the call option is initially "out-of-the-money" in that the exercise price exceeds the initial stock price.

The current demonstration program has a tentative "go/no-go" decision date to proceed with engineering of one year from now. Considering the developmental nature of this program, it is likely that as many as three years will be required to finish the retrofit and be ready to commence operations. Three years is then taken as the time period of the model. Twelve time periods are considered in this model with the final decision to begin firing the boiler with coal (exercise the option) being made at the terminal period of the model.

The payout rate, δ, is the difference between the investor's required rate of return and the rate of price appreciation earned on existing sources of supply (assuming that the fuel oil distributor is also the potential MCWM distributor). The payout rate is then the developer's opportunity cost of keeping the option open. Pickles and Smith argue that option pricing model should use a payout rate of 8 percent based upon their review of industry data and practice.

The values for p, u, and the other parameters of the model are calculated from the values given above following the equations given by Pickles and Smith. Table 9-1 shows the twelve period model using values for the relevant variables as used by Pickles and Smith[163]. A comparison of Table 9-1 to Pickles and Smith's data shows that the calculations are correctly specified and the spreadsheet model consistent with theirs.

Table 9-1.

Binomial Option Pricing Model Verification

MODEL STRUCTURE			
Initial Stock Price	S	1.00	$/bbl
Exercise Price	X	1.00	$/bbl
Risk-Free Interest rate	r	4	%
Payout Rate	δ	13	%
Option Life	T	1.00	Years
Number of Periods	n	12	
Time period length	dt	0.0833	Years
Upward price change	u	6.56	% per period
Downward price change	d	-6.15	% per period
Expected price change	ΔS*	-0.75	% per period
Up Probability	p	0.4253	
Down Probability	1 - p	0.5747	
Discount Rate	dr	-0.33	% per period

Period, $/bbl	0	1	2	3	4	5	6	7	8	9	10	11	12
Price	1.0000	1.0656	1.1354	1.2099	1.2892	1.3737	1.4638	1.5598	1.6621	1.7711	1.8872	2.0109	2.1428
Exercise Value	0.0000	0.0656	0.1354	0.2099	0.2892	0.3737	0.4638	0.5598	0.6621	0.7711	0.8872	1.0109	1.1428
Hold Value	0.0554	0.0886	0.1381	0.2007	0.2787	0.3623	0.4514	0.5463	0.6475	0.7553	0.8702	0.9926	0.0000
Option Value	0.0554	0.0886	0.1381	0.2099	0.2892	0.3737	0.4638	0.5598	0.6621	0.7711	0.8872	1.0109	1.1428
Exercise ?	No	No	No	Yes	Yes	Yes	Yes	Yes	Yes	Yes	Yes	Yes	Yes
Price		0.9385	1.0000	1.0656	1.1354	1.2099	1.2892	1.3737	1.4638	1.5598	1.6621	1.7711	1.8872
Exercise Value		-0.0615	0.0000	0.0656	0.1354	0.2099	0.2892	0.3737	0.4638	0.5598	0.6621	0.7711	0.8872
Hold Value		0.0312	0.0524	0.0858	0.1364	0.2002	0.2787	0.3623	0.4514	0.5463	0.6475	0.7553	0.0000
Option Value		0.0312	0.0524	0.0858	0.1364	0.2099	0.2892	0.3737	0.4638	0.5598	0.6621	0.7711	0.8872
Exercise ?		No	No	No	No	Yes	Yes	Yes	Yes	Yes	Yes	Yes	Yes
Price			0.8807	0.9385	1.0000	1.0656	1.1354	1.2099	1.2892	1.3737	1.4638	1.5598	1.6621
Exercise Value			-0.1193	-0.0615	0.0000	0.0656	0.1354	0.2099	0.2892	0.3737	0.4638	0.5598	0.6621
Hold Value			0.0157	0.0280	0.0489	0.0828	0.1343	0.2002	0.2787	0.3623	0.4514	0.5463	0.0000
Option Value			0.0157	0.0280	0.0489	0.0828	0.1354	0.2099	0.2892	0.3737	0.4638	0.5598	0.6621
Exercise ?			No	No	No	No	Yes	Yes	Yes	Yes	Yes	Yes	Yes
Price				0.8265	0.8807	0.9385	1.0000	1.0656	1.1354	1.2099	1.2892	1.3737	1.4638
Exercise Value				-0.1735	-0.1193	-0.0615	0.0000	0.0656	0.1354	0.2099	0.2892	0.3737	0.4638
Hold Value				0.0066	0.0127	0.0241	0.0444	0.0791	0.1310	0.2002	0.2787	0.3623	0.0000
Option Value				0.0066	0.0127	0.0241	0.0444	0.0791	0.1354	0.2099	0.2892	0.3737	0.4638
Exercise ?				No	No	No	No	No	Yes	Yes	Yes	Yes	Yes
Price					0.7757	0.8265	0.8807	0.9385	1.0000	1.0656	1.1354	1.2099	1.2892
Exercise Value					-0.2243	-0.1735	-0.1193	-0.0615	0.0000	0.0656	0.1354	0.2099	0.2892
Hold Value					0.0021	0.0044	0.0092	0.0189	0.0378	0.0733	0.1265	0.2002	0.0000
Option Value					0.0021	0.0044	0.0092	0.0189	0.0378	0.0733	0.1354	0.2099	0.2892
Exercise ?					No	No	No	No	No	No	Yes	Yes	Yes
Price						0.7279	0.7757	0.8265	0.8807	0.9385	1.0000	1.0656	1.1354
Exercise Value						-0.2721	-0.2243	-0.1735	-0.1193	-0.0615	0.0000	0.0656	0.1354
Hold Value						0.0004	0.0009	0.0021	0.0050	0.0118	0.0278	0.0574	0.0000
Option Value						0.0004	0.0009	0.0021	0.0050	0.0118	0.0278	0.0656	0.1354
Exercise ?						No	No	No	No	No	No	Yes	Yes
Price							0.6831	0.7279	0.7757	0.8265	0.8807	0.9385	1.0000
Exercise Value							-0.3169	-0.2721	-0.2243	-0.1735	-0.1193	-0.0615	0.0000
Hold Value							0.0000	0.0000	0.0000	0.0000	0.0000	0.0000	0.0000
Option Value							0.0000	0.0000	0.0000	0.0000	0.0000	0.0000	0.0000
Exercise ?							No	No	No	No	No	No	No
Price								0.6411	0.6831	0.7279	0.7757	0.8265	0.8807
Exercise Value								-0.3589	-0.3169	-0.2721	-0.2243	-0.1735	-0.1193
Hold Value								0.0000	0.0000	0.0000	0.0000	0.0000	0.0000
Option Value								0.0000	0.0000	0.0000	0.0000	0.0000	0.0000
Exercise ?								No	No	No	No	No	No
Price									0.6017	0.6411	0.6831	0.7279	0.7757
Exercise Value									-0.3983	-0.3589	-0.3169	-0.2721	-0.2243
Hold Value									0.0000	0.0000	0.0000	0.0000	0.0000
Option Value									0.0000	0.0000	0.0000	0.0000	0.0000
Exercise ?									No	No	No	No	No
Price										0.5646	0.6017	0.6411	0.6831
Exercise Value										-0.4354	-0.3983	-0.3589	-0.3169
Hold Value										0.0000	0.0000	0.0000	0.0000
Option Value										0.0000	0.0000	0.0000	0.0000
Exercise ?										No	No	No	No
Price											0.5299	0.5646	0.6017
Exercise Value											-0.4701	-0.4354	-0.3983
Hold Value											0.0000	0.0000	0.0000
Option Value											0.0000	0.0000	0.0000
Exercise ?											No	No	No
Price												0.4973	0.5299
Exercise Value												-0.5027	-0.4701
Hold Value												0.0000	0.0000
Option Value												0.0000	0.0000
Exercise ?												No	No
Price													0.4667
Exercise Value													-0.5333
Hold Value													0.0000
Option Value													0.0000
Exercise ?													No

Fuel Price Volatility Estimation

Particular care must be taken when estimating the stock volatility. [162], state that estimates of the stock's true volatility are generally taken from historical data or are implied by the market in the price of options. They point out that both historical and implied estimates of price volatility have drawbacks in predicting actual stock volatility during a particular period. The main reason is that stock price volatility is continually changing, therefore the use of historical data can be of limited value. Future stock price volatility is also difficult to predict even when using the accumulated knowledge represented by a market for options as demonstrated by Edwards and Ma. Johnson[164] offers a Monte Carlo method of option pricing with stochastic stock volatility; however, this paper does not pursue their approach.

The historical method of determining the future stock price volatility is used in this analysis as a "base case." The previous five years daily high and low prices for No. 2 fuel oil (Gulf Coast, f.o.b. pipeline) were obtained from Platt's Oil Price Handbook[165], the last year for which fuel oil consumption data from the Crane site are available). The monthly close, high, and low prices were taken as observations of the fuel oil price volatility and are shown in Figure 9-3. It can be seen from the figure that No. 2 fuel oil prices varied between just below 40 ¢/gal. to just over 60 ¢/gal. for most of the time period with the notable exception of late 1989 and the last half of 1990. The fuel oil price "shocks" experienced during these time periods correspond with uncertainty in the market regarding the invasion of Kuwait by Iraq, Operation Desert Shield, followed by Operation Desert Storm, and finally the relatively rapid recovery of oil field production capacity. This data set then, is a good representative sample of the price shocks of concern to policy makers.

The standard method for calculating the historical price volatility is performed by taking the difference between the natural logarithms of the current and previous prices. The standard deviation of the stock price is the standard deviation of the price changes themselves. The calculation procedure is:

$$\hat{\sigma}_0 = \sqrt{\frac{1}{N-1}\sum_{i=1}^{N}\left(X_i - \overline{X}\right)^2}$$

Where: $\hat{\sigma}_0$ = sample standard deviation calculated using first difference of stock price

N = number of observations

S_i = fuel oil end of month price at period i

$X_i = ln\left(S_i / S_{i-1}\right)$, the percentage price change

$\overline{X}$ = Arithmetic mean of X_i

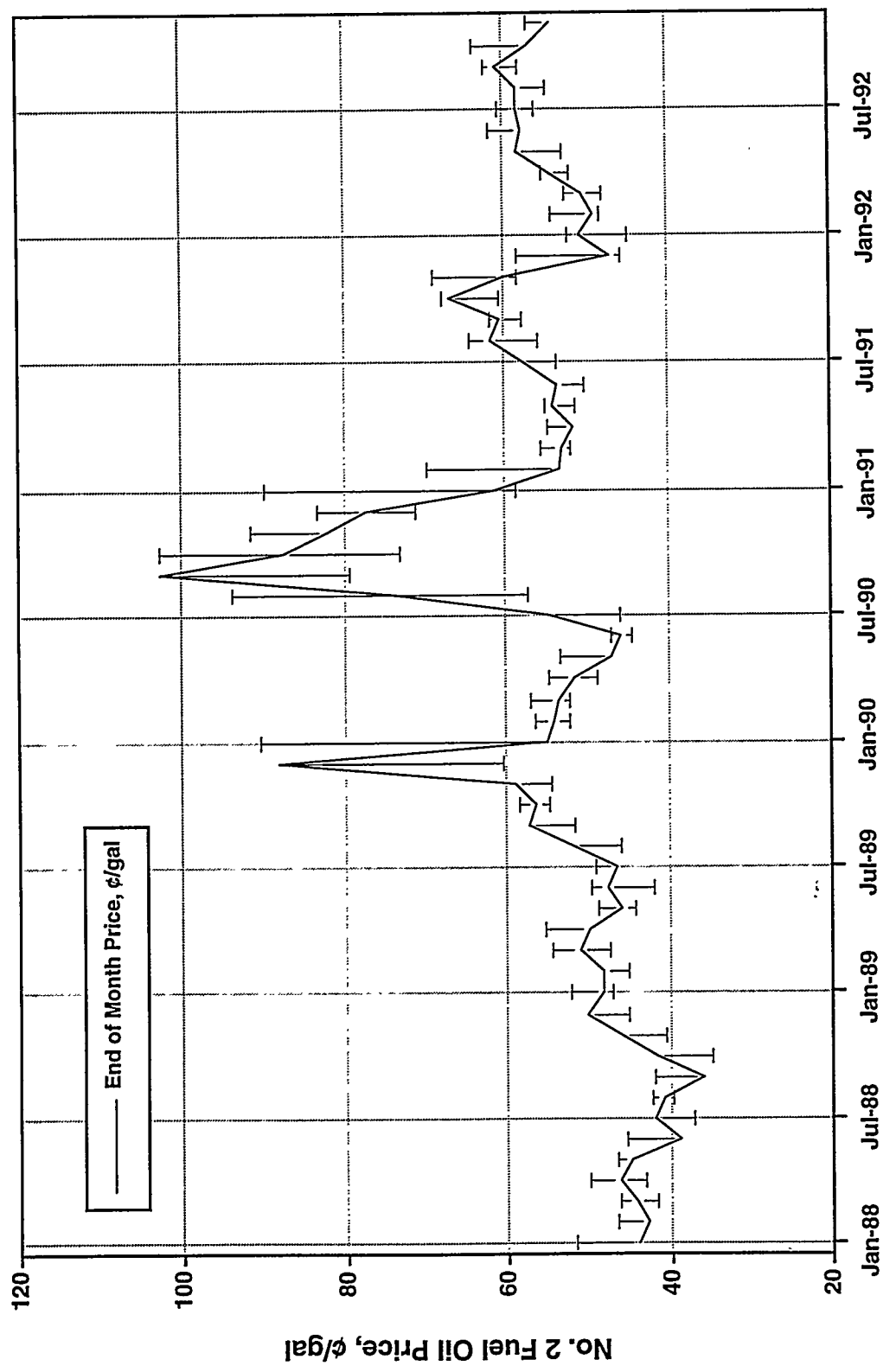

Source: "Platt's Oil Price Handbook," 65th to 69th Editions

Figure 9-3. END OF MONTH, HIGH AND LOW PRICES FOR GULF COAST NO. 2 FUEL OIL (f.o.b. Pipeline)

Table 9-2 shows the calculated monthly price volatility for the five year time period. Also calculated is the annualized standard deviation for the five year time period as well as the annualized standard deviations for each of the five years. These measures of the stock price volatility are summarized in Table 9-3.

It can be seen from the summary results in the table that the fuel oil price volatility changed fairly significantly throughout the time period for the same reasons as pointed out in the discussion of Figure 9-3. The 1988-1992 $\hat{\sigma}_0$ estimates of fuel oil price volatility can also be made using the instantaneous high and low prices recorded during the period in question. Parkinson[166] has developed the extreme value method for using the information contained in the high and low stock prices to provide an unbiased estimator of the stock price volatility. This model uses just the highest and lowest recorded stock price in the estimation of the price volatility.

Parkinson argues that the estimate of the stock price volatility using this method is over five times as efficient as that obtained using the classical approach. That is, about 80 percent fewer observations are required to construct an accurate estimator as compared to use of the classical approach. This level of data efficiency provides the opportunity to investigate time dependencies in the stock prices and to uncover, at an earlier time, sudden shifts in the stock price volatility.

The procedure for calculating the extreme value estimator of stock price volatility is:

$$\hat{\sigma}_2 = \sqrt{\frac{1}{4N\,ln(2)}\sum_{i=1}^{N} l_i^2}$$

Where: $\hat{\sigma}_2$ = sample standard deviation calculated using the extreme value method

N = number of observations

H_i = highest recorded fuel oil price during period i

L_i = lowest recorded fuel oil price during period i

$l_i = ln\left(\frac{H_i}{L_i}\right)$, the percentage difference in high and low price in period i

Table 9-2 also shows the calculated monthly price volatility using the extreme value method for the same five year time period. Also calculated is the annualized standard deviation for the five year time period as well as the annualized standard deviations for each of the five years. These measures of the stock price volatility are also shown in Table 9-4.

There appears to be a fairly good comparison of the stock volatility estimates provided by the classical, first difference, method and the extreme value method as shown in Tables 9-1 and 9-2 above. This is particularly true when considering the differences by which the Brownian movement of the stock price is being measured.

Table 9-2.

Monthly Close, High and Low Prices and Price Volatility Estimates for Gulf Coast No. 2 Fuel Oil (f.o.b. Pipeline) (Prices in ¢/gal)

Date	Close Price	High Price	Low Price	Percentage Change in Close, X%	Extreme Value Diff., L%	Bias Corrected*
Jan-88	44.00	51.50	44.00		15.74	18.30
Feb-88	42.75	46.50	42.00	-2.88	10.18	11.84
Mar-88	44.25	46.25	41.75	3.45	10.24	11.90
Apr-88	46.25	49.75	43.00	4.42	14.58	16.95
May-88	44.75	46.50	44.25	-3.30	4.96	5.77
Jun-88	38.75	45.25	38.50	-14.40	16.15	18.78
Jul-88	42.00	42.50	37.00	8.05	13.86	16.11
Aug-88	40.75	42.25	39.75	-3.02	6.10	7.09
Sep-88	36.00	42.00	36.00	-12.39	15.42	17.92
Oct-88	41.50	42.00	34.75	14.22	18.95	22.03
Nov-88	45.75	45.75	40.50	9.75	12.19	14.17
Dec-88	50.00	50.25	45.00	8.88	11.03	12.83
Jan-89	48.25	52.25	47.00	-3.56	10.59	12.31
Feb-89	48.25	48.75	45.00	0.00	8.00	9.31
Mar-89	51.00	54.25	47.25	5.54	13.82	16.06
Apr-89	49.75	55.25	49.00	-2.48	12.00	13.96
May-89	46.00	48.75	44.25	-7.84	9.68	11.26
Jun-89	47.50	49.50	42.00	3.21	16.43	19.11
Jul-89	46.50	49.00	45.75	-2.13	6.86	7.98
Aug-89	51.75	52.00	45.75	10.70	12.81	14.89
Sep-89	57.25	57.50	51.50	10.10	11.02	12.81
Oct-89	56.50	58.50	54.75	-1.32	6.62	7.70
Nov-89	59.00	59.50	54.50	4.33	8.78	10.21
Dec-89	88.25	88.75	60.25	40.26	38.73	45.04
Jan-90	55.00	90.50	55.00	-47.28	49.80	57.91
Feb-90	54.00	56.25	52.00	-1.83	7.86	9.14
Mar-90	53.50	57.00	52.00	-0.93	9.18	10.68
Apr-90	51.50	54.75	48.75	-3.81	11.61	13.50
May-90	47.00	53.25	47.00	-9.14	12.49	14.52
Jun-90	45.75	47.00	44.50	-2.70	5.47	6.36
Jul-90	54.75	55.00	45.75	17.96	18.41	21.41
Aug-90	73.75	94.00	57.25	29.79	49.59	57.66
Sep-90	102.75	103.00	79.25	33.16	26.21	30.48
Oct-90	87.75	102.75	73.25	-15.78	33.84	39.35
Nov-90	82.25	91.50	81.50	-6.47	11.57	13.46
Dec-90	77.50	83.25	71.25	-5.95	15.57	18.10
Jan-91	61.25	90.00	58.75	-23.53	42.65	49.60
Feb-91	53.25	69.75	53.25	-14.00	26.99	31.39
Mar-91	53.00	55.50	51.75	-0.47	7.00	8.13
Apr-91	51.50	54.75	50.75	-2.87	7.59	8.82
May-91	54.00	55.00	51.25	4.74	7.06	8.21
Jun-91	53.50	54.00	50.00	-0.93	7.70	8.95
Jul-91	57.75	58.00	53.50	7.64	8.08	9.39
Aug-91	61.75	64.25	55.75	6.70	14.19	16.50
Sep-91	60.75	61.75	57.75	-1.63	6.70	7.79
Oct-91	66.75	67.75	60.75	9.42	10.91	12.68
Nov-91	60.00	69.00	58.50	-10.66	16.51	19.20
Dec-91	47.00	58.25	45.50	-24.42	24.70	28.72
Jan-92	50.75	52.25	44.75	7.68	15.49	18.02
Feb-92	49.00	54.00	48.00	-3.51	11.78	13.70
Mar-92	50.50	52.50	47.75	3.02	9.48	11.03
Apr-92	54.25	55.25	51.75	7.16	6.54	7.61
May-92	58.25	58.75	52.75	7.11	10.77	12.53
Jun-92	57.75	61.75	57.75	-0.86	6.70	7.79
Jul-92	58.25	60.50	56.00	0.86	7.73	8.99
Aug-92	58.50	58.50	54.75	0.43	6.62	7.70
Sep-92	61.00	62.25	58.00	4.18	7.07	8.22
Oct-92	57.00	63.75	57.00	-6.78	11.19	13.01
Nov-92	54.00	57.00	54.00	-5.41	5.41	6.29
Dec-92	54.25	56.25	50.25	0.46	11.28	13.12
Daily standard deviations (%):						
1988–1992 σ				12.99	10.41	12.11
Annualized standard deviations (%):						
1988–1992 σ				44.99	36.07	41.94
1988 σ				31.88	27.21	31.64
1989 σ				43.25	31.95	37.16
1990 σ				73.61	53.58	62.31
1991 σ				40.15	38.36	44.61
1992 σ				16.83	20.00	23.25

* Assumes 100 transactions per day, Garman and Klass (1980, p. 75).

Source: "Platt's Oil Price Handbook," 65th to 69th Editions.

Table 9-3. Price Volatility Using the Historical First Difference Method

$1988\hat{\sigma}_o$	31.9	Percent per year
$1989\hat{\sigma}_o$	43.2	Percent per year
$1990\hat{\sigma}_o$	73.6	Percent per year
$1991\hat{\sigma}_o$	40.2	Percent per year
$1992\hat{\sigma}_o$	16.8	Percent per year
$1988-1992\hat{\sigma}_o$	45.0	Percent per year

Table 9-4. Price Volatility Using the Extreme Value Method

$1988\hat{\sigma}_2$	27.2	Percent per year
$1989\hat{\sigma}_2$	32.0	Percent per year
$1990\hat{\sigma}_2$	53.6	Percent per year
$1991\hat{\sigma}_2$	38.4	Percent per year
$1992\hat{\sigma}_2$	20.0	Percent per year
$1988-1992\hat{\sigma}_2$	36.1	Percent per year

[167] provide a different approach to evaluating the stock price volatility using historical data. They begin with Parkinson's extreme value model and add other stock price information, such as the previous stock close price, in successive steps to further improve upon the efficiency of the estimate of the volatility. They make a potentially troublesome observation regarding the non-classical volatility estimation methods in that for a low volume of trades (up to 500 transactions) even the extreme value method is subject to bias. In the case of the extreme value method, the bias results in a estimator that is 89% of its "actual" value for 100 transactions during that day. The difficulty with applying Garman and Klass's bias correction factor is a lack of knowledge of the actual number of transactions during the period. Table 9-2 also shows these 'bias corrected' volatility estimates using the extreme value method assuming that 100 transaction occurred during each day to allow comparison with the uncorrected and first difference volatility estimates.

Discussion of the Binomial OPM Results

A summary of the values for the specific variables used in the Crane-specific analysis are presented in Table 9-5. The results for the binomial option pricing model using the values shown in Table 9-5 above are presented in Table 9-6. The value of the call option was calculated at 65.6 ¢/MM Btu, or approximately 20 percent of the exercise price of the retrofit.

The volatility of the fuel oil price is an important variable of the model in which there is some doubt as to the actual future path of the stock price. Using the extreme value method of calculating the stock volatility over the five years of price data provided a $\hat{\sigma}_2$ of 36.1 %/annum. The price of the call option at this level of volatility is 49.5 ¢/MM Btu. Using the extreme value method and the last year's data provides a volatility measure of 20 %/annum with a corresponding call option price of 20.4 ¢/MM Btu.

The OPM pricing model results for the boiler retrofit appear to be very high, meaning that the model predicts that the value of the option to retrofit appears to be much higher than expected. There exist two possible explanations for this overpricing phenomenon. First, the OPM approach relies upon the use of historical price data to predict future price volatility. A related, and more likely explanation, is that the Brownian movement of oil prices may not be entirely a random walk over long time periods.

Care must be taken when using historical price data to estimate oil price volatility, as previously addressed. Edwards and Ma suggest that an alternative method to using historical data to estimate price volatility is to use volatility estimates derived from the current consensus outlook that underlay, or are implied by, the prices of option and futures contracts in the crude oil commodities markets. One obvious drawback is that the current sentiment regarding oil commodities, as represented by the aggregate attitudes and beliefs of economic agents in the market, is not a guarantee of the actual oil price volatility realized.

Table 9-5.

Twelve Period Binomial Option Pricing Model:
Summary of Given and Dervied Variable Values

Variable Description		Value	Units
Initial Stock Price	S	3.15	$/MMBtu
Exercise Price	X	3.40	$/MMBtu
Risk-Free interest rate	r	4	%
Payout Rate	δ	8	%
Option Life	T	3.00	Years
Number of Periods	n	12	
Time period length	dt	0.25	Years
Upward price change	u	25.23	% in a single period
Downward price change	d	-20.15	% in a single period
Expected price change	ΔS*	-1.00	%/period
Up Probability	p	0.4221	
Down Probability	1 - p	0.5779	
Discount Rate	dr	-1.00	%/period
Stock Volatilty	σ	45.0%	/annum

Table 9-6.

Twelve Period Binomial Option Pricing Model:
Crane Boiler Retrofit Case

Period, $/MMBtu	0	1	2	3	4	5	6	7	8	9	10	11	12
Price	3.1500	3.9446	4.9397	6.1858	7.7462	9.7003	12.1472	15.2115	19.0488	23.8540	29.8714	37.4068	46.8430
Exercise Value	-0.2500	0.5446	1.5397	2.7858	4.3462	6.3003	8.7472	11.8115	15.6488	20.4540	26.4714	34.0068	43.4430
Hold Value	0.6558	1.0884	1.7673	2.8042	4.2271	6.1426	8.5414	11.5453	15.3069	20.0175	25.9163	33.3032	0.0000
Option Value	0.6558	1.0884	1.7673	2.8042	4.3462	6.3003	8.7472	11.8115	15.6488	20.4540	26.4714	34.0068	43.4430
Exercise ?	No	No	No	No	Yes	Yes	Yes	Yes	Yes	Yes	Yes	Yes	Yes
Price		2.5155	3.1500	3.9446	4.9397	6.1858	7.7462	9.7003	12.1472	15.2115	19.0488	23.8540	29.8714
Exercise Value		-0.8845	-0.2500	0.5446	1.5397	2.7858	4.3462	6.3003	8.7472	11.8115	15.6488	20.4540	26.4714
Hold Value		0.3511	0.6114	1.0405	1.7264	2.7788	4.2271	6.1426	8.5414	11.5453	15.3069	20.0175	0.0000
Option Value		0.3511	0.6114	1.0405	1.7264	2.7858	4.3462	6.3003	8.7472	11.8115	15.6488	20.4540	26.4714
Exercise ?		No	No	No	No	Yes	Yes	Yes	Yes	Yes	Yes	Yes	Yes
Price			2.0087	2.5155	3.1500	3.9446	4.9397	6.1858	7.7462	9.7003	12.1472	15.2115	19.0488
Exercise Value			-1.3913	-0.8845	-0.2500	0.5446	1.5397	2.7858	4.3462	6.3003	8.7472	11.8115	15.6488
Hold Value			0.1670	0.3085	0.5575	0.9824	1.6819	2.7436	4.2271	6.1426	8.5414	11.5453	0.0000
Option Value			0.1670	0.3085	0.5575	0.9824	1.6819	2.7858	4.3462	6.3003	8.7472	11.8115	15.6488
Exercise ?			No	No	No	No	No	Yes	Yes	Yes	Yes	Yes	Yes
Price				1.6041	2.0087	2.5155	3.1500	3.9446	4.9397	6.1858	7.7462	9.7003	12.1472
Exercise Value				-1.7959	-1.3913	-0.8845	-0.2500	0.5446	1.5397	2.7858	4.3462	6.3003	8.7472
Hold Value				0.0666	0.1320	0.2567	0.4885	0.9047	1.6205	2.6974	4.2271	6.1426	0.0000
Option Value				0.0666	0.1320	0.2567	0.4885	0.9047	1.6205	2.7858	4.3462	6.3003	8.7472
Exercise ?				No	No	No	No	No	No	Yes	Yes	Yes	Yes
Price					1.2810	1.6041	2.0087	2.5155	3.1500	3.9446	4.9397	6.1858	7.7462
Exercise Value					-2.1190	-1.7959	-1.3913	-0.8845	-0.2500	0.5446	1.5397	2.7858	4.3462
Hold Value					0.0200	0.0431	0.0919	0.1930	0.3975	0.7973	1.5324	2.6974	0.0000
Option Value					0.0200	0.0431	0.0919	0.1930	0.3975	0.7973	1.5397	2.7858	4.3462
Exercise ?					No	No	No	No	No	No	Yes	Yes	Yes
Price						1.0229	1.2810	1.6041	2.0087	2.5155	3.1500	3.9446	4.9397
Exercise Value						-2.3771	-2.1190	-1.7959	-1.3913	-0.8845	-0.2500	0.5446	1.5397
Hold Value						0.0034	0.0082	0.0196	0.0470	0.1124	0.2689	0.6435	0.0000
Option Value						0.0034	0.0082	0.0196	0.0470	0.1124	0.2689	0.6435	1.5397
Exercise ?						No	No	No	No	No	No	No	Yes
Price							0.8169	1.0229	1.2810	1.6041	2.0087	2.5155	3.1500
Exercise Value							-2.5831	-2.3771	-2.1190	-1.7959	-1.3913	-0.8845	-0.2500
Hold Value							0.0000	0.0000	0.0000	0.0000	0.0000	0.0000	0.0000
Option Value							0.0000	0.0000	0.0000	0.0000	0.0000	0.0000	0.0000
Exercise ?							No	No	No	No	No	No	No
Price								0.6523	0.8169	1.0229	1.2810	1.6041	2.0087
Exercise Value								-2.7477	-2.5831	-2.3771	-2.1190	-1.7959	-1.3913
Hold Value								0.0000	0.0000	0.0000	0.0000	0.0000	0.0000
Option Value								0.0000	0.0000	0.0000	0.0000	0.0000	0.0000
Exercise ?								No	No	No	No	No	No
Price									0.5209	0.6523	0.8169	1.0229	1.2810
Exercise Value									-2.8791	-2.7477	-2.5831	-2.3771	-2.1190
Hold Value									0.0000	0.0000	0.0000	0.0000	0.0000
Option Value									0.0000	0.0000	0.0000	0.0000	0.0000
Exercise ?									No	No	No	No	No
Price										0.4160	0.5209	0.6523	0.8169
Exercise Value										-2.9840	-2.8791	-2.7477	-2.5831
Hold Value										0.0000	0.0000	0.0000	0.0000
Option Value										0.0000	0.0000	0.0000	0.0000
Exercise ?										No	No	No	No
Price											0.3322	0.4160	0.5209
Exercise Value											-3.0678	-2.9840	-2.8791
Hold Value											0.0000	0.0000	0.0000
Option Value											0.0000	0.0000	0.0000
Exercise ?											No	No	No
Price												0.2653	0.3322
Exercise Value												-3.1347	-3.0678
Hold Value												0.0000	0.0000
Option Value												0.0000	0.0000
Exercise ?												No	No
Price													0.2118
Exercise Value													-3.1882
Hold Value													0.0000
Option Value													0.0000
Exercise ?													No

Another method suggested in the literature is to model stochastic prices as a mean reverting process. With this method any significant deviation from 'normal' trends is eventually corrected for in the diffusion process. The question remains as to how to define what is a 'normal' long-term trend for oil prices.

It should be recognized that this is a first attempt at analyzing retrofit technology economics through the use of option pricing theory. One assumption made here is that the exercise price (i.e. the cost to retrofit) is known, when in fact it could be considered a random variable as discussed above. Other option pricing methods are available, such as Fischer's[168], that allow for the exercise price itself to behave stochastically. Future work in this area could be done to better define a value for research, development and engineering efforts directed towards decreasing the variance, as well as reducing the exercise price.

Another area for further work is consideration of operation of the boiler after retrofitting. The retrofit technology design currently being pursued by the EFRC is reversible in the sense that the option to switch back to firing fuel oil carries a low exercise price. This approach is taken up in the next section.

Despite the apparent drawbacks of using the current state of the art option pricing techniques to value decisions regarding investing capital in projects, this technique represents the 'cutting edge' in conducting such analysis. Much of the current theory and application using option pricing techniques are being developed for the electric utility, oil, and natural gas industries.

USING THE QUALITY OPTION MODEL TO QUANTIFY THE VALUE OF OWNING A FUEL SWITCHING CAPABILITY

The situation of the owner of a boiler can be viewed as being 'short' the fuels market since at some regular intervals of time the boiler owner must replenish fuel inventories in order to maintain production. In this situation, the boiler owner faces price risk as the future fuel price is uncertain. The owner of boiler retrofitted to fire two or more fuels has the advantage of being able to fire the minimum cost fuel now and in the future. This section will apply the "Quality Option" valuation technique to quantify the value of the benefits to a boiler owner of being able to use the minimum cost of two fuels. This model is presented here for the illustrative purposes of its potential value in quantifying the benefits of fuel flexibility.

Quality Option Background

The development of futures and options markets for commodities has provided the fuel-dependent producer a means to reduce price risk through hedging. The growth of the futures and options markets has also spurred the growth of methods to quantify the benefits inherent from the flexibility provided by such arrangements. One such option pricing model is the 'quality option.'

The quality option model was developed by Boyle[169] as an application of the Black and Scholes model to quantify the benefit to the short position of a futures contract resulting from

having flexibility over what is acceptable for delivery at the time of contract expiration. Futures contracts for commodities such as oil or wheat often include a variety of grades, or qualities, that are suitable for delivery since this improves market liquidity. For example, in the case of wheat futures traded on the Chicago Board of Trade (CBOT) there are eleven different varieties of wheat that can be delivered to fulfill the short position (In most cases a 'benchmark' or 'par' commodity is specified with a differential determined for all the other commodities of differing grades or quality that could be freely substituted for one another as a means to equalize prices at the inception of the futures contract.). Boyle found that, even with the drawback that the spot prices of the differing commodity grades generally move together over time (are highly correlated), there exists a definite and measurable advantage of owning the quality option from the standpoint of the short position of a futures contract in being able to deliver the cheapest commodity to fulfill the contract. In this case, the boiler owner has to 'deliver' the commodity to his boiler in order to fulfill production obligations. Moreover, he found that the quality option advantage grew with the number of commodities included in the contract.

The formal definition of the quality option is the option to exchange one risky asset for another at zero cost upon expiration of the option contract. Since the option is not exercised before expiration it is known as an European-type option. The mathematical development of this option model was done by Magrabe[170] and Stulz[171]. Boyle's own work was motivated by refinements in the model formulation made by Johnson[164].

Quality Option Model

The quality option model is based upon replicating the futures or forward price using portfolio consisting of a long position in a call option on the minimum of two commodities offset by the corresponding short position in a put option. This portfolio can be expressed as:

$$\text{Cmin}[S_1, S_2; F....] - \text{Pmin}[S_1, S_2; F....] = 0$$

The futures price, F, is that exercise price that causes the above relationship to hold. The additional parameters not shown include the parameters describing the relationship between the prices of the two commodities and other parameters of the contract.

The put-call parity relationship developed by Stulz that incorporates the above relationship for options on the minimum of two commodities is:

$$\text{Cmin}[S_1, S_2; F....] - \text{Pmin}[S_1, S_2; F....] = \text{Cmin}[S_1, S_2; 0....] - Fe^{-rT}$$

The call option on the right hand side of this equation has the zero exercise price. This call option entitles the owner to freely substitute between the two commodities in order to obtain his

own lowest cost. The zero exercise price call option can be evaluated using the same methodology as used in the Black and Scholes Model. This relationship is:

$$\text{Cmin}[S_1, S_2; 0....] = S_1 - S_1 \text{N}(d_1) + S_2 \text{N}(d_2)$$

where:

$$d_1 = \frac{ln\left(\frac{S_1}{S_2}\right) + \frac{1}{2}\sigma^2 T}{\sqrt{\sigma^2 T}}$$

$$d_2 = d_1 - \sqrt{\sigma^2 T}$$

This model will allow for the value of the quality option to be calculated. S_1 represents the lowest priced commodity where owning the option provides a zero cost means of exchanging this commodity at a future time if it is no longer the lowest priced commodity at that time.

Call Option Model for the Minimum Priced Fuel

The owner of a boiler that has been retrofitted to fire two or more fuels has thereby obtained an embedded call option on the minimum of two fuels. The value of owning this option can be quantified using the quality option model formulated above. In our case we will consider the case of No. 2 Fuel Oil and MCWM as the two fuels. The specific variables used in the model, along with their base case values is presented in Table 9-7.

As explained above, the value of the quality option results from the uncertainty in the future relative prices of two assets due to the existence of price volatility. In this illustrative example, we will assume the fuel oil price experiences a volatility of 22 %/annum and its present spot market price is $3/MM Btu. A sensitivity analysis will be conducted that demonstrates the effects of differing fuel oil price volatility on the value of the quality option. We will also assume that MCWM is obtained through long-term supply contracts resulting in its price volatility to be 0 %/annum. In addition, a 4% interest rate is assumed.

The reasons for and implications of long term contracting for MCWM require further explanation. MCWM is assumed to be made available only by entering into long-term contracts with suppliers. This constraint reflects the current lack of a developed MCWM supply market and the understandable reluctance on the part of potential suppliers and investors to commit capital to a project that will have very uncertain cash flows. However, to realize the benefits derived from a fuel switching capability it is necessary for boiler owners to actually follow through on fuel switching. This problem is endemic to adoption of technologies such as MCWM , as has been noted above with Manfred's observation of the 'chicken-and-the-egg' phenomenon. The model can be modified to recognize this constraint by specifying that boiler owners pay a premium for the

Table 9-7. Quality Option Base Case Assumptions

Variable Description		Value	Units
Initial "Adjusted" MCWSF Price	S_1	3.00	$/MMBtu
Initial Fuel Oil Price	S_2	3.00	$/MMBtu
Exercise Price	X	0.00	$/MMBtu
MCWSF Price Volatility	σ_1	0	%/annum
Fuel Oil Price Volatility	σ_2	22	%/annum
Fuels Price Correlation	ρ_{1s}	0	%/annum
Interest Rate	r	4	%
Option Expiry Intervals	T	1	Years

fuel oil that they use as compensation to the MCWM supplier for their unavoidable capital costs. In addition, boiler owners also have their own investment in the retrofit that requires payback. For the purposes of this example, all costs, inclusive of capital, are assumed to be captured in the MCWM price. Further, the retrofit technology is assumed to be just at the margin of being economically feasible when considering these costs.

With these arguments in mind the base case MCWM price will be assumed to be just equal to the initial fuel oil price of $3/MM Btu. Since MCWM price is time invariant due to the contracting assumption the further result is that there is a zero correlation between the price movements of the two fuels. Sensitivity analysis to be conducted will examine the effect of the retrofit economics moving to the either side of the margin of economic feasibility as reflected by variation in the breakeven price of MCWM .

The next model parameter to consider is time. Theoretically, fuel switching could occur instantaneously corresponding to the instantaneous crossings of MCWM and fuel oil prices. It is not realistically possible or practical to implement such a model however. The model could be formulated as an inventory control problem as addressed in operations research, however, it is likely adequate to simply specify periodic time intervals for obtaining new fuel supplies. An extension not pursued here would be to model 'actual' heating season fuel purchase decisions to replenish inventory. The purpose would be to take advantage of the additional volatility inherent in year-to-year variations in demand due to winter severity. For illustrative purposes only, the first year value will be calculated and considered due to the uncertainty as to how to handle option time periods extending out over long time periods.

Results and Conclusions

The implementation of the quality option model using the base case assumptions is shown in Table 9-8. The call option on the minimum price of two fuels is calculated to be $2.74/MM Btu. The futures price can be found through the use of the put-call parity relationship and is equal to:

$$2.74e^{1(0.04)} = 2.85$$

The significance of the quality option can be represented as the percentage of the base case futures price that would result from not owning the quality option. In this case, the futures price is calculated using the same equation as above resulting in $3.12 being the futures price of $3/MM Btu fuel oil. The ratio of the two futures prices is about 91%, or about a 9% advantage in fuel price due to owning the option to substitute freely between the two fuels

A sensitivity analysis of changes to MCWM price, reflecting a move either way from marginal viability of retrofits, is presented in Table 9-9. Not surprisingly, there is a decrease in the value of holding the option of substituting fuels when the initial fuel prices move further apart from

Table 9-8. Quality Option Sample Calculation

Variable Description		Value	Units
Combined Fuel Price Variance	σ_{12}	0.0484	
	d_1	0.11	
	d_2	-0.11	
	$N(d_1)$	0.5438	
	$N(d_2)$	0.5438	
Value of the Call Option on the Minimum Price of Two Fuels	Cmin	2.74	$/MMBtu

Table 9-9.

Quality Option Sensitivity to Differing MCWSF Prices
With Fuel Oil Price Held at $3.00/MMBtu

S2 $/MMBtu	Cmin	QF as a % of F		*d1*	*d2*
2.00	1.993	99.66		-1.7330	-1.9530
2.25	2.225	98.87		-1.1976	-1.4176
2.50	2.431	97.26		-0.7187	-0.9387
2.75	2.604	94.68		-0.2855	-0.5055
3.00	2.737	91.24		0.1100	-0.1100
3.25	2.833	94.45		-0.2538	-0.4738
3.50	2.899	96.62		-0.5907	-0.8107
3.75	2.940	98.01		-0.9043	-1.1243
4.00	2.966	98.87		-1.1976	-1.4176

one another. This is due to the fact that the introduction and increase of a price bias decreases the probability of a future crossing of the two fuel prices. With all other base case assumptions held constant it can be seen that the quality option loses most of its value with a fuel price differential of ±1/MM Btu.

A sensitivity analysis of the value of the quality option to volatility in fuel oil prices is presented in Table 9-10. As shown in the table, varying the fuel price volatility from 0.01 to 50 %/annum causes the quality option ratio to vary from 100 to 80.3%. Not surprisingly, this means that a reduction in the distribution of price changes of fuel oil decreases the value of owning the quality option and vice versa.

An extension not pursued here is to add to the analytical framework of the quality option by including three or more commodities. This would be useful for valuing the option to freely substitute for natural gas or even a whole suite of fuels.

This model should not be confused with substitutability as a means to increase competition among fuel suppliers and thereby obtain better pricing. While this consideration provides an additional potential benefit, the quality option derives its value from the current price levels, volatility, and correlation of commodities that can be freely substituted for one another at a future time of need and not from a competitive markers context.

CONCLUSION

This subtask has covered much ground regarding the issues involved with the economic viability of technologies that could utilize MCWMs, with an emphasis upon MCWMs. It is clear that success will most likely be achieved through those technologies that can achieve the margin of economic viability by reducing capital costs and not through a 'serendipitous' change in oil prices alone. In addition, those technologies that can reach that marginal level of viability could make their market entry by highlighting fuel flexibility as quantified by option pricing methods. The challenge then becomes translating these benefits into a form readily understandable and realized by consumers of fuels. These additional benefits that are available at the margin may also aid in the formulation of feasible contracts between fuel supplier(s) and consumers.

9.2 Subtask 3.2 Process Analysis

Subtask 3.2 focuses on the two technologies, slagging combustion and coal gasification. A literature search was conducted on these technologies to provide insight into the processes and to obtain necessary cost data required for their appraisal. The technologies are different from retrofitting to fire MCWM or DMC in that they require hardly any changes to existing boilers. Rather, they consist of additional units to provide hot gases into the boiler. Coal gasification produces gases which are combusted in the boiler and the heat recovered. In the case of slag combustion, combustion is carried out first and the hot gases produced are fed into the boiler for heat recovery. Technical feasibility of both technologies has been demonstrated for industrial

Table 9-10.

Quality Option Sensitivity to Differing Fuel Oil Price Volatilities

Fuel Oil Price Volatility, s2	Cmin	QF as a % of F		σ2	*d1*	*d2*
0.01	3.000	100.00		0.00000	0.00005	-0.00005
5	2.940	98.01		0.00250	0.02500	-0.02500
10	2.880	96.01		0.01000	0.05000	-0.05000
15	2.821	94.02		0.02250	0.07500	-0.07500
20	2.761	92.03		0.04000	0.10000	-0.10000
25	2.702	90.05		0.06250	0.12500	-0.12500
30	2.642	88.08		0.09000	0.15000	-0.15000
35	2.583	86.11		0.12250	0.17500	-0.17500
40	2.524	84.15		0.16000	0.20000	-0.20000
45	2.466	82.20		0.20250	0.22500	-0.22500
50	2.408	80.26		0.25000	0.25000	-0.25000

boilers firing pulverized coal[172-176]. In addition, it is technically feasible use coal water slurries in slagging combustors[177].

The economic evaluation of these technologies involves the determination of their respective net benefits over the life of the boiler. That is, a comparison of the capital required to set them up plus operating expenses, and the expected benefits to be derived over the life of plant. Below are tables that show annual fuel costs for a 25 MMBtu/hr (≅ 20,000 lb. steam/hr) boiler and a 50 MMBtu/hr boiler respectively, such as the Crane, Indiana boiler, when firing oil and gas. The costs are given for different utilization rates and boiler efficiencies. The combined oil/gas fuel price is taken at $2.83/MMBtu, and the utilization rates are selected to ensure consistency with the sensitivity analysis on MCWM retrofitting.

Annual Fuel Costs for a 25 MMBtu/hr boiler.

Boiler use (%)	50	50	33	33	70	70
Boiler efficiency (%)	85	95	85	95	85	95
Annual fuel costs ($,000)	327	327	216	216	457	457
Annual steam produced (thousand pounds)	74,460	83,220	49,144	54,925	104,244	116,508
Unit fuel cost (per thousand lb. steam, $)	4.39	3.93	4.39	3.93	4.39	3.93

Annual Fuel Costs for a 50 MMBtu/hr boiler.

Boiler use (%)	50	50	33	33	70	70
Boiler efficiency (%)	85	95	85	95	85	95
Annual fuel costs ($,000)	653	653	431	431	915	915
Annual steam produced (thousand pounds)	148,920	166,440	98,287	109,850	208,488	233,106
Unit fuel cost (fuel cost per thousand lb. steam, $)	4.39	3.93	4.39	3.93	4.39	3.93

The tables indicate that unit fuel cost is independent of boiler capacity and the percentage use of the boiler, and varies only with the boiler efficiency. Therefore, there are no economies of scale with regard to fuel utilization. In general, however, there are economies of scale with retrofit capital costs and O&M costs. Therefore, utility scale adoption of the technologies will become economically viable before industrial scale adoption. A detailed analysis as for MCWM was not performed for these technologies since Penn State did not undertake any demonstration of them. However, the two tables above provide cost data to which the cost of adopting of any new technology can be compared, to determine any economic advantage(s) from the adoption. On-site coal gasification has been found to be uneconomic relative to direct coal firing for industrial boilers [175, 176].

The benefits to be realized from adopting either technology is based on the cost differential between oil/gas and the fuel to be fired. Therefore, for viability, the sum of annualized capital costs, annual alternate fuel costs, and incremental annual O&M costs, must be less than the annual fuel costs shown in the tables. Alternatively, this annual cost sum per thousand pounds of steam generated must be less than the unit fuel costs shown. The unit fuel cost figures suggest a price for the steam produced. For example, the price of a thousand pounds of steam from a 25 MMBtu/hr boiler operating at 95% efficiency is $3.93 plus a correction for annualized capital and O&M costs per thousand pounds steam produced. This correction will be different for different boiler sizes given economies of scale. It is important to note that the quality of steam produced from an alternate technology may be different than that of the existing technology. Proper engineering economic adjustments must be made to account for any steam quality differences if these differences lead to variations in the use(s) of the steam produced.

9.3 Subtask 3.3 Environmental and Regulatory Impacts

The environmental regulations for Pennsylvania have been compiled for this subtask.

AIR QUALITY

Air pollution has adverse effects on human health, crops, the natural environment, aesthetics, materials, and climate conditions. The President's Science Advisory Committee estimates that air pollution is responsible for 9,000 deaths each year in the United States[178]. Over the past decade, Pennsylvania's air quality has been gradually improving. However, it still has immediate and long-term air quality problems in certain areas. Additional efforts are needed to restore the surrounding environments degraded by the past activities.

Under the Federal Clean Air Act Amendments of 1990, the Pennsylvania Department of Environmental Resources (DER) is obliged to promulgate air quality regulations which will protect the right to clean air for all Pennsylvanians. DER's Bureau of Air Quality Control (BAQC) fulfills this obligation by enforcing airborne emissions from thousands of sources. The DER has adopted the National Ambient Air Quality Standards (NAAQS) as the primary air quality standards for

Pennsylvania, in addition to several standards of its own. These standards are shown in Tables 9-11 and 9-12.

The DER of Pennsylvania monitors ambient air quality periodically in conjunction with NAAQS and its own standards. The main goals of the Air Monitoring Program are i) to evaluate compliance with Federal Air Quality Standards; ii) to develop data for trend analysis; iii) to develop and implement air quality regulations; and vi) to provide information to the public on daily air quality conditions in their area. The monitoring strategy of BAQC is to place monitors in areas having high population density, high levels of contaminants, or a combination of the two. The majority of all monitoring efforts take place in thirteen air basins defined by the BAQC regulations. The basins are listed in Table 9-13. The BAQC conducts surveillance in 12 of the basins; Allegheny County monitors itself.

Total Suspended Particulates (TSP)

Particulate matters are emitted mainly from fuel combustion and industrial processes. The smaller of these particulates can be inhaled into the lungs and cause respiratory disease. Over the past ten years, Pennsylvania's TSP levels have greatly improved. Since 1988, the TSP levels have improved by approximately 25 percent[179].

Particulate Matter-10 (PM-10)

PM-10 is small particulate matter in the air whose size is equal to or less than 10 micrometers. In 1987, TSP measurements were replaced with PM-10 standards because larger particles included in TSP do not penetrate into the lungs and have few health effects. The main sources of PM-10 are emissions from transportation and industrial processes. The monitoring of PM-10 began in 1985 in Pennsylvania. Since 1988, the PM-10 levels have improved by approximately 27 percent[179].

Sulfur Dioxide

Sulfur dioxide is emitted mainly by power plants burning fossil fuels. The major health effects associated with high exposures to sulfur dioxide include impairment of breathing and respiratory disease. Furthermore, sulfur dioxide damages trees, plants, and crops and causes acid rain. Over the past ten years, no Pennsylvania site exceeded the annual quality standard of 0.030 ppm. In 1992, sulfur dioxide levels were less than 50 percent of the annual air quality standard [179].

Nitrogen Dioxide

Nitrogen dioxide is a highly toxic brown gas that is generated by the burning of fossil fuels and vehicles. It causes an odorous brown haze that irritates the eyes and nose, blocks the sunlight, and reduces visibility. It also contributes to acid rain and adversely impacts forests and ecosystems. Over the past ten years, the level of nitrogen dioxide has been below the standard of 0.050 ppm[179].

Table 9-11. National Ambient Air Quality Standards (NAAQS)

Pollutant	Primary Standards	Averaging Time	Secondary Standards
Carbon Monoxide	9 ppm (10mg/m^3) 35 ppm (40mg/m^3)	8-hour* 1-hour*	None
Lead	1.5 ug/m^3	Quarterly average	Same as primary
Nitrogen Dioxide	0.053 ppm (100 ug/m^3)	Annual arithmetic mean	Same as primary
Particulate Matter (PM-10)	50 ug/m^3 150 ug/m^3	Annual arithmetic mean 24-hour**	Same as primary
Ozone	0.12 ppm (235 ug/m^3)	1-hour****	Same as primary
Sulfur Dioxide	0.03 ppm (80 ug/m^3) 0.14 ppm (365 ug/m^3)	Annual arithmetic mean 24-hour*	0.5 ppm (1300 ug/m3)

The numbers in Table 9-11 represent the maximum permissible ambient air quality levels.
* Not to be exceeded more than once per year
** The standard is attained when the expected number of days per calendar year with a 24-hour average concentration above 150 ug/m^3 is equal to or less than one.
*** The standard is attained when the expected number of days per calendar year with maximum hourly average concentration above 0.12 ppm is equal to or less than one.

Table 9-12. Pennsylvania Ambient Air Quality Standards (PAAQS)

	Averaging Time		
Pollutant	**1-Hour**	**24-Hour**	**30-days**
Settleable (tons/square mile/month)		43	23
Beryllium (ug/m^3)			0.01
Sulfates (ug/m^3)		30	10
Fluorides (ug/m^3) (total soluble as HF)		5	
Hydrogen Sulfide (ppm)	0.1	0.005	

The numbers in Table 9-12 represent the maximum permissible ambient air quality levels.
The PAAQS also includes the six pollutants in Table 9-11 and are identical to NAAQS.

Table 9-13. Pennsylvania Air Quality Basins

Allegheny County	Monongahela Valley
Allentown, Bethlehem, Easton	Reading
Erie	Scranton, Wilkes Barre
Harrisburg	Southeast Pennsylvania
Johnstown	Upper Beaver Valley
Lower Beaver Valley	York
Lancaster	

Carbon Monoxide

Carbon monoxide is a poisonous gas that inhibits the delivery of oxygen to the body's tissue, thereby causing asphyxia or shortness of breath. The main source of carbon monoxide is vehicle emissions. Since 1983, no air basins exceeded the annual quality standard of 9 ppm except Harrisburg Air Basin; the level of carbon monoxide in Harrisburg site was approximately 12 ppm in 1983, but it has been below the standard thereafter[179].

Ozone

Ozone is a secondary pollutant since it is not emitted directly to the atmosphere, but is formed by the reactions of hydrocarbons and nitrogen oxides in the presence of sunlight. Ozone is erratic and hampers breathing. It also damages crops and materials. Pennsylvania has experienced relatively high ozone concentrations in 1983, 1987, and 1988. Those levels are probably due in part to hot, dry, stagnant conditions that were conductive to ozone formation[179]. In 1992, only Norristown in Southeast Pennsylvania Air Basin exceeded the ozone standard. The improved levels of ozone seems to be attributable to control on volatile organic compounds and gasoline volatility.

Lead

Lead is a suspected carcinogen of the lungs and kidneys, and it has adverse effects on blood-formation and the nervous and renal systems. The main sources of lead are vehicles and industrial processes. The level of lead in Pennsylvania has met the Federal standards and shown little change for the past ten years.

Sulfates

Sulfates are classified into two types, primary and secondary. The former is created by industrial processes, but the latter is formed by photochemical processes. Sulfates are of concern because of their adverse effects on visibility and acid rain. The sulfate level in Pennsylvania has been above the 24-hour air quality standard of 30 μg/m3 over the past ten years. However, it has been improving since 1990[179].

WATER QUALITY

The 45,000 miles of streams in Pennsylvania are protected by state water quality standards. Approximately 13,000 miles are defined as major streams. The DER estimates that approximately 2,800 miles of the major streams are polluted by mine drainage and industrial and sewage discharge. Of the 2,800 miles of polluted streams, 2,000 miles (71 percent) are mainly attributed to abandoned coal mines. The cost estimate to control abandoned coal mine drainage is approximately three to four billion dollars[178]. The Pennsylvania Land and Water Conservation and Reclamation Act of 1968 allocated $130 million to correct acid mine drainage problems, $20 million to eliminate burning refuse piles, and $50 million to abate mine subsidence and mine fires. These funds have reduced acid mine drainage problems in 300 miles of streams, reclaimed 3,500

acres of strip mines and 38 refuse banks, extinguished 22 refuse bank fires, and protected 2,100 acres and $1.5 billion worth of property from mine subsidence[178],

Pennsylvania has made tremendous efforts in cleaning up water pollution. The Purity of Waters Act of 1905, Clean Streams Law of 1937, Land and Water Conservation and Reclamation Act of 1968, Federal Water Pollution Control Act of 1972 (The name was changed to the Clean Water Act in the 1977 amendments, and then to the Water Quality Act in the 1987 amendments), Federal Safe Drinking Water Act of 1974, and laws on mining and sewage facilities have been enacted and amended several times to improve the water quality in Pennsylvania.

Federal Water Quality Act (1977)

The goals of this act are to eliminate the discharge of pollutants to navigable water by 1985 and to attain water quality which provides for the protection and propagation of fish, shellfish, and wildlife and to provide recreation in and on the water by July 1, 1983. The Act allows two approaches to achieve these goals: water quality-based and technology based effluent limitations.

The technology based effluent limits are minimum degrees of requirements, under Section 301 of the Federal Water Quality Act, that must be achieved by industrial dischargers. These levels of requirements are based on Best Practical Control Technology Currently Available (BPT), Best Conventional Pollutant Control Technology (BCT), and Best Available Technology Economically Achievable (BAT). In contrast, the water quality-based effluent limitations are intended to protect both human health and aquatic life beyond the protection provided by the technology-based effluent limitations (Section 302).

Pennsylvania Clean Streams Law (1937)

The Pennsylvania Clean Streams Law was originally enacted in 1937 and provided a strong and comprehensive legislative framework for controlling water pollution. Article III of this law deals with industrial discharges to streams or rivers. It requires industrial dischargers to obtain permit to discharge industrial waste, to obtain approval of plans for the construction of industrial waste treatment facilities, and to obtain permits to construct these treatment facilities. The article also requires industrial dischargers to operate the industrial waste treatment facilities in accordance with the regulations.

SOLID WASTE

Traditionally, solid waste (which includes solid, liquid, semisolid, or contained gaseous substances and is classified into three types: municipal, residual, and hazardous waste) was regarded as a local problem, requiring local management. However, more than 85 million tons of solid waste have been generated in Pennsylvania and create potential hazards to public health and the environment. Approximately 4 million tons of that waste are hazardous[178]. For this reason, safe disposal of hazardous waste is of particular concern. In 1976, Congress passed the Resource

Conservation and Recovery Act (RCRA), giving EPA the authority to develop a nationwide program to regulate hazardous waste.

Pennsylvania responded to RCRA with the passage of the Solid Waste Management Act (SWMA) of 1980 (Act 97). The goal of this Act is to protect the residents of Pennsylvania from potential dangers involved in handling solid wastes through comprehensive management and stricter regulations. Upon the passage of SWMA, the State and Federal governments have taken the controlling role in solid waste management. However, deteriorated environmental conditions caused by past management practices such as open dumps, inadequate storage and transportation, combined landfilling of hazardous and non-hazardous wastes remained uncorrected.

The Comprehensive Environmental Response, Compensation, and Liability Act of 1980 (CERCLA, commonly known as Superfund) was enacted by the Federal government to establish the framework for cleanup of past releases of hazardous substances. Superfund called for a $1.6 billion fund to be used for the damages to natural resources caused by the release of hazardous substances.

To complement DER's existing waste management program, Pennsylvania Governor Robert Casey signed the Hazardous Sites Cleanup Act (HSCA) into law in 1988. HSCA offers incentives for industries to minimize hazardous waste generation and for municipalities to consider opportunities for siting new waste management facilities. HSCA also provides a long-term source of funding that enables Pennsylvania to participate in the federal Superfund program.

Under HSCA, 100 sites in Pennsylvania were projected to be cleaned up by 2000. During the 1990-91 fiscal year, 7 sites were cleaned with total expenditure of 38.4 million[180].

LAWS ASSOCIATED WITH MINING ACTIVITIES

Past mining activities in Pennsylvania have adversely affected the quality of the environment. Unreclaimed strip mines affect 225,000 acres of land, acid mine drainage from abandoned mines pollutes approximately 2,000 miles of streams, and more than 33,000 acres of abandoned non-burning coal refuse disposal piles remained uncorrected. According to the DER, Pennsylvania has 150,000 acres of urban land prone to subsidence[178].

To correct these problems, Pennsylvania enacted several laws including the Pennsylvania Clean Streams Law of 1937 and the Pennsylvania Surface Mining Conservation and Reclamation Act of 1968. In addition to these laws, the Federal Water Quality Act of 1987 and the Federal Surface Mining Control and Reclamation Act of 1977 also regulate the mining activities in Pennsylvania. Non-mining facilities such as iron and steel industries and coal dealers are also regulated by the Bureau's Industrial Waste Program or Storm Water Program.

9.4 Subtask 3.4 Transportation Cost Analysis

This subtask has mainly involved providing supporting data and cost functions for use in the market penetration model of Subtask 3.5, Technology Adoption. Both boilers and potential

fuel supply points in Indiana and Cambria counties were identified and located. The distances between each were determined and tabulated for the model. The fixed and mileage dependent transportation costs were found and expressed in a form suitable for use by the model. Finally, the transportation dependent component of the optimization model was specified.

9.5 Subtask 3.5 Technology Adoption

Market penetration models have been ascribed to a wide set of methods directed towards predicting the likely future adoption or emplacement of products, services, or technologies within an economy[181]. The models that have been developed and used in market penetration studies are tailored to fulfilling the objective of forecasting market share over time or estimating the potential, or equilibrium, market share. Models that forecast market share over time often must be explicitly defined with an estimate of the equilibrium market share toward which adoption proceeds. The types of models include:

- Time series models
- Econometric models
- Historical analogy
- Diffusion models
- Optimization models

Diffusion models are the most widely used in the literature with the seminal work of Zvi Griliches[182] laying the ground work for this type of analysis. The diffusion model is based upon the observation that the acceptance of a superior technology follows an 'S' shaped curve when measured over time. Such a curve can be estimated using a number of functions with cumulative normal and logistic among the most favored.

The model considered here is a partial equilibrium analysis since it is assumed that there would be no substitution effects on the oil or natural gas prices due to their displacement by MCWM. The extent to which this assumption holds will need to be examined.

9.6 Subtask 3.6 Regional Economic Impacts

BACKGROUND

Acid precipitation begins with the emission of sulfur dioxide and nitrous oxide gases into the atmosphere. These two gases mix, are absorbed by clouds, and eventually fall to the ground as acid rain and other forms of precipitation. The damage caused by acid rain include increased morbidity and mortality in humans and the destruction of flora and fauna. It can also cause corrosion in housing, factories, and equipment.

Efforts to mitigate acid rain by limiting emissions of its precursor pollutants have been a major part of various amendments to the Clean Air Act (CAA). The 1970 amendments were the start of more extensive regulations. They basically consisted of three parts for defining and controlling the minimum outdoor air quality in the U.S. First, the Act established the national

ambient air quality standards (NAAQS) and introduced the State Implementation Plan (SIP) for meeting these standards. Secondly, the Act specified the emission standards for stationary sources of pollution. Thirdly, the Act called for the control of pollution from mobile sources.

In 1977, the CAA was revised again to address issues uncovered by the experience with existing regulations. Important amendments cover the problem of fulfilling the NAAQS requirement in non-attainment areas, and the prevention of significant deterioration (PSD) of air quality in attainment areas. New provisions required all major new projects to adopt the best available control technology (BACT). In non-attainment areas, new entrants or modification of firms' production processes are required to use the lowest achievable emissions rate technology (LAER), the most stringent emission limitation contained in SIP. The mitigation option of using low-sulfur coal was made less attractive by forced use of the scrubbing technology required by BACT and LAER. This restriction on abatement tactics leads to inefficiencies and is, therefore, criticized by most economists[183, 184].

Under the 1990 CAA amendments, more stringent emission standards will be effective in 1995 and further tightened in 2000. The legislation tries to cover every aspect of air pollution by, for example, authorizing emission standards for 189 toxic air pollutants, stopping the use of chemicals believed to deplete ozone in the atmosphere, again requiring the reduction of air pollution in non-attainment areas, establishing an acid rain mitigation program, and raising the authority/liability of the Environmental Protection Agency (EPA). The most exciting aspect of the latest CAA revisions, in the eyes of an economist, is the greater emphasis on the use of tradable permits in meeting the acid rain provisions (The general category is usually referred to as emissions trading. A provision for this general approach was contained in the 1977 CAA Amendments but rarely implemented[185, 186].). Although the role of the tradable permit system in the 1990 amendments is not to substitute for the more prevalent command and control regulations but to coexist, it represents a step in the right direction towards achieving economic efficiency[187].

THE PENNSYLVANIA CGE MODEL

In this section, the Pennsylvania CGE model is summarized. The reader is referred to Li [188] for a detailed presentation of the model equations, data upon which it is based, and the manner of model construction.

Model Selection

The selection of a model framework was based on the following criteria:

1. It must reflect the economic characteristics of Pennsylvania — an industrialized and highly interdependent economy.
2. It must include the economy's ability to adjust to external shocks — industries' ability to substitute among inputs in the production process and consumers' ability to adjust spending patterns.

3. It must be able to address both microeconomic and macroeconomic aspects of environmental policy — both sectoral and economy-wide impacts.
4. It must readily incorporate policy instruments as variables in the model — emission standards, marketable permits, and taxes.

In applied economics, several modeling techniques are widely used to analyze environmental policy issues. These include input-output analysis, macro-econometric modeling, linear or non-linear programming, and computable general equilibrium (CGE) analysis. Each has its merits and shortcomings, but some are better suited than others to this area of research.

Computable general equilibrium analysis, a relatively new technique, depicts the economy-wide equilibrium, in which all agents independently maximize their own objective functions. (CGE modeling is a widely used approach in taxation, trade, and regulatory impact modeling [189, 190] It overcomes the drawbacks of other models by including aggregate macro information, detailed sectoral distinctions, extensive economic interdependencies, complete price-response mechanisms, resource constraints, and substitution possibilities. Furthermore, many policy instruments can be easily modeled as variables and incorporated into the model structure. Its strong features best satisfy our model selection criteria.

Overview of the Model

The Pennsylvania CGE model is a long-run, static, single-region model. It is specially designed to incorporate environmental policy variables and their regional economic impacts. This model is based on the following assumptions:

1. The product and factor markets are competitive, i.e., no economic agents are able to exercise monopoly power in the markets.
2. The State of Pennsylvania is modeled as a small, open economy, i.e., it has little or no influence on the supply and demand of goods in the national economy or their prices.
3. Monetary variables do not play an explicit role, i.e., transactions are in *real* terms.
4. Technological change (both embodied and disembodied), other than that associated with pollution control, is not explicitly taken into account in the period of study.
5. Prices are flexible enough to assure the existence of a general equilibrium; producers and consumers can fully adjust without any time lag after external shocks.

The major features of this model are its emphasis on production technology and its focus on trade theory. The structure of input demand in this model resembles that of several well-known national and regional CGE models[191, 192]. Important modifications are made in the specification of the production technology for energy and materials. The USDA/ERS CGE model[191, 192], for example, adopted a two-part production function, in which the intermediate inputs are assumed to follow a fixed-coefficient Leontief technology, and the two primary inputs, capital and labor, are modeled using the traditional Cobb-Douglas production function. In the Pennsylvania CGE

model, we use a two-tiered, or nested, Generalized Leontief cost function to describe the production technology. The first tier allows substitutions among capital (K), labor (L), energy (E), and materials (M). The second tier specifies interfuel and intermaterial substitutions inside the energy and material aggregates.

The other major difference between the model presented here and the other models cited above is the treatment of investment. In most models, the saving rates are exogeneously given with the investment variable adjusting indigeneously to equate total savings. In this study, however, fixed investment is set exogeneously so that the need for increased investment due to more stringent air quality regulations can be modeled explicitly. Savings rates are forced to change indigeneously to finance the purchase of new capital stocks.

The overall structure of this model is illustrated by a schematic diagram in Figure 9-4. (A list of the 18-sector aggregation of the model is presented in Appendix B.) Basically, there are four interrelated components: production, trade, demand, and income. Each component is further decomposed into several parts. The arrows in the diagram show the interlinkages of different parts in the model. When all economic agents interact together and jointly optimize their objective functions, a set of endogenous equilibrium prices is determined to clear all markets in the economy.

The Choice of Functional Form

The specification of production technology in an empirical analysis requires the selection of a suitable functional form. The Cobb-Douglas, CES, and Leontief were rejected functions because of their undesirable properties, such as predeterminate restrictions on the elasticities of substitution.

Flexible functional forms are local second-order approximations of a technology. They are flexible because no a priori restrictions are placed on the technology. For a smooth technology with n inputs, there exist $1/2(n + 1)(n + 2)$ separate economic effects at a point (EEP). Any linearized flexible function is capable of depicting these distinct effects if it contains exactly the same number of parameters. A partial list of commonly used flexible functions includes the generalized Leontief (GL), the transcendental logarithmic (TL), the generalized Cobb-Douglas (GCD), the generalized square root quadratic (GSRQ), and the normalized quadratic (NQ) function (The use of flexible functional forms is not always without limitations as many advocates originally expected. The separability assumption widely adopted in economic research imposes some restrictions on their flexibility. The other problem lies in the ability of flexible functions to approximate arbitrary technologies globally, because these functions are only second-order numerical or differential approximations at a point. Even worse are their applicabilities to maintain the desirable properties of technology, i.e., a well-behaved situation, over a wide range of observations[193]. For example, in their research on the U.S. agricultural production, Baffes and Vasavada[194] found that TL and NQ cost functions violate concavity conditions.).

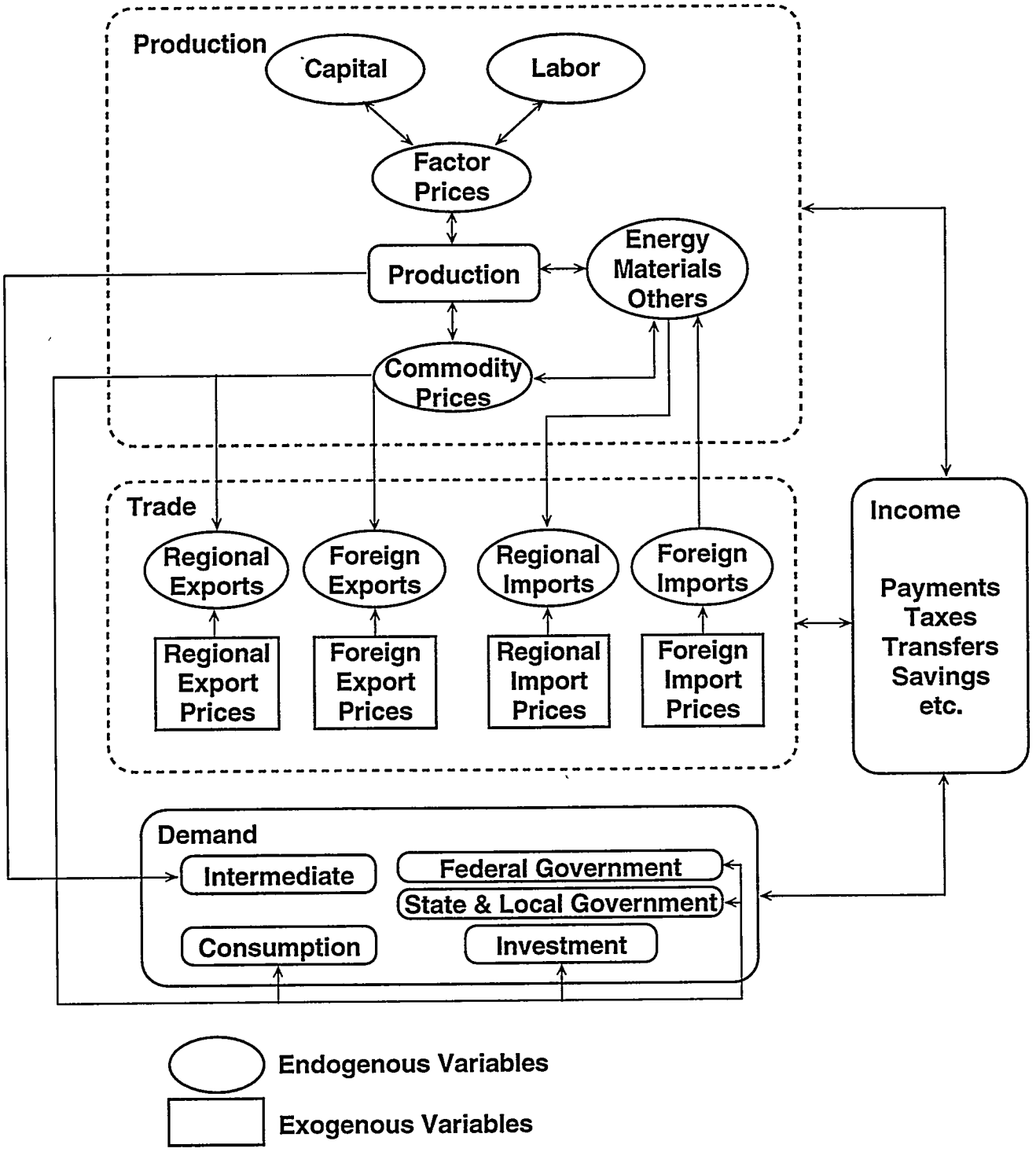

Figure 9-4. SCHEMATIC DIAGRAM OF THE PENNSYLVANIA CGE MODEL

The choice of a specific flexible function in the family of flexible functional forms definitely requires a comparison of their properties. Various criteria are used by researchers in the comparison. These include the ability to conform to neoclassical restrictions using the outer domain or inner domain of the function, and statistical properties such as best of fit. Although economists have been using well-designed experiments and reasonable criteria to compare the relative performance of flexible functional forms, they have found little consensus. The performance problem is indeed case-specific and closely relates to the magnitudes of the elasticities of substitution. The GL form generally performs better in cases with low elasticities or a mixture of high and low elasticities, while the TL form is apparently preferable for high elasticities (see, e.g., Caves and Christensen,[195]; Despotakis,[196]). In addition, different functional forms may yield quite different results for the same data set and the same economic assumptions[194]. In performing empirical analyses with flexible functional forms, pre-investigation of the substitution possibilities and careful understanding of case-specific differences are thus very important.

The flexible functional forms used in this study are two-tiered Generalized Leontief cost functions. They were selected based on the following concerns:

1. The elasticities of substitution between inputs may be a mix of low and high levels.
2. GL functions involve fewer parameters to be calibrated or estimated than other flexible functional forms.
3. For intermediate inputs other than K, L, E, and M, fixed input proportions were assumed. Since the GL form collapses to a Leontief function under certain conditions, intuitively, it seems desirable to choose the GL form for consistency.

Trade

For an open, regional economy like that of Pennsylvania, trade is very important and should be carefully handled conceptually and empirically. In CGE analysis, there are two approaches to modeling the terms of trade in a small, open economy. One method assumes product homogeneity among countries or regions. The other approach specifies product differentiation by country (or region) of origin into the demand structure using the Armington assumption.

The first approach can be regarded as an application of traditional trade theory. With perfectly competitive markets, a small, open economy faces a perfectly elastic supply of imports at constant world market prices and a perfectly elastic demand for its exports at exogeneously given export prices. Traditional trade theory stipulates that if n different goods are consumed and can be produced in the economy using m factor inputs at constant returns to scale ($n > m$), comparative advantage requires that, in equilibrium, no more than m goods will be produced and possibly exported, while the shortage of nonexport tradable goods will be imported[197]. This implies that each tradable good cannot be simultaneously exported and imported. Applying and extending this

theory to a CGE framework requires a high level of sectoral aggregation so that the number of tradable sectors will be equal to the number of nontradable factor inputs.

The above approach is theoretically attractive but may turn out to be too restrictive for a large scale CGE model. The widely accepted Armington[198] assumption can free CGE models from the limitation of traditional trade theory. According to Armington, similar goods originating from different countries (or regions) are imperfect substitutes. Thus, domestic consumers of commodities within one aggregated sector actually consume a mixture of domestically produced and imported goods. There are various reasons to justify this approach. Bergman[199] found that in a relatively aggregated CGE model, the aggregated indices for import prices, import quantities, domestic production costs, and domestic production are correlated. Another reason is the commonly observed cross-hauling problem associated with imperfect trade statistics or highly-aggregated data. This phenomenon can be easily explained and handled by the Armington assumption. In addition, the Armington assumption can avoid the occurrence of unrealistically strong specialization effects when a change in trade policy is modeled with traditional trade theory.

The treatment of trade in the Pennsylvania CGE model follows the traditional small, open economy assumption with the application of the Armington assumption only on the import demand side. Industries are distinguished between traded sectors and nontraded sectors. Trade with other regions and foreign countries is modeled as a two-stage decision process. From the small, open economy assumption, the world prices of imports, the prices of imports from other regions, the world prices of exports, and the prices of exports to other regions are all exogeneously given. On the import side, the consumer, at the first stage, maximizes the utility of consuming composite goods subject to a budget constraint by substituting between foreign goods and domestic goods. At the second stage, a choice is again made between locally produced goods and goods from other regions. At each stage, the Armington assumption is employed and a CES function is used to aggregate imperfect substitutes. On the export side, the producer, at the first stage, minimizes the cost of producing joint products to furnish domestic consumption and foreign demand. Then, at the second stage, the producer again makes supply decisions between local sale and export supply to other regions. At each stage, a constant elasticity of transformation function (CET) is used for aggregation (This two-stage decision structure and specification of imperfect substitution and transformation imply assumptions of separability and the lack of income effects.).

Factor Mobility

Factor mobility is another important issue in empirical analysis, especially in regional economic modeling. Two types of mobility are defined: factor mobility across sectors and factor movements across regions. In most CGE models, labor is usually assumed to be perfectly mobile across sectors, while capital is modeled as sector specific in the short run and fully mobile across sectors in the long run. In the Pennsylvania CGE model, both labor and capital are assumed to be

fully mobile across industries. Given the long-term nature of the model and the fact that the Pennsylvania economy is well developed and highly industrialized, this modeling decision should have less impact on the accuracy of the estimates than other simplifications that were adopted.

The problem of interregional factor mobility is critical. Interregional capital movement can be easily modeled by setting net regional savings as endogenous; interregional labor movement, on the other hand, is more difficult for modelers to deal with. Interregional labor movement may be the result of natural migration, a change of workers' preference, and a change in spatial employment patterns due to external shocks. For example, a more stringent environmental regulation may exert relatively heavier pressure on Pennsylvania coal industries compared to the other states. Therefore, the unemployed Pennsylvania coal miners may consider moving to adjacent coal producing states or exiting the industry.

The conventional approach to modeling interregional labor mobility is the expression of migration as a function of explanatory variables based on observed data. Such attempts in CGE analysis include the treatment of partial labor mobility by Whalley and Trela[200] and the impressive work by Norrie and Percy[201]. The treatment of interregional labor mobility in this model, however, takes another approach. We carry out a sensitivity analysis that allows total regional labor supply to be changed by in-migration or out-migration to balance labor demand. Thus, labor supply is modeled endogeneously but as a residual. This approach is consistent with long-run equilibrium conditions in most regional models.

Model Closure and Macro Balances

The model closure problem in general equilibrium models is actually a synonym for the overidentification problem in a mathematical simultaneous equation system. The tendency of modelers is often to impose as many restrictions as possible in a single model. In most cases, this will lead to an over-determination of the model (In general equilibrium analysis, if a model were to satisfy the following four conditions: (1) full labor employment, (2) factor prices equaling marginal value product, (3) personal consumption as a pure function of real incomes, and (4) a fixed amount of investment, then investment will not equal savings.).

To solve the overidentification problem, either one constraint has to be dropped from the model, or one previously exogenous variable or model parameter must be determined endogeneously. This process is called the imposition of a closure rule in general equilibrium models. Four types of closure rules are usually adopted by modelers in CGE analysis:

1. Classical: Full employment is achieved, and the economy-wide wage rate is forced to adjust endogeneously. Aggregate investment is endogenous and financed by total savings.
2. Keynesian: Unemployment is allowed to happen in the economy. The economy-wide average wage rate is fixed, and labor supply is determined indigeneously.

3. Kaldorian: Full employment is attained, and aggregate investment is set exogenously. Aggregate investment is equated to total savings through the endogenous adjustment of the price level and the functional distribution of income.
4. Johansen: Full employment is achieved and aggregate investment is set exogenously. Government expenditures and tax revenues adjust indigeneously to restore the savings-investment balance.

The closure rule adopted in this model is not exactly like any of the above categories. However, it most closely approximates Kaldorian closure. As mentioned in the beginning of this chapter, the level of fixed investment is set exogenously. Therefore, the profit-savings rate is forced to adjust indigeneously so that enough savings can be generated to finance increased investment requirements.

In addition to the closure rule, a set of macro balancing identities is necessary to make the CGE model consistent. These are producer's equilibrium, goods market clearing, the government budget deficit, the balance of trade, and an investment-savings identity.

ACID RAIN POLICY IMPACTS

Abatement Technology

Three broad categories of technical options are now available to industries to reduce acid-rain emissions: installing equipment to treat the discharge (end-of-pipe mitigation), substituting toward cleaner energy inputs (fuel-switching), and adopting a different production process (e.g., *clean coal technologies* in electricity generation). The development of these three technical options in the U.S. is closely related to air-quality regulations, notably, the Clean Air Act (CAA).

To meet the emission standards in the early years of the Clean Air Act, a major option was fuel switching, typically substitution within or between fossil fuels. For example, coal-fired plants in the electricity industry could substitute low-sulfur coal for high-sulfur coal. Alternatively, the boiler could be modified to use oil. The passage of the 1977 CAA amendments required industries in all areas to adopt the best achievable control technology (BACT) for new facilities, and required industries in non-attainment areas to use the lowest achievable emissions rate technology (LAER) to reduce the emissions of air pollutants. This movement accelerated the maturity of flue-gas desulfurization (or stack-gas scrubbers) technology, although this method is typically more costly compared to fuel-switching. The growing environmental concern since the mid-1980s stimulated the development of new technologies represented by low gas emission rate and improved fuel efficiency within several high air pollution industries. The most important recent technological innovation is the category of *clean coal technologies* in electricity generation, such as atmospheric fluidized-bed combustion (AFBC), pressurized fluidized-bed combustion (PFBC), and integrated gasification combined-cycle (IGCC)[202].

The passage of the 1990 CAA amendments marks a completely different stage in air-quality regulations. On the one hand, more stringent laws try to cover every aspect of air-quality regulations. To meet the strict emission standard, large cost increases are likely to be incurred in several high polluting industries (especially the electric utility industry). On the other hand, the new market incentive approach and the proved or emerging technologies seem to expand the opportunities for these industries to reduce their compliance costs.

Simulation Methodology

In this chapter, the potential economic impacts on the Pennsylvania economy of the 1990 CAA amendments for acid rain mitigation is simulated. Ideally, the above-mentioned three technical options should be incorporated in the model in order to capture the overall response of industries and the economy to acid rain regulations. However, most of the studies to date emphasize compliance through the adoption of the end-off-pipe mitigation strategy. In addition, the stringent 1990 CAA emission standards may eventually rule out fuel-switching as a practical option. And, given the fact that the new clean technologies that call for fully integrated new production processes will not be commercially available at least until early in the next century [203], end-of-pipe mitigation seems to be the most likely option over the next several years.

End-of-pipe mitigation can be considered as a production process which employs capital, labor, energy, and materials to reduce gaseous emissions, and which is separable from the remaining production structure. The increased capital investment in pollution control equipment (such as retrofitting and installation of FGD systems) and the subsequent expenditures on operating and maintaining it are the two major cost components. In this model, the increased capital investment in pollution control equipment is first assumed to offset or to *crowd out* ordinary investments on a dollar for dollar basis (an assumption of a 50% displacement is tested in a later sensitivity analysis). The increased operating and maintenance (O&M) costs are treated as the increase in costs of the overall industry production process. Since the expenditures to operate and maintain retrofitted or newly-installed pollution control equipment represents a supplemental production process, the cost structure of the old production process is modified accordingly.

Also, in modeling the new overall production process, it was assumed that the increased O&M costs can be completely passed on to consumers (a no cost pass-through assumption is analyzed in a sensitivity experiment later) and the firms' profits per physical unit of output stay the same as before. Therefore, the value of industry output rises by the amount of the O&M cost increase. The increased O&M costs on labor, capital, individual energy, and individual materials are translated into an increase in their derived demands. The input coefficients for those inputs not in the GL cost function are recalculated by dividing the value of inputs by the value of new industry output.

Data Preparation

The estimates of the annual compliance costs to meet the 1990 CAA emissions standard are quite uncertain. This ranges from the EPA's estimate of between $20 billion and $25 billion per annum for the U.S. by the year 2005 to the estimates of $51 billion/year by the Clean Air Working Group and Business Round Table. For the whole bill, $5 billion to $7 billion are expected to be spent per annum on acid rain compliance for the U.S.[204-207].

Estimates of the compliance costs at the regional level are few in number. In the May 1991 issue, Electrical World presented an estimate of compliance costs to mitigate SO_2 emissions for the electric utility industry, disaggregated by 9 electricity-supply regions. The compliance costs for the Mid-Atlantic Area, which consists of Pennsylvania, New Jersey, and New York, were reported as a total capital investment of $1.7 billion on FGD systems and annual O&M costs of $300 million by year 2005.

Since the current focus is on the economic impact of the end-of-pipe SO_2 mitigation strategy on the Pennsylvania economy, and because of lack of extensive information on Pennsylvania's compliance costs, existing data were adapted. At first, it was assumed that the compliance costs between 1991 and 2005 for Pennsylvania, New Jersey, and New York maintain the same proportion as year 1991. Then, the 1991 data on capital installation costs and average annual O&M costs from Electric Power Annual 1991[208] were obtained to disaggregate the cost estimates. The results are presented in Table 9-14. The power generated from coal-fired power plants for three states were multiplied by average O&M costs to obtain the total annual O&M costs for FGD operation. Then, the resulting values were used to calculate the distributional factor for O&M costs. In 1991, 96 percent of the O&M costs in Mid-Atlantic Area were distributed to Pennsylvania. Using this percentage, an increase in O&M costs of $289.44 million per year for the Pennsylvania electric utility industry was estimated in order to meet the 1990 CAA amendments.

The estimated total increase in capital investment on FGD systems consists of the retrofitting of existing FGDs and the installation of new systems. Since the 1991 average installed capital cost reported by EIA is an indicator of the charge per unit of combined retrofitting and installation, it is multiplied by the nameplate capacity of coal-fired power plants with FGDs installed to obtain the rough estimates of retrofitting investment on installed capacity for three states. The resulting values were then employed to calculate the distributional factor for capital investment. Roughly 73 percent of capital investment in FGD systems was allocated to the State of Pennsylvania. Using this factor, we estimated the total capital investment in FGD systems for the Pennsylvania electric utility industry to be $1.24 billion. Since it is unlikely that such a huge investment will be made within a year, we assume that the Pennsylvania electric utility industry will gradually put the new

Table 9-14. Estimation of Pennsylvania's Compliance Costs for Acid Rain Mitigation

	Mid-Atlantic Area			
	Total	N.J.	N.Y.	PA
Estimation of annual increase in operating costs in 2000 for PA				
Total power generated from coal-fired power plants (M Kwh)	130534	5237	24938	100359
Power generated from coal-fired power plants with FGDs installed (M Kwh)	26282	--	4585	21697
Average operating and maintenance costs for FGD operation (Mills/Kwh)	5.01	--	1.07	6.20
Total operating and maintenance costs for FGD operation ($ million)	139.43	--	4.91	134.52
Distributional factor for Operating and maintenance costs	1.00	--	0.04	0.96
Annual increase in operating costs in 2000 ($ million)	300.00	--	10.56	289.44
Estimation of annual increased inv. in FGD systems in 2000 for PA				
Nameplate capacity of coal-fired power plants with FGDs installed (Mw)	4727	--	691	4035
Average installed capital cost ($/Kw)	178	--	319	149
Distributional factor for increased capital investment	1.00	--	0.27	0.73
Total increased capital investment in FGD systems ($ billion)	1.70	--	0.46	1.24
Estimated annual increased capital investment in FGD systems ($ million)	113.33	--	30.40	82.93

Note: all values are in the 1990 constant dollars
Sources: Electrical World, 1991; Electric Power Annual 1991, EIA, February 1993

capital stock into place within the 1991 to 2005 time frame. If the investment is distributed uniformly in this period, the annual increased investment in FGD systems equals $82.93 million.

To modify the production process for the Pennsylvania electric utility industry, we required detailed O&M cost items for FGD systems installed in Pennsylvania. The FGD systems installed in the State are mostly wet-lime scrubbing technology. The largest FGD systems in Pennsylvania belong to three coal-fired power plants operated by the Pennsylvania Power Company, with their total nameplate capacity exceeding 60 percent of the Pennsylvania FGD capacity[209]. Since these three companies adopted magnesium enhanced lime process, we used the O&M costs estimate for this kind of FGD system to represent the typical O&M costs for all FGD systems installed in Pennsylvania[209]. Table 9-15 summarizes the detailed O&M cost items.

Since the data are restricted to the Pennsylvania electric utility industry, the natural choice is to perform model simulations for this industry only. Without the inclusion of compliance costs for other industries, the acid rain end-of-pipe policy simulations performed, therefore, underestimate the *overall* impact on the Pennsylvania economy. Fortunately, such an underestimate is only minor because over 70 percent of SO_2 emissions in the U.S. have typically come from electric utilities [210]. For Pennsylvania, the percentage of total compliance costs born by electric utilities is even higher. Since SO_2 is emitted mainly from the burning of coal, the percentage of coal use provides a good indicator. In 1992, over 84 percent of coal in Pennsylvania was consumed by electric utilities[211].

Results

The macro and micro simulation results for the end-of-pipe SO_2 mitigation strategy are presented in Tables 9-16 through 9-18, along with Figures 9-5 and 9-6. The end-of-pipe strategy to control the emissions of precursor gases that cause acid rain shows a small impact on the Pennsylvania economy. Real GRP in Pennsylvania decreases by a small 0.05 percent; the weighted price index increases by an insignificant 0.05 percent; total industry output falls by 0.18 percent. The results also show that Pennsylvania's trade declines. Total regional exports, foreign exports, and foreign imports are cut back by 0.38 percent, 0.22 percent, and 0.16 percent, respectively. Total regional imports rise by 0.30 percent. If the economic impact of the increased O&M costs is compared with that of the increased capital investment, it is evident that most of the economic impact is due to the increased O&M costs. This phenomenon is not difficult to understand. Since the annual capital investment increase for the Pennsylvania electric utilities to control SO_2 emissions is only $82.93 million per year, even though industries reduce productive investment by this amount, it is only a very small percentage of the total investment in Pennsylvania (If the real growth rate obtained from the REMI model is used to calculate the total capital investment in year 2000, this $82.93 million accounts for merely 0.19 percent of the total investment. The first simulation includes a complete offset in ordinary investment.). The small

Table 9-15. The Costs of a Representative Pennsylvania FGD System

	Value	Percentage
Total O&M costs (Mills/Kwh)	7.40	100.00
Fixed capital charges (Mills/Kwh)	2.81	37.97
Fixed O&M costs (Labor costs) (Mills/Kwh)	1.93	26.08
Variable O&M costs (Mills/Kwh)	2.66	35.95
Lime (Mills/Kwh)	1.01	13.65
Fixative lime (Mills/Kwh)	0.06	0.81
Raw water (Mills/Kwh)	0.01	0.14
Solids disposal (Mills/Kwh)	0.65	8.78
Reheat (Mills/Kwh)	0.40	5.41
Additional power (Mills/Kwh)	0.53	7.16

Table 9-16. Macro Results of the End-of-Pipe Mitigation Strategy for Acid Rain

Variable	Unit	O&M Costs	Capital Investment	Total Effect
Real GRP	%D	-0.05	-0.01	-0.06
Weighted price	%D	0.05	0.00	0.05
Total industry outputs	%D	-0.16	-0.02	-0.18
Total employment	%D	--	--	--
Regional exports	%D	-0.35	-0.03	-0.38
Regional imports	%D	0.31	-0.01	0.30
Foreign exports	%D	-0.19	-0.03	-0.22
Foreign imports	%D	-0.14	-0.02	-0.16

Table 9-17. Micro Results for Key Sectors of End-of-pipe Mitigation for Acid Rain

Variable	Unit	O&M Costs	Capital Investment	Total Effect
Coal				
Price	%D	0.04	0.00	0.04
Industry outputs	%D	-7.89	-0.05	-7.94
Employment	%D	-7.98	-0.05	-8.03
Regional exports	%D	-7.92	-0.05	-7.97
Regional imports	%D	-7.67	-0.03	-7.70
Foreign exports	%D	-7.83	-0.06	-7.89
Foreign imports	%D	-7.81	-0.02	-7.83
Petroleum Refining				
Price	%D	-0.09	0.00	-0.09
Industry outputs	%D	-0.22	-0.01	-0.23
Employment	%D	-0.32	-0.00	-0.32
Regional exports	%D	-0.09	-0.01	-0.10
Regional imports	%D	-0.46	-0.01	-0.47
Foreign exports	%D	-0.13	-0.01	-0.14
Foreign imports	%D	-0.59	0.00	-0.59
Iron & Steel				
Price	%D	0.45	0.00	0.45
Industry outputs	%D	-1.94	-0.07	-2.01
Employment	%D	-1.95	-0.07	-2.01
Regional exports	%D	-2.13	-0.07	-2.20
Regional imports	%D	0.83	-0.07	0.76
Foreign exports	%D	-2.03	-0.08	2.11
Foreign imports	%D	0.57	-0.05	0.52
Electric Utility				
Price	%D	2.06	0.00	2.06
Industry outputs	%D	-10.58	-0.02	-10.60
Employment	%D	-6.88	-0.02	-6.90
Regional exports	%D	-12.30	-0.03	-12.33
Regional imports	%D	5.31	0.01	5.32
Foreign exports	%D	-11.83	-0.03	-11.86
Foreign imports	%D	--	--	--
Gas Distribution				
Price	%D	-0.03	-0.00	-0.03
Industry outputs	%D	-2.37	-0.01	-2.38
Employment	%D	-2.43	-0.01	-2.44
Regional exports	%D	-2.29	-0.01	-2.30
Regional imports	%D	-2.50	-0.01	-2.51
Foreign exports	%D	-2.30	-0.01	-2.31
Foreign imports	%D	-2.43	-0.01	-2.44

Table 9-18. Percentage Change in the Intensity of Aggregate Inputs — End-of-Pipe Mitigation Strategy for Acid Rain

Sector	Labor Intensity	Capital Intensity	Energy Intensity	Material Intensity
O&M costs				
Agriculture	-0.29	0.34	-0.27	-0.00
Mining, except energy	-0.10	0.12	-0.20	-0.01
Coal mining	-0.10	0.40	-0.36	-0.02
Crude oil and natural gas	-0.19	0.15	-0.29	0.12
Construction	-0.02	0.18	-0.05	-0.01
Manufacturing	-0.03	0.19	-0.25	-0.09
Petroleum refining	-0.10	0.09	-0.01	0.03
Rubber and plastics	-0.06	0.20	-0.20	-0.04
Glass	-0.00	0.26	-0.16	-0.12
Stone	-0.05	0.17	-0.32	0.03
Primary iron and steel	-0.01	0.36	-0.15	-0.05
Nonferrous metal	0.07	0.27	-0.35	0.07
Transportation	-0.10	0.38	-0.12	-0.02
Communication	-0.28	0.17	-0.19	-0.03
Electric utility	4.14	0.19	-0.20	-0.07
Gas distribution	-0.06	0.40	-0.06	0.09
Trade and finance	-0.05	0.40	-0.23	0.00
Services	-0.12	0.34	-0.33	-0.01
Capital Investment				
Agriculture	0.01	-0.01	0.00	0.00
Mining, except energy	0.00	-0.00	0.00	0.00
Coal mining	0.00	-0.01	0.00	0.00
Crude oil and natural gas	0.00	-0.00	0.01	-0.00
Construction	0.00	-0.00	0.00	-0.00
Manufacturing	0.00	-0.00	0.00	-0.00
Petroleum refining	0.00	-0.00	0.00	-0.00
Rubber and plastics	0.00	-0.00	0.00	0.00
Glass	0.00	-0.00	0.00	-0.00
Stone	0.00	-0.00	0.01	-0.00
Primary iron and steel	0.00	-0.00	0.00	-0.00
Nonferrous metal	0.00	-0.00	-0.00	-0.00
Transportation	0.00	-0.01	0.00	-0.00
Communication	0.01	-0.00	0.00	0.00
Electric utility	0.00	-0.00	0.01	0.00
Gas distribution	0.00	-0.01	0.00	-0.00
Trade and finance	0.00	-0.01	0.00	-0.00
Services	0.00	-0.01	0:00	0.00

Table 9-18 (continued). Percentage Change in the Intensity of Aggregate Inputs — End-of-Pipe Mitigation Strategy

Sector	Labor Intensity	Capital Intensity	Energy Intensity	Material Intensity
Total Effects				
Agriculture	-0.28	0.34	-0.26	-0.00
Mining, except energy	-0.09	0.12	-0.20	-0.01
Coal mining	-0.09	0.39	-0.36	-0.02
Crude oil and natural gas	-0.18	0.14	-0.28	0.11
Construction	-0.02	0.18	-0.05	-0.02
Manufacturing	-0.03	0.18	-0.25	-0.09
Petroleum refining	-0.10	0.09	-0.01	0.03
Rubber and plastics	-0.06	0.20	-0.20	-0.04
Glass	-0.00	0.26	-0.16	-0.12
Stone	-0.05	0.17	-0.32	0.03
Primary iron and steel	-0.01	0.36	-0.15	-0.05
Nonferrous metal	0.07	0.27	-0.35	0.06
Transportation	-0.10	0.37	-0.12	-0.02
Communication	-0.27	0.16	-0.19	-0.03
Electric utility	4.15	0.18	-0.20	-0.07
Gas distribution	-0.06	0.39	-0.06	0.09
Trade and finance	-0.05	0.39	-0.23	0.00
Services	-0.12	0.33	-0.33	-0.01

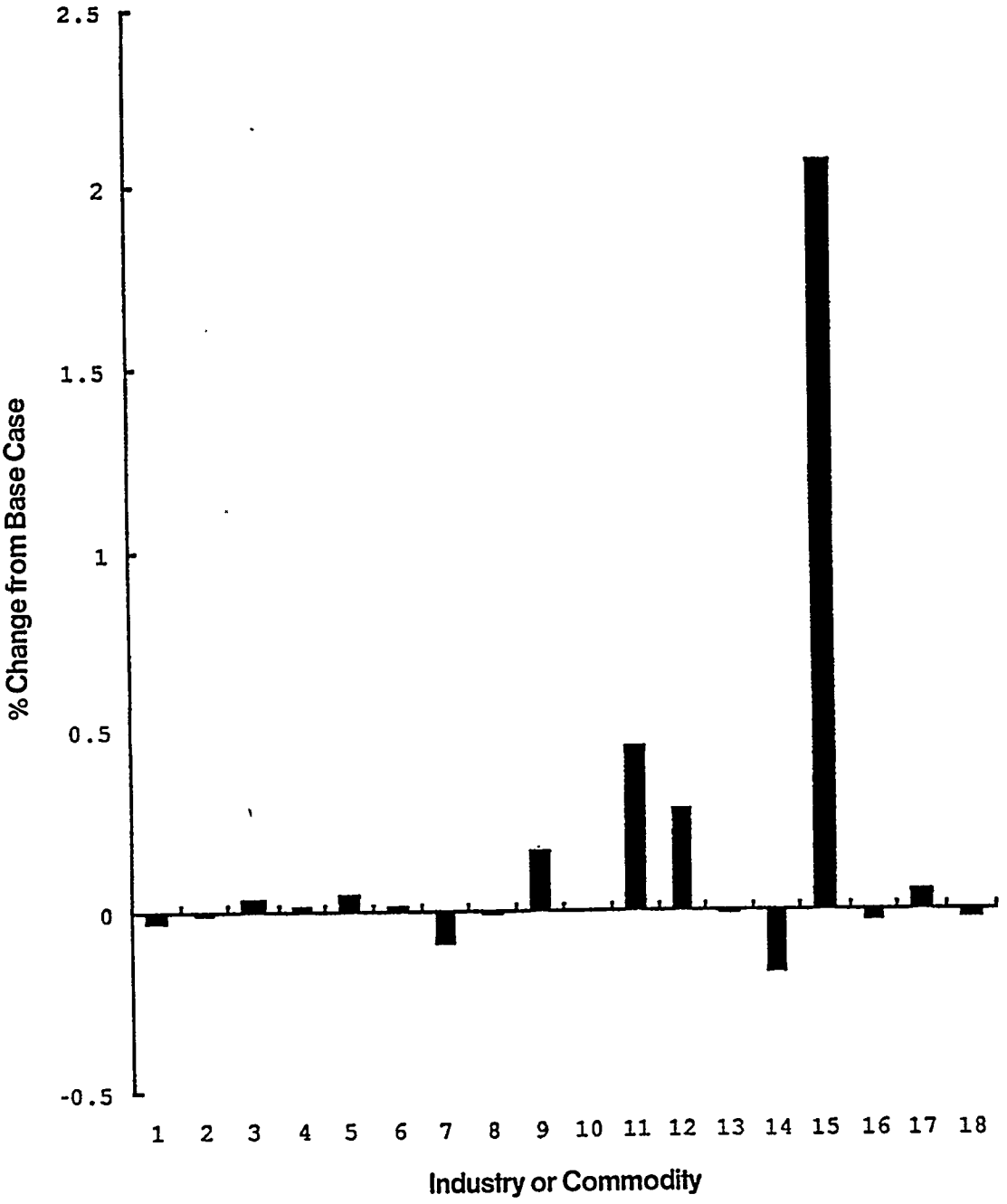

Figure 9-5. ACID RAIN END-OF-PIPE MITIGATION STRATEGY – EFFECT ON PRICES

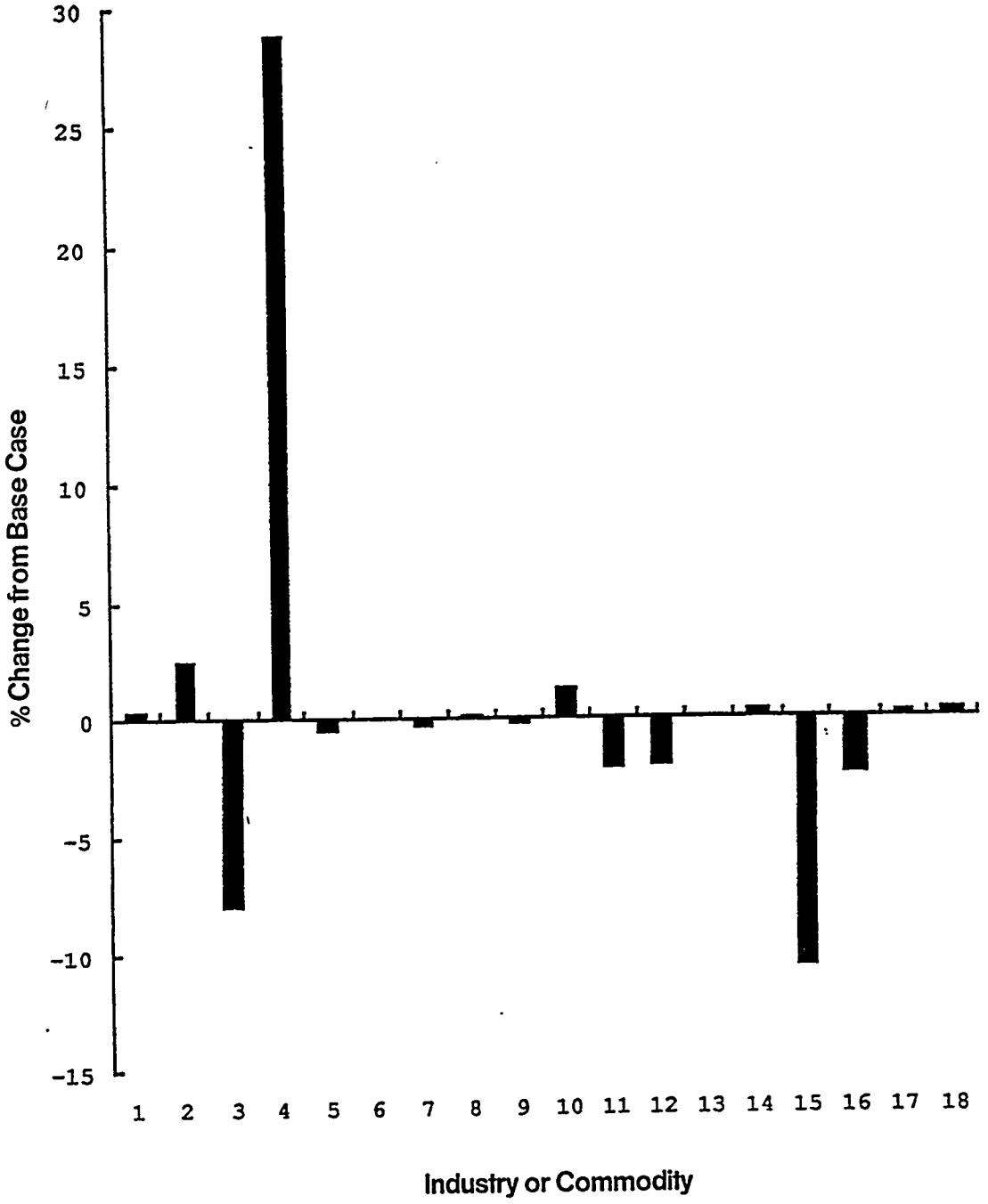

Figure 9-6. ACID RAIN END-OF-PIPE MITIGATION STRATEGY – EFFECT ON OUTPUT

percentage decrease in productive investment is unlikely to generate significant economic impacts. On the other hand, the increased O&M costs in the Pennsylvania electric utility industry will eventually be passed through as an electricity price increase, which will, in turn, lead to a decrease in electricity supply and an increase in the production costs of other industries. Therefore, the price effect multiplies and leads to various types of impacts on the Pennsylvania economy (see Table 9-17).

The micro aspect of the economic impact of the end-of-pipe mitigation strategy varies sizably. Figure 9-5 illustrates the price effect on 18 commodities measured in percentage change from the benchmark equilibrium. A significant price change only appears in the electricity sector. On the other hand, the output effect is much larger. Figure 9-6 shows the impact on the outputs of 18 industries measured in percentage change from the benchmark equilibrium. A significant decrease in production appears in the coal mining, iron and steel, nonferrous metal, electric utility, and gas distribution industries. Regardless of the difference in magnitude, the pattern of output effects is roughly inversely correlated to the price effects.

Table 9-17 shows the micro results for several key sectors in the Pennsylvania economy. The end-of-pipe SO_2 mitigation strategy will increase the price of electricity by 2.06 percent and decrease total electricity generation by 10.60 percent. The employment in the electric utility industry drops by 6.90 percent. The supply of electricity to other regions also decreases by a significant 12.33 percent, while the demand for electricity from other regions increases by 5.32 percent. The immediate effect of reduced power generation is reflected by the decline in input demands for fossil fuels. As expected, the largest impact is experienced by the coal mining industry. Although the price of coal falls by a small 0.04 percent, Pennsylvania coal output drops by a large 7.94 percent. Both coal imports and coal exports decrease significantly (we assume relatively equally stringent CAA influences in coal prices in competing states). Their magnitudes are comparable to the output decline. Petroleum refining and gas distribution industries also experience impacts to a certain extent. The output of refined petroleum falls by 0.23 percent, and the gas supply drops by 2.38 percent. The impact on the iron and steel industry is also significant because, today, a substantial amount of iron and steel is produced by electric arc furnace technology. The price of iron and steel increases by 0.45 percent and its production decreases by 2.01 percent. Regional exports and foreign exports of iron and steel decrease by 2.20 percent and 2.11 percent, respectively, while its regional imports and foreign imports rise by 0.76 percent and 0.52 percent, respectively.

Table 9-18 shows the percentage change in the intensity of use of aggregate labor, capital, energy, and materials inputs for 18 industries. The increase in capital investment in FGD systems leads to a drop in ordinary (often referred to in the literature as *productive*) investment. As indicated by this table, the capital intensity of use in each industry drops, while the labor intensity

of use and energy intensity of use increase accordingly. Although this change is a clear trend, its magnitude is negligible. On the other hand, increased O&M costs lead to a decrease in the energy intensity of use and an increase in the capital intensity of use. Therefore, increased capital investment in pollution control equipment and increased O&M costs appear to have inverse effects on the intensity of use of aggregate inputs. In my simulations, the impact of increased O&M costs outweighs the impact of the investment increase in FGD systems. In fact, the substitution of capital goods for energy inputs is the major result of the end-of-pipe strategy to mitigate the acid rain problem. This partly explains why energy sectors in the Pennsylvania economy will have much larger output changes than the price changes. In a general equilibrium context, any quantity changes are combinations of substitution effects and output effects.

From the above discussion, it is evident that the economic impact of acid rain mitigation on the Pennsylvania economy turns out to be relatively small in any given year. Nevertheless, one needs to remember that the compliance costs for acid rain mitigation account for at most 25 percent of the total compliance costs for the 1990 CAA amendments. If total compliance costs and the actions of all industries are taken into account, the economic impact on the Pennsylvania economy increases in significance.

SENSITIVITY ANALYSES

In the previous section, point estimates of policy simulations were reported. However, no information was provided to assure the accuracy of these results. The model will not only accurately estimate the response of endogenous variables to external shocks but is also structurally stable. Although various methods are possible to validate the model [212], sensitivity analyses were performed following the practice of most CGE modelers.

A weakness of most CGE models is their heavy reliance on literature surveys to determine elasticity values in the model calibration process. The reliability of this procedure is often questioned by non-CGE modelers. Therefore, the first type of sensitivity analyses in this research is to test how different elasticity values may affect the policy simulation outcomes. Four separate experiments were performed in turn on AES values for aggregate GL cost functions, AES values for energy GL cost functions, ES values for the two-stage import equation, and ET (elasticities of transformation) values for the two-stage export equations. The method employed here is an overall model sensitivity testing process, which arbitrarily chooses elasticity values within the proposed suitable ranges using a random generator provided in the GAMS software[213]. With each combination of elasticity values, the model was solved against the reference simulation scenario. One hundred computer runs were performed for each experiment to obtain a large sample size for the sensitivity analyses.

Three major conclusions can be drawn from the above experiments.

1. First, the point predictions are robust to uncertainty over elasticities. The mean values for major macro variables in the four experiments are of the same order of magnitude as the reference case.
2. The model generates policy simulation results without any difficulty over the proposed suitable ranges of elasticity values. This provides strong evidence that the model's structure is stable and reliable.
3. The extents to which elasticities may affect policy simulation results are ranked as follows from the largest effects to the smallest effects: AES for aggregate GL cost functions > ET for two-stage export equations > ES for two-stage import equations > AES for energy GL cost functions.

Sensitivity to Model Assumptions

The second type of sensitivity analysis is to test the effect of model assumptions on the policy simulation outcomes. Four kinds of model assumptions are tested. In the first sensitivity analysis, we changed the macro closure assumption to the classical closure rule for the investment-savings relationship. Instead of imposing factor immobility restrictions, the second sensitivity analysis allows for the possibility of interregional labor immigration. The third sensitivity analysis relates to the assumption on pollution equipment investment for acid rain mitigation. In the fourth sensitivity analysis, we assume no cost pass-through to consumers for SO_2 mitigation. The reference case for the last two analyses is the previous acid rain end-of-pipe mitigation strategy. As opposed to the *overall* model sensitivity analyses, only a *partial* test for each case was performed since one computer run is enough to obtain the required results for different model assumptions.

The macro results of sensitivity analyses on different model assumptions are illustrated in Table 9-19. The corresponding micro results for five key sectors are shown in Table 9-20.

In the previous simulation for the end-of-pipe mitigation strategy, it was assumed that the investment in pollution control equipment is totally unproductive in the conventional sense. However, in the real world, this is not necessarily the case[214-216]. Also, empirical studies have indicated that only one third to a half of the ordinary investment was displaced by pollution control investment[217]. Therefore, the investment displacement assumption was changed to see how this might affect the simulation results. In this experiment, a 50 percent investment displacement was assumed.

The simulation results for this experiment are shown in Tables 9-20. It was found that the investment displacement assumption does not have a significant influence on the simulation outcomes. This observation, of course, is due to the fact that the annual investment in FGD systems by the Pennsylvania electric utility industry is only a small portion of the total investment.

Table 9-19. Effects of End-of-Pipe SO_2 Mitigation Strategy — Macro Results of Sensitivity Analyses on Model Assumptions

Variable	Unit	50% Investment Displacement	No Costs Pass-through
Real GRP	%D	-0.06	-0.10
Weighted price	%D	0.05	0.05
Total industry outputs	%D	-0.17	-0.17
Total employment	%D	—	—
Regional exports	%D	-0.36	-0.42
Regional imports	%D	0.30	0.23
Foreign exports	%D	-0.21	-0.27
Foreign imports	%D	-0.15	-0.20

Table 9-20. Effects of End-of-Pipe SO_2 Mitigation Strategy — Micro Results of Sensitivity Analyses on Model Assumptions

Variable	Unit	50% Investment Displacement	No Costs Pass-through
Coal			
Price	%D	0.04	0.06
Industry outputs	%D	-7.91	-5.90
Employment	%D	-7.99	-5.94
Regional exports	%D	-7.93	-5.95
Regional imports	%D	-7.67	-4.94
Foreign exports	%D	-7.85	-5.90
Foreign imports	%D	-7.80	-5.08
Petroleum Refining			
Price	%D	-0.09	-0.03
Industry outputs	%D	-0.22	-0.18
Employment	%D	-0.32	-0.23
Regional exports	%D	-0.09	-0.14
Regional imports	%D	-0.46	-0.25
Foreign exports	%D	-0.13	-0.14
Foreign imports	%D	-0.59	-0.32
Iron & Steel			
Price	%D	0.45	0.29
Industry outputs	%D	-1.90	-1.42
Employment	%D	-1.91	-1.42
Regional exports	%D	-2.08	-1.55
Regional imports	%D	0.88	0.38
Foreign exports	%D	-1.99	-1.49
Foreign imports	%D	0.63	0.24
Electric Utility			
Price	%D	2.06	1.06
Industry outputs	%D	-10.59	-5.44
Employment	%D	-6.88	-2.71
Regional exports	%D	-12.31	-6.37
Regional imports	%D	5.33	2.86
Foreign exports	%D	-11.84	-6.11
Foreign imports	%D	—	—
Gas Distribution			
Price	%D	-0.03	-0.01
Industry outputs	%D	-2.37	-1.58
Employment	%D	-2.43	-1.61
Regional exports	%D	-2.28	-1.56
Regional imports	%D	-2.50	-1.62
Foreign exports	%D	-2.29	-1.55
Foreign imports	%D	-2.43	-1.60

If the percentage of pollution control investment is much higher, which is true in order for Pennsylvania to comply with the entirety of the 1990 CAA requirements, the displacement assumption on pollution control investment does appear to have a significant effect on the simulation results.

As opposed to the assumption of complete costs pass-through used in previous acid rain simulations, it was assumed that the increased costs are not passed on to the electricity consumers. Instead, the Pennsylvania electric utility industry reduces dividend payments by the amount of the increase in O&M costs. Therefore, total industry outputs before the policy simulation remain unchanged.

The micro results in Table 9-20 show that the economic impacts on the Pennsylvania electric utility industry are smaller than the reference case. This, of course, is due to the fact that the increased O&M costs are not passed through as an increase in electricity prices. The micro effects on other key sectors are also smaller in this experiment given their close supply and demand relationships with the electric utility industry. However, the impacts on the remaining industries are roughly the same as the reference case. This leads to macro results of the same order of magnitude as those in the reference simulation.

In the above sensitivity experiments, it was found that different model assumptions do affect the model simulation outcomes. However, in most cases, the extent is relatively mild as indicated by the macro and micro results. Therefore, the policy simulations results are robust with respect to different model assumptions.

CONCLUSIONS

The model simulations performed in this study provide insight into how the recent Clean Air Act Amendments may affect the economic performance of the State of Pennsylvania and its individual industries. The sensitivity analyses further indicate how different model assumptions and different parameters chosen for model calibration may influence the simulation results. Generally speaking, efforts to combat the acid rain problem are likely to have small impact on the Pennsylvania economy. The sensitivity analyses prove that the point predictions of the model simulations are robust and reliable.

Of course, there are still more environmental policy instruments and pollution abatement tactics that can be examined by this model. Performing additional analyses will help us better understand the ability of the Pennsylvania economy and its industries to withstand environmental policy shocks. This will also enable policy makers to design better environmental policies.

9.7 Subtask 3.7 Public Perception of Benefits and Costs

During this time period, data were obtained from the Vancouver Assessment Authority and related local agencies to undertake the hedonic property value analysis. This data includes property location and sales information and legal maps of the selected municipalities. Preliminary data

analysis has been undertaken and initial results have proven disappointing due to the uneven distribution of observations during the early years of the relevant time frame. During this reporting period, an alternative research path in was pursued in developing, testing and implementing a contingent valuation survey in the mid-Virginia area. Six hundred and thirty surveys were mailed from which roughly a 30% response (accounting for bad addresses) has been received. Preliminary data analysis indicates that the value of the environmental impact from coal transport is small but is important to people in close proximity to the railroads. Further analysis is planned for March and April using conditional logic modeling to fully examine the characteristics underlying individuals responses to the coal dusting problem.

9.8 Subtask 3.8 Social Benefits

In evaluating alternate energy technologies, one must first evaluate and assess the environmental and social damages associated with conventional coal and petroleum technologies. This summary will review the literature associated with energy emission cost estimates, and attempt to aggregate these estimates for use in comparison with clean coal technologies. Table 9-21 is a general emissions summary of conventional coal and oil technologies as well as that of a MCWM boiler.

Recent cost estimates of environmental damage from coal and oil emissions tend to focus on the social benefits of reduced emissions. Table 9-22a and b outlines the various estimates considered by some leading authors in the field. Darwin Hall reviews the literature and contends that most social cost estimates are understated, and attempts to provide a more accurate assessment of the social costs of energy emissions[218]. Hall estimates the incremental benefit (IB) associated with reduced air pollution. An incremental benefit shows what consumers are willing to pay for emission reductions from the current level to a proposed reduced concentration. The air pollution incremental benefit for reducing coal emissions is $16.80-$18.77/ short ton with a marginal cost estimate of abatement of $7.23-$7.67/short ton (1985$). Oil fired boilers have an incremental benefit of reduced emissions of $11.59 per barrel of oil (BBL). In comparison, the incremental benefit of reducing coal emissions would be $0.68-$0.76/million British thermal units (MM Btu) versus $1.93/MM BTU for oil emissions. (These conversions to MM BTU were estimated using the conversion rates provided by Hall, which states 1 barrel of oil = 6 MM BTU, and 1 short ton of coal = 24.7 MM BTU.)

For each energy source, Viscusi et al.[219] attempt to evaluate seven different components of the external costs of energy given in terms of contribution per unit of the fuel. These estimates (1986 $) include: damage from residual lead in gasoline, emitted particulates, sulfur oxides (excluding mortality), sulfur oxides (including mortality), ozone, visibility, and air toxics from motor vehicles. Table 9-22a,b describes the unit value of benefits of emission reduction, following compliance with current standards due to sulfur oxides emissions (including mortality)

Table 9-21. General Emission Levels for Conventional Coal and Oil Boilers and Clean Coal Technology Projects

	Particulate	SO_2	SO_3	NO_2	CO	N_2O	CO_2
Conventional Industrial Coal Boiler*	1.47kg /MMBTU	1.33kg /M.BTU		.38kg /M.BTU	.011kg /M.BTU		81.0kg/ M.BTU **
Conventional Industrial Oil Boiler*	.006kg /MMBTU	.319kg /M.BTU	.0041kg /M.BTU	.145kg /M.BTU	.016kg /M.BTU		65.8kg/ M.BTU **
Coal/Water Slurry Industrial Boiler***	2.37kg /MMBTU	.51kg /M.BTU	.0037kg /M.BTU	.42kg /M.BTU	.14kg /M.BTU	.054kg /M.BTU	
Penn State Project**** (Micronized Coal)		.403kg /M.BTU		.324kg /M.BTU	.329kg /M.BTU		

*Source: Air Pollution Engineering Manual. Fuel Sulfur levels weretaken from Sedwick, Todd and Carol Cole eds. Guide to Industrial Coal Users. Pasha Publications Incorporated, 1986. and Energy Information Administration. Electric Power Monthly, April 1991.
**Source: Barbir, F. and T. N. Veziroglu. "Environmental Damage Caused by Fossil Fuels Consumption," International Journal of Energy, Environment, Economics. vol. 1, no. 4, pp. 297-310, 1991.
***Source: Van Buren, D. and L.R. Waterland. "Environmental Assessment of a Coal/Water Slurry Fired Industrial Boiler: Project Summary," EPA/600/S7-86/012. May 1986.
****Source: Pennsylvania State University, Energy and Fuels Research Center. Spreadsheet of emissions when firing dry, micronized coal ; October to December 1994. note: daily emissions were averaged in order to compile a single factor.

Table 9-22. Conventional Technology Emission Reduction Valuation for (a) Coal and (b) Oil

(a) Coal

Estimates	Applicability	Particulates	SO_2	SO_3	NO_2	CO	N_2O	CO_2
Hall* (1985$)	Acid Rain Control Pre-1990		<----$16.80-$18.77 /short ton ---> ($0.68-$0.76/MMBTU)					
Viscusi** (1986$)	Non-Global Warming Externalities	$8.41 /short ton ($0.34 /MMBTU)	$151.51/short ton ($6.13 /MMBTU)					
Barbir*** (1990$)	Acid Rain and Global Warming Externalities (including particulates)	<----------$173.94/short ton----------> ($7.04/MMBTU)						$40.03 /s.t. $1.62/ MBTU

(b) Oil

Estimates	Applicability	Particulates	SO_2	SO_3	NO_2	CO	N_2O	CO_2
Hall* (1985$)	Acid Rain Control Pre-1990		<------$11.59/barrel of oil------> ($1.93/MMBTU)					
Viscusi** (1986$)	Non-Global Warming Externalites	$1.81/bbl. ($0.30 /MMBTU)	$15.34/bbl. ($2.56 /MMBTU)					
Barbir*** (1990$)	Acid Rain and Global Warming Externalities (including particulates)	<----------$34.29/short ton----------> ($5.72/MMBTU)						$7.34 /bbl. $1.22/ MBTU

*Source: Hall, Darwin C. "Preliminary Estimates of Cumulative Private and External Costs of Energy," Contemporary Policy Issues, July 1990.
**Source: Viscusi, W. Kip, Wesley A. Magat, Alan Carlin, and Mark K. Dreyfus. "Environmentally Responsible Energy Pricing," The Energy Journal, vol. 15, no.2. 1994.
***Source: Barbir, F. and T. N. Veziroglu. "Environmental Damage Caused by Fossil Fuel Consumption," International Journal of Energy, Environment, Economics. vol. 1, no. 4, pp. 297-310, 1991.

and emitted particulates from (a)coal and (b)oil consumption. The mortality effects of sulfur emissions from coal are nearly five times greater than the market price of coal.

Babir and Veziroglu[220] estimate world environmental damage of the three main fossil fuels in 1990$/ MM BTU and short ton. This study includes damages related to acid rain precursors as well as greenhouse gas emissions, namely carbon dioxide. The total cost of using coal, petroleum, and natural gas were assessed by adding the estimates of the external costs of using each of the fossil fuels and the market price of each fuel. For the purpose of this summary, the external costs are only considered and are outlined in the following tables. These external costs were computed using the environmental damages experienced by each component of the biosphere: humans, animals, farm produce plants and forests, aquatic ecosystems, buildings and other man-made structures, and also the effect of strip mining. Air pollution and Global Warming effects on each component were calculated separately.

The methods of calculating the external damages depend on the nature of the effects on each element of the biosphere. Health effects were found to be difficult to measure, but included health expenditures and the cost of premature death assumed to be cost of projected lost wages. Agriculture and timber production losses are estimated to be 15% due to air pollution. There are very little recorded data as to the effects of air pollution on animals. Barbir et. al. estimate the damage on farm livestock and animal production to be 10% of farm income. Aquatic ecosystems were found to be affected mainly by leaks and spills associated by fuel transportation. Effects on buildings and structures were calculated by estimates of repair and replacement costs, yet it is difficult to estimate the cost of lost cultural property. Other air pollution effects included loss of visibility in relation to transportation safety, property values, and aesthetics. Effects of strip mining are based on the extraction of coal. The total external costs reveal that the damage estimates associated with coal combustion are higher than that of petroleum combustion.

9.9 Subtask 3.9 Coal Market Analysis

Subtask 3.9 has been completed and is summarized in this section. Due to the length of the analysis, it can be found in its entirety in Appendix C.

Coal has become a predominately single use fuel. Since the late 1940's, electricity has gradually become the primary market for coal. Electric utility use of coal represented 17% of total coal use in 1949 compared to 85% in 1991. On the other hand, coal has historically held a considerable share of an expanding electricity generation fuel market. Not only did coal use become concentrated in the electric utility sector, but also, its consumption growth is attributable to large increases in use by this sector. While utilities were consuming more coal, other end use sectors experienced declining consumption.

On a state level, differences in coal consumption growth rates can be explained by differences in electric utility coal use from one state to another. Underlying the developments in

electricity coal use by states are changes in where the growth in coal consumption and output occurred. The majority of the production expansion has come from new western areas that correspond to areas of increasing electric utility coal consumption. In these western areas, coal, which is almost exclusively consumed by electric utilities, has increased its share of an expanding electricity market, while in the East coal lost share, primarily to nuclear gains. Even though coal lost its share of the electricity market in virtually every principal eastern coal consuming state, coal consumed by electric utilities still increased in these states because of the growing demand for electricity. Coal gains displaced gas as the fuel of choice for utilities in the West North Central, West South Central, and Mountain regions. Coal was also favored over hydropower, in light of the rising incremental costs of expanding these projects.

While most of the growth in coal consumption is in the West, nine of the ten largest consumers are still eastern states. Some eastern demand, and demand from West North Central states close to Illinois Basin producers is being met with low sulfur western coal.

9.10 Subtask 3.10 Integration of Analyses

The work in Task 3 is being integrated into a final report.

10.0 PHASE II, TASK 4 FINAL REPORT/SUBMISSION OF DESIGN PACKAGE

Work in preparing the final report has started. Subtask 3.1, 3.2, and 3.9 have been completed.

11.0 PHASE III, TASK 1 COAL PREPARATION/UTILIZATION

11.1 Subtask 1.1 Particle Size control

CONVENTIONAL BALL MILLING

The Bond method has been used traditionally to describe the behavior of ball mills. It is simple and has been quite successful for predicting mill sizes, but it is not suitable for optimization of mill or circuit conditions. Also, it does not predict the complete product size distribution, which is important for subsequent processes such as coal-water slurry preparation. Recently, commercial ball mill simulators have evolved based on the concepts of grinding kinetic theory using specific rates of breakage (S values) and primary breakage distribution (B values). Hence one can examine the performance of various full-scale grinding circuits.

The method employed here follows that developed by Austin et al.[138], which involves scale-up of the specific rates of breakage determined for the material in a laboratory test batch mill, allowing for the effects of the variables associated with milling. For ball milling, these variables typically include mill rotational speed, ball filling, powder filling, mill diameter, ball diameter, etc. Extensive work has been done to investigate the effect of these variables, and the methodology to incorporate these factors into simulations is well described by Austin et al.[138].

The functional forms used to characterize particle breakage during grinding can be summarized as follows:

1) Effect of particle size (x_i)

$$S(x_i) = a\left(\frac{x_i}{x_o}\right)^{\alpha} \frac{1}{1+\left(\frac{x_i}{\mu}\right)^{\Lambda}}$$

where $S(x_i)$ = specific rate of breakage for particle of size x_i

a = specific rate of breakage at x_o

α = an exponential constant, characteristic of a material

μ, Λ = characteristic constant for the description of decrease in the specific rates of breakage as the particle becomes too big to be broken effectively.

2) Effect of ball diameter (d)

$$a \propto 1/d,$$
$$\mu \propto d^2$$

3) Effect of mill diameter (D)

$$S(x_i) \propto a \propto D^{0.5}$$
$$\mu \propto D^{0.2}$$

4) Effect of rotational speed

$$S(x_i) \propto (\phi_c\text{-}0.1) / \{1+ \exp[15.7(\phi_c\text{-}o.94)]\}$$

where f_c: is the fraction of critical speed (Critical speed is the rotation speed at which a ball begins to centrifuge on the mill case and not tumble).

5) Effects of ball and powder loading

$$S(x_i) \propto \exp(-cU)/(1+ 6.6J^{2.3})$$

where J = the fraction of the mill volume filled by the ball bed at rest
U = the fraction of the interstices of the ball bed filled with powder at rest

The S values determined for the material in a laboratory test batch mill can be used to simulate the large-scale mills via the scale-up equations given above. On the other hand, the B values are

typically independent of the breaking size and milling environment. Therefore, scale-up is not necessary for B values.

For a retention grinding device such as the ball mill, the length of time that material spends in the mill controls the final degree of breakage. Moreover, some fraction of the feed stays in the mill for a short time, other fractions for a longer time, etc. Therefore, estimation of the residence time distribution (RTD) is required. It has often been shown that the experimental RTD can be matched against theoretical expressions derived for a number of fully mixed reactors in series. The one-large, two-small, fully mixed reactors in series model has been found to be appropriate for ball mills.

A grinding circuit is a comprised of one or more mills and classifiers. Industrial grinding circuits can be categorized into the following five types.

a) open circuit
b) normal closed circuit
c) open circuit with scalped feed
d) reversed closed circuit
e) combined closed circuit

These circuits are shown in Figure 11-1. The combined closed circuit can be used to represent the other circuits by assigning the appropriate classification parameters for the pre-classifier and the post-classifiers.

Classification is the splitting of a stream of particles into two streams, with separation by size (and density) e.g., one stream with mainly large particles, the other with fine particles. The classifier performance is characterized by a set of numbers, one for each size interval which describes how each size is split into the two product streams. The selectivity number for size i (s_i) is defined as the fraction of size i in the feed which is sent to the coarse stream. A plot of the selectivity numbers vs. size is called a size selectivity curve. This curve generally has an S shape and can often be described by a log-logistic function. Using this functional form, the complete set of size selectivity values can be calculated using three characteristic parameters: the sharpness index, cut size (d_{50}) and apparent by-pass. Finally, the different streams in the complete circuit can be described by the mass balance equations, a mill model, and two classifier models.

Simulations were performed for the two most common circuits: open and normal closed circuit. Capacities were obtained for three different diameter (3, 4, 5 meters) mills, giving a circuit product passing through the one-point specification of 80% passing 200 mesh. All mills were operated with a slurry density of 70 wt% coal and at 70% of critical speed. Ball loading was set at 30% filling with makeup of 50.8 mm balls. The residence time distribution was assumed to fit the one-large/two-small fully mixed reactor model in the ratio 0.5, 0.25, 0.25. The performance of the classifier was assumed to be constant with the characteristic parameters of sharpness index=0.7 and by-pass=0.3. The d_{50} values were changed to give results over a range of circulating loads.

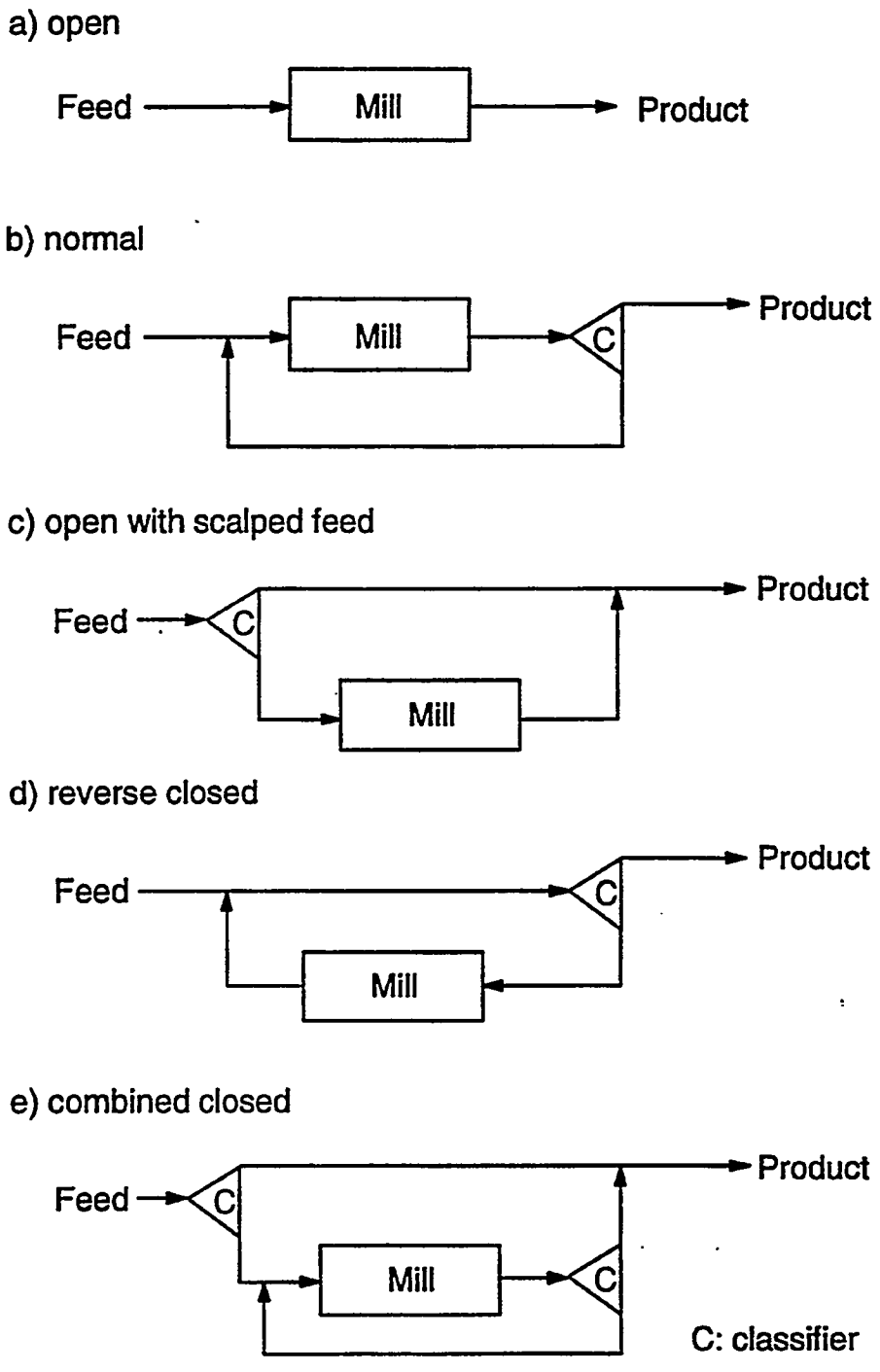

Figure 11-1. VARIOUS GRINDING CIRCUITS USED IN INDUSTRY

The coal feed was assumed to fit the Rosin-Rammler distribution with k=9.525 mm and m=1. The breakage parameters (a, a, g, f and b) measured in a laboratory batch mill at 70% solids are shown in Table 11-1.

The results of simulations are given in Table 11-2. As expected, the capacity is higher for easily ground coals (high HGI). For a given coal, capacity increases with the mill diameter and is proportional to $D^{3.5}$ as shown in Figure 11-2. This results from the fact that for the same grinding environment, the capacity is proportional to the mill volume, which is LD^2 (for the same L/D ratio it is D^3). Since the S values increase with the mill diameter by $D^{0.5}$ (relation No. 3), the overall effect of the mill diameter on the capacity is proportional to $D^{3.5}$. By closing the circuit with the classifier, the capacity increases substantially by minimizing the over-grinding of material that is already fine enough. Also, the closed circuit produces a steeper size distribution; i.e., produces less unnecessarily fine material. For a given classifier setting, as the feed rate is increased, the mill product coarsens, the classifier sends more material to recycle, the circulation ratio C (ratio of the amount of recycle to that of the product) increases, and the circuit product becomes coarser. However, there is only one feed rate that will meet the one-point product specification. By changing the classifier setting (d_{50}), it is possible to obtain the one-point match for a range of feed rates and circulation ratios. Figure 11-3 shows the results. A lower value of d_{50} gives a higher circulation ratio and a steeper size distribution. Also, the production rate increases as the circulation ratio increases, as seen in Figure 11-4. At low circulation ratio, the product is sufficiently fine that the classifier has no effect, so the production rate is the same as that of the open circuit. On the other hand, high recycle leads to increased overfilling, causing inefficient grinding: thus an optimum circulation ratio exists. Generally, the optimum circulation ratio is function of the fineness of the final product. In this case, the optimum circulation ratio is found to be in the range of 1.5-2.0. At this optimum circulation ratio, the increase in capacity given by closing the circuit is also in the range of 1.5-2.0. The energy required for grinding to a one-point product specification is less for the closed circuit than for open-circuit grinding.

The same approach can be used to predict grinding behavior in a stirred ball mill. However, the engineering and mill scale-up procedure needs further study. It has often been suggested that the median size of the product is related to the energy input, independent of the mill size and operation conditions[221, 222]. This suggests that the relation of power draw to the mill dimensions and operating variables can be used to predict the product fineness. However, in recent studies[223-226], it was reported that the energy efficiency is affected by operation conditions such as media density and size, slurry concentration and agitation speed. Also, the design procedure for scaling up the laboratory mill data to the full scale mill has not been completely established. In an earlier project, we evaluated a 4 liter stirred ball mill. Currently a 0.5 liter

Table 11-1. Breakage Parameters for the Various Seam Coals at 70% Solids

Coal Seam	a	α	ϕ	γ	β
Taggart	0.85	1.37	0.52	0.44	5.0
Pittsburgh	1.90	1.33	0.45	0.58	5.0
Lower Kittanning	3.47	1.56	0.45	0.36	5.0

Table 11-2. Comparison of Circuit Capacity Between Open and Closed Circuits.

Open Circuit

Mill Diameter (meters)	Taggart (HGI=47) (TPH)	Pittsburgh (HGI=56) (TPH)	Lower Kittanning (HGI=68) (TPH)
3	8.45	14.82	22.58
4	21.13	39.37	61.66
5	44.02	81.12	131.25

Closed Circuit

Mill Dia. (meters)	Taggart			Pittsburgh			Lower Kittanning		
	C	d_{50}, µm	TPH	C	d_{50},µm	TPH	C	d_{50}, µm	TPH
3	0.53	244	9.14	0.50	244	15.01	0.54	211	25.02
	1.03	137	13.13	0.97	133	21.47	1.03	133	32.60
	1.44	120	15.04	1.47	113	23.03	1.50	119	34.19
	2.10	112	17.09	1.97	104	23.17	1.98	108	33.23
	2.47	105	16.65						
4	0.48	305	22.39	0.50	244	38.91	0.48	264	61.51
	0.98	141	35.06	0.99	133	59.16	1.00	141	92.41
	1.52	119	41.86	1.46	115	63.48	1.54	117	92.32
	1.91	112	45.23	2.06	106	64.38	1.74	111	91.02
	3.33	99	44.55						
5	0.47	305	43.90	0.50	244	81.90	0.49	264	139.91
	0.97	139	71.31	0.95	132	118.42	0.96	141	191.2
	1.56	122	92.66	1.54	115	136.86	1.47	117	193.67
	2.04	112	97.73	2.07	105	135.48	1.97	111	197.62
	2.50	103	95.10						

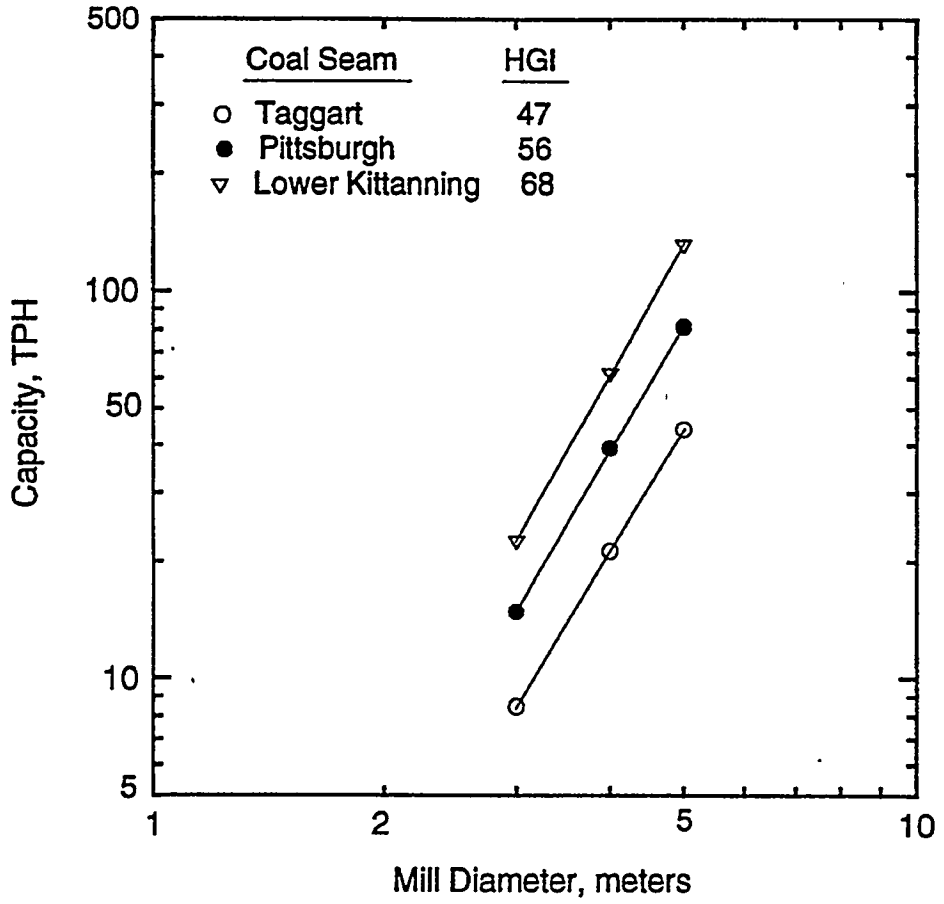

Figure 11-2. VARIATION OF THE CAPACITY WITH MILL DIAMETER

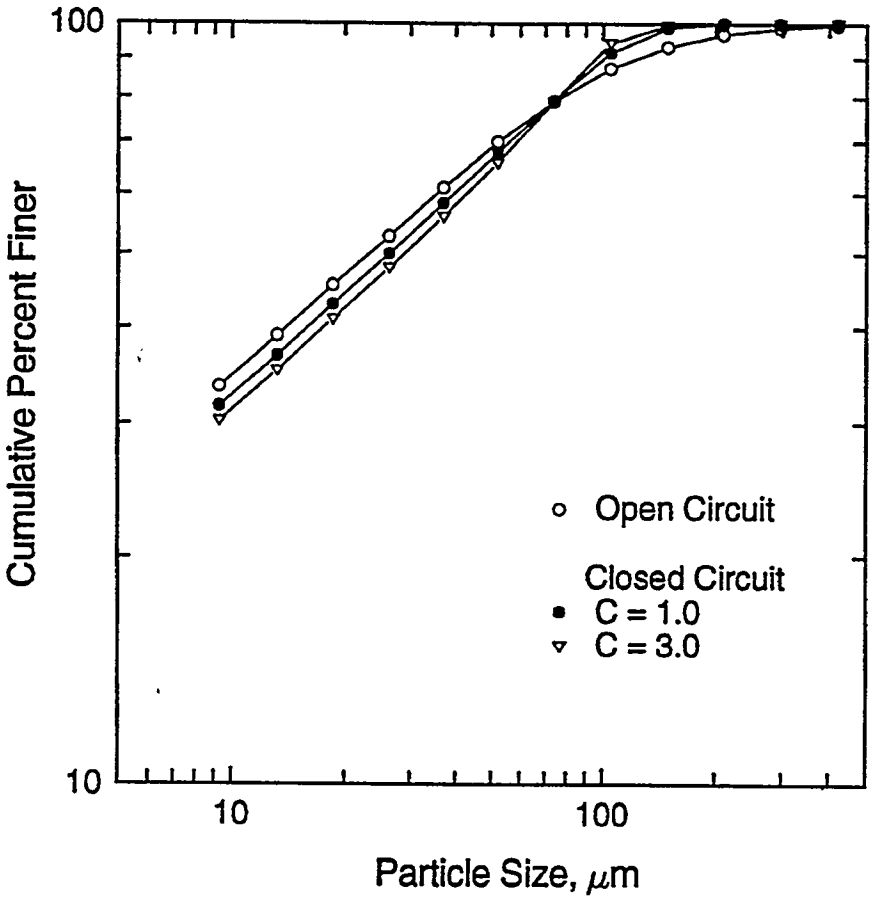

Figure 11-3. COMPARISON OF SIZE DISTRIBUTIONS BETWEEN OPEN AND CLOSED CIRCUIT GRINDING

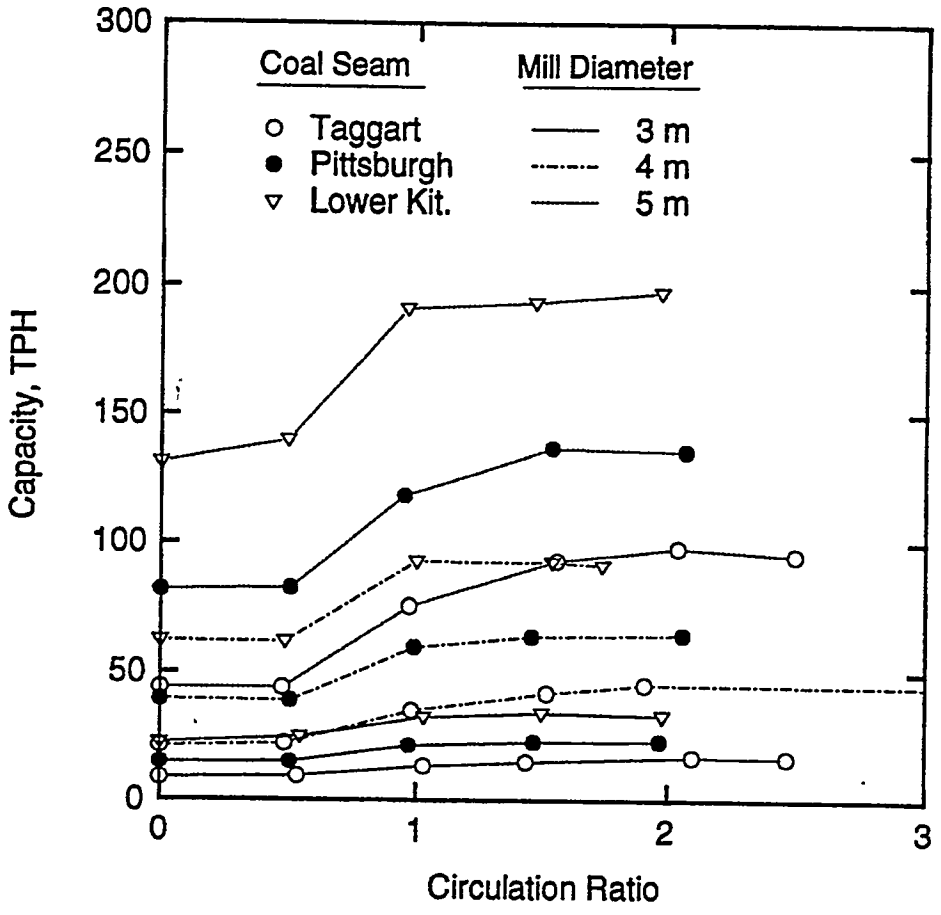

Figure 11-4. EFFECT OF CIRCULATION RATIO ON CAPACITY

stirred ball mill is being built. The test results obtained with the small mill in conjunction with the data from the large mill will be used to develop scale-up criteria.

11.2 Subtask 1.2 Physical Separations

MAGNETIC FLUID

Magnetic-fluid testing of the modified Franz separator continued. Separations were performed under static conditions to calibrate the device. Narrow size (i.e., 6x8 mesh) and narrow relative density (e.g., 1.28x1.30) fractions of coal were prepared by heavy liquid fractionation. One of the coal fractions was placed in the magnetic fluid of a fixed concentration. The magnetic field intensity was increased until the material just began to float. This was repeated for ten relative density fractions to establish a calibration curve (Figure 11-5). Subsequent tests, which were carried out using purchased plastic tracer particles of a fixed density, confirmed the calibration curve.

After calibration, a series of separations was made using a sample of the nominal -1/4" Upper Freeport seam coal, which was screened to produce 12x14 mesh and 28x100 mesh size fractions. Separations were made at 1.3, 1.4, 1.5, 1.6, and 2.0 relative densities using the magnetic fluid separator under static conditions. A parallel approach was used whereby a separate sample was used for each test thereby providing cumulative float and sink values at each relative density.

Prior to immersion in the magnetic fluid, the coal was wetted using a small amount of 0.1% Aerosol OT solution followed by rinsing with the magnetic fluid. After setting the relative density, the coal was added to the separator and allowed to stand for one hour. At that time, the products were separated by first collecting the float material followed by removal of the sink material. The samples were washed with water to remove any remaining liquid, dried, and weighed to determine the yield at each relative density. An ash analysis was done on each fractionated sample.

The resulting values, along with those obtained using heavy-liquid fractionation, are plotted in Figures 11-6 and 11-7 for the 12x14 mesh and 28x100 mesh size fractions, respectively. Ideally, both liquids should produce the theoretically best separation possible at a given relative density, i.e., the washability curve for the given size fraction. Therefore, the differences in the results can be attributed, in part, to the differences in the properties of the two liquids. That is, the magnetic fluid is water based, while the heavy liquids are organic.

Testing of the continuous separator is continuing. Initially, the separations will be made under gravity alone using the flow-through separator described previously. Subsequent separations will be made using a centrifugal separator. The design of this unit is in progress.

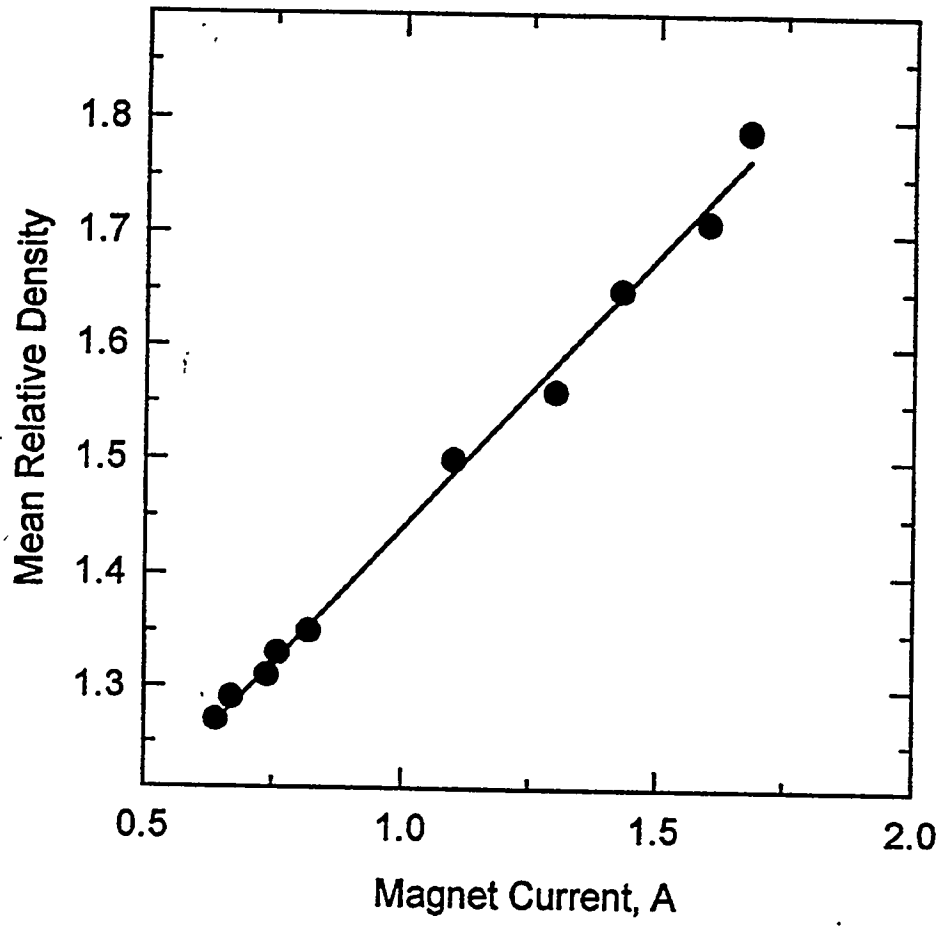

Figure 11-5. VARIATION OF THE RELATIVE DENSITY OF SEPARATION AS A FUNCTION OF THE CURRENT FOR THE MAGNETIC-FLUID SEPARATOR

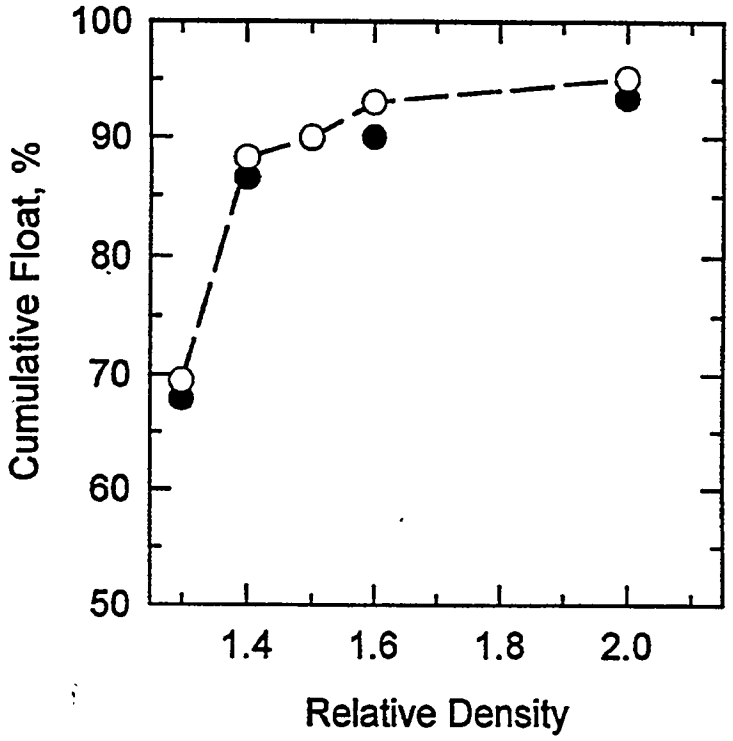

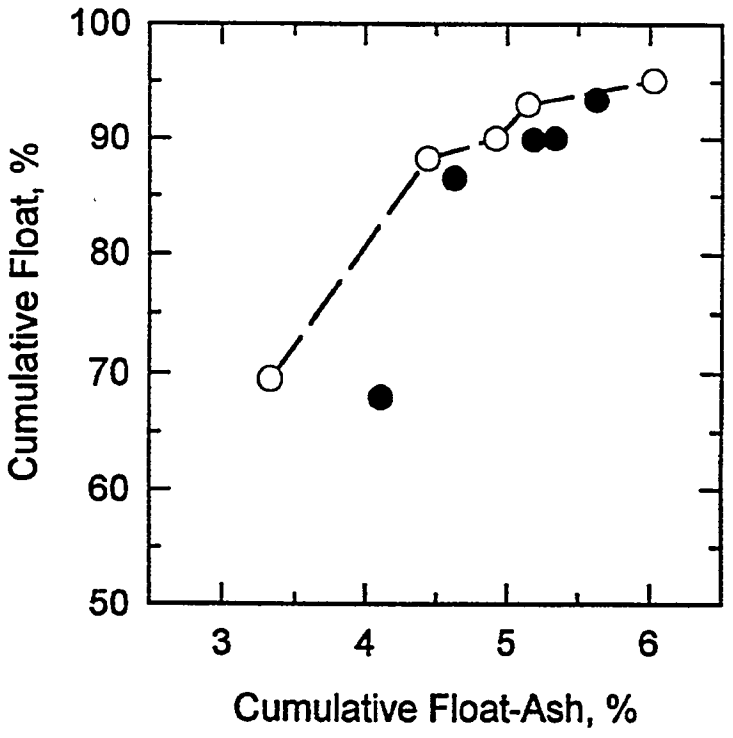

Figure 11-6. WASHABILITY CURVES FOR THE 12 x 14 MESH UPPER FREEPORT SEAM COAL
(○ organic liquids, ● magnetic fluid)

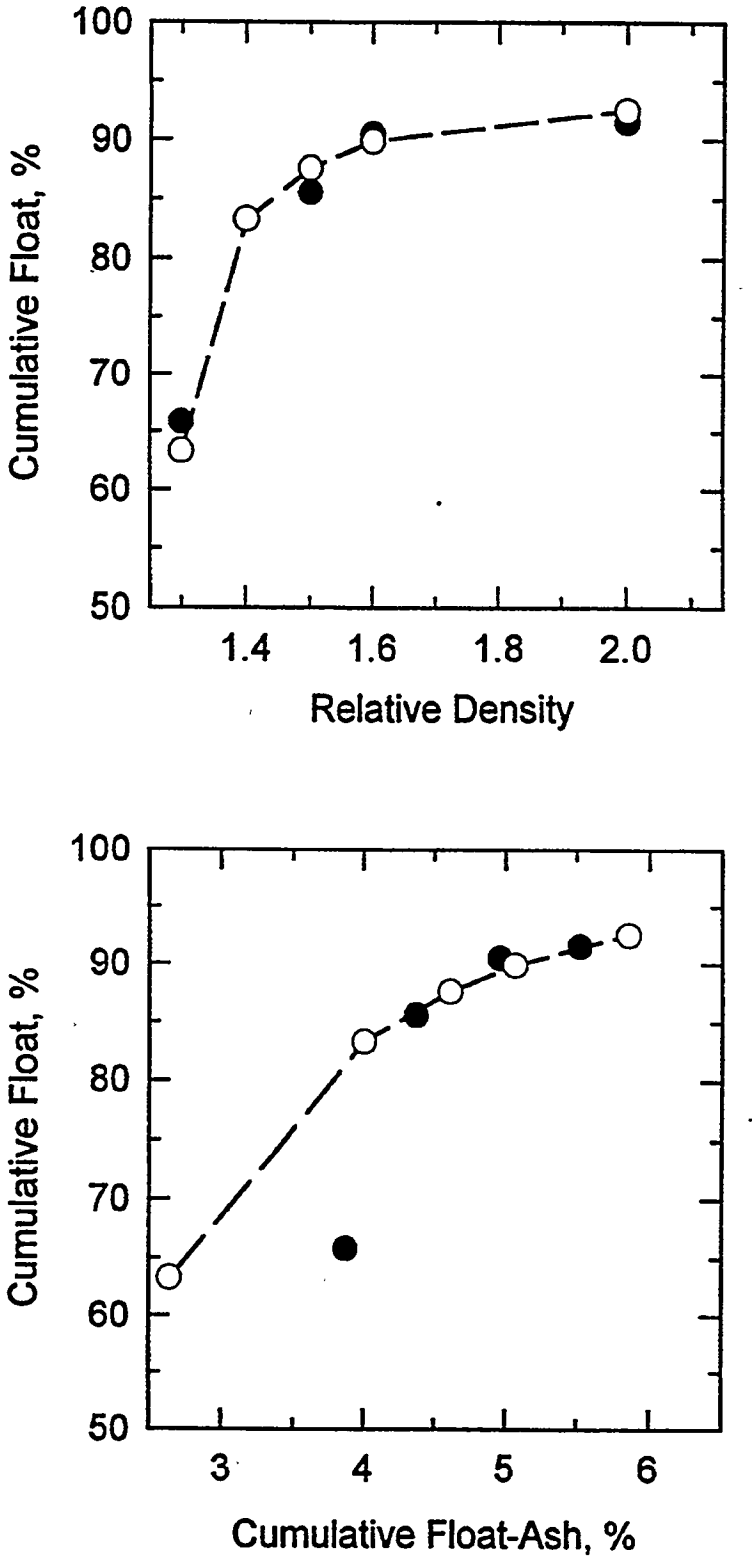

Figure 11-7. WASHABILITY CURVES FOR THE 28 x 100 MESH UPPER FREEPORT SEAM COAL
(○ organic liquids, ● magnetic fluid)

11.3 Subtask 1.3 Surface-Based Separation Processes

The continuous froth flotation circuit consists of two stages:

(a) the rougher stage, and
(b) the cleaner stage.

The flotation circuit is designed for deep cleaning of coal to obtain target ash and sulfur contents. The raw coal to be fed to the flotation circuit is ground in a stirred ball mill with a total capacity of 30 gallons and a working capacity of about 20 gallons, so that a size distribution of 90% passing 28 mesh is produced. During grinding, a coal water slurry containing 20-35% solids is produced which is pumped to the 500 gallon capacity head tank. The slurry from the head tank is pumped by a Moyno pump to the head tank for the flotation cells. The flow rate is set depending on the rougher circuit requirements and the percent solids in the feed slurry. A flow meter is connected after the pump to monitor the slurry flow rate from the head tank.

The rougher stage of the circuit consists of:

1. A 20 gallon feed tank with mixer
2. Four WEMCO flotation cells of 2 cubic feet capacity each
3. A 5 gallon collector/frother tank
4. A 1 gallon reagent tank with mixer
5. A Quinn forth pump, with a flow meter
6. Sampling system

The coal-water slurry at 20-35% solids from the head tank comes into the feed tank where it is diluted with water to make a slurry containing about 5% solids. The amount of water added to the feed tank depends on the solids content of the feed slurry from the head tank. A rotometer is present in series with the water line to measure the flow rate. The water flow rate is adjusted so as to achieve the desired percent solids for flotation.

The frother (typically MIBC), and the collector (Dodecane or full oil) are mixed with water in a ratio of 1:400 times in the frother and collector tanks, respectively, and pumped at the required rate into the feed tank. During some tests, the collector was fed into cells 3 and 4 only, to avoid overloading of the froth in cells 1 and 2, and increase recovery in cells 3 and 4.

The coal-water slurry containing 5% solids, and frother and collector is fed to the series of four rougher cells. The impellers in the cells rotate at a fixed speed, and the cells are self-aerated. The froth containing coal rises above the lip of the cells and is removed into the launders on each side of the cells by the rotating paddles. The froth in the launders is washed down by the wash water. The wash water flow rate is typically around 1 gpm, and is monitored by a water rotometer. The froth product from the rougher circuit flows down into a froth sump, from where it is pumped to the cleaner circuit. The tailings coming out of the last cell went into the trench sump. Simultaneous samples are taken from the washed down froth product from all the four rougher cells, and tailings stream. Samples are being analyzed to evaluate the performance.

CLEANER CIRCUIT

The cleaner circuit consists of:

1. A 20 gallon feed tank with mixer
2. Two WEMCO flotation cells of 2 cubic feet capacity each
3. A 5 gallon frother tank
4. A 1 gallon collector tank with mixer

The froth product from the rougher circuit are brought into the feed tank where it is diluted to about 5% solids with water. The water flow rate into the feed tank is adjusted to obtain the desired total flow rate, and is monitored using a water rotometer. The frother and collector are fed into the feed tank and mixed with the slurry as described in the previous section.

The slurry is fed to the cleaner flotation cells. The froth product from the cleaner cells is collected in drums, and the tailings from the last cell flows down to the trench sump. Samples are taken simultaneously from the washed down froth product streams of both the cells, and the tailings stream.

The product collected from the cleaner circuit is filtered on the vacuum filter. The tailings in the trench sump, now containing very low percent solids, are pumped by the trench pump to a overhead tank, where it is mixed with a solution of dissolved calcium chloride, and the solids are allowed to flocculate and settle overnight. The clear water on the top is drained out, and the slurry with settled solids is pumped to the vacuum filtration system.

Several tests have been made with the Upper Freeport coal but some difference are observed in the flotation behavior of the coal even though the operating conditions are kept constant. The reason for such a behavior are under investigation.

11.4 Subtask 1.4 Dry Processing

The development of a tribocharging-electrostatic separation system continued. Fabrication of a newly designed continuous separator has been completed (Figure 11-8). The test unit consists of two, 600 mm diameter, rotating copper plates, which are spaced 100 mm apart. The plates are enclosed within a 810 mm high by 725 mm deep by 115 mm wide box constructed of 6.35 mm thick Plexiglas. The entire unit is mounted on a table. The diameter of the plates was based on the results from the batch testing, which showed that the bulk of the particles separated within a distance of 600 mm from the feed end.

The voltage is applied to each plate by attaching the positive or negative electrode from each power supply to a metal washer that "rides" on a rotating copper shaft, which is attached directly to a plate. The drive pulleys are insulated from the copper shafts. The plates are belt driven using a variable-speed motor.

The coal is fed with a vibrating feeder into a venturi feeder where it is entrained in a nitrogen stream. The solids are passed through an in-line copper static mixer to charge the particles. The solids are then discharged downward into the separator where they are collected

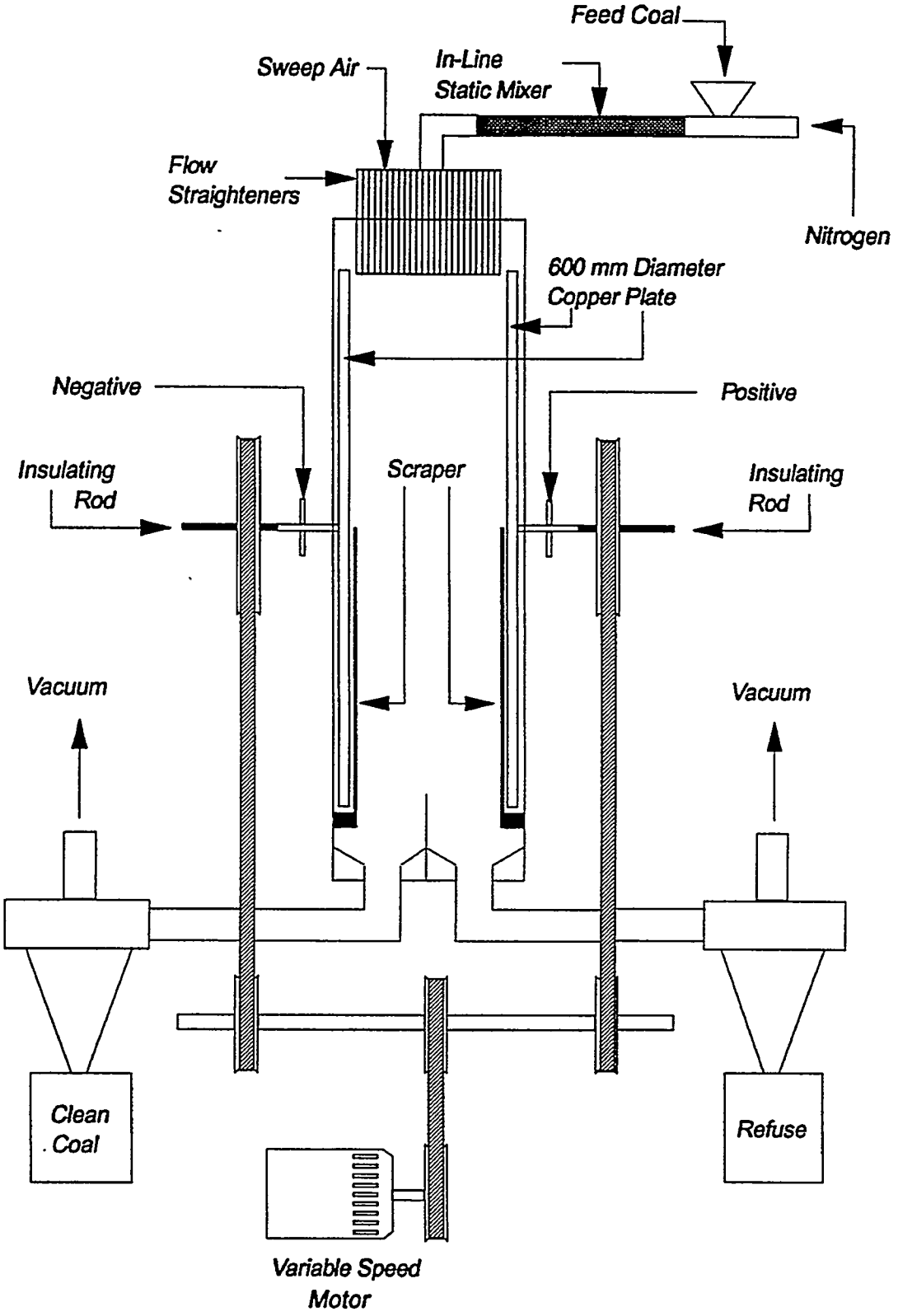

Figure 11-8. SCHEMATIC OF THE CONTINUOUS TRIBOELECTROSTATIC SEPARATOR

electrostatically on the rotating plates. The separated material is scraped off at the bottom of the plates and allowed to fall into collection ports. The products are withdrawn under vacuum into separate Plexiglas cyclones where the solids are separated from the gas stream. The vacuum is provided by separate sweepers. The sweepers are also used to draw sweep air through the flow straighteners at the top of the separator. Testing of this unit has been initiated.

Integrating a grinding device prior to triboelectrostatic separation is also being investigated. The emphasis will be on minimal grinding to achieve sufficient liberation for separation. This study will be held in conjunction with an investigation of the mechanisms responsible for the charging of the coal and mineral matter particles. This will include an investigation of the factors that contribute to the agglomeration of fine particles.

11.5 Subtask 1.5 Stabilization of Coal-Water Mixtures

OVERVIEW

The purpose of this part of the project is to obtain an understanding of the hydrodynamic properties of coal-water mixtures in order to

a) obtain stable slurries
b) be able to predict (calculate) the viscosity of a slurry, given its particle size distribution
c) be able to design blends of different size distribution that will give optimal loading

In recent reports, a new theory that describes the optimal size distribution has been presented. This is presently being refined, as in its original form it is complex and needs to be reduced, to a model that can be simply applied to practical problems. One way of accomplishing this is to simply "hide" the mathematical machinery in the form of a user friendly computer program for personal computers that will be made available to any potential user. Progress in this area is described below. The other way is to consider theoretical simplifications. This is also being pursued but will not be discussed here, as the work is incomplete.

THE CALCULATION OF POLYDISPERSE SLURRY VISCOSITIES

The main factor that determines the viscosity of highly concentrated slurries is the random close packing ratio, that is, the maximum possible loading of a given slurry. The theory mentioned above describes how to calculate this for a polydisperse system. Recent work on using this parameter in the form of a semiempirical equation for slurry viscosity is described.

The viscosity of complex systems like concentrated slurries is highly sensitive to how this property is defined and measured and also on the rate at which stress is applied. Only the simplest variant – the effective shear viscosity at zero frequency shear rate will be discussed. For dilute suspensions the classical result of Einstein shows that the effective viscosity depends only on the loading:

$$\mu = \mu_0\left(1+\frac{5}{2}\phi\right), \phi << 1 \qquad (1)$$

where μ is the effective viscosity, μ_0 is the viscosity of the solvent, and ϕ is the loading (volume fraction of the solid phase). As loading is increased, the universality of Equation 1 is lost, and the effective viscosity should depend on the details of interparticle interactions, particle shapes, etc. The surprising fact is that in the limit of large ϕ universality is recovered. This was first recognized by Dougherty and Krieger. Its validity will be shown here in a slightly more general framework than originally proposed.

The viscosity of a slurry grows quickly as the loading approaches the maximal value, ϕ_{max} and can be assumed to be infinite at ϕ_{max}. It can therefore be represented in the following form:

$$\mu = \mu_0\left(1-\frac{\phi}{\phi_{max}}\right)^{-p(\phi)\phi_{max}} \qquad (2)$$

where $p(\phi)$ is some 'well-behaved' function of ϕ. If ϕ is close enough to ϕ_{max}, the main contribution to Equation (2) is from the singularity at $\phi \rightarrow \phi_{max}$. Accordingly, the unknown function $p(\phi)$ can be substituted by the intrinsic viscosity, $p = p(\phi_{max})$. To determine the error involved in such an approximation, Equation (2) is taken and differentiated obtaining:

$$\frac{1}{\mu}\frac{d\mu}{d\phi} = \frac{p(\phi)}{1-\frac{\phi}{\phi_{max}}} - \phi_{max}\ln\left(1-\frac{\phi}{\phi_{max}}\right)\frac{dp}{d\phi} \qquad (3)$$

The first term in Equation (3) describes the influence of the divergent factor $1-\frac{\phi}{\phi_{max}}$ in Equation (2), while the second term describes the influence of the variation in the function $p(\phi)$. If $p(\phi)$ is substituted by the constant value $p = p(\phi_{max})$, an error of the order of the ratio of the second and first terms in Equation (3) is made. This error is negligible as long as:

$$\frac{1}{p}\left|\frac{dp}{d\phi}\right| << -\left[\phi_{max}\left(1-\frac{\phi}{\phi_{max}}\right)\ln\left(1-\frac{\phi}{\phi_{max}}\right)\right]^{-1} \qquad (4)$$

Experimental data in the literature indicates that when ϕ changes from 0 to ϕ_{max}, $p(\phi)$ changes from 2.5 to 2.7. Therefore $\frac{1}{p}\left|\frac{dp}{d\phi}\right| \sim 0.1$. On the other hand, the minimal value of the right hand side of

Equation (4) is $e/\phi_{max} \approx 4$, and is achieved at $\phi = \frac{e}{e-1}\phi_{max} = 0.63\phi_{max}$. The condition Equation (4) is always satisfied. Therefore,

$$\mu = \mu_0 \left(1 - \frac{\phi}{\phi_{max}}\right)^{-p\phi_{max}} \qquad (5)$$

where the intrinsic viscosity p is a *constant* coefficient, approximately equal to 2.7.

This simple argument shows why the Dougherty-Krieger correlation (Equation (5)) has been so successful when applied to concentrated slurries, and why other equations suggested for the concentration dependence of viscosity give essentially the same results as Equation (5). Since Equation (5) has the simplest and most general form, this is what will be used for the calculation of viscosity.

If the slurry is polydisperse, p and ϕ_{max} depend on the distribution of sizes and shapes of the solid particles. Repeating the preceding considerations, it can be shown that Equation (5) is still valid, but the parameters p and ϕ_{max} are now some function of the composition of the solid phase. The variations in p will be neglected, concentrating on the almost singular contribution $\left(1 - \frac{\phi}{\phi_{max}}\right)$.

The recipe for the calculation of slurry viscosity is therefore the following:

- Calculate the maximal random packing loading ϕ_{max}.
- Using the generalized Dougherty-Krieger correlation, Equation (5), to calculate μ at a given loading ϕ.

Now it is evident that the only way of decreasing the viscosity at a given loading is to increase ϕ_{max}. This is the problem of *optimal packing of particles* described in previous reports.

Computer programs are being developed to calculate this parameter and hence slurry viscosity. The progress in this area is described in the following section.

DEVELOPMENT OF PROGRAMS FOR CALCULATING SLURRY VISCOSITIES

Common grinding processes produce polydisperse powders that form polydisperse slurries. The aim is therefore to control this process and produce an "optimal" blend of particles of different sizes. Consider the following typical situation. Suppose two different grinders that produce particles of different sizes (e.g., "fine" and "coarse" powders) are used. Both outputs are polydisperse, but the particle sizes distributions are different. How to blend these outputs to produce the slurry of the lowest possible viscosity at a given loading must be determined. Of course, the answer to this question depends on the particle shapes, the details of their interactions, etc., and is a prohibitively complex problem. This problem cannot be solved exactly, but a simple

semiempirical theory has been constructed, which is described above and in previous reports, that allows this calculation. These will be made available in the form of software.

The initial version of the program that has been developed is called *Coal 0.1*. This reads text files containing size distributions and loadings of the samples of coal slurries. The input files can be obtained directly from measurements using particle counting devices like the Malvern Particle and Droplet Sizer. The program can plot a histogram of the mixture and a viscosity graph showing dependence of viscosity on the composition. Sample windows of the program are shown in Figures 11-9 and 11-10. The histogram and viscosity graph data can be saved as text files that can be read by programs like *Cricket Graph, Deltagraph,* etc. At present, the program is being modified to broaden and simplify its application by:

1. Improving the user interface of the *Coal* program.
   - The program should start with a Main window containing file areas and a toolbar. Clicking the mouse in the corresponding areas of the Main window should open input files, or enable plotting or printing. This will greatly enhance the intuitive character of the program.
   - The program should also contain multiple windows that allow the user to compare histograms and viscosity graphs corresponding to different mixing options.
   - Various modes of saving and printing plots *and* textual data need to be supported.
2. Design of a new program *Quick Mixer*. This program is meant to be a primary tool for an operator of a MCWM preparation plant. It should read the data on coarse coals (from a main grinder) and fine coals (from a secondary grinder) and given an instant recommendation of the amount of mixing and dilution. This program is being designed for an inexperienced user, and therefore must have a very intuitive and simple interface. This is presenting some programming difficulties, but none that cannot be solved.

12.0 PHASE III, TASK 2 STOKER COMBUSTION PERFORMANCE ANALYSIS AND EVALUATION

12.1 Subtask 2.1 Determine DOD Stoker Operability and Emissions

No work was conducted in Subtask 2.1.

12.2 Subtask 2.2 Conduct Field Test of a DOD Stoker

No work was conducted in Subtask 2.2.

12.3 Subtask 2.3 Provide Performance Improvement Analysis to DOD

No work was conducted in Subtask 2.3.

12.4 Subtask 2.4 Evaluate Pilot-Scale Stoker Retrofit Combustion

No work was conducted in Subtask 2.4.

12.5 Subtask 2.5 Perform Engineering Design of a Stoker Retrofit

No work was conducted in Subtask 2.5.

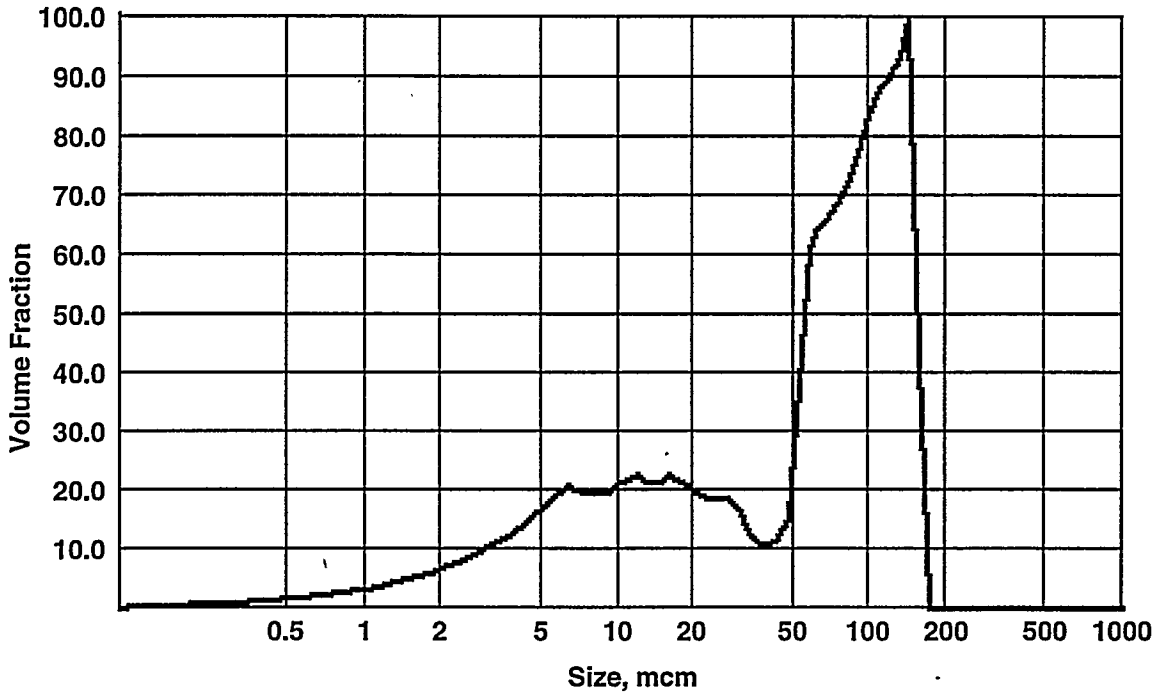

Figure 11-9. EXAMPLE OF A HISTOGRAM OF A BLEND OF TWO PARTICLE SIZE DISTRIBUTIONS PRODUCED BY COAL 0.1

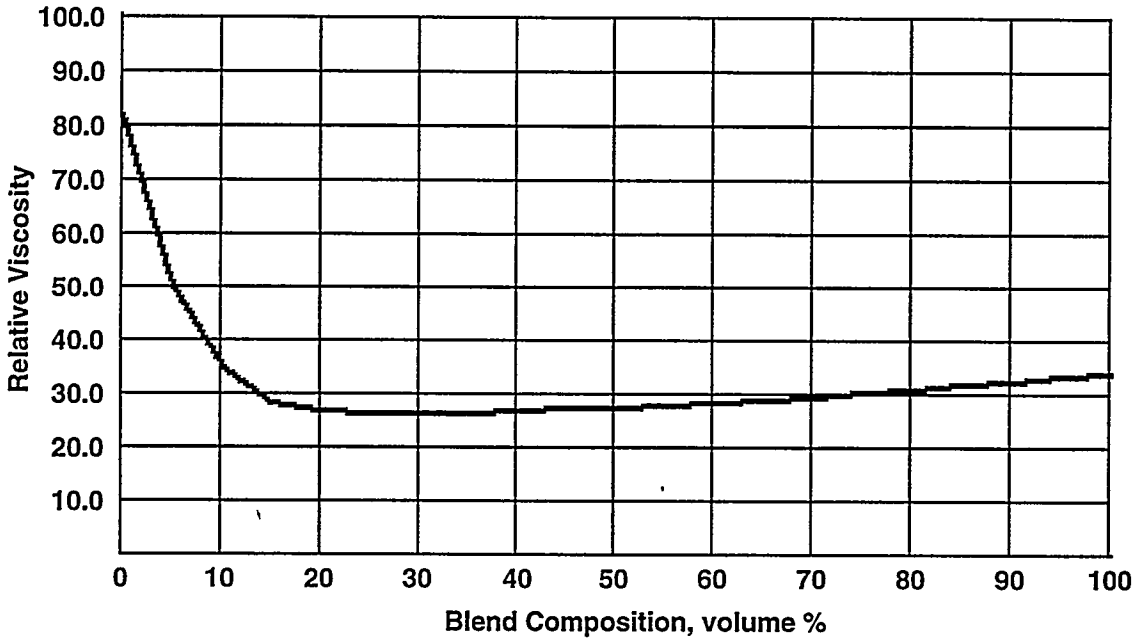

Figure 11-10. EXAMPLE OF A VISCOSITY GRAPH OF TWO BLENDED COAL SLURRIES

13.0 PHASE III, TASK 3 EMISSIONS REDUCTION

13.1 Subtask 3.1 Demonstrate Advanced Pollution Control System

No work was conducted in Subtask 3.1.

13.2 Subtask 3.2 Evaluate Carbon Dioxide Mitigation and Heavy Metal Removal in a Slipstream System

In this subtask, a study to examine the refossilization of algal biomass as a means of simultaneous mitigation of CO_2, NO_X, SO_X, and trace metals from coal-fired emissions is being performed.

PROJECT DESCRIPTION

The emission of flue gases from the combustion of fossil fuels contributes to a steady increase in greenhouse gases, to the problems of acid rain and to the production of health-hazardous trace metals. This study seeks to examine the feasibility of a novel strategy for multiple component mitigation by growth of the unique alga *Botryococcus braunii* directly on flue gas emissions, followed by anaerobic digestion and refossilization. The strategy will target concurrent reductions in the emissions of CO_2, NO_X, SO_X and major toxic trace metals. THE goal is to bury carbon assimilated in, nitrogen and sulfur incorporated into and trace metals absorbed onto a recently discovered refractory biopolymer produced during growth of *Botryococcus braunii* for geologic time scales. Following growth on flue gases, algal biomass grown on coal combustion effluents, is digested anaerobically to reduce labile cellular fractions of the algae to CO_2 and CH_4 which can be recycled for power generation. The refractory algal biopolymer, comprising up to 30% of the original algal biomass, undergoes vulcanization (sulfur cross-linking) during digestion as sulfur is incorporated and accumulates as a natural kerogen where upon it can be fossilized by disposal or reused depending upon economic and environmental factors.

Perhaps the most compelling factors for implementation of this strategy are the facts that existing or new power plants can be fitted with this proposed technology at a cost that is less than that required for conventional mitigation of sulfur species alone, and combustion effluents vented to atmosphere can be easily made to pass through algal ponds prior to venting.

PLANNED STUDY

The feasibility of this strategy will be tested by use of laboratory experiments to optimize algal growth and maximize production of the refractory biopolymers. The mitigation efficiency for NO_X, SO_X, CO_2 and trace metals will be evaluated under simulated and natural flue gas exposure conditions using individual and multiple component mixtures. Anaerobic digestion of algal biomass will be conducted to determine overall capture efficiency for each component and the feasibility for fossilization as a mechanism for long term removal.

PRELIMINARY RESULTS

Optimization of the Isolation Technique for Refractory Biopolymers

A new technique for isolation refractory biopolymers has been developed. Compared to methods described in literature the extraction procedure was shortened from several weeks to four days. The new technique will be presented as a talk at the Second Annual Meeting Central-Atlantic Region Association of Biogeochemists (CARAP) (May 27, 1995).

Characterization of Refractory Algal biopolymers by thermochemolysis with tetramethylammoniumhydroxid (TMAH)

This technique was developed for the characterization of polar compounds in macromolecules. The first application on refractory biopolymers from algae showed that this technique can also be used for their characterization.

Establishing Acquisition Parameters for ^{13}C and ^{15}N Solution NMR for the Chemical Characterization of Algal Material and its Degradation Products

The low sensitivity of the isotopes ^{13}C and ^{15}N in a NMR experiment makes it impossible to obtain ^{13}C and ^{15}N solution NMR spectra of algal biomass with standard NMR acquisition parameters. Optimal conditions had to be tested and established using the Department of Chemistry NMR facilities. ^{15}N NMR spectra of the algal residues can now be obtained.

NMR Spectroscopic Comparison of Torbanite and Algaenan

The nature of nitrogen in refractory biopolymers (algaenan) and its preservation during sediment diagenesis is still not completely understood. The first application of ^{15}N solid state NMR was achieved for algaenan in sediments which are derived from algal biomass and for Torbanite, an ancient algal coal. The results showed that, in algaenan and recent sediments, nitrogen is mainly bound in amide structures. In Torbanite the nitrogen is mainly bound in pyrrole/indole structures. In a previous study of composted grass material which was exposed to heat, it was shown that the transformation of amide functional groups to indoles and pyrroles can be accomplished by thermal alteration. Similar processes may be responsible for the alteration of amide functional groups to heterocyclic nitrogen functional groups during thermal maturation which is responsible for Torbanite formation. These data will be presented at the 17th International Meeting of Organic Geochemistry (September 4-8, 1995) and in two publications with the titles "^{15}N and ^{13}C NMR spectroscopic Examination of the Transformation of Organic Nitrogen in Plant Biomass during Thermal Treatment" (Soil Biol. Biochem.) and "^{13}C and ^{15}N NMR Spectroscopic Investigation on the Formation of Torbanite" (Org. Geochemistry).

CHARACTERIZATION OF NITROGEN IN COALS BY ^{15}N SOLID STATE NMR

Project Description

NO_X produced during coal combustion is well known to be a major contributor to the increase of greenhouse gases in the atmosphere. In order to develop successful strategies to

decrease NO_X emission during coal combustion a better understanding of the nature of nitrogen in coal is necessary. In spite of its importance, the chemistry of nitrogen in coal is not very well understood. The reason for this may be its low concentration of less than 2% and that macromolecules, which are insoluble in most solvents cannot be analyzed by the most common analytical techniques. A non degradative technique such as ^{15}N solid state NMR spectroscopy may contribute to a better understanding of the nature of nitrogen in coal and its chemistry during coal combustion.

Preliminary Results

The first ^{15}N solid state NMR spectra have been obtained from three different coals and their chars. The spectra display the main signal intensities in the region of pyrrole and indole derivatives. No signals assigned to pyridine derivatives were identified. This contradicts the most common belief that pyridine-like structures comprise a major form of nitrogen in coal. The successful application of ^{15}N solid state NMR to coal samples introduces a new technique which may help to provide a new level of understanding of coal-nitrogen chemistry. The results of this study will be presented at the 95th International Congress of Pacific Basin Chemical Societies held in Hawaii, December 17-23, 1995. A publication for *Energy and Fuels* is in preparation.

13.3 Subtask 3.3 Study VOC and Trace Metal Occurrence and Capture

No work was conducted in Subtask 3.3.

14.0 PHASE III, TASK 4 COAL-BASED FUEL WASTE COFIRING

14.1 Subtask 4.1 Coal Fines Combustion

No work was conducted in Subtask 4.1

14.2 Subtask 4.2 Coal/Rocket Propellant Cofiring

An informational meeting was attended at the U.S. Department of Energy Pittsburgh Energy Technology with attendees from industry (Energy and Environmental Research Corporation, Science Application International Corporation), government (DOE, NASA, Bureau of Mines), and a university (Penn State). Topics of discussion included the types of propellants, the current methods for removing them from rockets and their disposal, and current research.

15.0 PHASE III, TASK 5 ECONOMIC ANALYSIS

15.1 Subtask 5.1 Cost and Market Penetration of Coal-Based Fuel Technologies

No work was conducted on this subtask during this reporting period.

15.2 Subtask 5.2 Selection of Incentives for Commercialization of the Coal Using Technology

During this reporting period, data collection, organization and processing were performed. A list of 6,823 watertube boiler locations in the Commonwealth of Pennsylvania was generated from a database obtained from the Pennsylvania Department of Labor and Industry (PDL&I).

Consequently, these locations were cross referenced against the names of publicly traded corporations or their subsidiaries for the entire United States. This cross reference revealed 128 corporations, or their subsidiaries have water tube boiler locations in the Commonwealth of Pennsylvania. The latest and past one, three and five year annual financial statements, i.e. income statements and balance sheets, and key financial and operating ratios for the aforementioned 128 corporations were obtained.

The data was then tabulated and organized into a convenient format to facilitate quantitative analysis of the impacts of various government incentives for commercialization of the new technology. For given levels of boiler capacity the switch in technology is treated as a real investment and the net return on investment is calculated.

Preliminary data analysis reveals the result that firms under consideration respond to tax and depreciation allowances more than partial capital subsidies and reduced interest loan policies.

Further data analysis is planned where the effect of incentives will be analyzed by taking each firm's historical trends into account. Operational and financial leverages and other key financial ratios will be employed in calculating firms' sensitivities to various types of government incentives.

15.3 Subtask 5.3 Community Sensitivity to Coal Fuel Usage

During this reporting period, a literature review of the relevant risk perceptions literature was started. In addition, the research plan was reviewed with a risk perceptions expert to assist in developing a viable methodology. Beginning in mid-March, site characteristics will be compiled in order to proceed with a study site selection.

15.4 Subtask 5.4 Regional Economic Impacts of New Coal Utilization Technologies

A computable general equilibrium (CGE) model of the United States was updated and refined for subsequent analysis of technology adoption and energy policy issues. The original CGE model was developed by Dr. Shih-Mo Lin as part of his Ph.D. dissertation at West Virginia University in 1991. The base year was extended from 1982 to 1987 and the utility sector disaggregated into gas and electric components (see Appendices D and E for the mathematical representation of the model). The model is being updated to a 1992 base.

An analysis of the economic impacts of generic clean coal technologies, a carbon tax, and an oil price spike will be performed. Finally, this analysis will be integrated with the work on new technology adoption being performed by other researchers. The latter work will involve recalibration of production functions for specific clean coal technologies under development by Penn State. A spreadsheet program is being prepared that translates engineering cost estimates into standard industry classification categories used in economic models. Also, ways to map

differentials in scale, fuel quality, and fuel prices into distinct production vectors is being investigated.

15.5 Subtask 5.5 Economic Analysis of the Defense Department's Fuel Mix

In this subtask, current and future energy technology and fuel use in the military are being examined. This is in line with the Government's dual objectives of strategic diversification away from imported petroleum and to improve air quality standards.

The research has so far identified key sources of information for the final report regarding past, current and potential changes in fuel use in the military. This has included meeting with DOE to request material that was difficult to obtain at Penn State. Various other people in research institutions such as branches of the DOE and other government institutes have been contacted to request general information on subjects considered to be of interest.

The research is divided into two fairly distinct areas: 1) fuel use in transportation; and 2) fuel use for power generation and other stationary uses such as space heating.

In terms of transportation, data have been found on jet fuel, residual and distillate usage together with some predictions for future use (EIA). It has not been found how these figures break down in terms of specific types of vehicle. For now, distillate and residual fuel are assumed to be in use in navy ships, and kerosene fuel is assumed to be used for jets, with naphtha aviation fuel used in helicopters and other rotary/turbo-prop engines.

Alternative fuels have characteristics that make them more attractive than conventional fuels on strategic and/or environmental grounds. The report will include discussion of currently known alternative "fuels" in the broad sense and the conventional fuels that they replace and the technologies that are now being developed to exploit them (either in the military or private/civilian sectors).

Some on-going programs introducing alternative fuels into the military fleet have been identified and will be discussed in the report. Most of the available information refers to programs underway regarding civilian applications; some of these will also be discussed as the applications are very much the same as in the vast majority of military activity (logistic transport, for example).

Contact has been made with the military and data will be forthcoming. With respect to alternative fuel use and new technology, some alternative power generation sources have been identified covering alternative coal burning technologies and fuel cell use. Fuel cells are expensive to install but have low fuel costs due to their dramatically higher fuel efficiency. Other technology that could affect fuel use patterns includes the "E-scrub" coal scrubber technology that is being developed by DOD.

Demand side management programs are also being currently investigated by DOD as a means to reduce fuel consumption. The success of these could affect fuel usage significantly.

15.6 Subtask 5.6 Constructing a National Energy Portfolio which Minimizes Energy Price Shock Effects

During this reporting period, the necessary computer program and algorithm to efficiently estimate time-varying variances and covariances was obtained. The program was obtained in November and required a substantial amount of debugging before it was operational. The program now runs and has been used in trials to estimate several similar models.

A literature review has also been undertaken, revealing a relative shortage of research in this particular field. One potential paper exists examining the Nigerian energy mix. That study used a linear programming approach to choose an efficient mix. The literature survey has led to the belief that the form of the model should be based on the following assumptions:

a) the goal of the government is to maximize sustainable growth,
b) cheap energy encourages growth, and
c) volatile energy prices inhibit growth.

These assumptions imply that we should be able to determine the energy portfolio that meets a country's goals of expected low prices and low volatility. This will not be a unique portfolio but instead will be a portfolio set. The appropriate portfolio would then be chosen by the government based on the society's risk profile.

15.7 Subtask 5.7 Proposed Research on the Coal Markets and their Impact on Coal-Based Fuel Technologies

Two projects were undertaken under this topic. The first provided a survey of the history of U.S. coal consumption from since World War II. For years prior to 1960, only national total figures on consumption are available. However, for subsequent years, data by states are available. For the years 1957 to 1989, data also exist on interregional coal shipments. A draft report on these trends was completed in the Summer of 1994. Examination of this draft report disclosed numerous problems of form and substance. Consequently, the difference between 1960 and 1991 was examined. To see whether this mattered, numerous graphs were prepared to show behavior in the years between 1960 and 1991. The effort disclosed that it was useful to examine and report on the most important movements between these years. This effort was completed in early 1995. The draft report was completely reedited, comments were inserted in the main text, and appendices were added. The numerous graphs were all put into final form, but because of their large number, were not included in the report.

The work verified what was expected--that coal had changed from a fuel directly used in many parts of the economy to one predominantly (87 percent in 1983) employed to generate electricity, that the lost nonutility markets were predominantly served by coal mines east of the Mississippi, that the electric utility coal markets grew more west of the Mississippi, that a further but smaller problem for eastern coal mines was the shift of some midwestern states to coal

produced west of the Mississippi, and thus that the greatest growth in coal consumption was west of the Mississippi.

On the basis of this effort it was decided to proceed to study historic and prospective electric utility coal use in greater detail. The effort is designed to focus on differences among states over time in the growth of electricity generation and of the fuels used. The various major shifts that have occurred will be conveyed. Among the subjects of interest are the rise of oil use in electricity on the East Coast from 1966 to 1978 and its rapid decline from 1978 to the early 1980s, the rise of nuclear power, the shift of West Central and Mountain states to coal as the fuel for expanding electricity generation, and the tendencies from about the middle 1980s for electric utilities to shift to natural gas as the fuel for new capacity (with much of this capacity provided by firms outside the industry.).

A supplementary study was undertaken and recently completed on the forces in electric power that caused the shift to gas-firing in new plants.

15.8 Subtask 5.8 Integrate the Analysis

No work was scheduled in Subtask 5.8

16.0 PHASE III, TASK 6 FINAL REPORT/SUBMISSION OF DESIGN PACKAGE

No work was scheduled in Task 6.

17.0 MISCELLANEOUS ACTIVITIES

A paper was prepared and will be presented at the 20th International Technical Conference on Coal Utilization & Fuel Systems to be held at Clearwater, Florida on March 20-23, 1995. The title of the paper is "A Comparison Between Firing Coal-Water Slurry Fuel and Dry, Micronized Coal in an Oil-Designed Industrial Watertube Boiler."

18.0 NEXT SEMIANNUAL ACTIVITIES

During the next reporting period, the following will be done:

- Complete draft of the Phase I final report.
- Appropriate commercial NO_x and SO_2 technologies for installation on an industrial boiler will be identified, the systems will be designed, and component procurement will begin for installing them on the demonstration boiler.
- Work will begin on installing a ceramic bagfilter on the demonstration boiler.
- Bench-scale and pilot-scale emissions activities will continue with algal capture of trace metals and CO2, and will begin with low-temperature NO_x and SO_2 catalyst development.
- Work will continue in the refinement and optimization of coal grinding and MCWM preparation procedures.

- Work will continue on determining cost and market penetration, selection of incentives, and regional impacts of coal-based fuel technologies. In addition, work will continue in developing a national energy portfolio.

19.0 REFERENCES

1. Davidson, J. E., Hartsock, D. K., Conley, A. D., Hein, R. L. and Schanche, G. W., Overview of Slagging Coal Combustor Systems as Applied to Army Central Heat Plants, Technical Report, USACERL, E-91/04, (1991).

2. Sadler, L. Y. and Sim, K. G., Minimize Solid-Liquid Mixture Viscosity By Optimizing Particle Size Distribution, Chemical Engineering Progress, p. 68, (1991).

3. Skolnik, E. G., Scheffee, R. S. and Henderson, C. B., Effect of Particle Size Distribution on Viscosity of Coal Water Fuels, *Proceedings of the 8th International Symposium on Coal Slurry Fuels Preparation and Utilization*, Orlando, Florida, (1986).

4. Xie, J., Walsh, P. M., Miller, B. G. and Scaroni, A. W., Evaluation of Erosion-Corrosion and Ash Deposition in the Convection Section of an Industrial Watertube Boiler Retrofitted to Fire Coal-Water Fuel, *Proceedings of the 19th International Technical Conference on Coal Utilization & Fuel Systems.*, Clearwater, Florida, (1994).

5. Miller, e. a., Bartley, D. A., Morrison, R., Poe, R. L., Sharifi, R., Shepard, J. F., Xu, G., Scaroni, A. W., Hogg, R., Chander, S., Cho, H., Ityokumbul, M. T., Klima, M. S., Luckie, P. T., Rose, A., Addy, S., Considine, T. J., Gordon, R. L., Lazzo, J., Li, P., McClain, K., Schaal, A. M., Szczesniak, P., Walsh, P. M., Xie, J., Painter, P. C., Veytsman, B., Morrison, D., Englehardt, D. and Sommer, T., The Development of Coal-Based Technologies for Department of Defense Facilities, Semiannual Technical Progress Report, U.S. Department of Energy, Pittsburgh Energy Technology Center, DE-FC22-92PC92162, (1995).

6. Rassk, E., Erosion Wear in Coal Utilization, Hemisphere Publishing Corporation, ., (1988).

7. Finnie, I., p. 87, (1960).

8. Levy, A. V., p. 1, (1986).

9. Bouillard , J. X. and Lyczkowski, R. W., p. 37, (1991).

10. Sundarajan, G., p. 111, (1991).

11. Flament, G., International Fire Research Foundation(IFRF), K20/a/118, (1982).

12. Cen, K., Theory and Calculation of Multi-Phase Flow in Engineering (in Chinese), Zhejiang, China: Zhejiang University Press, ., (1990).

13. Khalil, E. E., Modeling of Furnaces and Combustors, Abacus Press, ., (1982).

14. Launder, B. E., Mathematical Models of Turbulence, Academic Press, ., (1972).

15. Sloan, D., Smith, P. J. and Smoot, L. D., Modeling of Swirl in Turbulent Flow Systems, *Prog. Energy Combust. Sci*, 12, 163, (1986).

16. Visser, B. M., Ph.D. Thesis, University of Delft: The Netherlands. (1991).

17. FLUENT, v. 4.25 Users Guide, FLUENT Inc., (1994).

18. Lawn, C. J., Principles of Combustion Engineering for Boilers, Orlando, Florida: Academic Press, ., (1987).

19. Truelove, J. S., The Modeling of Flow and Combustion in Swirled, Pulverized-Coal Burners, *Twentieth Symposium (International) on Combustion*, 523pp., (1984).

20. Weber, R., Dugue, J., Sayre, A. and Visser, B. M., Quarl Zone Flow Field and Chemistry of Swirling Pulverized Coal Flames: Measurements and Computations, *Twenty-Fourth Symposium (International) on Combustion*, 1373pp., (1992).

21. Truelove, J. S., Prediction of the Near-Burner Flow and Combustion in Swirling Pulverized-Coal Flames, *Twenty-First Symposium (International) on Combustion*, 275pp., (1986).

22. Lockwood, F. C., Salooja, A. P. and A., S. S., The Prediction of Coal Fired Flames, *Combustion and Flame*, 38, (1), (1980).

23. Magnussen, B. F. and Hjertager, J., On Mathematical Models of Turbulent Combustion with Special Emphasis on Soot Formation and Combustion, *Sixteenth Symposium (International) on Combustion*, Pittsburgh, PA, (1976).

24. Smoot, L. D., Hedman, P. O. and Smith, P. J., Pulverized-Coal Combustion Research at Brigham Young University, *Energy and Combustion Science*, 10, (4), 359, (1984).

25. Beer, J. M. and Chigier, N. A., Combustion Aerodynamics, London: John Wiley and Sons, ., (1972).

26. Gupta, A. k., Lilly, D. G. and Syred, N., Swirl Flows, ABACUS Press, ., (1984).

27. Truelove, J. S., Wall, T. F., Dixon, T. F. and Stewart, M., Flow, Mixing and Combustion Within the Quarl of a Swirled, Pulverized-Coal Burner, *Nineteenth Symposium (International) on Combustion*, 1181 - 1187 pp., (1982).

28. Visser, B. M., Smart, J. P., Van De Kamp, W. L. and Weber, R., Measurements and Predictions of Quarl Zone Properties of Swirling Pulverized Coal Flames, *Twenty-Third Symposium (International) on Combustion*, 949pp., (1990).

29. Truelove, J. S. and Williams, R. G., Coal Combustion Models for Flame Scaling, *Twenty-Second Symposium (International) on Combustion*, 155pp., (1988).

30. Truelove, J. S. and Holcombe, D., Measurement and Modeling of Coal Flame Stability in a Pilot-Scale Combustor, *Twenty-Third Symposium (International) on Combustion*, 963pp., (1990).

31. Weber, R. and Dugue, J., Combustion Acclerated Swirling Flows in High Confinements, *Prog. Energy Combust. Sci.*, 18, 349, (1992).

32. Milosavljevic, V. D., Taylor, A. M. K. P. and Whitelaw, J. H., Stability of Pulverized Coal burners, *Twentieth Symposium (International) on Combustion*, 957pp., (1990).

33. Milosavljevic, V. D., Taylor, A. M. K. P. and Whitelaw, J. H., The Influence of Burner Geometry and Flow Rates on the Stability and Symmetry of Swirl-Stabilized Nonpremixed Flames, *Combustion and Flame*, 80, 196, (1990).

34. Chang C, L. I., Chang I, Chou Y, Liu S, Shih S, Hwang D, Film Model for sulfur dioxide absorption into quiescent water with interfacial resistance, 28, (6), 1217, (1994).

35. Gage C, R. G., Modeling of SO2 removal in slurry scrubbing as a function of limestone type and grind, *EPRI SO2 Control Symposium*, New Orleans, Louisiana, (1990).

36. Makansi, J., Special Report: Reducing NOx Emissions from Today's Powerplants, p. 11, (1993).

37. Sloss, L. L., Hjalmarsson, A.-K., Soud, H. N., Campbell, L. M., Stone, D. K., Shareef, G. S., Emmel, T. M., M., Livengood, C. D. and Markussen, J., Nitrogen Oxides Control Technology Fact Book, New Jersey: Noyes Data Corporation, ., (1992).

38. Smith, D. J., Low-NOx Burners Lead Technologies to Meet CAA's Title IV, p. 40, (1993).

39. Yagiela, A. S., Maringo, G. J., Newell, R. J. and Farzan, H., Update of Coal Reburning Technology for Reducing NOx Cyclone Boilers, *Proceedings of the EPRI/EPA 1991 Joint Symposium on Stationary Combustion NOx Control*, Washington, D.C., (1991).

40. Chagger, H. K., Goddard, P. R., Murdoch, P. L. and Williams, A., Effect of SO2 on the Reduction of NOx by Reburning with Methane, *Fuel*, 70, (10), 1137, (1991).

41. Farzan, H., Rodgers, M., Maringo, G., Kokkinos, A. and Pratapas, J., Pilot Evaluation of Reburning for Cyclone Boiler NOx Control, *Proceedings of the EPRI/EPA 1989 Symposium on Stationary Combustion NOx Control*, San Francisco, CA, 6pp., (1989).

42. Borio, R. W., Kwasnik, A. F., Anderson, D. K., Kirchgessner, D. A., Lott, R. A., Kokkinos, A. and Durriani, S., Application of Reburning to a Cyclone Fired Boiler., *Proceedings of the EPRI/EPA 1989 Joint Symposium on Stationary Combustion NOx Control*, San Francisco, CA, (1989).

43. Knill, K. J. and Morgan, M. E., The Effect of Process Variables on NOx Species Reduction in Coal Fuel Staging, *Proceedings of the EPRI/EPA 1989 Joint Symposium on Stationary Combustion NOx Control*, San Francisco, CA, 6pp., (1989).

44. Cobb, D., Glatch, L., Ruud, J. and Snyder, S., Application of Selective Catalytic Reduction (SCR) Technology for NOx Reduction From Refinery Combustion Sources., *Environ. Prog.*, 10, (1), 49, (1991).

45. Prins, W. L. and Nuninga, Z. L., Design and Experience with Catalytic Reactors for SCR-DENOX., p. 187, (1993).

46. Cho, S. M. and Dubow, S. Z., Design of a Selective Catalytic Reduction System for NOx Abatement in a Coal-Fired Cogeneration Plant., *Proceedings of the American Power Conference, sponsored by Illinois Institute of Technology*, 54, 717, (1992).

47. Gutberlet, H. and Schallert, B., Selective catalytic Reduction of NOx from Coal Fired Power Plants, p. 207, (1993).

48. Vogt, E. T. C., Van Dillen, A. J., Geus, J. W. and Janssen, F. J. J. G., Selective Catalytic reduction of NOx with NH3 over a V205/Ti02 on Silica Catalyst, p. 569, (1988).

49. Chen, J. P. and Yang, R. T., Role of WO3 in mixed V205-WO3/TiO2 catalysts for selective catalytic reduction of nitric oxide with ammonia, p. 135, (1992).

50. Byrne, J. W., Chen, J. M. and Speronello, B. K., Selective Catalytic Reduction of NOx using Zeloitic Catalysts for High Temperature Applications, p. 33, (1992).

51. Matsuda, S., Kama, T., Kato, A., Nakajima, F., Kumura, T. and Kuroda, H., Deposition of Ammonium Bisulfate in the Selective Catalytic Reduction of Nitrogen Oxides with Ammonia, p. 48, (1982).

52. Richter, E., Schmidt, H. J. and Schecker, H. G., Adsorption and Catalytic Reactions of NO and NK3 on Activated Carbon, p. 332, (1990).

53. Makansi, J., Developments to Watch: Activated Coke Emerges as Cleaning Agent for Stack Gas, p. 60, (1992).

54. Juntgen, H., Richter, E., Knoblauch, K. and Hoang-Phu, T., Catalytic NOx Reduction by Ammonia on Carbon Catalysts, p. 419, (1988).

55. Yang, R. T., Chen, J. P., Kikkinides, E. S., Cheng, L. S. and Cichanowicz, J. E., Pillared Clays as Superior Catalysts for Selective Catalytic Reduction of NO with NH3., *Ind. Eng. Chem. Res.*, 31, (6), 1440, (1992).

56. Chen, J. P., Yang, R. T., Buzanowski, M. A. and Cichanowicz, J. E., Cold Selective Catalytic Reduction of Nitric Oxide for Flue Gas Application, p. 1431, (1990).

57. Fewel, K. J. and Conroy, J. H., Design Guidelines for NH3 Injection Grids Optimize SCR NOx Removal, *Oil & Gas Journal*, 91, (48), 56, (1993).

58. Redinger, K., Personal Communication, (1994).

59. Wang, J., Personal Communication, (1994).

60. Sczudlo, G., Personal Communication, (1994).

61. Reed, C., Personal Communication, (1994).

62. Perry, R. A. and Siebers, D. L., Rapid Reduction of Nitrogen Oxides in Exhaust Gas Streams, p. 657, (1986).

63. Lodder, P. and Lefers, J. B., Effect of Natural Gas, C2H6&CO on the Homogeneous Gas Phase Reduction of NOx by NH3., *Chem. Eng. Journ.*, 30, (3), 161, (1985).

64. Wood, S. C., Select the Right NOx Control Technology, p. 32, (1994).

65. Irons, R. M. A., Price, H. J. and Squires, R. T., Tailoring Ammonia-Based SNCR for Installation on Power Station Boilers, *Proceedings of the EPRI/EPA 1991 Joint Symposium on Stationary Combustion NOx Control*, Washington D.C., 25pp., (1991).

66. Tirpak, D. A., The Role of Nitrous Oxide (N20) in Global Climate & Stratospheric Ozone Depletion., *Proceedings of the EPRI/EPA 1987 Joint Symposium on Stationary Combustion NOx Control*, New Orleans, LA, (1987).

67. Muzio, L. J., Montogomery, T. A., Quartucy, G. C., Cole, J. A. and Kramlich, J. C., N20 Formation in Selective Non-Catalytic NOx Reduction Processes., *Proceeding of the EPRI/EPA 1991 Joint Symposium on Stationary Combustion NOx Control*, Washington, D.C., 25pp., (1991).

68. Jodal, M., Lauridsen, T. L. and Dam-Johansen, K., NOx Removal on a Coal-Fired Utility Boiler by Selective Con-Catalytic Reduction, p. 296, (1992).

69. Grisko, S., Personal Communication, (1994).

70. Epperly, W. R., The World of NOx Reduction Chemicals, Chemtech: p. 429, (1991).

71. Comparato, J. R., Buchs, R. A., Arnold, D. S. and Bailey, L. K., NOx Reduction at the Argus Plant Using the NOxOUT Process, *Proceedings of the EPRI/EPA 1991 Joint Symposium on Stationary Combustion NOx Control*, Washington, D.C., (1991).

72. Lyon, R. K. and Colè, J. A., A Reexamination of the RapreNOx Process, *Combust. & Flame.*, 82, 435, (1990).

73. Pletcher, D. and Weinber, N. L., The Green Potential of Electrochemistry, Part 2: The Applications, p. 132, (1992).

74. Aurousseau, M., Lapicque, F. and Storck, A., Simulation of NOx Scrubbing by Ceric Solutions: Oxidation of Nitrous Acid by Ce(IV) Species in Acidic Solutions, p. 191, (1994).

75. Pont, J. N., Evans, A. B., England, G. C., Lyon, R. K. and Seeker, W. R., Evaluation of the CombiNOx Process at Pilot Scale., p. 140, (1993a).

76. Pont, J. N., Evans, A. B., England, G. C., Lyon, R. K., Seeker, W. R. and Schmidt, C., Development of Advance NOx Control Concepts for Coal-Fired Utility Boilers, *Proceedings of the 9th Annual Coal Preparation, Utilization, and Environmental Control Contractors Conference*, Pittsburgh, PA, 19pp., (1993b).

77. Dasu, B. N., Deshmange, D., Shanmugasundram, V. and Lee, R., Microbial Reduction of sulfur dioxide and Nitric Oxide, *Fuel*, 72, (1993).

78. Apel, W. A. and Turick, C. E., The Use of Denitrifying Bacteria for the Removal of Nitrogen Oxides from Combustion Gases., *Fuel*, 72, (12), 1715, (1993).

79. Engineering, C., Chementator: UV Light Knocks out NOx from Flue gas., p. 19, (1994a).

80. Engineering, C., Chementator: Microwaves Destroy NOx on Coal Char., p. 29, (1994b).

81. Leonard, C. A., Haslbeck, J. L., Friedrich, J. J. and Woods, M. C., NOXSO Process Economics, Technical Paper, Noxso Corp., (1994).

82. Haslebeck, J. L., Woods, M. C., Ma, W. T., Harkins, S. M. and Black, J. B., NOXSO SO2/NOx Flue Gas Treatment Process:Proof -of-Concept Test., Technical Paper, Noxso Corp., (1993).

83. Livengood, C. D. and Markussen, J. M., FG Technologies for Combined Control of SO2 and NOx, p. 38, (1994).

84. Redinger, K. E. and Corbett, R. W., SOx-NOx-ROx-BOx Demonstration Project Review, Technical Paper, Babcock & Wilcox, (1993).

85. Evans, A. P., Kudlac, G. A., Wilkinson, J. M. and Chang, R., SOx-NOx-ROx-High Temperature Baghouse Performance., Technical Paper, Babcock & Wilcox, (1993).

86. Doyle, J. B., Redinger, K. E., Evans, A. P. and Kudlac, G. A., SNRB - Multiple Emissions Control with a High-Temperature Baghouse., (1993).

87. Hyland, M., WSA-SNOX Takes on North American Boilers, p. 59, (1990).

88. Olms, N., DESONOX Process for Flue Gas Cleaning., p. 247, (1993).

89. Systems, M. P., DESONOX is Put Through its Paces in Munster, p. 41, (1991).

90. Shah, P. P. and Leshock, D. G., Sorbent Life Cycle Testing Fluidized-Bed Copper Oxide Process, *Fourth EPRI Symposium on Integrated Environmental Control*, Washington D.C., (1988).

91. Roberts, A. E., Conceptual Design for Fluidized Bed Copper Oxide Process., *Proceedings of the 9th Annual Coal Preparation, Utilization, and Environmental Control Contractors Conference*, Pittsburgh, PA, (1993).

92. Harriot, P. and Markussen, J. M., Kinetics of Sorbent Regeneration in the Copper Oxide Process for Flue Gas Cleanup., p. 373, (1992).

93. Sato, S., Electron Beam Treatment Reduces SO2 and NOx in Coal Combustion Flue Gas, p. 211, (1993).

94. Besedina, E. A. and Kremkov, M. V., The prospects for the use of physico-chemical methods of removing sulfur and NOx from flue gases, *Thermal Engineering*, 39, (6), 318, (1992).

95. Shoichi, S., Electron beam treatment reduces SO2 and NOx in coal combustion flue gas., *Colliery Guardian*, 241, (6), 211, (1993).

96. Kremkov, M. V. and Besedina, E. A., The Prospects for the Physico-Chemical Methods of Removing Sulphur and Nitrogen Oxides from Flue Gases, p. 318, (1992).

97. Gangwal, S. K. and Silverston, P. L., A Novel Carbon-Based Process for Flue Gleanup., *Proceedings of the 9th Annual Coal Preparation, Utilization, and Environmental Control Contractors Conference*, Pittsburgh, 19pp., (1993).

98. Tamaki, H., Kawamura, K. and Yoshida, H., Effects of Temperature, Water Vapour, Sulfur Dioxide and Ammonia on the Discharge Oxidation of Nitrogen Monoxide, *Journ. of the Chem. Soc. Japan*, 11, 1597, (1979).

99. Makansi, J., Will Combined SO2/NOx Processes Find a Niche in the Market, p. 26, (1990).

100. Novoselov, S. S., Gavrilov, A. F., Svetlichnyi, V. A., Chmovzh, V. E., Simachev, V. Y. and Zaplatinskaya, I. M., Ozone Method of Removing SO2 and NOx from the Flue Gases of Thermal Power Stations, p. 496, (1986).

101. Mangal, R., Mozes, M. S., Feldman, P. L. and Kumar, K. S., Ontario Hydro's SONOX Process for Controlling Acid Gas Emissions, *Proceedings of the EPRI/EPA 1991 Joint Symposium on Stationary Combustion NOx Control*, Washington D.C., 25pp., (1991).

102. Helfritch, D., Bortz, S., Beittel, S., Bergman, P. and Toole-O'Neil, B., Combined SO2 and NOx Removal by Means of Dry Sorbent Injection, p. 7, (1992).

103. Bartok, W., Folsom, B. A., Elbl, M., Kurzynske, F. R. and Ritz, H. J., Gas Reburning-Sorbent Injection for Controlling SOx and NOx in Utility Boilers., p. 18, (1990).

104. Bartok, W., Folsom, B. A., Sommer, T. M., Opatrny, J. C., Mecchia, E., Keen, R. T., May, T. J. and Krueger, M. S., Application of Gas Reburning-Sorbent Injection Technology for Control of Nox and SO2 Emissions, *Proceedings of the EPRI/EPA 1991 Joint Symposium on Stationary Combustion NOx Control.*, Washington, D.C., (1991).

105. Gullett, B. K., Bruce, K. R., Hansen, W. F. and Hofmann, J. E., Sorbent/Urea Slurry Injection for Simultaneous SO2/NOx Removal, p. 155, (1992).

106. Narita, E., Sato, T., Shioya, T., Ikari, M. and Okabe, T., Formation of Hydroxylamidobis (sulfate) Ion by the Absorption of NO in Aqueous Solutions of Na2SO3 containing Fe(2+)EDTA Complex., p. 262, (1986).

107. Harriot, P., Smith, K. and Benson, L. B., Simultaneous Removal of NO and SO2 in Packed Scrubbers or Spray Towers., p. 110, (1993).

108. Tsai, S. S., Bedell, S. A., Kirby, L. H. and Zabick, D. J., Field Evaluation of Nitric Oxide Abatement with Ferrous Chelates, p. 126, (1989).

109. Engineer, C., Technology in Perspective: Argonne Chemistry offers deNOx/deSOx Solution, p. 30, (1989).

110. Chang, S. G. and Lee, G. C., LBL PhoSNOX Process for Combined Removal of SO2 and NOx From Flue Gas, p. 66, (1992).

111. Smock, R., Acid rain bills point to wet-scrubber retrofits, *Power Engineering*, 94, (6), 34, (1990).

112. Nolan, P. S., Flue-Gas Desulfurization in Thermal Power Plants, *Thermal Engineering*, 41, (6), 434, (1994).

113. Radcliffe, P. T., Economic evaluation of flue gas desulfurization systems, 1610-6, EPRI, GS-7193, (1991).

114. Moser, R. E., Evaluation of the Chiyoda Thoroughbred 121 Flue Gas Desulfurization Process at the University of Illinois Abbott Plant, EPRI, GS-7042, (1990).

115. IEA, The problems of sulfur, (1989).

116. Jansson, L. and Vannergerg, N. G., The Effect of the Oxygen Pressure and the Growth of Whiskers on the Oxidation of Pure Fe, p. 453, (1971).

117. Reeves, A., New scrubber process is sludge-free, *Coal mining and processing*, 16, (6), 50, (1979).

118. Jahnig, C. a. S., H, A comparative assessment of flue gas treatment processes. Part 1-Status and design basis, *Journal of the air pollution control association*, 31, (4), 421, (1981).

119. IEA, The problems of sulphur, *Reviews in Coal Science*, (1989).

120. Pruce, L., Why so few regenerative scrubbers ?, *Power*, 125, (6), 73, (1981b).

121. Report, M. P. S., High sulphur coal demo for US LIFAC, *Modern Power*, 60, (4), 67, (1990).

122. Gosman, A. D., p. 81, (1981).

123. Griffen, R. D., Principles of Air Quality Management, Lewis Publishers, ., (1994).

124. Tillman, D. A., Trace Metals in Combustion Systems, Academic Press, ., (1994).

125. Akers, D. and Dospoy, R., An overview of the use of coal cleaning to reduce air toxics, *Minerals and Metallurgical Processing*, August 1993, 124, (1993).

126. Drohan, D., Different Routes to VOC Control, *Pollution Engineering*, (September, 1992), 30, (1992).

127. McInnes, R., Jameson, K. and Austin, D., Scrubbing Toxic Inorganics, *Chemical Engineering*, September 1990, 116, (1990).

128. Cross, F. L. and Howell, J., New Technology to Meet Air Toxics Regs, *Pollution Engineering*, (March, 1992), 41, (1992).

129. Chedgy, D. G., Watters, L. A. and Higgins, S. T., Heavy-Media Cyclone Separations at Ultralow Specific Gravity, *Tenth International Coal Preparation Congress*, Edmonton, 60pp., (1986).

130. Berndt, E. R., The Practice of Econometrics: Classic and Contemporary, Reading, MA: Addison-Wesley Publishing Company, ., (1991).

131. Cen, K., *Particulate Science and Technology*, 21, 81, (1988).

132. Cumberland, D. J. and Crawford, R. J., The Packing of Particles, Elsevier, ., (1987).

133. Chong, J. S., Christiansen, E. B. and Baer, A. D., Rheology of Concentrated Suspensions, *Journal of Applied Polymer Science*, 15, 2007, (1971).

134. Farris, R. J., Prediction of the Viscosity of Multimodal Suspensions from Unimodal Viscosity Data, *The Society of Rheology*, 12, (2), 281, (1968).

135. Henderson, C. B. and Scheffee, R. S., The Optimum Particle-Size Distribution of Coal for Coal-Water Slurries, , 28, 11pp., (1983).

136. Miller, B. G., Morrison, R., Sharifi, R., Shepard, J. F., Scaroni, A. W., Hogg, R., Chander, S., Cho, H., Ityokumbul, M. T., Klima, M. S., Luckie, P. T., Rose, A., Addy, S., Considine, T. J., Gordon, R. L., McClain, K., Schaal, A. M., Walsh, P. M., Xie, J., Painter, P. C., Veytsman, B., Morrison, D., Englehardt, D. and Sommer, T., The Development of Coal-Based Technologies for Department of Defense Facilities, Semiannual Technical Progress Report, Department of Energy,
Pittsburgh Energy Technology Center, DE-FC22-92PC92162, (1993).

137. Austin L.G., R. R. K., P.T. Luckie, Process Engineering of Size Reduction: Ball Milling, (1984).

138. Tangsathitkulchai, C. and Austin, L. G., The Effect of Slurry Density on Breakage Parameters of Quartz, Coal and Copper Ore in a Laboratory Ball Mill, p. 287, (1985).

139. Pandya, K., Bahadur, p., Nagar, T. N. and Bahadur, P., Mecellar and Solubilizing Behavior of Pluronic L-64 in Water, p. 219, (1993).

140. Schick, M. J., *Nonionic Surfactants,* in "Colloids and Surfaces", Marcel Dekker: New York. (1987).

141. Hecht, E. and Hoffman, H., Interaction of ABA Block Co-Polymers with Ionic Surfactants in Aqueous Solution, p. 86, (1994).

142. Mular, A. L. and Musara, W. T., Batch Column Flotation: Rate Data Measurement, *Column '91*, Sudbury, Ont., (1991).

143. Huettenhain, H., Chari, M. V. and Schaal, M., Advanced Physical Fine Coal Cleaning: Microbubble Flotation, Final Report, DOE, GS-2704-5, (1990).

144. Ityokumbul, M. T., Maximum gas velocity for column flotation, p. 1279, (1993).

145. Bensley, C., Roberts, T., Nicole, S., Lamb, R. and Holtham, P., The Development of the Tower Flotation Cell, *Proc. 4th Australian Coal Preparation Conf.*, Queensland, (1988).

146. Ityokumbul, M. T., Upgrading of oil sand coke residues, p. 127, (1994).

147. Buscall, R. and White, L. R., The Consolidation of Concentrated Suspensions, *Journal of Chem. Soc. Faraday Trans.*, 1, (83), 873, (1987).

148. Tiller, F. M. and Khatib, The Theory of Sediment Volumes of compressible, Particlate Structures, *Journal Coll. Interf. Sci.*, 100, 55, (1984).

149. Kos, P., Sedimentation and Thickening - General Overview in Flocculation Sedimentation and Consolidation, New York: Engineering Foundation, ., (1985).

150. Weiland, R., Bunnaul, P. and Hogg, R., Centrifugal Dewatering of Flocculated Clays, p. 37, (1994).

151. Hogg, R., Lutsky, M. and Suharyono, H., A Simulation Model for Thickening of Flocculated, Fine-Particle Suspensions, *Proceedings, XIX International Mineral Processing Congress,*, San Francisco, CA, (1995).

152. U.S. National Technical Information Service, U. S. D. o. c., SilverPlatter 3.11 CD-ROM Database, (1985-1994).

153. Manfred, R. K., Quo Vadis, Coal Slurry, *10th International Conferene On Slurry Technology*, Lake, Tahoe, Nevada, 7pp., (1985).

154. Adelman, M. A., The World Ail Market: Past and Future, *The energy Journal*, 15, (special issue, Internationla Association of Energy Economics), 3, (1994).

155. Addy, S. N. and Considine, T. J., Retrofitting Oil-Fired Boilers to Fire Coal-Water Slurry: An Economic Evaluation, *19th International Technical Conference on Coal Utilization & Fuel Systems*, Clearwater, Florida, 341pp., (1994).

156. Schaal, A. M. and Gordon, R. L., A Comparison of Premium Coal Fuel Supply Options for the Conversion of Industrial Sized Boilers, *19th International Technical Conference On Coal Utilization & Fuel Systems*, Clearwater, Florida, 371pp., (1994).

157. Green, L., Developments to Watch, p. 65, (1993).

158. Black, F. and Scholes, M., The Pricing of Options and Corporate Liabilities, *Journal of Political Economy*, 81, 637, (1973).

159. Cox, J. C., Ross, S. A. and Rubenstein, Option Pricing: A Simplified Approach, *Journal of Financial Economics*, 7, 229, (1979).

160. Edwards, F. R. and Ma, C. W., Futures and Options, New York: 1st ed. HcGraw-Hill, ., (1992).

161. Pickles, E. and Smith, J. L., Petroleum Property Valuation: A Binomial Lattice Implementation of Option Pricing Theory, *The Energy Journal*, 14, 1, (1993).

162. Johnson, H., Options on the Maximum or the Minimum of Several Assets, *Journal of Financial and Quantitative Analysis*, 22, 277, (1987).

163. Report, P. O. G. P., Platt's Oil Price Handbook and Oilmanac, New York: ., (1988-1992).

164. Parkinson, M., The Extreme Value Method for Estimating the Variance of the Rate of Return, *Journal of Business*, 53, 61, (1980).

165. Garman, M. B. and Klass, M. J., On the Estimation of Security Price Volatilities from Historical Data, *Journal of Business*, 53, 67, (1980).

166. Fischer, S., Call option Pricing when the Exercise Price is Uncertain, *Journal of Finance*, 7, 169, (1978).

167. Boyle, P. P., The Quality Option and the Timing Option in Futures Contracts, *The Journal of Finance*, 44, (1), 101, (1989).

168. Magrabe, W., The Value of an Option to Exchange One Asset for Another, *The Journal of Finance*, 33, 277, (1987).

169. Stulz, R. M., Options on the Minimum or the Maximum of Two Risky Assets, *Journal of Financial Economics*, 10, 161, (1982).

170. Mann, A. P. and Kent, J. H., A COmputational Study of Heterogeneous Char Reactions in a Full-Scale Furnace, *Combustion and Flame*, 99, 147, (1994).

171. Zauderer, B. and Fleming, E. S., Demonstration of an Advanced Cyclone Coal Combustor, with Internal Sulfur, Nitrogen, and Ash Control for the Conversion of a 23 MMBtu/hr Oil Fired Boiler to Pulverized Coal, Department of Energy, DE-FC22-87PC-79799, (1991).

172. Lab, A.-E. R., Devlopment of Retrofit External Slagging Combustor, Department of Energy, DE-AC22-84PC-60417, (1987).

173. Kleeper, O. H., Delene, J. G., Drago, J. P., Fox, E. C. and Kahl, W. K., Comparative Assessment of Industrial Boiler Options Relative to Air Emission REgulations, Department of Energy, DE-W7405ENG26, (1983).

174. Klepper, O. H., Economics of Industrial Steam Options for the 1980's, *Annula Symposium on Industrial Coal Utilization*, Pittsburgh, (1984).

175. Corp., C. T., Design, Fabrication and Testing of an Advanced Cyclone Coal Combustor of an Industrial Boiler, Using Coal Slurries as a Fuel, Final Report, Department of Energy, DE-FG22-86PC-90266, (1987).

176. Board, P. E. Q., Environmental Master Plan, Environmental Quality Board, Commonwealth of Pennsylvania, (1982).

177. DER, P., 1992 Pennsylvania Air Quality Report, Department of Environmental Resources, DER #407-6/93, (1993).

178. DER, P., Annual Report to the General Assembly Pursuant to the Hazardous Sites Cleanup Act: Fiscal Year July 1, 1990 to June 30, 1991, Bureau of Waste Management, Department of Environmental Resources, Commonwealth of Pennsylvania, (1991).

179. Bodington, J. C. and Quinn, A. C., Methods for Analyzing the Market Penetration of End-Use Technologies: A Guide for Utlity Planners, Electric Power Research Institute, EPRI-EA-2702, (1982).

180. Griliches, Z., Hybrid Corn: An Exploration in the Economics of Technological Change, p. 501, (1957).

181. Gordon, R. L., An Economic Analysis of World Energy Problems, Cambridge, MA: The MIT Press, ., (1981).

182. Ackerman, B. A. and Hassler, W. T., Clean Coal/Dirty Air or How the Clean Air Act Became a Multibillion-Dollar Bail-Out for High-Sulfur Coal Producers and What Should Be Done about It., New Haven: Yale University Press, ., (1981).

183. Tietenberg, T. H., Transferable Discharge Permits and the Control of Stationary Sourcy Air Pollution: A Survey and Synthesis, p. 391, (1980).

184. Tietenberg, T. H., Emissions Trading: An ExerC.I.S.e in Reforming Pollution Policy, Washington, DC: Resources for the Future, (1985).

185. Malueg, D. A., Welfare Consequences of Emission Credit Trading Programs, *Journal of Environmental Economics and Management*, 18, 66, (1990).

186. Li, P.-C., Environmental Policy, Coal, and the Macroeconomy: The Impact of Air Quality Regulations on the Pennsylvania Economy, unpublished Ph.D. dissertation, Mineral Economics, Pennsylvania State University, (1994).

187. Shoven, J. B. and Whalley, J., Applied General-Equilibrium Models of Taxation and International Trade: An Introduction and Survey, *Journal of Economic Literature*, 22, (3), 1007, (1984).

188. Bandara, J. S., Computable General Equilibrium Models for Development Policy Analysis in LDCs, *Journal of Economic Surveys*, 5, (1), 1, (1991).

189. Kraybill, D. S., A Computable General Equilibrium Analysis of Regional Impacts of Macroshocks in the 1980's, Unpublished Ph.D. Dissertation, Department of Agricultural Economics, Agricultural Economics, uirginia Institute of Technology, (1990).

190. Robinson, S., Kilkenny, M. and Hanson, K., The USDA/ERS Computable General Equilibrium Model of the United States, USDA, (1990).

191. Lau, L. J., The Measurement of Raw Material Inputs, *Explorations in Natural Resource Economics*, Washington, DC, Resources for the future, 167pp., (1982).

192. Baffes, J. and Vasavada, U., On the Choice of Functional Forms in Agricultural Production Analysis, p. 1053, (1989).

193. Caves, D. W. and christensen, L. R., Global Properties of Flexible Functional Forms, p. 422, (1980).

194. Despotakis, K. A., Economic Performance of Flexible Functional Forms, p. 1107, (1986).

195. Samuelson, P., Prices of Factors and Goods in General Equilibrium, p. 1, (1953).

196. Armington, P., A Theory of Demand for Products Distinguished by Place of Production, IMF Staff Papers: p. 159, (1969).

197. Bergman, L., A system of Computable General Equilibrium Models for a Small Open Economy, p. 421, (1982).

198. Whalley, J. and Trela, I., Regional Aspects of Confederation, Toronto: University of Toronto Press, ., (1986).

199. Norrie, K. H. and Percy, M. B., Freight Rate Reform and Regional Burden: A Regional Equilibrium Analysis of Western Freight Rate Proposals, *Canadian Journal of Economics*, 116, 325, (1983).

200. Rose, A. Z., Labys, W. and Torries, T., Clean Coal Technologies and Future Prospects for Coal, p. 59, (1991).

201. World, E., The Nuclear-power Option: CAA Punishes Coal, Improves Nuclear Outlook, p. 16, (1991).

202. Kuckro, R. and Rubin, D. K., Industry Poised for Clean Air Bill, p. 12, (1990).

203. Yates, M., Washington and the Utilities: Congress Approves Historic Clean Air Legislation, p. 53, (1990).

204. World, E., News Analysis: The Impact of the New Acid-rain Laws, p. 9, (1990).

205. Jorgenson, D. W. and Wilconxen, P. J., The Economic Impact of the Clean Air Act Amendments of 1990, *The Energy Journal*, 159, (1992b).

206. Administration, E. I., Electric Power Annual 1991, U.S. Department of Energy, (1993).

207. Institute, E. P. R., Economic Evaluation of Flue Gas Desulfurization Systems, United Engineers and Constructors, Inc., (1991).

208. Dowlatabadi, H. and Harrington, W., Policies for the mitigation of Acid Rain: A Critique of Evaluation Techniques,, p. 116, (1989).

209. Association, P. C., Pennsylvania Coal Data 1993, Pennsylvania Coal Association, (1993).

210. Labys, W. C. and Wood, D. O., Energy Modeling, *Economics of the Mineral Industries*, 303pp., (1985).

211. Brooke, A., Kendrick, D. and Meeraus, A., GAMS: A User's Guide, REdwood City, CA: The Scientific Press, ., (1988).

212. Jenrich, J., Environmental Control, Nation's Business: p. 72, (1979).

213. Royston, M., Making Pollution Prevention Pay, p. 6, (1980).

214. Rose, A. Z., Discussion of Macroeconomic Models of the Economic Impact of Climate Change, *Hundred and Second Annual Meeting of the American Economic Association*, Atlanta, GA, (1989).

215. French, R., Aggregate Aconomic Impacts of Environmental Expenditures, *Social Science Journal*, 15, 73, (1979).

216. Hall, D., C., Preliminary Estimates of Cumulative Private and External Costs of Energy, p. 283, (1990).

217. Viscusi, W. K., Magat, W. A., Carlin, A. and Dreyfus, M., Environmentally REsponsible Energy Pricing, *The Energy Journal*, 15, (2), (1994).

218. Barbir, F. and Veziroglu, T. N., Environmental Damage caused by Fossil Fuels Consumption, *International Journal of Energy, Environment, Economics*, 1, (4), 297, (1991).

219. Herbst, J. A. and Sepulveda, J. L., Fundamental of Fine and Ultrafine Grinding, *The Powder and Solid Handling Conference*, Chicago, ILL, 452pp., (1978).

220. Stehr, N. and Schwedes, J., Investigation of the Grinding Behavior of a Stirred Ball Mill, p. 337, (1983).

221. Mankosa, M. J., Adel, G. T. and Yoon, R. H., Effect of Media Size in Stirred Ball Mill Grinding of Coal, p. 75, (1986).

222. Mankosa, M. J., Adel, G. T. and Yoon, R. H., Effect of Operation Parameters in Stirred Ball Mill Grinding of Coal, p. 255, (1989).

223. Gao, M. W. and Forssberg, E., A Study on the Effect of Parameters in Stirred Ball Milling, *International Journal of Mineral Processing*, 38, 45, (1993).

224. Zheng, J. and Harris, C. C., A Study on Grinding and Energy Input in Stirred Media Mills, *AIME Annual Meeting*, Denver, CO, (1995).

20.0 SELECTED NOMENCLATURE

G_ϕ = annular momentum
G_X = axial momentum
r = density of gas
u = axial component of gas velocity
w = tangential velocity
r = radius
S = swirl number
S' = modified swirl number
w = vorticity
Ω = angular velocity
Γ = circulation

21.0 ACKNOWLEDGMENTS

Funding for the work was provided by the U.S. Department of Defense (via an interagency agreement with the U.S. Department of Energy) and the Commonwealth of Pennsylvania under Cooperative Agreement No. DE-FC22-92PC92162. The project is being managed by the U.S. Department of Energy, Pittsburgh Energy Technology Center (PETC). John Winslow of PETC is the project manager.

The following Penn State staff were actively involved in the program: Michael Anna, Paul Colose, Howard R. Glunt, Ruth Krebs, Scott Lyons, Bradley Maben, Joseph Suefert, Christopher Snyder, and Ronald T. Wincek.